Climatic reconstruction of the last 1000 years from bristlecone pine tree rings at Blanco, White Mountains, California, USA.

Bale, Roderick Jon

Climatic reconstruction of the last 1000 years from bristlecone pine tree rings at Blanco, White Mountains, California, USA

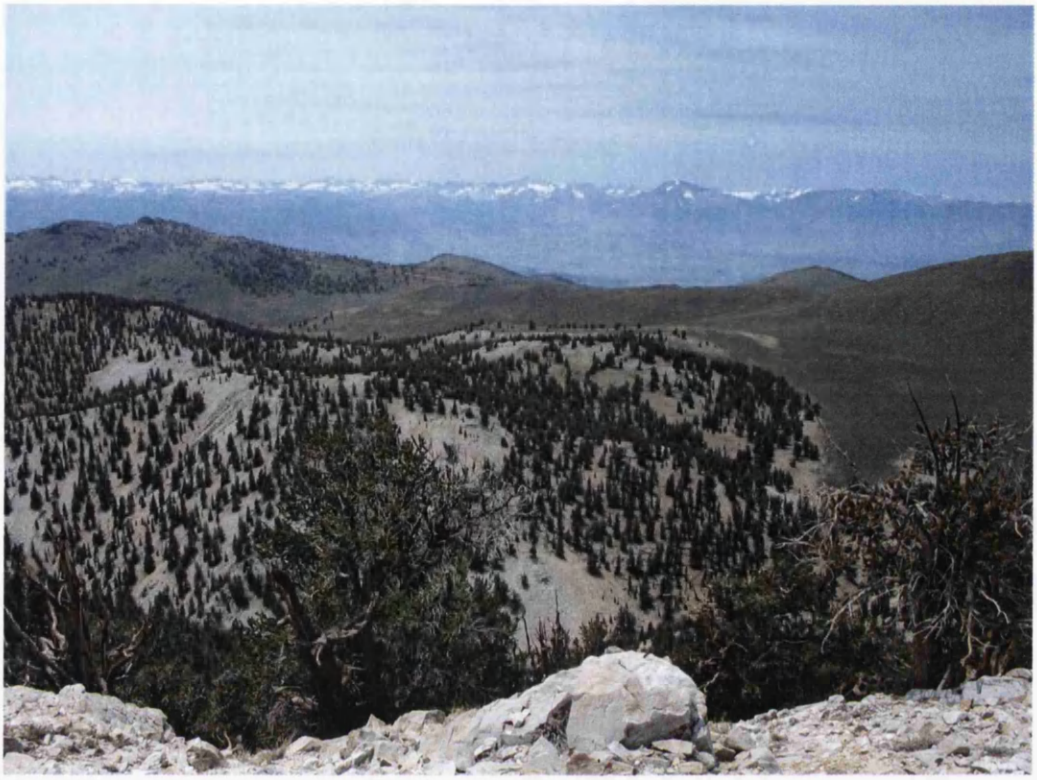

Roderick Jon Bale

Submitted to Swansea University in fulfilment of the requirements for the Degree of Doctor of Philosophy

Department of Geography

School of the Environment and Society

Swansea University

May 2008

SUMMARY

As the first decade of the 21st century draws to a close, a key issue facing humanity is that of climate change. Understanding past climate should improve future predictions and climate models. Stable isotope ratios from tree rings may be free from some of the problems associated with tree ring width studies. This research creates a millennial (AD1005-2005) annually resolved $\delta^{13}C$ based temperature and precipitation reconstruction from bristlecone pine trees growing at an elevation of *c.*3000m at Blanco in the White Mountains of south central California. Samples were cross dated, cut into annual increments and extracted to α-cellulose. Following this measurements of $\delta^{13}C$ were made. The $\delta^{13}C$ results were corrected for increasing atmospheric $\delta^{12}C$ concentration due to fossil fuel combustion ($\delta^{13}C_{cor}$), and for increasing CO_2 over the last 150 years ($\delta^{13}C_{pin}$). Summer temperature and precipitation are demonstrated to influence $\delta^{13}C$ ratios. Annual $\delta^{13}C$ fluctuations correlate strongly with summer precipitation, while lower frequency variations appear to follow changes in summer temperature. The mid 12th, late 16th, late 17th and early 18th century appear to have been warmer, or drier than the 20th century. The late 11th/early 12th, early 15th, early 17th and late 19th centuries appear to have witnessed wetter or colder periods than the 20th century. The data compares favourably with previous climate reconstructions from the Western United States.

DECLARATION

This work has not been accepted in substance for any degree and is not being concurrentlv submitted in candidature for any degree.

Signed.. .....(Candidate)

Date.....10:10:2008

STATEMENT 1

This thesis is the result of my own investigations, except where otherwise stated. Other sources are acknowledged in Harvard (author-year) style. A bibliography is appended.

Signed.... .....(Candidate)

Date.....10:10:2008

STATEMENT 2

I hereby give consent for my thesis, if accepted, to be available for photocopying and for inter-library loan, and for the title and summary to be made available to outside organisations.

Signed.. .....(Candidate)

Date.....10:10:2008

ACKNOWLDGEMENTS

This is an opportunity to thank those people and organisations that have made the completion of this thesis possible.

Firstly, my supervisors Dr Iain Robertson, Dr Mary Gagen and Professor Steve Leavitt, for their help and support throughout this research. Professor Leavitt kindly made available the bristlecone pine isotope data from previous research. Professor Danny McCarroll provided help and ideas with the data analysis and $\delta^{13}C$ corrections undertaken in this research and Dr Neil Loader shared his knowledge and expertise during fieldwork, with mass spectrometry and provided help with the interpretation of the data. Tom Harlan, the bristlecone pine fieldwork leader provided invaluable support, expertise and insight during fieldwork and with both preparation and cross dating of some of the samples used in this research. Rex Adams provided able assistance with increment borer maintenance and field sampling. All of the bristlecone pine fieldwork volunteers deserve thanks, and of particular help during the collection of samples for this thesis were; Dr Cynthia Froyd, Dr Kath Ficken, Dave and Ann Marie Clarke, Bob and Debbie Buecher, Adelia Barber and Rebecca Franklin.

There are many others who have helped during the last three and a half years; Paula Santillo and Jonathan Woodman Ralph for their help in the laboratory at Swansea. Other members of the Swansea geography department who helped and gave advice include Joanne Demmler, Dr Giles Young, Nathan Scott, Dr Tamsin Davies, Phil Bevan, Tommy Wils, Rochelle Campbell, Alan Cutliffe, Dr Sietse Los, Dr Graham Weedon and Steve Shaw.

Outside of Swansea Deni Vorst, Jemma Bezant, Nigel Nayling, Mark Blake and Richard Matthews also deserve thanks. My parents John and Ruth Bale have provided support throughout this thesis. Jessie, Morris and Lex provided welcome diversion from work.

Both Swansea University and the Natural Environment Research Council (NERC) deserve thanks for giving me the opportunity and funding to do this PhD and for providing the facilities to ensure successful completion.

Table of contents

Climatic reconstruction of the last 1000 years from bristlecone pine tree rings at Blanco, White Mountains, California, USA

LIST OF FIGURE AND TABLES

Section 1

Section 2

Section 3

Section 4

Section 5

Section 6

Section 7

Section 8

1.1: Introduction

Bristlecone pine trees are the oldest living trees on the planet, with some individuals nearly 5000 years old (Brown, 1996; Schulman, 1958). An 8700 years long absolutely dated sequence has been developed since the 1950s which may, in time, be linked with a 3000 year 'floating' sequence to be extended some 12000 years back toward the end of the last ice age (Ferguson, 1968; Ferguson, 1979; Schulman, 1958). The geographical range of bristlecone pine is restricted to mountainous regions of the southwestern USA. The bristlecones growing at an elevation of 3000-3500m are climatically sensitive due to a relatively arid environment with an average rainfall of 305-340mm. They survive on highly alkaline dolomite soil, with the Sierra Nevada to the west creating a rain shadow. Sparse ground cover results in few forest fires and little competition from other tree and plant species. High resin content provides resistance to moisture and decay and long retention of needles enable a tree to survive several years of stress (Ferguson, 1968).

Most previous research on bristlecone pine has focused on ring widths. Using ring width analysis, LaMarche (1974) was able to tentatively reconstruct warm season temperatures over the last 5500 years from the differing response of timberline bristlecone pine trees to climate. Although the early ring width studies of *Pinus longaeva* presented problems in terms of climate calibration and annual reconstruction of climate parameters due to the short, and sparse instrumental weather records available, more success with climate calibration has been achieved with *Pinus balfouriana* (foxtail pine) from the Sierra Nevada to the West (Scuderi, 1993; Graumlich, 1993) and from *Pinus aristata* (Rocky Mountain bristlecone pine) from the Colorado Plateau (Salzer and Kipfmueller, 2005) where detrended ring width series have been used to reconstruct millennial temperature changes. For example, in the study by Salzer and Kipfmueller (2005), mean annual temperatures and mean annual precipitation of the previous year are used to calibrate ring width records rather than an individual season or month. These and other studies are referred to in Chapters 6 and 8 where comparison of the data from this thesis and that of other climate reconstructions is considered. Likewise extreme ring width minima and anatomical abnormalities have been linked to environmental phenomena including

drought and volcanic activity (LaMarche and Hirschboeck, 1984; Salzer and Hughes, 2007).

There have however been several isotope studies on bristlecone pine tree rings. These studies were limited by now outdated techniques, either through analysis of bulk samples (Epstein and Yapp, 1976) or from selected years (Tang *et al.*, 1999). These reconstructions were based upon single trees often joined together in an almost arbitrary manner (Feng and Epstein, 1994). However, several common features were found, a warm or wet period centred around AD1100 (Leavitt, 1994; Leavitt and Long, 1992) and a possible cooler period around AD1450-1650 (Epstein and Yapp, 1976; Grinsted *et al.*, 1979). The increasing influence of anthropogenic $\delta^{13}C$ depleted fossil fuel burning on the isotopic composition of the atmosphere since the mid-19th century is also evident in the form of increasingly depleted $\delta^{13}C$ values from bristlecone pine cellulose (Epstein and Krishnamurthy, 1990; Feng, 1998; Feng, 1999). The most recent isotope study (Leavitt, 1994) utilised more trees, in the form of pooled five year 'blocks' of cellulose from two groups of trees from the Methuselah Walk site, 'Meth A' comprising four trees from AD1420-1984 and `Meth B` comprising two trees from AD925-1654. In addition, Leavitt and Long (1992) created a similar five year pooled series from higher elevation bristlecone pine from the Patriarch site (around 3500m a.s.l) comprising four trees and running from AD1380-1984.

However, owing to the extremely laborious preparation techniques that were used in the past, previous isotopic work on bristlecone pine was based on pooled samples from a few trees. Any trends apparent in the data from previous studies may not portray a true picture of isotopic variability between trees, and any climate calibration will be limited. Technological advances mean it is now possible to analyse very small amounts of wood or cellulose (McCarroll and Loader, 2004).

The approach taken in this research is analysis of absolutely dated annually resolved cellulose samples from seven trees of various ages (from 300 to 1000 years old). Being very long lived, bristlecone pine trees are, in theory, relatively free from the problems of

traditional 'short', overlapping tree ring sequences (Cook *et al.*, 1995) that often results in a loss of low frequency climate signal. Recent research (Gagen *et al.*, 2007) suggests that in any case cambial age (excluding the juvenile effect) may have little effect on the potential of overlapping tree ring isotope series to reconstruct high and low frequency climate changes. In addition to the information contained within ring widths, tree ring isotope series require minimal detrending and in many cases may exhibit a far stronger climate signal than ring widths alone (Robertson *et al.*, 1997). By using annually resolved samples from individual trees, this research demonstrates that both extreme high frequency environmental events and low frequency environmental information are demonstrated to be present in the data. In addition, using annually resolved, absolutely dated cellulose samples will allow direct comparison with other annually resolved climate records, an approach that is more difficult with records of lower resolution. Low frequency $\delta^{13}C$ appear to be strongly influenced by summer maximum temperature and annual variations appear to be dominated by total summer precipitation. Comparison with other millennial length proxy data is considered and the limitations and benefits of using stable isotopes in bristlecone pine tree rings are highlighted in this research.

1.2: Climate change over the last millennium – what is known?

Over the last twenty or so years scientists have become increasingly concerned that human activity is causing climate change, namely through greenhouse gas emissions and global warming, at an intensity and rate that in some cases has not been witnessed throughout the last several hundred thousand years (Jansen *et al.*, 2007). The IPCC (Intergovernmental Panel on Climate Change) reports of 1990, 1995, 2001 and 2007 all highlight how understanding of climate change has progressed. Increasing concern over the role of human activity in affecting climate throughout the 20th century has resulted in a situation where a large amount of time and money has been increasingly invested in climate research.

1.3: Long term proxy records of climate change.

Since the 1970's the science of palaeoclimatology has developed rapidly. The publication of the long polar ice core isotopic and chemical record (Hays *et al.*, 1976) provided clear evidence of astronomically driven insolation changes and the link between greenhouse

gases and glacial/interglacial cycles in a proxy record that is in places of annual resolution. The longest polar ice core (EPICA from Antarctica) record now extends back some 740000 years and ocean sediment cores and loess records extend back over the last 2 or 3 million years (Jansen *et al.*, 2007).

It is these archives that bear witness to the periodic changes in the orbit of the Earth around the Sun, that lead to changes in solar insolation. These orbital cycles, known as Milankovitch cycles, are well known from astronomical calculations. Changes in the tilt of the earths axis (obliquity) have a quasi periodic cyclicity of 41kyr (Jansen *et al.*, 2007) and the eccentricity of the earths orbit around the sun also modulates the distance between the sun and earth. Longer cycles of 400kyr and 100kyr occur due to eccentricity of orbit. In addition to the general procession of the equinoxes and the longitude of perihelion, shifts in the position of the solstices and equinoxes relative to the perihelion occur and these occur with a 19 and 23 kyr (thousands of years) periodicity (Jansen *et al.*, 2007). The result is relatively minor changes in latitudinal and seasonal distribution of insolation. Low insolation periods (such as 400kyr and the next 100kyr) seasonal insolation changes are less strong than larger eccentricity events (Jansen *et al.*, 2007). High frequency orbital variations are associated with far smaller insolation changes. The direct measurement of solar irradiance began 30 years ago and only small changes are evident. Cosmogenic isotope production as recorded in ice cores (^{10}Be) and tree rings (^{14}C) clearly show 11 year solar cycles, during which time isotope values are higher during times of low or absent sunspot numbers (Muscheler, 2007). Volcanic climate forcing is also difficult to gauge as location, persistence and temporal accuracy vary with each eruption. Indirect evidence is available in the form of acidity and sulphate levels. Regional and hemispheric changes due to volcanism are therefore difficult to detect and the choice of ice core data used also influences any reconstruction (Jansen *et al.*, 2007).
However the long term cycles of ice ages and interglacials associated with orbital and volcanic forcing, and evidenced in the long ocean and ice cores are also associated with large changes in greenhouse gas concentrations (Hays *et al.*, 1976; Imbrie *et al.*, 1984; Petit *et al.*, 1999; Raynaud *et al.*, 2000). The levels of these gases have increased rapidly over the last 100 or so years as a result of human activity and rapid industrialisation

throughout the world. Levels of the 3 main greenhouse gases, carbon dioxide (CO_2), methane (CH_4) and nitrous oxide (N_2O) are probably higher now than during the last 16kyr (Jansen *et al.*, 2007). Observations of greenhouse gas concentrations from ice core data show that changes in greenhouse gases during the last 10kyr were small and were probably the result of natural processes. Current atmospheric CO_2 concentrations (379ppm) are probably higher now than at any point during the last 650kyr and levels of CH_4 (1744ppb) exceed by far the natural range observed in ice core data from the last 650 kyr, these being 180-330ppm for CO_2 and 320-1790ppb for CH_4 (Raynaud *et al.*, 2000). As temperature and CO_2 levels co vary in the Antarctic a close relationship between CO_2 levels and climate is indicated. It is likely that atmospheric CO_2 levels amplify the large glacial/interglacial cycles but are not responsible for their occurrence. Antarctic CO_2 levels in previous interglacials rose several centuries before atmospheric CO_2 levels (Raynaud *et al.*, 2000). Although it is probable that there have been warmer interglacials on long term timescales (thousands of years), it is likely that the rate of warming has been much slower than that evidenced for the 20th century. For example, the warming of 4° to 7°C that has occurred since the last glacial maximum probably occurred ten times slower than the rate of 20th century warming. Warm periods evident in centennial scale proxy records indicate that warm periods during the last 10kyr are likely to have been regional in nature and cannot explain the global warming of the 20th century. There was orbitally forced glacial retreat in some areas due to warmth between 11 and 5kyr and at times before 5kyr were smaller or the same size as in the 20th century (Jansen *et al.*, 2007). The almost global retreat of mountain glaciers during the 20th century cannot be explained in the same way because summer insolation has actually been decreasing over the last few millennia in the Northern Hemisphere and should be favourable to the growth of glaciers. GCMs (Global Circulation Models) reveal regional temperature and monsoon changes in the mid Holocene compatible with orbital forcing. Climate and vegetation models suggest Holocene boreal treeline shifts in response to changing temperatures Studies suggest that treeline changes are likely to result in significant positive climate feedback (McDonald, 2003).

Palaeoclimatic data suggest decadal to centennial-scale changes in the regional frequency of tropical cyclones, floods, decadal droughts, and Africa/Asia monsoon intensity have likely occurred over the last 10kyr but the mechanisms behind these events are neither well understood or fully investigated (Jansen *et al.*, 2007).

1.4: Shorter timescales of environmental change

Narrowing down the timescale of analysis to 2000 years more detail can be added still. The dating resolution of the proxy data used over these timescales is often annual or near annual. It has long been thought that in addition to solar forcing, volcanoes may have a great impact on short term climate variability (Rampino and Self, 1982) and recent observations (McCormick *et al.*, 1995) of volcanic activity demonstrate how, in addition to recent human activity, natural events such as volcanism can also change the composition of the atmosphere and have effects on climate for several years after an eruption. That volcanism affects climate cannot be disputed, but the issue of whether volcanic eruptions and their climatic effects are evident in proxy climate data or the archaeological record has been, and remains a contentious issue (LaMarche and Hirschboeck, 1984; Scuderi, 1990; Baillie, 1991, 1994, 1999; Briffa *et al*, 1998; Hantemirov *et al*, 2003; Schindell *et al*, 2003; Salzer and Hughes, 2007; Larsen *et al*, 2008). Abrupt, rare temperature declines during the growing season (i.e spring/summer) result in frosts and multiday temperature declines that affect the structure of cells in trees prior to the completion of an annual ring and lignification in late summer/autumn (LaMarche and Hirshcboek, 1984). In places (such as the western United States) where instrumental meteorological data only extend back to the late 19th century evidence of such extreme events in proxy data can provide clues as to the nature and extent of extreme climates in preinstrumental times. Frost damaged tree rings offer one way of reconstructing extremes to annual or even seasonal resolution. Frost rings are anatomically distinctive, ice damaged, dehydrated layers of the outermost tree cells caused by prolonged sub zero growing season temperatures. In coniferous species these rings consist of underlignified and crumpled tracheids, collapsed cells and traumatised parenchyma cells. Two nights of temperatures below -5°C and one day of freezing temperatures are sufficient to lead to a frost ring (Glock, 1951; Hantemirov *et al.*, 2004;

Hantemirov and Shiyatov, 2002; LaMarche and Hirschboeck, 1984). Incompletely lignified tree rings are known as 'light' rings. These are the result of unfavourable, though perhaps not so extreme weather during the growing season and are often the result of a short, cool summer (Hantemirov *et al.*, 2004). As the factors affecting the fractionation of carbon isotopes are at least as well understood as the factors that lead to the formation of frost and light rings additional information about extreme climatic events may be gleaned through the analysis of extreme positive and negative isotope values on an annual basis. For example, Kuhn and Shepherd, (1984) attribute a 'stormy' period in California that lasted intermittently from 1883-1891 to the after effects of the eruption of Krakotoa in 1883. 1891 is the most negative $\delta^{13}C$ value in the period from 1850-2005 and is also picked up as an extreme in diverse tree ring data. Hantemirov *et al* (2004) attribute a frost ring in Siberian juniper in 1891 to a cold spell that lasted from July 5-7 and LaMarche and Hirschboeck (1984:121) attribute a frost ring in AD1884 from trees in the White Mountains and Snake Pass, Nevada to an event on the 9-10 September and a similar latewood frost ring in AD1965 to the 17-19 September. In 1902 an earlywood frost ring probably resulted from freezing temperatures from 3-4 July when temperatures at treeline may have fallen to -10° C. Stahle *et al* (2007) suggest that the weather in the early 20th century may have been the most severe pluvial period in the North America in the last 500 or perhaps 700 years. All the trees used in this research display negative values (suggestive of wet/cold) during the latter half of the 19th and the first quarter of the 20th century and though these are not the most extreme negatives in the whole chronology it is interesting to note that in tree 4123 (AD1453-2004) the extreme values in the late 19th century (notably 1853, 1863, 1891, 1922 and 1925) are the most negative in the whole of the 549 year period covered by this tree.

1.5: Tree rings

Tree ring sequences provide the most accurately dated record with annual or seasonal dating resolution possible for much of the Holocene. The Bristlecone pine trees of the southwest USA are the oldest living trees in the with a chronology of living and dead trees extending back to 8681 BP (Ferguson, 1979) with the possibility existing to extend

this back 10000 years BP. There are many shorter chronologies from other species in North America, spanning from 1000 to several thousand years (Scuderi, 1993). South America's longest tree ring sequences come from Chile where a 3622 year chronology has been created from *Fitzroya cupressoides* tree ring data (Lara and Villalba, 1993).

Tree ring chronologies from Western Europe are just as long as the North American chronologies but are made up of much shorter overlapping sequences (typically around 100-300 years) of living trees and dead trees from building timbers, archaeological contexts, river gravels and bogs. Oak chronologies from Britain and Ireland extend to 7272 BP (Pilcher *et al.*, 1984).German oak chronologies extend to 9971 BP, and when crossdated with subfossil pine specimens that grew when climate was too cold for oaks, extend the record back to 11370 BP (Becker, 1993; Kromer and Spurk, 1998). Aegean chronologies total 6500 years and are made up of long lived oak, juniper and pine, with some segments of this chronology over 1000 years long (Kuniholm *et al.*, 1996). The longest Scandinavian chronology, from overlapping Scots Pine samples is 7400 years long (Grudd *et al.*, 2002). Multi-millennial sequences from Russian Holocene deposits are of 4000 years in length, and are made up for the most part of short (samples of sixty to one hundred years in length) overlapping larch tree ring series (Hantemirov and Shiyatov, 2002). It is likely that in the near future the Russian chronologies will be extended further, as wood already ^{14}C dated to 9000 years BP old has been found in the same deposits (Hantemirov and Shiyatov, 2002). Many 'floating' chronologies exist for all the aforementioned areas, both in North America and Europe that may in time be tied into existing chronologies and extend an annually resolved record back several thousand more years. Work is ongoing to fill in many of the regional 'gaps' in annually resolved tree ring chronologies throughout the world but compared to the northern hemisphere, the southern hemisphere has far fewer tree ring chronologies.

Creating tree ring chronologies in tropical areas is difficult as the seasonality that causes trees in temperate areas to grow for an optimal seasonal period and therefore lay down annual rings is often absent from tropical areas. However tree ring work from mountain and other areas with pronounced seasonality has led to the creation of some multi millennial and more centennial records. Early African tree ring records were in the region

of 400 years long from South African cedar (Dunwiddie and LaMarche Jr, 1980). Work to further develop African tree ring chronologies is ongoing, with a 600 year tree ring isotope record recently developed from *Breonadia salicina* (Norström *et al.*, 2005) and work on Northern African trees promising millennial length sequences.

Multi species chronologies (pine, elm, juniper, hemlock and spruce) have been created for the Himalyan regions for up to the last 1200 years (Cook *et al.*, 2003). New Zealand and Australia have tree ring chronologies that are approaching 2000 years in length. Silver pine (*Lagarostrobos colensoi*) chronologies have been created for New Zealand from AD816-1998 (Cook *et al.*, 2002) and Kauri chronologies from New Zealand back to 1724 BC have recently been created (Boswijk *et al.*, 2006) and continue to be developed further. In Australia Huon Pine trees can live up to 2000 years and a 4000 year long chronology has been developed from Tasmanian specimens (Cook *et al.*, 2006).

1.6: 20th century climate change

It is likely that the combined radiative forcing from anthropogenically created greenhouse gases over the period 1960-1999 has occurred five times faster than at any time over the past two millennia prior to the industrial era (Jansen *et al.*, 2007). Between the 2001 IPCC report and the 2007 IPCC report re-analysis of the proxy datasets used for reconstructing temperature for the last millennium shows that there has probably been more variability than was shown in the 2001 report. The 12th to 14th and 17th to 19th centuries may have been cooler according to one study, while the 11th century may have been warmer according to another. The 2007 report strengthens the claim that the last 50 years are the warmest over the last 500 years and on a hemispheric level it is probably the hottest 50 year period over the last 1.3kyr. The warming over the last 50 years cannot be reproduced by palaeoclimatic model simulations without including anthropogenic greenhouse emissions. The report also acknowledges that most of the proxies used for reconstructing climate are from the northern hemisphere and that southern hemisphere has a low spatial density of proxy records. El Niño – Southern Oscillation (ENSO) teleconnections are more spatially varied in climate reconstructions for the last millennium than instrumental records suggest for the 20th century. Palaeoclimatic data from North and East Africa as well as the Americas suggest that decadal length droughts are a common feature of the last 2kyr (Jansen *et al.*, 2007).

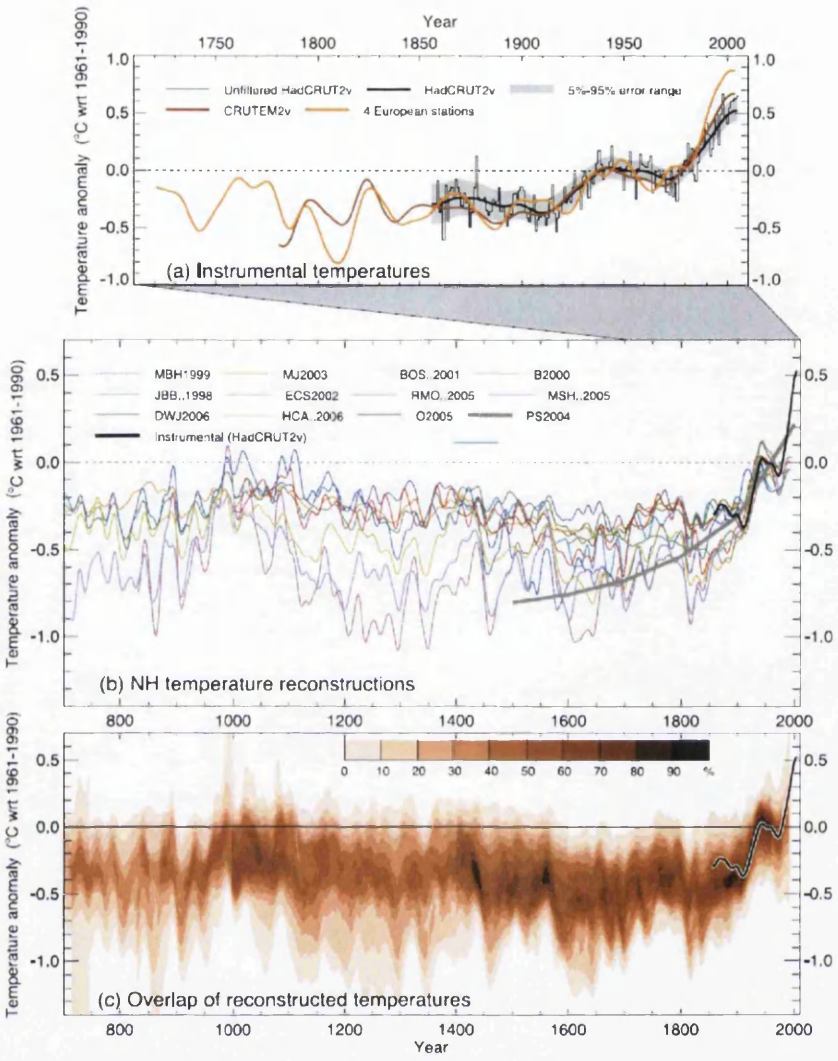

Figure 1.1. Northern Hemisphere temperature reconstruction for the last 1.3kyr . (a) Annual mean instrumental temperature records, identified in Table 6.1. (b) Reconstructions using multiple climate proxy records, identified in Table 6.1, including three records (JBB..1998, MBH..1999 and BOS..2001) shown in the TAR, and the HadCRUT2v instrumental temperature record in black. (c) Overlap of the published multi-decadal time scale uncertainty ranges of all temperature reconstructions identified in Table 6.1 (except for RMO.2005 and PS2004), with temperatures within ±1 standard error (SE) of a reconstruction 'scoring' 10%, and regions within the 5 to 95% range 'scoring' 5% (the maximum100% is obtained only for temperatures that fall within ±1 SE of all 10 reconstructions). The HadCRUT2v instrumental temperature record is shown in black. All series have been smoothed with a Gaussian-weighted filter to remove fluctuations on time scales less than 30 years; smoothed values are obtained up to both ends of each record by extending the records with the mean of the adjacent existing values. All temperatures represent anomalies (°C) from the 1961 to 1990 mean (Jansen et al., 2007).

The scientific community's current understanding of Northern Hemisphere temperature variability over the last 1300 years is best shown in figure 1 from the IPCC 2007 report (Jansen *et al.*, 2007).

1.7: Instrumental climate data

The uncertainties represented in figure 1.1 are chiefly a result of incomplete spatial coverage of instrumental climate data through time, and inherent errors in the longest instrumental records such as the central England temperature series that extends back to AD 1659 (Manley *et al* ,) . This is especially apparent in the 19th century where there is far less spatial cover of instrumental climate data. The data shows the last 20-30 years to be anomalously warm in the context of the last 150 years, with the land only data exhibiting a greater rate of warming (Jansen *et al.*, 2007). Land only data goes back to AD1781 with 23 European stations but only 1 North American station for the first two decades. The first instrumental Asian data begins in the 1820s. Four European records (central England, De Bilt, Berlin and Uppsala) that extend back in to 17th century show greater warming in the last 20 or 30 years than for the Northern Hemisphere (NH) as a whole. In fact, the European data as a whole, including instrumental, proxy and documentary evidence suggests that the 20th century may be anomalously warm in the context of the last millennium and the summer of 2003 may have been the warmest in the last 500 years (Guiot *et al* , 2005; Jansen *et al.*, 2007; Luterbacher and *et al.*, 2004).

1.8: Millennial temperature reconstructions

The third IPCC report of 2001 concentrated on three main temperature reconstructions for the last 1000 years. The first of these (Mann *et al.*, 1999) is a mean annual temperature reconstruction based on a range of proxy evidence including tree rings, ice cores and documentary evidence in addition to instrumental temperature and precipitation data from the 18th century on. For the first 900 years of this reconstruction multi decadal fluctuations are observable in the range of 0.3°C superimposed on a negative trend of 0.15°C followed by an abrupt warming of ~0.4°C during the first half of the 20th century. This trend has become known as the famous 'hockey stick' curve. The other temperature reconstructions (Jones *et al.*, 1998) and Briffa *et al* (2001) are based on a much smaller number of proxies and a tree ring density series back to AD1400 respectively. These reconstructions are warm season temperature reconstructions and are geographically focused on extratropical areas. They show more variability on centennial time scales prior to the 20th century and suggest cooler conditions during the 17th century than those in the Mann (1999) series. Naturally there have been a number of studies that are critical of these reconstructions. A study that examined regionally diverse proxy data (Soon and Baliunas, 2003) noted relatively warm (or cold), or alternatively dry (or wet) conditions occurring at any time within pre defined periods assumed to include the 'Medieval Warm Period' and 'Little Ice Age.

McIntyre and McKitrick, (2003) were unable to replicate the 'hockey stick' results of Mann *et al* (1998). However, a recent study (Wahl and Ammann, 2007) has been able to replicate the findings of Mann *et al.*, (1998) and showed that McIntyre and Mckitrick (2003) had not implemented the method used by Mann *et al.*, (1998). Further criticism was made (McIntyre and McKitrick, 2005a; McIntyre and McKitrick, 2005b) about the details of the Mann *et al.*, (1998) method, chiefly relating to the independent verification of the reconstruction against 19th century instrumental temperature data and to the extraction of the dominant modes of variability present in a network of western North American tree ring chronologies using Principal Components Analysis (PCM). This may

have some basis, but Wahl and Amman (2006) show that the impact on the amplitude of the final reconstruction is small (~0.05°C).

The most recent map of worldwide proxy data covering the last 1000 years is contained within the 2007 IPCC report and shown in figure 1.2 (Jansen *et al.*, 2007).

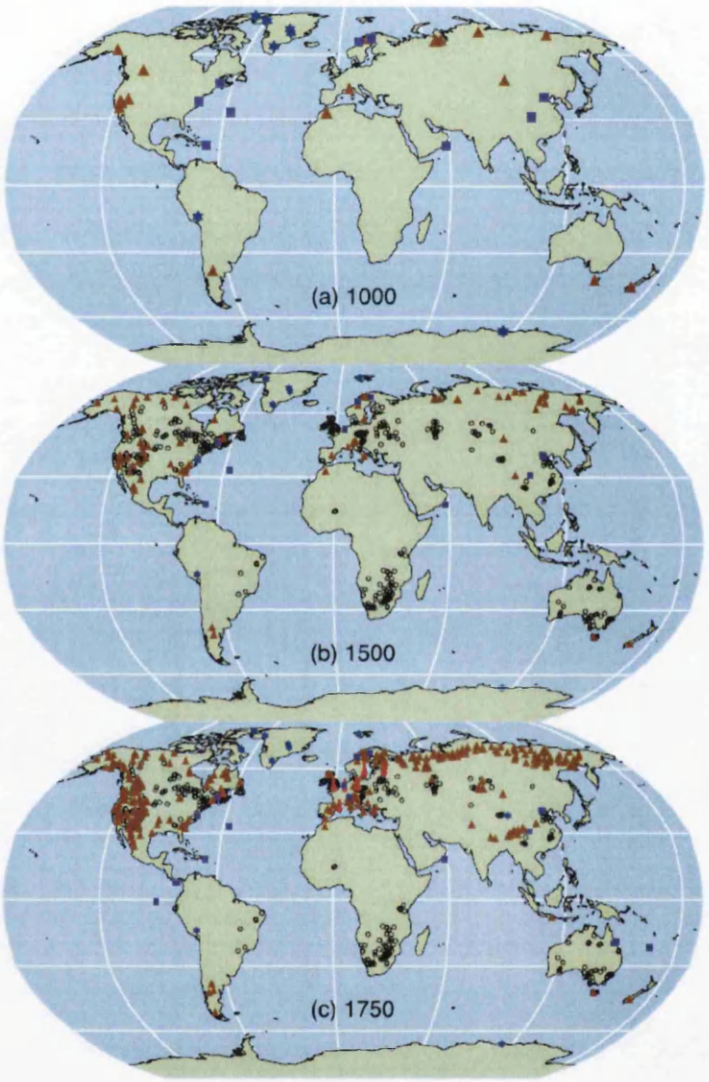

Figure 1:2.Locations of proxy records with data back to AD 1000, 1500 and 1750 (instrumental: red thermometers; tree ring: brown triangles; borehole: black circles; ice core/ice borehole: blue stars; other including low-resolution records: purple squares) that have been used to reconstruct NH or SH temperatures by studies shown in Figure 6.10 (see Table 6.1, excluding 2005) or used to indicate SH regional temperatures (Jansen et al., 2007).

Using tree ring data from Fennoscandia and Russia, Briffa (2000) developed a statistical technique capable of retaining multi-centennial time scale variability. These records are inherently bias toward recording Northern European summer conditions but when scaled using a NH mean temperature model a reconstruction of temperatures over Fennoscandia for the last 2kyr has been possible (Briffa, 2000). Esper *et al.*, (2002) analysed tree ring data from 14 Eurasian and North American sites that when smoothed and scaled against the Mann curve (Mann, 1998) showed markedly cooler temperatures between the mid-12th to the end of the 14th century. Mann and Jones (2003) selected eight temperature sensitive NH records to represent annual temperatures over the past 1.8kyr. Some of these are integrations of many individual site records, others are $\delta^{18}O$ ice core records and there is also tree ring and documentary data. A weighted average of decadally smoothed data was scaled and weighted so it fitted the mean and standard deviation of a combined land and marine instrumental NH temperature series between 1856-1980. Moberg *et al.*, (2005) used a mixture of tree ring and other proxy data to represent changes at short and long timescales respectively across the NH. The data was made up of seven tree ring series and a whole array of less well dated proxies including ice melt series, lake diatoms, pollen data, marine shell chemistry and foraminifera in addition to the borehole temperature record from the Greenland Ice Sheet were combined and scaled to match the mean and standard deviation of the instrumental record between 1856-1979. This displays the warmest temperature of any reconstruction during the 10th and 11th centuries but these are still below the level of warmth since 1980. Many of these individual proxies have been combined in a new reconstruction back to AD1400 based on a climate field reconstruction technique. The reconstruction proved robust to changes in the input of proxy data and different statistical reconstruction techniques. A climate reconstruction of North America (D'Arrigo *et al.*, 2006) based on tree ring data shows a large range of variability throughout the past millennium, with cool conditions during the 9th, 13th and 14th centuries. Of 14 proxies used by Hegerl *et al.*, (2006) only 3 were not tree ring based. Their reconstruction used least squares regression for scaling that is intended to reduce the loss of low frequency variance. This reconstruction lies close to the centre of the reconstruction by D'Arrigo *et al.*, (2006).

There are various ways in which proxy data are converted into different estimates of NH temperature as shown in figure 1.1. Regional data can be simply averaged and the resulting series scaled so the mean and standard deviation match the observed record with some period of overlap (Jones *et al.*, 1998) to more complex climate field reconstructions where large scale modes of spatial climate variability are linked to variations in a given proxy record via a multivariate transfer function that explicitly provides estimates of spatial and temporal changes in past temperatures, from which larger scale averages can be derived by averaging data across a given area (Mann *et al.*, 2005; Rutherford, 2005). Regionalisation of the data leads to fewer, but more robust, regional predictors (D'Arrigo *et al.*, 2006; Mann and Jones, 2003). However, such studies reconstruct temperatures for the tropics, based on data from the extratropics and assume stationarity in association between climatic regions.

A reconstruction of global temperature based on 169 glacier length records (Oerlemans, 2005) suggests moderate global warming occurred after around AD1850, and rose by around 0.6°C to the middle of the 20th century. Following cooling to around AD 1970 temperatures rose after, though there is a great deal of regional and high frequency variability superimposed on this interpretation. Other studies indicate that glacier advance in the western European Alps between AD 1760-1830 was driven by precipitation levels 25% above those of the 20th century while average temperatures remained stable. Retreat following 1830 was related to reduced winter precipitation with summer warming becoming important in the 20th century (Jansen *et al.*, 2007).

A major difficulty in determining what is affecting any proxy data series is identifying the relative influence of any climate parameter. With physical changes such as isotopic variations in ice core layers, or biological changes such as tree ring width variations or tree ring stable isotope ($\delta^{13}C$, $\delta^{18}O$, δD) variations, it is not possible to solely define these variations in terms of one climate parameter or to changes that occur within one season (e.g June to August temperature). Proxies must be calibrated by comparing the measured record of proxy data against instrumental records of climate. This enables an' optimum' period of climate influence to be identified. This inherently brings a degree of

compromise regarding the dependant variable selected. The differences observed in figure 1.1 reflect this and also the use of different predictor series. The approaches taken to statistical scaling also differ in the reconstructions and also accounts for differences observed in figure 1.1. There is considerable uncertainty with all the main NH temperature reconstructions. At the multi decadal time scale this is in the region of ±0.5°C and is generally calculated from the error apparent in the calibration of the proxies. No account is made of the statistical robustness of the period before instrumental data (Jansen *et al.*, 2007). Additional problems are introduced with tree ring data due to the way in which ring width and density chronologies are constructed. Statistical processing is undertaken to remove non-climatic trends that would obscure the climate signal in the data. Such processing can unfortunately obscure long term climate trends in the data, and in effect filters the data. As already mentioned, the calibration of tree ring records involves linear regression against a particular climate variable, an over simplification of what is in reality a complex biological system altered by a myriad of environmental influences. In addition non-climatic influence such as changes in atmospheric CO_2 and changes in soil chemistry may influence the assumption of uniformity in a long tree ring record. A group of ring width chronologies from the western USA display marked growth increases over the last 100 years that LaMarche (1984) attributed to increasing atmospheric CO_2. This data, which includes bristlecone pine ring width data, was used in the reconstruction by Mann *et al.*, (1998, 1999). Several analyses of ring width and density chronologies, with known temperature sensitivity do not emulate the general warming trend evident in instrumental temperature records over the last few decades. The early 20^{th} century warming is detected and over the whole instrumental period a good correlation with observed temperatures is apparent (Briffa *et al.*, 2004; D'Arrigo *et al.*, 2006). This 'divergence' between the tree ring and instrumental record is apparently restricted to northern high latitude regions but does not occur at all sites even there (Jansen *et al.*, 2007). Briffa *et al.*, (2001) excluded the post 1960 data in their calibration due to this problem, thereby assuming this is a recent problem. This argument is supported by (Cook *et al.*, 2004a). An alternative argument is that there has been a breakdown in the assumed linear relationship between warming and tree growth and this may have exceeded some threshold level whereby moisture stress is

now the limiting factor on growth (Jansen *et al.*, 2007). Whether this may also be the case for warm times in the past is uncertain, with investigation hampered by the lack of recent (last 20 years) tree ring data for most of the sites discussed here.

For the NH as a whole, there are in fact surprisingly few long well dated proxies, particularly prior to the 17th century (see figure 2). Those there are concentrated in extratropical, terrestrial locations and are bias towards summer sensitivity, rather than winter or annual conditions. There are very few long temperature series for the tropics. Stable isotope data from high elevation ice cores provide long records but modelling of such data indicates a dominant sensitivity to precipitation changes on seasonal and decadal time scales (Jansen *et al.*, 2007). Rapid melting of the tropical ice caps has been observed for the last few decades, this may be associated with enhanced warming at high elevations (Thompson, 2000). Coral $\delta^{18}O$ and Sr/Ca ratios reflect sea surface temperature (SST) but are often short (a few hundred years at most) and are not annually dated. The 20th century stands out in all these records as being the warmest period in the last few hundred years (Jansen *et al.*, 2007).

The proxy evidence points toward greater 20th century warmth than was reported in the third IPCC report in comparison with the last 400 years. The new reconstructions that extend further than 1000 years suggest the 20th century was the warmest in the last 1.3ky. The same evidence suggests the second half of the 20th century to be the warmest in the last 500 years. There is too much uncertainty with the proxy data to gauge the significance of individual years such as the very hot years of 1998 and 2005 in the context of the last millennium (Jansen *et al.*, 2007).

1.9: Bristlecone Pines – previous isotope work

In his paper detailing the creation of a 7500 year bristlecone pine tree ring series that had taken place over the previous 20 years, Ferguson (1979) commented on the strengths of this tree, in terms of ^{14}C timescale calibration and chronology building, also stressing the potential of these trees as a unique source of palaeoenvironmental and geophysical investigation. Moreover, in the same year Grinsted *et al.*, (1979) published a paper

detailing $^{13}C/^{12}C$ ratio variations in α-cellulose extracted from *Pinus longaeva* tree rings for the last millennium.

Leavitt (1994) has studied $\delta^{13}C$ values of cellulose from bristlecone pine for the last millennium. The chronology was made up of five year ring groups pooled from nine trees, and made up of two 'spliced' chronologies with an overlap of 235 years. The two most notable aspects of this study are progressively more negative $\delta^{13}C$ values (^{13}C-depletion) after AD 1800 and a temporary excursion to more negative isotopic values during AD 1080-1129. The high frequency $\delta^{13}C$ fluctuations in these chronologies are likely to be dominated by moisture stress and there is significant correlation with regional summer Palmer Drought Severity Indices (PDSI). The AD1080-1129 moisture excursion falls between 2 equally long periods of dry conditions. The results of the research described in this thesis compare favourably with those of Leavitt (1994) with extra information provided by annual resolution and the analysis of individual trees $\delta^{13}C$ instead of pooling samples.

Ring width index patterns do not reveal the full extent or magnitude of these climatic events as evidenced by $\delta\ ^{13}C$ chronology. Once a maximum ring size is attained under favourable conditions, any further improvement in conditions (e.g. more water) cannot increase growth further. Carbon isotopes however, continue to be a valuable proxy indicator of physiological responses to moisture conditions when ring size no longer responds to such extreme climatic conditions (Leavitt, 1994). This is an important finding with relevance to this research. If, as Leavitt (1994) and others (Robertson *et al.*, 1997, McCarroll and Pawellek, 1998) suggest, carbon isotopes represent a stronger climate signal than ring widths alone, the results of annually resolved carbon isotope tree ring series over the last 1000 years may enhance understanding of climate change

Epstein and Yapp (1976) present a δD chronology from bristlecone pine (decadal pooled samples of multiple trees) for AD 970-1974. The elevation of the chronology was given as 3000m, corresponding to the site studied by Leavitt (1994). The most notable feature of their curve is isotopically light (more negative) δD values for AD 1450-1650, which they interpreted as 'Little Ice Age' (LIA) signal. Short departure to less negative δD

values centres on AD 1100. Standard interpretation of δD in plant cellulose is that less negative values imply warmer conditions and more negative values imply cooler conditions, although there are questions as to the exact interpretation of δD values (DeNiro and Cooper, 1989). If the δD curve does represent temperature then in conjunction with the $\delta^{13}C$ chronology, the implication is a 50-year warmer and wetter period in the White Mountains around AD 1100. This event appears to fall between 2 equally long periods of dry conditions. A further study of δD and $\delta^{13}C$ values from bristlecone pine (Epstein and Krishnamurthy, 1990) shows a drop in δD values of 10‰ between AD 1090-1100. Citing the work of Lamb (1982), Epstein and Krishnamurthy (1990) link this fall in $\delta^{13}C$ values to the start of a possible cool period that led to the loss of colonies due to increased sea ice and cooling in Greenland around AD 1100. Lamb (1995) mentions the volcanic ash layer of AD 1090 that is present stratigraphically above the wealthiest of the medieval settlements at Kvisker in southeast Iceland.

Bristlecone pines in the White Mountains grow in two forms; full bark and strip bark form. Young trees are often covered by ring forming cambium (bark) but older bristlecone pine may have only a narrow strip of active cambium on one side of the trunk (Tang *et al.*, 1999). These two forms have been observed to have experienced different cambial growth rates over the last century or longer, with strip bark trees exhibiting the greatest growth. Increasing CO_2 has been shown to have a positive effect on plant photosynthesis and plant water use efficiency (WUE), and a negative effect on the stomatal conductance of plant leaves. A study of $\delta^{13}C$ values of both full bark and strip bark bristlecones from Sheep mountain (Tang *et al.*, 1999) aimed to test whether the WUE of trees at this site has increased over the last 200 year and whether the magnitude of any increase in iWUE (Intrinsic water use efficiency) for the 2 tree forms corresponds to the differing rates of stem growth. The results show the trend of tree $\delta^{13}C$ form a mirror image of the CO_2 concentration of the atmosphere for the past 200 years.

The $\delta^{13}C$ of trees in arid environments often correlates well with the amount of annual or seasonal precipitation, with a rainy season influencing growth for the next 1-3 years (Leavitt, 1989). In the study of full and strip bark trees by Tang *et al*, (1999), no

significant difference was observed between the full and strip bark trees in terms of WUE. Error may be introduced into these results when constant climate conditions are assumed for factors that may not be constant. Both types of tree demonstrate increased WUE in response to elevated CO_2 levels, with no significant difference between the two. Elevated atmospheric CO_2 concentration may lead to increased biomass allocation to roots in order to compensate for increased photosynthetic rate, though long term studies of this are lacking (Tang *et al.*, 1999).

The study by Tang *et al* (1999) correlates well with $\delta\ ^{13}C$ studies from the same area (Epstein and Krishnamurthy, 1990; Leavitt and Long, 1992). Leavitt and Long (1992) pooled multiple 5 year pentad cellulose samples for the period 1800-1983. The two study sites demonstrated consistently lower $\delta\ ^{13}C$ values at lower altitudes. Feng and Epstein (1995) used the same White Mountain trees as Epstein and Krishnamurthy (1990) as part of a study of carbon isotopes of trees from arid environments. The highest correlations were observed for fifteen year running averages of 5 year ring width/ $\delta\ ^{13}C$ values and may be interpreted as evidence of strong climatic response of bristlecone pine on decadal timescales. Due to the irregular growth of *Pinus longaeva* there are wide variations in an individual trees rings around the trees circumference. This has the potential to lower inter-tree correlation and also affect the signal strength as expressed as express population signal (EPS). In their study of δ D values of *Pinus longaeva* over 8000 years Feng and Epstein (1994) also report the differences in δ D values due to asymmetrical growth across different radii. The variations are reported as being coherent though access to full cross sections would enable full climatic variation to be assessed.

In addition to the ring width and isotope work undertaken on bristlecone pine there have also been a number of studies that examine the physiology of bristlecone pine. Net photosynthesis and dark respiration measurements were taken from bristlecone pine trees and big sagebrush growing close to each other at around 3000m above sea level (a.s.l) in the White Mountains (Mooney *et al.*, 1966). The bristlecone saplings in this study appeared relatively insensitive to environmental conditions during the summer of study, which included a period of drought. Carbon dioxide exchange rates of terminal branches

were stable from the initiation of bud elongation to the end of the growing season. Analysis of different aged needles also proved similar, as did transpiration rates during the active growth period. The sagebrush plants conversely showed marked fluctuations in metabolic responses during the growing season. Mooney *et al*, (1966) explain the differential reactions in terms of apparent water supply differences between the two plants.

Winter rates of photosynthesis and respiration have also been undertaken on White Mountain timberline bristlecones (Schulze *et al.*, 1967). Photosynthesis was observed to decline sharply following the onset of severely cold temperatures. By midwinter net photosynthesis was zero and remained so until early spring. Respiration rates were high from summer until late winter and then dropped rapidly in early spring as the air temperature increased and the ground thawed. This suggests a large CO_2 balance by the end of winter. Schulze *et al.*, (1967) suggest that approximately 117 hours of summer photosynthesis at peak rates are needed to equalize the winter loss of 140mg CO_2 per gram dry weight of photosynthetically active tissue.

There is a clear need to increase the number of annually resolved proxies at a regional scale to enhance understanding of the context of present climate in the last 1kyr. Annually resolved stable isotope values from tree rings offer are now obtainable on very small samples, so that even trees with very narrow rings such as bristlecone pine can be used. The bristlecone pine is one of the few annually resolved proxies present in figure 1.2 that covers the last 1000 years, and the use of bristlecone ring width data in NH climate reconstructions is at the forefront of the climate change debate. This research should complement the diverse research into bristlecone pines that has been undertaken over the last 60 years, providing additional information using techniques that have not been possible until the last decade.

1.10: Aims and research objectives.

The aims of this research are as follows:

- The primary aim of this research is to create a 1000 year annually resolved $\delta^{13}C$ chronology from α-cellulose extracted from individual tree cores. By using individual trees a clearer picture of inter tree variability may be gained, and more confidence can be placed in subsequent climate reconstruction.
- The aim of producing high quality annually resolved isotope data is to reconstruct annual variations in summer temperature and precipitation. As particularly long lived trees, bristlecone pine ring width data have been used as a key component of millennial length climate reconstructions, and their suitability in reconstructing northern hemisphere temperatures has been the source of much debate (Mann, 2005, McIntyre, 2005). Stable isotopes may contain a less ambiguous climate signal and help resolve some of the debate regarding climatic influence on bristlecone pine trees.
- The data generated from this thesis may contribute to the debate on the 'hockey stick' shape of millennial reconstruction and the unusual nature of 20^{th} century warming. This research complements previous bristlecone ring width and isotope research by using a novel technique to further understanding of how the trees are responding to climate change. By using annually resolved data the record can be compared directly to annually (or seasonally) resolved instrumental climate data, and also to other proxy and documentary evidence.

2: Methods

2.1: Introduction

This chapter firstly describes the rationale behind using bristlecone pine tree ring isotopes for this research. The field methods employed are then described. The laboratory methods are outlined in conclusion.

2.2: Stable isotopes in tree rings

The potential for large scale, regional annual climatic reconstruction is unrivalled in tree rings. The use of stable isotopes in tree rings has the added advantage that the environmental controls over their relative abundances in tree rings are relatively well understood compared to the myriad of factors that can affect the width of an annual tree ring. An isotope refers to the different forms of a given element that have different atomic masses. The isotopes within an element have nuclei with the same number of protons but a different number of neutrons. The mass number refers to the total number of nucleons, the number of protons plus neutrons.

Isotopic fractionation refers to the selective separation of chemical elements during natural physical, chemical or biochemical processes such as evaporation, condensation, transpiration and metabolism (Lowe and Walker, 1997). There are three main elements in wood: carbon, oxygen and hydrogen.

- $^{2}H/^{1}H = \delta D/\delta^{2}H$ (deuterium/hydrogen)
- $^{18}O/^{16}O = \delta^{18}O$ (oxygen)
- $^{13}C/^{12}C = \delta^{13}C$ (carbon)

2.21: Stable carbon isotopes in tree rings

Discrimination against ^{13}C during carbon fixation by trees (and other C3 plants) can be expressed as:

$$\Delta‰ = a + (b-a)(c_i/c_a)$$

Where a is the discrimination against ^{13}C during stomatal diffusion ($\approx$+4.4‰), b is the net discrimination due to carboxylation ($\approx$+27‰), c_i refers to intercellular CO_2 concentration and c_a refers to ambient CO_2 concentration (Farquhar *et al.*, 1982; Vogel, 1980).

Isotopic analysis of tree growth rings should provide a record of past climate related to the time of compound synthesis, thus forming the basis of $\delta^{13}C$ tree ring series as a climate proxy (Leavitt, 1993; Switsur and Waterhouse, 1998). The logic behind using stable carbon isotopes is as follows. If the tree is suffering from water stress or the temperature of the atmosphere around the tree is high this will lead to narrowing of the stomata in the leaves or needles. The lighter isotope (^{12}C) will evaporate in preference to the heavier isotope (^{13}C) due to the higher temperature, or water stress. This will lead to more positive discrimination against ^{13}C, as reflected in the tree ring cellulose.

$\delta^{13}C$ values from tree rings have been used to reconstruct relatively recent atmospheric $\delta^{13}C$ changes and climate. On longer timescales $\delta^{13}C$ values obtained from geological material reflect atmospheric changes in $\delta^{13}C$.
Difficulty in climatic reconstruction from tree ring isotope series occurs as the carbon isotope fractionation model indicates that the ratio of intercellular CO_2 to atmospheric CO_2 is driven by a variety of factors such as light, moisture, relative humidity and CO_2 concentration (Farquhar *et al.*, 1982).

WUE is defined by (Farquhar *et al.*, 1989) as the ratio of the net carbon fixed to the total water cost. Intrinsic plant water use efficiency (iWUE), the ratio of biomass production to

water loss, is also dependent on c_i/c_a and therefore related to $\delta^{13}C$ values. High $\delta^{13}C$ values correspond to high WUE and vice versa.

$$iWUE = A/g = C_a [1-(c_i/c_a)] (0.625)$$

Where A is photosynthetic rate, g is stomatal conductance and 0.625, also referred to as 1/1.6 derives from the ratio of binary diffusivity of CO_2 and water vapour in the air (Farquhar *et al.*, 1989).

The two processes of fractionation are constant, but are additive. The net effect depends on the isotopic ratios of the source gas. The value of ^{13}C in leaf sugars is controlled dominantly by $c_i;c_a$. If c_i is high relative to c_a stomatal conductance is much higher than the rate of photosynthesis resulting in a strong carboxylation discrimination against ^{13}C, yielding low $\delta^{13}C$ values. Low stomatal conductance compared to photosynthetic rate will have the opposite effect, internal CO_2 concentration will drop, and there will be less discrimination against $\delta^{13}C$ leading to higher values. The patterns of seasonal $\delta^{13}C$ changes in tree rings contain a record of seasonal environmental factors as they affect c_i/c_a (Helle and Schleser, 2004; Leavitt and Long, 1991). Therefore the dominant environmental controls on stable carbon isotope ratios in tree rings should be those that control the rate of stomatal conductance and photosynthesis (McCarroll and Loader, 2004).

Increases in atmospheric carbon dioxide concentration have the following effects on the isotopic composition of tree rings. CO_2 and O_2 compete for reaction sites on Rubisco. Increasing atmospheric CO_2 will result in increased carboxylation and decreased oxygenation. Photosynthetic rate is increased as oxygenation is followed by photorespiration that releases CO_2. This can allow plants to develop faster. Overall litter production rate may rise, leading to increased soil carbon. This has been observed in C_3 plants. Increased CO_2 levels allow partial closure of the stomata, restricting water loss during transpiration and producing an increase in the ratio of carbon gain to water loss

(WUE). This can lengthen the growing season in seasonally dry ecosystems and increase productivity (McCarroll and Loader, 2004).

In C_3 plants, this includes all the trees used in dendroclimatology, there are two major processes contributing to carbon isotope fractionation. These are CO_2 diffusive resistance for CO_2 entering the leaf through stomatal regulation and carboxylation by the photosynthetic enzyme, that is a measure of photosynthetic rate and capacity (Ehleringer *et al.*, 1993; Francey and Farquhar, 1982; Saurer and Siegenthaler, 1989). Furthermore a relationship has been demonstrated between leaf $\delta^{13}C$ levels, stomatal density, air pressure and altitude (Hultine and Marshall, 2000; Leavitt and Long, 1992; Woodward and Bazzaz, 1988).

Studies of $\delta^{13}C$/climate relationships from tree rings since the 1970s have enabled a detailed understanding of the factors which influence carbon isotope variations in tree rings, these being the balance between stomatal conductance and photosynthetic rate. Diffusion through the stomata represents the strongest physical control over CO_2 uptake. When fully open stomata can assimilate as much ^{12}C as possible. When atmospheric temperature is high or the tree is suffering from moisture stress, narrowing of the stomatal openings occurs in order to limit the amount of water lost by the tree. This however limits the amount of CO_2 available for photosynthesis. Gas exchange and photosynthetic systems within the tree will accordingly use more ^{13}C, which should be reflected in the isotope ratios in tree annual rings. At dry sites carbon isotope ratios in tree rings are dominated by relative humidity and soil water status and at moist sites by summer irradiance and temperature (McCarroll and Loader, 2004).

Stable oxygen and hydrogen isotope ratios record source water that contains a temperature signal, and leaf transpiration controlled dominantly by vapour pressure deficit. Variable exchange with xylem (source) water during wood synthesis determines the relative strength of the source water and leaf enrichment signals (McCarroll and Loader, 2004). This can be extremely useful in climatic reconstruction as the isotopic

composition of precipitation varies spatially according to environmental conditions (Edwards, 1993)

2.3: Species selection and isotopic differences between tree species.

Between species differences in isotope ratios, and the environmental signal imparted in different species are to be expected. Hydraulic conductivity, for example is more efficient in ring porous species than conifers. Such a process would influence the values of carbon, oxygen and deuterium (McCarroll and Loader, 2004). Conifers tend to yield higher $\delta^{13}C$ values than angiosperms (Stuiver and Braziunas, 1987). Leaf morphology is also important and Barbour *et al.,* (2002) suggest that it affects the environmental signal imparted. Needle temperature is closely correlated to air temperature, so the dominant control on enrichment is vapour pressure deficit. Flat leaves have a greater potential for evaporative cooling so stomatal conductance becomes important (McCarroll and Loader, 2004). Differences in rooting depth will affect water availability, and therefore stomatal conductance. Root depth will also affect the residence time of water in the soil, and hence its isotopic composition (Warren *et al.*, 2001). The $\delta^{18}O$ from shallow rooted trees may contain a better signal of annual variations in precipitation, whereas deep rooted trees, tapping into groundwater, may contain a clearer evaporative enrichment signal. Radiation levels (and therefore $\delta^{13}C$ values) will be strongly influenced by position in the canopy (McCarroll and Loader, 2004). Large differences in isotope values among trees of the same species from a given site have been shown to exist (Leavitt and Long, 1984; McCarroll and Pawellek, 1998). Others have demonstrated that $\delta^{13}C$ of two pine species was almost identical, despite ring width and density differences (Gagen *et al.*, 2004), and that the δD variation of different species at a site was less than that from within a species (Tang *et al.*, 2000). From a Quaternary perspective the trees that offer the greatest potential are those that form the long chronologies (McCarroll and Loader, 2004).

2.4: Site selection:

Stomatal conductance is controlled by soil water status and relative humidity (RH). Carbon isotope results from wet sites will often produce very different ratios than those from dry sites, which will be more sensitive to changes in precipitation, though this is not

always the case (Robertson *et al.*, 1997). The effects of moisture stress will be most observable in carbon isotopes, where stomatal conductance may be the strongest control, but will also affect oxygen and deuterium through evaporative enrichment in the leaf. Trees on dry sites (e.g bristlecone pine) are ideal for reconstructing moisture regimes, though where precipitation is seasonal the isotopic signature of source water may relate to winter, and the leaf enrichment signal to summer environmental conditions (Robertson *et al.*, 2001). Deliberately sampling dry sites, as is often the case with ring width studies, may, on the basis of isotope theory produce very misleading results, especially if the findings are applied to areas with different environmental influence.

2.5: Tree age

One of the major problems of deriving palaeoclimatic information from tree ring width series is that as a tree ages the ring width declines in an exponential fashion. Much effort has been devoted to detrending tree ring width series, while retaining as much climate signal as possible (Briffa, 2000). However, detrending may remove any climate signal that is equal to or longer than the tree's age. This may mean it is difficult to reconstruct climate over timescales longer than individual trees ages and has become known as the 'segment length curse' (Cook *et al.*, 1995). It is a common feature of many tree ring chronologies made up of short overlapping sequences.

A major question faced in isotope dendroclimatology is whether such age-related trends are present in tree ring isotope series. Unfortunately the methods of data treatment often adopted do not provide a clear, equivocal answer to this problem. Time and financial constraints often mean that trees are pooled prior to isotopic analysis, making it impossible to examine age related trends in individual trees. Age related trends in carbon isotopes have been observed in studies that use individual trees (McCarroll and Pawellek, 1998). Through sampling different age classes of beech trees (Duquesnay *et al.*, 1998) reported clear differences for the same years. More recently, using carbon isotope data, Gagen *et al.*, (2007) demonstrated that the cambial age (excluding juvenile effect) of Finnish trees had little effect on the long term trends in the record.

One interpretation of age-related changes has been the so called 'juvenile effect'. This has been observed in young trees and may be the result of trees closer to the forest floor recycling air already depleted in ^{13}C (Schleser and Jayasekera, 1985). However this trend has also been observed in Alpine settings where tree cover is sparse and recycled air is unlikely to be a factor (McCaroll and Loader, 2004). It has been suggested that a decreasing fixation from bark may be responsible, as the tree ages and bark thickens access to light diminishes (Cernusak *et al.*, 2001). Alternatively it may be that changes in hydraulic conductivity as a tree ages are responsible for depleted ^{13}C values in young trees (Ryan and Yoder, 1997). Due to gravity, leaf water potential decreases as tree height increases and the hydraulic conductance from soil to leaf declines with increasing path length. A decline in leaf-water potential should cause stomatal conductance to decline as trees grow higher, which would have a marked effect on fractionation of carbon and a lesser effect on the water isotopes. In some species this will be offset because the sapwood to leaf area ratio increases, making more water potentially available (McCarroll and Loader, 2004). Carbon isotope discrimination has also been correlated with height for two pine species (*Pinus moniticola* and *Pinus ponderosa*), and in both cases the sapwood to leaf area ratio also increased (Monserud and Marshall, 2001). They found no such trend for Douglas fir (*Pseudotsuga menziesii*), although for the same species McDowell *et al.*, (2002) demonstrated a clear trend of declining discrimination and stomatal conductance for three different height classes. More data are required from individual trees, of varying age and longevity, before this problem can be fully understood.

Again, pooling trees prior to isotopic analysis presents a problem with regard to identifying age related trends, as trends in individual trees will not be observable. An alternative is to use only those rings that formed after any 'juvenile effect' ceased, although this limits the length of series that can be used. This is the method commonly applied, and the first 30-50 years of a trees growth are often removed before isotope analysis.

An estimation of a tree cores distance from the pith maybe obtained by the apparent radius of the innermost rings. By placing a tree core on a 'bulls eye' drawing of concentric circles it is possible to make estimates about how far a core is from the pith.

With regard to the bristlecone pine trees used in this research only one of the cores from the material analysed reached anywhere near the pith (tree 001c). Isotopic analysis was carried out on this tree back to the 'pith' to see if any 'juvenile effect' is observed in bristlecone pine. The results from this single tree do not show a depletion in ^{13}C toward the pith and in fact the opposite occurs with the tree following the same trend as the older trees in the series. Obtaining pith estimates with such long-lived trees clearly presents a problem. With the oldest bristlecone specimens it is estimated that up to 800 years may be missing from the heart of the tree (Schulman, 1954).

BCP tree 001 appeared to be very close to the pith, and using the aforementioned 'bulls eye' method it was estimated that the core was perhaps 20 annual rings from the pith. However, bristlecone pine trees grow in many different forms and in young trees growth and form may be highly variable. For example, a tree of 1m could be 50 or 500 years old, as is evident in the picture of BCP tree001 (figure 2.6). An added problem is that this core was taken at breast height (around 1.2 m). The tree may have already been well over 100 years old by the time it reached the height at which it was cored. The carbon isotope values from this core do not show any pronounced 'juvenile effect', and in fact the innermost rings carbon isotope ratios follow the same pattern as the other trees and it may be assumed that the age of the innermost rings of the core are out of the range of this effect. Undertaking isotopic analysis of other relatively young bristlecone pine trees would help in answering the question of the extent and nature of a 'juvenile effect' in this particular species.

2.6: Individual samples over pooling:

Early tree ring isotope studies of the mid 20th century were limited by the technology available at the time and were dependant on large sample sizes and slow throughput, though precision was often better than with modern machines. Early studies were either based on small numbers of trees (one or two), pooled from multiple trees and often used 'blocks' of years, ranging from five- fifty years (Craig, 1954; Epstein and Yapp, 1976; Yapp and Epstein, 1982). Pooling samples can yield the same results as individual cores (Treydte *et al.*, 2001) but pooling samples prior to isotope analysis severely limits the ability to place confidence limits around inter tree variability. Defining variability, and thus precision, by placing confidence limits around mean values and resulting reconstructions is a great advantage of tree rings over other climate proxies (lake and ice cores for example) which only normally yield one value for each time period. Pooling samples also prevents removal of non-climatic (e.g. age) trends in the individual trees isotope record (McCarroll and Loader, 2004).

2.7: Field sampling:

12mm and 5mm increment cores were obtained from bristlecone pine trees growing at the Blanco West site in the White Inyo Mountain range, California, USA. (37°27'N, 118°10'W) and at around 3000m elevation. The locations of all trees used in the $\delta^{13}C$ chronology are described below.

Table 2.1: Location of bristlecone pine trees used in this research.

tree	Lat/long	altitude	d.b.h	slope	aspect	Full/strip bark
001	N37 ° 27 722' W118° 10 724'	3240m	102cm	20°	NE	full
523	N37 ° 27 577' W118° 10 474'	3240m	95 cm	20°	S	strip
362	N37 ° 27 670' W118° 10 485'	3243m	160cm		W	full
123	N37° 27.642' W118° 10.315'		87cm			full
527	N37° 27.642' W118° 10.501'	3230m	124cm	10°	NW	strip
007	N37° 27.716' W118° 10.418'	3230m	123cm	35°	NW	strip
487	N37 ° 27 672' W118° 10 296'	3404m	110cm			strip

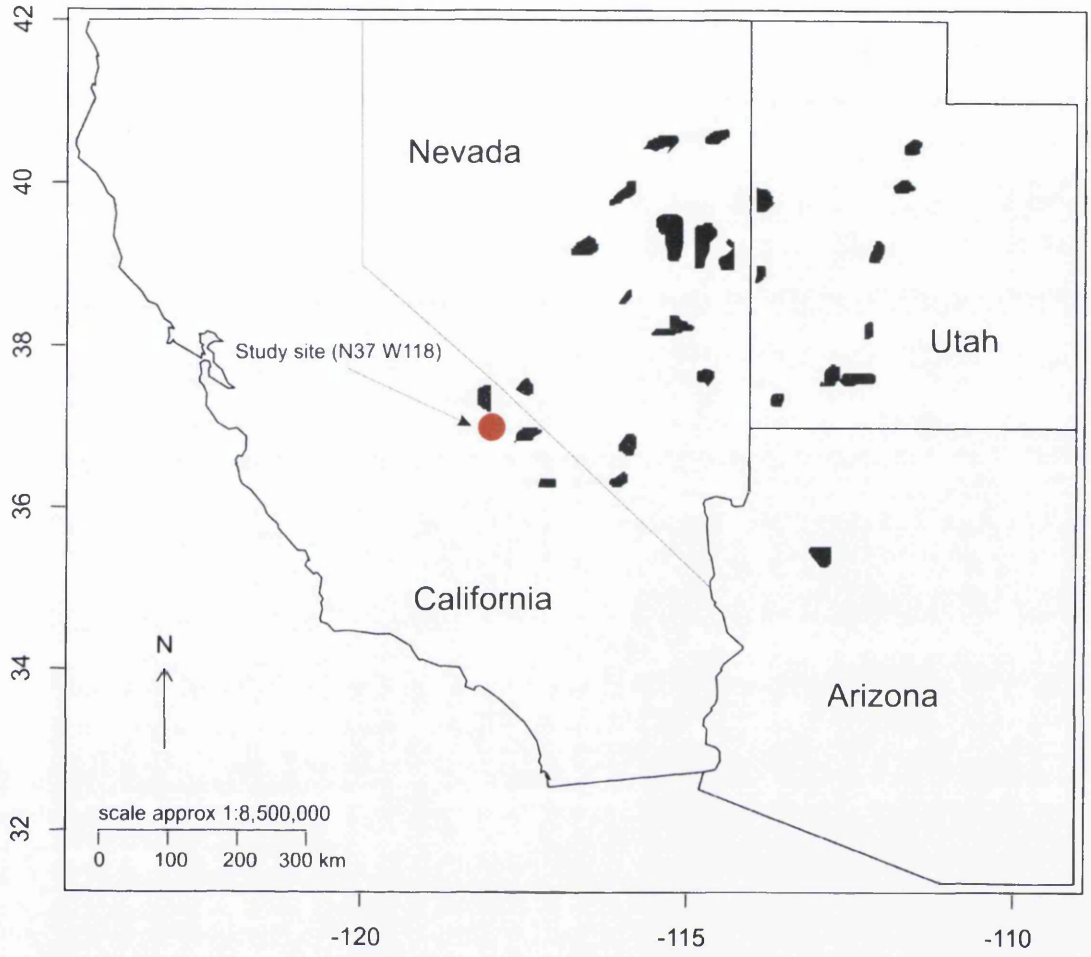

Figure 2.1. Approximate distribution of bristlecone pine indicated by shading (Pinus longaeva, D.K Bailey) and the location of the study site. Rocky mountain bristlecone pine (Pinus aristata) grows to the east in the Colorado Rockies. The range of bristlecone pine (Pinus longaeva D.K Bailey) is patchy and restricted to mountainous areas of the south western United States.

Figure 2.2(upper): GPS points of sampled trees on U.S Department of Agriculture/Forest Service map (1:24000).

Figure 2.3(lower): 1950s aerial photo of Blanco West and sampled trees. The highest tree density is apparent on north facing slopes, followed by west facing slopes. North and west facing slopes receive less daytime sunlight and are therefore subject to less harsh growing conditions. The cooler temperatures on these slopes also means that snow is held longer providing more favourable growing conditions.

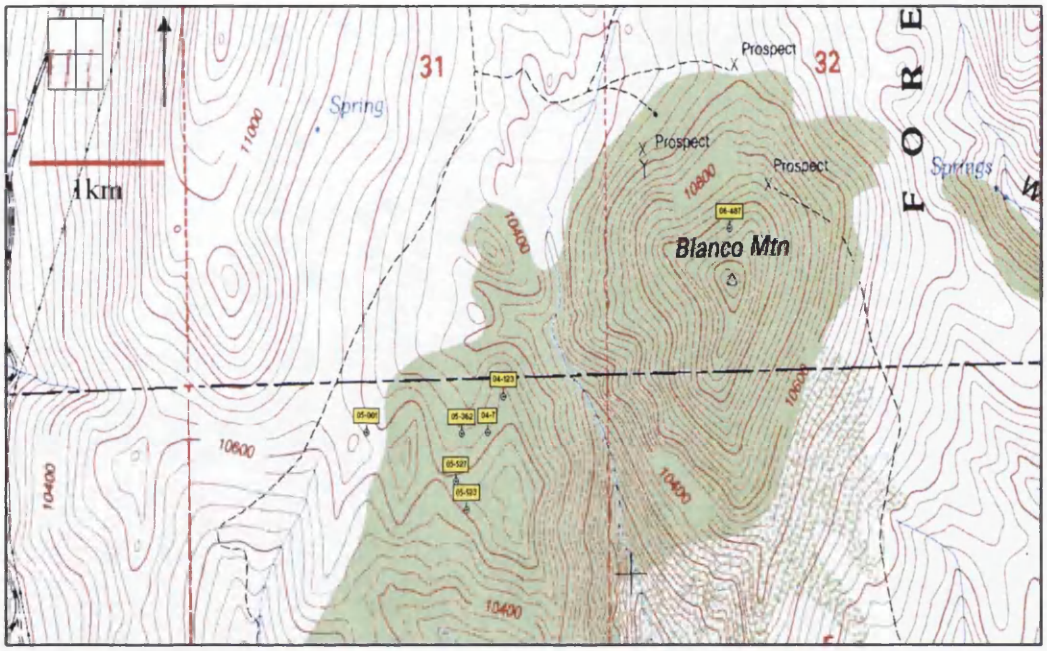

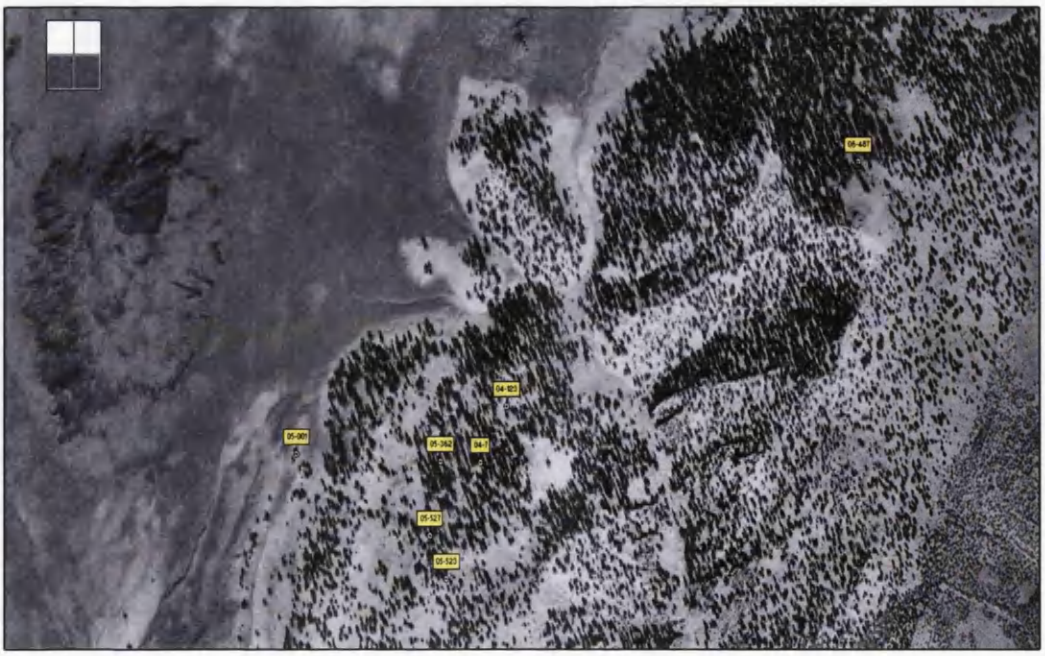

Figure 2.4: Aspect analysis of fieldwork site also showing location of trees used for isotopic analysis. The numbers on the legend refer to the degree and direction of slope. This figure shows detailed aspect data for the trees used in this research. It demonstrates the relatively homogenous sampling on north and north westerly slopes, and the variable slope aspect present at the site. Such detailed aspect analysis could prove useful when prospecting for trees for particular research aims prior to fieldwork taking place.

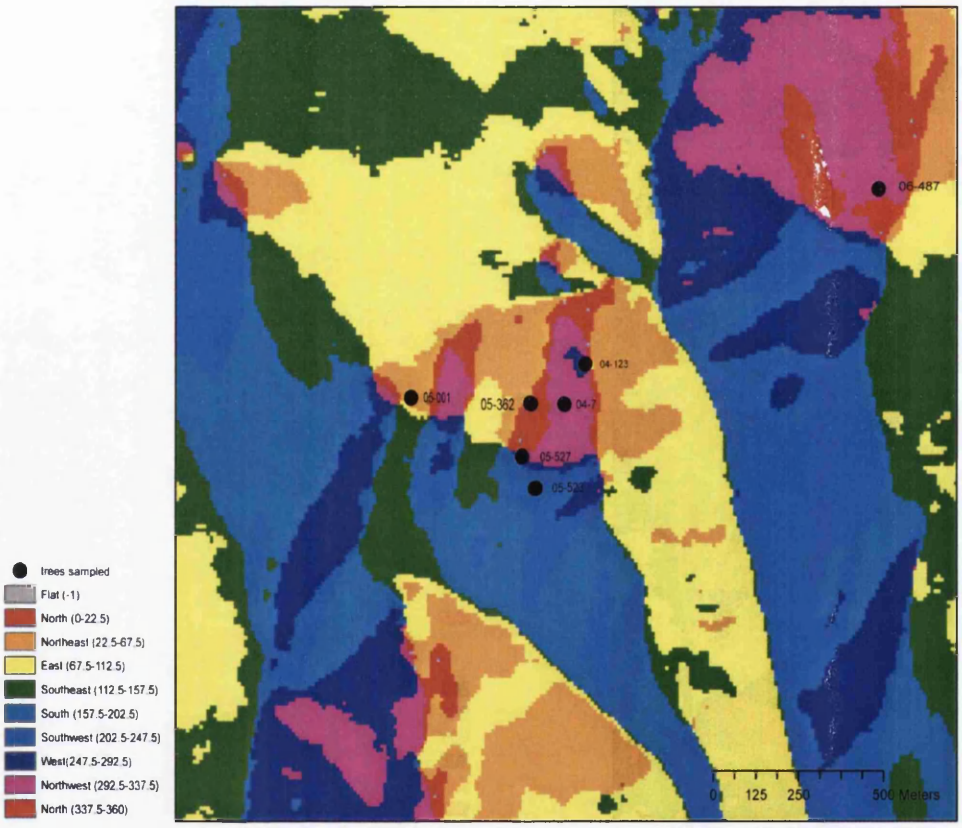

Tree 001 (figure 2.5) view south

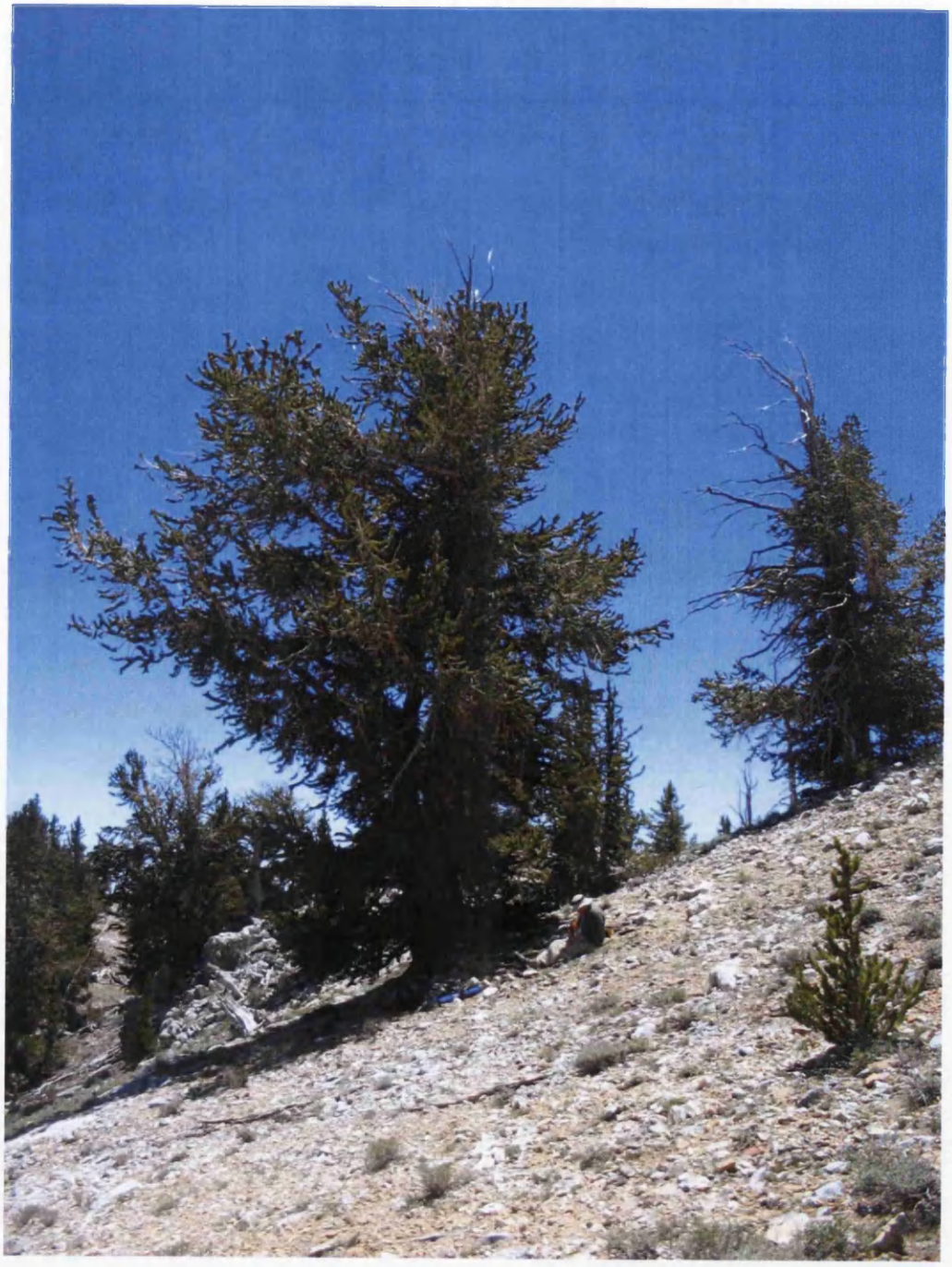

Tree 001 (figure 2.6) view east

Tree 523 (figure 2.7) view west

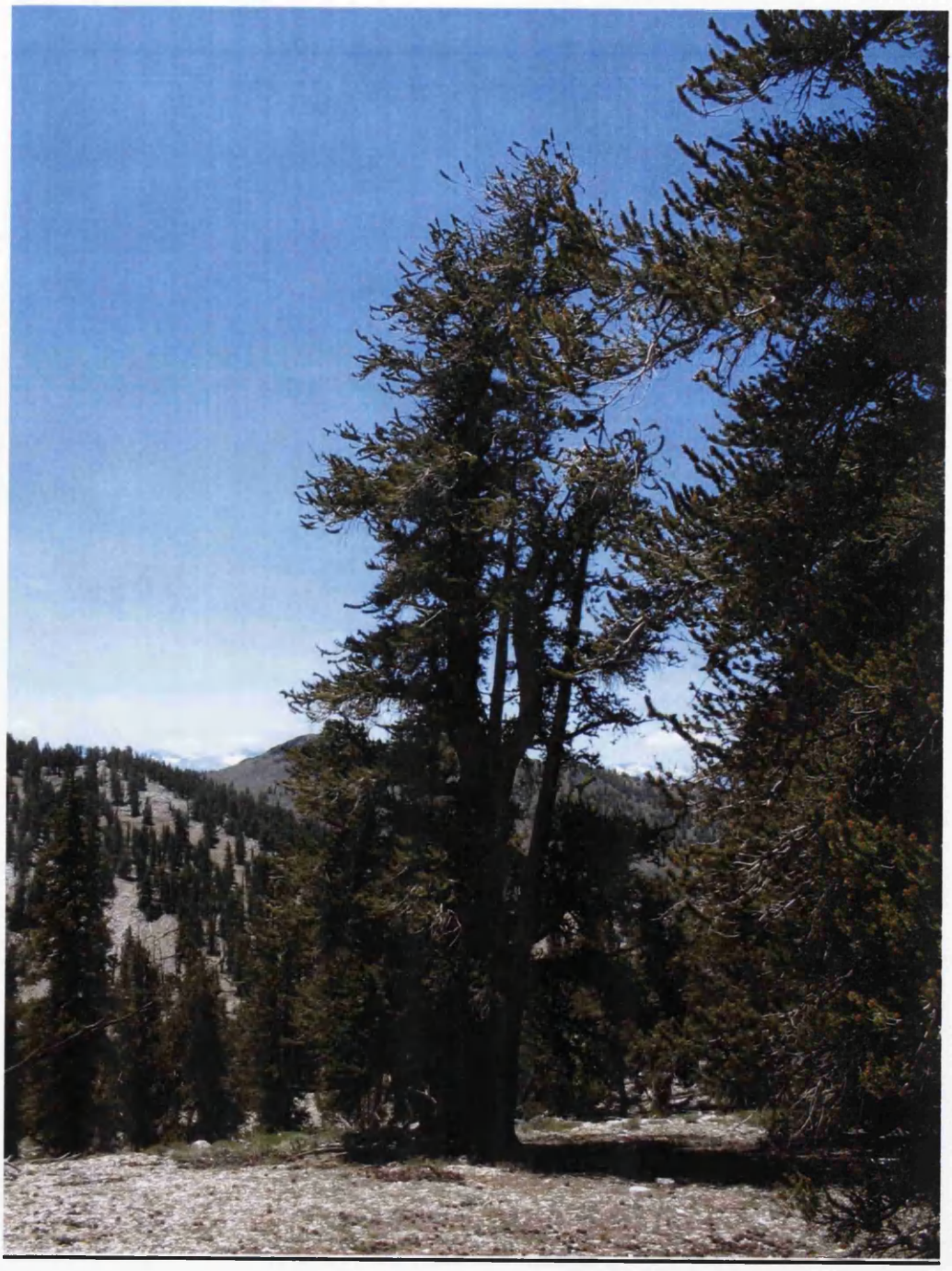

Tree 523 (above figure 2.8) view west

Tree 523 (below figure 2.9) view west

Tree 362 (figure 2.10) view east

Tree 527 (figure 2.11) view north east

Tree 527 (figure 2.12) view north east with position of cores C and D

Tree007 (figure 2.13)

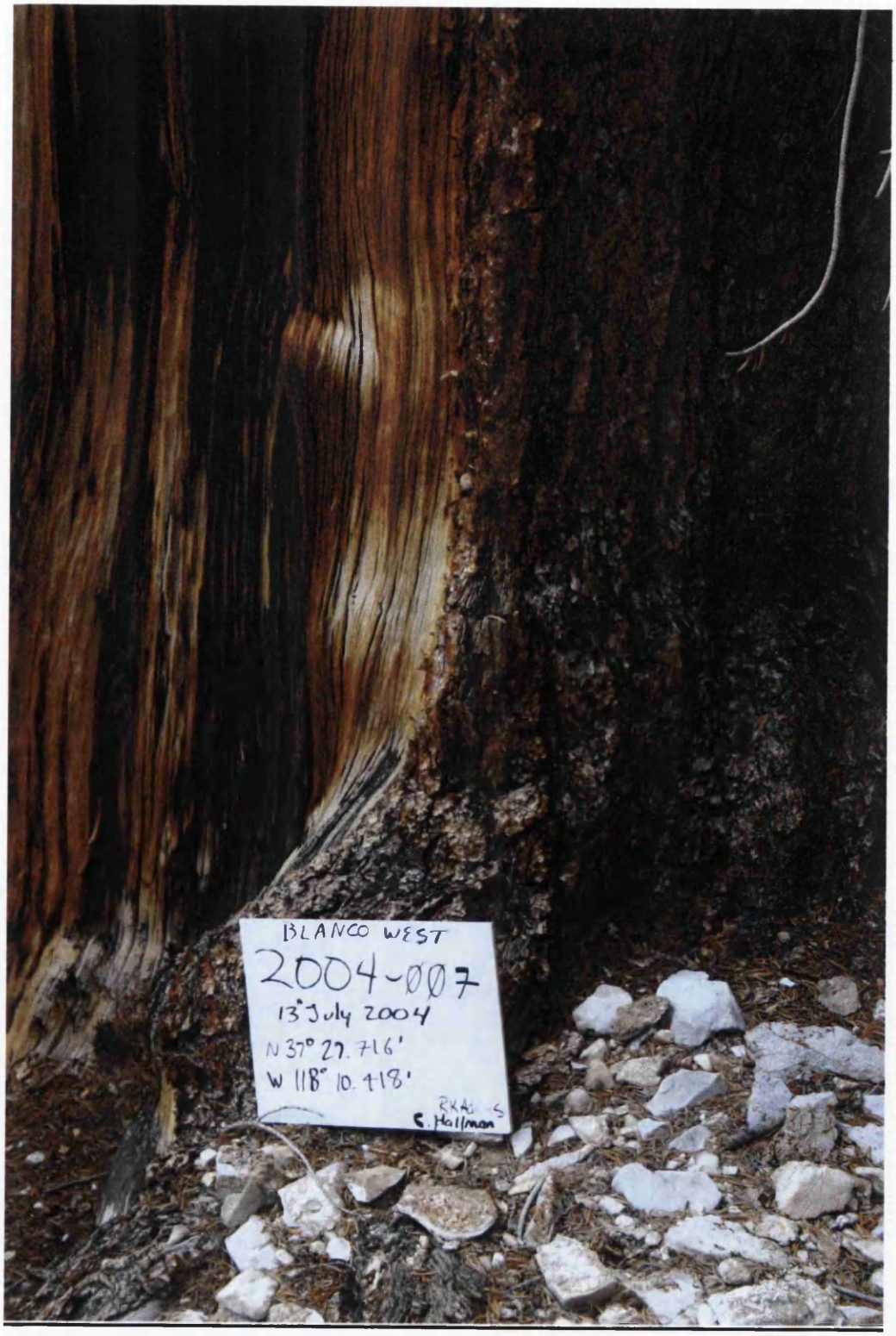

Tree 487 (figure 2.14) view south west

An attempt was made to select trees that reflected the influence of regional climate, rather than micro-climatic conditions. Trees that resided on windy ridges with lopsided crowns, trees suffering from insect damage and those on unstable slopes liable to avalanche should not be generally selected (Schweingruber, 1996), though this proved difficult due to the effects of a harsh environment on the trees and the highly variable mountainous rocky terrain of the White Mountains. This is to avoid the effects of non-climatic influence on annual growth and allows the creation of a tree ring chronology based on a common limiting factor for a group of trees.

Soil composition has been shown to be of significance in differences in ecology and form of bristlecone pine (Beasley and Klemmedson, 1980). They found that trees growing on sites with high clay and carbon content showed significantly more favourable growth than trees on soil low in clay and carbon. Soils with higher clay and carbon content are likely to hold snowpack moisture longer into the growing season than those with lower water holding capacity (Beasley and Klemmedson, 1980). The influence of aspect on tree growth and density is explored further in chapter 2.12 and is clearly evident in figure 1 with more tree growing on North facing slopes that receive less sun and hold snow longer.

The field site (Blanco West 37°27'N, 118°10'W) is situated within the central area of the White/Inyo mountain range of south central California and forms part of the Inyo National Bristlecone pine forest, created in the 1950s to protect what had become known through dendrochronology as the worlds oldest living things (Schulman, 1954; Schulman, 1958)

Figure 2.15: (left): White Inyo range location map taken from Powell and Klieforth (1991:39).
Figure 2.16: (right): View west from Blanco Mountain Summit (taken in July 2006).

2.8: Geology

The White Inyo range represents the westernmost range of the Basin and Range structural province and extends for 110miles from Montgomery Pass, south-southeastward to Malpais Mesa opposite Owens Lake and is 22 miles at its maximum width east of the town of Bishop. As is typical of ranges in the area it is bounded by normal faults of large magnitude slip (Nelson *et al.*, 1991). Rock types in the range span from the late Precambrian (700 million years old) to the Holocene. A detailed geological history of the White Inyo range is provided by Nelson *et al.*, (1991), and a 1:62, 500 geological map is available for the Blanco Mountain area (GQ529-1966).

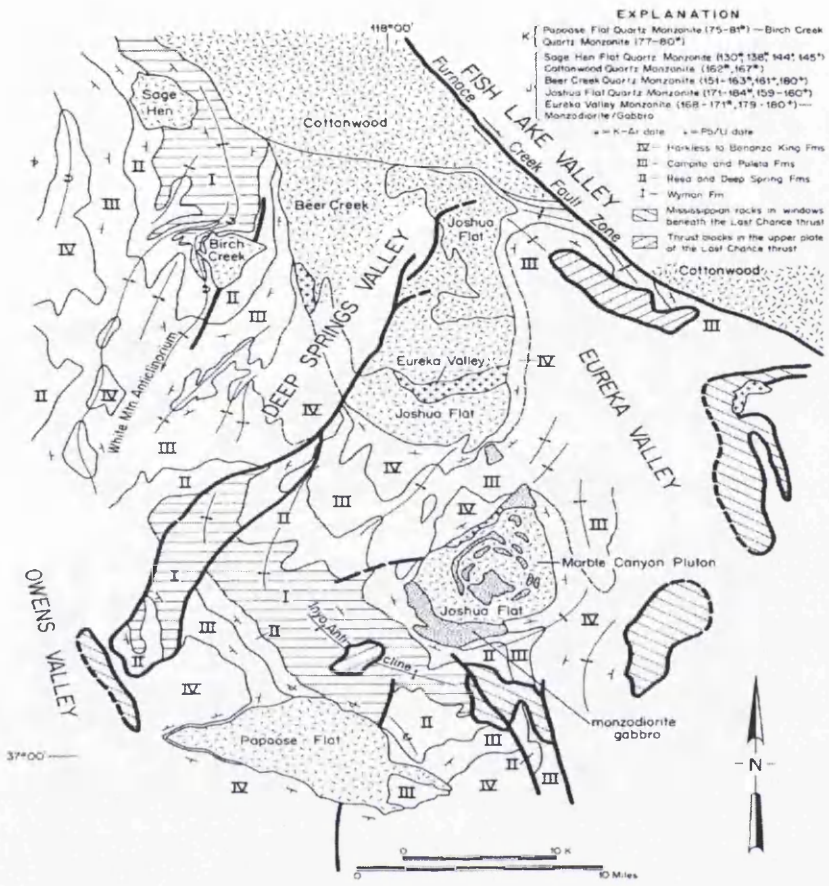

Figure 2.17: Major geological features of the White Inyo range and surrounding area (Nelson et al., 1991).

Most of the landforms created today are the result of late Cenozoic processes. Many of the high peaks (such as Blanco Mountain) formed over millions of years of weathering and erosion. It is likely that the peaks have always been exposed to the subaerial environment, perhaps as nunataks above a hypothetical White Mountain ice cap (Elliot Fisk, 1991). More recent (Holocene) landforms are the result of glaciation of the range or the result of fluvial activity (Elliot Fisk, 1991). Using tree ring evidence LaMarche (1968) measured weathering on slopes inhabited by bristlecone pine, with tree roots gradually exposed through time as material is removed. This and other studies show that weathering is a relatively slow process in the dry climate of the White Mountains. As precipitation increases with altitude weathering may be more rapid at higher elevations, with increased frost and ice leading (Elliot Fisk, 1991).

2.9: Weather and climate

The climate of western North America is dominated by Pacific influence. Precipitation in the White/Inyo range is from continental polar air, recycled maritime polar air, moist Pacific air and less frequently very moist tropic air from the Hawaii area. Extreme cold air invades every few years from interior Alaska or the Yukon bringing extreme cold temperatures (Powell and Klieforth, 1991).

Precipitation along the Pacific coast of North America is strongly affected by the orientation of the North Pacific storm track. Of particular importance are changes in wintertime atmospheric circulation that strongly influence regional precipitation (Castello and Shelton, 2004). Over much of North America south of 45° North, the major climatic influences are the state of the circumpolar vortex, the strength of the subtropical westerlies and large scale sea surface temperature (SST) anomalies, particularly those associated with the El Niño Southern Oscillation (ENSO) and North Atlantic Oscillation (NAO) (Hughes and Graumlich, 1998). Storms moving inland from the Pacific result in large amounts of precipitation falling on the Sierra Nevada, leaving the White Mountains in a rain shadow. Precipitation is low, but highly variable and freezing temperatures dominate from November to April (Fritts, 1969) .The bristlecone pine trees growing at an elevation of 3000-3500m are climatically sensitive due to a relatively arid environment (average rainfall 305-340mm). The site lies right on the transition between maritime Pacific influence and the more extreme continental influence of interior North America. The large difference in altitude in the range (from 1200m at the base to 4343m at the highest summit) leads to large changes in temperature and precipitation over short distances (Powell and Klieforth, 1991). Air masses reaching the White Mountains must pass over smaller or equally sized ranges and the least impeded approach for air masses is from the southeast. Air movement from the southeast is uncommon, apart from in July and August (key months for tree growth) when heavy storms may occur bringing a large volume of precipitation, as has been the case in 1955, 1956, 1967, 1976, 1983 and 1984 (Powell and Klieforth, 1991). Most of the air that passes over California will at some point have crossed the Pacific. In summer the Pacific anticyclone brings cool maritime air inland and cool dry air to the White Inyo range. At the same time the Great Basin

Anticyclone develops over the desert areas of Nevada and Utah, that when shifting west allows a flow of moist maritime tropical to persist in the range until the dry Pacific air once again dominates.

Unlike the Sierra Nevada, the White Inyo range receives much moisture during spring from northeasterly to southeasterly air flow, known as a 'Tonopah low' which brings low cloud and heavy snow. Extreme winter cold (-31°C) may occur occasionally when Northern Arctic air is brought in from Alaska or Yukon. This happens infrequently and has been noted in January 1937, January 1949, December 1972, February 1989 and December 1990 (Powell and Klieforth, 1991). Winters normally also include some 'warm' storms that can bring devastating flooding to much of California and the freezing level may be above 3000m (Powell and Klieforth, 1991). Westerly winter storms may bring large snowfalls but those from the northwest contain less moisture and bring less snow.

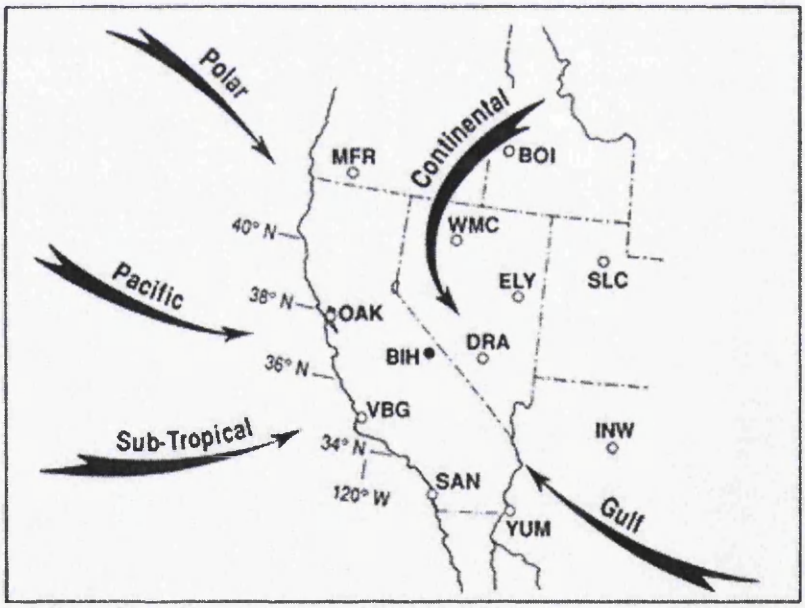

Figure 2.18: Air masses affecting the White Inyo range. The White Inyo mountain range is just east of Bishop (BIH). Map source: Powell and Klieforth, (1991:5).

2.10: Climate observations

A sparse permanent population coupled with the inaccessible nature of the terrain are the main factors why there is little in the way of reliable weather records for the region. There are gaps in the data that does exist, especially during extreme events and in winter. The stations in Owens valley and Nevada offer the longest records and there are two weather stations in the mountains themselves (figure 2.19). The station at Bishop is at an elevation of 1250m and has records back to 1947. The stations in the mountains (White Mountain 1 and 2) are at 3095m and 3800m respectively. White Mountain 1 (Crooked Creek Research Station) is the nearest weather station to the field site (figure 2.19). Unfortunately, due to maintenance costs and access problems, records were only kept all year at White Mountain 1 from 1955 to 1977 and at White Mountain 2 (Barcroft) until the year 1980. Spring and summer measurements are still taken at these 2 stations and automated weather recording equipment was installed at both stations, although problems with maintenance still occur in winter months.

The lowland valleys to the east of the White Inyo range are represented by stations at Dyer and Deep springs (both at around 1520m). The record from Deep Springs starts at 1947. Stations to the northwest have short and incomplete records and are unsuitable for use in this research. Longer weather records are available from stations further away. Independence, to the southeast in Owens valley has records back to 1927 and Mina, 100 miles to the east, near Tonopah in Nevada has records back to 1897.

Figure 2.19: Location of nearest weather stations, from Powell and Klieforth, (1991:13).

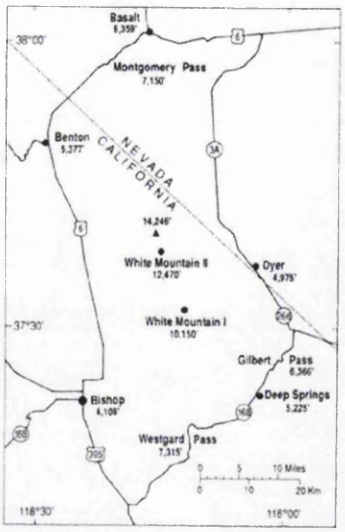

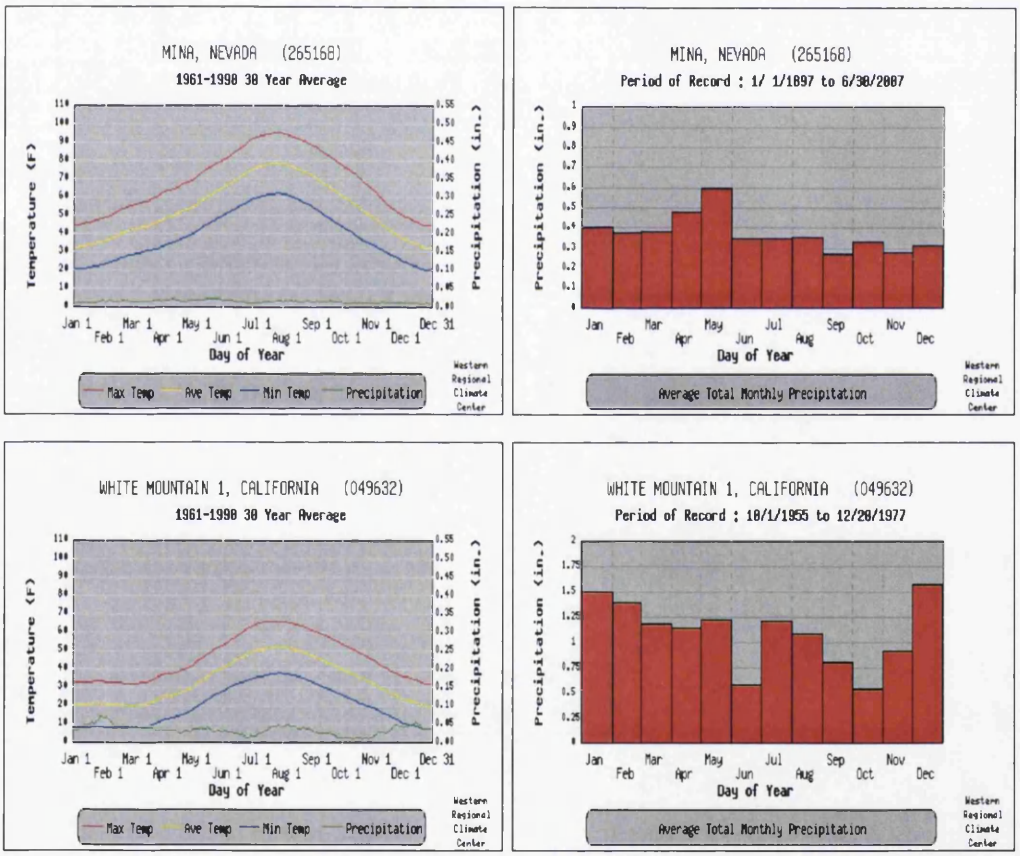

Figure 2.20: Temperature and precipitation averages from Mina (Nevada) and White Mountain 1. Source: (http://www.wrcc.dri.edu/summary/Climsmnv.html)

2.11: Temperature

The White Mountains appear from the Owen's Valley as somewhat barren and dry, especially in comparison to the Sierra Nevada to the west. However, within the mountain range at around 3000m the temperature is in fact quite cool. In July (the warmest month) average temperature at White Mountain 1 is around 11°C and the highest recorded temperature in July has been 26° C in July 1967. The valley floors are much warmer in July with 42°C recorded at Bishop in June 1969 and July 1982 (Powell and Klieforth, 1991) and the hottest instrumental temperature ever at this station of 43°C recorded on July 22nd 2003. The normal lapse rate for temperature is around 6.5°C per km elevation gained. At least once every summer temperatures in both the lowland valleys and mountains fall below 0°C. Of particular note is the fact that at White Mountain 1 the average temperature in the warmest month (July) is above 10° C, thought to be the threshold value for tree growth. The average temperature for July at White Mountain 2 is below this and there are in fact trees at White Mountain 1 but none at White Mountain 2 (Powell and Klieforth, 1991).

Winter temperature decrease with altitude is less pronounced than in summer, with the average temperature for January (coldest month) at White Mountain 1 being -6.3° C, and the all time lowest temperature at this station of -31.5° C in March 1968 (Powell and Klieforth, 1991). Temperatures to the east of the range are on average cooler due to decreased Pacific influence and increased likelihood of cold air being brought in from the north and east. Variation in temperature is greater in winter than summer, with cold air excursions from the north occasionally bringing record cold temperatures. This occurred in January and February 1949 and January 1937, where a temperature of -41° C was recorded at Fish Valley 100 km to the east (Powell and Klieforth, 1991). Anomalous for the latitude is the fact that March is colder than December, possibly the result of the passage of closed low pressure systems in late winter and spring over the range. Significant warming occurs in mid-May, when snowmelt starts and following summer, cooling starts in late September (Powell and Klieforth, 1991).

2.12: Precipitation

Annual precipitation varies from around 150mm on the valley floors to around 500mm at the highest elevations. Applying a linear lapse rate correction to precipitation (around 125-150mm per km) is difficult as the increase in precipitation becomes exponentially greater at high elevations. In addition precipitation can be extremely localised, particularly in the mountains themselves (Fritts, 1969). Average monthly precipitation is shown in figure 2.21 for White Mountain 1 and Mina. Again the mountains are at a transition point between the seasonal precipitation patterns of Pacific influence, and the more evenly spread annual precipitation of the interior (Powell and Klieforth, 1991). All stations in the area show that 1967, 1969, 1982 and 1983 were extreme wet years and 1960 was a very dry year (Powell and Klieforth, 1991). At both mountain stations, neither 1976 or 1977 were drought years unlike the rest of central California. Precipitation in the range is more evenly distributed than in the Owens Valley or Sierra Nevada and there is no pronounced dry season (Powell and Klieforth, 1991). With its winter wet, summer dry precipitation regime, California weather stations often use a year from 1 July to 30 June the following year. Even more appropriate for the White Mountains could be to use the year as from 1 October to 30 September. This means that July and August precipitation is included, all important months for plant growth (Powell and Klieforth, 1991).

It would be impossible to discuss the precipitation of the White Mountains without reference to snowfall. At elevations above 3050m 80% of annual precipitation is snowfall, as compared to 15 to 25% on the valley floor (Powell and Klieforth, 1991). Regardless of air mass temperature, rainfall is extremely rare at White Mountain 1 from November to April, and snow has in fact been recorded during all months at White Mountain 2 (Powell and Klieforth, 1991). Snowfall occurs every year in the mountains. At White Mountain 1 seasonal totals range from 432cm (1969) to 123cm (1960). Daily accumulation can be from 25-60cm (Powell and Klieforth, 1991). Continuous snow cover at around 3000m usually begins in late October, but may start in September and even start as late as February. Snow disappears around May or June at this elevation, and at

White Mountain 1 snow cover is on average 160 days (Powell and Klieforth, 1991). Snow cover rapidly disappears on western slopes, where the afternoon sun brings warm temperatures. North and east facing slopes, receiving less sunlight, hold the snow longer, often for many more weeks and often into June.

2.13: Wind

Wind data for the mountain stations are of an incomplete nature, the measuring machines are often of doubtful accuracy, and as with precipitation local differences due to topography make generalisations problematic. For about two thirds of the year the prevailing wind direction in the mountains is westerly. Easterly winds are less common, though can be important in certain years (Powell and Klieforth, 1991). Winds in the mountains can reach 100m.p.h in winter, but on average winter wind speed is 30m.p.h and in summer 20m.p.h (Powell and Klieforth, 1991). Wind is significant in terms of snow movement and texture, and also in terms of wind chill. The updrafts and downdrafts created by the Sierra Nevada, the Owens Valley and the White Inyo range lead to warm dry winds, known as *foehn* winds.

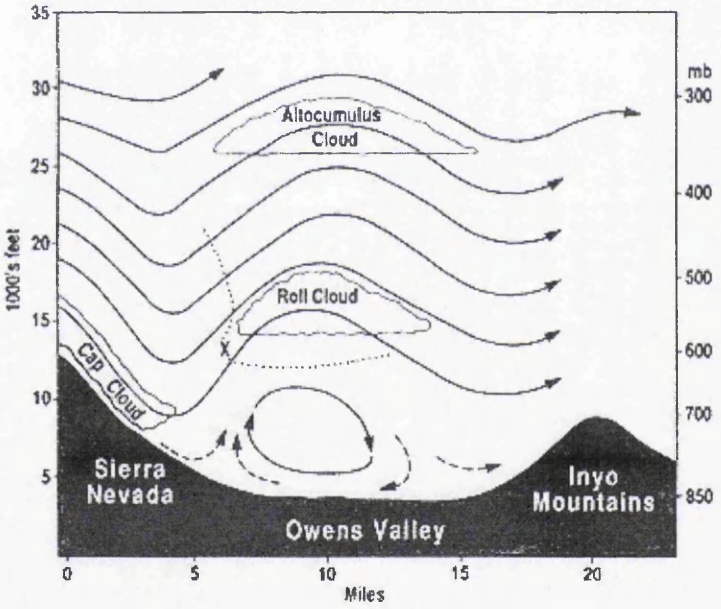

Figure 2.21: Effect of Sierra Nevada, Owens valley and Inyo range on circulation. From Powell and Klieforth, (1991:9).

For the bristlecone pine trees wind is important in that it removes snow from west facing or exposed slopes, displacing it to dense forest stands or valleys leading to sharply contrasting moisture regimes within a relatively small area (Fritts, 1969; Wright and Mooney, 1965). The most eroded and damaged trees are those on exposed ridges subject to strong winds and the effects of ice being blasted against them.

2.15: Bristlecone pine physiology.

The dendrochronological work that has taken place since the 1950s has been complemented by a range of research examining the physiology of the species. The findings of these studies may be important in interpreting the findings from the $\delta^{13}C$ values in the bristlecone pine tree ring cellulose. The dominance of Bristlecone pine for dolomite substrate is well documented and these trees survive almost competition free, able to tolerate the poor nutrient and water status of these soils (Elliot Fisk and Peterson, 1991) that are in fact around 75% rock cover (Fritts, 1969). The light colour of the dolomite means there is a 15-25% greater reflection of sunlight compared to sandstone. This results in a lower soil temperature and lower evaporation, meaning the dolomite remains consistently wetter compared to sandstone (Fritts, 1969). The contrast in vegetation due to geology is often striking, with Sagebrush scrub inhabiting the darker Campito sandstone, and bristlecone pine, generally but not always restricted to dolomite. The oldest trees, those at Methuselah Walk are also those at a lower altitude and suffer more moisture stress than trees at higher elevations.

Bristlecone pine is commonly 5-15m in height, and the trunk is commonly thick and contorted. Young specimens are often straight and full bark whereas older specimens are multi stemmed with strip bark growth. There are five needles per fascicle, slender around 2-3cm long, with a characteristic bristle like appearance. Male catkins are around 1cm long and are red purple. Female cones are ovoid, dark brown to purple when rip, 7-9 cm long and seeds up to 8mm long (Elliot Fisk and Peterson, 1991). Roots are often no more than 50cm deep, most numerous at around 10-20cm of depth and the substrate is mostly rock (Fritts, 1969). The species is common in the subalpine zone (3000-3500m a.s.l) occasionally extending down to 2600m where it forms mixed Pinyon woodland (Elliot Fisk and Peterson, 1991). These trees have been extensively studied through traditional ring width analysis and information indicates environmental influence over a wide geographical portion of North America. High corrleations are evidenced between bristlecone pine tree ring widths and other tree ring width chronologies from 1600km to

the east and south and about 480 kilometres to the North (Ferguson, 1968). This indicates similar climatic variations over a wide geographical area. The narrow rings that form the basis of most of the correlations between these chronologies are more than likely a reflection of regional drought, occurring in the years proceeding and composing a narrow ring. Bristlecone pine has a very short summer growing season and in some years this may be as little as 45 days. However at high latitude and high altitude photosynthesis continues into autumn even though cell division takes place in a short time (Fritts, 1976). Using living trees, standing dead wood and fallen sub-fossil material, well replicated tree ring chronologies exist for different areas of the White Mountains, now extending back to almost 12000 years (Harlan and Robertson *pers. comm*).

Bristlecone pine growth is thought to be moisture limited at low to mid elevations and temperature limited at high elevations (Cook *et al.*, 2004b; Hughes and Funkhouser, 1998; Hughes and Graumlich, 1998; Scuderi, 1993). However while traditional site selection for ring width studies is based on the principal of ecological limiting factors as defined by Fritts (1976) the limiting factors with regard to $\delta^{13}C$ series may not be of the same nature.

Infra red gas analyser studies indicate that photosynthesis decreases as trees grow older. Older trees show lower rates of respiration to photosynthesis than younger trees (Wright and Mooney, 1965). Reduced photosynthesis of leaves in old trees appears to be compensated for by trunk dieback. The crown starts to dieback and the amount of living material becomes more restricted, resulting in the older trees (over around 800 years old) surviving on a narrow strip of cambium. This reduction in cambium means slower growth rate. Wind damage and soil erosion contribute to dieback in strip bark trees (LaMarche, 1969).

Freezing temperatures in November mark the start of photosynthetic dormancy. In mid winter photosynthesis is not thought to occur (Schulze *et al.*, 1967) though in this infra red gas analyser based study respiration was still observed under warm conditions during winter.

In spring as the snow melts and soil thaws, photosynthesis increases. Schulze *et al.*, (1967) believe that 117 hours of summer daylight is necessary to equalize the loss of energy due to winter respiration.

A dendrograph study by Fritts (1969) over the period 1962, 1963 and 1964 indicate the highest growth rates during cool moist seasons. Cambial activity is centred on late June to early July after freezing temperatures cease (Fritts, 1969). The same dendrograph study study suggests that early July drought strongly limits the number of xylem cells. The growing period does not seem to be shortened by soil moisture or by day length changes but by internal phonological factor associated with growth initiation (Fritts, 1969). However the number and size of cells produced under different moisture regimes are different. The growing season can be as little as 45 days. Younger trees generally start growth earlier and finish cambial growth later than older trees (Fritts, 1969)

In cool years lower temperatures limit cell size on north slopes. In mid season there is expansion that may be the result of soil moisture replenishment. The change from wide earlywood cells to narrow latewood cells occurs during lignification and the timing is highly variable between trees, especially during wet years (Fritts, 1969).

Bristlecone pine growing on south facing slopes generally experience more stressful conditions. In spring drift snow supplements soil moisture in upper and middle north facing slopes. The highest inter tree ring width correlations are found between trees on south facing slopes (Fritts, 1969), that is those trees that, in general suffer more climatic stress.

It can be seen that there are many factors affecting the growth of each annual tree ring in bristlecone pine trees. In addition to the factors which directly influence cell division and growth there is a strong possibility that environmental processes have changed over time and the degree of influence of different environmental factors on the trees may have changed. Moisture, in the fact that it influences cell water balance, and temperature, as it affects the rate of photosynthetic assimilation are two of the most important factors in the development of plant tissue. Day length, wind and other disturbances will also influence cell growth (Fritts, 1969).

A decrease in the uptake of water through roots, or an increase in leaf transpiration will produce a water deficit in the tree. The dendrogram studies undertaken by Fritts (1969) indicate that there are major changes in the water balance of bristlecone pine during the growth season. Fritts (1969) suggests that only in the youngest trees is cell production influenced by rainfall late in the growing season. The well attested absence of 'false rings' in bristlecone pine (Ferguson, 1968; Fritts, 1969; LaMarche, 1969) also supports the theory that the midsummer climate has little influence on the structure of the annual ring. Moisture, although it may not directly affect cell growth, will have an effect on photosynthesis. Fritts (1966) suggests that water deficits reduce the cooling power of leaves and induce higher needle temperature, inhibiting photosynthesis particularly during May and June. The fact that growing season moisture abundance may not be reflected in growing season cell division (and therefore ring width), but does have an effect on growing season photosynthesis is of great relevance to this research. If tree ring $\delta^{13}C$ is a reflection of growing season photosynthetic processes, themselves dependant on moisture abundance, then tree ring $\delta^{13}C$ may be a better reflection of growing season climate than ring widths.

Respiration and assimilation of cell material is often a function of temperature, particularly at high altitudes. The cool late June and early July of 1963 and 1964 led to decreased xylem production in the trees studied by Fritts (1969). Cambial activity started 10 to 12 days later at high elevation trees in these two years as compared to 1962. However, although growth started later in these trees it also lasted longer than in the comparatively warm summer of 1962. Fritts (1969) concluded that temperature during the growing season did not significantly affect the width of the annual ring of the bristlecone pine trees in his study. The infra red gas analyser studies undertaken (Mooney *et al.*, 1966; Schulze *et al.*, 1967) indicate that respiration and photosynthesis in bristlecone pine, may at times be dependent on temperature fluctuations. These studies were undertaken during June, August, November, January and April. Net photosynthesis was found to be highest in June and lowest in January and April. During winter, needles are yellow and cannot photosynthesise (Mooney *et al.*, 1966). Moderate day temperature and cool night temperatures during June would lead to rapid accumulation of photosynthate just prior to the main growth season in July (Mooney *et al.*, 1966). Fritts

(1969) suggests that after cambial activity is initiated in late June, much of the recent photosynthate is utilised in meristems within the tree crown. Ring growth in the trunk is probably more dependant on reserves of food produced at an earlier time. Roots and shoots all compete for food reserves that would otherwise be used for cambial tissue formation. In addition Fritts (1969) analysis of needle length indicates that needle growth in the crown may depend on winter assimilated foods. Bud swelling has been observed to precede cambial growth, with needle emergence taking place in mid season. When the needles are mature and the last cells of the annual ring are formed, pollination occurs (Fritts, 1969). As mentioned needles can be retained in bristlecone pine for up to 30 years and may remain active for their entire life span (LaMarche, 1974). Therefore the total needle mass and photosynthetic capacity for any one year represents the cumulative effects on needle production over many years. The needle mass in these trees does not vary a great deal from year to year and may only change as a result of longer term climate. Extreme drought in any given year is therefore represented by a single narrow ring, not by reduced growth in the several years therafter.

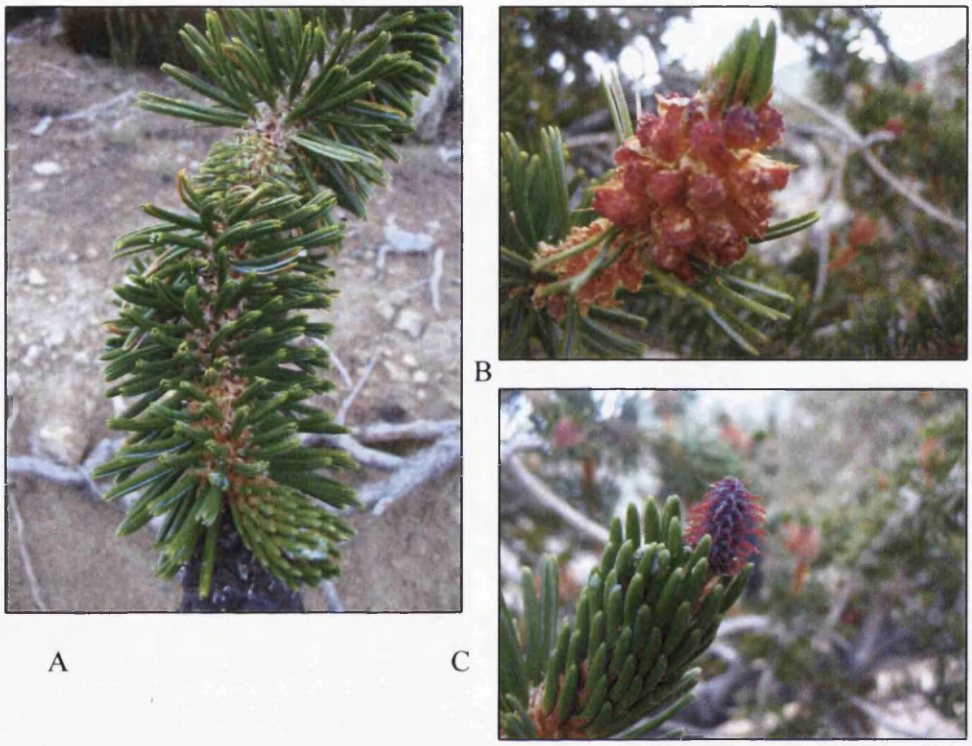

Figure 2.22: A) Bristlecone pine needles (July 2006). The needles here represent 6 years growth (2001-2006). The very small needles are from 2002 and probably represent extreme spring drought. B) Pollen bearing male flower (July 2006) C) Bristlecone pine female flower (July 2006).

The large, stable needle mass is probably a major factor in the ability of bristlecone pines to withstand adverse conditions (Fritts, 1969). As temperatures cool during late summer, and meristematic activity ceases photosynthesis may continue that can be utilised in the next years growth. Schulze *et al.*, (1966) report that rates of respiration are higher than photosynthesis in winter for bristlecone pine. Fritts (1966) suggests this may be due to impaired water transport due to freezing. Schulze *et al.*, (1967) suggest that cold winters lead to inactivity and depletion of food reserves. Fritts (1969) suggests that early summer drought (May, June) limits photosynthesis and can be correlated with narrow rings.

2.16: Cross dating- Introduction

As with other tree ring proxies, creating an annually resolved $\delta^{13}C$ series is dependant on absolute dating, that is, dendrochronology, and many of the criteria applied to ring width studies or the dating of trees or wood should also be applied to $\delta^{13}C$ chronologies. Ring counting, from either the bark edge or pith, from either one or more samples is insufficient in assigning precise calendar dates to every single year to be analysed either isotopically or otherwise. Results will be rendered invalid if a year is missed or a year added that does not actually exist. There can be a huge amount of variation in ring growth between different trees from the same area due to local site differences, particularly in mountainous areas (Cook and Kairiukstis, 1990), but in many parts of the world, particularly in the northern hemisphere, seasonality leads to the creation of annual increments of wood, and there is enough coherence in the pattern of annual rings laid down in different trees to permit calendar dates to be assigned to each layer of wood. The pioneering work of Andrew Douglass on trees and archaeological specimens from the southwestern USA in the early 20th century led to the later creation of many tree chronologies throughout the world. By creating regional chronologies from many tens or hundreds of trees the background 'noise' associated with individual tree samples may be ironed out and the common environmental signal imparted to a group of trees can be identified. Long annually resolved ring width chronologies (up to 12460 years) have been compiled since the early 20th century using living trees, dead wood, sub fossil and archaeological material (Baillie, 1995. Friedrich *et al.*,2004).

2.17: Sample preparation

Of key importance in successful cross dating of samples is the ability to see the annual rings clearly under magnification. A poorly prepared sample that has not been surfaced properly will only create problems. Careful preparation of a clean, visible surface to a core must be done as a first step in successful cross dating. While machine sanding, using progressively finer abrasive paper is commonly used to prepare dendrochronological samples, cores may also be prepared for analysis by hand, using a razor blade followed by hand sanding with progressively finer abrasive paper (150, 300, 600 grit). This is the method preferred by those working with bristlecone pine samples. Samples are first

mounted with the grain of the wood facing vertically upwards so a clear section is visible after cleaning. For dating purposes and ring width measurement, cores are normally mounted in wooden blocks using wood glue. 5mm cores obtained from the same trees as the 12mm isotope cores were mounted this way as an aid to cross dating the 12mm cores, and as a permanent record of each tree once the 12mm core had been processed for isotope analysis. As carbon based glue would contaminate isotope samples, the 12mm cores were mounted in a small vice and surfaced using a razor blade. Neither sanding nor hand surfacing should cause contamination of individual tree rings. A slight amount of surface wood dust may move between annual years but is an insignificant amount compared to the total amount of wood in any given annual ring.

Once a flat surface was obtained the core was sanded with small pieces of progressively fine abrasive paper. Samples were then ready to be cross dated. Any areas of the core that were not clean enough, or particularly narrow groups of rings were resurfaced during cross dating.

2.18: Skeleton plots

Fundamental to tree ring chronology building is the fact that through cross dating of individual tree samples each annual growth increment may be assigned a calendar (absolute) date according to the year it was formed (Stokes and Smiley, 1996). The pattern of wide and narrow rings over different radius and of different specimens forms the basis for cross dating and chronology building. Dating of bristlecone pine has traditionally been carried out using the skeleton plot method. This method utilises strips of graph paper onto which the pattern of a trees ring widths are plotted using vertical lines, and then compared to other samples or chronologies. This method is highly suited to dating of bristlecone pine. Unlike other conifer species, especially those at low elevations or of southern latitude, the problems of dating bristlecone pine are not associated with 'multiple' growth rings but are caused by 'missing' or locally absent rings due to the extremely low growth rate and semi arid nature of the White Mountains. In extreme cases up to 5% of rings may be absent along a given radii (Ferguson, 1968). The location of missing rings is verified by cross dating ring patterns from different cores

from the same and other trees and identifying missing rings common to some or all of the samples. The skeleton plot method involves identifying the narrowest rings in relation to adjacent rings and using a line to indicate the narrowness of the ring. Longer lines indicate narrower rings in comparison to neighbouring rings. Skeleton plots are traditionally plotted on strips of graph paper and the strips 'moved' across each other until a satisfactory correlation is made. As with all dendrochronological dating, replication is all important. Each sample should correlate at the same date with other samples from the same site and with relevant master chronologies. With living trees there is the benefit of knowing the year in which the core was taken and a calendar date may be assigned to the outermost (bark edge) ring. Although not every narrow ring may correlate directly in different trees over a period of 100 to 1000 years, a match is considered adequate when most of the narrow rings match each other, and the same match, at the same dates is repeatedly obtained. The very narrow, or missing rings are generally the same in a group of trees from the same site, and with experience it becomes possible to quickly identify distinctive groups of rings. For example, with the bristlecone pines from Blanco West (and in the bristlecone master chronologies) the years AD2002, 1960, 1929 and 1899 act as the most distinctive narrow, or missing 'marker' years in the last 100 or so years. With experience the dendrochronologist is able to memorise distinctive ring patterns over a long time period, and is quickly able to identify problems encountered during cross dating. Through identification of these distinctive narrow or missing years it is possible to assign exact calendar years to each annual ring. Anatomical features should always be noted during crossdating, as should the amount of sapwood rings. A computerised version of the skeleton plot method (crossdate) was used in this research (Lazear and Harlan 2001). The program operates in the same way as the traditional paper skeleton plot, but with several benefits. This is because the work is painstaking, and while computers make the job easier and faster they are no replacement for the dendrochronologist's judgement. Thousands of individual tree samples and master chronologies are easily available for reference on computer file. The master bristlecone chronologies are up to 8500 years long, a very long paper skeleton plot , so while initial skeleton plots from Blanco West were done on paper strips, it soon became necessary to use the crossdate computer software that was available.

Once the samples from each Blanco West core had been skeleton plotted a comparison was made between that sample and master chronologies made up of many trees using 'cross date' (Lazear and Harlan, 2001). With paper plots this has done by sliding the two papers alongside each other until a visually satisfactory match is made. Crossdate also does this, but it is also possible to find the best match in terms of a correlation value. Instead of comparing a full 1000 year core against a master chronology, the most satisfactory and quickest method of cross dating is to look for the highest correlation in a given segment. Problems can be identified quickly and more importantly before further errors are made. Segments of 100 or 250 years were used for cross dating of the Blanco cores against master chronologies (Table 2.2). The highest correlations always placed each measured core in the correct place in time, against chronologies up to 8500 years long. The results from each core may be replicated against a whole series of independently constructed master chronologies. Any missing rings may be clearly identified using this method.

However, no amount of correlation can replace the need to visually match tree ring sequences (Cook and Kairiukstis, 1990). This is usually done either through the skeleton plot method, while referring back to the core in question, or by overlaying ring width patterns over each other, looking in minute detail to identify any problems such as missing rings. This was traditionally done using ring widths plotted on semi logarithmic graph paper overlaid on a light box, but is also achievable using graphics utility computer software. If the dendrochronologist can be certain that a match is correct, problem areas adjacent to a successfully dated segment can be re-examined and any missing rings identified. The process is laborious and time consuming, and while the method may appear somewhat unscientific, the same results and dates are obtained by different researchers working on the same material, and can therefore be relied upon with a high level of confidence.

Cross dating of the Blanco West cores to be used for isotopic analysis was initially carried out during fieldwork in July 2004 by colleagues from Swansea University under the guidance of Tom Harlan, fieldwork leader from the Laboratory of Tree Ring Research (LTRR), University of Arizona. A Blanco West skeleton plot chronology was established

using dated segments from up to 10 trees that extended from AD1250 to 2005. Additional cores obtained by myself and others from the fieldwork team were obtained during fieldwork in July 2005 and July 2006. These were cross dated during the field season and back in the laboratory at Swansea. Detailed notes were taken during cross dating to help identify the location of missing rings. Traditionally cores are marked every 10^{th} ring, every 50^{th} ring and every 100^{th} ring in order to aid dating (Stokes and Smiley, 1996) and to give good convenient reference points and to help those working with cores in the future. With ring width studies this is done using a pen or sharp pencil. This was not possible for the isotope cores due to the risk of carbon contamination and so each 10^{th} ring was marked by 1 pin mark, every 50^{th} ring by 2 pin marks and every 100^{th} ring by 3 pin marks. The main chronologies used for cross dating are the Methuselah Walk, Campito and Sheep Mountain chronologies created in the 1950s, 60s and 70s (Ferguson, 1979; Ferguson *et al.*, 1962; Graybill, 1980; LaMarche, 1974; Schulman, 1958). Table 2.2 shows the highest Pearson's rank correlation (*r* value) for each of the trees used for isotope analysis. The *r* value refers to the best 250 yr fit for each of the trees against a master chronology.

Table 2.2 – correlations of isotope cores against bristlecone pine master chronologies. The fact that high correlations are evident in any 250 year segment should not prelude ensuring that there are no missing rings in other segments. This is done by carefully going through all segments and checking for missing rings.

chronology	**tree**	**r value - best 250 year segment**
Campito 5230BC-AD1961	001c	0.69 at AD1679-2005
	523b	0.60 at AD1086-2005
	362b	0.69 at AD1221-2005
	4123	0.63 at AD1454-2004
	527d	0.62 at AD923-2005
	007	0.62 at AD802-2004
	487d	n/a- only 100 years (AD1907-2006) used
		r value - best 250 year segment
Blanco West AD1250-AD2004	001c	0.74 at AD1679-2005
	523b	0.83 at AD1086-2005
	362b	0.71 at AD1221-2005
	4123	0.71 at AD1454-2004
	527d	0.73 at AD923-2005
	007	0.74 at AD802-2004
	487d	n/a- only 100 years (AD1907-2006) used
		r value - best 100 year segment
Sheep Mountain AD460-1979	001c	0.59 at AD1679-2005
		r value - best 250 year segment
Sheep Mountain AD460-1979	523b	0.65 at AD1086-2005
	362b	0.64 at AD1221-2005
	4123	0.57 at AD1454-2004
	527d	0.64 at AD923-2005
	007	0.71 at AD802-2004
	487d	n/a- only 100 years (AD1907-2006) used
		r value - best 250 year segment
Methuselah Walk 6700BC-AD1981	001c	0.70 at AD1679-2005
	523b	0.92 at AD1086-2005
	362b	0.64 at AD1221-2005
	4123	0.70 at AD1454-2004
	527d	0.80 at AD923-2005
	007	0.876 at AD802-2004
	487d	n/a- only 100 years (AD1907-2006) used

An example of a skeleton plot is provided here. All the skeleton plots for each individual tree against master chronologies are included as an appendix, along with the ring width pattern for each tree.

Figure 2.23– Two examples of skeleton plots and associated ring widths. The skeleton plots (upper section) match up with the ring widths (lower section). The r values refer to the correlation between the individual trees and the master skeleton plot for the period of overlap.

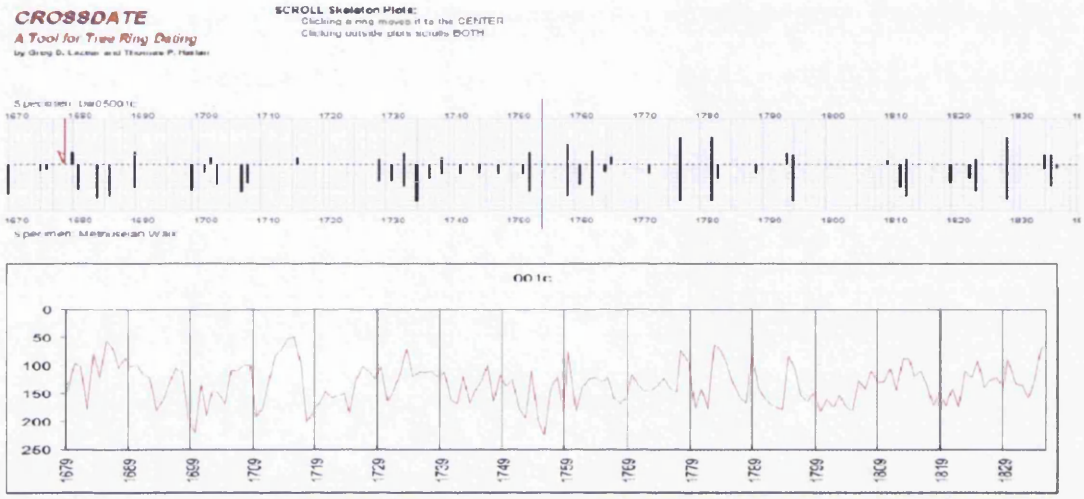

Top: 001c/Meth Walk AD1679-1835 r= 0.790 Below: ring widths AD1679-1835

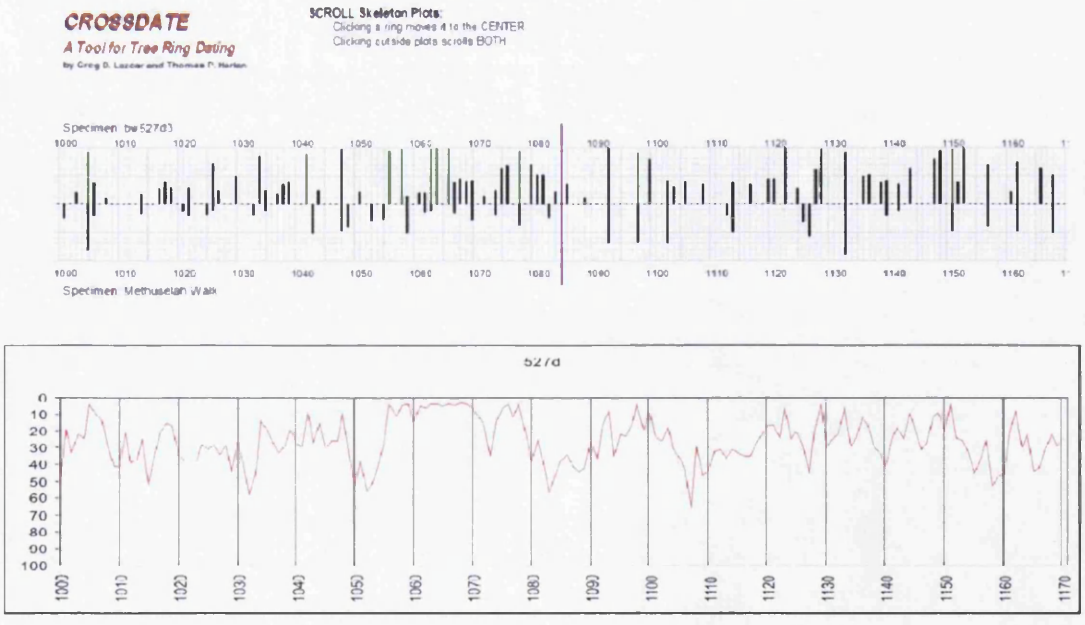

Top: 527d/Meth Walk AD1000-1170 r= 0.489 Below: ring widths AD1000-1170

These examples of skeleton plots demonstrate how skeleton plots are compiled. The first of the two figures represents the ring pattern from the youngest tree used for isotopic analysis, skeleton plotted against the Methuselah Walk master chronology for the period AD1679-1835. BCP tree core 001c is dated to AD1679-2005. The ring width pattern is typical of what is known as a 'complacent' ring width series (i.e relatively low variation in annual ring widths from one year to the next) although there are several 'pointer' narrow rings that match with the Methuselah master. The red arrow on the plot marks the first ring of core 001c. The ring width pattern for 1679-1835 is plotted below the skeleton plot. The scale (0-250) represents 0.01mm. The 2nd skeleton plot example shows one of the more difficult samples, core 527d, again with the Methuselah master skeleton plot, for the period AD1000-1170. The green dashes on the skeleton plot represent missing rings and can be seen against the ring width pattern for this tree, again measured to 0.01mm. Plotting ring widths adjacent to skeleton plots is commonly used (Stokes and Smiley, 1996) to illustrate the physical nature of a given sample. Whereas the dashes on a skeleton plot represent the size of any given ring as compared to its neighbouring rings, showing the ring widths shows the actual size of the rings and also demonstrates that a sample has been correctly cross dated. The location of any missing rings in the Blanco West samples was compared against missing, or narrow rings from the bristlecone pine master chronologies, and against several individual trees that make up these chronologies.

Table 2.3 – Location of years of missing rings in each of the Blanco West tree cores. Number of sapwood years for each tree is indicated at the bottom of the table.

001c AD1679-2005	523b AD1086-2005	362b AD1220-2005	4123 AD1453-2004	527d AD1005-2005	007 AD1005-2004	487d AD1907-2006
none	AD1686	AD1580	none	AD1005	AD1065	none
		AD1759		AD1042	AD1083	
		AD1855		AD1056	AD1133	
		AD1899		AD1058	AD1668	
				AD1063	AD1782	
				AD1064	AD1960	
				AD1066		
				AD1078		
				AD1098		
				AD1151		
				AD1285		
				AD1579		
				AD1899		
				AD1929		

	001c	523b	362b	4123	527d	007	487e
Sapwood years	52	71	69	42	73	76	55

2.19: Ring widths

Following successful cross dating, ring widths were measured using a Velmex travelling stage interfaced to a computer running the dendrochronology program- TSAPWin version 4 for Windows. Ring widths were measured to 0.01 mm. Ring width measurements are used to verify cross dating, and to complement the isotopic data in any climatic reconstruction. Ring width patterns were visually compared to some of the bristlecone pine chronologies available on the International Tree Ring Database (ITRDB). Individual tree ring patterns are available for Methuselah Walk, Campito and Sheep Mountain and there are also master ring width chronologies compiled from many trees (Ferguson, 1979; Ferguson *et al.*, 1962; Graybill, 1980; LaMarche, 1974; Schulman, 1958). As can be seen in the following figures the dating of all the Blanco West samples is absolutely secure. The trees have all been dated satisfactorily and both the skeleton plot and actual ring width data indicates that the dating is absolute. In addition the ring width data generated can be used in any climate reconstruction, as with previous $\delta^{13}C$ studies of bristlecone pine (Feng, 1998; Feng and Epstein, 1996; Leavitt, 1994; Leavitt and Long, 1992). Ring widths from the Blanco West cores were visually compared against

bristlecone master chronologies and are shown below. The location of missing, and narrow rings is also shown in the following figures.

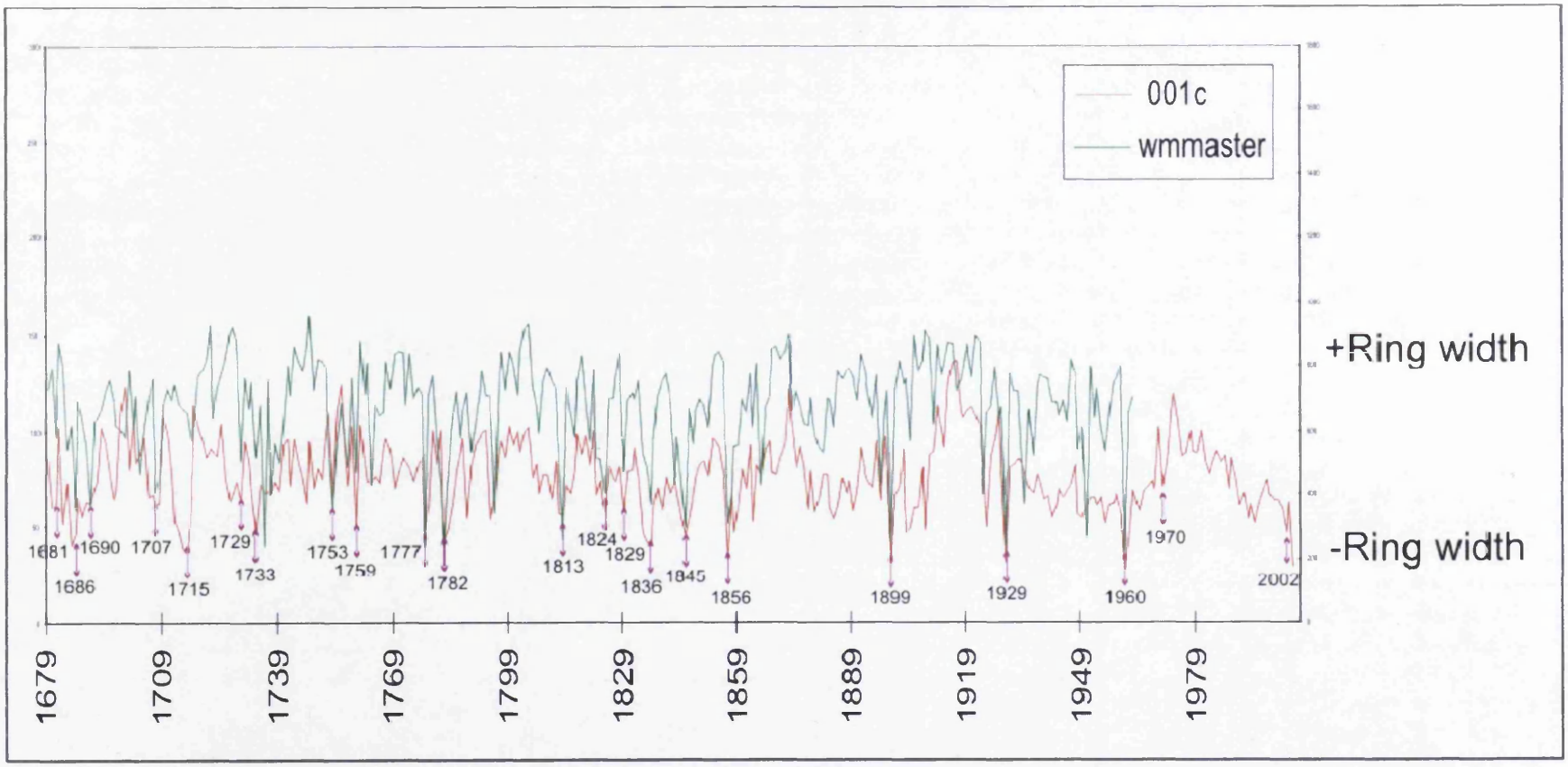

Arrows indicating key years used in cross dating The White Mountain master extends to year AD 1962. 001c is dated from AD1679-2004.

Figure 2.24: Ring widths of BCP core 001c and White Mountains master ring width chronology (Ferguson et al , 1962).

The two figures above show firstly core 523b against the White Mountain master chronology (Ferguson *et al.*, 1962). The location of narrow 'pointer' years is indicated, and missing rings are indicated in red. The White Mountain master (for the period AD1000- 1962) is made up of 18 to 31 trees. The second figure shows tree 523b and an individual specimen from Methuselah Walk, sample mwlk995 (Graybill, 1980). For the White Mountains master and 523b almost all of the narrow rings match up. Even when comparing individual trees, as in the lower figure the degree of similarity between the two series is very high.

The above figure shows the location of the most important narrow 'pointer' rings that aided cross dating of samples for the last 1000 years. The Y axis indicates growth increment with 0 being very narrow or missing and 1 being larger rings. The tree or chronology name is on the left hand axis. All the Blanco trees are shown in this figure, as is the White Mountain master chronology and a tree each from the Methuselah and Campito chronologies. The blue text (AD1227) indicates an early wood frost ring present in Blanco 523b and 362b. The red text (AD1055-1070) is used to indicate a period of extremely narrow rings that was present in Blanco 007 and Blanco527d.

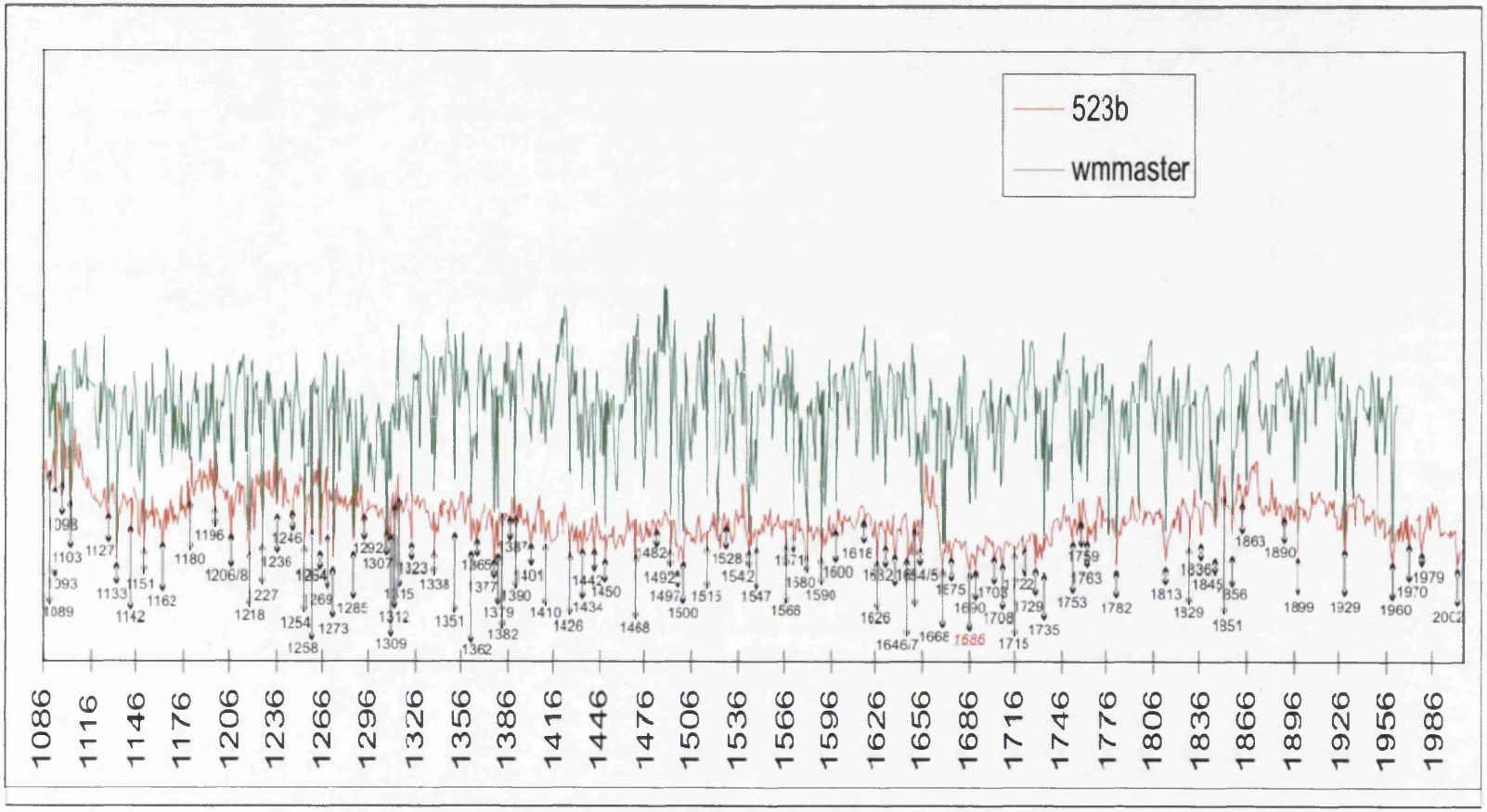

Location of 'pointer' narrow ring years in tree core 523b(AD1086-2005). AD 1686 is a missing ring in the sample.White Mountain master chronology(AD1086-1962).

Figure 2.25:Ring widths for tree core 523b and White Mountain master chronology.

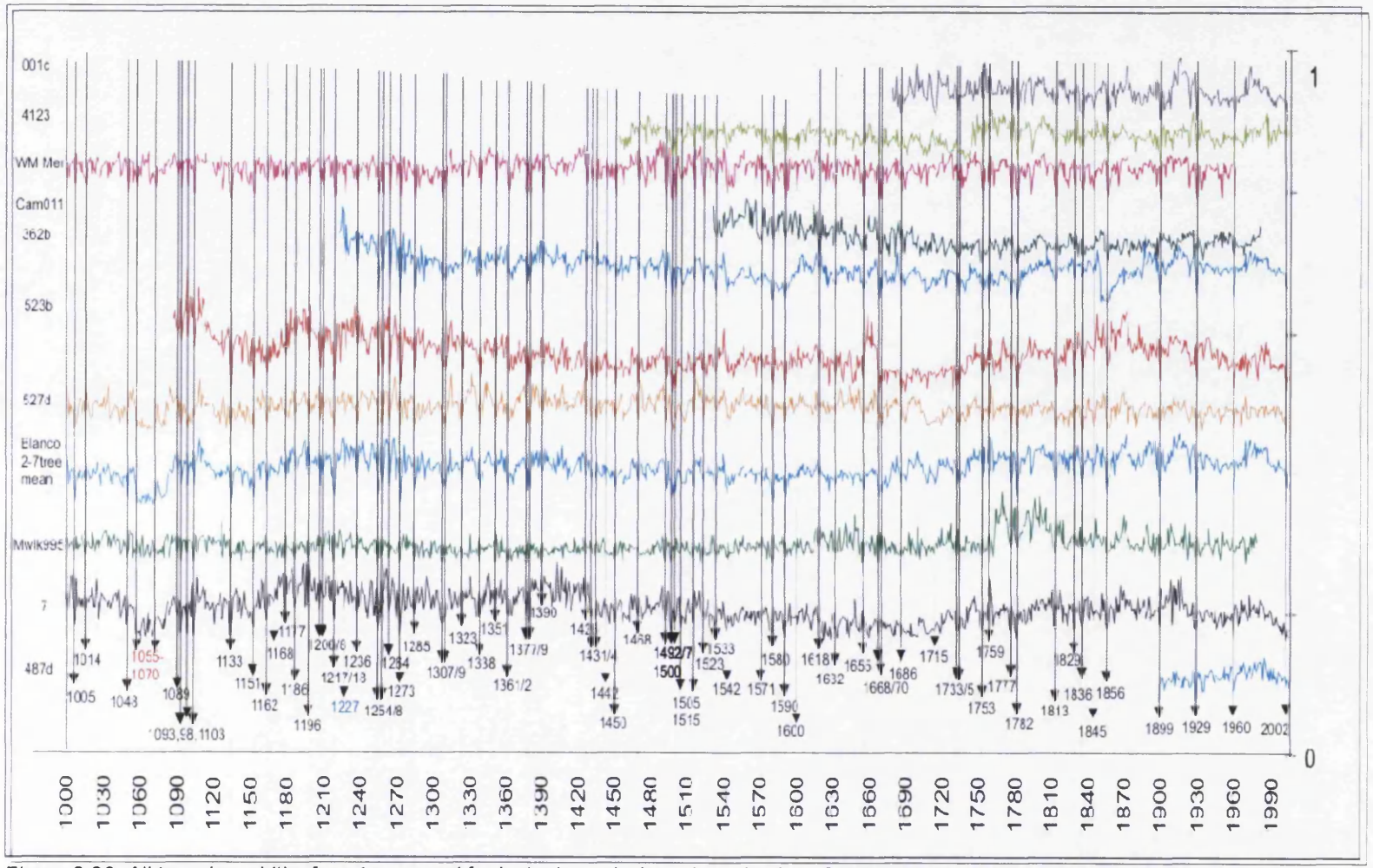

Figure 2.26. All tree ring widths from trees used for isotopic analysis and a selection of ring width master chronologies. Both wide and narrow rings are used to cross date samples as are anatomical features present in the wood. The year AD1227, for example was noted to contain an earlywood 'frost ring' signature that was visible in two of the trees selected for isotopic analysis.

2.20: Cutting

Introduction

Many $\delta^{13}C$ tree ring studies utilise latewood as, particularly in broadleaf species it is free from the effect of previous years carbon remobilisation (Hill *et al.*, 1995). However, the latewood of Bristlecone pine is too small an amount to slice separately. With regard to the isotopic values of early wood and latewood, conifers exhibit a gradual rise in $\delta^{13}C$ during earlywood formation and a sharp decrease during latewood formation (Schulze *et al.*, 2004). This contrasts with broadleaf species that rely on rapid utilization of previous years carbon for spring growth. Carbon in conifer earlywood formation is usually assimilated directly from current supply and the more gradual earlywood formation does not require the high physiological activity associated with earlywood formation in hardwoods (Schulze *et al.*, 2004). The ring structure of *Pinus longaeva* is such that latewood is very limited (Epstein and Yapp, 1976). This means that the whole year (combined early and late wood) has been used in this research. Previous investigations into bristlecone pine (Epstein and Yapp, 1976; Feng and Epstein, 1994; Leavitt, 1994; Leavitt and Long, 1992) have used pooled samples and 'blocks' of annual rings ranging from 5 to 30 years.

This research project used annually resolved α-cellulose from individual trees so greater confidence can be placed in the accuracy of climatic reconstruction. The only time annual resolution has not been possible has been in the case of where there are missing rings (table2.3). In the case of these few missing rings a small amount of cellulose was weighed out from the two adjacent years (if there was any left).

Procedure:

In order to accurately cut each annual increment from the tree cores it is necessary to surface cores 360° using a razor blade and a small piece of high grit abrasive paper. Wood was cut into thin sections using a scalpel to allow thorough penetration of the wood with chemical reagents. Each years wood slivers (combined early and late

wood) were placed in labelled sealed glass containers to await cellulose extraction. Problem rings (missing/ narrow rings/ cutting errors) were noted during cutting.

2.21: Cellulose extraction

Early studies used wholewood (Craig, 1954; Farmer and Baxter, 1974). The different constituents of wood differ isotopically (Wilson and Grinsted, 1977) and the method of cellulose extraction from wood slivers used in this research involves several chemical steps based on the 'Jayme and Wise' methodology outlined by (Green, 1963; Loader *et al.*, 1997) and has the advantage of not requiring a Soxhlet resin cellulose extraction (Rinne *et al.*, 2005).

Wood is a complex polymer made of varying proportions of different compounds. These are:

α-Cellulose	**40%**	
Hemicelluloses	**30%**	
Lignin	**25%**	
Others (resins and waxes)	**5%**	(Pettersen, 1984)

The structure of cellulose is made up of various polysaccharides including the alkali soluble hemi-celluloses and insoluble α-celluloses. Molecules of α-cellulose comprise the cell walls within each annual ring. The remaining polysaccharides make up a hemi-cellulose matrix which gives strength to cell walls. These units are added to cell walls prior to the final addition of lignin that has a high molecular weight, is least resistant to decay and provides cellular support (Loader, 1995).

Borella *et al.*, (1997) concluded that wholewood samples can also be used for isotopic analysis although this technique may not be applicable to conifers due to the high proportion of resins and waxes. These contain a different isotopic signature that could mask any common signal in a group of trees (Robertson *et al.*, 2004). In view of the possible problems associated with using holocellulose or wholewood,

processing samples to α-cellulose was the method of preparation for isotope analysis in this research.

There are arguments for stopping extraction at the holo-cellulose stage and there are studies that investigate climate- $\delta^{13}C$ relationships in this way (Saurer *et al.*, 1995). In addition $\delta^{13}C$ variations between holo and α-cellulose can be as little as 0.15 ‰ (Borella *et al.*, 1998), almost insignificant when compared to the variations that can exist between different trees. When dealing with small samples Macfarlane *et al.*, (1999) suggest using an acid-catalysed solvolysis method using di-glycol methyl ether, a quick method that does not require large amounts of laboratory equipment. However as this method may be of primary use for small samples and as powdered wood is processed on filter papers there is a risk of contamination from the filter paper cellulose that could potentially invalidate any results. The solvolysis method does also not remove all lignin and may be unsuitable for highly resinous species (Macfarlane *et al.*, 1999).

An advantage of the cellulose isolation procedure described by Loader *et al.*, (1997) is that milling of samples into powder is not required prior to processing. Samples are kept in modified glass Soxhlet thimbles throughout processing and transfer contamination is avoided.

Procedure:

The methodology used is a modified version of the method outlined by Loader (1997). Each annual wood sample was placed in a labelled borosilicate extraction thimble (Figure 2.27) Extraction of α-Cellulose was carried out in batches of 100 samples (figure 2.28).

This first step involves six 50 minute acidified sodium chlorite washes in a water bath heated to 80°C. This process oxidises non-cellulose compounds (waxes and resins).

Following five deionised distilled water rinses samples were suspended in 10%NaOH for 45 minutes in a water bath heated to 70°. Following filtration samples were suspended in 17%NaOH for 45 minutes in a water bath at room temperature. This procedure leaches carbohydrates such as mannan and xylan from the holocellulose.

Following five deionised washes the samples were subjected to two final acidified sodium chlorite washes for 50 minutes in a water bath heated to 80°C. Samples were then filtrated using deionised water five times.

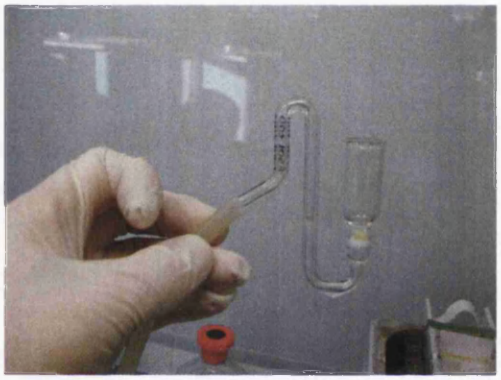

Figure 2.27. Extraction tube

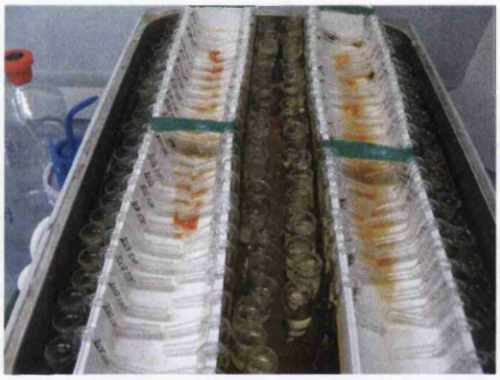

Figure 2.28. 100 Soxhlet tubes in water bath

2.22: Homogenisation

Rationale:

The amount of latewood in bristlecone pine is generally a very small amount, often little more than one or two layers of cells thick. The short growing season, often as little as 45 days in June, July or August, means that the climate signal is likely to be fairly homogenous across single rings. Cell size in bristlecone pines has been shown, in all apart from the youngest trees, to be largely unaffected by storms late in the growing season (Fritts, 1969). In addition conifer physiology means that carbon assimilation is generally more gradual in conifers (Schulze *et al.*, 2004) as compared to hardwoods where remobilisation of previous years food reserves may be evident in isotope series (Helle and Schleser, 2004). Although the risk of skewed results due to latewood inclusion is therefore probably minimal it was decided to homogenise

all samples to be as certain as possible that the isotopic value given for each year is representative of the whole of the growing season, with early and latewood well mixed.

Procedure:

Following the extraction process cellulose samples were removed from their extraction tubes and placed in labelled eppendorf tubes with one ml of deionised water. Individual samples were then homogenised ultrasonically using a Hielchsher homogeniser (figure 2.32) for up to one minute each in a method outlined by Loader *et al.*, (2008). Each sample was covered with a pierced foil lid (to allow ventilation during freeze drying) and batches of 100 were frozen overnight.

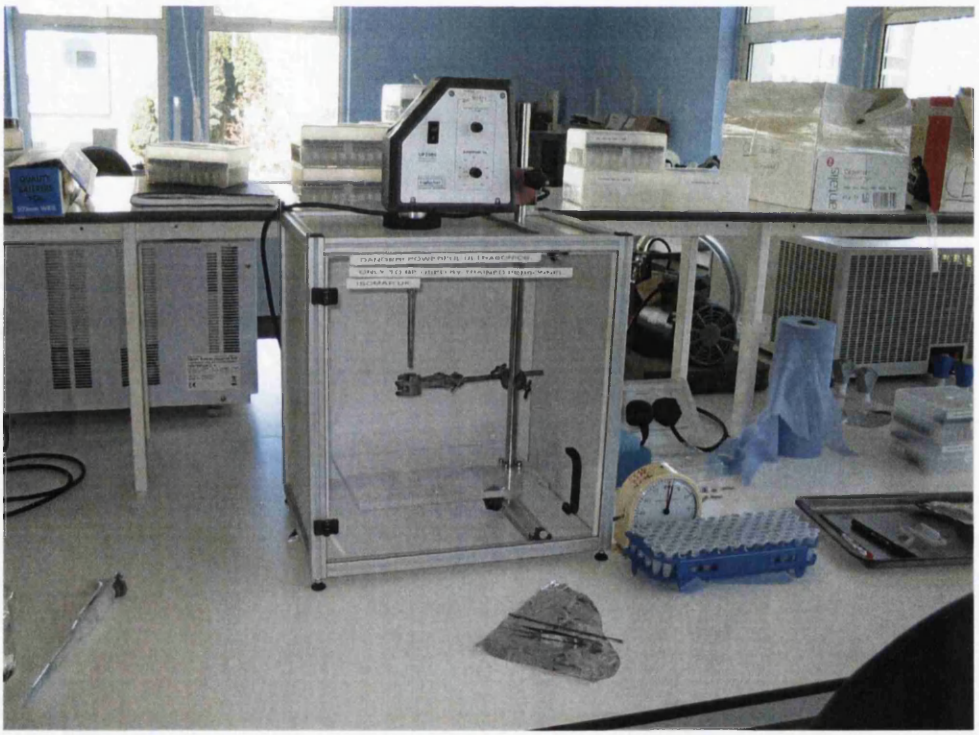

Figure 2.32 Hielchsher ultrasonic homogeniser.

2.23: Freeze drying

Frozen samples were dried under vacuum (<80mbar) for up to three days in order to ensure all traces of water were removed. The fully dried homogenised samples were then ready for weighing for isotope analysis.

2.24: Sample weighing

Samples for $\delta^{13}C$ analysis were weighed to 0.30-0.35 μg and were placed into tin foil capsules. High levels of precision (0.1‰) with rapid sample throughput (8-12 minutes per sample) can typically be obtained on samples of 0.30-0.35μg.

2.25: Mass spectrometry (GC-IRMS)

Isotopic samples were analysed using a PDZ Europa 20/20 stable isotope ratio mass spectrometer interfaced to a ANCA GSL elemental analyzer.

On line carbon isotope analysis:

Sample gases are admitted to the mass spectrometer where they are ionised. The charged particles are accelerated by high voltage to a magnetic field where they are deflected according to mass to Faraday cups or detectors. The sample values are compared against standards of known isotopic composition. Traditional dual inlet machines run single or small batches of samples. These were used in many early studies but are limited by low sample throughput and are relatively time consuming as compared to on line methods (McCarroll and Loader, 2004).

Samples drop into a tube heated to 1000°C through which a stream of helium is passed. A pulse of oxygen is admitted on the carrier gas and the combustion products are carried in a stream of helium through a silica column packed reduction reagents, usually chromium(III) oxide and copper(II) oxide. These act as further oxygen sources ensuring complete combustion so that the carbon in the sample is completely oxidised to CO_2. The sample gas is admitted into the mass spectrometer via a capillary tube and split where the carbon dioxide (and/or nitrogen) can be analysed. Some nitrogen oxides are still present and could potentially contaminate the carbon isotope measurements, so the sample is reduced to nitrogen gas in a second furnace heated to 600°C over copper. Traces of water are removed, typically using a chemical trap, and the resulting gases, a mixture of CO_2 and N_2, resolved to separate peaks by a gas chromatography column. The results are compared with standard reference gases and samples of known isotopic composition. Addition of an autosampler enables many samples (100+) to be prepared and run as a batch. From

entry into the elemental analyser to the production of an isotope result takes between eight and twelve minutes (McCarroll and Loader, 2004).

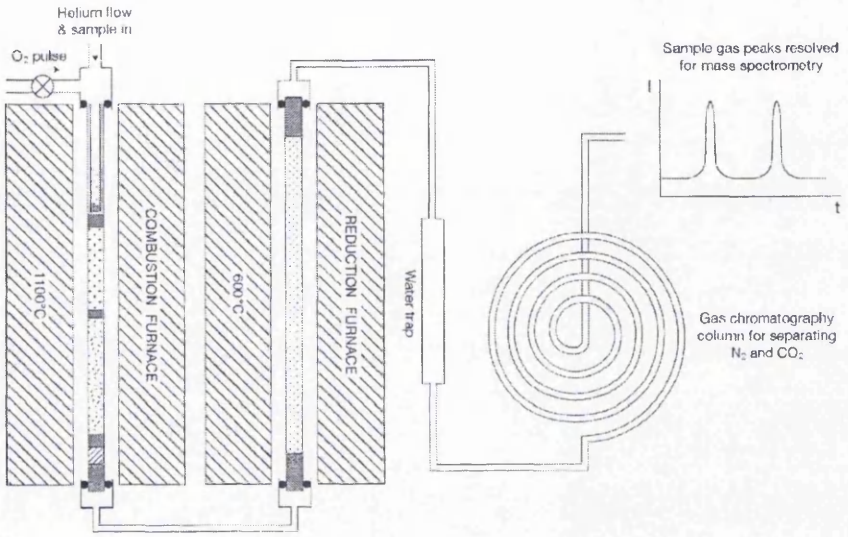

Figure 2.33. Schematic diagram of elemental analyser setup for online $\delta^{13}C$ analysis (From McCarroll and Loader, 2006)

3: $\delta^{13}C$ Corrections

3.1: Introduction

Prior to calibration with instrumental climate data two corrections must be made to carbon isotope data over the 'industrial' period from AD1850 onwards. Firstly, fossil fuels are of organic origin and are therefore already depleted in $\delta^{13}C$ (Keeling, 1979). Industrially related changes in the isotopic composition of CO_2 in the atmosphere have resulted in the lowering of the $\delta^{13}C$ value of air by about 1.5‰ since AD 1850 (McCarroll and Loader, 2004). An incremental adjustment is made to the $\delta^{13}C_{raw}$ results based upon what is known of changes in atmospheric CO_2 over the last 150 years. A second correction (chapter 3.3) made is that proposed by McCarroll *et al.*, (in press) to account for the response of trees to increased CO_2 concentration in the atmosphere, resulting in the final 'pre-industrially corrected' or PIN ($\delta^{13}C_{pin}$) values to be used for climate calibration. Following detailed analysis of the raw $\delta^{13}C$ ($\delta^{13}C_{raw}$) values, the fossil fuel corrected $\delta^{13}C$ ($\delta^{13}C_{cor}$) values, and the PIN corrected data ($\delta^{13}C_{pin}$), variability is discussed in terms of significant trends and inter tree correlation and the data are standardised. A measure of the common signal, express population signal (EPS) between the seven trees that cover the calibration data set is presented in conclusion of this chapter.

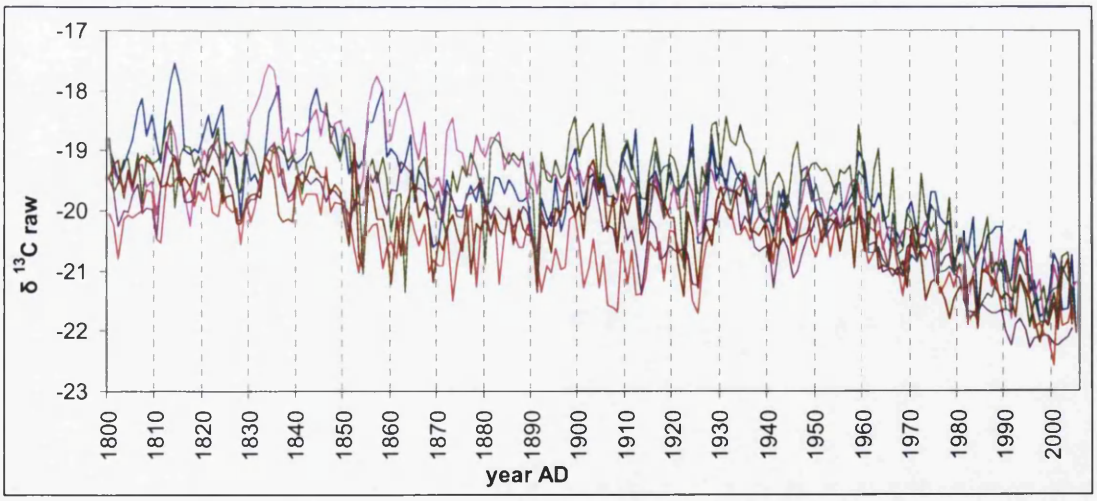

Figure 3.1 Raw $\delta^{13}C_{raw}$ values for all 7 trees from AD1800-2005

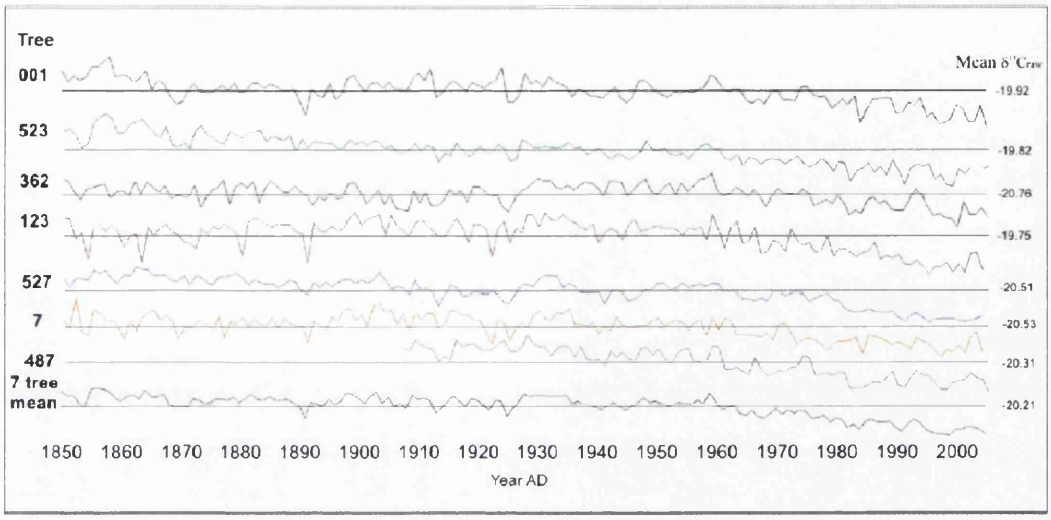

Figure 3.2. Raw $\delta^{13}C$ results from AD1850-2005 for 7 individual trees and mean for all trees.

3.2: Correction for atmospheric decline in $\delta^{13}C$

Anthropogenic burning of fossil fuels, themselves of an organic origin and already depleted in $\delta^{13}C$, has changed the relative concentration of $\delta^{13}C$ in the atmosphere. Fossil plant and animal material that forms the basis of fossil fuels has already taken in CO_2 and is therefore depleted in $\delta^{13}C$. As fractionation is additive this trend should be reflected in tree ring $\delta^{13}C$ series with significantly depleted values of $\delta^{13}C$ since AD1850 evident in many tree ring series (McCarroll and Loader, 2006). It is clearly apparent in the $\delta^{13}C_{raw}$ values of bristlecone pine trees from the Blanco West site and, in the context of the last 1000 years is particularly pronounced for the second half of the 20th century to a large degree in all trees (Figure 3.3). The $\delta^{13}C_{raw}$ values show a strong trend towards depletion

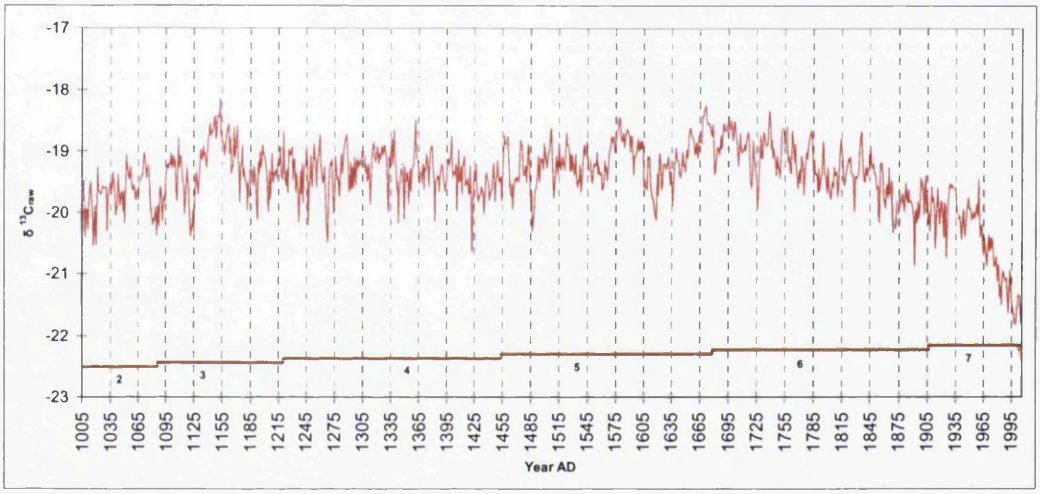

Figure 3.3. Mean of all trees $\delta^{13}C_{raw}$ values AD1005-2005. Number of trees comprising the mean value is also shown.

This trend is present in many tree-ring $\delta^{13}C$ series (Epstein and Krishnamurthy, 1990; Feng and Epstein, 1995; Feng and Epstein, 1996; Freyer, 1981; Robertson *et al.,* 2008), though is not seen in others (Anderson *et al.*, 1998). Statistical detrending, by fitting a line or curve and adding or subtracting values that deviate from this curve would be an approach used to remove growth related trends in tree ring width studies, and is the simplest way to remove this, although this would also remove trends associated with climatic or other environmental controls present in

isotope series and render them liable to the same sorts of problems associated with ring width/climate studies (Duquesnay *et al.*, 1998).

A particular feature of this problem is that the period over which $\delta^{13}C$ declines is also a time in which major factors such as CO_2 enrichment of the atmosphere may have influenced tree growth and response to climate (McCarroll and Loader, 2004). There is a considerable scatter in both ice core and atmospheric measurements of CO_2 (McCarroll and Loader, 2006, Francey *et al.*, 1999) and there is local CO_2 variations particularly over forested areas that act as 'carbon sinks'. However, McCarroll and Loader (2004) argue that although sampling CO_2 from each individual tree ring site would be an ideal solution the data are precise enough to allow a standard approach to $\delta^{13}C$ correction over the last 150 years. In addition to removing any effect on trees from declining $\delta^{13}C$ of the atmosphere any physiological response to increased CO_2 concentrations will be removed, as will any changes in climate due to rising CO_2. Where the aim of study is to focus on high frequency extreme events (e.g droughts), detrending will not present as much of a problem as studies that seek to extrapolate a low frequency signal from $\delta^{13}C$ series (Briffa *et al.*, 1998). This research aims to identify both and high and low frequency climate events and it is necessary to examine in detail any trends that are apparent in the time period (AD1850-2005) used for climate calibration. To achieve this aim, both raw, fossil fuel corrected and PIN corrected carbon isotope data have been broken down into 50 year 'blocks' and described in terms of the high and low frequency trends and also in terms of inter-tree correlation, the range of error among the trees used and any observed divergence in the tree ring isotope series. This has been done to examine the significance of any trends and high frequency fluctuations apparent in the $\delta^{13}C$ series.

Two approaches may be used that avoid the problems associated with statistical detrending, these are removing the trend mathematically, or expressing isotope ratios in terms of discrimination against ^{13}C rather than relative to a standard. Both require annual estimates, or actual measurements of the $\delta^{13}C$ of the atmosphere (McCarroll

and Loader, 2004). Ice cores provide evidence for the early and pre-industrial period and air sampling provides recent air measurements. A non-linear decline is evident in this incomplete data with a marked scatter of points, meaning a certain amount of generalisation is needed to obtain annual correction values. Various line fitting methods have been used to correct data each giving slightly different results and making corrected data difficult to compare (McCarroll and Loader, 2004). A common approach should preclude the use of polynomials as adding a few points can have a unpredictable effect on the rest of the curve. McCarroll and Loader (2004), Bert *et al.*, (2004) and Saurer *et al.*, (1997) propose dividing data into a series of segments with inflection points rather than a curve. Here, accrued data cannot change earlier values, and if future research discovers an error in one segment only values from that segment need be amended. Saurer *et al.*, (1997) compiled a record of atmospheric $\delta^{13}C$ based on Antarctic ice cores that can be summarised into two segments. Between 1850 and 1961 an annual decline of 0.0044‰ and between 1962 and 1980 a calculated decline of 0.0281‰. Although there are other local data sets this data is thought to be sufficient to provide a means of removing the atmospheric $\delta^{13}C$ decline from tree ring series (Francey *et al.*, 1999).

Quoting $\delta\ ^{13}C$ values for a long dataset such as that from the Blanco West bristlecone pines in terms of discrimination against ^{13}C would involve adjusting all the values in the whole dataset, even though only a small part of the 1000 year record, from around 1850-2005 (see figure 3.3) is affected by the anthropogenic effect.

McCarroll and Loader (2004) propose a method whereby changing atmospheric $\delta\ ^{13}C$ can be corrected for by simply adding the difference between the atmospheric value for each year to the uncorrected value for the $\delta^{13}C$ of each tree ring (see table below). A logical standard value is the 'pre-industrial' value of $\delta^{13}C$ of the atmosphere (-6.4‰ is an estimate of this).

Year	$\delta^{13}C$	Δ	CO_2	Year	$\delta^{13}C$	Δ	CO_2	Year	$\delta^{13}C$	Δ	CO_2
1850	−6.41	0.01	285.2	1901	−6.64	0.24	297.0	1952	−6.86	0.46	312.8
1851	−6.42	0.02	285.3	1902	−6.64	0.24	297.3	1953	−6.87	0.47	313.2
1852	−6.42	0.02	285.4	1903	−6.65	0.25	297.6	1954	−6.87	0.47	313.6
1853	−6.43	0.03	285.5	1904	−6.65	0.25	297.9	1955	−6.88	0.48	314.1
1854	−6.43	0.03	285.6	1905	−6.66	0.26	298.2	1956	−6.88	0.48	314.6
1855	−6.43	0.03	285.7	1906	−6.66	0.26	298.5	1957	−6.89	0.49	315.1
1856	−6.44	0.04	285.8	1907	−6.66	0.26	298.9	1958	−6.89	0.49	315.7
1857	−6.44	0.04	285.9	1908	−6.67	0.27	299.2	1959	−6.90	0.50	315.8
1858	−6.45	0.05	286.0	1909	−6.67	0.27	299.6	1960	−6.90	0.50	316.8
1859	−6.45	0.05	286.2	1910	−6.68	0.28	299.9	1961	−6.90	0.50	317.5
1860	−6.46	0.06	286.3	1911	−6.68	0.28	300.2	1962	−6.92	0.52	318.3
1861	−6.46	0.06	286.5	1912	−6.69	0.29	300.5	1963	−6.95	0.55	318.8
1862	−6.47	0.07	286.6	1913	−6.69	0.29	300.9	1964	−6.98	0.58	319.4
1863	−6.47	0.07	286.8	1914	−6.70	0.30	301.2	1965	−7.01	0.61	319.9
1864	−6.47	0.07	287.0	1915	−6.70	0.30	301.5	1966	−7.03	0.63	321.2
1865	−6.48	0.08	287.2	1916	−6.70	0.30	301.8	1967	−7.06	0.66	322.0
1866	−6.48	0.08	287.4	1917	−6.71	0.31	302.2	1968	−7.09	0.69	322.9
1867	−6.49	0.09	287.6	1918	−6.71	0.31	302.5	1969	−7.12	0.72	324.5
1868	−6.49	0.09	287.8	1919	−6.72	0.32	302.9	1970	−7.15	0.75	325.5
1869	−6.50	0.10	288.0	1920	−6.72	0.32	303.2	1971	−7.17	0.77	326.2
1870	−6.50	0.10	288.2	1921	−6.73	0.33	303.5	1972	−7.20	0.80	327.3
1871	−6.51	0.11	288.4	1922	−6.73	0.33	303.9	1973	−7.23	0.83	329.5
1872	−6.51	0.11	288.7	1923	−6.74	0.34	304.2	1974	−7.26	0.86	330.1
1873	−6.51	0.11	288.9	1924	−6.74	0.34	304.6	1975	−7.29	0.89	331.0
1874	−6.52	0.12	289.1	1925	−6.74	0.34	304.9	1976	−7.32	0.92	332.0
1875	−6.52	0.12	289.4	1926	−6.75	0.35	305.2	1977	−7.34	0.94	333.7
1876	−6.53	0.13	289.7	1927	−6.75	0.35	305.6	1978	−7.37	0.97	335.3
1877	−6.53	0.13	289.9	1928	−6.76	0.36	305.9	1979	−7.40	1.00	336.7
1878	−6.54	0.14	290.2	1929	−6.76	0.36	306.2	1980	−7.43	1.03	338.5
1879	−6.54	0.14	290.5	1930	−6.77	0.37	306.5	1981	−7.46	1.06	339.8
1880	−6.55	0.15	290.8	1931	−6.77	0.37	306.8	1982	−7.48	1.08	341.0
1881	−6.55	0.15	291.1	1932	−6.78	0.38	307.1	1983	−7.51	1.11	342.6
1882	−6.55	0.15	291.4	1933	−6.78	0.38	307.4	1984	−7.54	1.14	344.3
1883	−6.56	0.16	291.7	1934	−6.78	0.38	307.7	1985	−7.57	1.17	345.7
1884	−6.56	0.16	292.0	1935	−6.79	0.39	308.0	1986	−7.60	1.20	347.0
1885	−6.57	0.17	292.3	1936	−6.79	0.39	308.3	1987	−7.62	1.22	348.8
1886	−6.57	0.17	292.6	1937	−6.80	0.40	308.5	1988	−7.65	1.25	351.3
1887	−6.58	0.18	292.9	1938	−6.80	0.40	308.8	1989	−7.68	1.28	352.8
1888	−6.58	0.18	293.1	1939	−6.81	0.41	309.1	1990	−7.71	1.31	354.0
1889	−6.58	0.18	293.4	1940	−6.81	0.41	309.3	1991	−7.74	1.34	355.5
1890	−6.59	0.19	293.7	1941	−6.82	0.42	309.5	1992	−7.77	1.37	356.3
1891	−6.59	0.19	294.0	1942	−6.82	0.42	309.8	1993	−7.79	1.39	357.0
1892	−6.60	0.20	294.3	1943	−6.82	0.42	310.0	1994	−7.82	1.42	358.9
1893	−6.60	0.20	294.6	1944	−6.83	0.43	310.2	1995	−7.85	1.45	360.9
1894	−6.61	0.21	294.9	1945	−6.83	0.43	310.5	1996	−7.88	1.48	362.7
1895	−6.61	0.21	295.2	1946	−6.84	0.44	310.8	1997	−7.91	1.51	363.8
1896	−6.62	0.22	295.5	1947	−6.84	0.44	311.0	1998	−7.93	1.53	365.5
1897	−6.62	0.22	295.8	1948	−6.85	0.45	311.3	1999	−7.96	1.56	367.0
1898	−6.62	0.22	296.1	1949	−6.85	0.45	311.7	2000	−7.99	1.59	368.5
1899	−6.63	0.23	296.4	1950	−6.86	0.46	312.0	2001	−8.02	1.62	370.0
1900	−6.63	0.23	296.7	1951	−6.86	0.46	312.4	2002	−8.05	1.65	371.5
								2003	−8.07	1.67	373.0

Figure 3.4 from McCarroll and Loader, (2004:788). Estimated annual values for the $\delta^{13}C$ of atmospheric CO_2 together with the correction factor necessary to quote tree-ring $\delta^{13}C$ values relative to a pre-industrial standard value of -6.4%. Note: Data are interpolated using the high precision records of atmospheric $\delta^{13}C$ obtained from Antarctic ice cores (McCarroll and Loader, 2004) . Estimated values for the atmospheric concentration of CO_2 (ppm) are taken from (Francey et al., 1999).

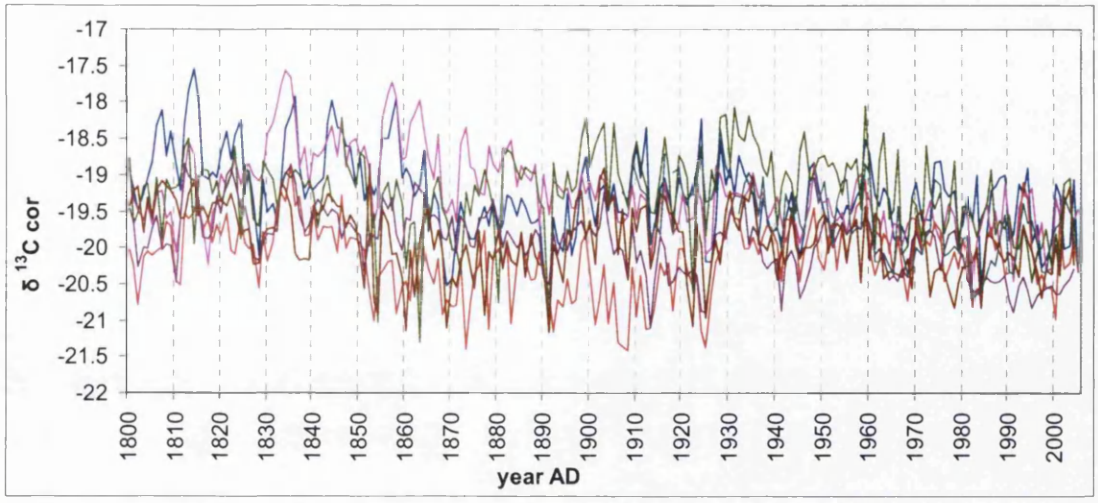

Figure 3.5. Fossil fuel corrected $\delta^{13}C$ ($\delta\ ^{13}C_{cor}$) values for all 7 trees AD1800-2005.

As can be seen in figures 4, 5 and 6 the Suess correction does remove most of the fossil fuel trend apparent in the raw $\delta^{13}C$ tree ring data although there is still a significant declining trend in all the trees.

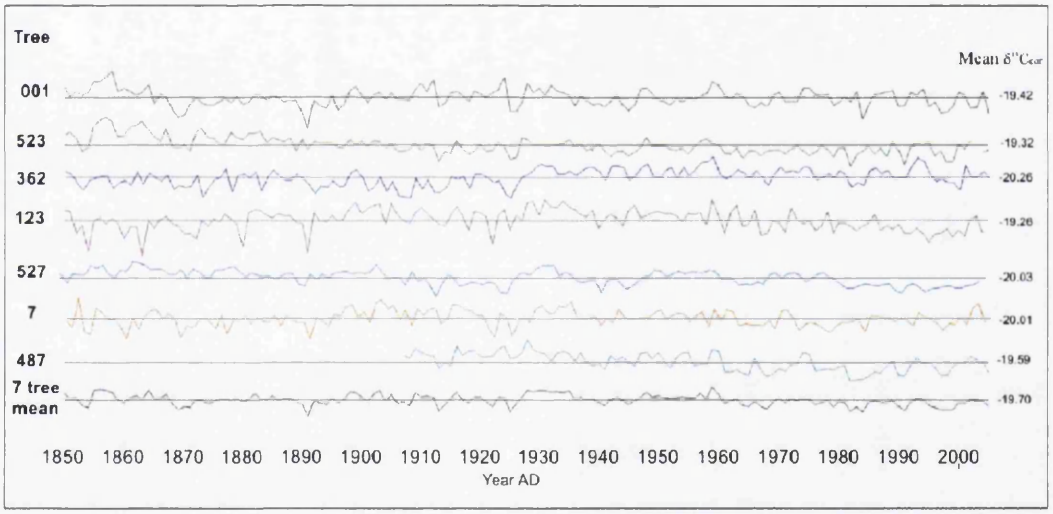

Figure 3.6. fossil fuel corrected $\delta^{13}C$ results from AD1850-2005 for 7 individual trees and mean for all trees.

3.3: PIN correction.

The correction for the isotopic composition of fossil fuels shown above does not however account for the trees response to elevated CO_2 concentrations. McCarroll *et al.*, (in press) agreed to perform a correction on the data presented in this thesis that they term a PIN correction. Their justifications for undertaking the PIN correction to tree ring isotope data are outlined in the following paragraphs taken directly from McCarroll *et al.*, (in press).

"*Fossil fuel burning since industrialisation has led to changes in the* $\delta^{13}C$ *of the atmosphere* ($\delta^{13}C_{atm}$). *Since annual values of* $\delta^{13}C_{atm}$ *are available (Robertson et al., 2001) tree ring* $\delta^{13}C$ *values can be corrected against a pre industrial standard of -6.4‰* ($\delta^{13}C_{cor}$) *using:*

$$\delta^{13}C_{cor} = \delta^{13}C_{plant} - (\delta^{13}C_{atm} - 6.4)$$

This equation shows that the only non-constant factors that control fractionation are c_i *and* c_a, *that is the intercellular and ambient concentrations of* CO_2. *It is generally assumed that pre-industrial Holocene rises in atmospheric carbon dioxide were gradual. Ice core and atmospheric measurements show a rise from about 260ppm at 8ka BP to 285ppm in about AD1850 (Freidli et al., 1986; Leuenberger et al., 1992; McCarroll and Loader, 2004). Stable carbon isotopes from tree rings represent a palaeo record of internal changes in* CO_2 (c_i). *The concentration of* CO_2 *in the leaf is determined by the balance between the rate at which it enters (stomatal conductance) and the rate at which it is removed (photosynthetic rate). If* c_a *is stable an increase in* $\delta^{13}C$ *represents a decline in stomatal conductance or a decrease in photosynthetic rate (or some combination of the two). The climatic controls that may be reconstructed from* $\delta^{13}C$ *are those that influence these two factors, with the dominant controls being tree species, location and climatic regime (Robertson et al., 2001). Dry environments or trees with shallow roots on well drained soils tend to*

provide stronger correlations with air relative humidity or antecedent precipitation (McCarroll and Loader, 2004). In moist environments where trees suffer less moisture stress, photosynthetic rate may dominate giving strong correlations with sunlight and temperature (McCarroll et al., 2003; Robertson et al., 1997; Schleser et al., 1999).

If the values of $\delta^{13}C_{atm}$ are considered to be reliable then any remaining decline in the $\delta^{13}C_{cor}$ of tree rings that cannot be explained by environmental change must be the result of an increase in ci as a result of increasing CO_2 content of the atmosphere (c_a).

The largest declines in $\delta^{13}C_{cor}$ will occur where trees display a passive response to increased c_a and do not display either changes in stomatal conductance or photosynthetic rate. Every increase in ca will result in an equal incremental increase in ci so the relationship remains constant. For example, a tree with a stable pre-industrial $\delta^{13}C$ value of –23‰, which would equate to a c_i of 154ppm assuming pre-industrial values of c_a and $\delta^{13}C_{atm}$ of 285ppm and –6.4‰, would have ci values at AD1950 and AD2000 of 181ppm and 237ppm, assuming no influence from climate fluctuations. This would give $\delta^{13}C_{cor}$ values of –23.90‰ and –25.35‰ respectively (Tans and Mook, 1980).

The afore described increase in c_i that results from a passive response to increased ca may be regarded as the maximum effect that can be attributed directly to an increase in atmospheric CO_2. However, in many published $\delta^{13}C$ series a decline is still evident that is too small to be attributed to a passive response. In some cases the increase in c_i-c_a is enough to maintain a near constant c_i/c_a, so that the decline in measured ratios ($\delta^{13}C_{plant}$) is explained by the changes in $\delta^{13}C_{atm}$ and there is no declining trend in $\delta^{13}C_{cor}$.

An increase in c_a-c_i as an active response to increasing atmospheric CO_2 may be understood in terms of a trees water use efficiency. This means the amount of water lost compared to each carbon unit gained (McCarroll et al., In press) and at the plant level includes respiratory losses. At the leaf level water use efficiency (W_i) is proportional to c_a-c_i. (Ehleringer and Cerling, 1995; Saurer et al., 2004). This may be expressed as :

$$W_i = (C_i - C_a)/1.6$$

Here, 1.6 represents the ratio of diffusivity of water to CO_2. Increased intrinsic water use efficiency can be the result of decreased stomatal conductance and/or in increase in assimilation rate. Both effects may be observed in simulated elevated CO_2 experiments although whether the results of such experiments may be related to trees living in natural conditions is debatable (Saurer et al., 2004). Some trees display a near constant c_i/c_a throughout the industrial period, but many show a non-linear response to increased ca, with a switch from near constant c_i/c_a (active response) to near constant c_a/c_i (active response) in recent decades. A simple incremental approach is not enough to capture or understand this change in response (Korner, 2003), who propose a new correction for carbon isotope tree ring data.

The aim of the PIN correction is to remove any changes in increased c_i (and therefore the decline in $\delta^{13}C_{cor}$) that is due directly to increasing c_a while retaining any trends that are related to changes in climate. The procedure is based on a non-linear de-trending of the data after 1850, but the de-trending is constrained. The argument is that a rise in CO_2 cannot cause delta values to rise (that would be a decline in wue) and the maximum decline in delta is that which would occur if the rise in ca was mirrored by exactly the same rise in ci, ie completely passive response. The effect is that rising values of delta are not changed and the amount of correction to falling values increases through time as the rate of increase in ca has accelerated.

The $\delta^{13}C$ values obtained from these equations should represent the values that would have been obtained had the carbon dioxide concentration of the atmosphere remained at 285ppm and the stable carbon isotopic ratio of atmospheric carbon dioxide remained at -6.4‰). Any declining trends in $\delta^{13}C$ that can be explained by changes in the isotopic composition of the atmosphere, or in response to increased atmospheric CO_2 concentration should be removed. Any trends that remain should therefore carry important signals of climate change" McCarroll *et al.*, (in press)

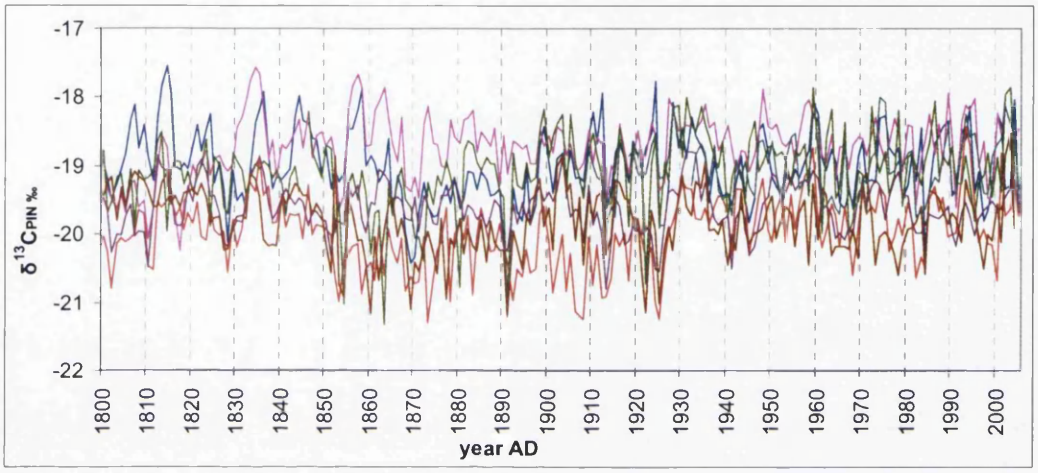

Figure 3.7. $\delta^{13}C$ ($\delta^{13}C_{pin}$) values for all 7 trees AD1800-2005.

Figure 3.8. PIN corrected $\delta^{13}C$ results from AD1850-2005 for 7 individual trees and mean for all trees.

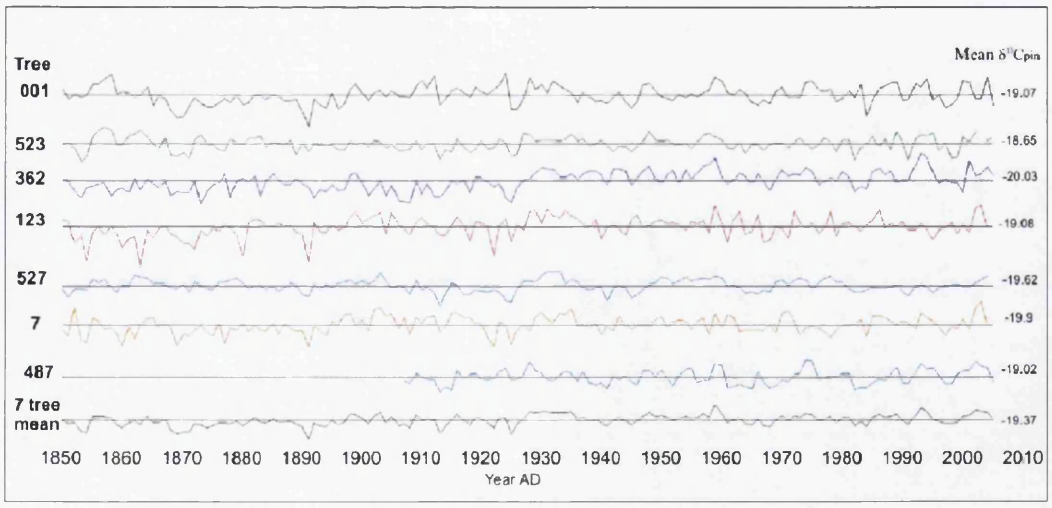

Figure 3.9 A

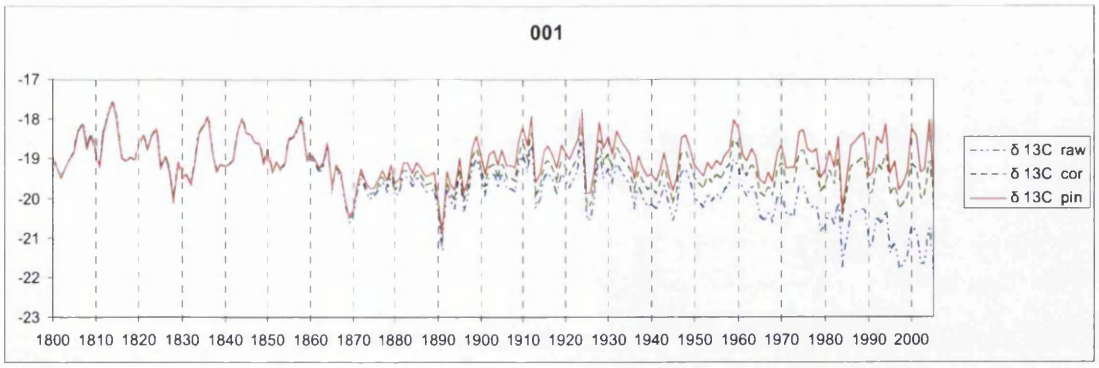

Figure 3.9 B

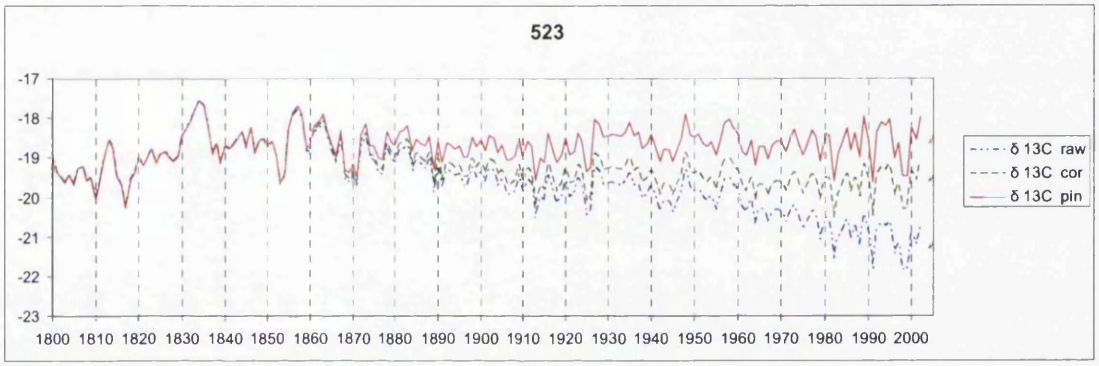

Figure 3.9 C

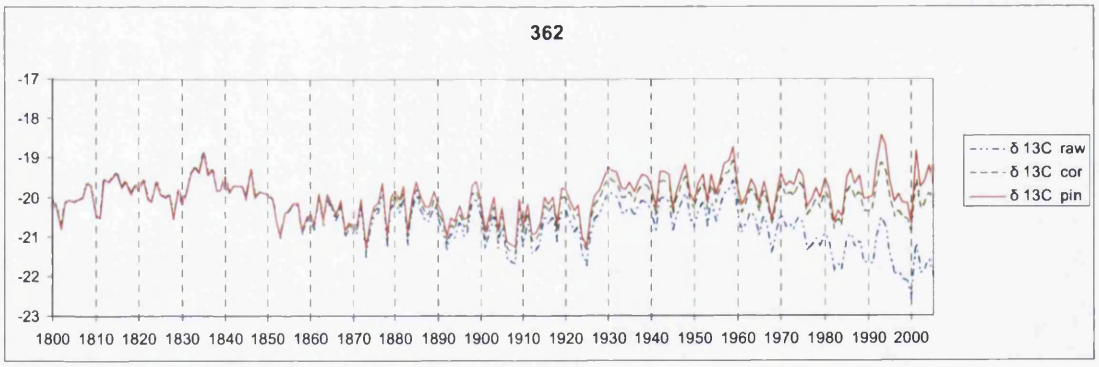

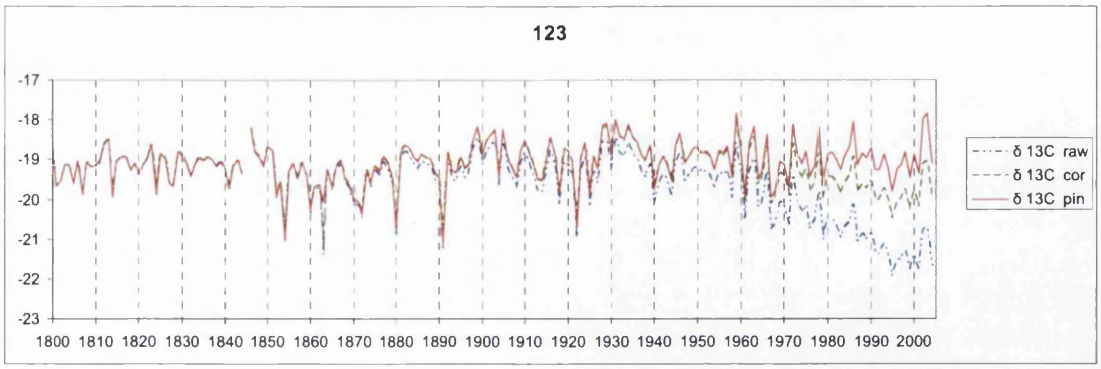

Figure 3.9 D

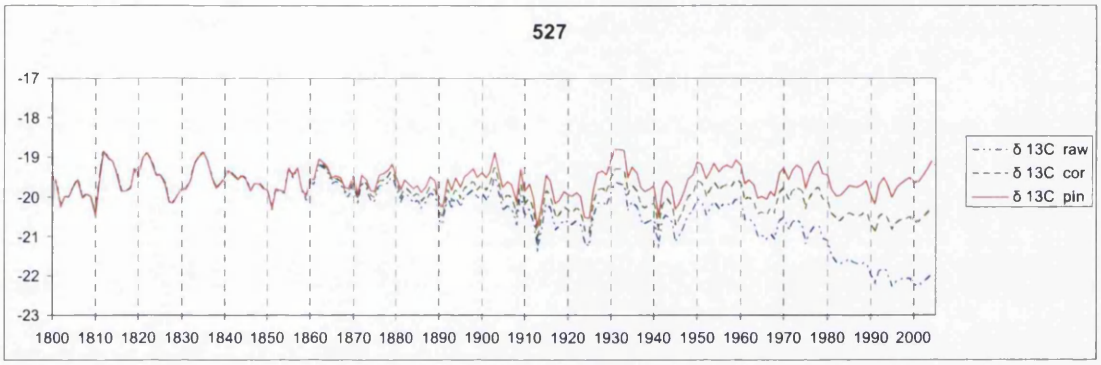

Figure 3.9 E

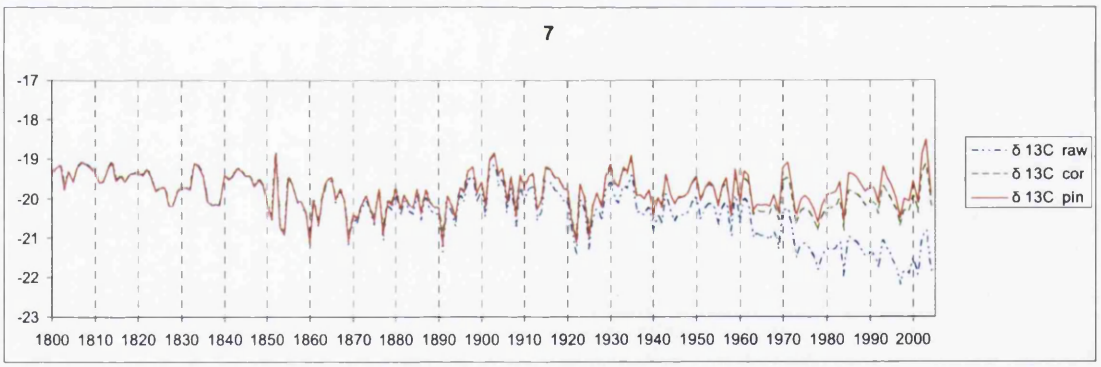

Figure 3.9 F

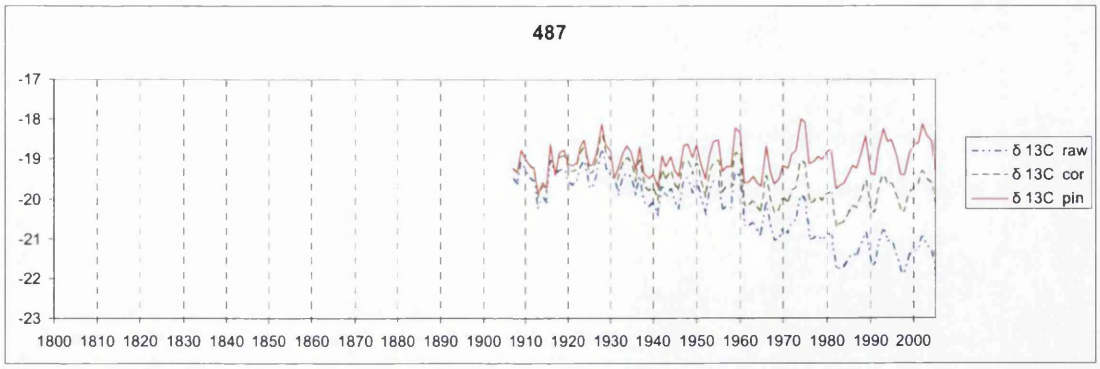

Figure 3.9 G

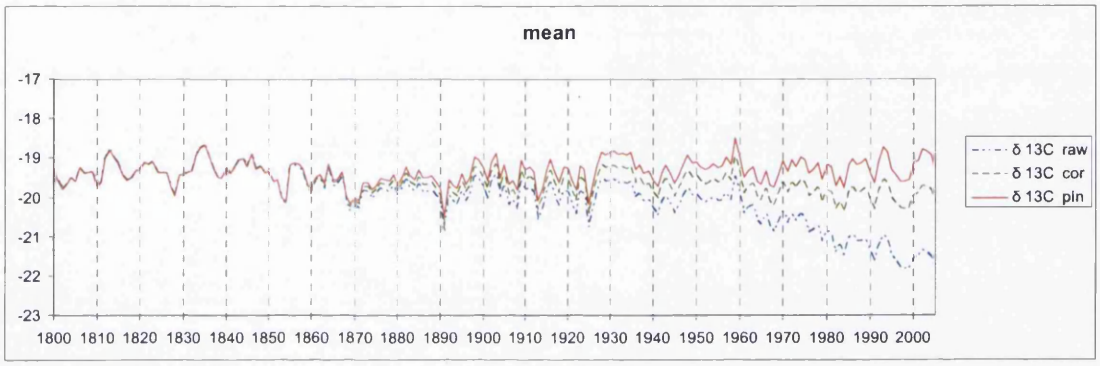

Figure 3.9 H

Figure 3.9 (A,B,C,D,E,F,G,H) Raw, Cor and PIN corrected $\delta^{13}C$ data trees and mean of 6/7 trees values) for correction period (AD 1820-2005).

According to the criteria outlined by McCarroll *et al.,* (in press):

"A declining trend will remain that represents an increase in internal concentration of CO_2, and therefore an increase in either stomatal conductance and/or a decrease in photosynthetic rate. Likely climatic scenarios for this would be a decrease in temperature or an increase in moisture availability. In situations where there is a trend toward rising $\delta^{13}C$ values, this will be indicative of warmer/drier conditions"

This would appear to be the case for the bristlecone pine, at least over the last 150 years. The increase is significant with the mean of all trees (figure 3.9H) (r^2=.168 AD1850-2005). When looking at shorter periods of time other trends are apparent, in some or all of the seven trees. There are periods of divergence, both in terms of inter

tree correlation and with instrumental climate data calibration. It is more than likely that the carbon isotope ratios, for which the most data is available for this thesis, reflect an integration of environmental factors. High and lower frequency anomalies may be explained by drought (e.g AD2002 and 1929-1935) or extreme summer heat (e.g AD1959), or can be related to local or more regional climate phenomena such as volcanoes and ENSO activity (e.g AD1913, 1991, 1982-1984). It may be that western North American tree ring data is not particularly suited to reconstructing temperature, but it is difficult to explain the trends in terms of precipitation alone.

As can be seen in Figures 3.1, 3.2 and 3.3 the decline in $\delta\ ^{13}C_{raw}$ values really takes effect, to a varying degree from around 1925-1930 and is most pronounced since 1960. The largest decline occurs in the second half of the 20th century and, based on the correction proposed by McCarroll *et al.*, (in press) could be explained by a change in the reaction of the tree to increasing CO_2 concentration. Up until the mid-20th century the trees may be increasing their water use efficiency (maintaining near constant c_i/c_a and displaying an active response) to a more passive response (maintaining a constant c_i/c_a).

The bristlecone pine data from Blanco West was compared to climate data both in $\delta\ ^{13}C_{cor}$ and $\delta^{13}C_{pin}$ form. Correlation with temperature was improved by applying the PIN correction, but with precipitation the correlations were either slightly lowered or remained the same (chapter 6). In particular, the significant decline evident in the fossil fuel corrected $\delta^{13}C$ data after 1950 appears to be related to the reaction of the trees to increased CO_2, and is not a function of temperature or precipitation. The application of the PIN correction can thus be justified with this data set. Inter tree correlation (in terms of *r* values) is much higher with the raw data, due to the very strong declining trend from 1850 onwards. Inter tree correlation and EPS are lower when the fossil fuel correction is applied and lower still with the application of the PIN correction.

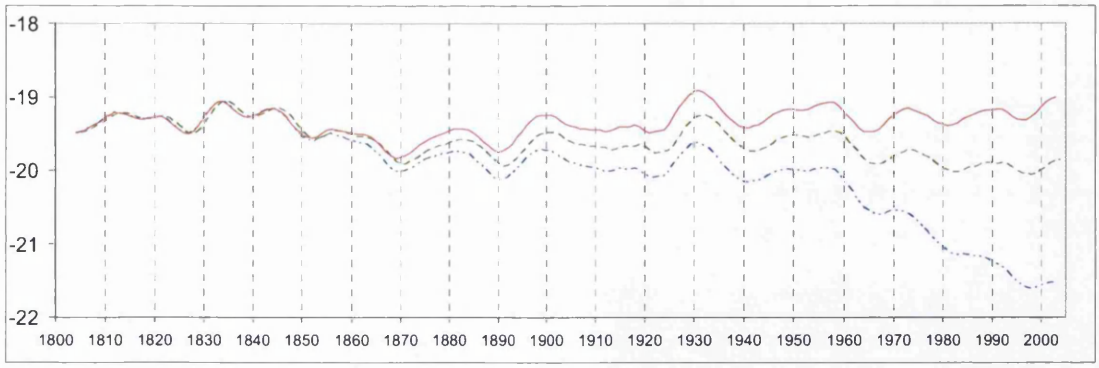

Figure 3.10. Weighted 11 year mean of $\delta^{13}C_{raw}$, $\delta^{13}C_{cor}$ and $\delta^{13}C_{pin}$ data from AD1800-2005.

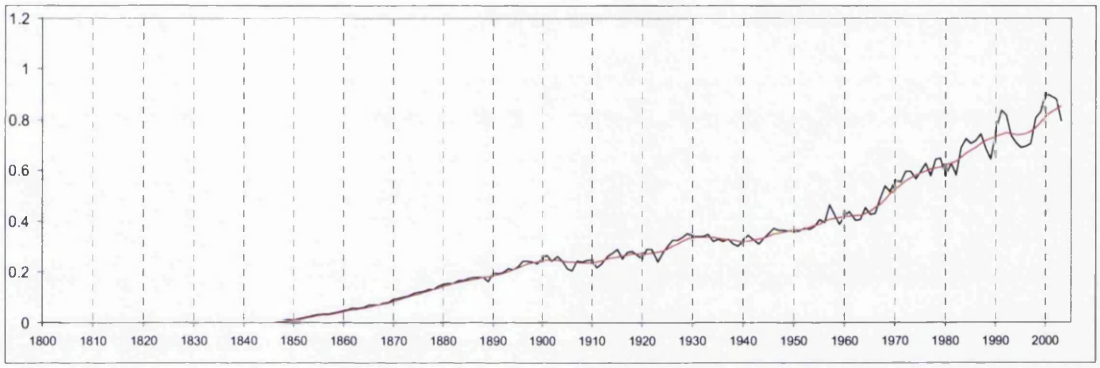

Figure 3.11. $\delta^{13}C_{pin}$ - $\delta^{13}C_{cor}$ and weighted 11 year running mean.

Figure 3.10 illustrates the changes that each $\delta^{13}C$ correction makes over time from AD1800 to 2005 at decadal level. The most rapid $\delta^{13}C_{raw}$ depletion occurs in the decades after 1960. Figure 3.11 illustrates $\delta^{13}C_{pin}$ - $\delta^{13}C_{cor}$. The fluctuations over time in $\delta^{13}C_{pin}$ - $\delta^{13}C_{cor}$ from AD 1800-2005 represent the effect that the PIN correction as undertaken by McCarroll *et al.*, (in press) has at the decadal level as a response to increasing CO_2.

4.0: Data analysis and inter tree variability- Introduction.

Before any climate calibration can be undertaken it is important to understand the range of variability that is present in the individual tree data. The following chapter demonstrates how isotope values from different trees may be offset, and individual trees may display different, significant trends during the same time period. The data are broken down into 50 year blocks and any trends are described. This includes any significant rises or decreases in $\delta^{13}C$ for each tree and the mean of all trees during each 50 year period. In addition a measure of inter tree correlation for each 50 year period is shown in order to understand the degree of coherence between the trees in any given time period. This is expressed as the EPS (express population signal) and is used in tree ring studies to ascertain the suitability of a group of trees for climate reconstruction (Wigley *et al.*, 1984). The EPS values used throughout this research were calculated in the following way:

*EPS= NUMBER OF TREES * AVERAGE r VALUE*
*/ (NUMBER OF TREES * AVERAGE r VALUE*
+ (1- AVERAGE r VALUE))

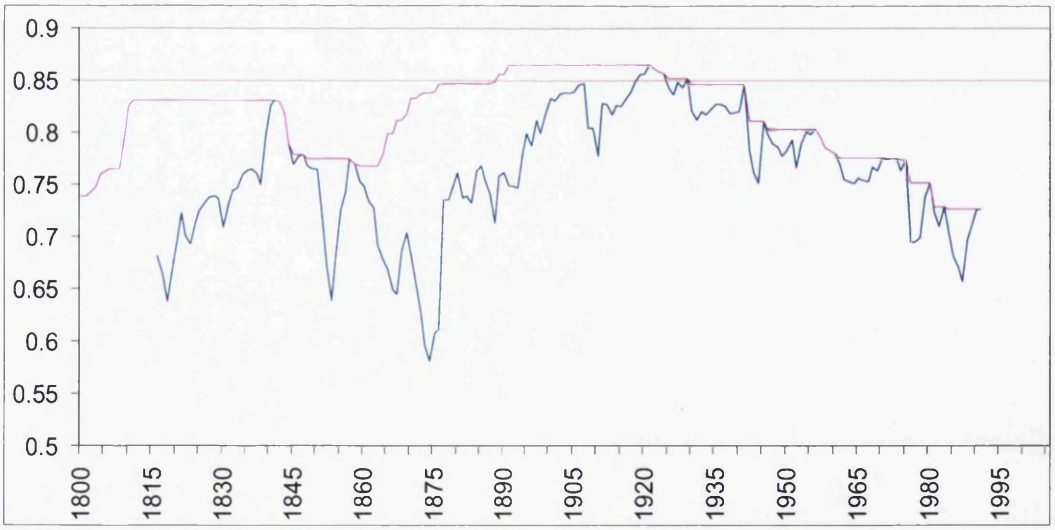

Figure 3.12. 30 year moving EPS value between 6/7 trees. The blue line shows the EPS for each 30 year block. The pink line shows the maximum EPS value for any 30 year period. 0.85 is generally considered to be the value necessary for climate reconstructions. Axes

Although an EPS value of 0.85 is used as a benchmark to assess trees suitability for use in palaeoclimate work (Cook and Kariukistis, 1995), it does not mean that trees

that attain this level are totally suitable for climate study, or that inter tree correlations that do not meet this level are unsuitable for climate reconstruction. It is evident from figure 3.12 that the EPS and the degree of common variance in the trees is well below 0.85 and may well be related to the wide variation in trunk morphology and growth form of individual trees. The dating of the trees followed established procedures and protocols (Stokes and Smiley, 1996). Cores were first skeleton plotted against master chronologies. Every 10^{th} ring was pinned, every 50^{th} ring pinned twice and every 100 rings pinned 3 times. Missing rings were noted during crossdating. In addition ring widths were measured and all the ring width measurements were analysed in COFECHA (Holmes, 1983, Grissino Meyer, 2001) to see if any rings had been missed. All the dating procedures point to the fact that there is not a cross dating error in the bristlecone pine trees from Blanco West.

As the period AD1850-2005 is to be used for climate calibration, the $\delta\ ^{13}C_{raw}$,$\delta^{13}C_{cor}$ and $\delta^{13}C_{pin}$ data for this period are initially described in 50 yr blocks. After analysis of the 50 year blocks the $\delta\ ^{13}C$ data for the last 150 years is examined for trends and extreme values. The rationale behind breaking the data up into 50 year blocks is that 50 years is considered a long enough amount of time in which to deduce both meaningful trends in the data and the significance of extreme annual events. The data is made more manageable by dividing it into 50 year blocks. The rationale behind using both uncorrected and corrected data is to demonstrate the effect that increasing CO_2 has had in the last 150 years. In addition, by analysing both raw and corrected data the effect that the corrections have on the $\delta^{13}C$ data is clear. How these trends may be explained in environmental terms (i.e correlation with instrumental climate data) is described in chapter 5 that deals with calibration of carbon isotope data with instrumental climate records.

4.1: $\delta^{13}C$ data analysis- raw values ($\delta^{13}C_{raw}$) AD1950-2005

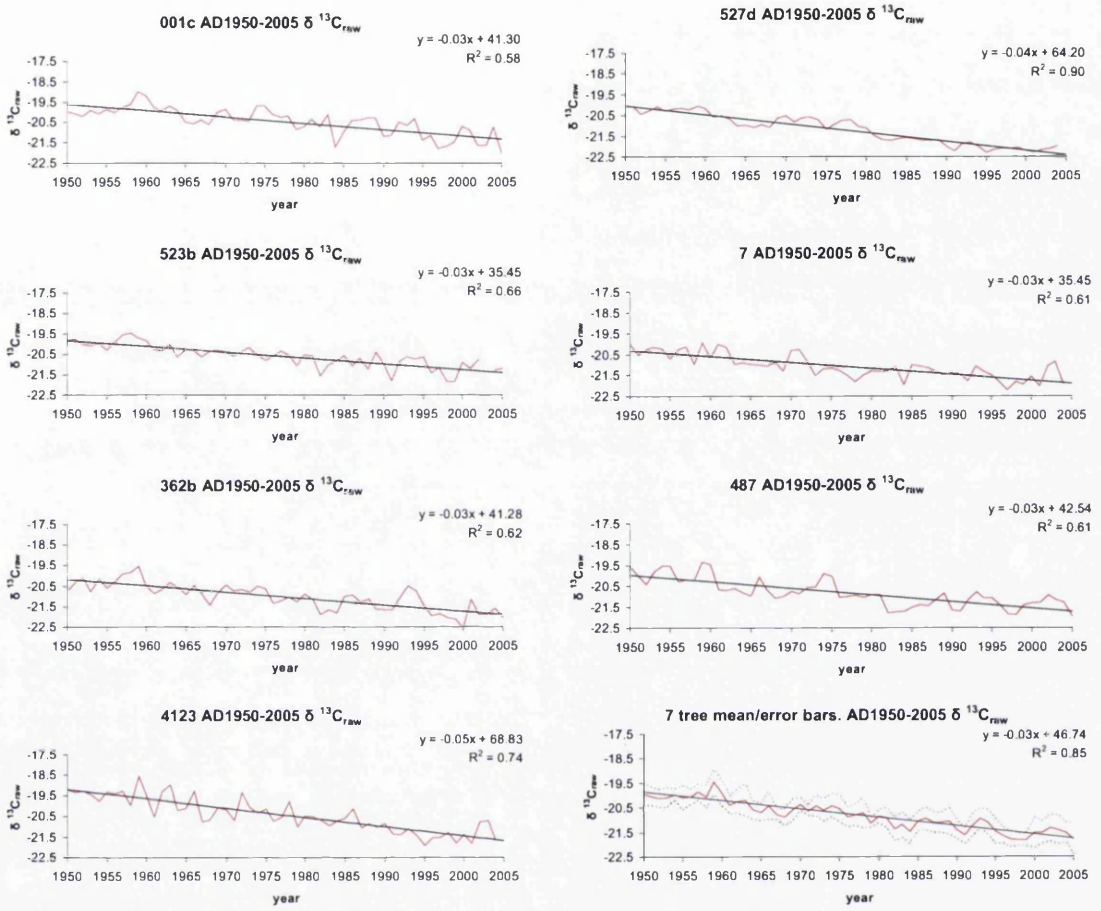

Figure 4.1: All trees and mean $\delta^{13}C_{raw}$.

Below:Table 4.1:Tree details and inter tree correlation

Tree	Most positive year (AD)	Most negative year(AD)	mean $\delta^{13}C_{raw}$
001c	1959	2005	-20.47
523b	1958	1999	-20.60
362b	1959	2000	-21.05
4123	1959	1995	-20.42
527d	1950	1995	-21.18
007	1959	1997	-21.07
487d	1959	2005	-20.84
mean	**1959**	**1999**	**-20.81**

	001c	523b	362b	4123	527d	007
523b	0.71					
362b	0.79	0.79				
4123	0.69	0.78	0.76			
527d	0.79	0.84	0.80	0.87		
007	0.63	0.71	0.68	0.74	0.74	
487d	0.75	0.78	0.78	0.76	0.81	0.68
		Mean r	**0.76**		**EPS**	**0.96**

Description: $\delta^{13}C_{raw}$ 1950-2005

A large significant decline in $\delta^{13}C_{raw}$ values is apparent in all trees and the mean. 1959 is the most positive value in five trees and the mean. 1950 and 1958 the most positive values in one tree each. 2005 is the most negative value in 2 trees. 1995 the most negative value in two trees. 1997 the most negative value in one tree. 2000 the most negative value in 1 tree and 1999 the most negative mean value.

Interpretation: $\delta^{13}C_{raw}$ 1950-2005

In the context of the last 1000 years the $\delta^{13}C_{raw}$ values for this period stand out as being unusually depleted due to the anthropogenic combustion of fossil fuels (figure3.3).

The strong significant decline in $\delta^{13}C$ is related to the rapid increase in the use of fossil fuels by humans over the second half of the 20th century and is well observed in many, though not all $\delta^{13}C$ tree ring series (McCarroll and Loader, 2005) and ice core and atmospheric measurement. The combustion of organically based fossil fuels (already depleted in $\delta^{13}C$) increases the amount of ^{13}C in the atmosphere and this is reflected in the $\delta^{13}C$ values. The period from 1995-2005 exhibits the most depleted values in all trees and demonstrates how strong the anthropogenic combustion of fossil fuels is altering the isotopic composition of the atmosphere. The most positive values, 1950 in one tree and 1959 in all the others and the mean is more a reflection of climatic conditions than the most negative values. 1959 was an unusually hot and dry year in the instrumental weather data, though locally was not the hottest in the last 50 years (see chapter 6.1). The strong negative decline is most evident after 1960. This decline in $\delta^{13}C$ values obscures any climatic signal in the data and also accounts for the high inter tree correlation and EPS (0.96).

4.2: $\delta^{13}C$ data analysis- raw values ($\delta^{13}C_{raw}$) AD1900-1949

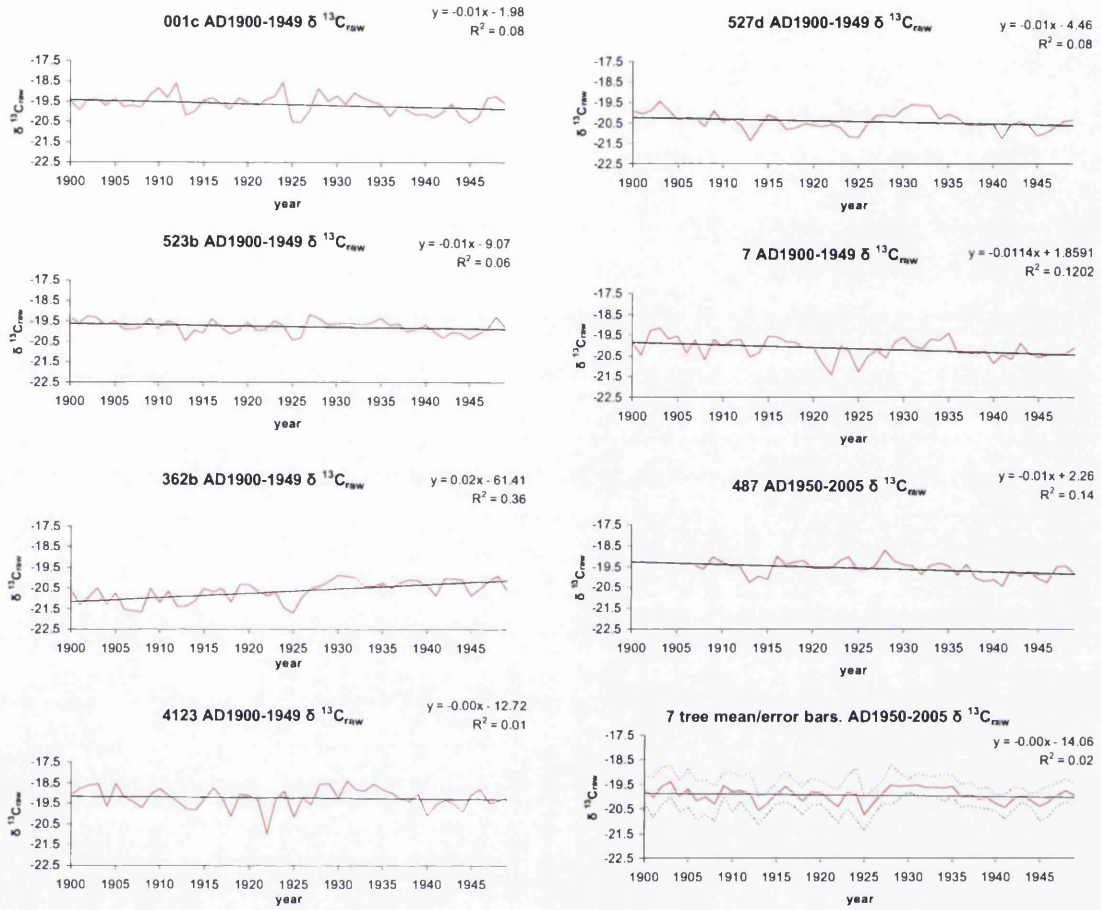

Figure 4.2: All trees and mean $\delta^{13}C_{raw}$.

Below:Table 4.2:Tree details and inter tree correlation

Tree	Most positive year (AD)	Most negative year(AD)	mean $\delta^{13}C_{raw}$
001c	1924	1945	-19.66
523b	1927	1913	-19.78
362b	1930	1925	-20.66
4123	1931	1922	-19.25
527d	1903	1913	-20.44
007	1903	1922	-20.15
487d	1928	1941	-19.62
mean	**1928**	**1925**	**-19.94**

	001c	523b	362b	4123	527d	007
523b	0.59					
362b	0.08	0.26				
4123	0.36	0.46	0.28			
527d	0.37	0.65	0.35	0.48		
007	0.44	0.52	0.17	0.57	0.59	
487d	0.66	0.58	-0.02	0.31	0.35	0.30
		Mean r	**0.40**		**EPS**	**0.82**

Description: $\delta^{13}C_{raw}$ AD 1900-1949

There is a significant rise in one tree (362b) and a significant decline in one tree (487d). No significant trend is found in the other trees or the mean. 1903 is the most positive value in two trees. 1924, 1927, 1930 and 1931 are the most positive values in one tree each. 1928 is the most positive value in tree 487d and the mean.

Interpretation: $\delta^{13}C_{raw}$ AD 1900-1949

In the context of the last 1000 years the average $\delta^{13}C_{raw}$ values for this period are the second most depleted values due to the anthropogenic combustion of fossil fuels (figure 3.3). The decline is not significant in the mean series and suggests that the level of increase in anthropogenic carbon emissions has been greatest in magnitude in the second half of the 20th century. The most positive values reflect the known 'dustbowl' drought of the (1928-1935) the most negative values are known from the instrumental climate data to be cool or wet summers.

4.3: $\delta^{13}C$ data analysis- raw values ($\delta^{13}C_{raw}$) AD1850-1899

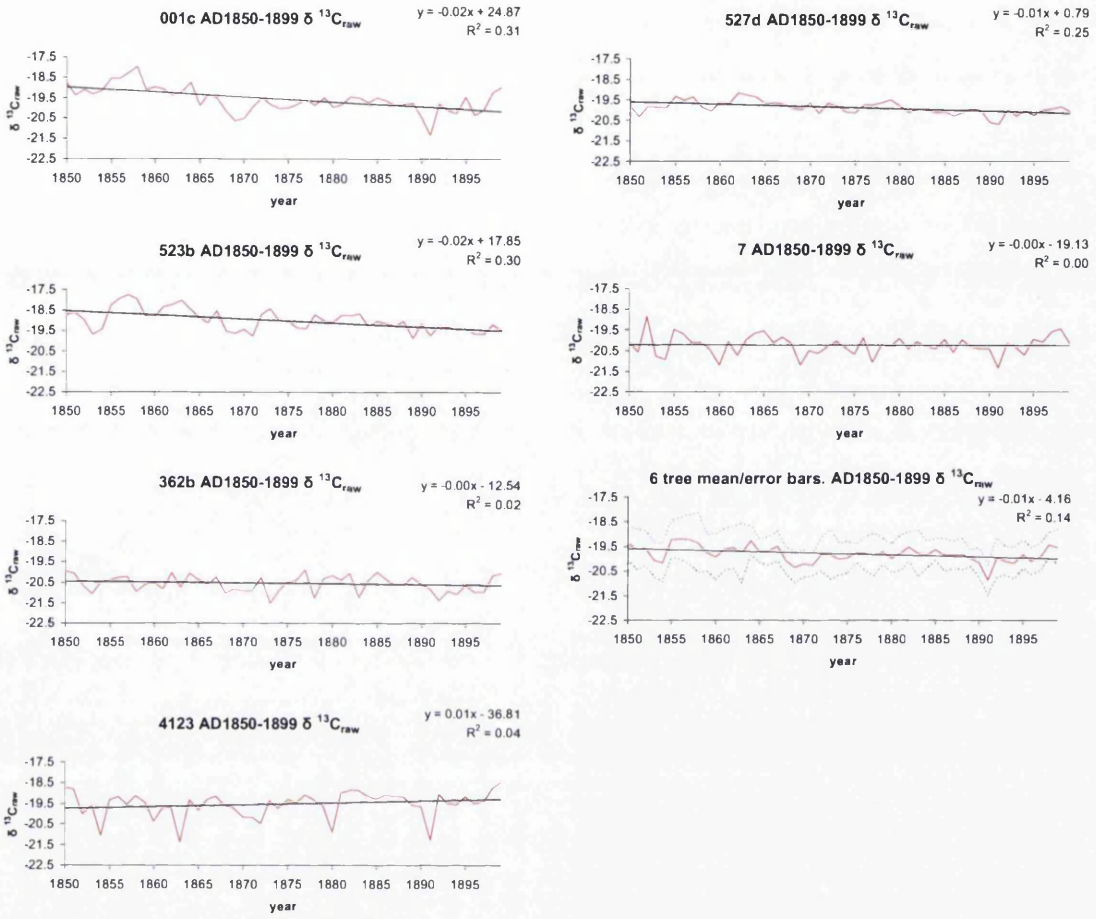

Figure 4.3: All trees and mean $\delta^{13}C_{raw}$.

Below: Table 4.3:Tree details and inter tree correlation

Tree	Most positive year (AD)	Most negative year(AD)	mean $\delta^{13}C_{raw}$
001c	1858	1891	-19.57
523b	1857	1889	-19.00
362b	1877	1873	-20.56
4123	1899	1863	-19.52
527d	1862	1891	-19.89
007	1852	1891	-20.25
mean	**1856**	**1891**	**-19.80**

	001c	523b	362b	4123	527d	007
523b	0.68					
362b	0.37	0.20				
4123	0.26	0.07	0.16			
527d	0.55	0.59	0.21	-0.11		
007	0.37	0.32	0.10	0.26	0.33	0.30
		Mean r	**0.29**		**EPS**	**0.71**

Description: $\delta^{13}C_{raw}$ AD 1850-1899

There is a significant declining trend in three of the six trees, and the mean at both 95 and 99% probability. Three of the most positive values occur in the 1850s (four including mean). 1 in 1899, 1 in 1877 and 1 in 1862. 1891 is the most negative value in three trees (four including mean). 1873, 1863 and 1889 are the lowest values in the other trees.

Interpretation: $\delta^{13}C_{raw}$ AD 1850-1899

The $\delta^{13}C_{raw}$ data during this 50 year period are on average one of the lowest. The extreme positive and negative values appear to represent real climatic events although both significant negative and positive trends are evident in the individual trees and the mean. AD 1891 witnessed extreme winter precipitation that caused extensive damage to many parts of California (Kuhn and Shepherd, 1984).

4.4: $\delta^{13}C$ data analysis-raw values ($\delta^{13}C_{raw}$) AD1850-2005

Figure 4.4A

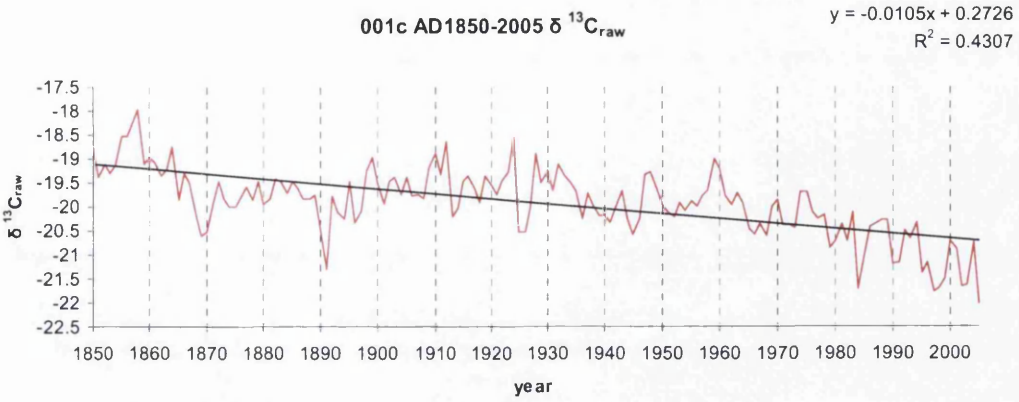

Figure 4.4B

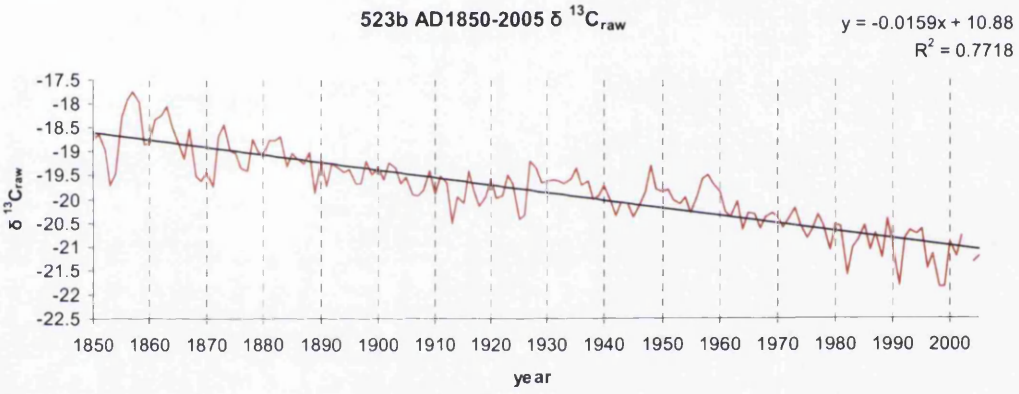

Figure 4.4C

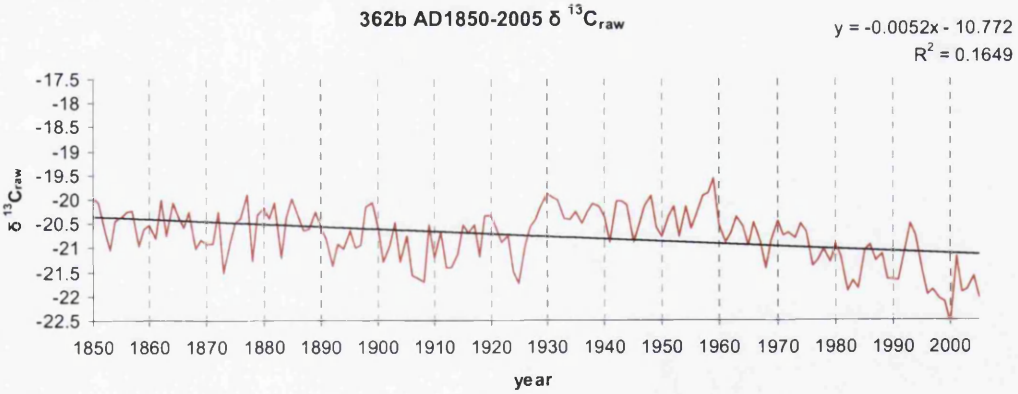

Figure 4.4D

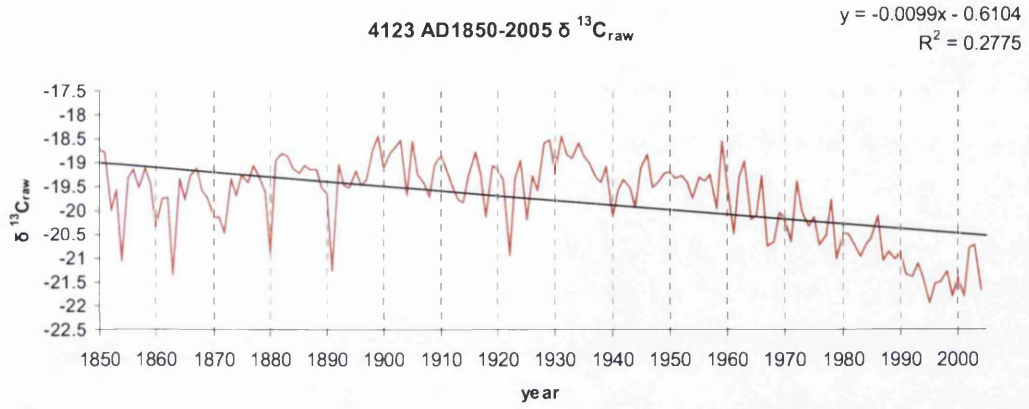

Figure 4.4E

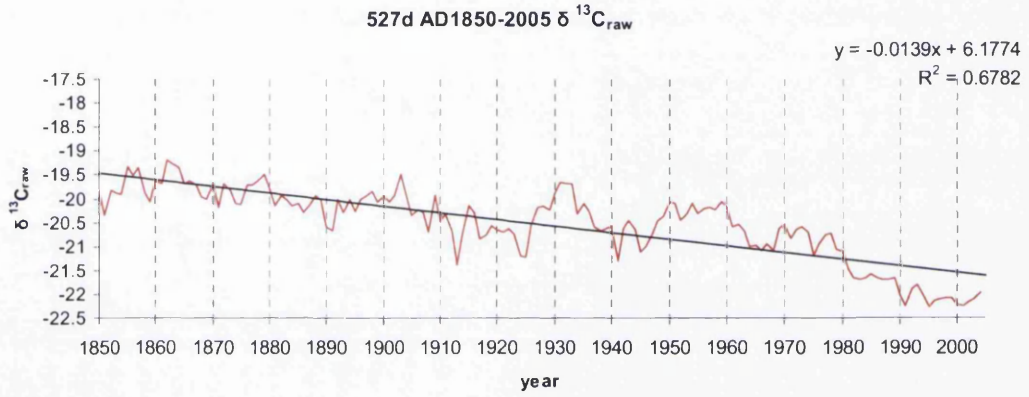

Figure 4.4F

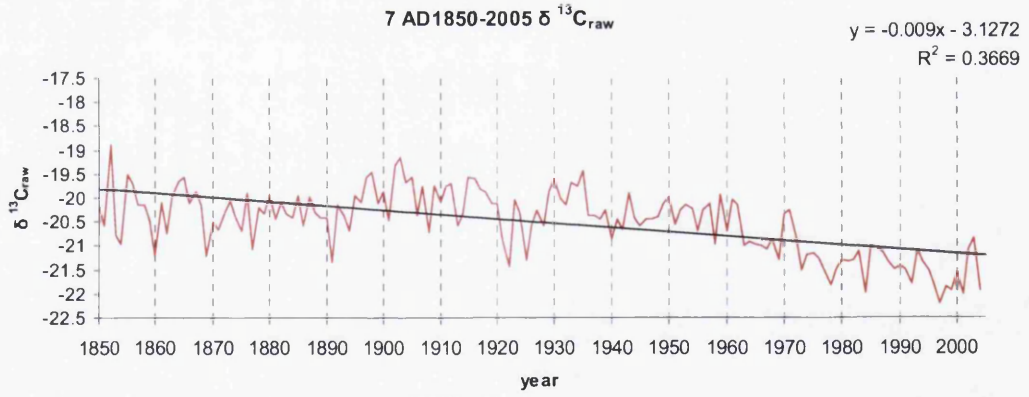

Figure 4.4G

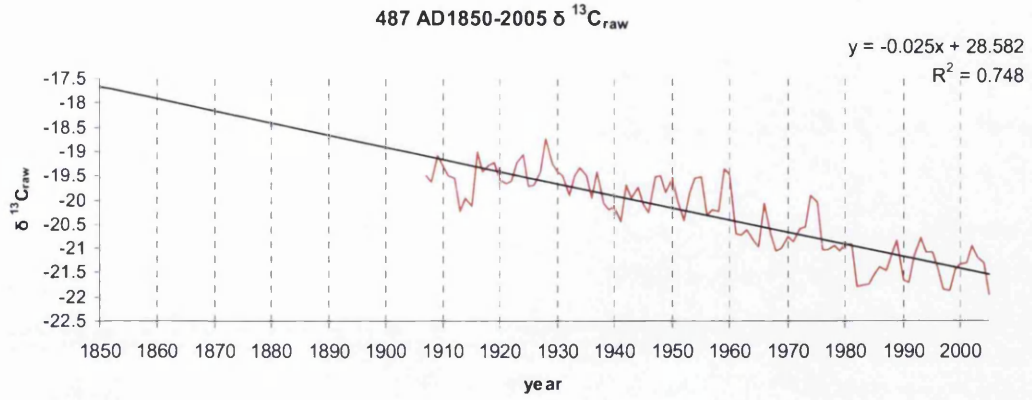

Figure4.4H

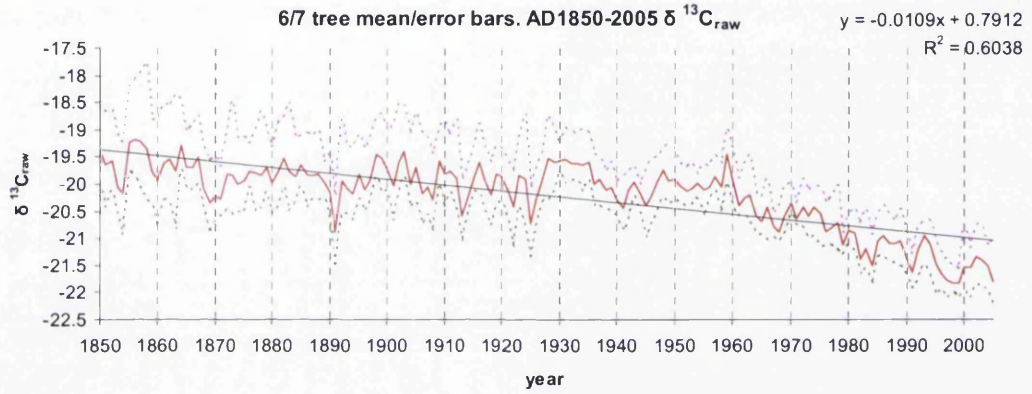

Figure 4.4 (A,B,C,D,E,F,G,H)- Individual trees and mean $\delta^{13}C_{raw}$ 1850-2005.
Below: Table 4.4 Tree details and inter tree correlation 1850-2005.

Tree	Most positive year (AD)	Most negative year(AD)	mean $\delta^{13}C_{raw}$
001c	1858	2005	-19.92
523b	1857	1999	-19.82
362b	1959	2000	-20.76
4123	1899	1995	-19.75
527d	1862	1995	-20.53
007	1852	1997	-20.51
487d	1928	2005	-20.31
mean	**1856**	**1999**	**-20.21**

	001c	523b	362b	4123	527d	007
523b	0.75					
362b	0.59	0.56				
4123	0.64	0.60	0.57			
527d	0.74	0.87	0.64	0.68		
007	0.67	0.67	0.51	0.73	0.72	
487d	0.81	0.86	0.62	0.81	0.78	0.77
	Mean r	0.69		**EPS**	0.94	

Description: $\delta^{13}C_{raw}$ AD 1850-2005

The decline $\delta^{13}C_{raw}$ in all trees and the mean of all trees since 1850 is significant. The 1850's are again well represented in the most positive values in three trees and the mean. 1862, 1899, 1928 and 1959 are the most positive values in the other trees. The most negative values are all in the period from 1995-2005, with 1999 being the most negative value for the mean.

Interpretation: $\delta^{13}C_{raw}$ AD 1850-2005

The anthropogenic effects from fossil fuel combustion on the $\delta^{13}C_{raw}$ are clearly evident in the strong decline in values during the period from 1850-2005, particularly in the period from 1950- 2005 (chapter 5.2). This trend obscures any climatic signal that may be present in the data.

4.5: $\delta^{13}C$ data analysis- Fossil fuel corrected values ($\delta^{13}C_{cor}$) AD1950-2005

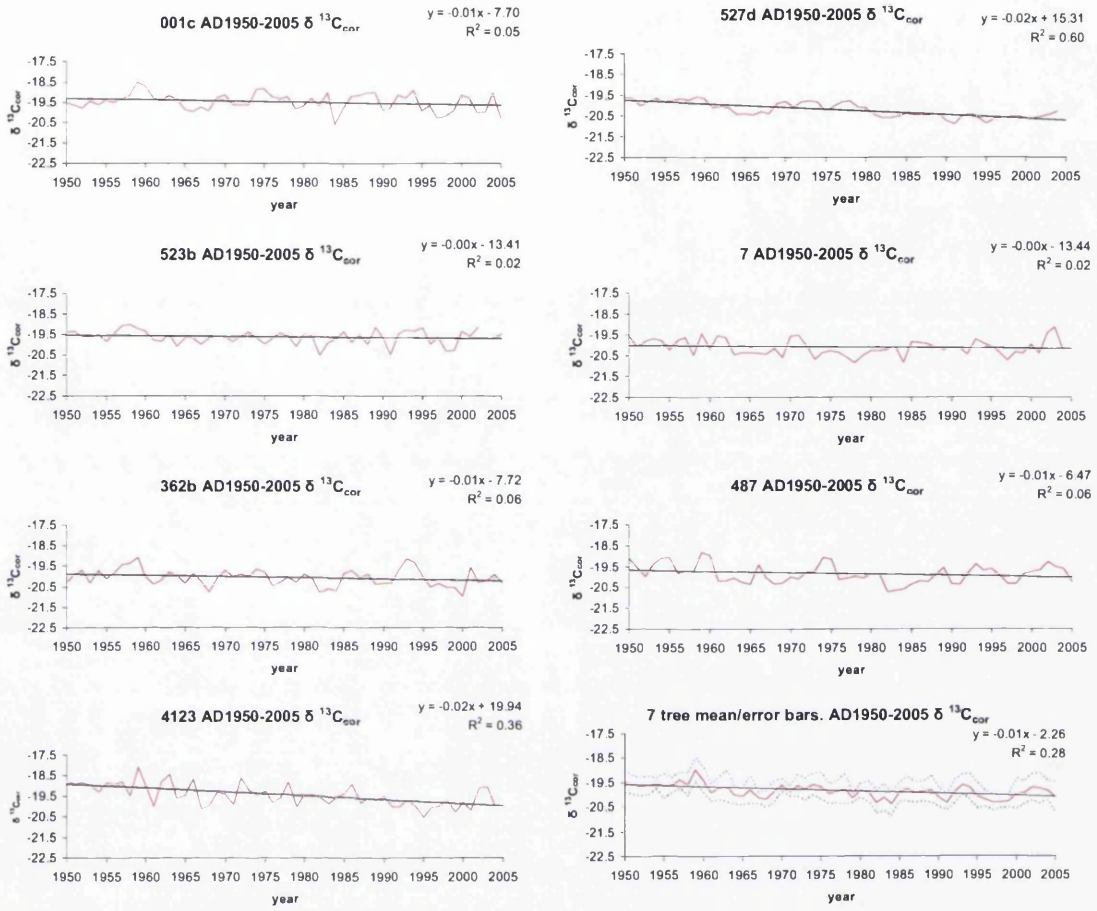

Figure 4.5: All trees and mean $\delta^{13}C_{cor}$.

Below: Table 4.5:Tree details and inter tree correlation

Tree	Most positive year (AD)	Most negative year(AD)	mean $\delta^{13}C_{cor}$
001c	1959	1984	-19.48
523b	1958	1982	-19.62
362b	1959	1982	-20.06
4123	1959	1995	-19.45
527d	1950	1991	-20.21
007	1959	1978	-20.10
487d	1959	1982	-19.86
mean	**1959**	**1984**	**-19.83**

	001c	523b	362b	4123	527d	007
523b	0.25					
362b	0.47	0.46				
4123	0.19	0.30	0.35			
527d	0.34	0.38	0.37	0.63		
007	0.13	0.22	0.22	0.28	0.14	
487d	0.41	0.47	0.49	0.40	0.45	0.30
		Mean r	**0.34**		**EPS**	**0.79**

Description: $\delta^{13}C_{cor}$ AD 1950-2005

The fossil fuel correction (chapter3.2: $\delta^{13}C_{cor}$) corrects the large decline in evident in $\delta^{13}C_{raw}$ values for five of the seven trees. There is still a significant decline in two of the seven trees and in the mean data. 1959 remains the most positive year in five of the seven trees and the mean, and also becomes the most positive year in tree 527d. The most negative year changes in all the trees. 1982 is the most negative year in three trees.1984 is the most negative value in one tree and the mean. 1978, 1991 and 1995 are the most negative values in one tree each.

Interpretation: $\delta^{13}C_{cor}$ AD 1950-2005

The fossil fuel correction removes some, but not all of the strong decline from the raw data in the period from 1950-2005. The decline is still strong but the data is more meaningful in climatic terms. The most negative values in four of seven trees and the mean are 1982 and 1984, years that represented extreme El Niño related moisture in the western United States. The most positive years for this period remain the same as with the raw values. The nearest instrumental weather data indicates that 1959 may not have been the hottest or driest year in the last 55 years and that the significant decline may be evidence that the fossil fuel correction is not entirely removing a non climatic trend during the period 1950-2005.

4.6: $\delta^{13}C$ data analysis- Fossil fuel corrected values ($\delta^{13}C_{cor}$) AD1900-1949

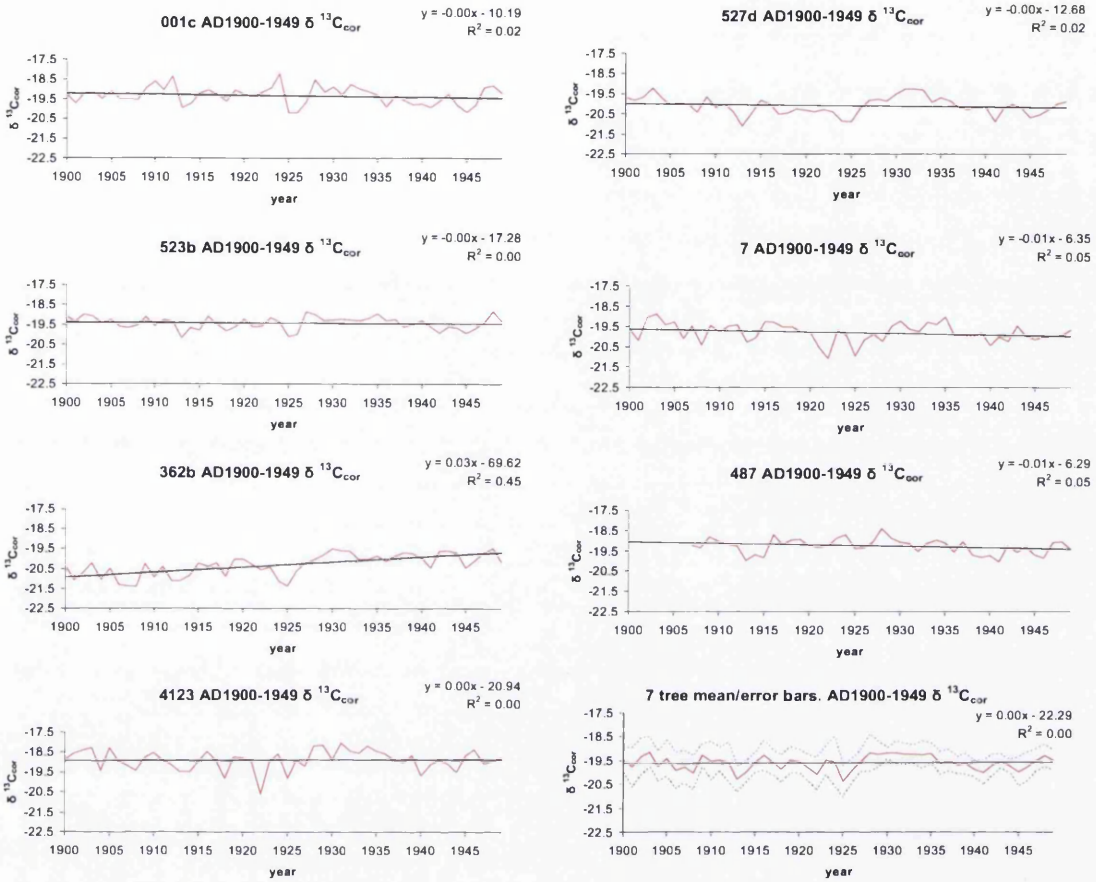

Figure4.6: All trees and mean $\delta^{13}C_{cor}$.

Below: Table 4.6:Tree details and inter tree correlation

Tree	Most positive year (AD)	Most negative year(AD)	mean $\delta^{13}C_{cor}$
001c	1924	1925	-19.32
523b	1948	1913	-19.44
362b	1948	1908	-20.32
4123	1931	1922	-18.91
527d	1903	1913	-20.10
007	1903	1922	-19.80
487d	1928	1941	-19.26
mean	**1903**	**1925**	**-19.60**

	001c	523b	362b	4123	527d	007
523b	0.56					
362b	0.14	0.35				
4123	0.34	0.45	0.33			
527d	0.34	0.62	0.40	0.47		
007	0.40	0.47	0.21	0.55	0.55	
487d	0.64	0.55	0.04	0.31	0.34	0.25
		Mean r	**0.40**		**EPS**	**0.82**

Description: $\delta^{13}C_{cor}$ AD 1900-1949

The fossil fuel correction increases the rise in $\delta^{13}C_{cor}$ tree 362b. The decline in tree 487d is reduced and is no longer significant. The extreme positive values are altered. 1948 replaces 1927 and 1930 in trees 523b and 362b respectively. 1903 becomes the most positive value in the mean series. The most negative values are less changed, although in 001c 1925 replaces 1945 as the most negative year, and in 362b 1908 replaces 1925 as the most negative value.

Interpretation: $\delta^{13}C_{cor}$ AD 1900-1949

The fossil fuel correction appears to have little effect on the most positive and most negative $\delta^{13}C_{cor}$ values during this time period.

4.7: $\delta^{13}C$ data analysis- fossil fuel corrected values ($\delta^{13}C_{cor}$). AD1850-1899

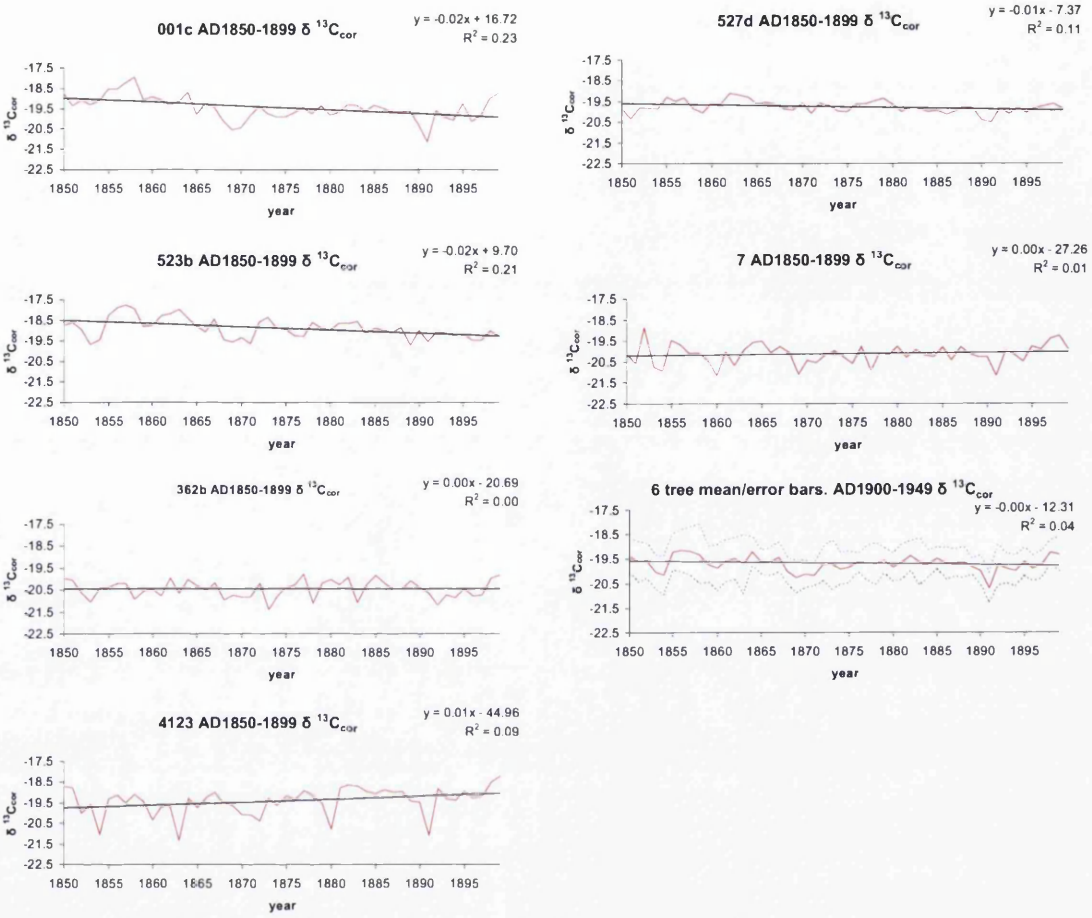

Figure 4.7: All trees and mean $\delta^{13}C_{cor}$.

Below: Table 4.7:Tree details and inter-correlation

Tree	Most positive year (AD)	Most negative year(AD)	mean $\delta^{13}C_{cor}$
001c	1858	1891	-19.44
523b	1857	1889	-18.88
362b	1877	1873	-20.44
4123	1899	1863	-19.40
527d	1862	1891	-19.77
007	1852	1891	-20.13
mean	**1856**	**1891**	**-19.67**

	001c	523b	362b	4123	527d
523b	0.64				
362b	0.30	0.12			
4123	0.25	0.06	0.19		
527d	0.47	0.51	0.14	-0.11	
007	0.32	0.27	0.09	0.29	0.31
	MeanR	**0.26**		**EPS**	**0.67**

Description: $\delta^{13}C_{cor}$ AD 1850-1899

The fossil fuel corrected data for 1850-1899 removes some of the decline apparent in the $\delta^{13}C_{raw}$ data. The decline is now only significant in two trees. None of the most positive or negative values differ from the raw data.

4.8: $\delta^{13}C$ data analysis- fossil fuel corrected values ($\delta^{13}C_{cor}$) AD1850-2005

Figure 4.8 illustrates the $\delta^{13}C_{cor}$ values for the period 1850 to 2005. The change that the fossil fuel correction makes to the $\delta^{13}C$ values of each tree is clearly visible, as is the effect on the most positive and negative $\delta^{13}C$ values of each tree and the mean. The effect on inter tree correlation (EPS) is evident in table 4.8.

Figure 4.8A

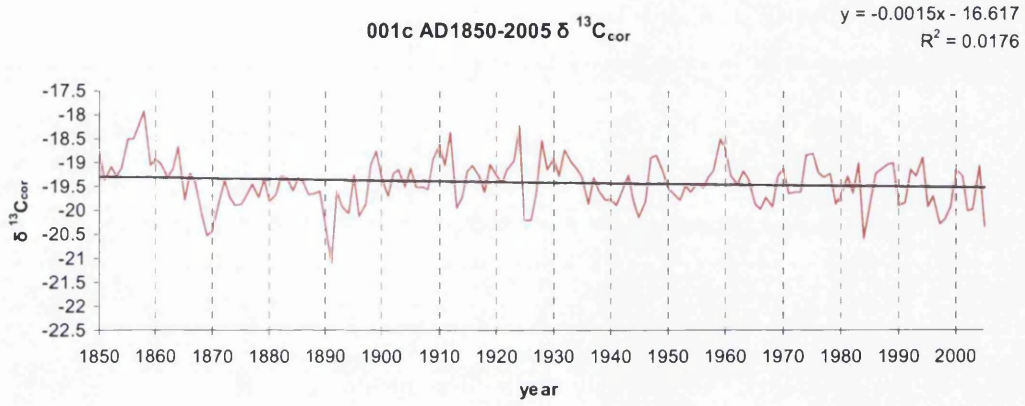

Figure 4.8B

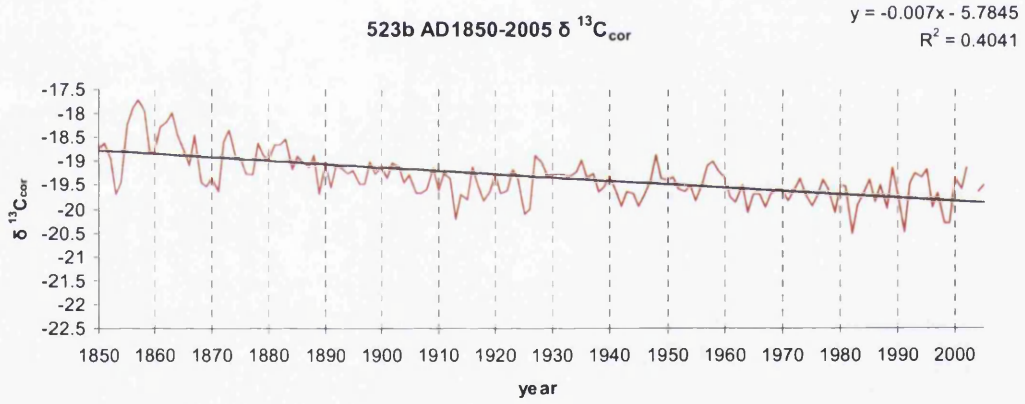

Figure 4.8C

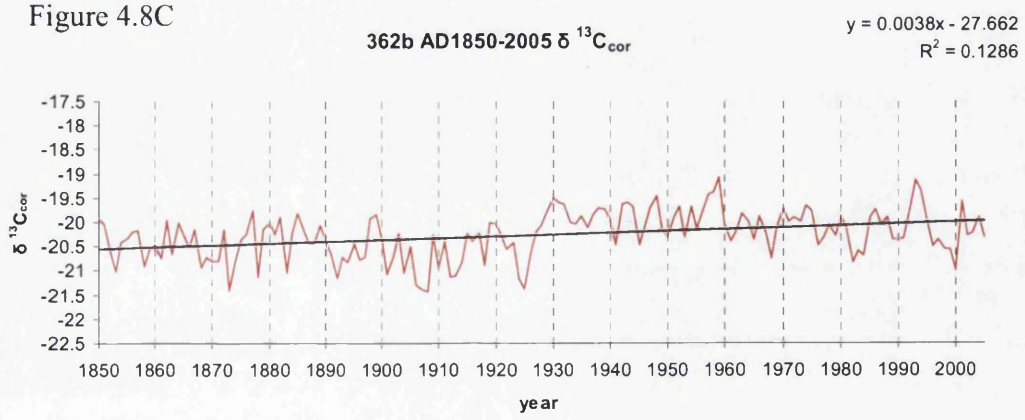

Figure 4.8D

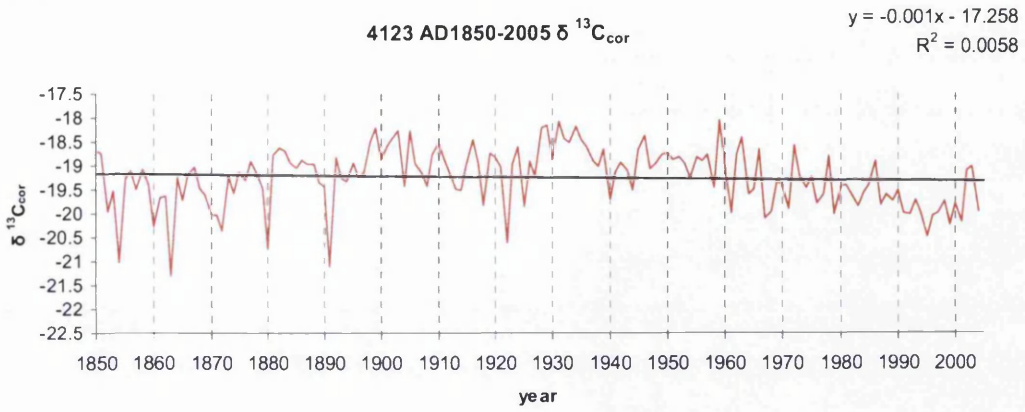

Figure 4.8E

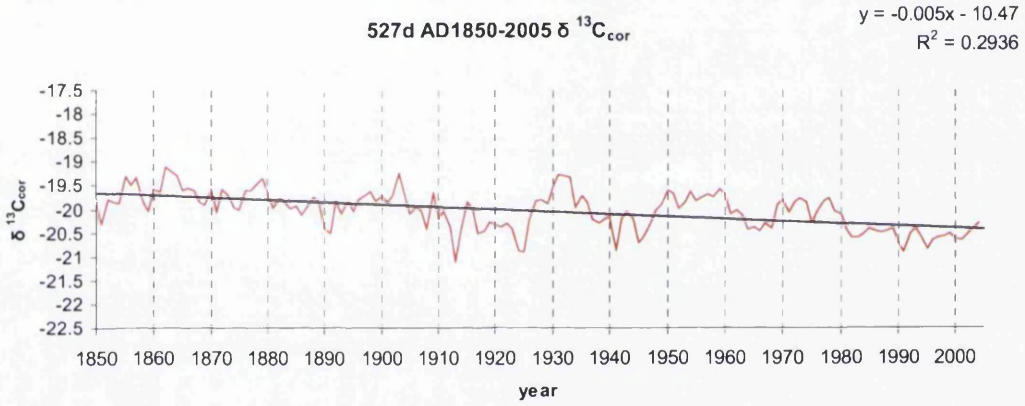

Figure 4.8F

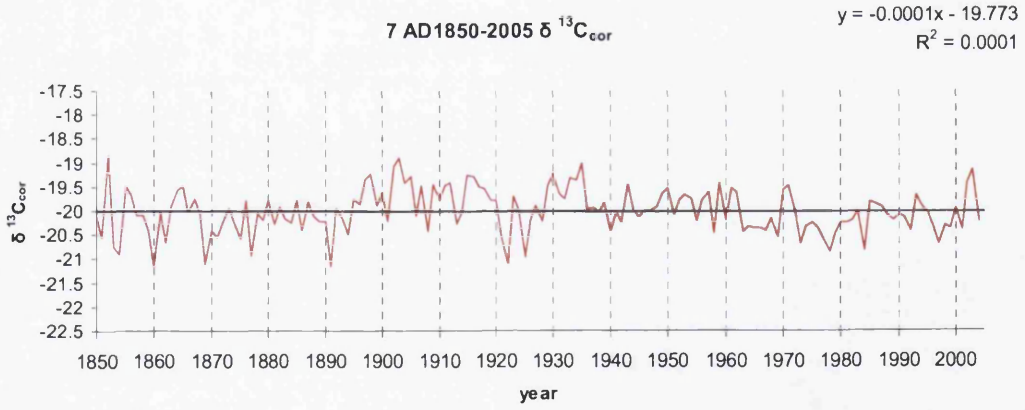

Figure 4.8G

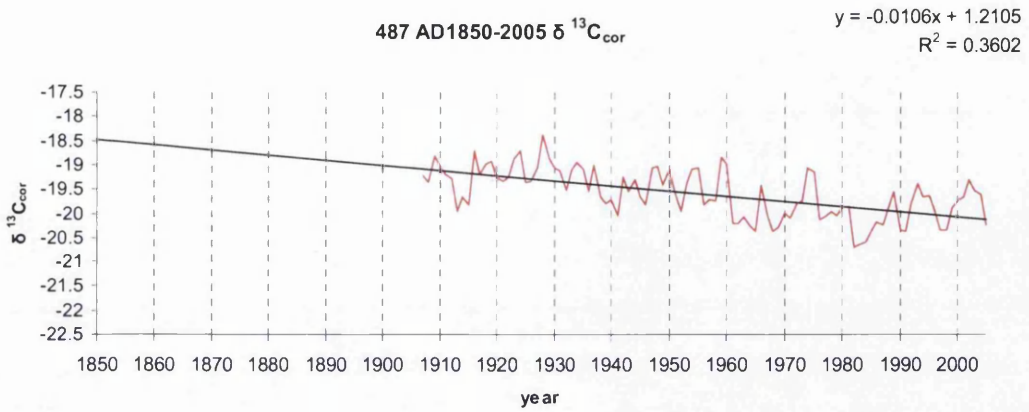

Figure 4.8H

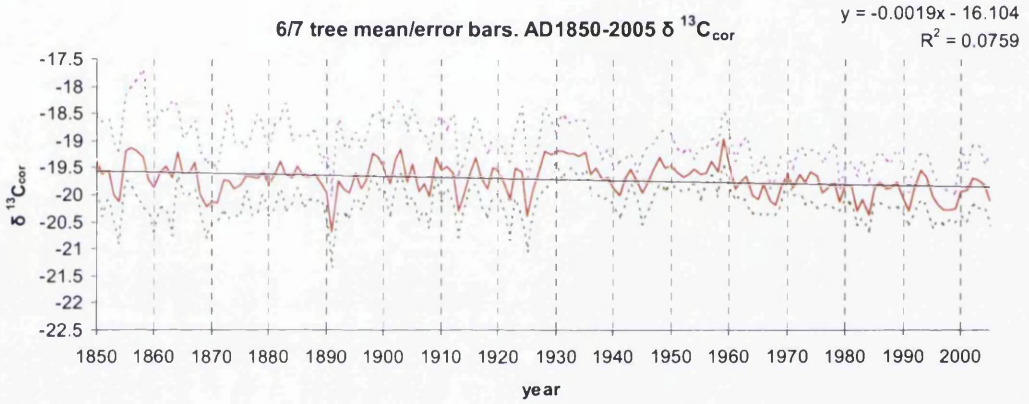

Figure 4.8 (A,B,C,D,E,F,G,H)- Individual trees and mean $\delta^{13}C_{cor}$ 1850-2005.
Below: Table 4.8 Tree details and inter-tree correlation 1850-2005.

Tree	Most positive year (AD)	Most negative year(AD)	mean $\delta^{13}C_{cor}$
001c	1858	1891	-19.42
523b	1857	1982	-19.32
362b	1959	1908	-20.26
4123	1959	1863	-19.26
527d	1862	1913	-20.03
007	1852	1891	-20.01
487d	1928	1982	-19.61
mean	**1959**	**1891**	**-19.71**

	001c	523b	362b	4123	527d	007
523b	0.39					
362b	0.24	0.02				
4123	0.28	0.12	0.20			
527d	0.31	0.62	0.14	0.24		
007	0.32	0.17	0.14	0.44	0.24	
487d	0.51	0.53	0.11	0.52	0.36	0.38
	Mean r	0.30		**EPS**	0.75	

Description: $\delta^{13}C_{cor}$ AD 1850-2005

Over the period 1850-2005 the fossil fuel correction reduces the significant decline evident in the $\delta^{13}C_{raw}$ data in four of the seven trees and the mean. A strong decline is still evident in three of the seven trees. The most positive values remain the same in six of the seven trees but in tree 4123 the most positive value changes from 1899 to 1959. The most negative values are changed in all trees. 1863 is the most negative value for one tree, 1891 for two trees and the mean. 1908 for one tree, 1913 for one tree and 1982 for two trees.

Interpretation: $\delta^{13}C_{cor}$ AD 1850-2005

The significant decline in $\delta^{13}C_{cor}$ is evident in four of the seven trees over this time period is less evident in the mean series. The significant decline in $\delta^{13}C_{cor}$ that is evident from 1950-2005 suggests that the fossil fuel correction is not removing all non-climatic trends, particularly in the last 50 years (1950-2005).

4.9: $\delta^{13}C$ data analysis- PIN corrected values ($\delta^{13}C_{pin}$) AD1950-2005

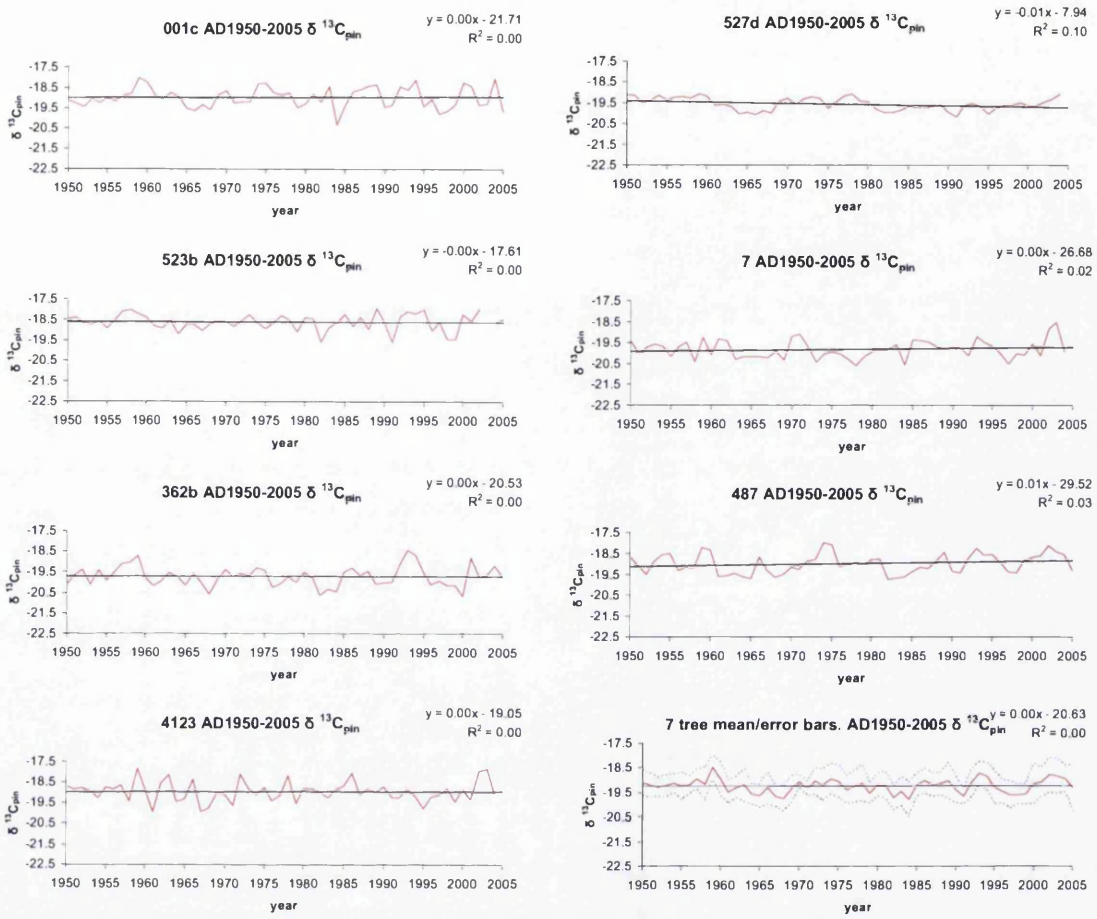

Figure 4.9- Individual trees and mean $\delta^{13}C_{pin}$ 1950-2005.

Below:Table 4.9Tree details and inter tree correlation $\delta^{13}C_{pin}$ 1950-2005.

Tree	Most positive year (AD)	Most negative year(AD)	mean $\delta^{13}C_{pin}$
001c	1959	1984	-19.01
523b	1989	1982	-18.65
362b	1993	1982	-19.73
4123	1959	1967	-19.00
527d	1959	1991	-19.57
007	2003	1978	-19.87
487d	1974	1982	-19.04
mean	**1959**	**1982**	**-19.27**

	001c	523b	362b	4123	527d	007
523b	0.26					
362b	0.44	0.43				
4123	0.09	0.25	0.24			
527d	0.27	0.38	0.31	0.32		
007	0.16	0.17	0.21	0.27	0.05	
487d	0.48	0.41	0.48	0.31	0.41	0.21
		Mean r	**0.29**		**EPS**	0.74

Description of $\delta^{13}C_{pin}$ data AD 1950-2005

Any significant declining trend present in the fossil fuel corrected 1950-2005 data ($\delta^{13}C_{cor}$) is removed by the PIN correction, aside from tree 527d where there is a slight declining trend. The most positive values are changed for trees 523 (from 1958 to 1989), from 1959 to 1993 (tree 362b), and in tree487d from 1959 to 1974. The mean most positive value remains at 1959. The most negative value for tree 4123 is changed from 1995 to 1967. 1982 becomes the most negative mean value as opposed to 1984 for the fossil fuel corrected data.

4.10: $\delta^{13}C$ data analysis- PIN corrected values ($\delta^{13}C_{pin}$) AD1900-1949

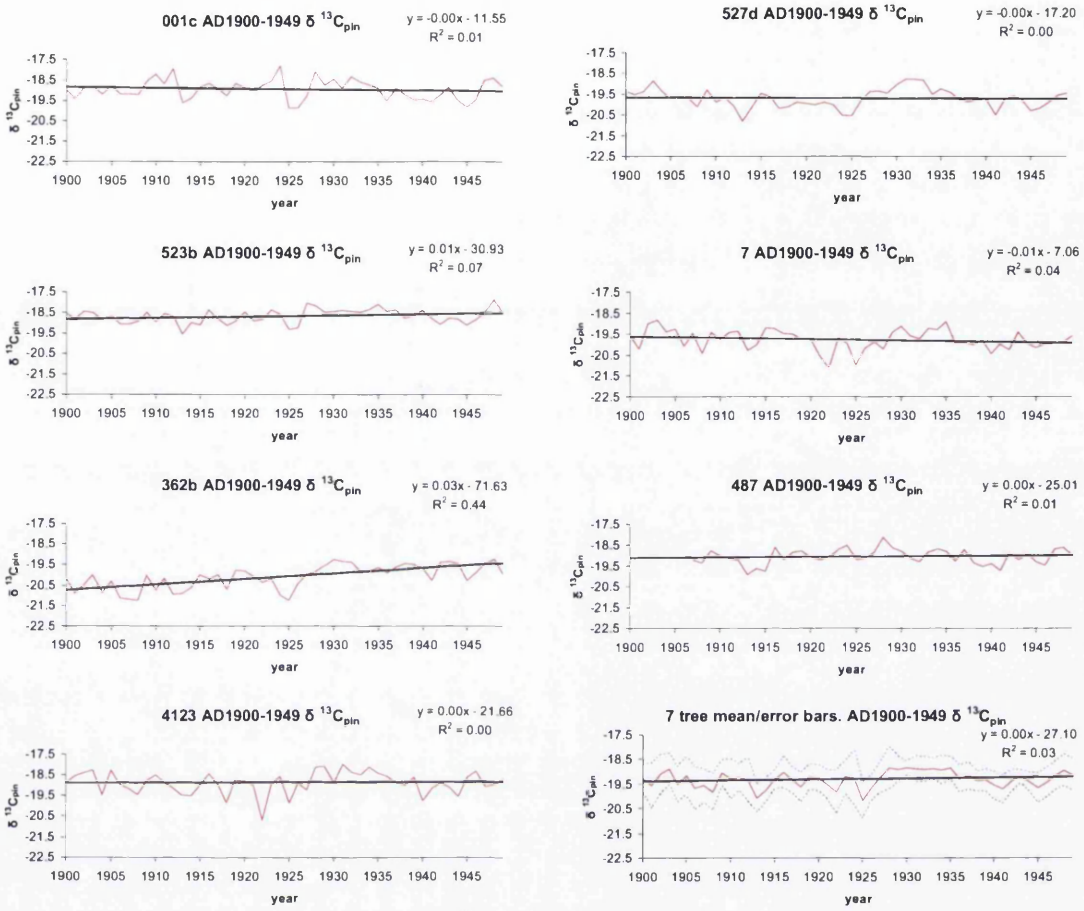

Figure 4.10: Individual trees and mean $\delta^{13}C_{pin}$ 1900-1949.

Tree	Most positive year (AD)	Most negative year(AD)	mean $\delta^{13}C_{pin}$
001c	1924	1926	-18.94
523b	1948	1913	-18.67
362b	1948	1908	-20.09
4123	1931	1922	-18.90
527d	1931	1913	-19.70
007	1903	1922	-19.77
487d	1928	1913	-19.05
mean	**1931**	**1925**	**-19.31**

	001c	523b	362b	4123	527d	007
523b	0.51					
362b	0.17	0.55				
4123	0.34	0.44	0.34			
527d	0.33	0.58	0.47	0.47		
007	0.39	0.39	0.24	0.56	0.54	
487d	0.59	0.60	0.26	0.36	0.39	0.22
	MeanR	0.42		**EPS**	0.83	

Table 4.10: Tree details and inter tree correlation $\delta^{13}C_{pin}$ 1900-1949.

Description of $\delta^{13}C_{pin}$ data AD1900-1949

The increasing trend in $\delta^{13}C_{pin}$ for 362b is made more significant by the PIN correction. All the other trees and the mean contain no significant trend. The most positive value for tree 527d is changed from 1903 (fossil fuel corrected) to 1931. All the other trees most positive values remain the same, although the most positive mean value is changed to 1931 by the PIN correction. The most negative value for tree 487d is changed to 1913 by the PIN correction. All other most negative values remain the same, including the mean.

4.11: $\delta^{13}C$ data analysis- PIN corrected values ($\delta^{13}C_{pin}$) AD1850-1899

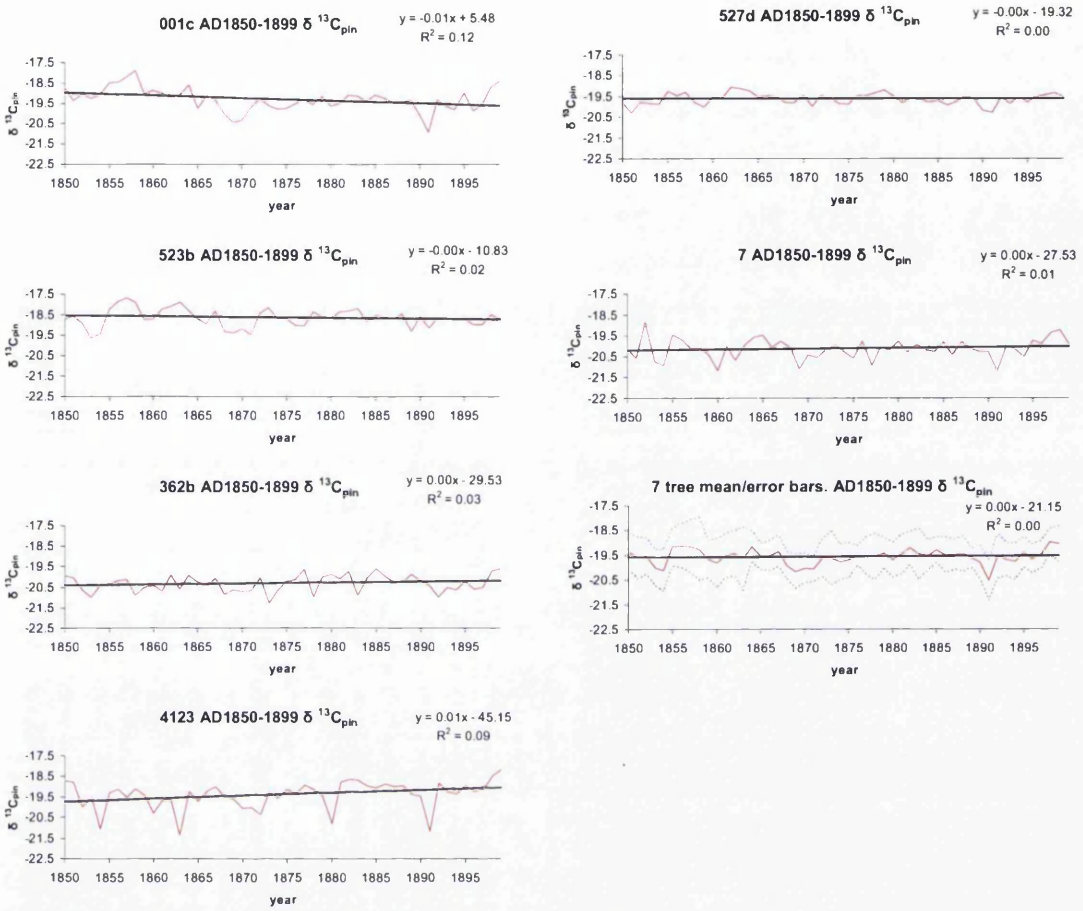

Figure 4.11: Individual trees and mean $\delta^{13}C_{pin}$ 1850-1899.

Below: Table 4.11.Tree details and inter tree correlation $\delta^{13}C_{pin}$ 1850-1899.

Tree	Most positive year (AD)	Most negative year(AD)	mean $\delta^{13}C_{pin}$
001c	1858	1891	-19.30
523b	1857	1853	-18.64
362b	1899	1873	-20.31
4123	1899	1863	-19.40
527d	1862	1851	-19.62
007	1852	1891	-20.13
mean	**1898**	**1891**	**-19.56**

	001c	523b	362b	4123	527d
001c					
523b	0.56				
362b	0.26	0.11			
4123	0.32	0.19	0.24		
527d	0.36	0.41	0.15	0.00	
007	0.36	0.35	0.11	0.29	0.38
	Mean r	0.27		**EPS**	0.69

Description of data

The PIN correction removes any declining trend in the $\delta^{13}C_{pin}$ for all the trees. The most positive $\delta^{13}C_{pin}$ value for 362b is changed from 1877 to 1899. The other most positive $\delta^{13}C_{pin}$ values remain the same, apart from the mean where 1898 becomes the most positive value instead of 1856 for the fossil fuel corrected and raw data. The most negative values are changed from 1889 to 1853 in tree 523b, and from 1891 to 1851 in tree 527d. The other most negative $\delta^{13}C_{pin}$ values remain unchanged.

4.12: $\delta^{13}C$ data analysis- PIN values ($\delta^{13}C_{pin}$) AD1850-2005

Figure 4.12A

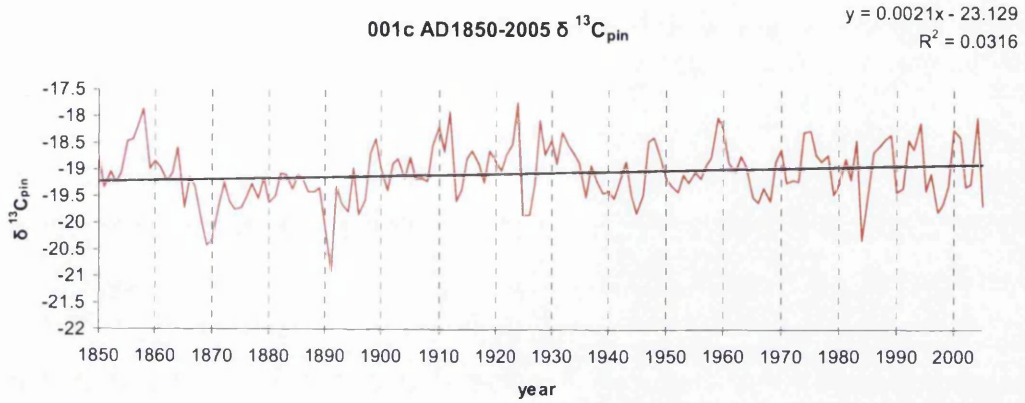

Figure 4.12B

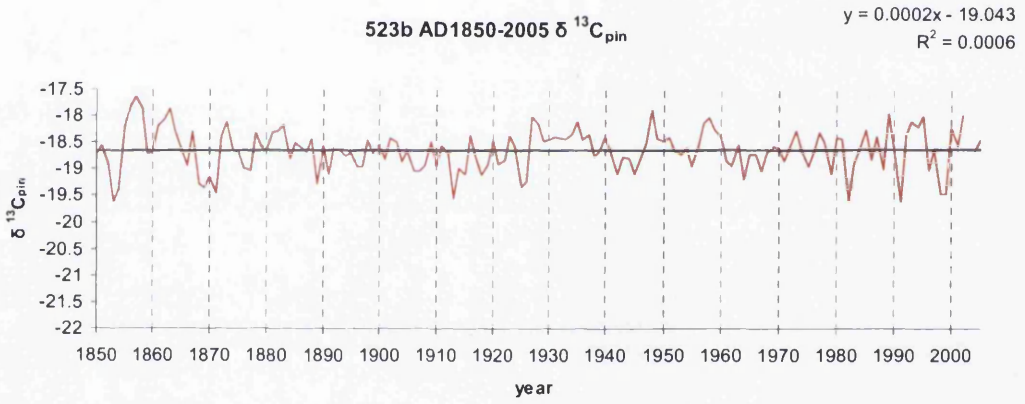

Figure 4.12C

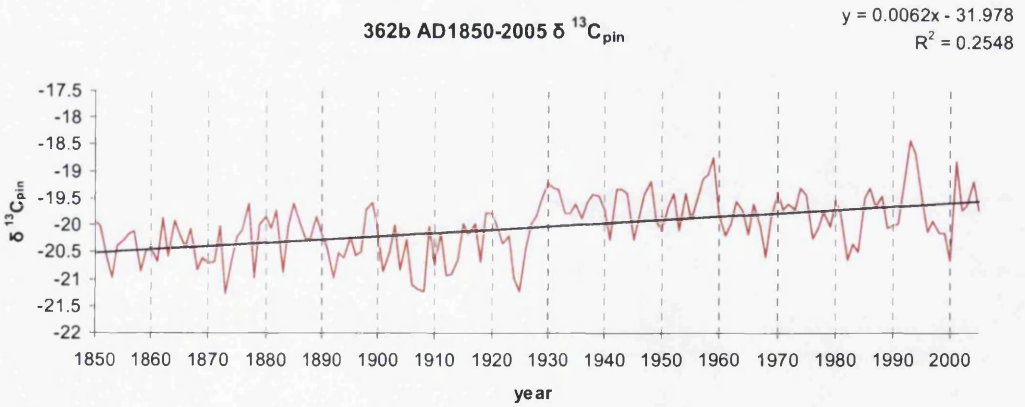

Figure 4.12D

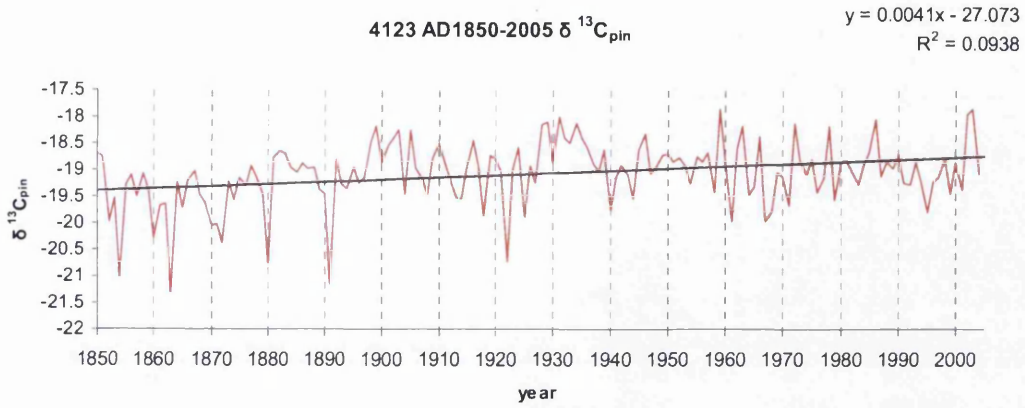

Figure 4.12E

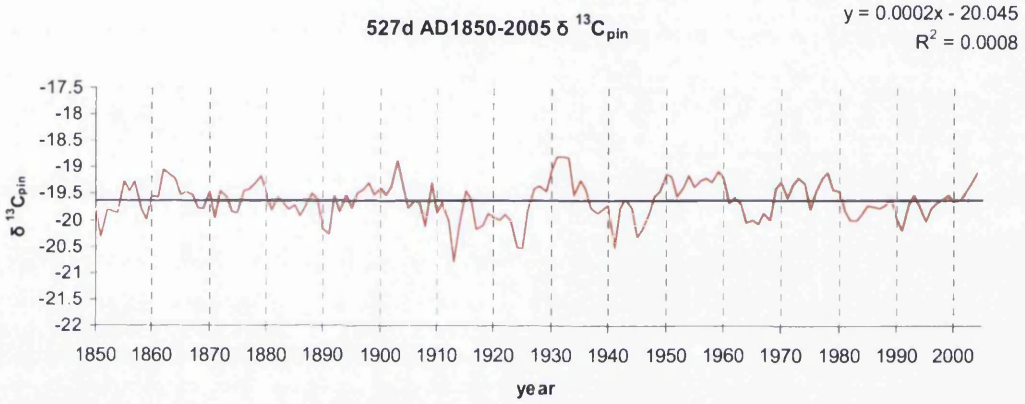

Figure 4.12F

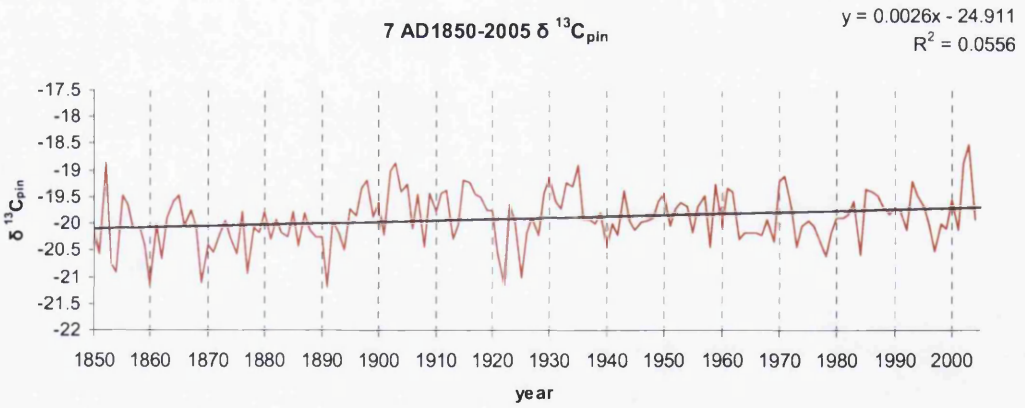

Figure 4.12G

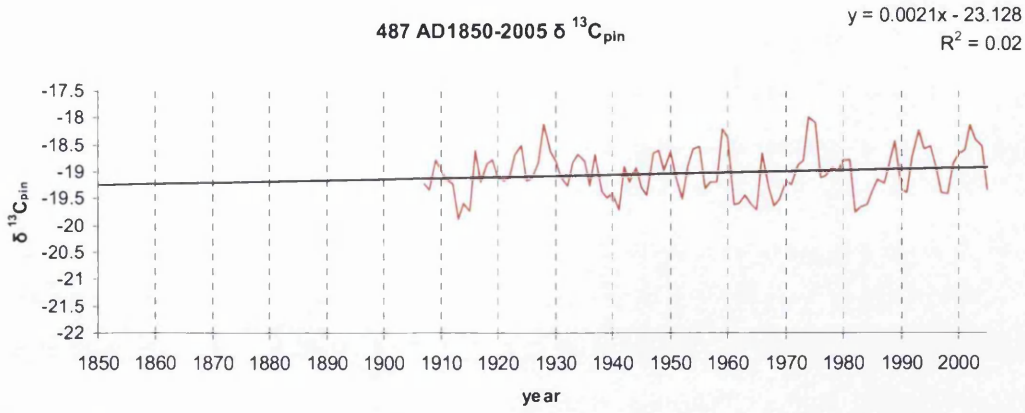

Figure 4.12H

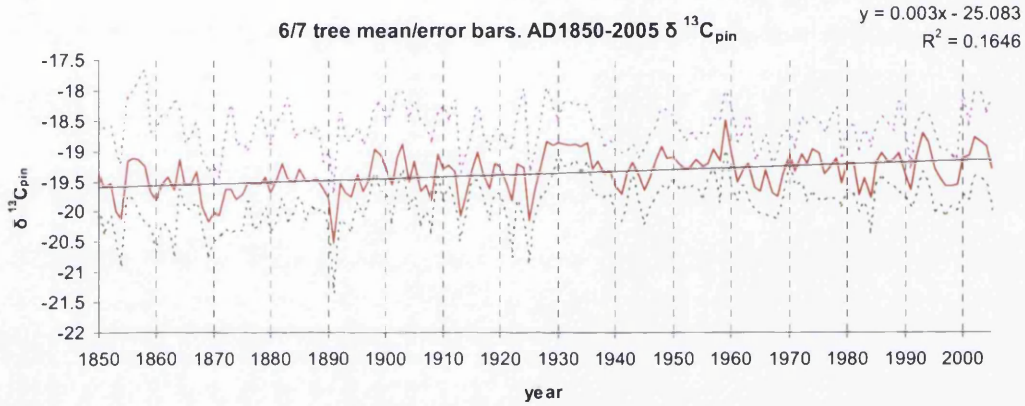

Figure 4.12 (A,B,C,D,E,F,G,H)- Individual trees and mean $\delta^{13}C_{pin}$ 1850-2005.

Table 4.12 Tree details and inter-tree correlation $\delta^{13}C_{pin}$ 1850-2005

Tree	Most positive year (AD)	Most negative year(AD)	mean $\delta^{13}C_{pin}$
001c	1924	1891	-19.07
523b	1857	1853	-18.65
362b	1993	1873	-20.03
4123	1959	1863	-19.08
527d	1931	1913	-19.62
007	2003	1891	-19.90
487d	2002	1913	-19.02
mean	**1959**	**1891**	**-19.37**

	001c	523b	362b	4123	527d	007
523b	0.42					
362b	0.34	0.34				
4123	0.34	0.25	0.34			
527d	0.28	0.45	0.36	0.23		
007	0.37	0.28	0.26	0.44	0.31	
487d	0.51	0.48	0.38	0.31	0.37	0.21
	Mean r	0.35		**EPS**	0.79	

Description of $\delta^{13}C_{pin}$ AD 1850-2005

Applying the PIN correction results in a significant rise in the $\delta^{13}C_{pin}$ mean values over the period 1850-2005. Tree 362 also contains a significant rising trend, as does tree 4123. 1959 remains the most positive value for the mean and for tree 4123. Tree 001's most positive value changes from 1858 to 1924. Tree 362 most positive value changes from 1959 to 1993. The most positive value for tree 527d changes from 1862 (fossil fuel corrected) to 1931. 2003 replaces 1852 as the most positive value in tree 007 and 2002 replaces 1928 as the most positive value in tree 487. 1891 remains the mean most negative value. 1913 replaces 1982 as the most negative value for tree 487. 1853 replaces 1982 as the most negative value in tree 523.

In order to test the effectiveness of both the fossil fuel ($\delta^{13}C_{cor}$) and PIN ($\delta^{13}C_{pin}$) correction both sets of data are compared to instrumental climate data in chapter 5.

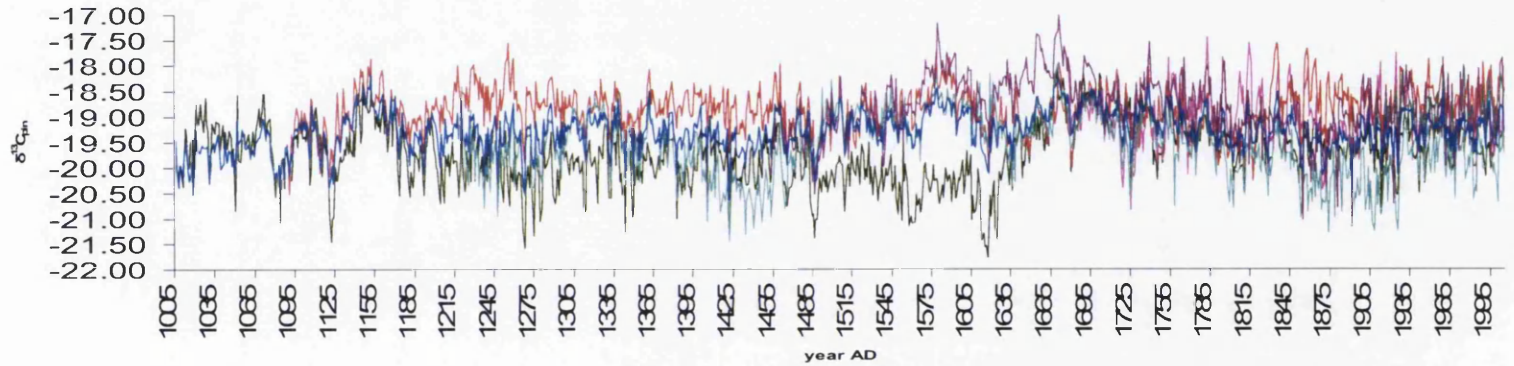

Figure 4.13 All 7 trees $\delta^{13}C_{pin}$ together on same axis.

Figure 4.14 All 7 trees $\delta^{13}C_{pin}$ separate The axis on the left (0 to +1) refers to positive and negative values.

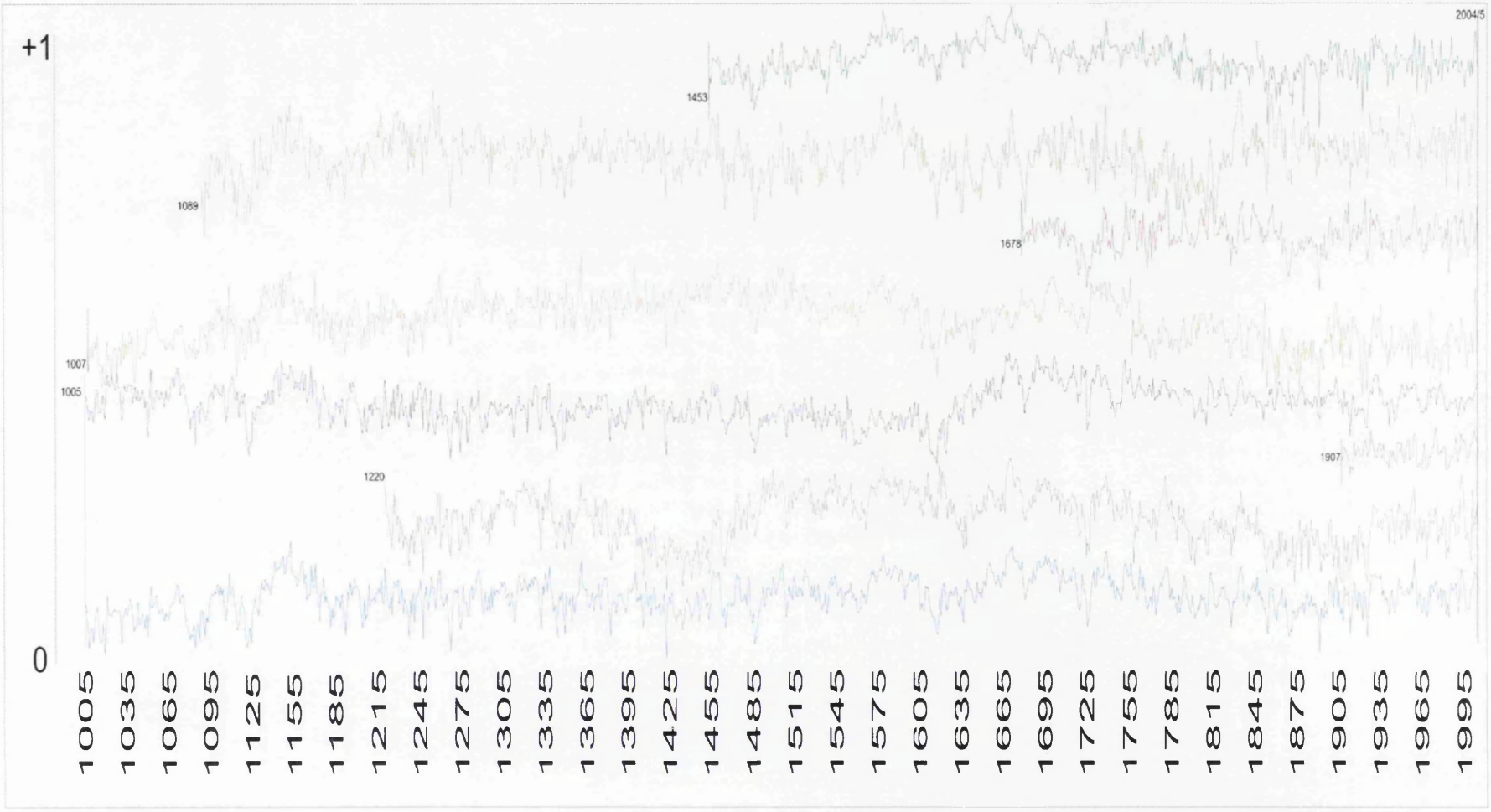

5.1: Climate correlations.

The nearest weather stations to the sampling site are the White Mountain Research Stations (chapter 2.10). Unfortunately, the records from these stations are quite short so it has also been necessary to compare the isotope data with weather stations from further away that have longer, more complete records. This will also determine whether significant correlations from the short instrumental records are spurious, or are reflecting the influence of regional climate.

In addition it is necessary to examine if the trends present in the $\delta^{13}C_{pin}$ data are related to climate variables. Any significant trend left in the $\delta^{13}C_{pin}$ data should be related to climate. In order to assess the significance of the PIN correction both the $\delta^{13}C_{pin}$ and $\delta^{13}C_{cor}$ will be compared to climate data. In addition the individual trees comprising the isotope chronology will be compared to the meteorological data to assess the degree and nature of climate sensitivity for each of the trees that comprise the mean.

As a logical place to start, the isotope data was first compared to the meteorological data from the two White Mountain Research Stations. The nearest station is White Mountain 1 (WM1). Full annual meteorological data was compiled for the period 1955-1977. The highest correlations from this station is between average maximum temperature (June/July/August) and mean $\delta^{13}C_{pin}$.

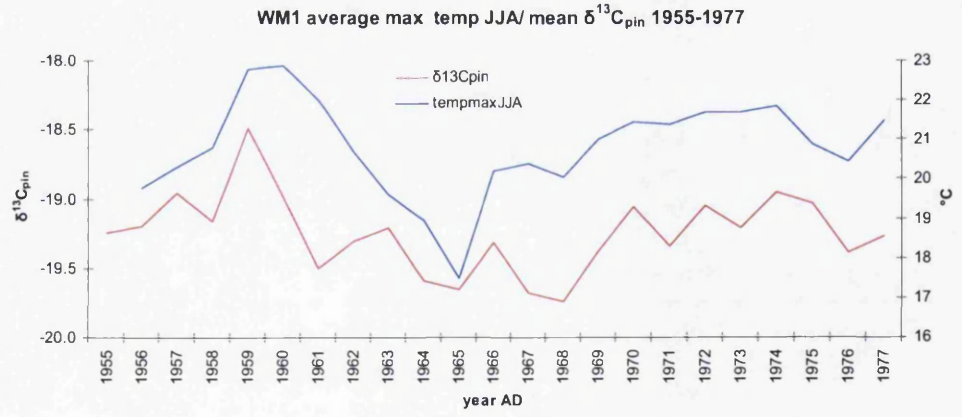

Figure 5.1. Mean $\delta^{13}C_{pin}$ and White Mountain 1 JJA maximum temperature (°C) (r=0.62)

The highest correlation from this station is between average maximum temperature for June/July/August and $\delta^{13}C_{pin}$ for core 527d (r=0.67). The correlation between average maximum temperature for June/July/August and mean $\delta^{13}C_{pin}$ is r=0.62 (figure 5.1). The full list of correlations for WM1 average max temperature (June/July/August) for $\delta^{13}C_{pin}$ and $\delta^{13}C_{cor}$ are shown below (Table 5.1).

Table 5.1 Correlations between $\delta^{13}C$ and White Mountain 1 June/July/August maximum temperature (*indicates significance at p<0.01)

Tree	1	523	362	123	527	007	487	mean
$\delta^{13}C_{pin}$	0.57	0.34	0.32	0.20	0.67*	0.31	0.59*	0.62*
$\delta^{13}C_{cor}$	0.57	0.30	0.29	0.16	0.64*	0.27	0.57	0.54

There are no significant correlations with the precipitation record (1955-1977) from WM1. The next nearest weather station is White Mountain 2, at an elevation (12500ft) with a longer climate record. Continuous readings are available from 1955-1980.

The immediate lowlands of the Owen's Valley to the west are represented by Bishop Airport, situated at 1263 m (N 37° 22.4' W 118° 21.8') that has records from 1948 to 2007. Although much lower in altitude, and therefore much warmer, the weather data from this station mirrors the data from WM1 and is close enough to share much of the same weather as the White Mountains themselves.

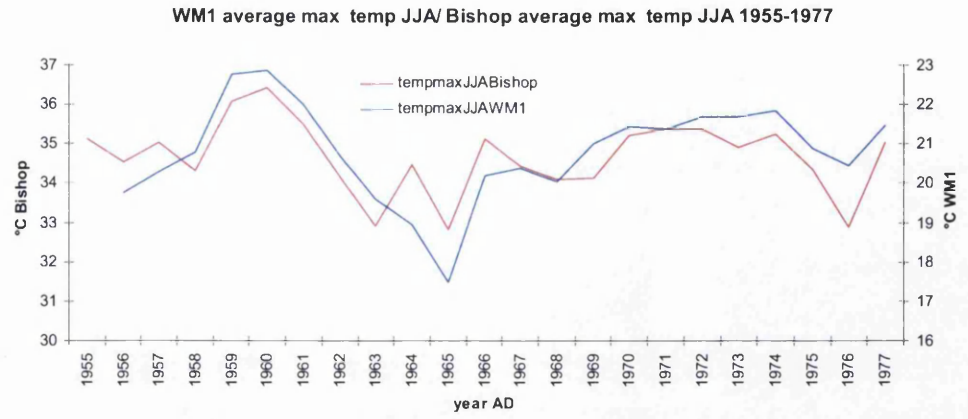

Figure 5.2. Comparison of summer (June/July/August) maximum temperature (°C) from Bishop Airport (left y axis) and White Mountain 1(right y axis) (r=0.78).

Again, the highest found correlations with the Bishop Airport data are for total summer precipitation and average maximum summer temperature. The correlations with average maximum summer temperature for both $\delta^{13}C_{pin}$ and $\delta^{13}C_{cor}$ are shown in Table 5.4.

*Table 5.2 Bishop Airport correlations with average maximum summer temperature for both $\delta^{13}C_{pin}$ and $\delta^{13}C_{cor.}$ *=significant at both 95 and 99% confidence limits*

Tree	1	523	362	123	527	007	487	mean
$\delta^{13}C_{pin}$	0.29	0.35*	0.33	0.30	0.31	0.37*	0.51*	0.55*
$\delta^{13}C_{cor}$	0.23	0.36*	0.28	0.20	0.14	0.37*	0.50*	0.43*

As can be seen the highest correlation is with mean $\delta^{13}C_{pin}$.

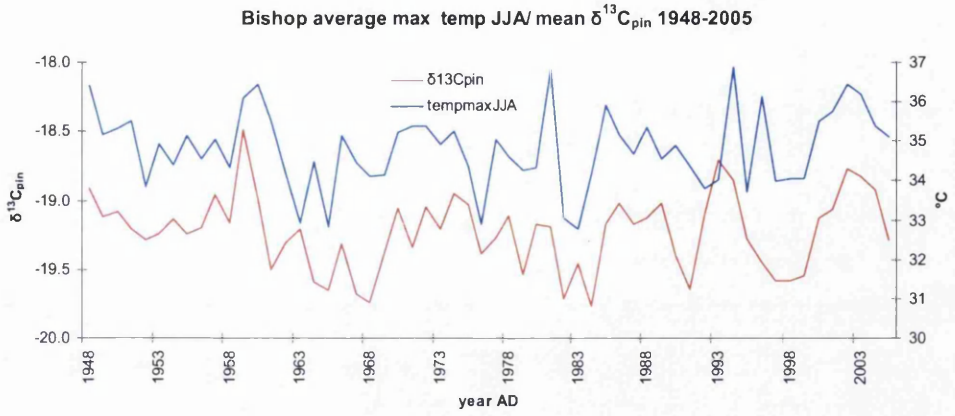

Figure 5.3. Mean $\delta^{13}C_{pin}$ and Bishop average maximum JJA temperature 1948-2005 (r=0.55).

The correlations for both mean $\delta^{13}C_{pin}$ and $\delta^{13}C_{cor}$,as shown in table 5.4 and figure 5.5 are *=significant at both 95 and 99% confidence limits.

There are also significant correlations with summer (June/July/August) precipitation data from Bishop, though none were evident with the precipitation data from WM1. The temperature data from WM1 and Bishop do correlate significantly with each other (figure 5.2), but the problems of extrapolating precipitation data from low to altitudes are highlighted (McCarroll *et al.*, in press).

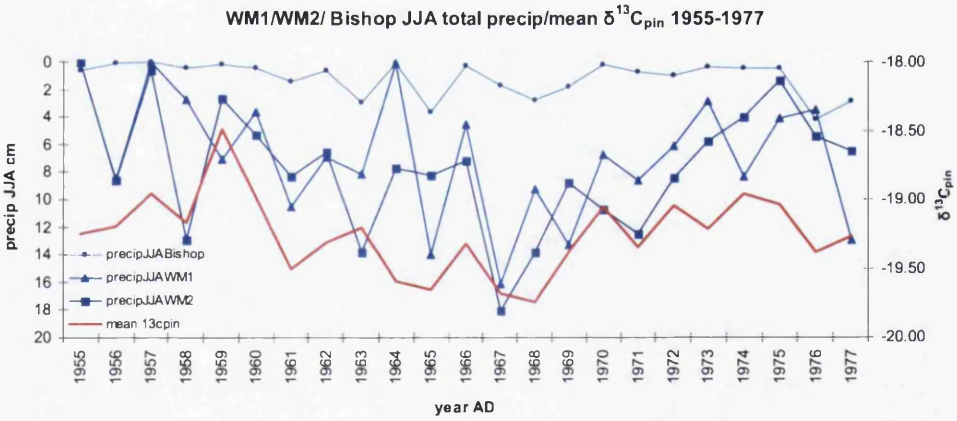

Figure 5.4 – WM1/WM2/ Bishop summer (June/July/August) total precipitation and Mean $\delta^{13}C_{pin}$ 1955-1977. The highest correlation with mean $\delta^{13}C_{pin}$ is with WM2 (r=-0.52 significant at 95% confidence level).

The differences between the two sets of data may be the result of instrumental error but they may also be explained climatically. Significant airflow from the southeast is uncommon, even though it is the least impeded route, topographically speaking. On the occasions it does occur, in June or July, there are often spectacular thunderstorms with high precipitation intensities. Summer storms in the mountains may bring more precipitation in a few hours than are recorded during the whole of the summer during most years (Powell and Klieforth, 1991). For example, nearly 22cm was recorded in under 3 hours at Chiatovich Flats, California on July 23 1955 (Powell and Klieforth, 1991).

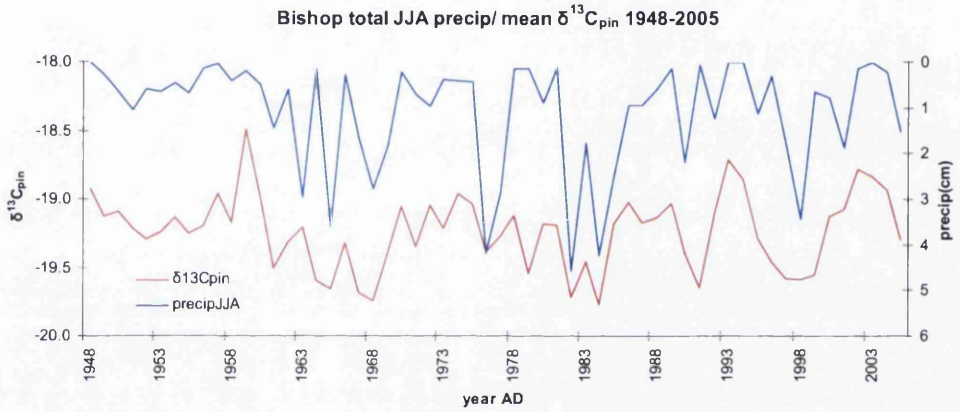

Figure 5.5. Total summer (JJA) precipitation (Bishop) and mean $\delta^{13}C_{pin.}$ (r=.-0.58).Note: precipitation is plotted on an inverse scale.

Tree	001	523	362	123	527	007	487	mean
$\delta^{13}C_{pin}$	-0.38*	-0.26	-0.49*	-0.19	-0.34	-0.32	-0.56*	-0.58*
$\delta^{13}C_{cor}$	-0.36*	-0.29	-0.49*	-0.22	-0.24	-0.37*	-0.61*	-0.54*

*Table 5.3. Correlation for individual trees/mean $\delta^{13}C_{pin}$ and $\delta^{13}C_{cor}$ and Bishop Airport JJA total precipitation 1948-2005. *=significant at both 95 and 99% confidence limits*

The nearest weather station to the east of the White Mountains is at Deep Springs College (N37° 371' W 117° 984'- 1583m a.s.l). This is slightly higher in altitude than Bishop and this is reflected in lower summer temperatures that correlate highly with the Bishop record for the same period.

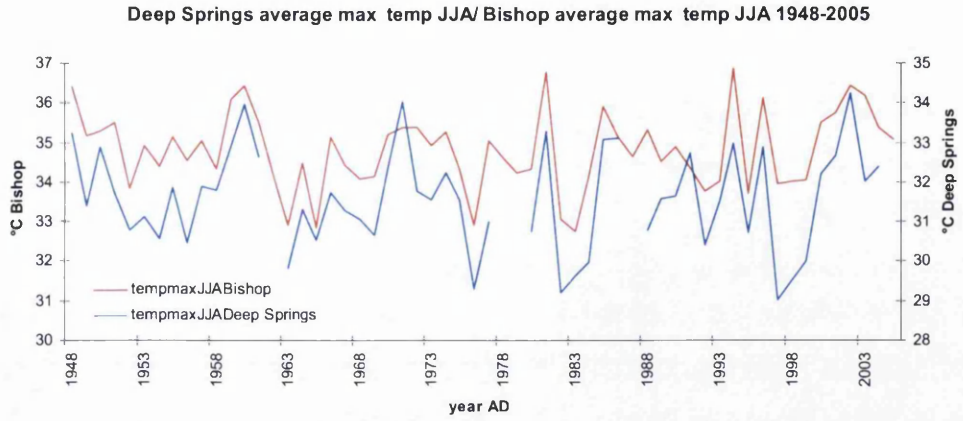

Figure 5.6 Bishop/Deep Springs average max summer (JJA) temp 1948-2005 (r=0.84)

Table 5.4. Deep Springs average max summer temp/$\delta^{13}C$ correlations.

Tree	001	523	362	123	527	007	487	mean
$\delta^{13}C_{pin}$	0.34	0.32	0.34	0.21	0.20	0.46*	0.45*	0.53*
$\delta^{13}C_{cor}$	0.31	0.33	0.32	0.18	0.13	0.47*	0.45*	0.45*

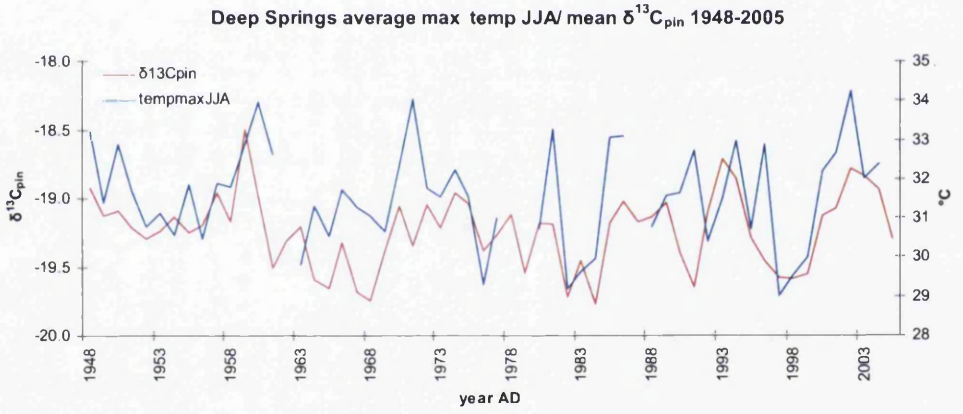

Figure 5.7. Deep Springs JJA temperature/ mean $\delta^{13}C_{pin}$.

*Table 5.5 Deep Springs JJA precipitation and $\delta^{13}C$ correlation values. *=significant at both 95 and 99% confidence limits*

Tree	001	523	362	123	527	007	487	mean
$\delta^{13}C_{pin}$	-0.27	-0.36*	-0.45*	-0.11	-0.31	-0.16	-0.43*	-0.47*
$\delta^{13}C_{cor}$	-0.27	-0.39*	-0.47*	-0.23	-0.31	-0.25	-0.53*	-0.51*

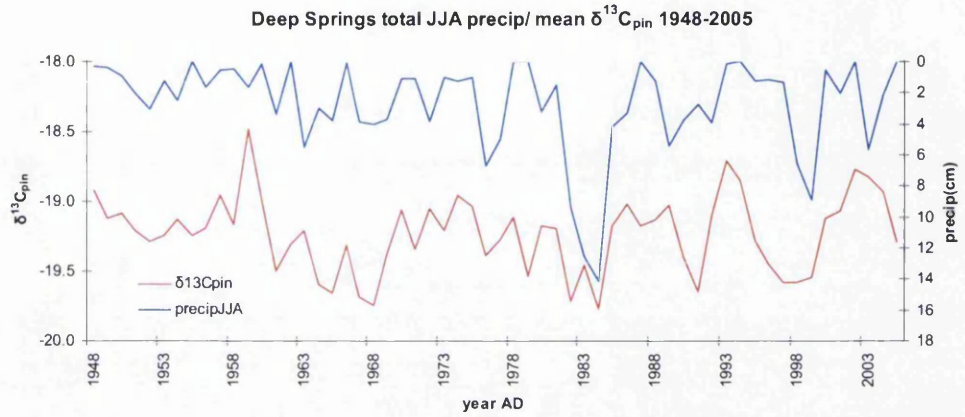

Figure 5.8 Deep Springs JJA total precipitation $\delta^{13}C_{pin}$ (r=-0.47).Note: precipitation is plotted on an inverse scale.

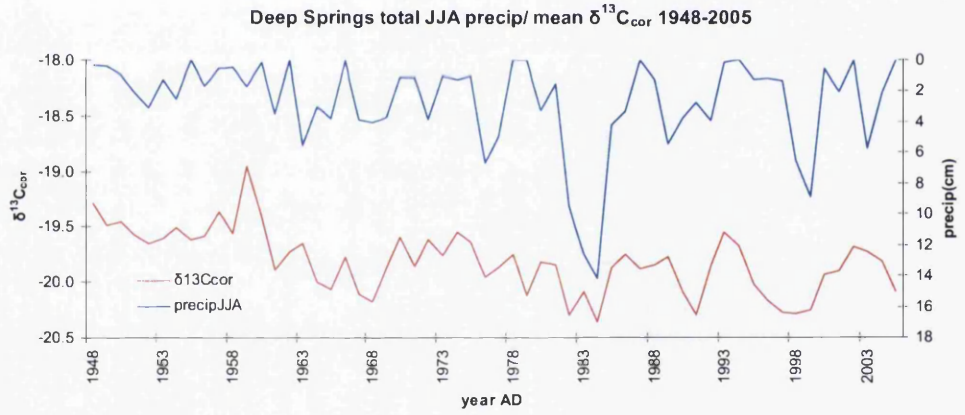

Figure 5.9 Deep Springs JJA total precipitation and $\delta^{13}C_{cor}$ (r=-0.51).Note: precipitation is plotted on an inverse scale.

Longer instrumental climate records back to the late 19th century are available from further away in Nevada. Mina (N 38° 23' 25" W 118° 06' 30" elevation. 1390m) is around 100 miles to the northeast from the location of the sampled trees and has temperature and precipitation data back to 1897 (Powell and Klieforth,1992). In addition there are less complete records from Austin, Nevada (230 miles away from the sampled trees at 39°29'35.73"N 117° 4'18.57"W elevation. 2030m) that extend back to 1887. Additional climate data are available from Lovelock, Nevada (N 40°10'49.30" W 118°28'30.40" elev. 1210m) that extends back to 1895.

Table 5.6.Mina, Nevada average summer max temp/ $\delta^{13}C_{pin}$ and $\delta^{13}C_{cor}$ correlations

Tree	001	523	362	123	527	007	487	mean
$\delta^{13}C_{pin}$	0.16	0.15	0.15	0.20	0.29*	0.21	0.31*	0.30*
$\delta^{13}C_{cor}$	0.14	0.22	0.14	0.21	0.27*	0.25	0.32*	0.31*

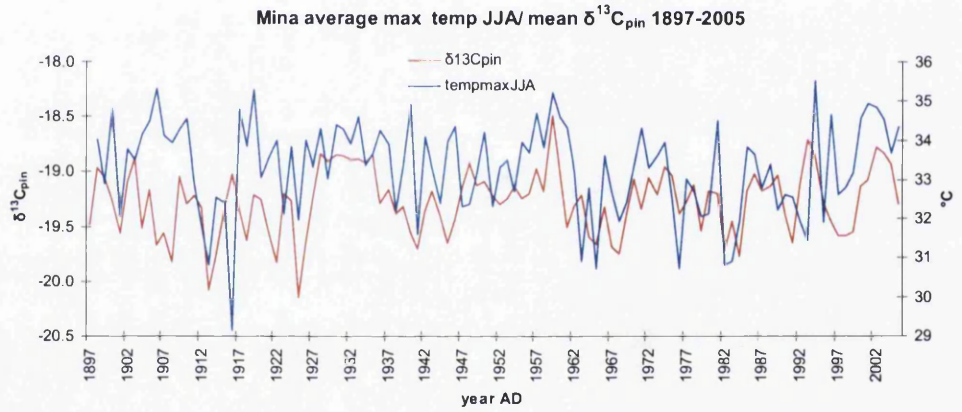

Figure 5.10. Mina JJA average max temp and mean $\delta^{13}C_{pin}$ (r=0.30).

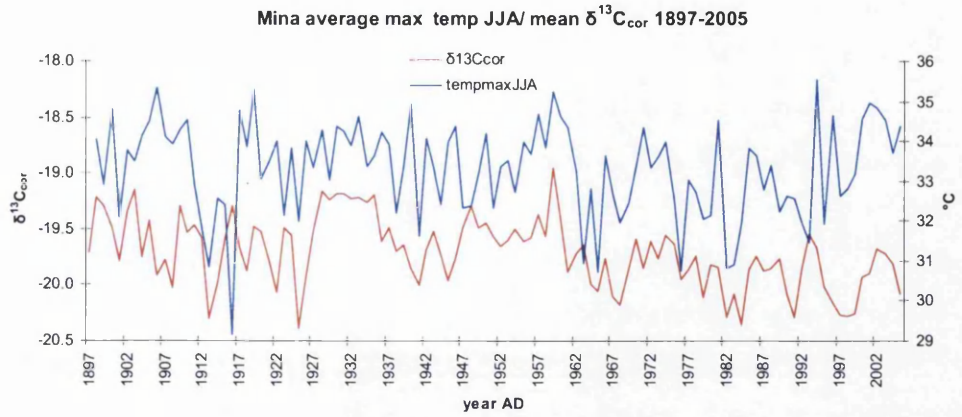

Figure 5.11. Mina JJA average max temp and mean $\delta^{13}C_{cor}$ (r=0.31).

Table 5.7. Correlations with Mina JJA precipitation

Tree	001	523	362	123	527	007	487	mean
$\delta^{13}C_{pin}$	-0.33*	-0.29*	-0.17	-0.30*	-0.21	-0.20	-0.39*	-0.40*
$\delta^{13}C_{cor}$	-0.35*	-0.39*	-0.18	-0.37*	-0.27*	-0.27*	-0.51*	-0.49*

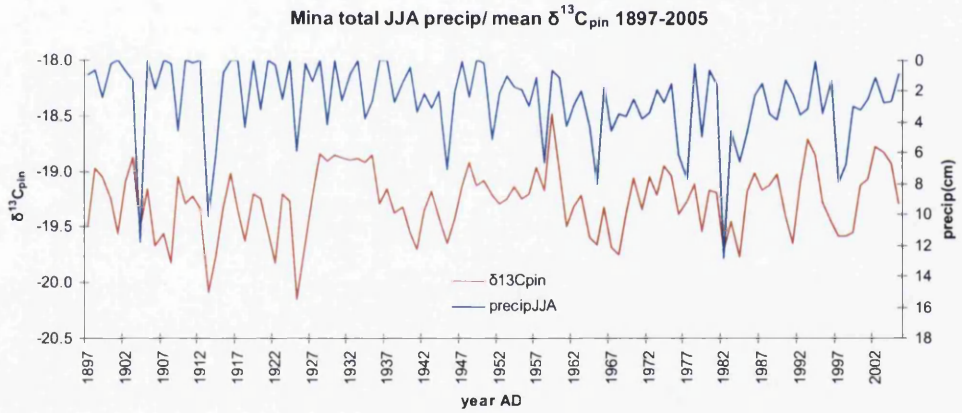

Figure 5.12. Mina JJA precipitation/ mean $\delta^{13}C_{pin.}$ (r=-0.40). Note: precipitation is plotted on an inverse scale.

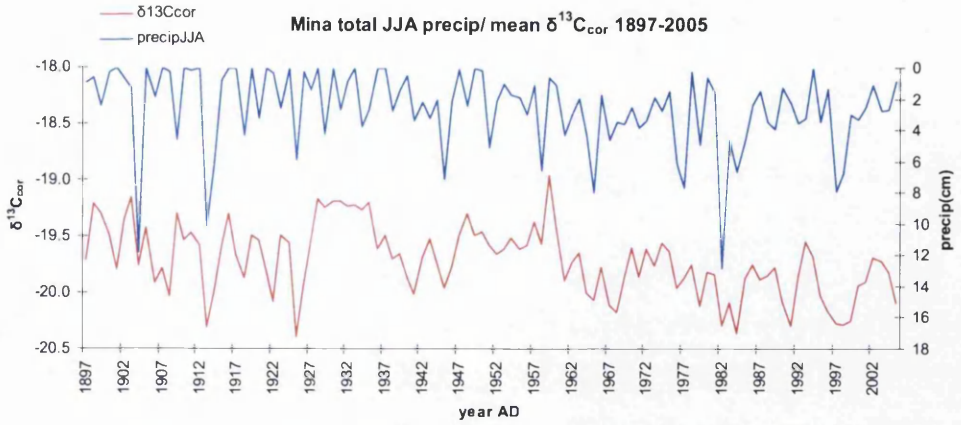

Figure 5.13. Mina JJA precipitation/ mean $\delta^{13}C_{cor.}$ (r=-0.49). Note: precipitation is plotted on an inverse scale.

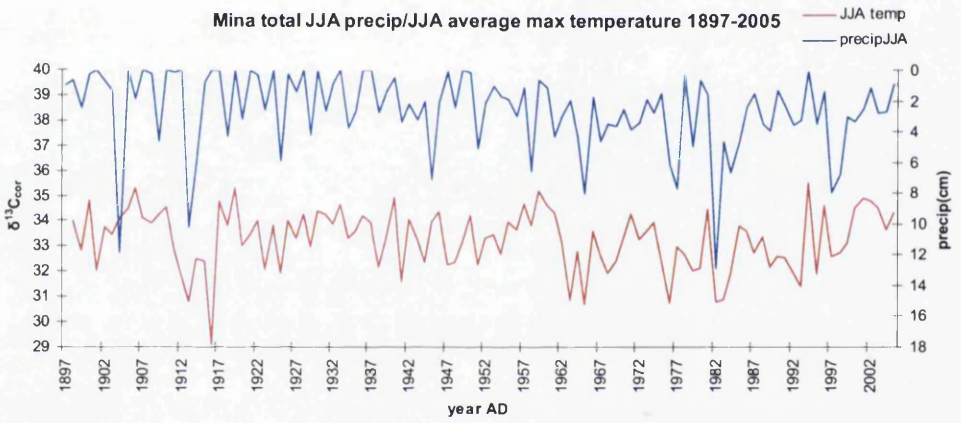

Figure 5.14. Mina JJA temperature and precipitation. (r=-0.39). Note: precipitation is plotted on an inverse scale.

5.2: Regional/ gridded data

Temperature, precipitation and PDSI data from 1895-2005, made up of averaged station were obtained from the NOAA website (http://www.wrcc.dri.edu/summary/Climsmnv.html).

The White Mountains are on the edge of two different climate sub divisions, California division 7 and Nevada division 3. The highest correlations were found with Nevada climate division 3.

(http://www.cdc.noaa.gov/cgi-bin/Timeseries/timeseries1.pl)

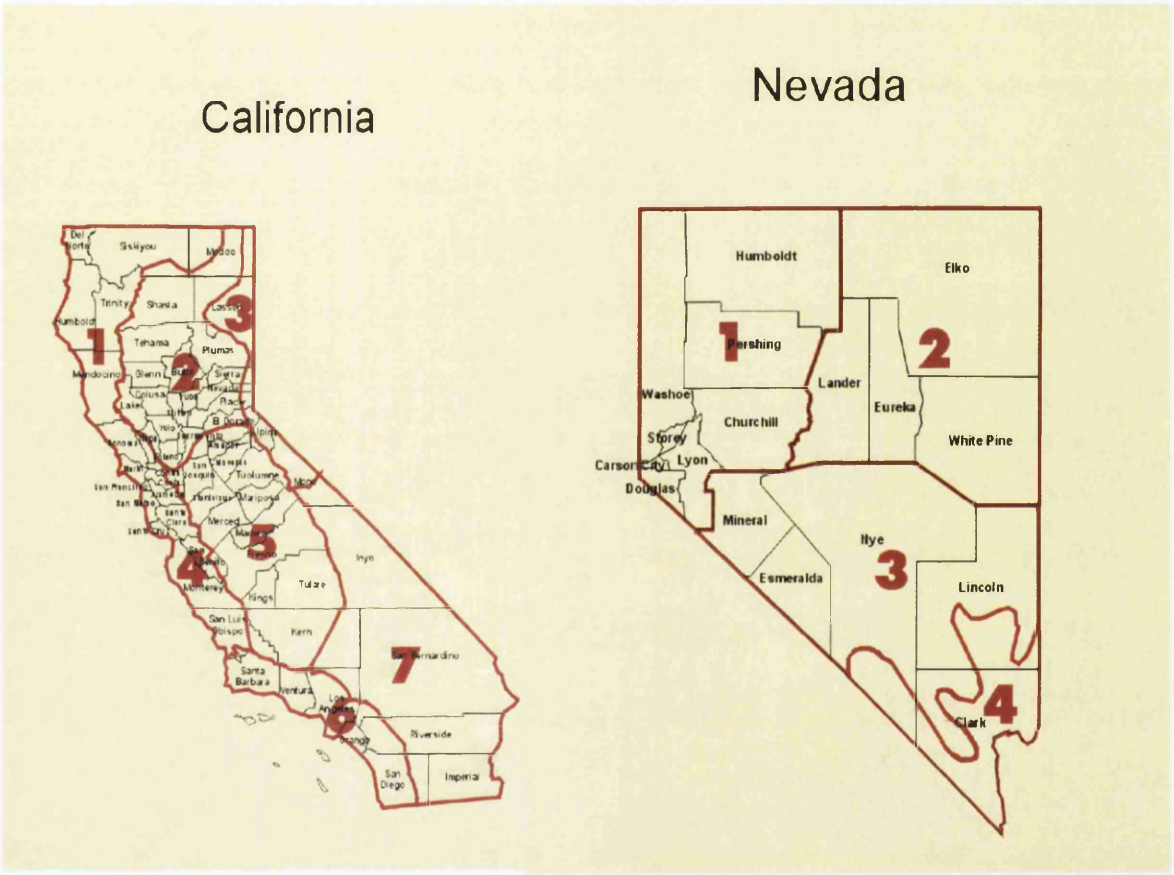

Figure 5.15- California and Nevada climate divisions

5.3 Correlations with temperature.

Table 5.8. Nevada sub division 3.Significant correlations with temperature $\delta^{13}C_{pin}$. (*indicates significance at p<0.01)

Tree $\delta^{13}C_{pin}$	001	523	362	123	527	007	487	mean
june	0.19	0.27*	0.30*	0.08	0.27*	0.12	0.28*	0.32*
jj	0.11	0.26	0.37*	0.12	0.25	0.05	0.32*	0.32*
jja	0.09	0.26	0.46*	0.15	0.26	0.05	0.25	0.34*
julaug	-0.02	0.16	0.44*	0.15	0.16	-0.02	0.15	0.25
jjas	0.12	0.30*	0.52*	0.14	0.27*	0.02	0.30*	0.37*
julas	0.05	0.23	0.51*	0.13	0.20	-0.04	0.23	0.30*
as	0.08	0.22	0.50*	0.10	0.19	-0.02	0.15	0.29*
mjjas	0.10	0.33*	0.51*	0.12	0.20	-0.08	0.30*	0.33*
amjjas	0.11	0.37*	0.49*	0.17	0.21	-0.01	0.30*	0.37*
am	0.07	0.33*	0.30*	0.17	0.07	-0.05	0.20	0.25
amj	0.13	0.38*	0.36*	0.16	0.17	0.01	0.27*	0.33*
amjj	0.11	0.37*	0.40*	0.18	0.18	-0.01	0.31*	0.34*
mam	0.10	0.30*	0.32*	0.19	0.10	-0.04	0.27*	0.28*
july	-0.04	0.14	0.30*	0.13	0.13	-0.07	0.26*	0.19
August	0.00	0.13	0.42*	0.13	0.14	0.04	-0.02	0.21
Sept	0.12	0.22	0.39*	0.05	0.16	-0.06	0.24*	0.26*

Table 5.9 Nevada sub division 3.Correlations with temperature $\delta^{13}C_{cor}$.(*indicates significance at p<0.01)

Tree $\delta^{13}C_{cor}$	001	523	362	123	527	007	487	mean
june	0.12	0.16	0.28*	-0.07	0.11	0.03	0.06	0.14
jj	0.04	0.10	0.35*	-0.03	0.08	-0.04	0.10	0.12
jja	0.01	0.08	0.44*	-0.01	0.07	-0.03	0.06	0.13
julaug	-0.09	-0.01	0.43*	0.04	0.02	-0.07	0.04	0.08
jjas	0.04	0.09	0.51*	-0.03	0.07	-0.06	0.08	0.15
julas	-0.02	0.03	0.50*	0.01	0.02	-0.10	0.07	0.11
as	0.03	0.05	0.49*	-0.01	0.03	-0.07	0.02	0.12
mjjas	0.01	0.10	0.49*	-0.06	-0.01	-0.17	0.06	0.09
amjjas	0.02	0.15	0.47*	-0.01	0.00	-0.09	0.09	0.13
am	-0.01	0.17	0.27	0.02	-0.09	-0.10	0.08	0.07
amj	0.04	0.20	0.33*	-0.01	-0.02	-0.06	0.08	0.11
amjj	0.01	0.17	0.37*	0.00	-0.02	-0.09	0.11	0.11
mam	-0.01	0.12	0.27	-0.02	-0.11	-0.12	0.09	0.04
july	-0.09	-0.02	0.29*	0.03	0.01	-0.12	0.13	0.04
August	-0.05	0.01	0.41*	0.03	0.03	0.01	-0.07	0.09
Sept	0.08	0.06	0.39*	-0.04	0.02	-0.10	0.08	0.11

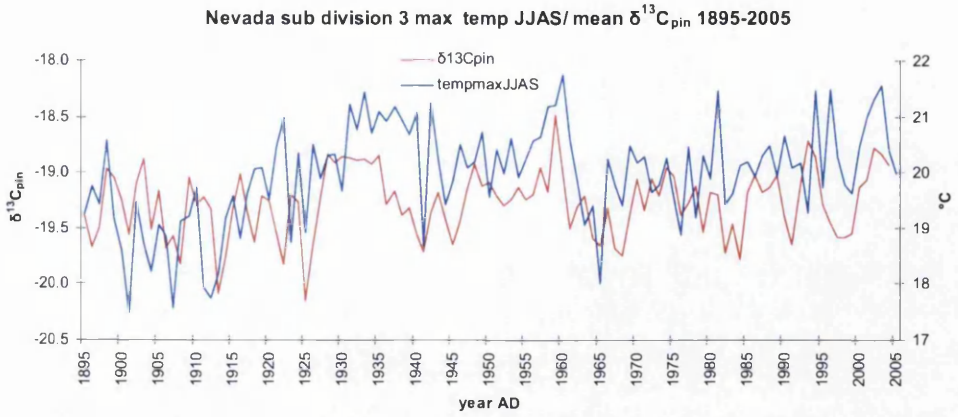

Figure 5.16. 6/7 tree mean (all data) $\delta^{13}C_{pin}$ Nevada division 3 June/July/August/September average temperature (r=0.37)

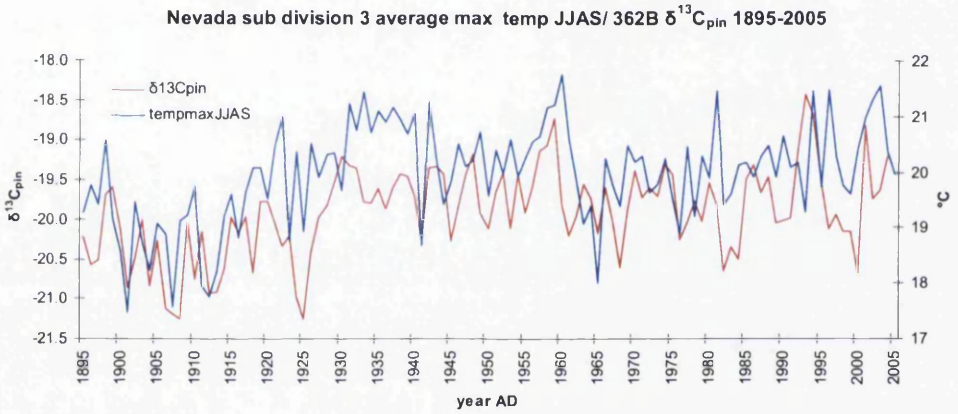

Figure 5.17 tree 362b $\delta^{13}C_{pin}$ June/July/August/September average temperature (r=0.52)

The temperature data of Nevada climate division 3 correlates significantly with the $\delta^{13}C_{pin}$ data (table 5.8). The only significant correlations with the $\delta^{13}C_{cor}$ data (table 5.9) are with tree 362b, and with combined April, May, June average temperature for 523b. Tree 362b appears to be highly responsive to summer temperatures, with correlations higher for this tree alone (figure 5.17) than with the mean of all trees (figure 5.16). The earliest part of the series (from 1895 to around 1918) appears to present the most difficulty in terms of correlation with $\delta^{13}C_{pin}$ mean. Using three or four trees for this first period and then using seven trees for the rest of the series increases the correlation with this temperature data from r=0.37 to r=0.60.

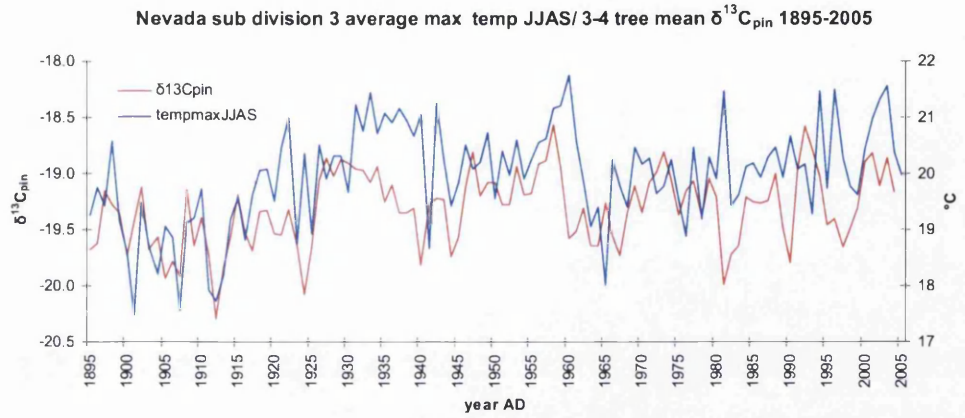

Figure 5.18. 3-4 tree $\delta^{13}C_{pin}$ and June-September average maximum summer temperature, Nevada climate division 3 (r=0.50). 3 tree s(362,527 and 007) are used from 1895 to 1907. 4 trees are used from 1908 to2005 (362,527,487 and 007) (r=0.50).

The correlation can be improved further by using all seven trees from 1916-2005 (r=0.64). This type of approach presents obvious problems when deciding which trees to use for the majority of the data for which no instrumental climate data are available, but this involves dropping trees in and out of the series for the earliest part, and is not really an appropriate method for calibrating all of the $\delta^{13}C_{pin}$ data. It is however useful for demonstrating that the low frequency trends in the $\delta^{13}C_{pin}$ data are influenced by fluctuations in summer temperature to a significant degree. Smoothing the data to 3 yr centred means also improves the correlation to a large degree. This is especially evident when undertaking spatial analysis of the data, where correlations well over r=0.7 are evident (chapter 6.7).

5.4 Precipitation

The Nevada climate division 3 total precipitation data also correlates significantly with the Blanco carbon isotopes. The following correlations were observed with both $\delta^{13}C_{pin}$ and $\delta^{13}C_{cor}$ data.

Table 5.10 Nevada sub division 3. Correlations with precipitation $\delta^{13}C_{pin}$(*indicates significance at p<0.01)

Tree $\delta^{13}C_{pin}$	001	523	362	123	527	007	487	mean
july	-0.36*	-0.36*	-0.37*	-0.21	-0.25	-0.24	-0.32*	-0.46*
jja sum	-0.34*	-0.35*	-0.34*	-0.25	-0.25	-0.31*	-0.41*	-0.49*
jjsum	-0.39*	-0.35*	-0.31*	-0.27*	-0.29*	-0.35*	-0.41*	-0.50*
julaug	-0.30*	-0.34*	-0.37*	-0.21	-0.21	-0.23	-0.35*	-0.44*
jan-aug	-0.29*	-0.29*	-0.18	-0.28*	-0.27*	-0.32*	-0.43*	-0.43*
jjas	-0.34*	-0.40*	-0.34*	-0.21	-0.25	-0.32*	-0.41*	-0.49*
mjjas	-0.33*	-0.37*	-0.30*	-0.26*	-0.25	-0.28*	-0.42*	-0.47*
jjaso	-0.29*	-0.33*	-0.33*	-0.18	-0.24	-0.29*	-0.34*	-0.43*
mjj	-0.34*	-0.29*	-0.24	-0.31*	-0.26*	-0.26*	-0.40*	-0.45*
mjja	-0.32*	-0.31*	-0.29*	-0.30*	-0.24	-0.26*	-0.42*	-0.46*
oct-may	-0.16	-0.11	0.01	-0.16	-0.17	-0.18	-0.25	-0.20

Table 5.11 Nevada sub division 3. Correlations with precipitation $\delta^{13}C_{cor}$(*indicates significance at p<0.01)

Tree $\delta^{13}C_{cor}$	001	523	362	123	527	007	487	mean
july	-0.34*	-0.36*	-0.37*	-0.16	-0.20	-0.23	-0.24	-0.40*
jja sum	-0.35*	-0.40*	-0.35*	-0.28*	-0.26*	-0.36*	-0.46*	-0.52*
jjsum	-0.38*	-0.41*	-0.32*	-0.26*	-0.28*	-0.36*	-0.36*	-0.49*
julaug	-0.30*	-0.36*	-0.37*	-0.21	-0.19	-0.26*	-0.39*	-0.44*
jan-aug	-0.34*	-0.38*	-0.23	-0.36*	-0.32*	-0.39*	-0.56*	-0.54*
jjas	-0.36*	-0.47*	-0.35*	-0.29*	-0.28*	-0.38*	-0.48*	-0.55*
mjjas	-0.35*	-0.45*	-0.31*	-0.33*	-0.28*	-0.35*	-0.52*	-0.55*
jjaso	-0.33*	-0.42*	-0.35*	-0.27*	-0.30*	-0.36*	-0.45*	-0.52*
mjj	-0.34*	-0.36*	-0.25	-0.33*	-0.26*	-0.30*	-0.42*	-0.47*
mjja	-0.33*	-0.37*	-0.30*	-0.33*	-0.25	-0.32*	-0.50*	-0.51*
oct-may	-0.20	-0.16	-0.04	-0.22	-0.20	-0.22	-0.36*	-0.30*

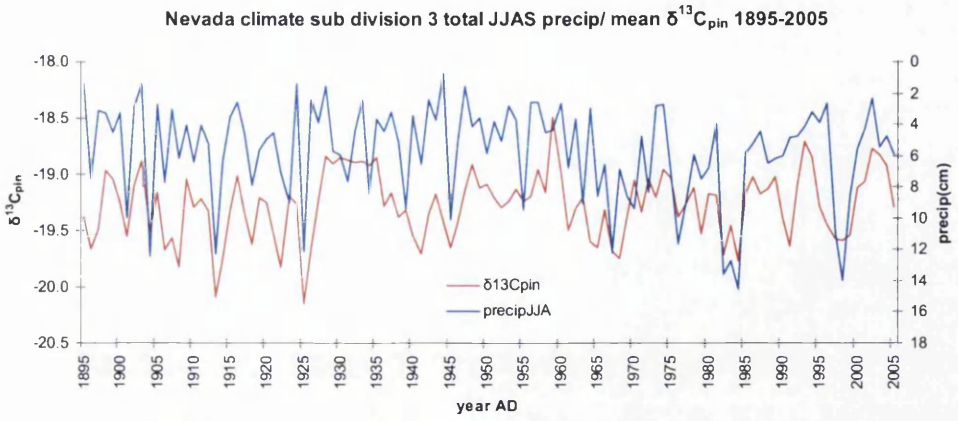

Figure 5.19. Total June/July/August/September precipitation/mean $\delta^{13}C_{pin}$(r=-0.49). Note: precipitation is plotted on an inverse scale.

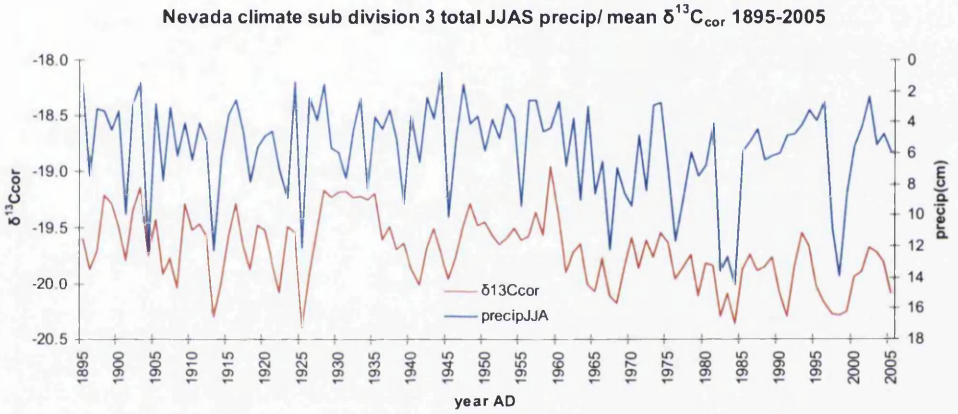

Figure 5.20. June-September total precipitation and mean $\delta^{13}C_{cor}$ (r=-0.55). Note: precipitation is plotted on an inverse scale.

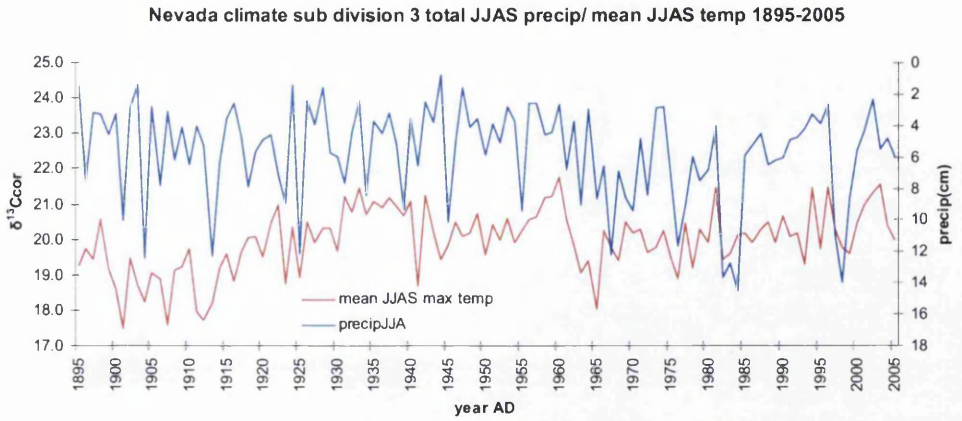

Figure 5.21. June-September total precipitation and June-September averaged temperature data for Nevada climate division 3 (r=-0.27). Linear upward trend in temperature data (r=0.40) is significant at p<0.01. The increasing trend in precipitation (r=0.18) is not significant. Note: precipitation is plotted on an inverse scale.

5.5: Validation of data.

The role of a validation period is to provide an independent assessment of the accuracy of any climate reconstruction. By reserving a subset of data it is possible to independently assess the predictive value of the proxy data. If the validation period is independent of the calibration period, the quality of any reconstruction will not be biased by the potential overfit during the calibration period. Any climate reconstruction is limited by the length of the instrumental weather record, so no estimate is available of the reconstruction skill of the period outside the period of the instrumental record. Due to the problem of autocorrelation in most geophysical time series, the validation period adjacent to the calibration period cannot be truly independent, although if the autocorrelation is short term the validation results should not be seriously biased (National Research Council, 2006).

Common measures used to assess the accuracy of statistical predictions are the mean squared error (MSE), reduction of error (RE), coefficient of efficiency (CE), and the squared correlation (r^2). MSE is a measure of how close predicted values are to actual values and is widely used in geophysical studies. The value is usually normalised and presented in the form of the RE statistic or the CE statistic. RE is a comparison of the MSE of the reconstruction to the MSE of a reconstruction that is constant in time with a value that is equal to the sample mean for the calibration data set. Should the reconstruction possess any predictive value it would be expected to do better than the sample average over the calibration period, and should therefore produce an RE value of greater than zero (National Research Council, 2006).

The CE compares the MSE to the performance of a reconstruction that is constant in time with a value equivalent to the sample mean for the validation data. This second, constant reconstruction depends on the validation data, withheld from the calibration process, and therefore presents more demanding comparison. CE is always lower than RE, and the difference increases as the difference between the sample means

for the validation and calibration periods increases. (National Research Council, 2006).

If the calibration has predictive value, it would be expected to do better than just the sample average over the validation period, making CE a particularly useful measure of predictive value. R^2 is used to provide a measure of association between two variables. Specifically, r^2 measures the strength of a linear relationship between two variables when the linear fit is determined by regression. R^2 measures how well the linear functions of a prediction match the data, not how well the predictions themselves perform. The coefficients cannot be calculated without knowing the values being predicted, so it is not a particularly useful measure of prediction alone. A high CE value will however always have a high r^2, and having high r^2 supports the use of CE.

In order to assess the potential climate reconstruction accuracy of the Blanco West bristlecone pines carbon isotope series some of the significant climate relationships were examined in this way. Firstly temperature relationships were examined in this way and then precipitation was examined. The ability of the $\delta^{13}C$ of bristlecone pines from Blanco West to reconstruct climate was considered in conclusion.

Temperature 1895-2005.

Let y_t denote a temperature at time and $\hat{y}_t$ is the prediction based on a proxy reconstruction.

Equation 1.

Mean squared error(MSE)

$$MSE(\hat{y}) = \frac{1}{N}\sum(y_t - \hat{y}_t)^2$$

The sum on the right side of equation 1 represents the time of interest (either calibration or validation) and N is the number of time points. The instrumental temperature record used here is 110 years so that and the isotope data are split into two 55 year blocks.

The four bristlecone pine trees (trees 523,362,527 and 487) that correlate best (i.e statistically significant r values) with the Nevada division 3 June-September average maximum temperature record (r=0.50) are used in the example below. Firstly the data was divided into two sections.

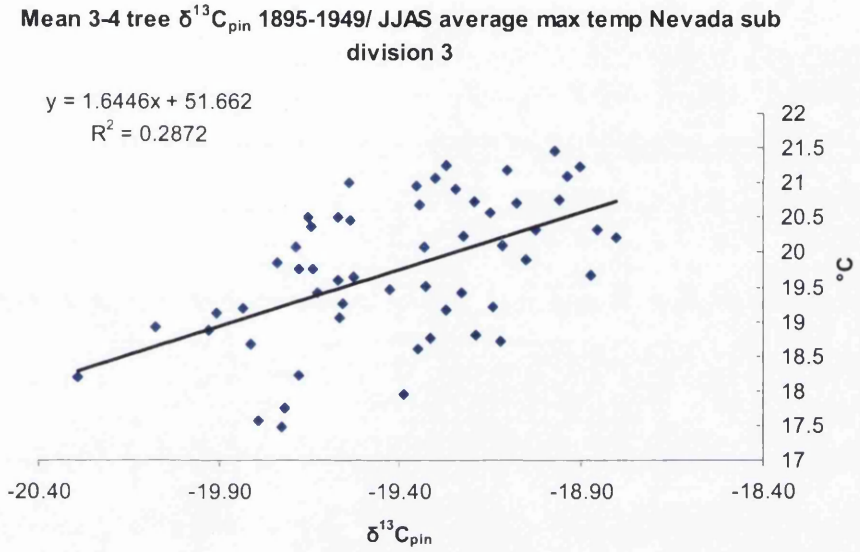

Figure 5.22 Linear relationship between 3-4 tree $\delta^{13}C_{pin}$ and June-September average maximum temperature Nevada division 3,(1895-1949).

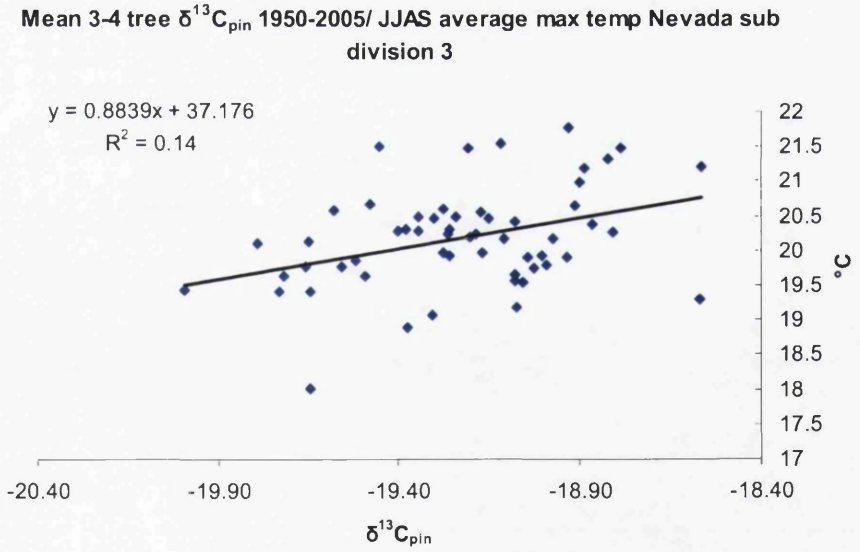

Figure 5.23. Linear relationship between 3-4 tree $\delta^{13}C_{pin}$ and June-September average maximum temperature Nevada division 3 (1950-2005).

As can be seen above the linear relationship between temperature and the four tree mean $\delta^{13}C_{pin}$ is different in the two sub sections of data. To evaluate the predictive ability of this data using the first half of the data (1895-1949) the following procedure was undertaken.

The values in column 'Calib1895-1949' and referred to in example 1 for the year AD1895 on the following page are reconstructed $\delta^{13}C_{pin}$ values based upon the known linear relationship between observed temperature and $\delta^{13}C_{pin}$ for the period 1895-2005 (figure 5.22).This is worked out for each value by the following formula:

$$Calib1895-1949 = 1.6446 * \delta^{13}C_{pin} + 51.662$$

The MSE of each value is worked out using equation 1.

$$MSE(\hat{y}) = \frac{1}{N}\sum(y_t - \hat{y}_t)^2$$

The MSE for the period 1895 to 1949 is the average of all the individual MSE values for the same period, e.g MSE (Calibration 1895-1949)= 0.06.

The numbers in the column 'Calib 1950-2005' and referred to in example 1 for the year AD1895 on the following page are reconstructed values based on the linear relationship between temperature and $\delta^{13}C_{pin}$ for the period 1950-2005 (figure 5.23).

Example 1:

Year	$\delta^{13}C$	temp	calib1895-1949	MSE	calib1950-2005	MSE
1895	-19.55	19.26	19.50	0.06	19.89	0.39

In example 2 (below) the opposite analysis is undertaken. Here the value in column 'calib 1950-2005' is reconstructed based on the known relationship between temperature and $\delta^{13}C_{pin}$ for the period 1950-2005 (figure 5.34). The data in column'calib 1895-1949' is a reconstructed values for the year 1950 based on the linear relationship between temperature and $\delta^{13}C_{pin}$ for the period 1895-1949 (figure 5.33).

Example 2.

Year	$\delta^{13}C$	Temp	calib1950-2005	MSE	calib1895-1949	MSE
1950	-19.08	19.57	20.31	0.56	20.29	0.52

*Table 5.12(below): Reconstructed temperature values for **1895-1949** based on temperature/ $\delta^{13}C_{pin}$ relationship for 1895-1949 (calib 1895-1949) and on temperature/ $\delta^{13}C_{pin}$ relationship for 1950-2005 (calib1950-2005). Mean actual temperatures are also shown as are the MSE of mean temperatures necessary to calculate RE and CE.*

$\delta^{13}C_{pin}$ /temp r=0.54(r^2=.29)	**Mean MSE(1895-1949)**= 0.73	**Temp 1895-1949/calib1950-2005** r=0.54	**Mean MSE $\hat{y}$ (1950-2005)**=0.87	**$\bar{y}_c$ Mean MSE (1950-2005)**= 1.21	**Mean temp mean MSE $\bar{y}_t$ (1895-1949)**=1.03

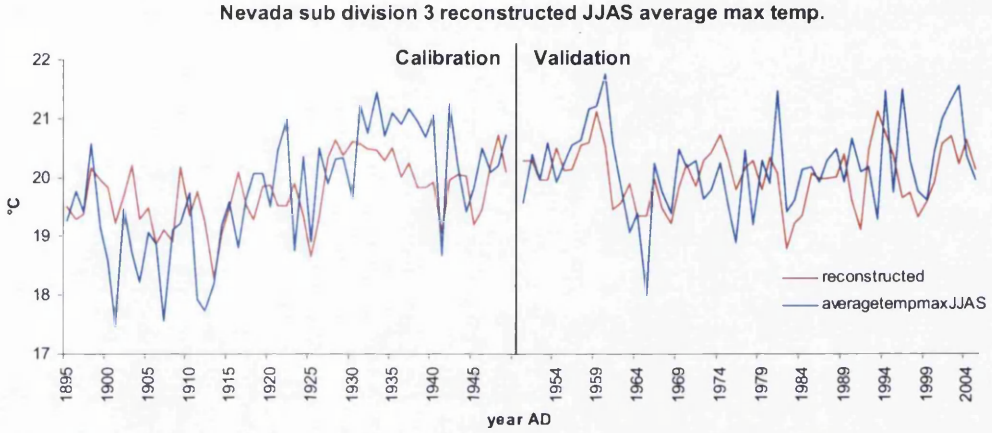

Figure 5.24. Calibration based on the relationship between temperature and 4 tree $\delta^{13}C_{pin}$ relationship for the period 1895-1949 (r^2=0.29).

Table 5.13 Statistical measures of using the first period for calibration and validation (observed temperature/ $\delta^{13}C_{pin}$ relationship for 1895-1949).

Calibration 1895-1949	
MSE	0.73
RE	0.29
CE	NA
r^2	0.29
Validation 1950-2005	
MSE	0.87
RE	0.28
CE	0.15
r^2	0.29

Table 5.14 (below): Reconstructed temperature values for 1950-2005 based on temperature/ $\delta^{13}C_{pin}$ relationship for 1950-2005 (calib 1950-2005) and on temperature/ $\delta^{13}C_{pin}$ relationship for 1895-2005 (calib1895-2005). Mean actual temperatures are also shown as are the MSE of mean temperatures necessary to calculate RE and CE.

$\delta^{13}C_{pin}$/temp r=0.37(r^2=0.14)	**Mean MSE(1950-2005)**= 0.44	**Temp 1950-2005/calib1895-1949** r=0.37	**MSE mean $\hat{y}$ (calib 1895-1949)**= 0.52	**Mean MSE $\bar{y}_c$ (1895-1949)** =0.70	**Mean temp mean MSE $\bar{y}_t$ (1950-2005)**=0.52

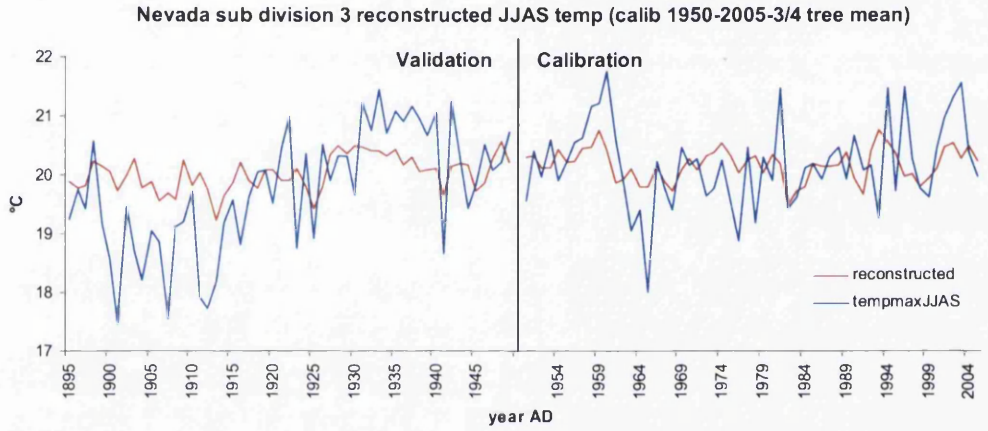

Figure 5.25. Calibration based on the observed relationship between June-September average maximum temperature and 4 tree $\delta^{13}C_{pin}$ relationship for the period 1950-2005(r^2=0.14).

The blue line represents actual temperature for both periods and the red line represents the reconstruction of $\delta^{13}C_{pin}$ values to temperature values based on the calibration period 1950-2005 (figure 5.23).

The results indicate that the relationship between average maximum summer temperature and $\delta^{13}C_{pin}$ values appears to differ for the two split time periods that the instrumental data covers (AD1895-1949 and AD1950-2005). The data for AD1895-1949 appears to more effective (as evidenced by positive RE and CE values) at reconstructing temperature than the period AD1950-2005. The temperature relationship for the AD1895-1949 is stronger in terms of r^2 and it is interesting to note that generally lower temperatures occur from around AD1895-1925. It may be

the case that the relationship between average maximum summer temperature and $\delta^{13}C$ for the period AD1950-2005 is such that the lower temperatures from AD1895-1949 cannot be reconstructed by the linear relationship between AD1895-1949.

It is immediately apparent that the first half of the data (temperature/ four tree $\delta^{13}C_{pin}$ relationship for 1895-1949) better predicts climate than the second half (1950-2005). This is evidenced both in the higher r^2 values and higher RE/CE values, and also in the figure 5.24 and table 5.13. It would seem that the r^2 value for the whole calibration period between temperature and four tree $\delta^{13}C_{pin}$ is high enough ($r^{2=}$ 0.25) to permit some sort of temperature reconstruction, albeit with more error.

1950-2005calibration	
MSE	0.44
RE	0.14
CE	NA
r^2	0.14
validation1895-1949	
MSE	0.52
RE	0.26
CE	0.00
r^2	0.14

Table 5.15 *Statistical measures of using the second period (AD1950-2005) for calibration and validation (observed temperature/ $\delta^{13}C_{pin}$ relationship for 1950-2005(r^2=0.14).*

Reduction of error (RE) statistic.

$$RE = 1 - \frac{MSE(\hat{y})}{MSE(\bar{y}_c)}$$

Where MSE($\bar{y}_c$) is the mean squared error of using the sample average temperature over the calibration period (a constant $\bar{y}_c$) to predict temperatures during the period of interest.

$$MSE(\hat{y}) = \frac{1}{N}\sum(y_t - \bar{y}_c)^2$$

RE=1-(1.59/2.27

Coefficient of efficiency (CE)

$$CE = 1 - \frac{MSE(\hat{y})}{MSE(\bar{y}_t)},$$

Where $MSE(\bar{y}_t)$ is the mean squared error of using the sample average of the period of interest ($\bar{y}_t$) as a predictor of temperatures during the period of interest:

$$MSE(\bar{y}_t) = \frac{1}{N}\sum(y_t - \bar{y}_c)^2$$

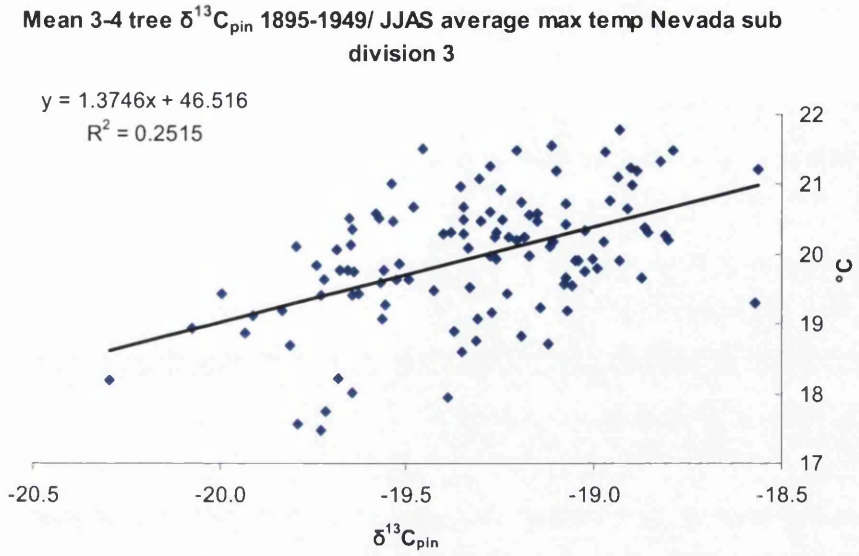

Figure 5.26. Linear relationship between temperature (1895-2005) and 3-4 tree $\delta^{13}C_{pin}$

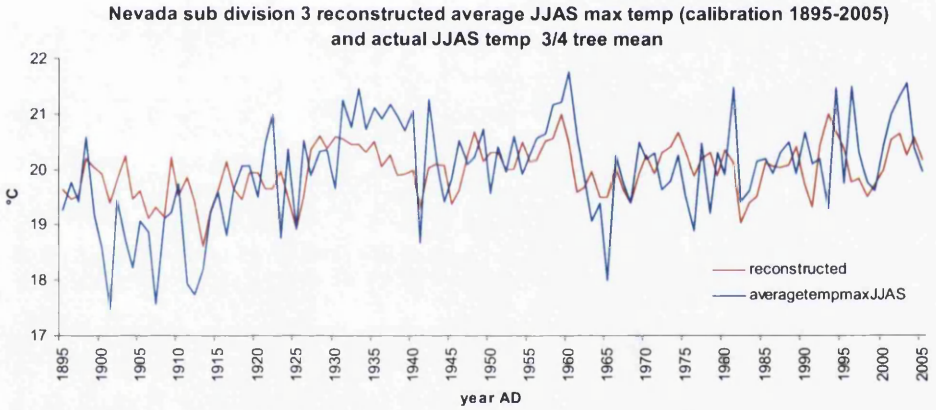

Figure 5.27. Reconstructed 3/4 tree $\delta^{13}C_{pin}$ based on the relationship between temperature and 3/4 tree $\delta^{13}C_{pin}$ relationship for the whole period 1895-2005(r^2=0.25)

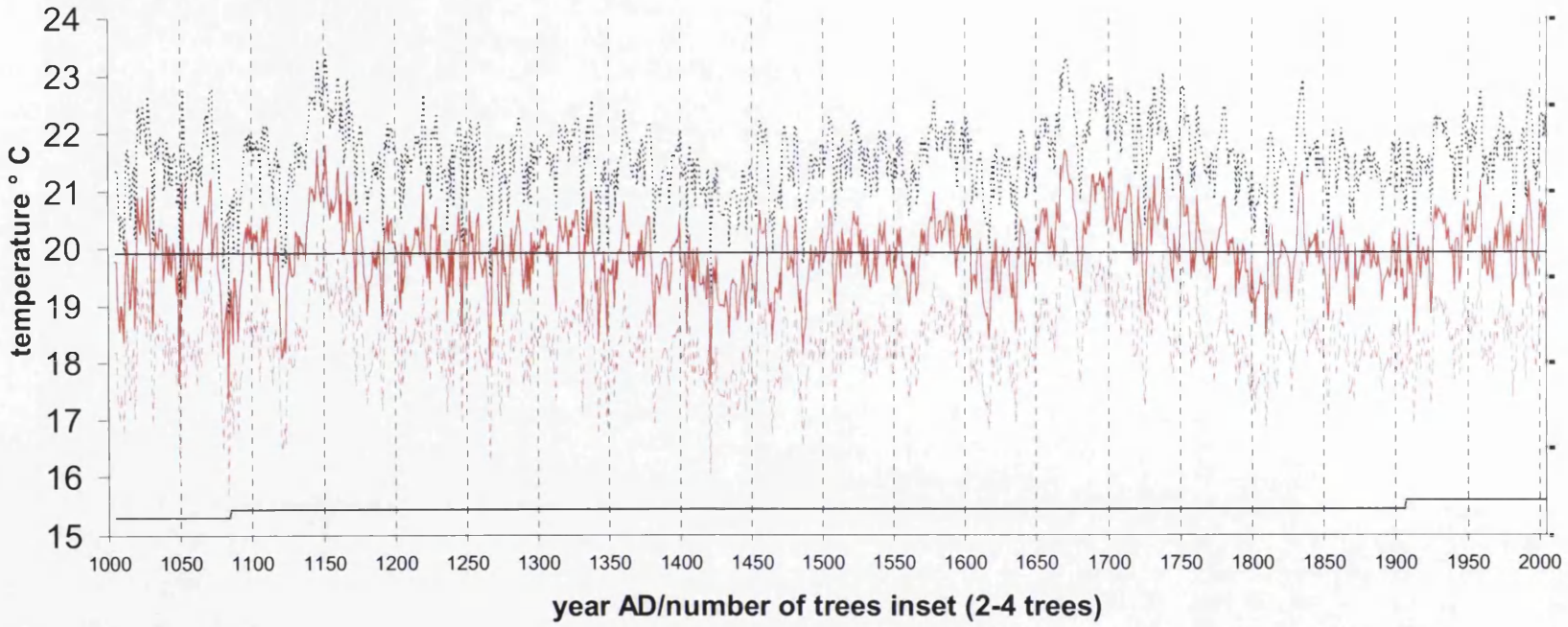

Figure 5.28. Reconstructed average maximum summer temperature for the last 1000 years with error bars (2σ) based on linear relationship between 2-4 tree $\delta^{13}C_{pin}$ for Nevada division 3 mean June-September (JJAS) average maximum temperature AD1895-1949.

When the same validation procedure is carried out with the mean series from all seven trees the prediction ability is not so good for either half of the data. The data again split into two sets.

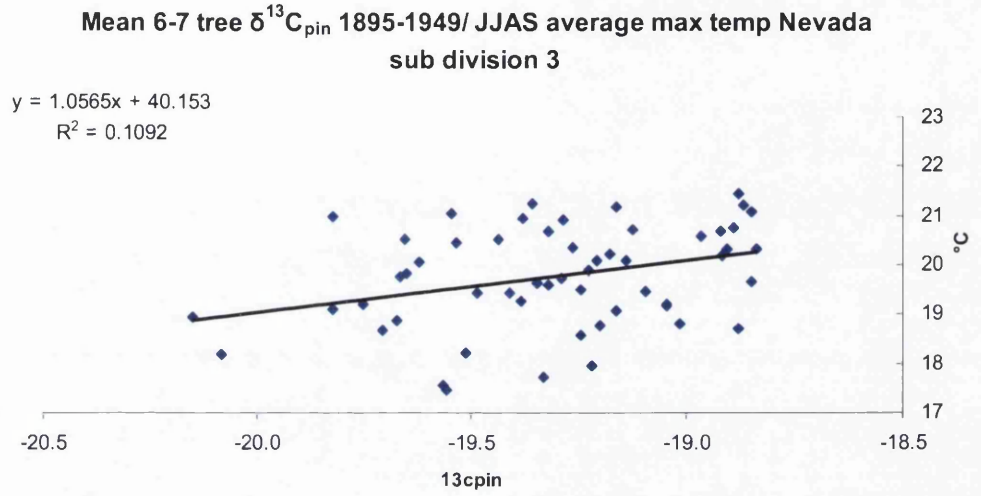

Figure 5.29 (1895-1949) Linear relationships between temperature and 6/7tree mean $\delta^{13}C_{pin}$

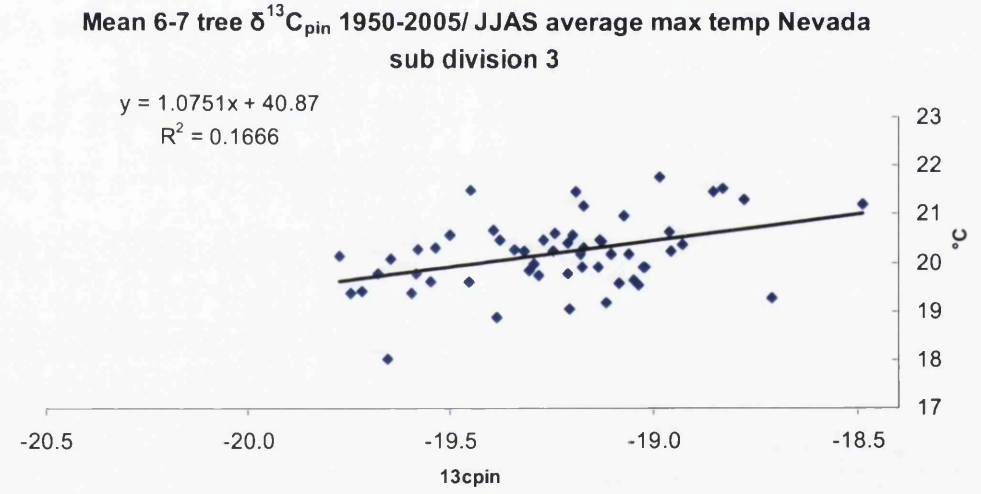

Figure 5.30 Linear relationships between temperature and 6/7tree mean $\delta^{13}C_{pin}$ (1950-2005).

calibration1895-1949	
MSE	0.92
RE	0.11
CE	NA
r^2	0.11
1950-2005	**validation**
MSE	1.04
RE	0.14
CE	-0.01
r^2	0.11

calibration1950-2005	
MSE	0.43
RE	0.17
CE	NA
r^2	0.17
1895-2005	**validation**
MSE	0.56
RE	0.21
CE	-0.08
r^2	0.17

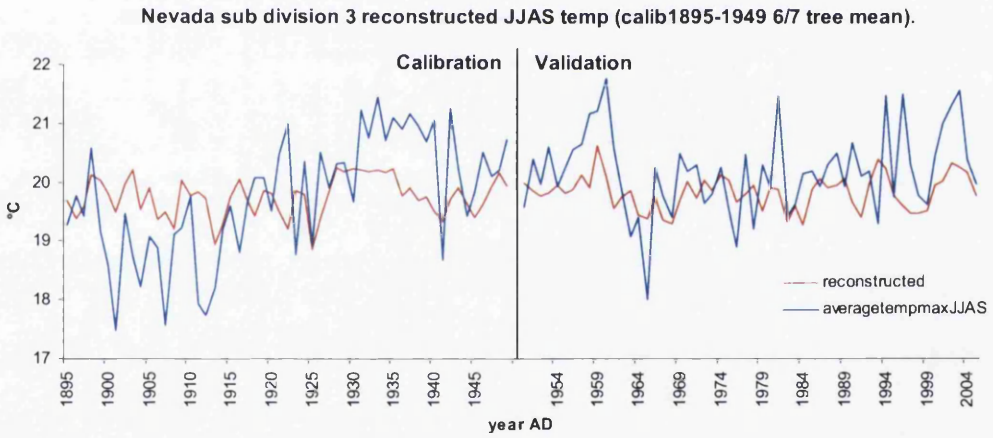

Figure 5.31. Using mean $\delta^{13}C_{pin}$/temperature relationship for 1895-1949 to reconstruct temperature values for 1950-2005.

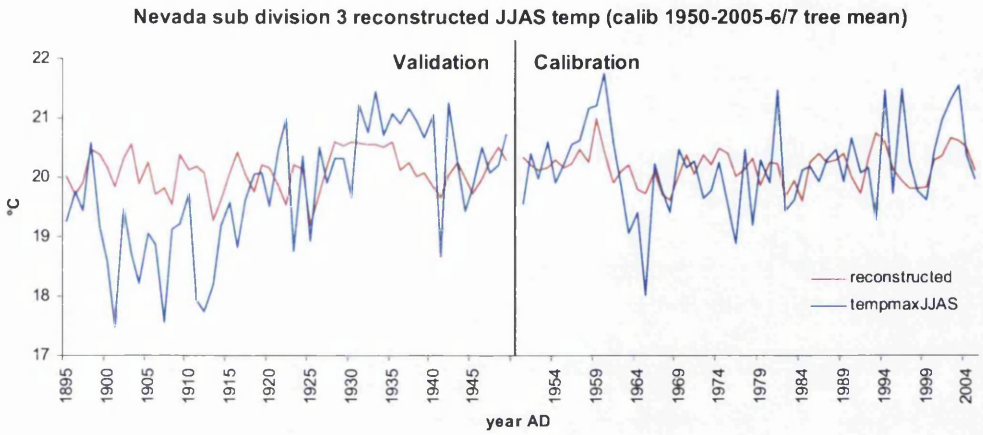

Figure 5.32. Using mean $\delta^{13}C_{pin}$/temperature relationship for 1950-2005 to reconstruct temperature values for 1895-1949.

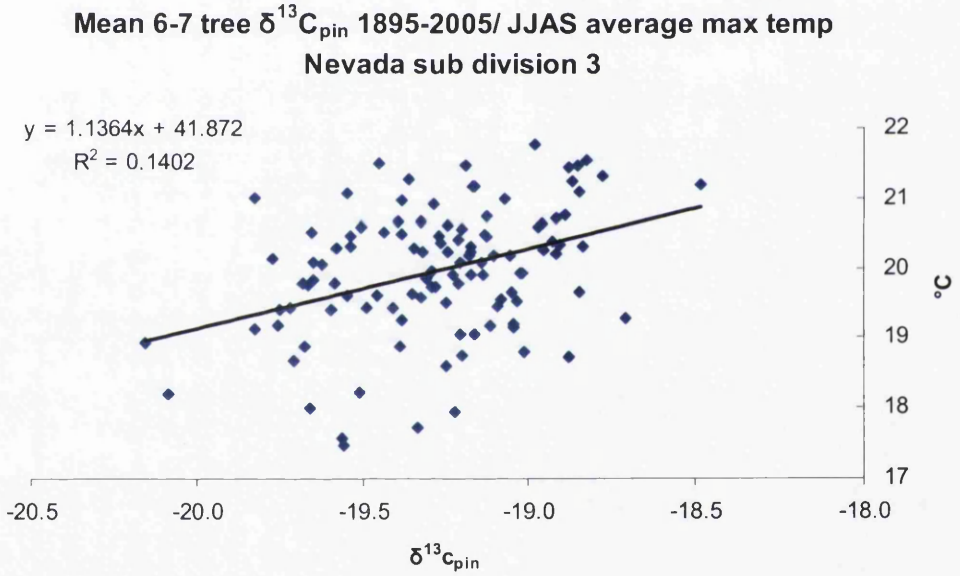

Figure 5.33. Mean $\delta^{13}C_{pin}$ and temperature linear relationship AD1895-2005

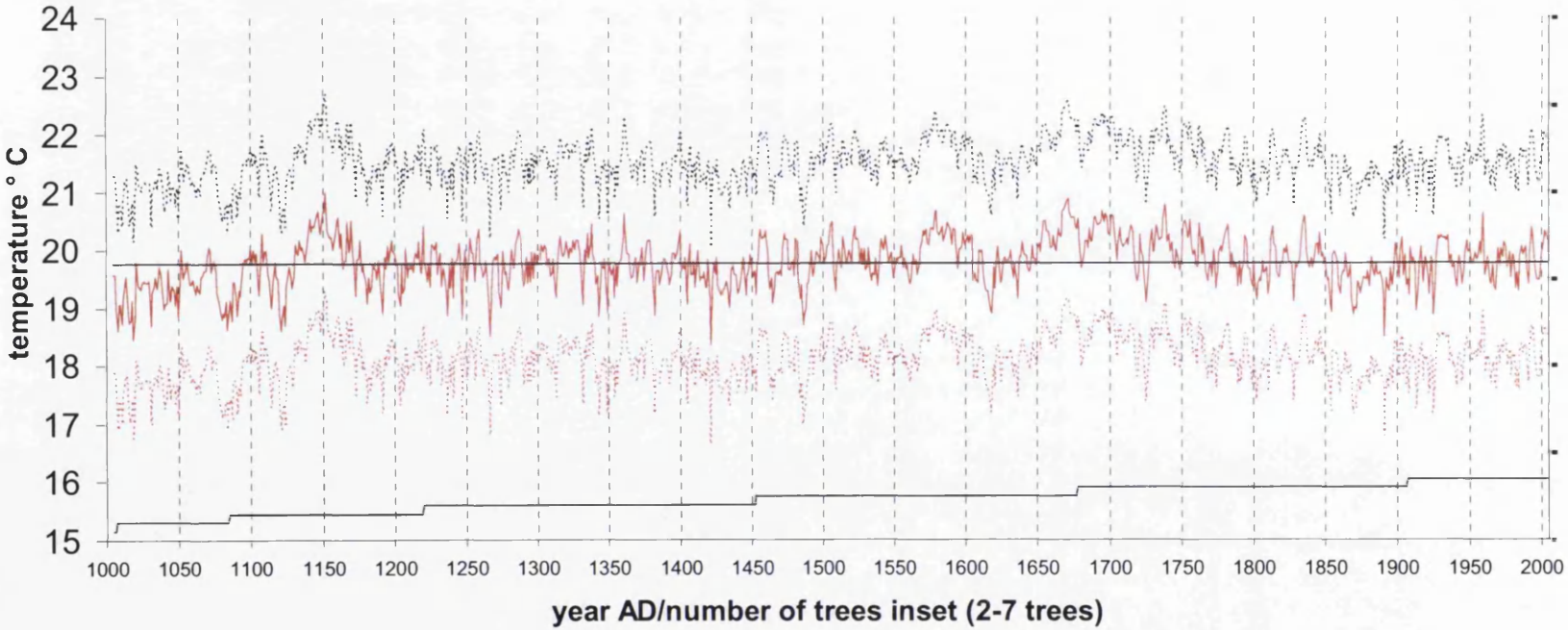

Figure 5.34.Reconstructed summer temperature for last 1000 years with error bars (2б) based on linear relationship between all tree (2-7) mean $\delta^{13}C_{pin}$ and actual Nevada sub division 3 June-September (JJAS) average maximum temperature AD1895-1949.

Bearing in mind the high degree of correlation between the 3-4 tree and 6-7 tree means (r=0.92) it is likely that both time series reflect summer temperature. A future research objective could involve adding further trees to the mean series may make a summer temperature reconstruction possible back to AD1000 that meets the necessary statistical standards for climatic reconstruction.

5.6: Precipitation

With all of the trees exhibiting significant negative correlation with total June to September (JJAS) precipitation it is more likely that all trees could be used in any accurate precipitation reconstruction. The same procedure to assess the degree of accuracy to which the calibration dataset is able to reconstruct climate was used with the precipitation data. The data was divided into two sets, 1895-1949 and 1950-2005.

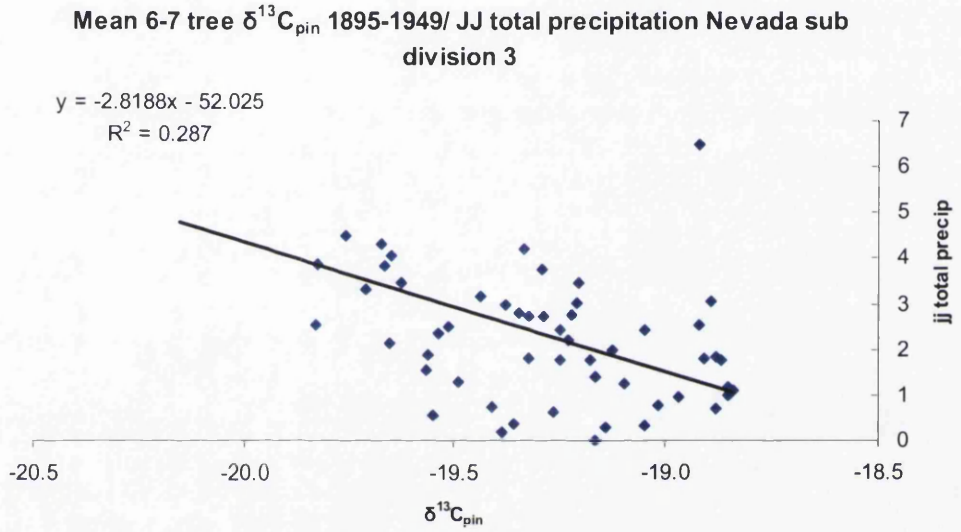

Figure 5.35. Mean $\delta^{13}C_{pin}$ and summer precipitation(cm) AD1895-1949

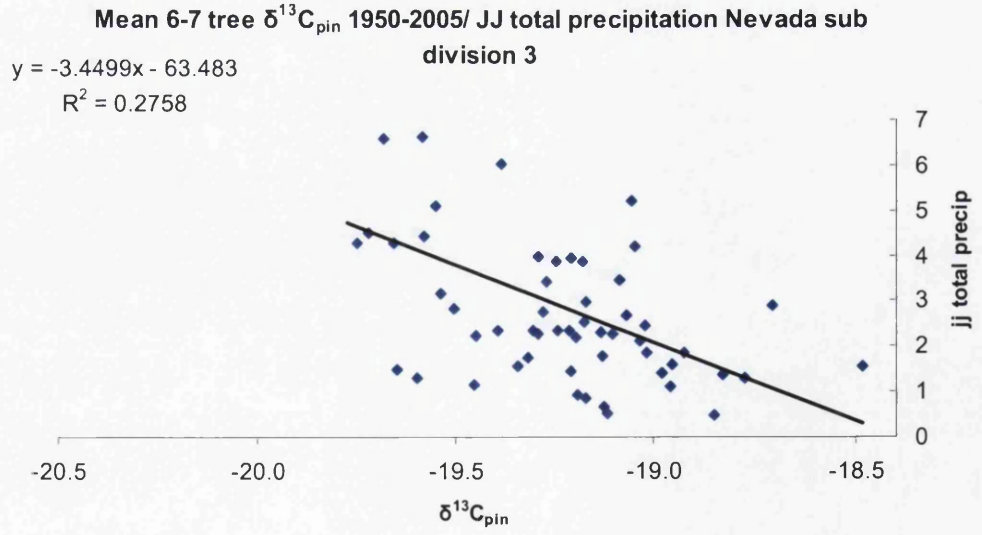

Figure 5.36. Mean $\delta^{13}C_{pin}$ and summer precipitation(cm) AD1950-2005

The ability of each data set to predict the precipitation of the other data set is assessed Firstly the 1895-1949 $\delta^{13}C_{pin}$ and precipitation relationship is used to reconstruct precipitation for 1950-2005.

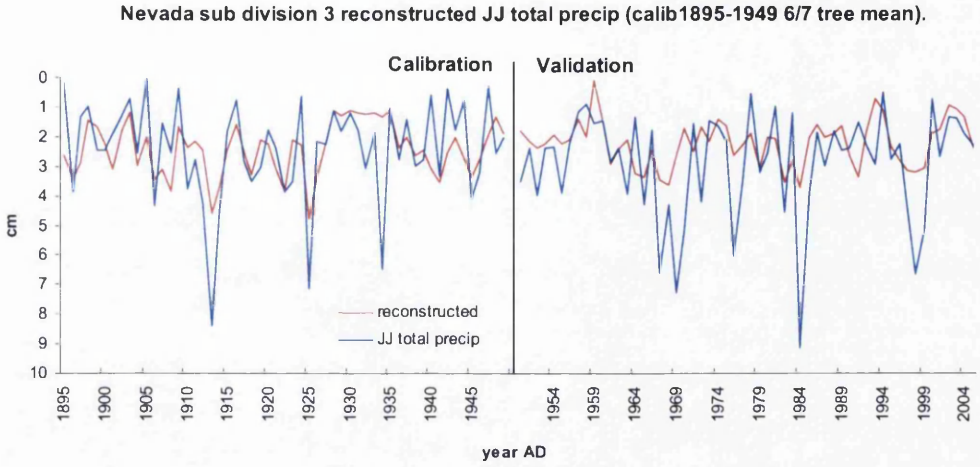

Figure 5.37. Mean $\delta^{13}C_{pin}$ and reconstructed summer precipitation based on 1895-1949 calibration.

1895-1949		**calibration**
MSE		2.73
RE		0.02
CE		NA
r^2		0.29
1950-2005		**validation**
MSE		2.56
RE		0.15
CE		0.08
r^2		0.29

Table 5.15. Measures of predictive ability for 1895-1949 calibration period.

Secondly the 1950-2005 $\delta^{13}C_{pin}$ and precipitation relationship is used to reconstruct precipitation for 1895-1949.

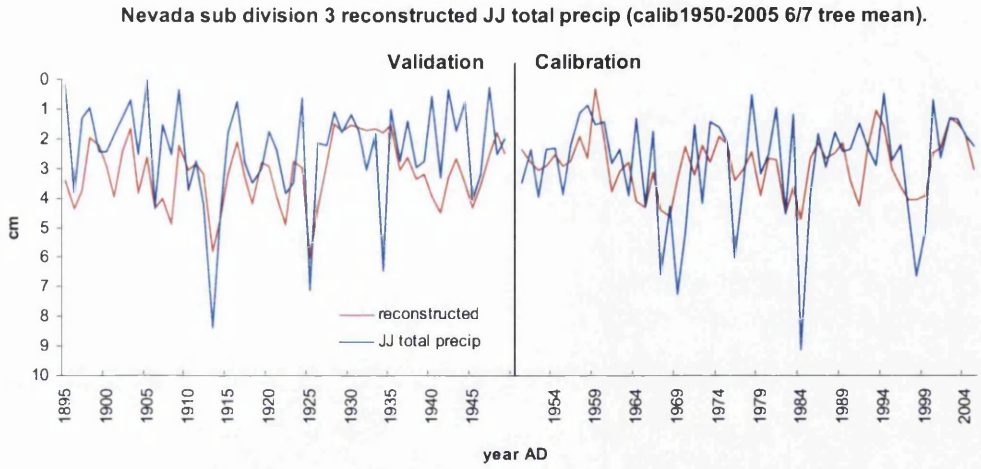

Figure 5.38. 6-7 tree mean $\delta^{13}C_{pin}$ reconstructed summer precipitation based on 1950-2005 calibration and JJ total precipitation 1895-2005.

1950-2005		**calibration**
MSE		2.32
RE		0.28
CE		NA
r^2		0.28
1895-1949		**validation**
MSE		2.82
RE		0.18
CE		0.12
r^2		0.28

Table 5.39. Measures of predictive ability for 1950-2005 calibration period.

As is evidenced both halves of the data are able to reconstruct precipitation for the other half of the data. Using the 1950-2005 period as calibration presents a slightly better reconstruction in terms of CE value but both sets seem to predict precipitation with some accuracy.

It is possible to use the mean of all trees for a precipitation reconstruction, using the 1895-1949 calibration period as the basis for the climate reconstruction. Both sets of data are effective in reconstructing precipitation so the relationship for the whole period can be applied to a reconstruction for the pre instrumental period.

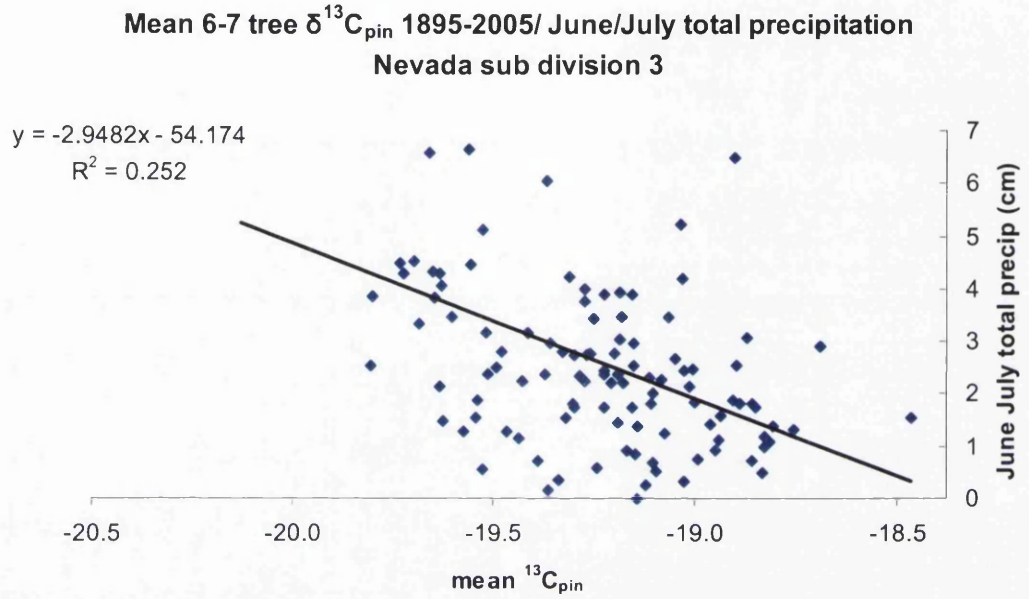

Figure 5.40. Linear relationship between mean $\delta^{13}C_{pin}$ and summer precipitation 1895-2005

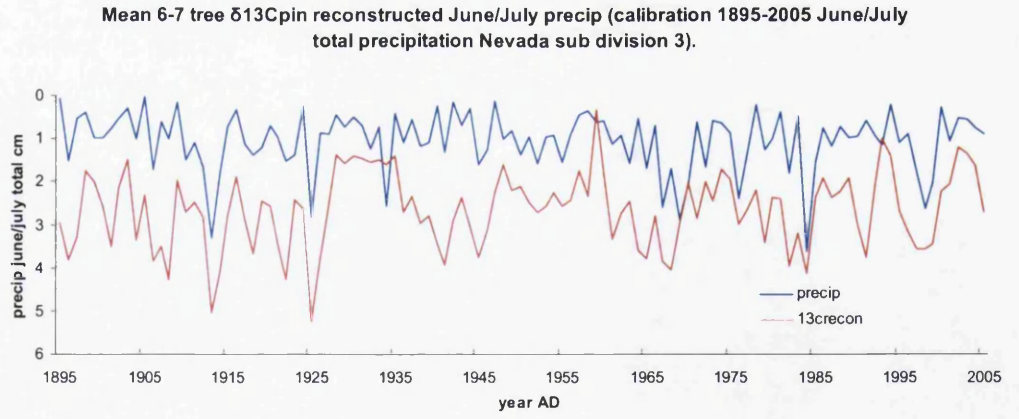

Figure 5.41. Reconstructed June/July precipitation (red) using calibration period 1895-2005 (r=0.51).

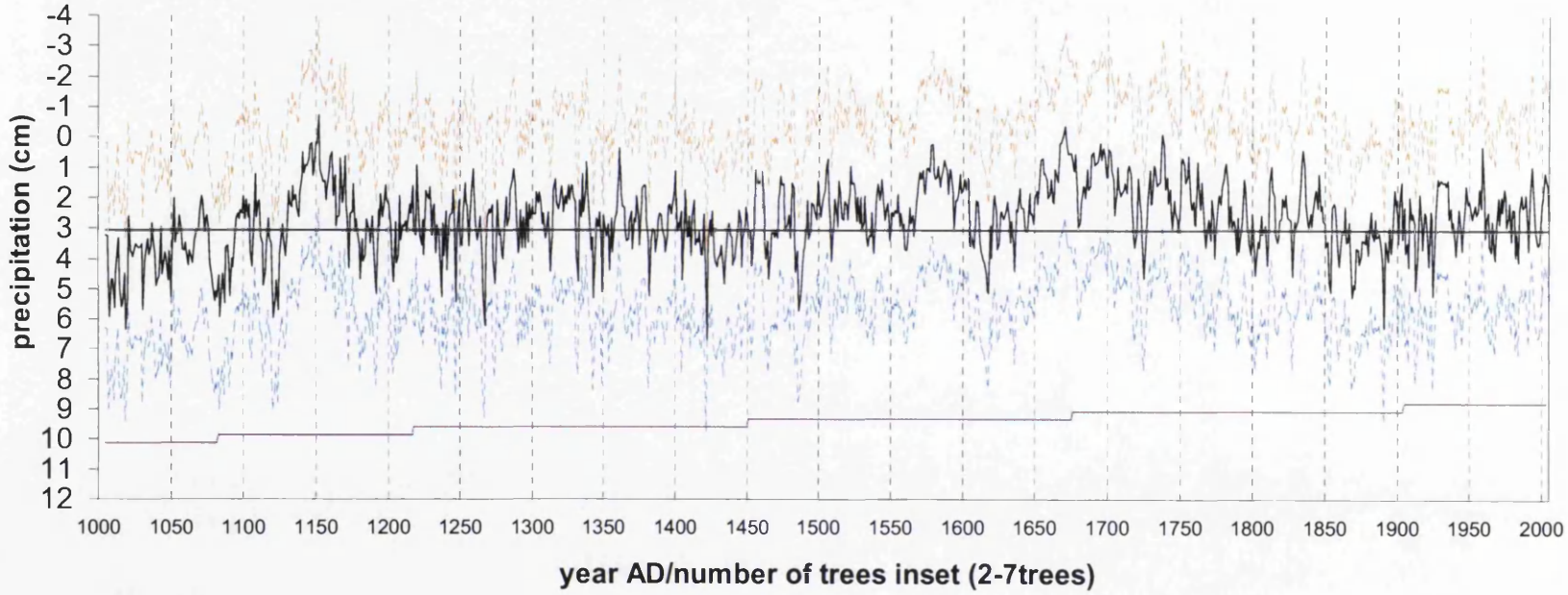

Figure 5.42. Reconstructed June/July precipitation (AD1005-2005) with error bars (2σ) based on calibration/validation relationship with total June/July (JJ) precipitation data (Nevada division 3 AD 1895-2005.) Precipitation is plotted on an inverse scale.

5.7: Spatial analysis

Worldwide instrumental climate data are also available from the Royal Netherlands Meteorological institute climate explorer webpage (Oldenborgh and Burgers, 2005). Climatic Research Unit (CRU) 0.5°, 1° and 2.5° meteorological data are available on this website along with a whole suite of other instrumental weather observations. The Blanco $\delta^{13}C_{pin}$ series was uploaded to the webpage and compared against instrumental data (chapters 5.8 to 5.13). The results confirm the findings from the comparisons with individual climate stations (chapter 5.5 and 5.6) and also give some idea of the range and nature of climatic influence on the $\delta^{13}C_{pin}$ ratios of the Blanco series. The CRU 0.5° data was used for this analysis.

5.8: June – September averaged maximum temperature.

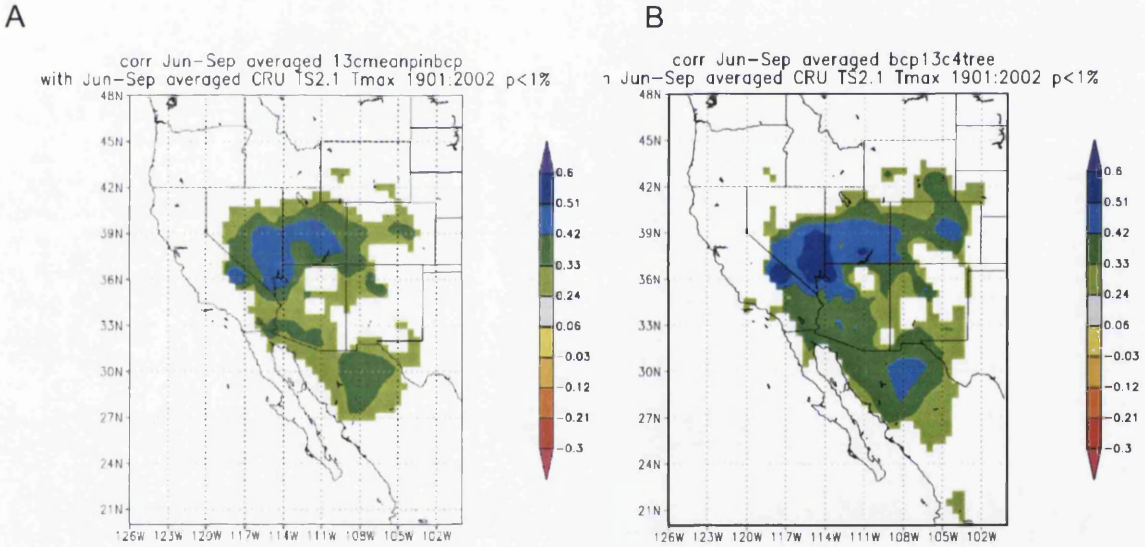

Figure 5.43. A) CRU 0.5° New World average Maximum JJAS temperature data and 7 tree mean $\delta^{13}C_{pin}$. The values on the legend refer to correlation (r) values. B) CRU 0.5° New World Maximum JJAS temperature data and 4 tree mean $\delta^{13}C_{pin}$.

5.9: Individual months June-September averaged maximum temperature

Figure 5.44 3-4 tree $\delta^{13}C_{pin}$ and individual months averaged maximum temperature (A=June, B=July, C=August, D=September).

A

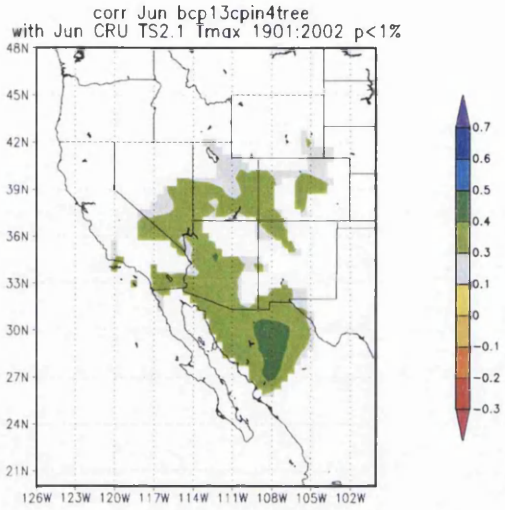

B

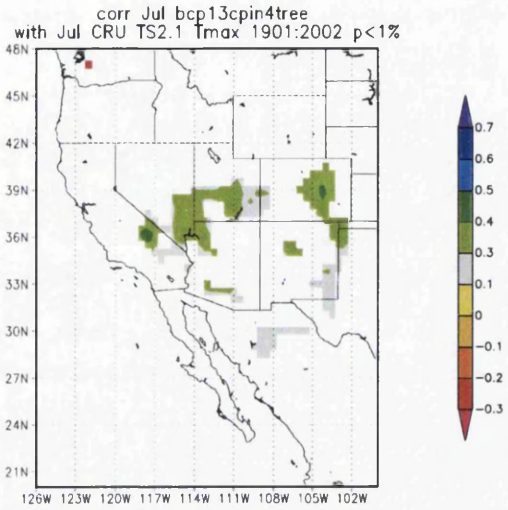

C

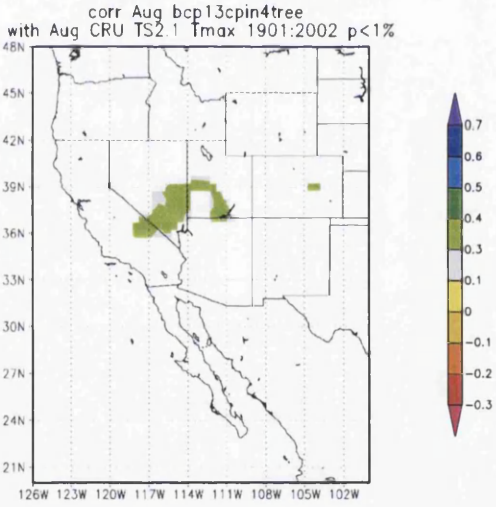

D

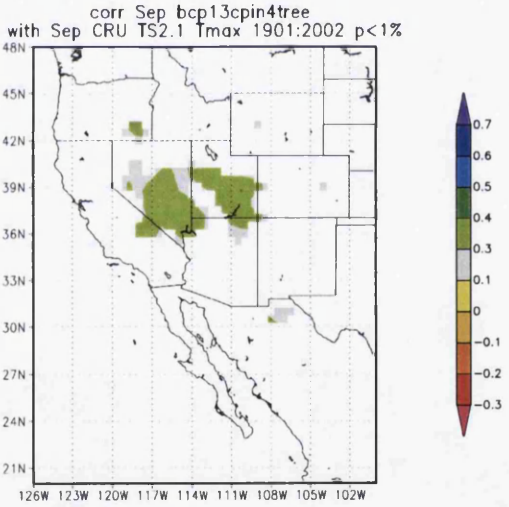

5.10: Individual months June-September maximum temperature

Figure 5.45 7tree $\delta^{13}C_{pin}$ and individual months averaged max temperature (A=June, B=July, C=August, D=September). June appears to be the month in which average maximum temperature has the strongest effect on $\delta^{13}C_{pin}$.

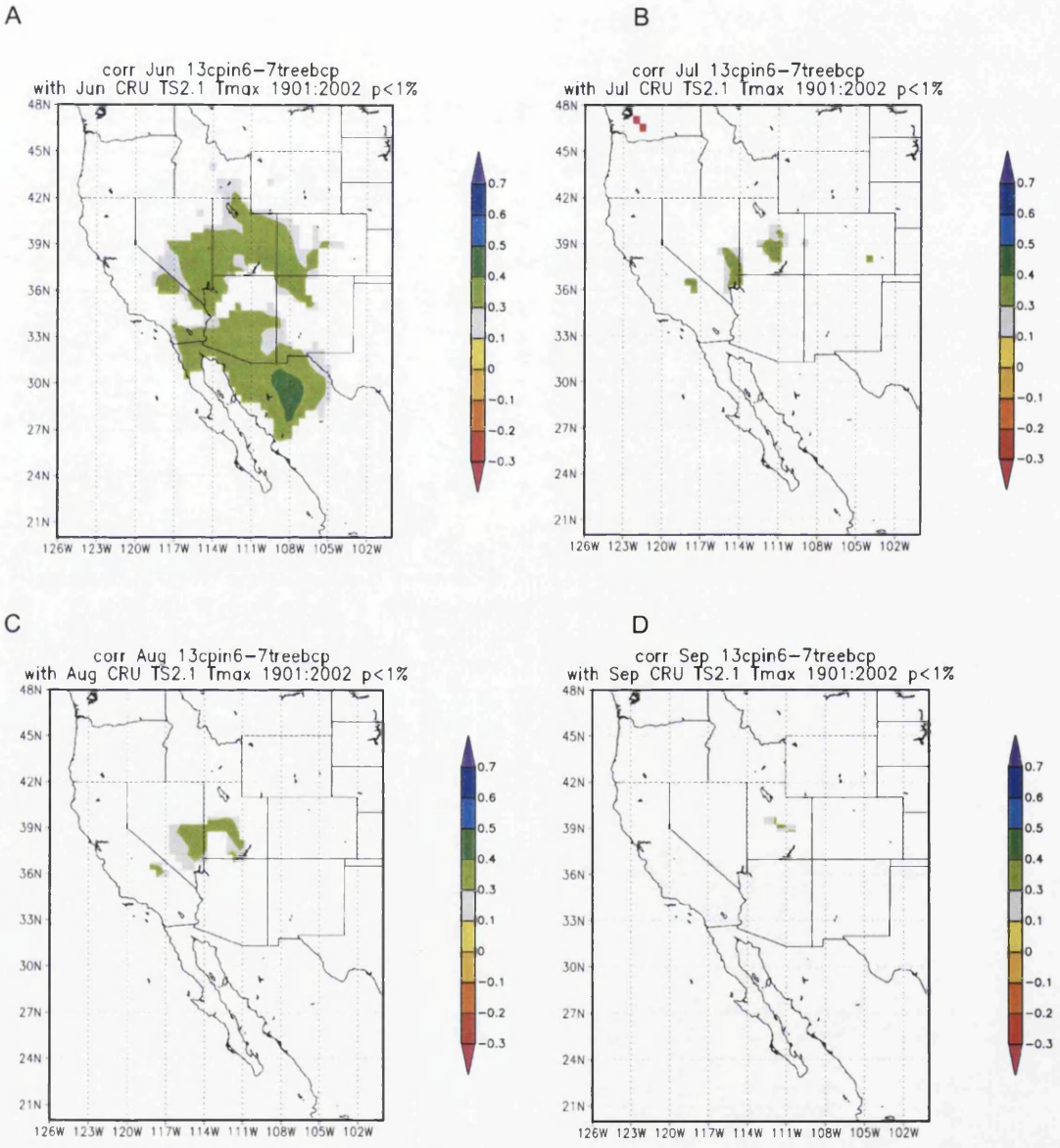

5.11 3 year smoothed June – September maximum temperature

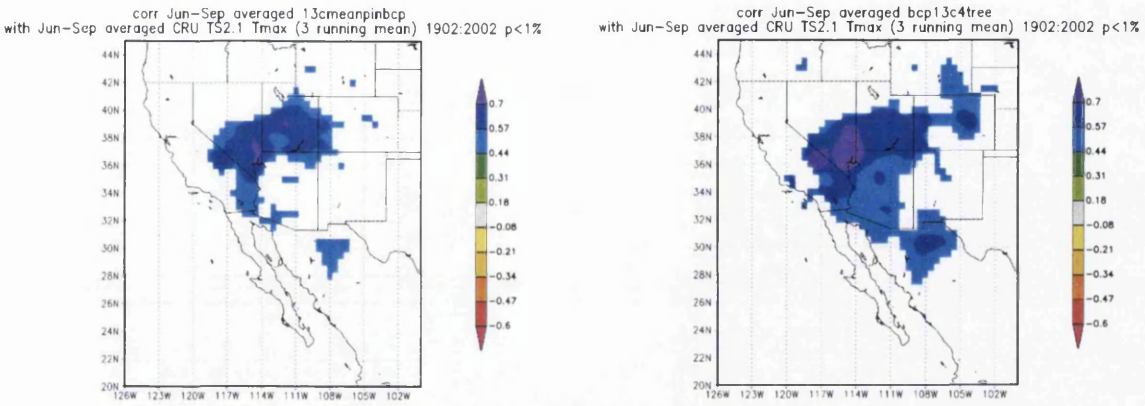

Figure 5.46. 3 year running mean June-September averaged maximum temperature/ $\delta^{13}C_{pin.}$ (Left) 7 tree mean. (Right) 4 tree mean. This figure demonstrates the improvement in correlation with average maximum summer temperature when the data is smoothed.

5.12: Individual months June-September precipitation

Figure 5.47: 7tree $\delta^{13}C_{pin}$ and individual months (A=June-September averaged/mean $\delta^{13}C_{pin}$, B= June-September averaged and reconstructed precipitation (all trees) C=June-August averaged precipitation, D=August precipitation, E=June precipitation, F= July precipitation).

A

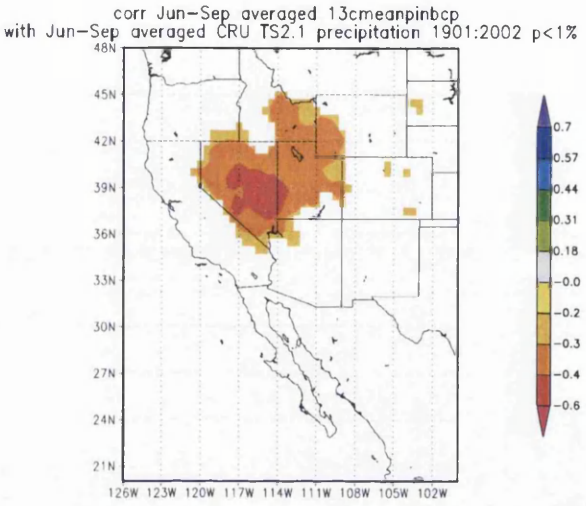

B

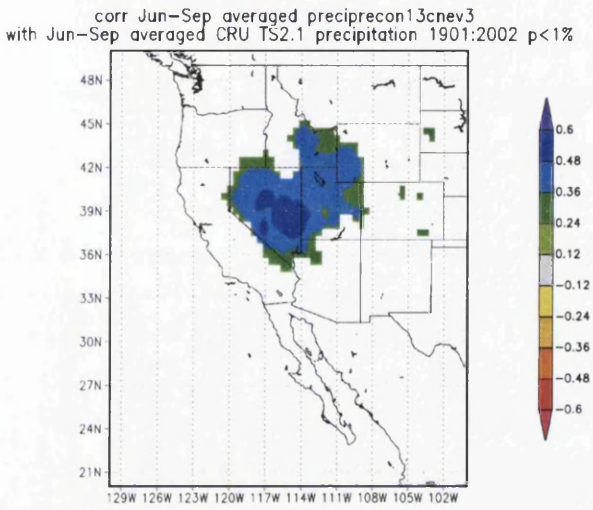

C

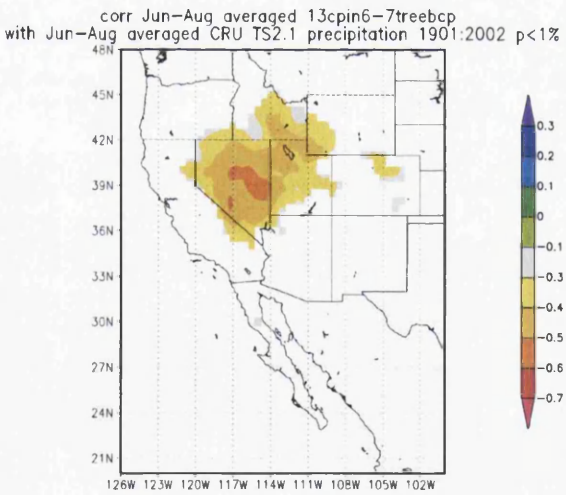

D

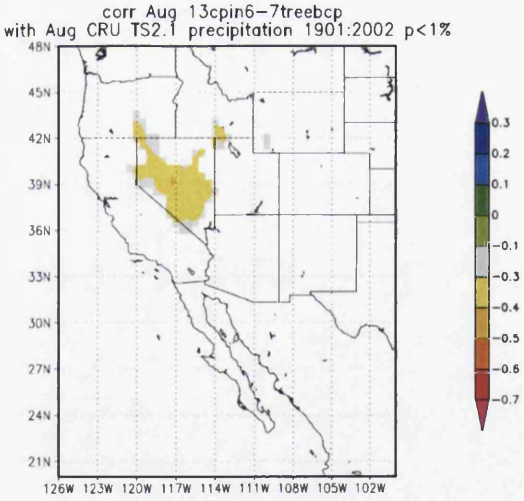

E

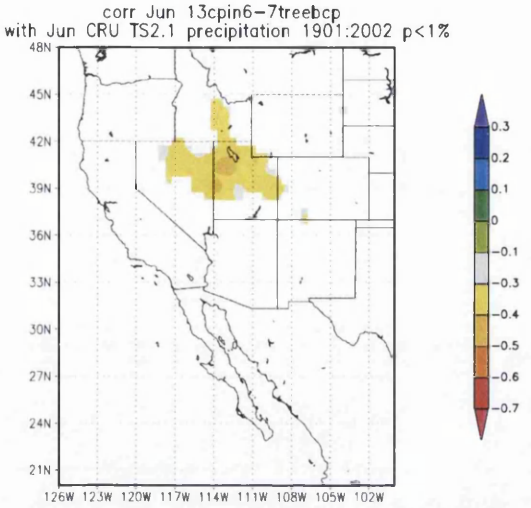
corr Jun 13cpin6–7treebcp
with Jun CRU TS2.1 precipitation 1901:2002 p<1%
48N
45N
42N
39N
36N
33N
30N
27N
24N
21N
126W 123W 120W 117W 114W 111W 108W 105W 102W
0.3
0.2
0.1
0
−0.1
−0.3
−0.4
−0.5
−0.6
−0.7

F

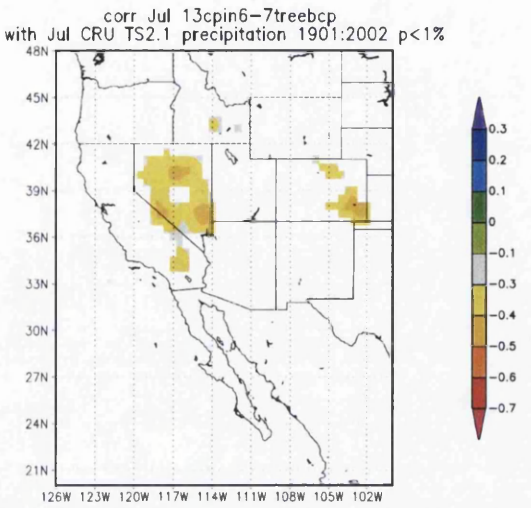
corr Jul 13cpin6–7treebcp
with Jul CRU TS2.1 precipitation 1901:2002 p<1%
48N
45N
42N
39N
36N
33N
30N
27N
24N
21N
126W 123W 120W 117W 114W 111W 108W 105W 102W
0.3
0.2
0.1
0
−0.1
−0.3
−0.4
−0.5
−0.6
−0.7

5.13: Individual months May-September Palmer Drought Severity Indices (PDSI)

Figure 5.48. Individual months (A=May, B= June, C=July, D= August, E=September, F=October, G=November, H=December) and precipitation/7tree $\delta^{13}C_{pin}$

A

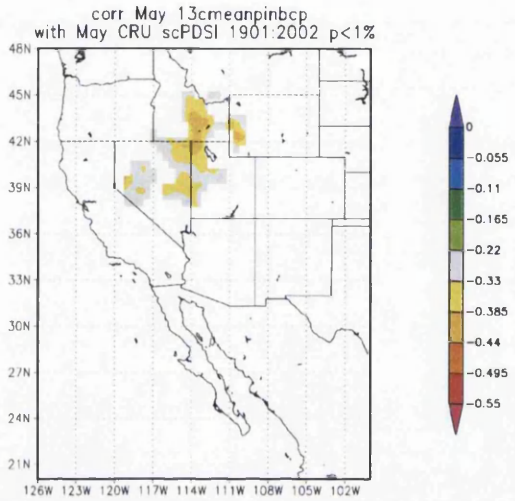

B

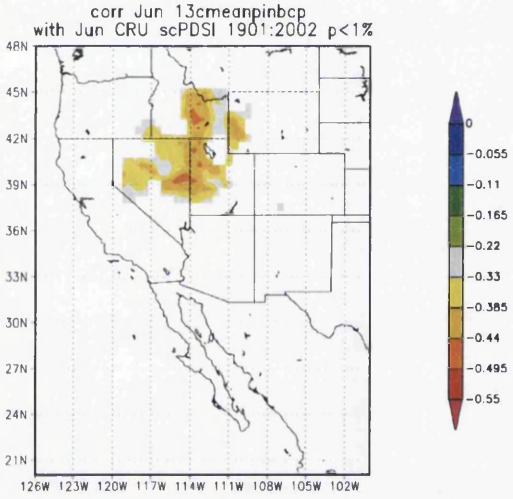

C

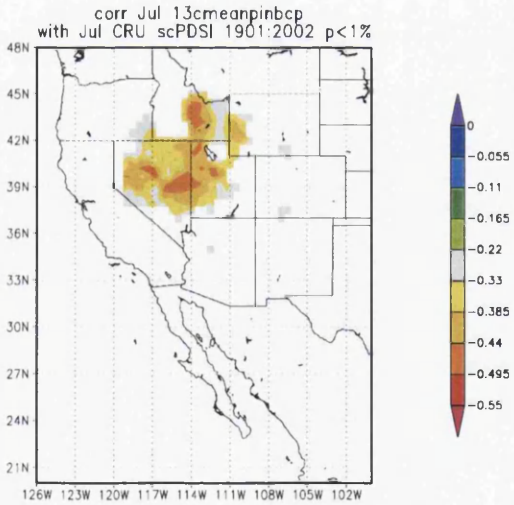

D

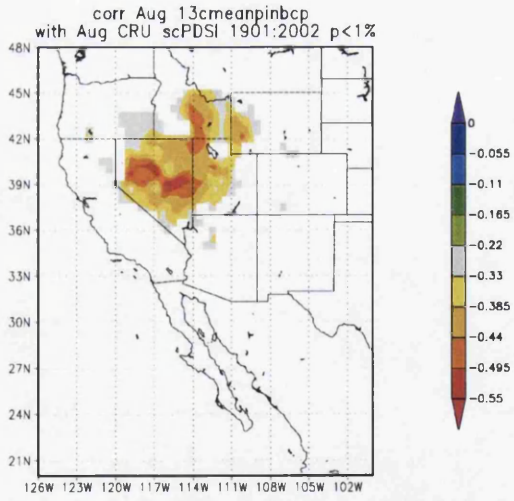

E

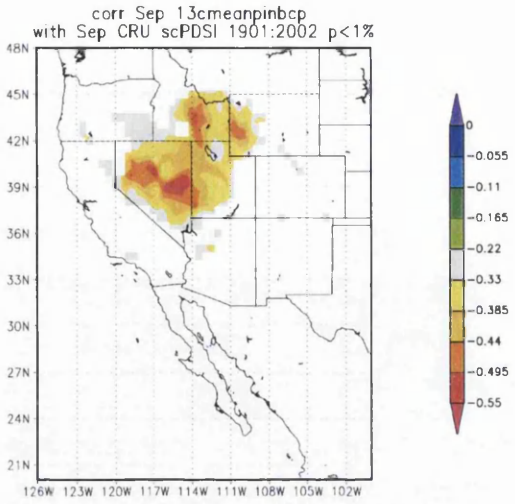
corr Sep 13cmeanpinbcp
with Sep CRU scPDSI 1901:2002 p<1%
48N
45N
42N
39N
36N
33N
30N
27N
24N
21N
126W 123W 120W 117W 114W 111W 108W 105W 102W
0
-0.055
-0.11
-0.165
-0.22
-0.33
-0.385
-0.44
-0.495
-0.55

F

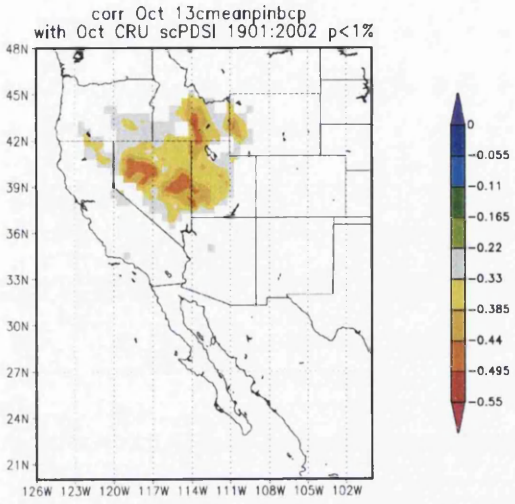
corr Oct 13cmeanpinbcp
with Oct CRU scPDSI 1901:2002 p<1%
48N
45N
42N
39N
36N
33N
30N
27N
24N
21N
126W 123W 120W 117W 114W 111W 108W 105W 102W
0
-0.055
-0.11
-0.165
-0.22
-0.33
-0.385
-0.44
-0.495
-0.55

G

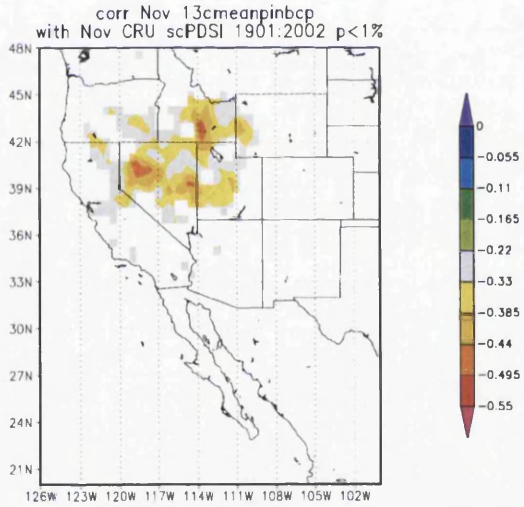
corr Nov 13cmeanpinbcp
with Nov CRU scPDSI 1901:2002 p<1%
48N
45N
42N
39N
36N
33N
30N
27N
24N
21N
126W 123W 120W 117W 114W 111W 108W 105W 102W
0
-0.055
-0.11
-0.165
-0.22
-0.33
-0.385
-0.44
-0.495
-0.55

H

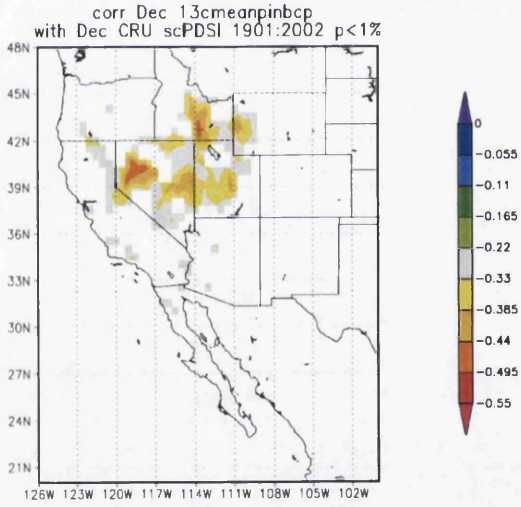
corr Dec 13cmeanpinbcp
with Dec CRU scPDSI 1901:2002 p<1%
48N
45N
42N
39N
36N
33N
30N
27N
24N
21N
126W 123W 120W 117W 114W 111W 108W 105W 102W
0
-0.055
-0.11
-0.165
-0.22
-0.33
-0.385
-0.44
-0.495
-0.55

5.14: Interpretation of $\delta^{13}C_{pin}$ data- summary

The $\delta^{13}C$ values of the Blanco bristlecone pines are being influenced primarily by summer weather conditions. The correlations with both summer temperature and precipitation are statistically significant ($p \leq 0.01$) when compared with the closest meteorological data and gridded data. Stronger lower frequency (two-seven years) correlations are evident with temperature and higher annual correlations are evident for comparison with instrumental precipitation data. Correlation between precipitation and $\delta^{13}C$ is not improved by smoothing the time series. Low frequency $\delta^{13}C$ values are influenced by average maximum summer June-September (JJAS) temperature as evidenced by the high correlation (*r*) values that occur when the data are smoothed to three, four, five, six and seven year means (for example figures 5.46, 7.18, 7.19 and 7.20). That the high frequency variations in frequency $\delta^{13}C$ values are influenced by growing season total June and July (JJ) precipitation is evidenced by high correlation (*r*) values for annually resolved data (figure 5.50 to figure 5.57) with little, if any improvement in correlation if the time series are smoothed. This may be due to the long retention of needles (LaMarche, 1974). In effect, the temperature signal contained within the $\delta^{13}C$ series could be 'smoothed' over several years due to the large stable needle mass. The $\delta^{13}C$ variations also reflect the importance of actual growing season moisture availability on photosynthetic activity, as evidenced in the correlations between $\delta^{13}C$ and total June/July precipitation.

Strong continental influence is evidenced particularly with precipitation data. Spatial analysis demonstrates that the area of climate correlation, with temperature and precipitation, corresponds roughly to the areas in bristlecone pine predominates, that is eastern California, Nevada and western Arizona. It is interesting that Powell and Klieforth (1991) note that airflow from the east (i.e continental) only occurs during the summer months, at the same time of year that tree growth is taking place. The correlations evident in the north of Mexico may indicate Gulf influence. However caution must be exercised when interpreting the spatial analysis. The density of weather stations in this part of the United States is low and 'hot spots' of correlation may simply reflect the location of isolated desert weather stations. High frequency

correlations with regional summer temperature are highest in three of the trees $\delta^{13}C_{pin}$ data and the $\delta^{13}C_{pin}$ mean. Extreme annual $\delta^{13}C$ events that fall within the instrumental period can be linked to real weather/climate events and documentary evidence.

Now that the $\delta^{13}C$ data has a climatic 'context', the data in its entirety is reviewed in detail and suggestions offered for both the high and low frequency events that are apparent in this millennial length data set. To achieve this the data was broken down into 50 year and then 150 year blocks to identify any significant trends or climatic episodes of both high and low frequency, With reference to other climate reconstructions from the western United States the Blanco $\delta^{13}C$ was put into a regional context and any similarities or differences between it and the other data were identified. The first period that was examined was the last 150 years, the period for which instrumental and documentary evidence was most readily available.

6.1. $\delta^{13}C$ data analysis

The annually resolved data, from individual trees, from AD1005-2005 allows greater confidence to be placed into the significance of any environmental event as reflected in the $\delta^{13}C$ ratios. Unusual weather events that have occurred in historic times, recorded in documentary and instrumental records can be related to the $\delta^{13}C$ record and the significance of environmental events in a given year may be ascertained, as can the 'recovery' period of the tree as evidenced in the $\delta^{13}C$ values. Considering the annual nature of the record the extreme values present both in the $\delta^{13}C$ data and the reconstructed temperature and precipitation values are examined. The two tables (tables 6.1 and 6.2) list extreme events (both positive and negative) for each century that comprises the $\delta^{13}C$ chronology. Linked with this is a set of figures (6.1 to 6.12) illustrating the $\delta^{13}C$ values as normalised indices for each century. The $\delta^{13}C_{raw}$, $\delta^{13}C_{cor}$ and $\delta^{13}C_{pin}$ data is included as an appendix (appendix 1) that contains annual $\delta^{13}C$ values for individual trees and the mean. The annual, and lower frequency fluctuations are a sensitive reflection of summer moisture and temperature conditions in a fragile semi arid environment, that can be interpreted in terms of both a trees physiological response over a millennium and also in terms of the effects that droughts, volcanoes and other environmental phenomena may have had on human communities over the last 1000 years.

Table 6.1: Most extreme 20 years (the 10most positive years(+) and 10 most negative years (-) in each century based on temperature reconstruction. The years presented are for the temperature reconstruction based on the $\delta^{13}C$ values for 3- 4 tree mean. Temperature was reconstructed using the regression equation apparent from the relationship between instrumental June, July, August, September average maximum temperature (Nevada division 3) and Blanco $\delta^{13}C$ for the period 1895-1949.

	(+)	(-)		(+)	(-)		(+)	(-)
11th century	1021	1008	15th century	1400	1405	19th century	1832	1802
	1022	1011		1404	1422		1833	1803
	1024	1015		1407	1434		1834	1810
	1025	1019		1410	1440		1835	1817
	1028	1031		1413	1446		1836	1828
	1052	1050		1456	1463		1856	1853
	1068	1080		1460	1465		1857	1868
	1070	1084		1473	1486		1862	1869
	1071	1087		1474	1487		1864	1871
	1072	1091		1481	1488		1898	1891
12th century	1141	1120	16th century	1505	1509	20th century	1928	1906
	1142	1121		1506	1533		1930	1908
	1143	1122		1522	1534		1931	1913
	1146	1123		1525	1538		1935	1914
	1147	1124		1544	1549		1948	1925
	1150	1173		1578	1560		1959	1968
	1152	1180		1579	1561		1974	1982
	1160	1181		1588	1562		1993	1983
	1161	1191		1591	1566		1994	1991
	1167	1192		1598	1567		2002	1998
13th century	1220	1204	17th century	1601	1615			
	1226	1206		1604	1616			
	1227	1237		1639	1617			
	1229	1241		1640	1618			
	1245	1247		1641	1636			
	1253	1266		1667	1663			
	1258	1267		1669	1679			
	1259	1274		1670	1680			
	1286	1279		1671	1681			
	1287	1280		1672	1682			
14th century	1316	1313	18th century	1701	1718			
	1327	1331		1702	1725			
	1328	1332		1715	1726			
	1335	1343		1732	1744			
	1338	1349		1738	1745			
	1360	1354		1751	1774			
	1361	1381		1752	1789			
	1377	1382		1762	1791			
	1378	1386		1780	1798			

Table 6.2: Most extreme 20 years(10most positive years (+) and 10 most negative years (-) in each century based on precipitation reconstruction. The years presented here are from the precipitation reconstruction based on the $\delta^{13}C$ values from 7 tree mean. Precipitation is reconstructed using the regression equation apparent from the relationship between total June/July precipitation (Nevada division 3) and $\delta^{13}C$ for the period 1895-2005).

	(+)	(-)		(+)	(-)		(+)	(-)
11th century	1005	1008	15th century	1400	1405	19th century	1813	1801
	1006	1011		1407	1422		1834	1802
	1021	1016		1413	1429		1835	1803
	1037	1019		1444	1434		1836	1810
	1043	1031		1449	1446		1846	1828
	1052	1050		1456	1465		1856	1854
	1070	1080		1459	1484		1857	1869
	1071	1082		1460	1486		1864	1870
	1072	1084		1473	1487		1898	1871
	1098	1087		1499	1488		1899	1891
12th century	1141	1114	16th century	1505	1509	20th century	1903	1908
	1143	1120		1506	1534		1928	1913
	1145	1121		1514	1538		1930	1914
	1146	1122		1522	1539		1931	1922
	1147	1124		1544	1549		1935	1925
	1150	1173		1578	1550		1959	1965
	1151	1181		1579	1560		1993	1967
	1152	1183		1583	1561		1994	1968
	1161	1191		1587	1562		2002	1982
	1170	1192		1588	1566		2003	1984
13th century	1217	1203	17th century	1600	1615			
	1220	1204		1601	1616			
	1226	1237		1603	1617			
	1229	1241		1604	1618			
	1245	1247		1639	1636			
	1253	1266		1667	1652			
	1258	1267		1669	1663			
	1259	1273		1670	1680			
	1286	1274		1671	1681			
	1287	1275		1695	1682			
14th century	1316	1313	18th century	1701	1718			
	1325	1331		1702	1719			
	1327	1332		1737	1724			
	1335	1343		1738	1725			
	1338	1349		1739	1726			
	1360	1354		1751	1768			
	1361	1356		1752	1774			
	1377	1382		1756	1789			
	1378	1386		1762	1791			
	1379	1393		1782	1799			

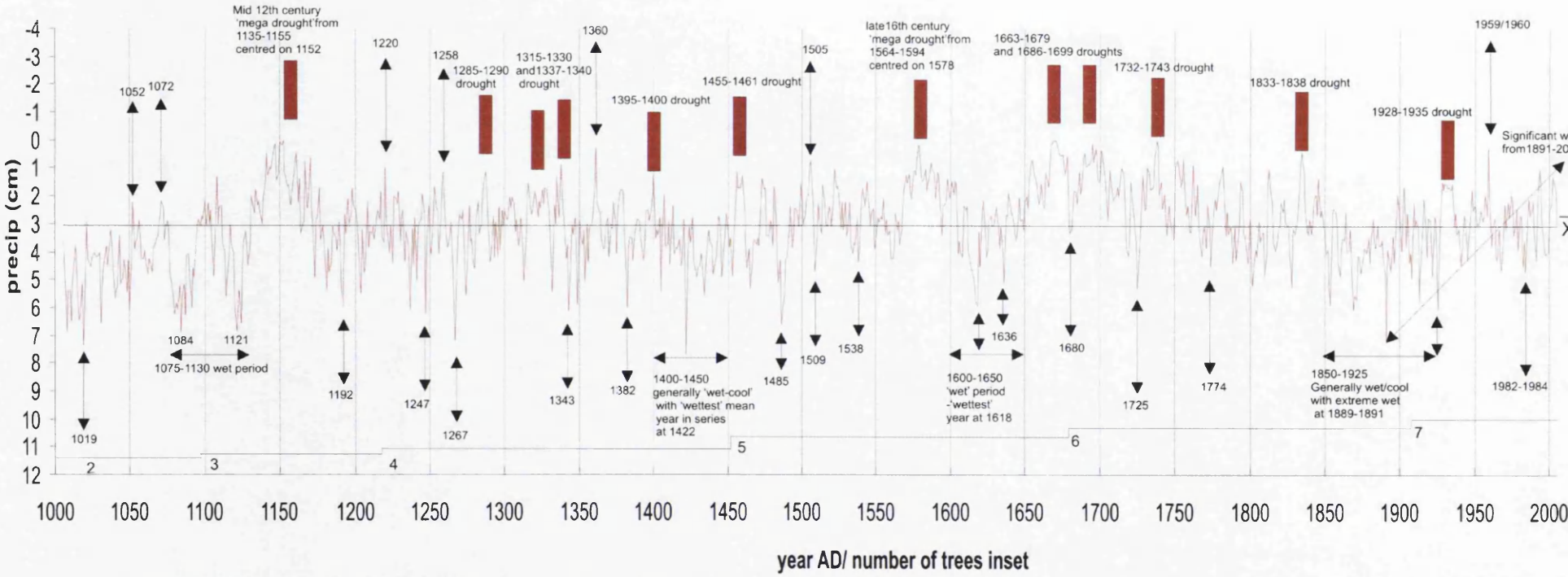

Figure 6.1: Major climatic events of the last 1000 years as evidenced by $\delta^{13}C$ values of the from bristlecone pine tree ring cellulose. The major droughts are indicated as are 'wet/cool' intervals. The 2 most extreme positive and negative values in each century are also indicated. Although the 2-7 tree precipitation reconstruction has been used for this figure, the similarities between this and the temperature reconstruction suggest that both temperature and precipitation influence the $\delta^{13}C$ values, and subtle differences in extreme years may be observed with reference to tables 6.1 and 6.2. Tables 6.1 and 6.2 can be used to add further detail to this figure. Number of trees comprising the Blanco $\delta^{13}C$ chronology is inset at bottom of figure(2-7 trees). The following figures (figures 6.3 to 6.13 illustrate the Blanco $\delta^{13}C$ series in more detail, century by century). Precipitation scale is inverse.

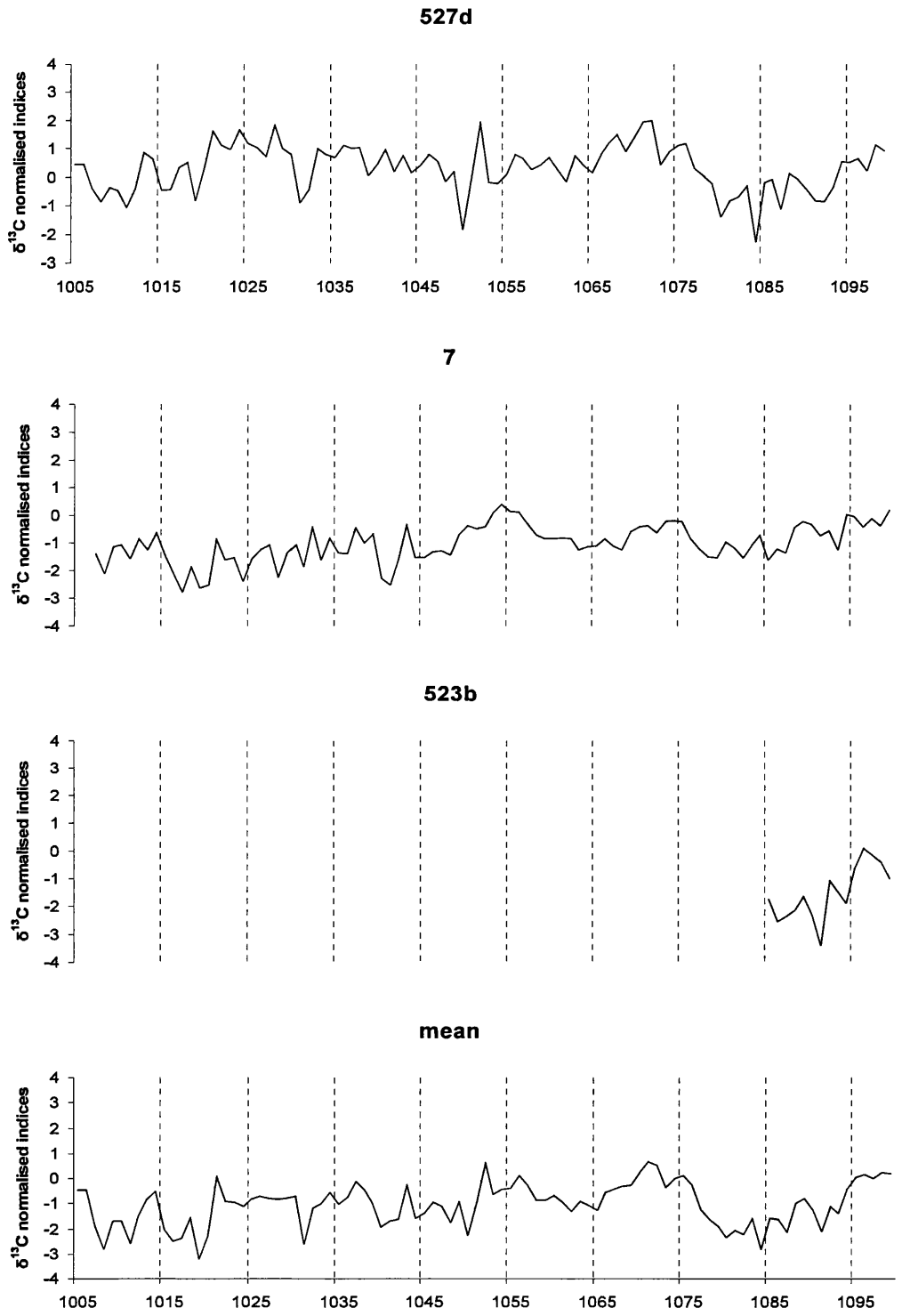

Figure 6.2: 11th century AD normalized raw $\delta^{13}C$ indices for individual trees and mean.

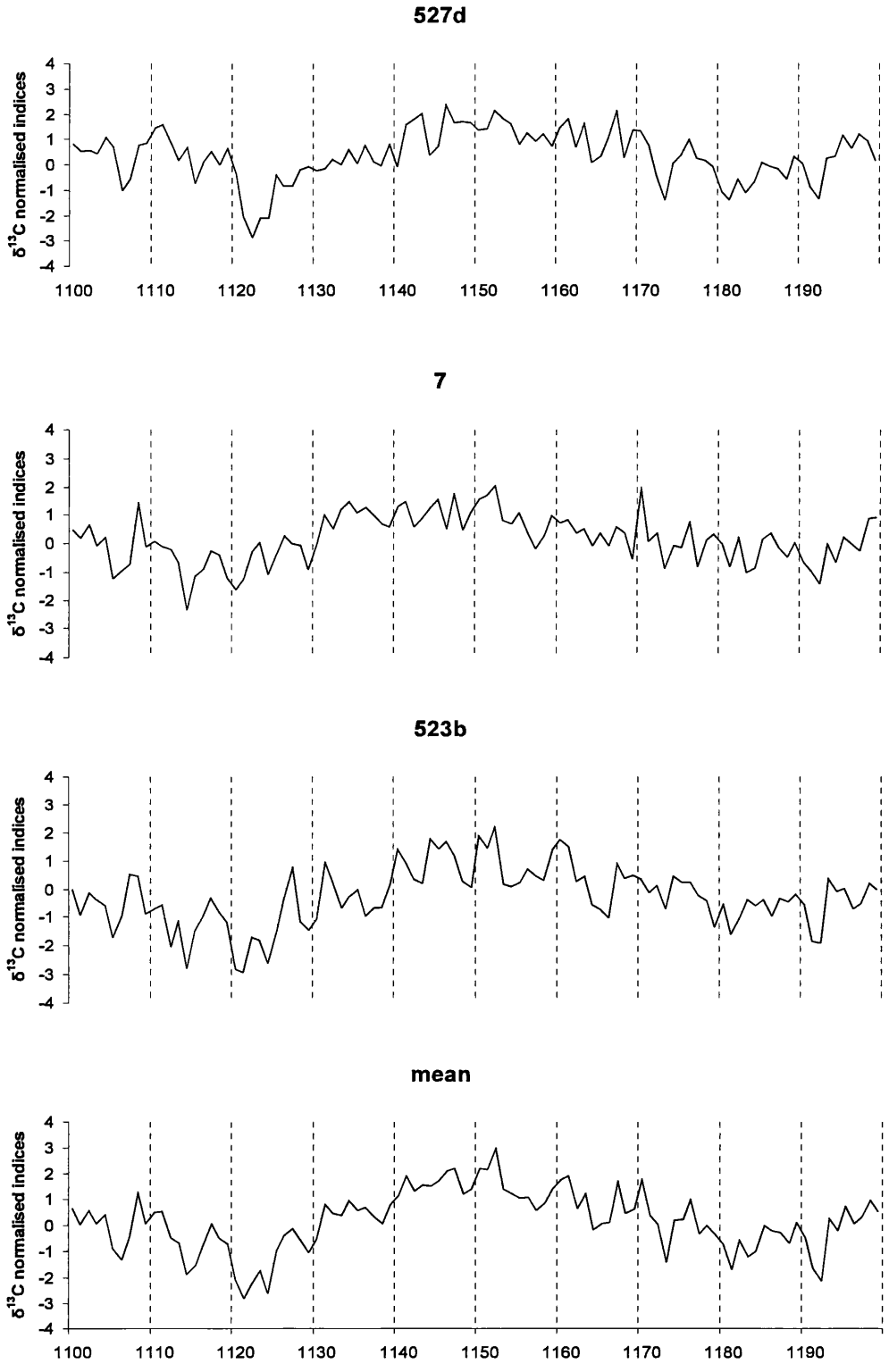

Figure 6.3:12th century AD normalized raw $\delta^{13}C$ indices

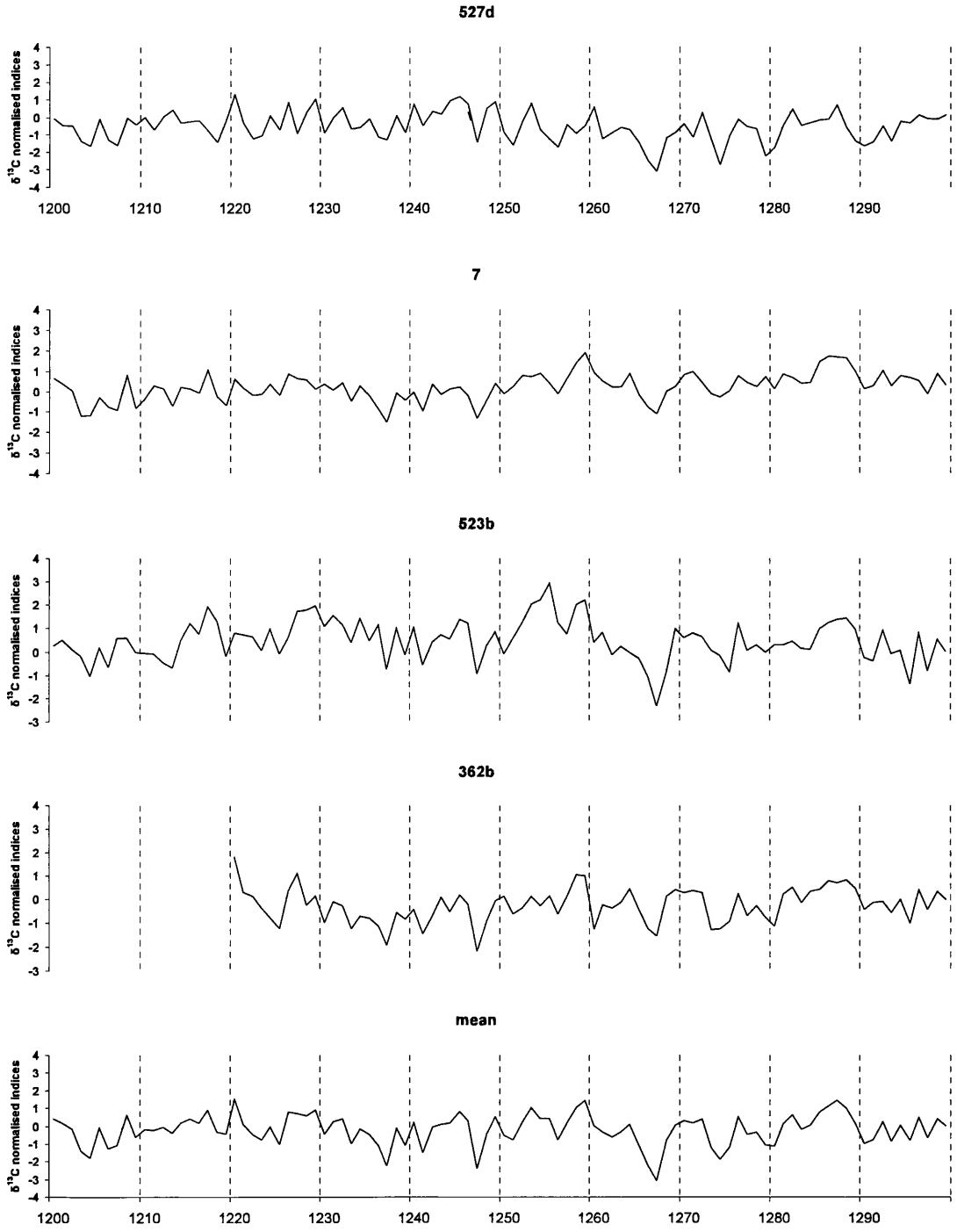

Figure 6.4: 13th century AD normalized raw $\delta^{13}C$ indices

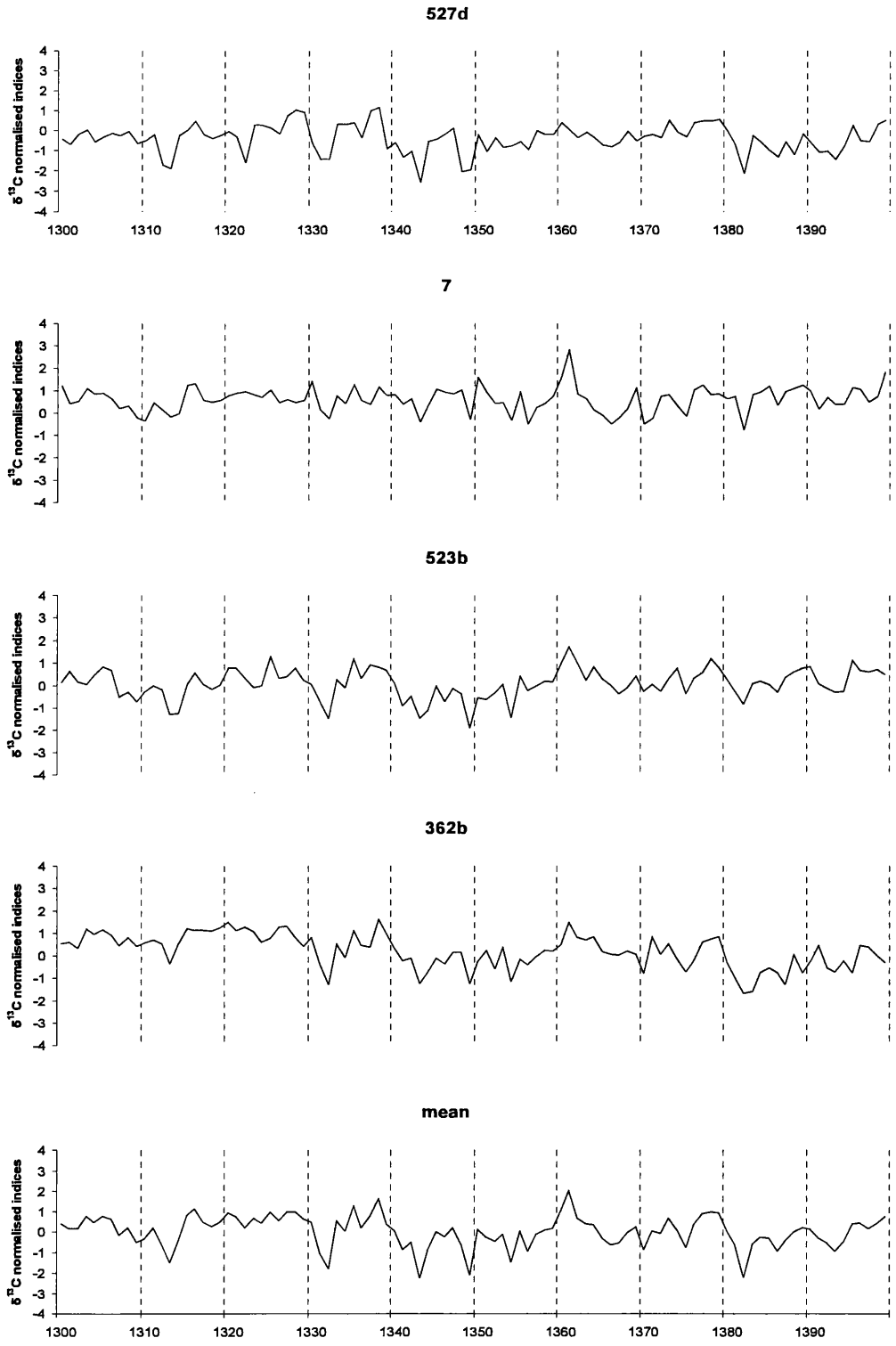

Figure 6.5: 14th century AD normalized raw $\delta^{13}C$ indices

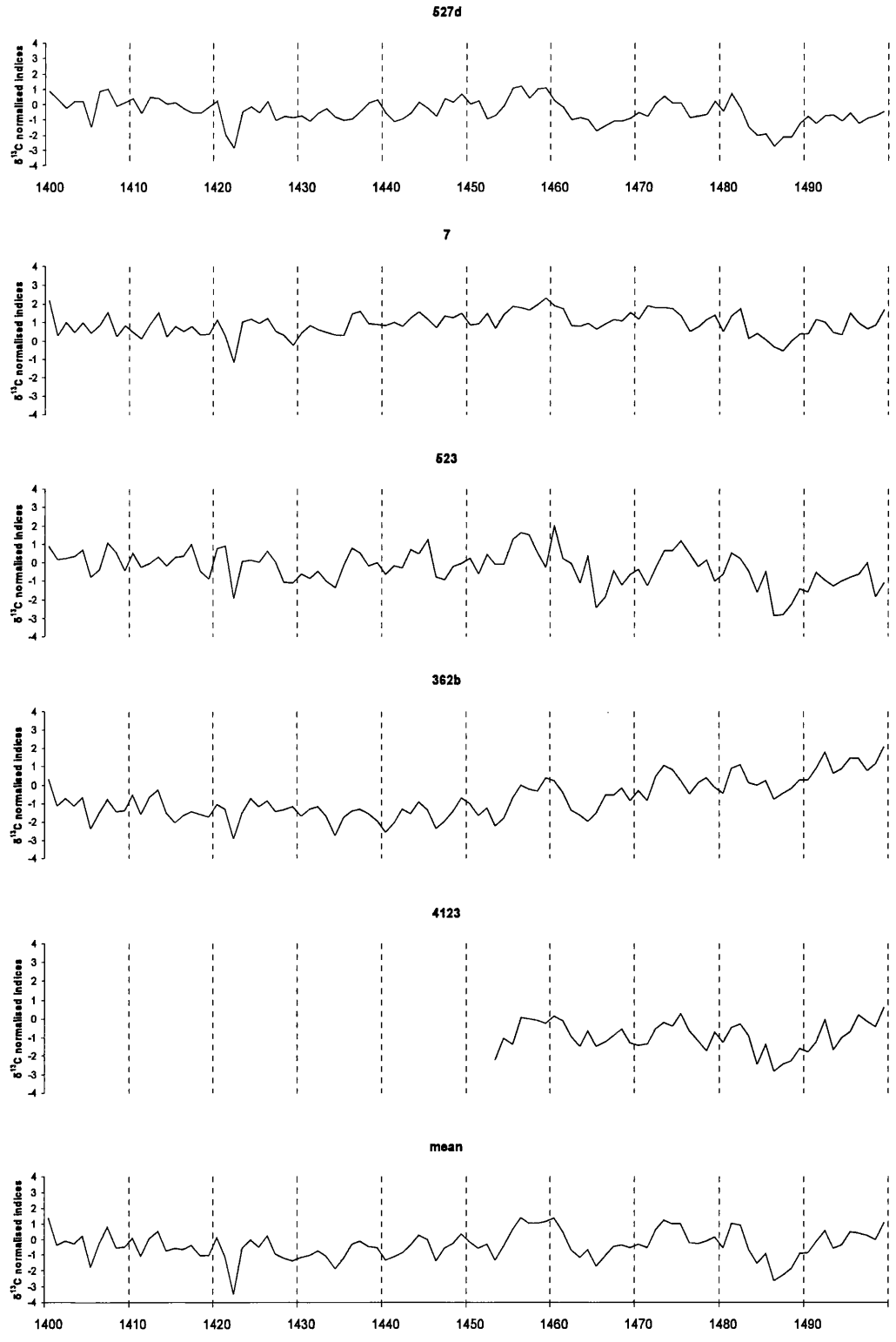

Figure 6.6: 15th century AD normalized raw $\delta^{13}C$ indices

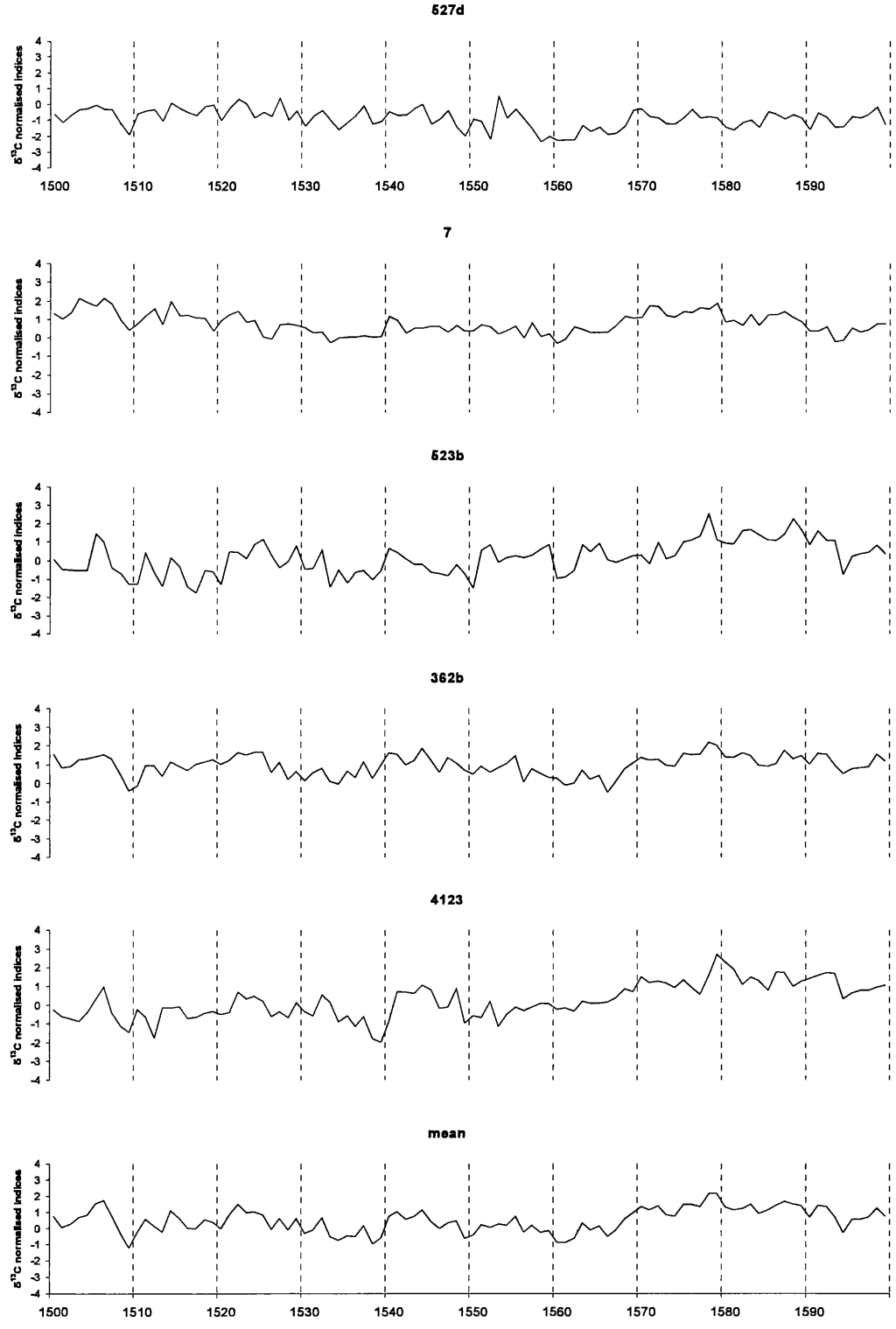

Figure 6,7: 16th century AD normalized raw $\delta^{13}C$ indices

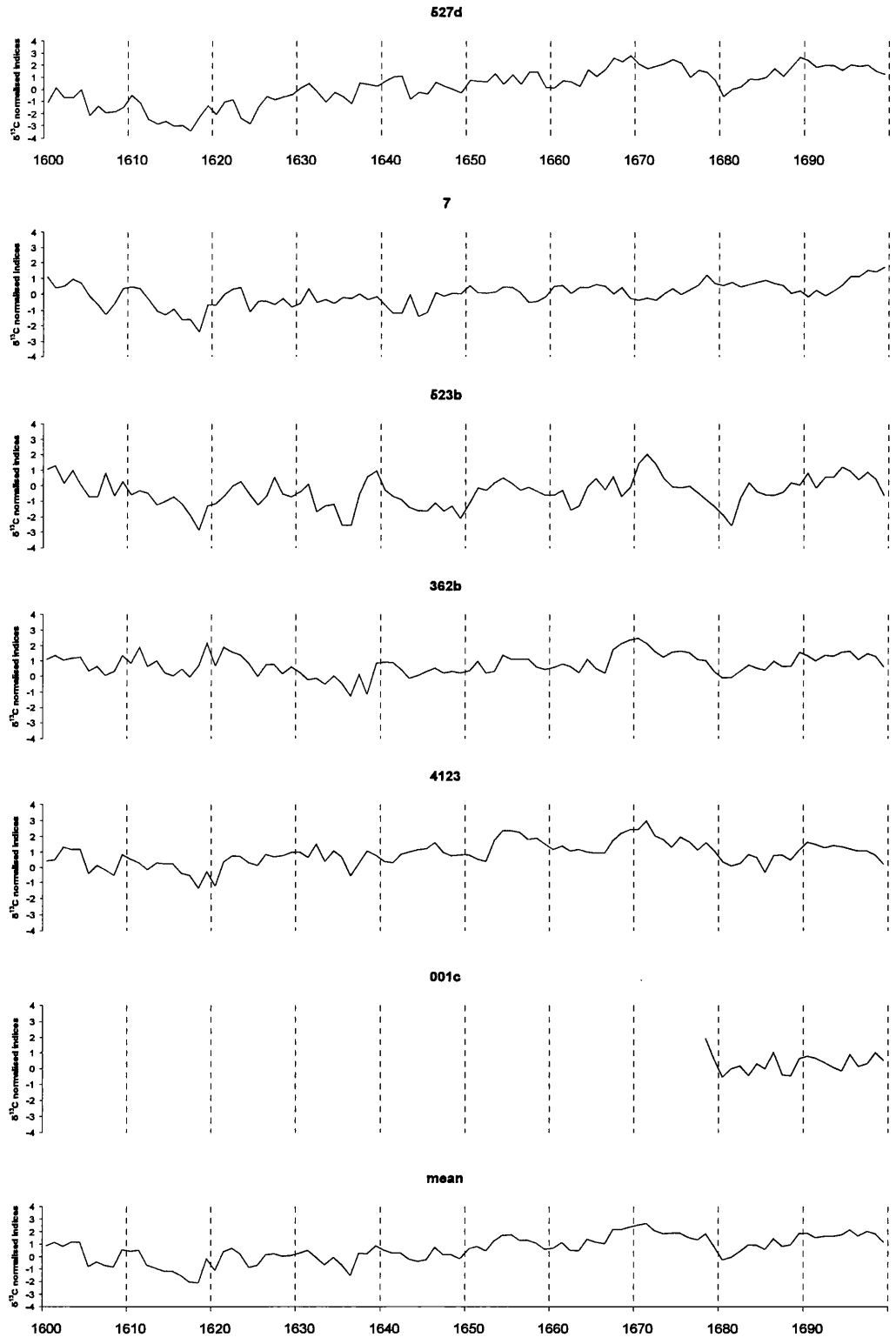

Figure 6.8: 17th century AD normalized raw $\delta^{13}C$ indices

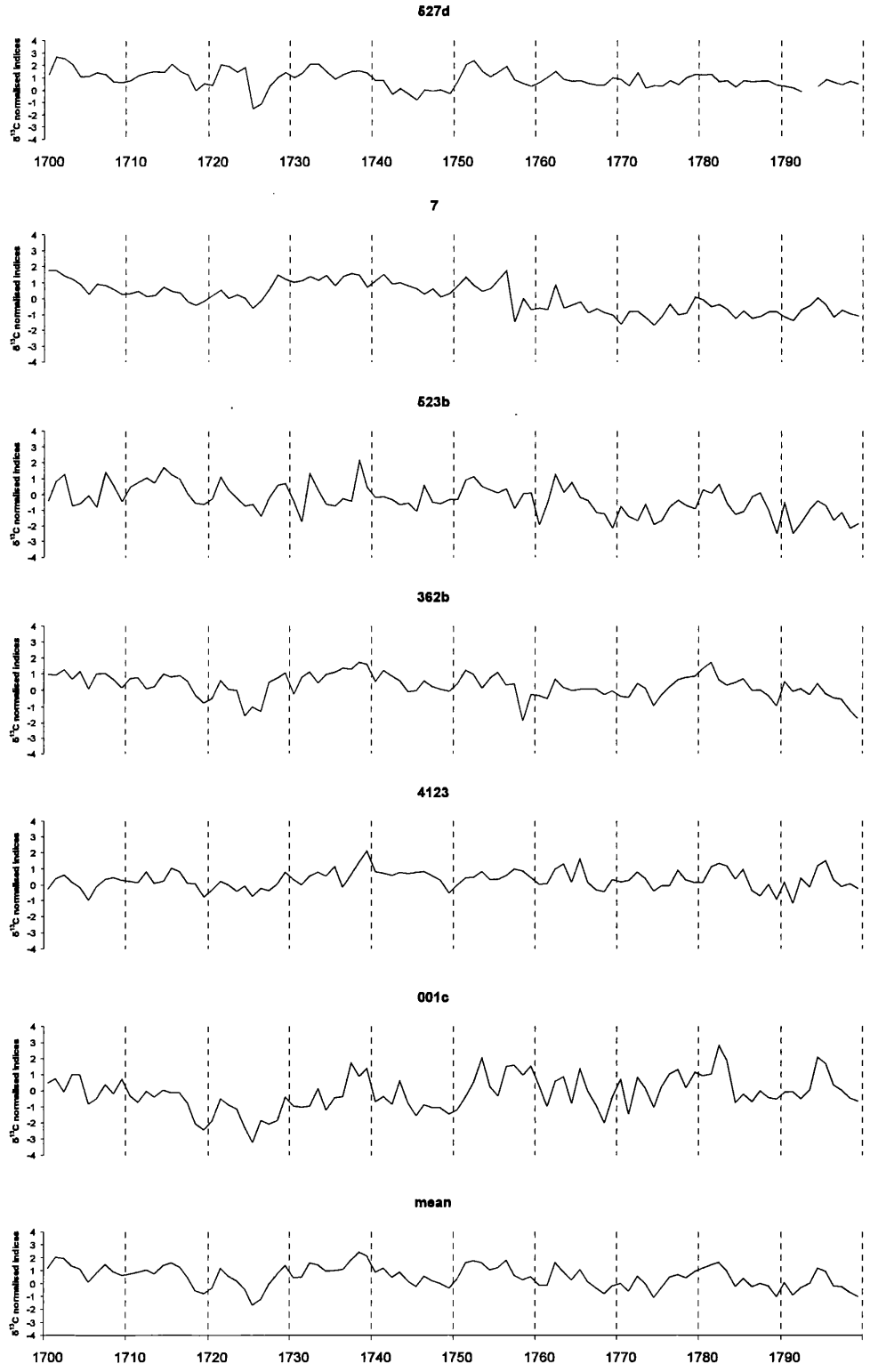

Figure 6.9: 18th century normalized raw $\delta^{13}C$ indices

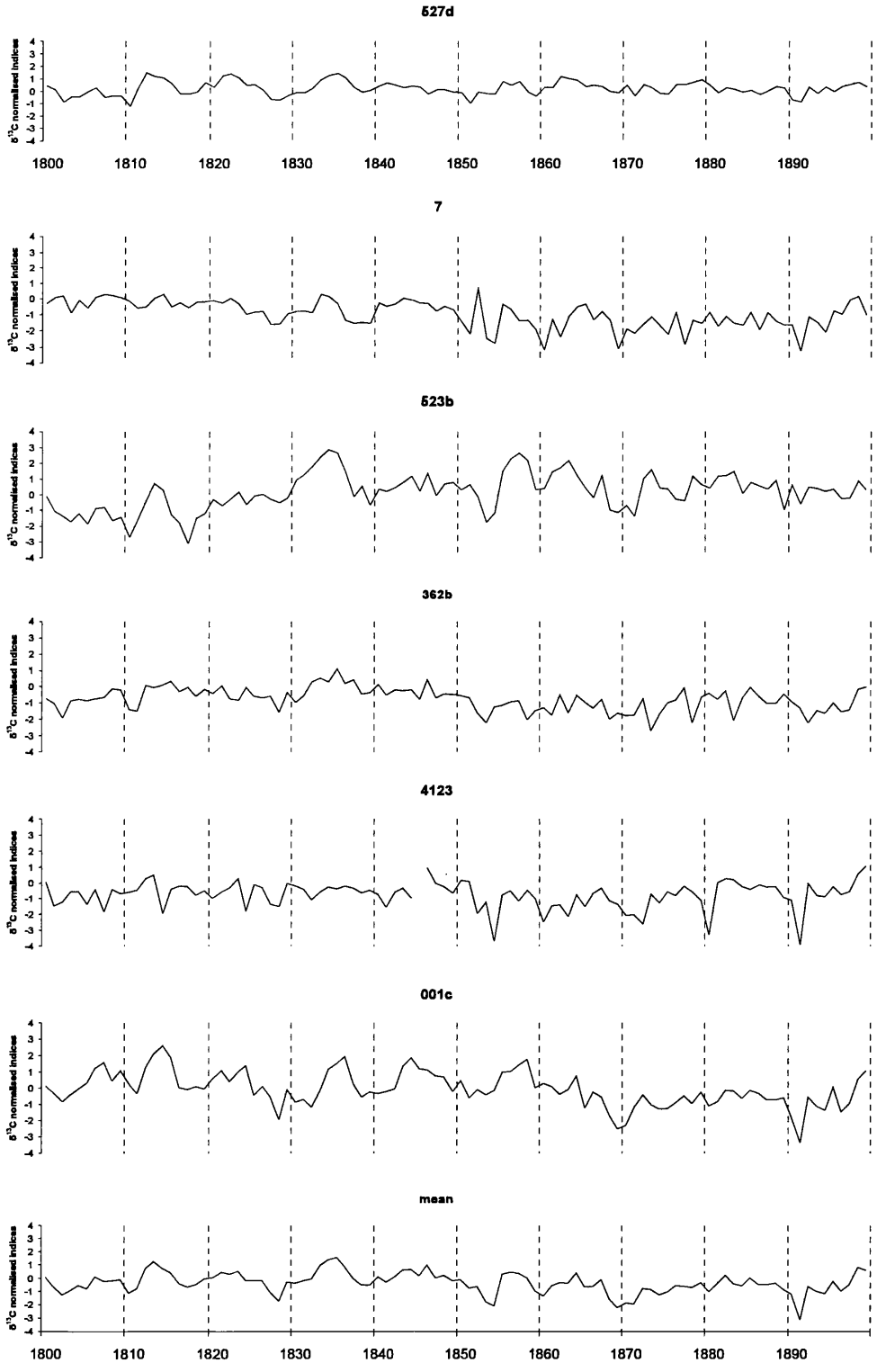

Figure 6.10: 19th century AD normalized raw $\delta^{13}C$ indices ($^{13}C_{pin}$ from 1820).

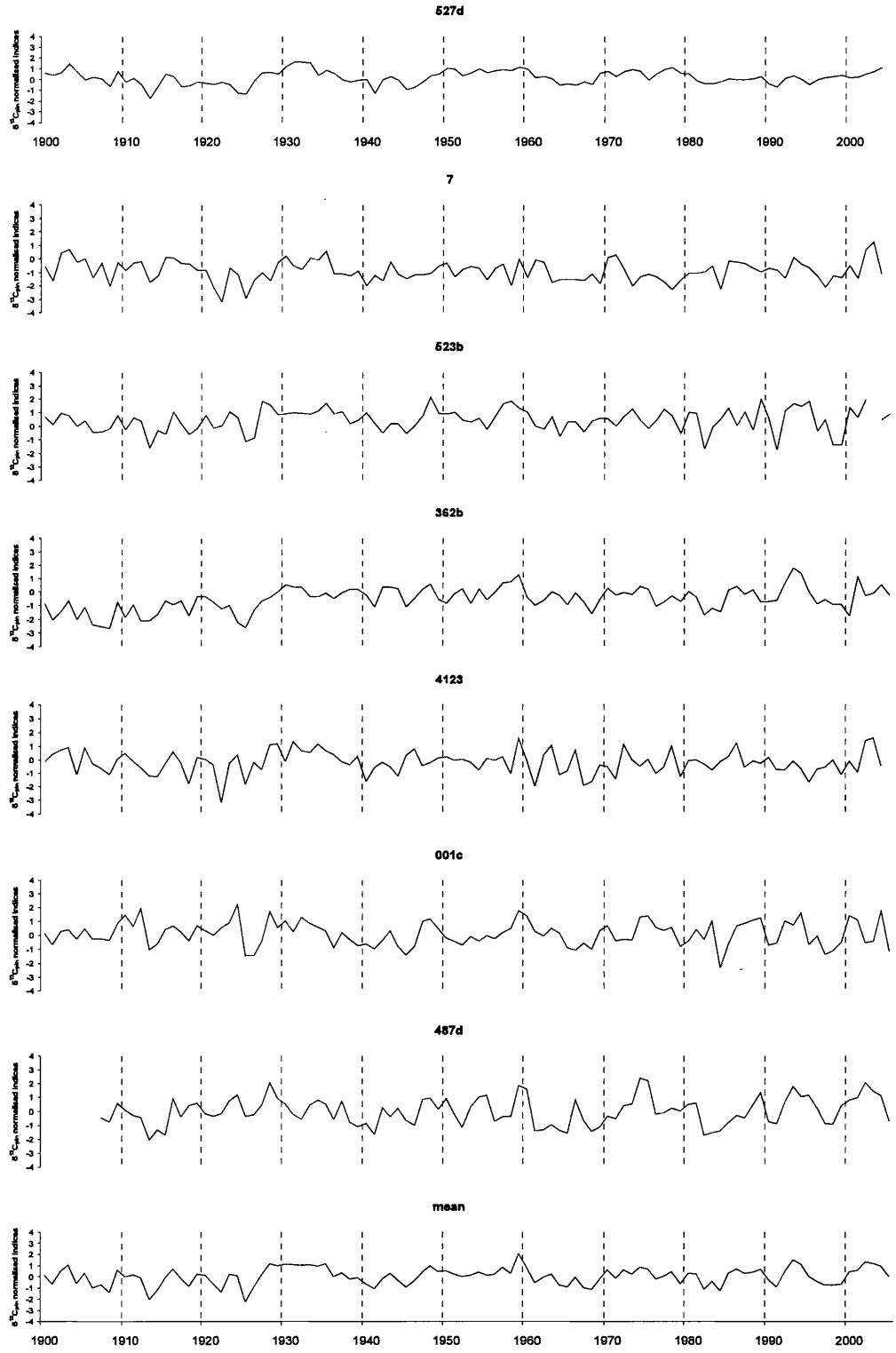

Figure 6.11: 20th century normalized $\delta^{13}C_{pin}$ indices

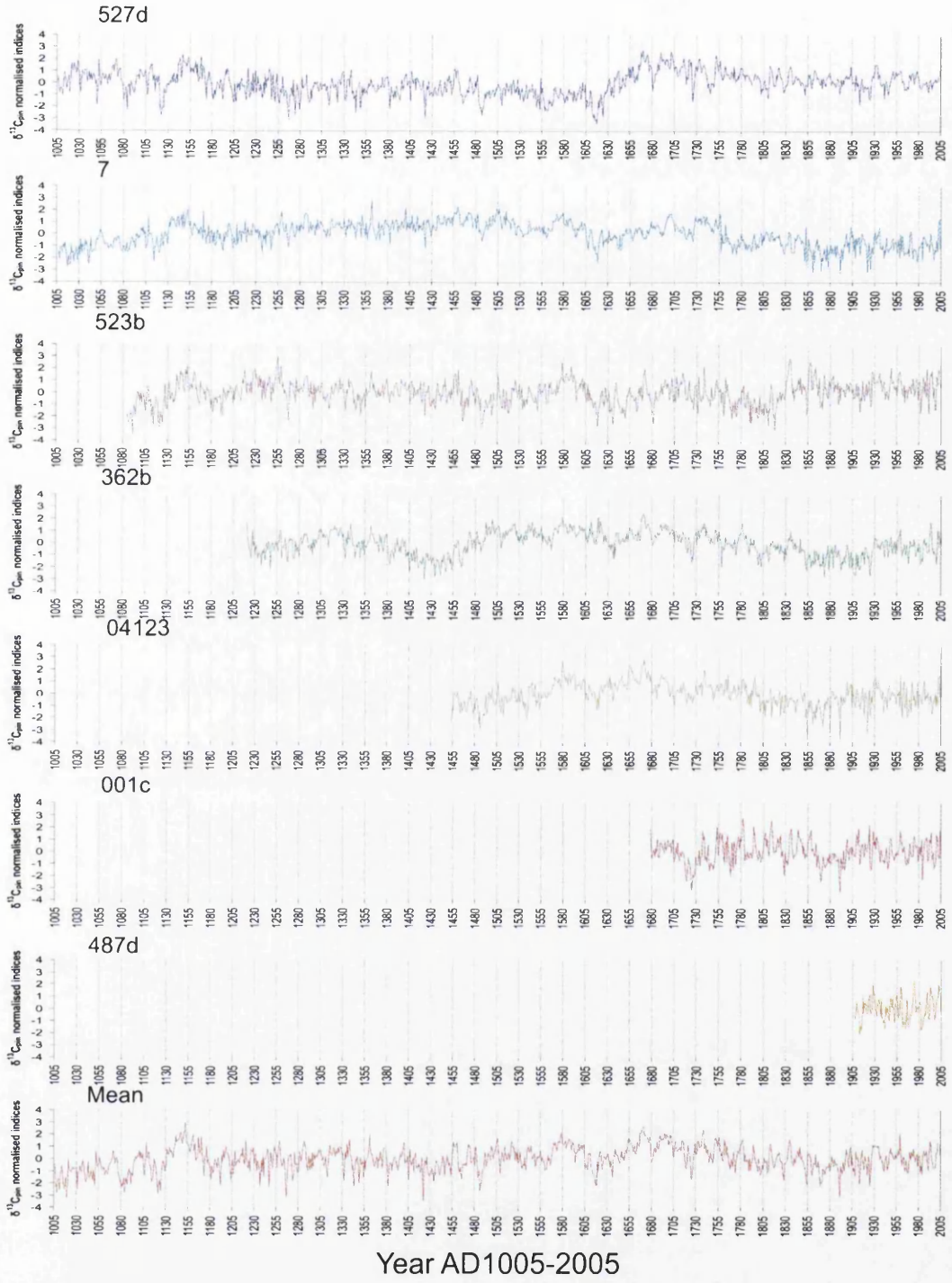

Figure 6.12: All trees normalized $\delta^{13}C$ indices for the last millennium (AD1005-2005).

6. 2: 1850-2005 $\delta^{13}C$ data analysis- PIN values AD1850-2005

Figure 6.13(A,B,C,D,E,F,G,H) Individual trees $\delta^{13}C_{pin}$.

6.13A

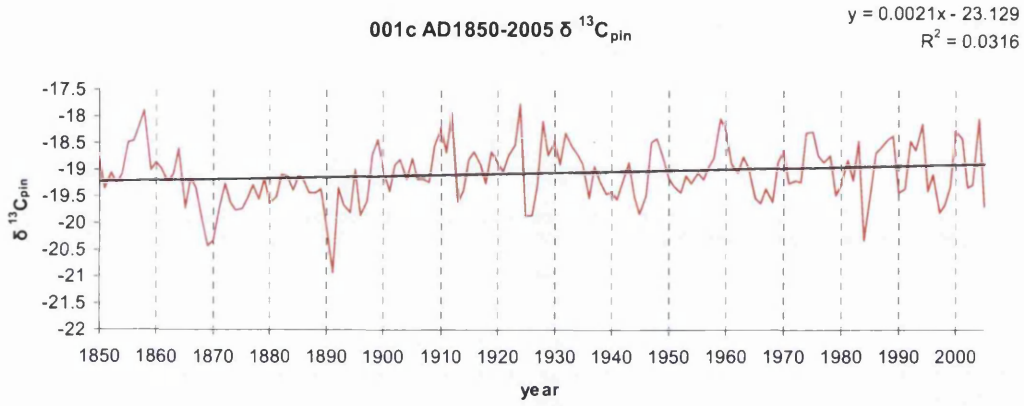

6.13B

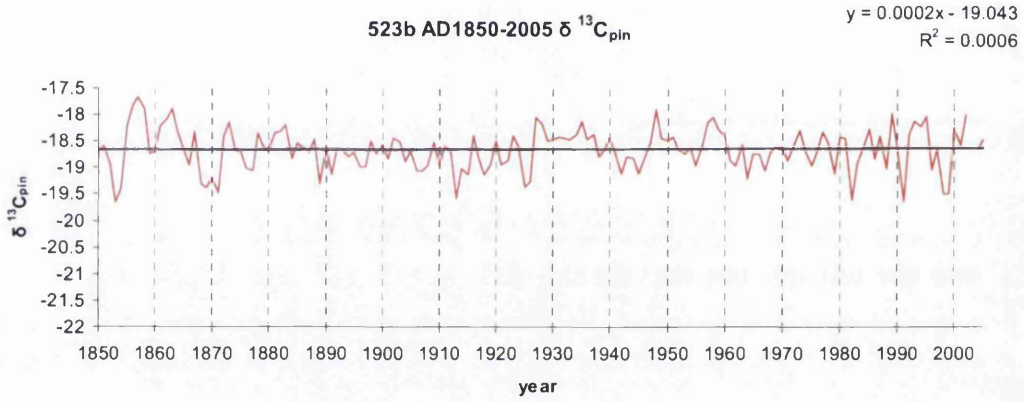

6.13C

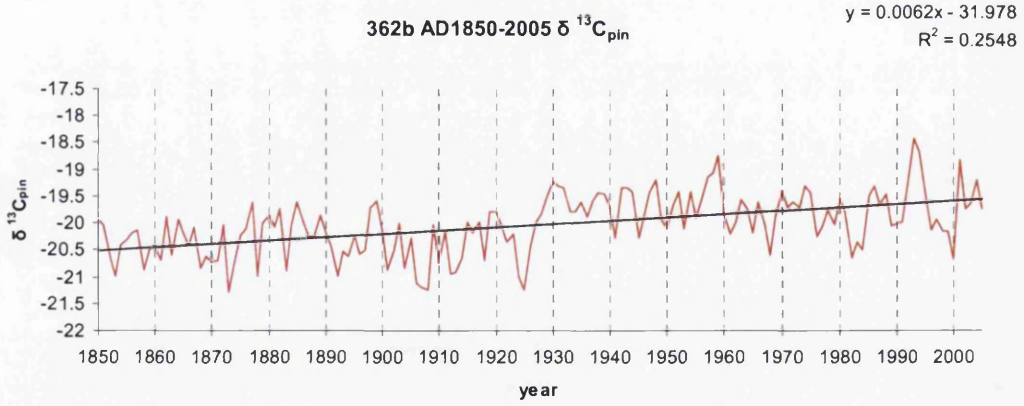

6.13D

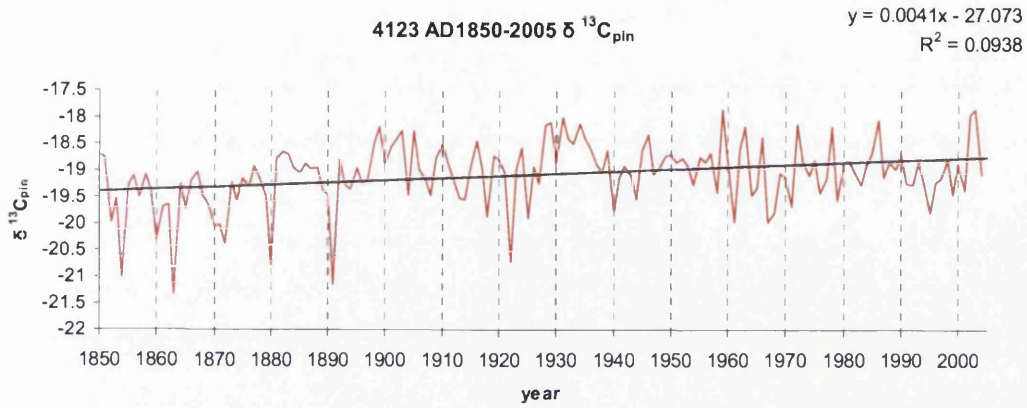

6.13E

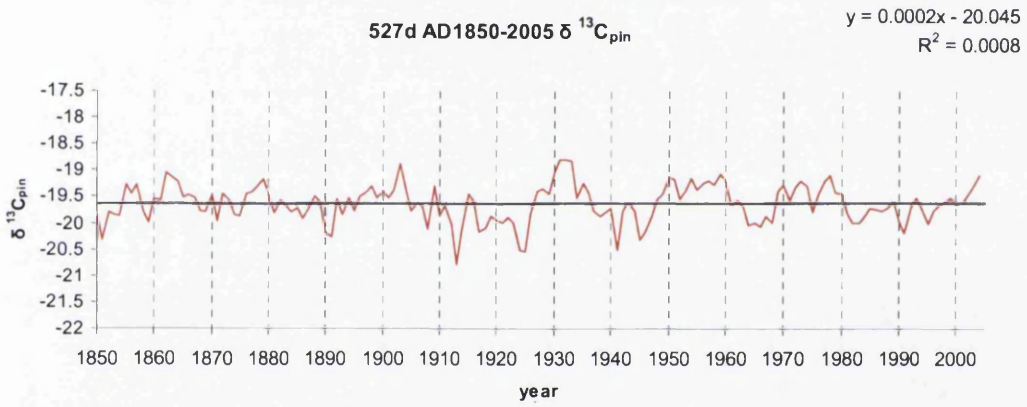

6.13F

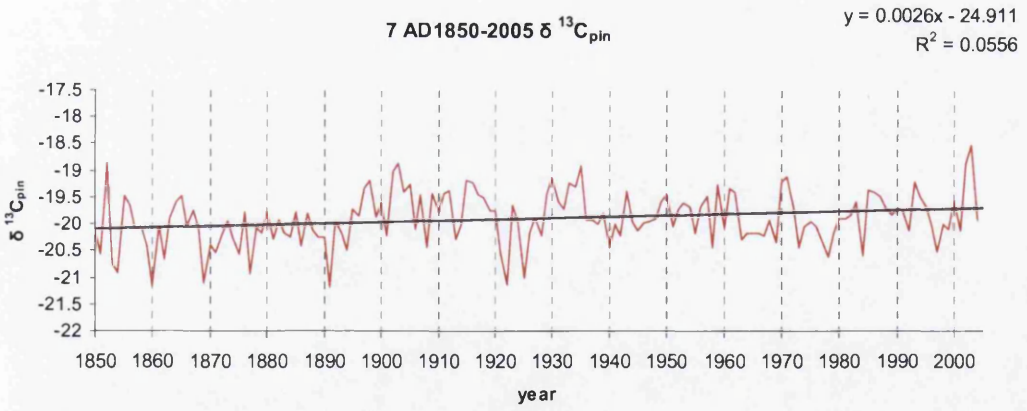

6.13G

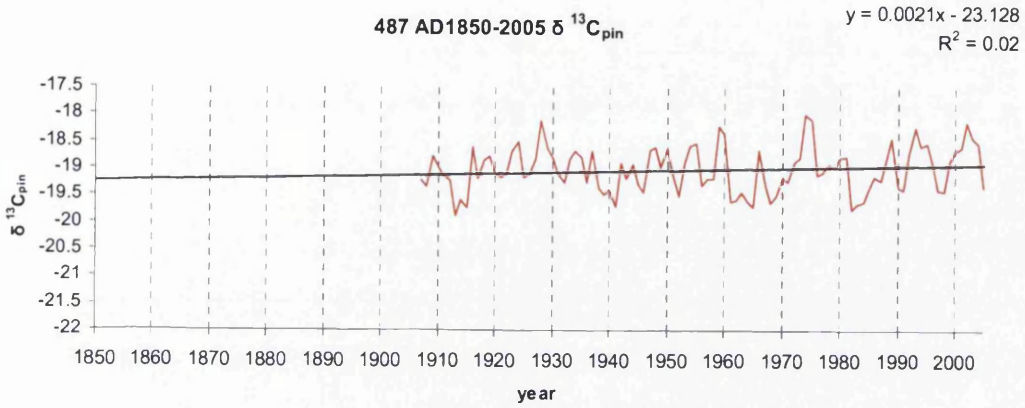
487 AD1850-2005 δ 13Cpin
y = 0.0021x - 23.128
R2 = 0.02
δ 13Cpin
-17.5
-18
-18.5
-19
-19.5
-20
-20.5
-21
-21.5
-22
1850 1860 1870 1880 1890 1900 1910 1920 1930 1940 1950 1960 1970 1980 1990 2000
year

6.13H

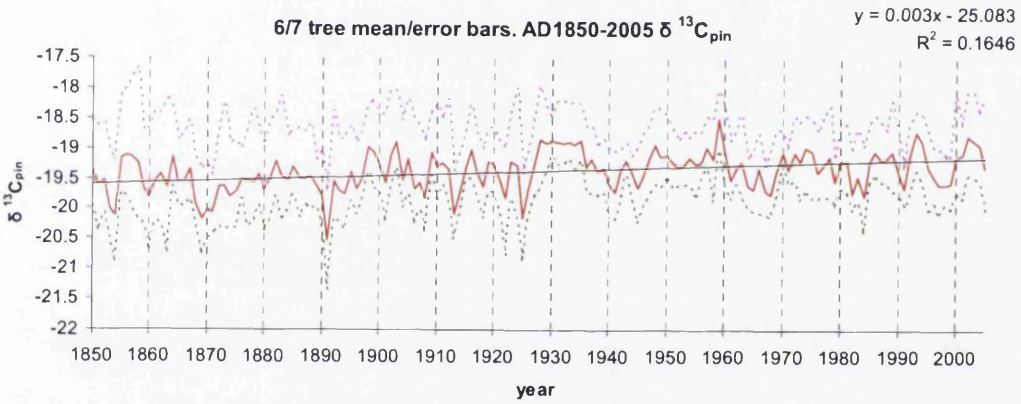
6/7 tree mean/error bars. AD1850-2005 δ 13Cpin
y = 0.003x - 25.083
R2 = 0.1646
δ 13Cpin
-17.5
-18
-18.5
-19
-19.5
-20
-20.5
-21
-21.5
-22
1850 1860 1870 1880 1890 1900 1910 1920 1930 1940 1950 1960 1970 1980 1990 2000
year

Table 6.3 Tree details and inter tree correlation $\delta^{13}C_{pin}$ 1850-2005

Tree	Most positive year (AD)			Most negative year(AD)		mean $\delta^{13}C_{pin}$
001c	1924			1891		-19.07
523b	1857			1853		-18.65
362b	1993			1873		-20.03
4123	1959			1863		-19.08
527d	1931			1913		-19.62
007	2003			1891		-19.90
487d	2002			1913		-19.02
mean	**1959**			**1891**		**-19.37**
	001c	**523b**	**362b**	**4123**	**527d**	**007**
523b	0.42					
362b	0.34	0.34				
4123	0.34	0.25	0.34			
527d	0.28	0.45	0.36	0.23		
007	0.37	0.28	0.26	0.44	0.31	
487d	0.51	0.48	0.38	0.31	0.37	0.21
	Mean r	0.35		**EPS**	0.79	

The period between1928-1935 represents a prolonged period of positive $\delta^{13}C$ values in all trees (although not so pronounced in tree 487) and is especially evident in the mean $\delta^{13}C_{pin}$ as an unusual episode where the $\delta^{13}C_{pin}$ of all trees show the same trend. The 'dust bowl' drought of the 1930s and the drought of the 1950s are well replicated through tree ring width reconstruction (Stahle *et al.*, 2007) and include distinctive sub-decadal droughts (figure 6.21), and there are detailed historic accounts of the misery that the drought and heat during the 1930s brought to communities of the west (Bonnifield, 1979). The period between 1929-1934 represents the most severe period of drought in the Nevada/California border region during the 20th century according to the reconstruction by Stahle *et al.,* (2007), and the bristlecone pines reflect this with a period of positive $\delta^{13}C_{pin}$ values from 1928 to 1935. Significant rising trends in $\delta^{13}C_{pin}$ values are observed in the period 1850-2005 in trees 362b and 4123 and also the mean of all trees. The period between 1850 and 1925 is marked by generally negative $\delta^{13}C$ values in all trees.

Superposed Epoch Analysis (SEA) of proxy data has been used in the past to identify the effects of large volcanic eruptions and is used in this research in a similar way to the technique used by Adams *et al.*, (1974) in their analysis of the

effects of volcanoes on El Niño events as represented in a range of proxy evidence. Salzer and Hughes (2007) also apply the approach in their study of bristlecone frost rings and volcanic influence. The approach is further outlined by Lough and Fritts (2003). In the aforementioned studies ten years either side of a known, or supposed volcanic, or other climatic event are used to assess the significance of that event. The normalised values referred to here and elsewhere throughout this and other chapters were calculated using the following equation:

$\delta^{13}C$ indices or ring width indices = (annual value – mean value of series) / standard deviation of series

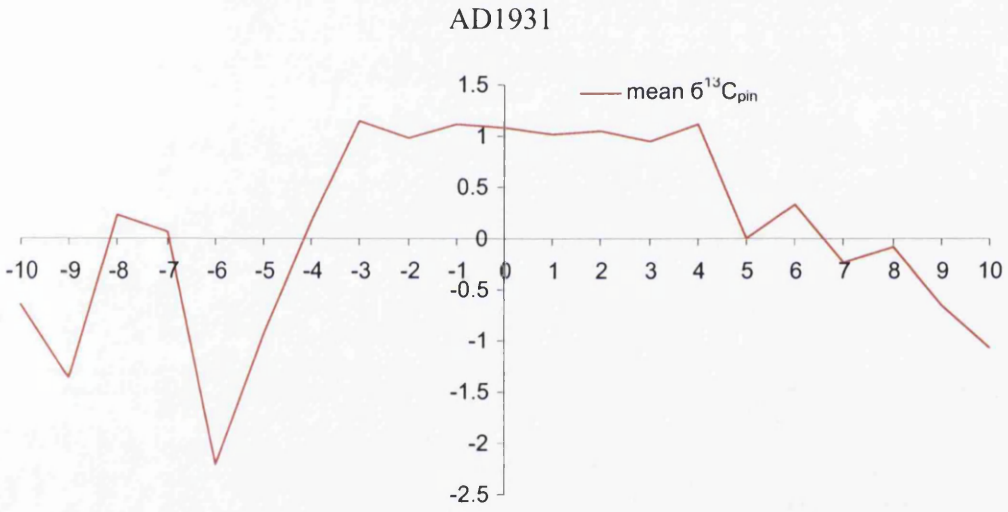

Figure 6.14: 1931 centred drought (1928-1935). Normalised indices of $\delta^{13}C_{pin}$ are shown on the Y axis and the period AD1921 to AD1941 is shown on the X axis.

In the mean series the $\delta^{13}C_{pin}$ values between1928 to 1935 display little variance and the drought appears unusual in the context of at least the last 150 years, and possibly the last millennium. The drought of the 1950s is evident in the $\delta^{13}C$ series between 1957 and 1962 and corresponds well to the drought reconstruction (figure 6.21) by Stahle *et al.,* (2007).

The most negative $\delta^{13}C$ can also be explained by weather or climate. During the period between 1889 and 1891 the western United States witnessed severe winter and spring flooding and unusually high intensity summer storms and landslides that had devastating socio-economic effects, particularly on the coast of southern California (Kuhn and Shepherd, 1981:33). As they state:

"Between 1889 and 1891, southern California was again battered by violent subtropical storms and exceptionally heavy rainfall. During this period the U. S. Coast and Geodetic Survey (USCGS) was conducting topographic and bathymetric surveys along the coast of San Diego County. The USCGS (1889) topographic notes indicate that the bluffs show "new erosion during each winter storm as the characteristic feature of this coast." One thunderstorm hit Encinitas on the evening of 12 October 1889 (U. S. Signal Service 1889), and in eight hours 7.58 inches of rain fell there, while only 0.44 of an inch was measured at San Diego, and 0.04 of an inch at Los Angeles on the same date.

Examination of the 1889–90 San Diego County Tax Assessor records of land parcels located at the mouth of Cottonwood Creek, Encinitas, and south of there indicate that seaward property was greatly devalued or stricken from the tax roles, and land parcels directly inland increased temporarily in value. The weather varied greatly from month to month throughout the world during the winter of 1889–90. A stormy condition seems to have prevailed generally throughout much of the United States. During February 1891, there were destructive floods in California, Arizona, and on all major rivers east of the Rockies. Extremely large snowpacks existed in southern California prior to the warm rain that fell from 17–27 February 1891. Pourade noted:

For its brief duration, scarcely more than a week, the storm that struck Southern California and Arizona in February of 1891 was probably the worst on record. . . .

The San Diego River quickly rose to flood level and hundreds of residents flocked to ride the cable cars to the pavilion park overlooking Mission Valley. A solid sheet of

water spread across the valley floor and over the tide flat to False Bay [Mission Bay]. Every telephone and telegraph line was out, railroad connections were severed and a heavy storm at sea with gale winds interrupted shipping. Virtually everything that had been built in the riverbeds or on the alluvial plains between the great watersheds and the sea was gone or reduced to wreckage [presumably referring to much of the coast of southern California]. . . .

Bear Valley [south of Escondido near the present Wild Animal Park] reported thirty inches of rain in thirty-seven hours; Cuyamaca, eighteen inches in forty-eight hours, the City [of San Diego] recorded only 2.57 inches for the storm and 4.77 inches for the month.

As these storms moved east, Arizona was devastated. Flooding in Arizona reached a peak in the last week of February 1891, and the U. S. Army reported that the Colorado River was twenty miles wide at the former crossing at Yuma.

August 1891 was the warmest August recorded up until that time along the Pacific coast (U. S. Signal Service 1891:188, 191). Although no rainfall was reported over the greater part of California, a world record rainfall was verified at Campo (near the Mexican border) on 12 August 1891 when 11.5 inches fell in only eighty minutes!

Perhaps the significance of these floods, as far as coastal erosion is concerned, is that the rains that produced them were very concentrated. In more recent times such rains have caused immediate erosion of sea cliffs. One can imagine how this much more concentrated rainfall would have cut deeply into the cliffs and canyons and would have been responsible for landslides of far greater devastation than those we have experienced in recent years.

When stormy seas and heavy rain of this magnitude attack the sea cliffs, erosion can be so disastrous that any buildings on top of the bluffs, so common now, can be seriously damaged if not destroyed. The one foreseeable alternative to this scenario is that the rivers, swollen by the floods, might carry such a large quantity of

sediment to the sea that wide beaches would be formed which would, for a time, protect the cliffs from the waves."

Kuhn and Shepherd (1981) attribute this period of storminess to the after effects massive explosive eruption of Krakotoa in 1883.

Figure 6.15 shows SEA for the year 1883 with the Blanco mean $\delta^{13}C_{pin}$ values. As can be seen the most significant event in the data are the depleted $\delta^{13}C_{pin}$ values that occur in 1889-1891.

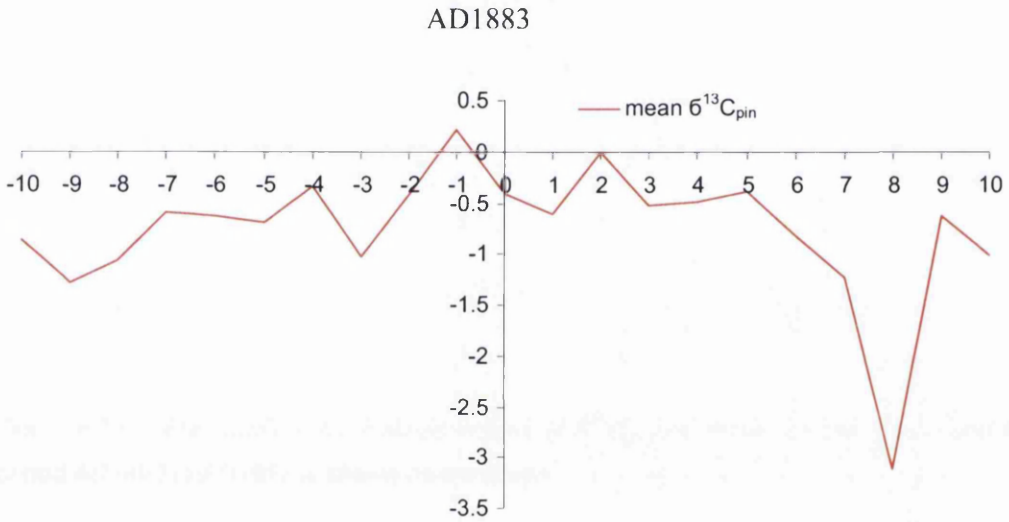

Figure 6.15 1883 eruption SEA also showing exceptional 'stormy period' 1889-1891. Normalised indices of $\delta^{13}C_{pin}$ are shown on the Y axis and the 21 year years between AD1883 and AD1893 are shown on the X axis. No major deviation from the mean is apparent between AD1881 and 1888. The negative $\delta^{13}C_{pin}$ values between AD1889 and AD1891 represent the most negative excursion in the last 150 years corroborate the documentary evidence of a long term period of extreme storminess in California between AD1889 and AD1891. The absence of a negative isotopic excursion associated with the AD1883 eruption of Krakotoa may represent the limited climatic effects that this volcano had in the White Mountains.

Devastating floods are also documented for the year 1862 in California (Kuhn and Shepherd, 1981) and are reflected in the negative $\delta^{13}C$ in the bristlecone carbon

isotope series in 1863. Conversely 1864 is well known across North America as the year of the 'Yankee' or Civil war drought (Stahle *et al.*, 2007). 1864 is also one of the most positive five $\delta^{13}C_{pin}$ values in the period from 1850 to 1899 (figure 6.25). The summer of 1913 is evident in instrumental weather data to be abnormally cold and wet. 1902 witnessed three volcanic eruptions. These are Peleé, Martinique, Soulfriére, St Vincent and Santa Maria, Guatemala. Although an early wood frost ring was noted by LaMarche and Hirschboeck (1984) the effects in the Blanco $\delta^{13}C_{pin}$ appear as a positive value in 1903 (figure 6.16).

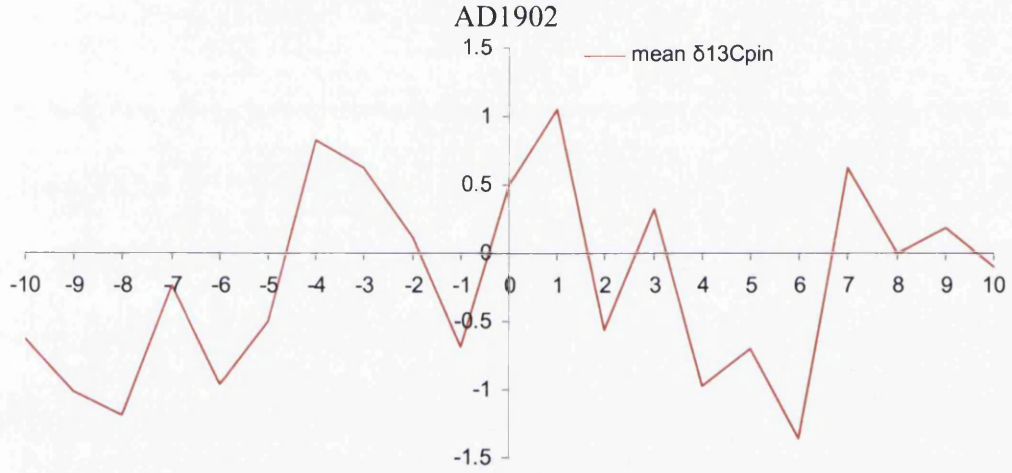

Figure 6.16: 1902 eruption. Normalised indices of $\delta^{13}C_{pin}$ are shown on the Y axis and the period AD1892 to AD1912 is shown on the X axis.

The cool wet summer of 1913 evident in the instrumental data (e.g figure 5.25) and $\delta^{13}C$ may have been a result of the eruption of the Alaskan volcano Katmai in 1912. SEA is also used for the year 1912 and the effects are clearly noticeable (figure 6.17).

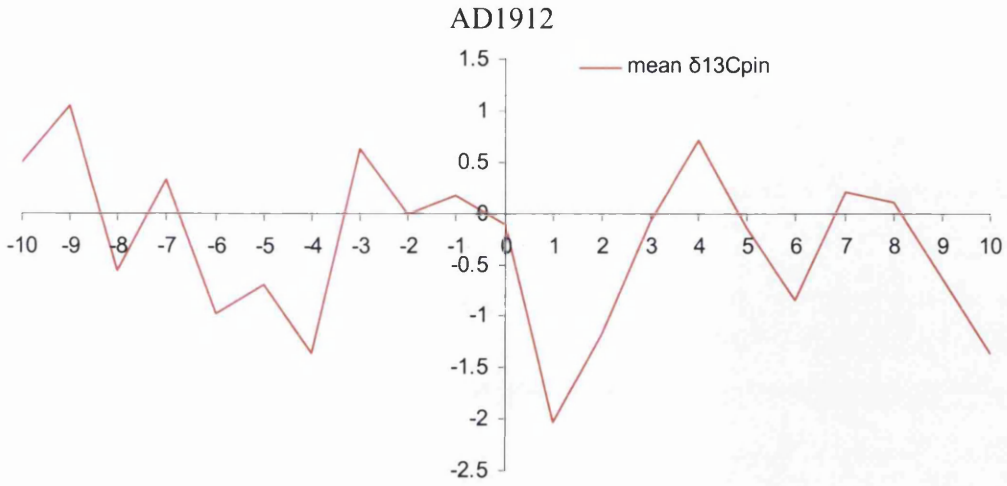

Figure 6.17: 1912 eruption SEA. The years between 1902 to 1922 are shown.

Likewise the mid 1960s negative $\delta^{13}C_{pin}$ values may be related to the large volcanic eruption of Agung in Bali in 1963 that is represented as a bristlecone frost ring in 1965 (Salzer & Hughes, 2007) and in the Blanco $\delta^{13}C$ as depleted values.

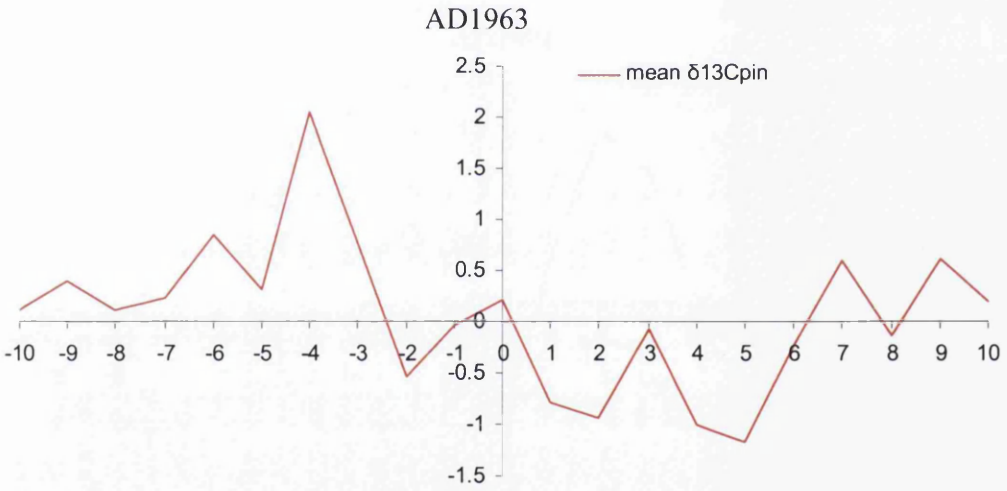

Figure 6.18: 1963 eruption SEA. The period 1953 to 1973 is shown.

The major El Niño event of the early 1980s is also reflected in the $\delta^{13}C_{pin}$ data. The years 1982 and 1984 are extreme negative $\delta^{13}C$ values reflecting the heavy rains that affected the western United States. The depleted $\delta^{13}C_{pin}$ values may be related to the eruption of El Chichon in 1982.

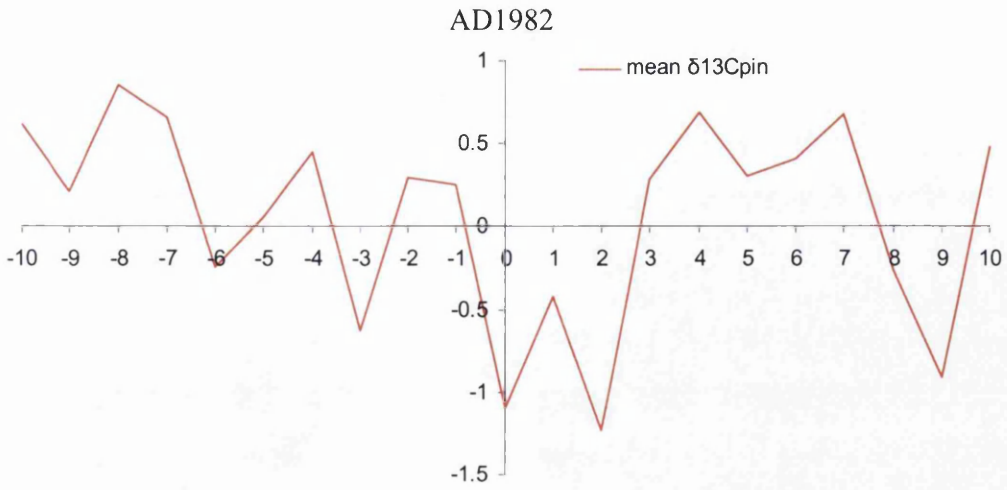

Figure 6.19: 1982 eruption SEA. The period 1972 to 1992 is shown.

The eruption of Pinatubo in the Philippines in 1991 is perhaps the best understood volcanic eruption. Both the eruption and its after effects have been studied in greater detail with more advanced technology than any other eruption (McCormick *et al.*, 1995).

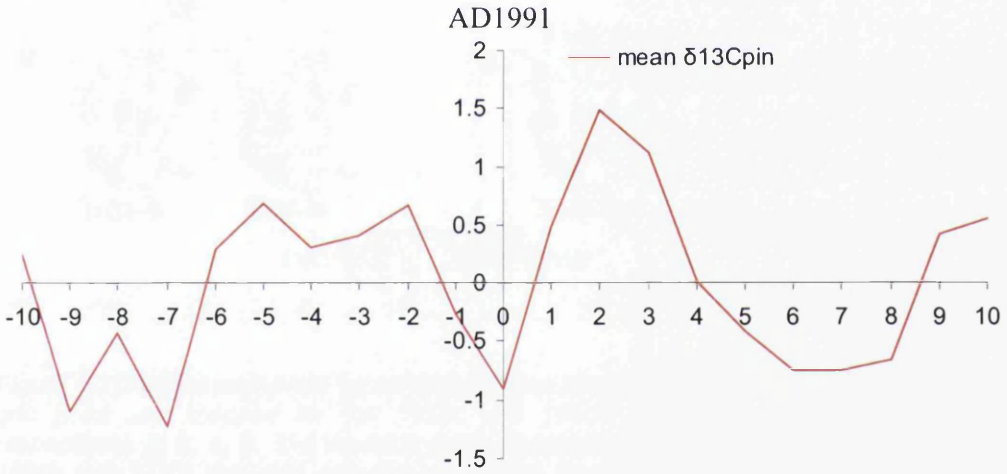

Figure 6.20: 1991 eruption SEA. The period 1981 to 2001 is shown.

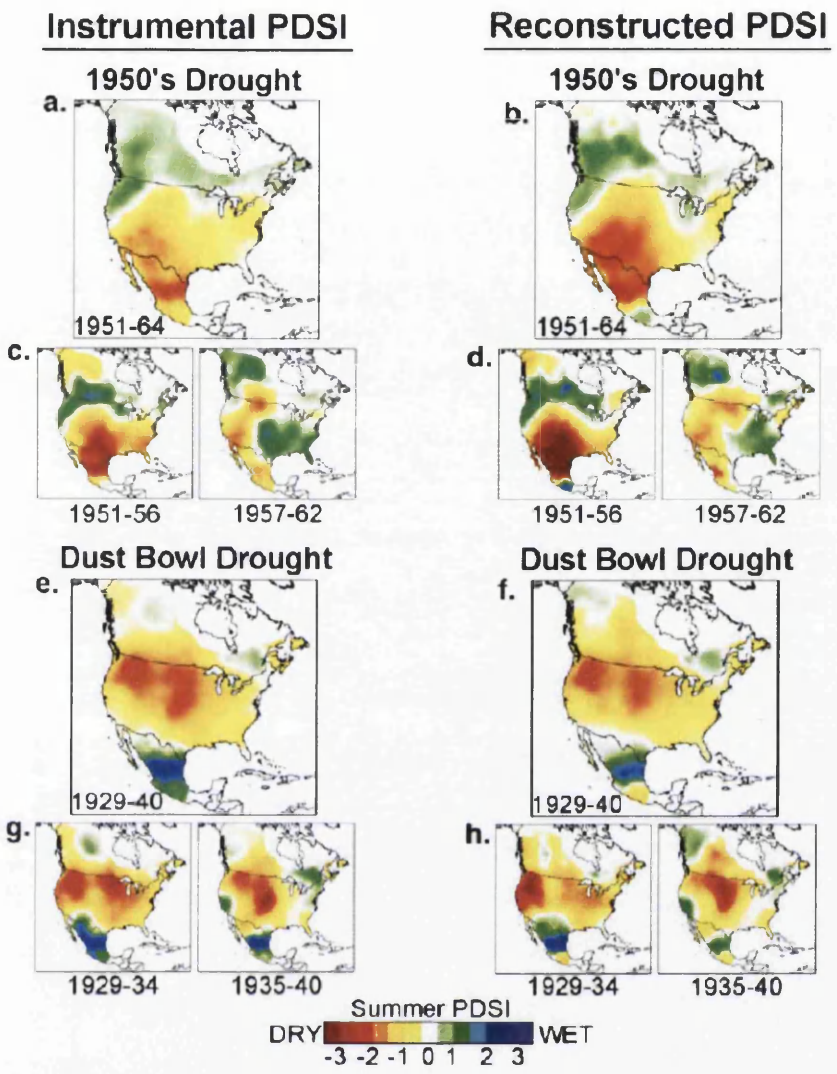

Figure 6.21. Instrumental and tree-ring reconstructed summer PDSI were averaged at each grid point and mapped for the 1950s and 1930s droughts (1951–64 and 1929–40, respectively, a, b, e, f). The tree-ring reconstructions reproduce the spatial patterns of the 1950s and 1930s droughts, but over-emphasize the 1950s drought. Each decadal drought regime was split in half, and shorter subdecadal averages were computed and mapped (1951–56 and 1957–62; 1929–34 and 1935–40). The 1950s and 1930s droughts both included distinctive sub-decadal regional drought cells that are well replicated with the tree-ring reconstructions. Figure and text from Stahle et al., (2007:138).

The most positive and most negative $\delta^{13}C$ values during this period (1850-2005) also represent observed climate events that are evident in the instrumental climate data and documentary sources. With the most positive $\delta^{13}C_{pin}$ (representing dry/hot conditions) it is known that 2003 was the hottest year in the meteorological record

from Bishop and 2002 was a very dry spring. 1993, 1959 and 1931 are also hot/dry years that fall within the period covered by instrumental weather data. Drought conditions in the southern Great Plains are documented from native American accounts for the year 1855, and positive $\delta^{13}C$ values, and narrow ring widths are evident in 1855, 1856 and 1857.

The year 1855 is evidenced in both proxy and historical evidence as an extreme drought year in the mid west and was known among native Americans of the mid-west as the 'sitting summer' (Stahle *et al.*, 2007).

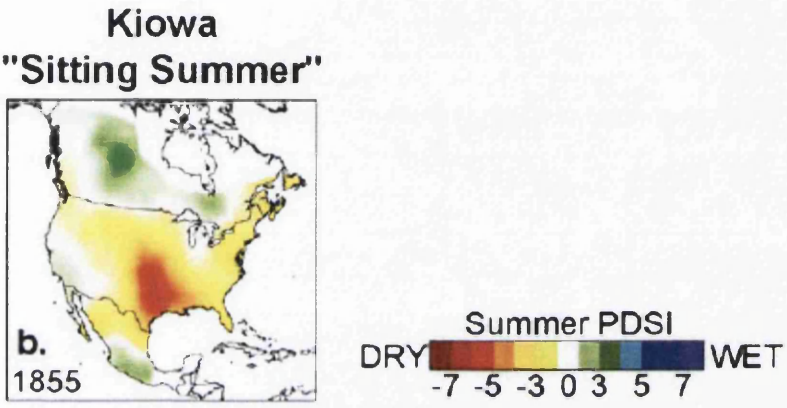

Figure 6.22 Tree ring width reconstructed drought for the year 1855 (Stahle et al., 2007:139).

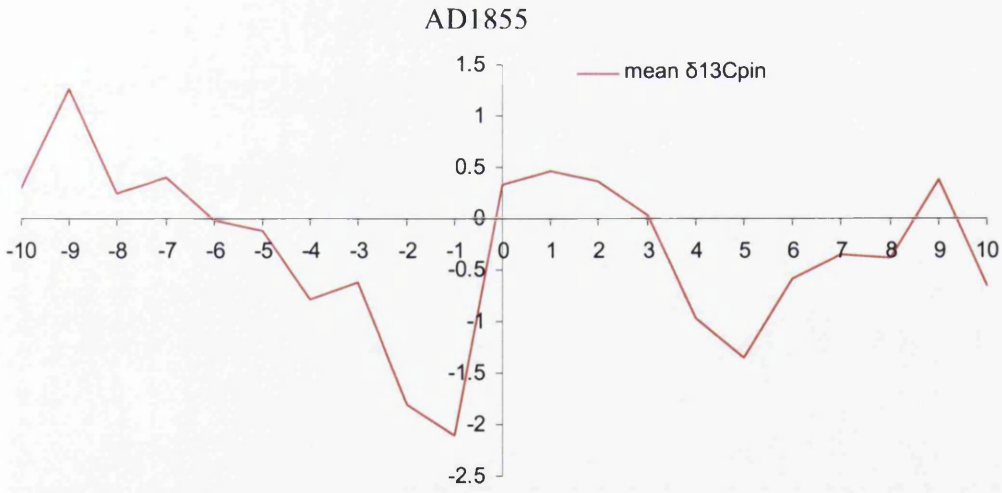

Figure 6.23: 1855 SEA showing the period 1845 to 1865.

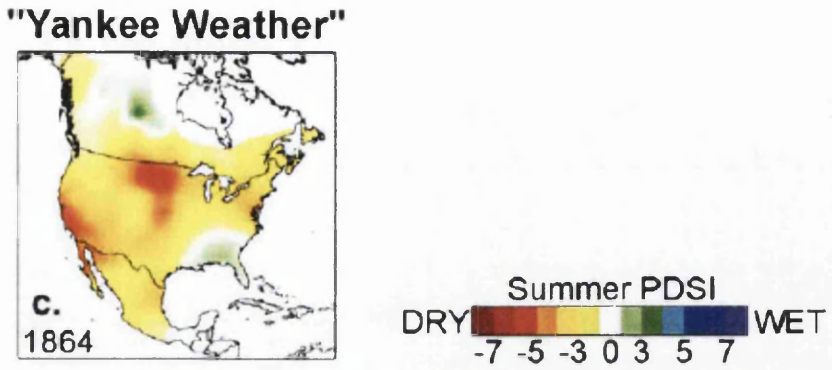

Figure 6.24: Tree ring width reconstructed drought for the year 1864 (Stahle et al., 2007:139).

AD1864

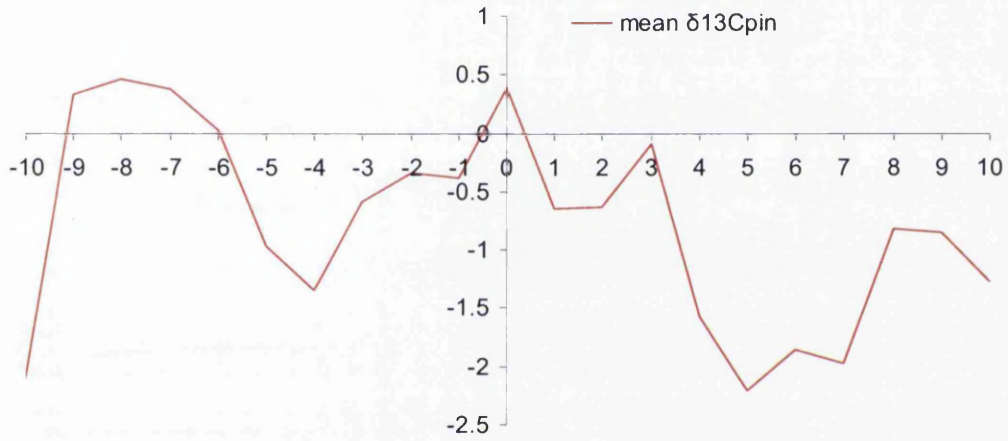

Figure 6.25: 1864 SEA showing the period 1854 to 1874

6.3. $\delta^{13}C$ data analysis- PIN corrected values AD1800-1849

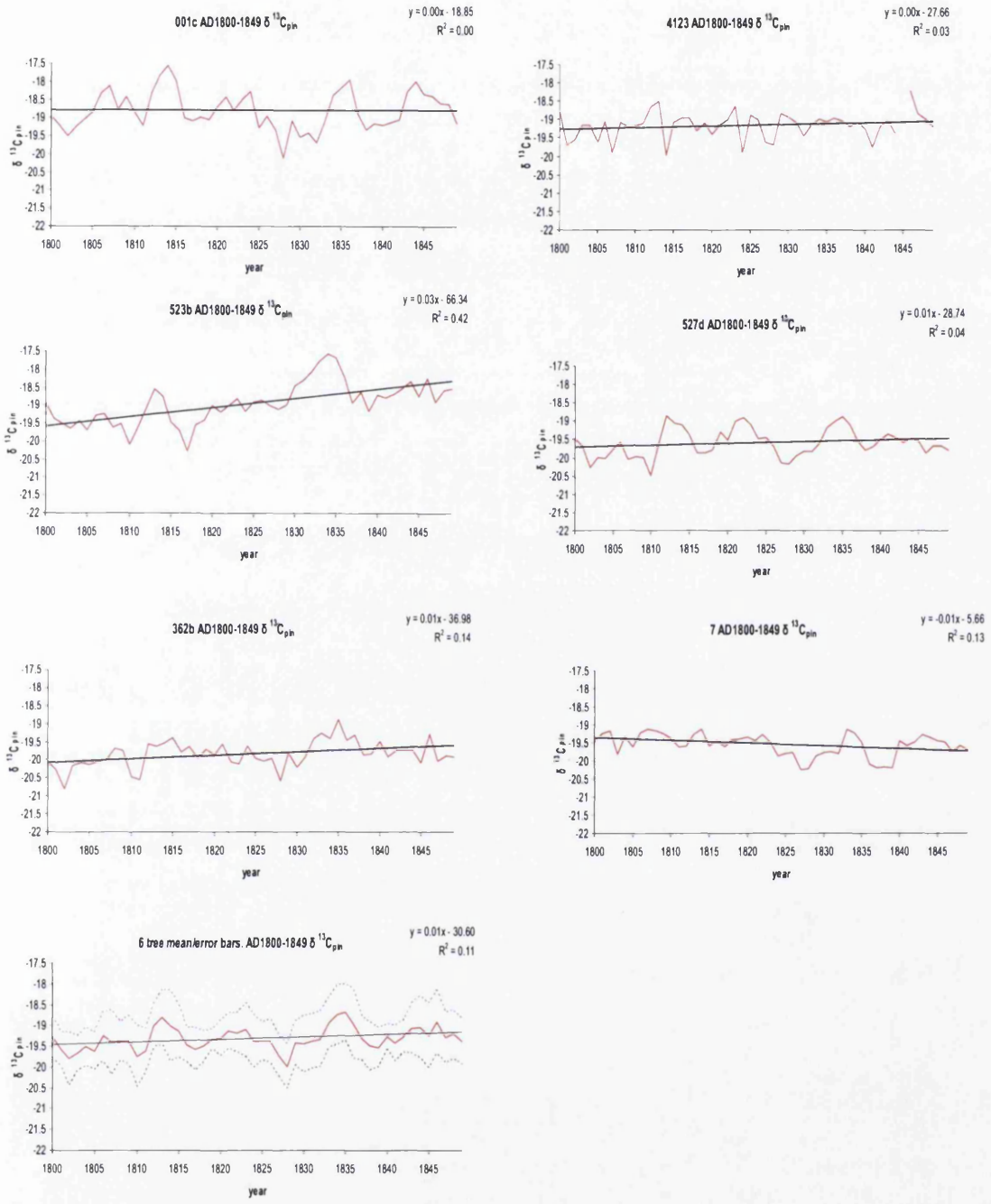

Figure 6.26. Individual trees $\delta^{13}C$ 1800-1849

Table 6.4 Tree details
Below: inter tree correlation $\delta^{13}C_{pin}$ 1800-1849

Tree	Most positive year (AD)	Most negative year(AD)	mean $\delta^{13}C_{pin}$
001c	1814	1811	-18.79
523b	1834	1817	-18.93
362b	1835	1802	-19.82
4123	1846	1814	-19.15
527d	1812	1810	-19.59
007	1807	1827	-19.54
mean	**1835**	**1828**	**-19.36**

	001c	523b	362b	4123	527d
523b	0.17				
362b	0.47	0.51			
4123	0.14	0.19	0.24		
527d	0.52	0.50	0.57	0.23	
007	0.42	-0.04	0.04	-0.02	0.19
Mean r	0.28			**EPS**	0.69

A significant rising trend in $\delta^{13}C$ values is observed in two of six trees (523 and 362). Depleted values around 1810/1811 (lowest in 001,527d) were replaced by positive $\delta^{13}C$ values in 1812-1814 (527d/001c) with depleted values following in 1814-1817(523/123). With the mean, low values in 1827/1828 are followed by extreme positive values from 1832 to 1837 with a peak in 1834/1835.

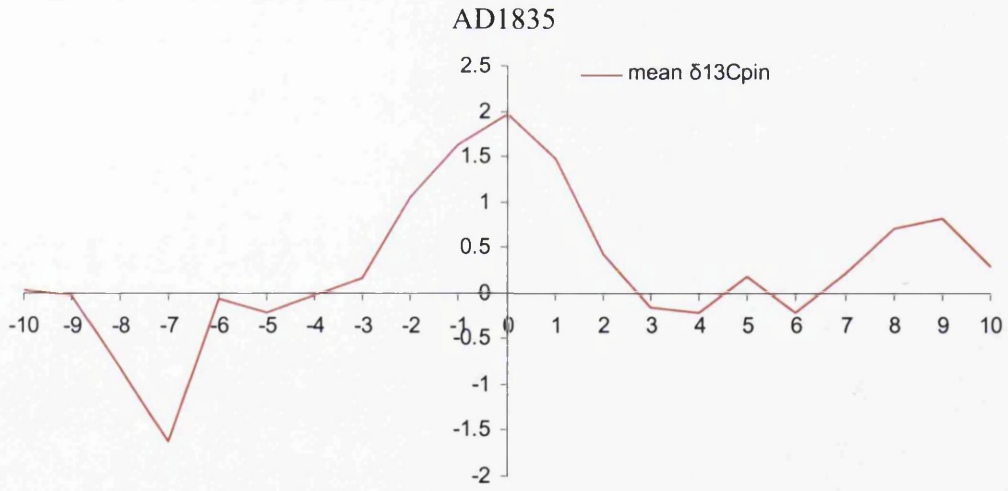

Figure 6.27 1835 eruption SEA showing the period 1825 to 1835.

This period of positive $\delta^{13}C_{pin}$ suggests extreme drought or heat. It is interesting that Stahle *et al.*, (2007:137) note from historical and tree ring evidence that 1833 may

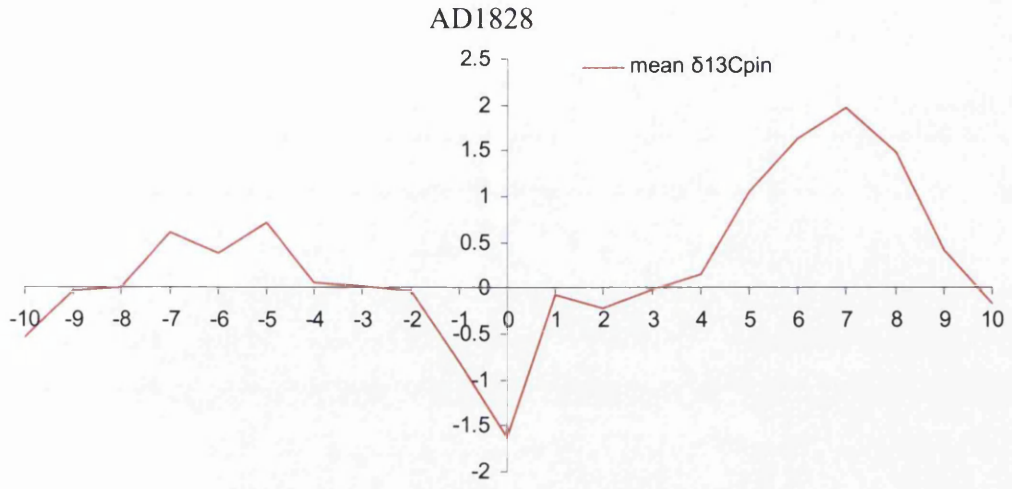

Figure 6.29 1828 'event' SEA showing the period 1818 to 1838.

Perhaps the largest volcanic eruption of the first half of the 19th century, and possibly the largest known historic eruption was that of Tambora, Indonesia in April 1815. Around 71000 people were killed by this eruption and the climatic after effects led to what has been termed 'the year without a summer' in much of the Northern Hemisphere in the year 1816 (LaMarche and Hirschboeck, 1984). A smaller eruption occurred in 1814 at Mayon in the Philippines (Oppenheimer, 2003).

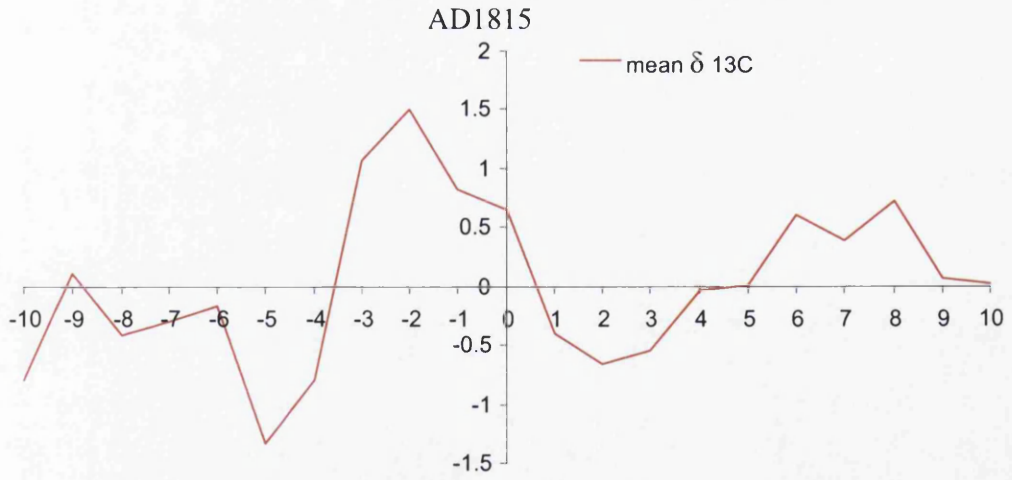

Figure 6.30 1815 eruption SEA showing the period 1805 to 1825

have been the wettest year in the last 500 years in the area from the Great Plains into central Mexico. The Blanco isotopes suggest completely the opposite for the White Mountains, and that dry or hot conditions prevailed from 1832 to 1837 in this part of western North America. The eruption of Avachinskaya Sopka, Kamchatka in 1837 does not appear so strongly represented in the $\delta^{13}C$, but was noted as a widespread bristlecone frost ring by LaMarche and Hirschboeck (1984).

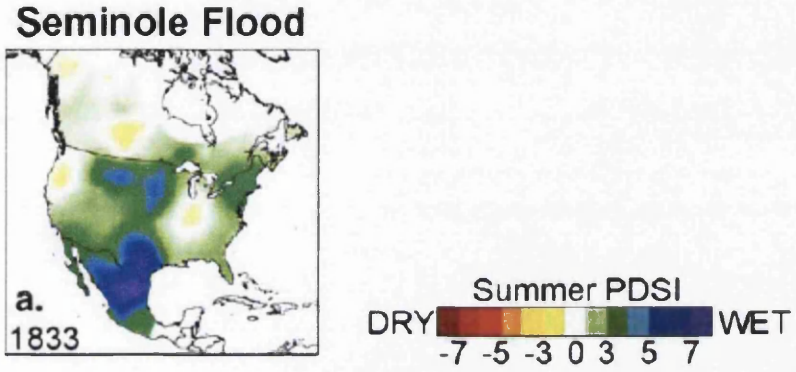

Figure 6.28 1833. Extreme continental wetness as described by Stahle et al., (2007:139).

Volcanic eruptions also occurred in 1821 (Eyjaffjallajökull, Iceland) and in 1822 (Vesuvius, Italy and Galunggung, Java). Bristlecone frost rings are also noted in bristlecone pines in 1828 and 1831 but no volcanic eruption has been identified as their cause (LaMarche and Hirschboeck, 1984). 1828 does appear as an extreme $\delta^{13}C$ negative and is reported to be a more widespread bristlecone frost ring than the one that occurred in 1831. A cool period between AD1817 and 1836 is identified in tree ring widths from the Sierra Nevada by Scuderi (1993).

Although the values for 1816/1817 and 1818 are depleted suggestive of cold or wet weather the most negative isotopic event occurs in 1810, while the most positive occurs in 1813.The year 1817 is a widespread frost ring in bristlecone pines (LaMarche and Hirschboeck, 1984) and a sulphate peak occurs in ice cores at 1810 (Oppenheimer, 2003). The year 1813 is a ring width minima in Finnish tree rings, 1815 in trees from the Yamal peninsula, Siberia (Hantemirov *et al.*, 2004).

The year 1805 is a notable frost ring in the bristlecone pines (LaMarche and Hirschboeck, 1984) though no eruption is identified for its cause. No similar event appears to occur with the Blanco $\delta^{13}C$.

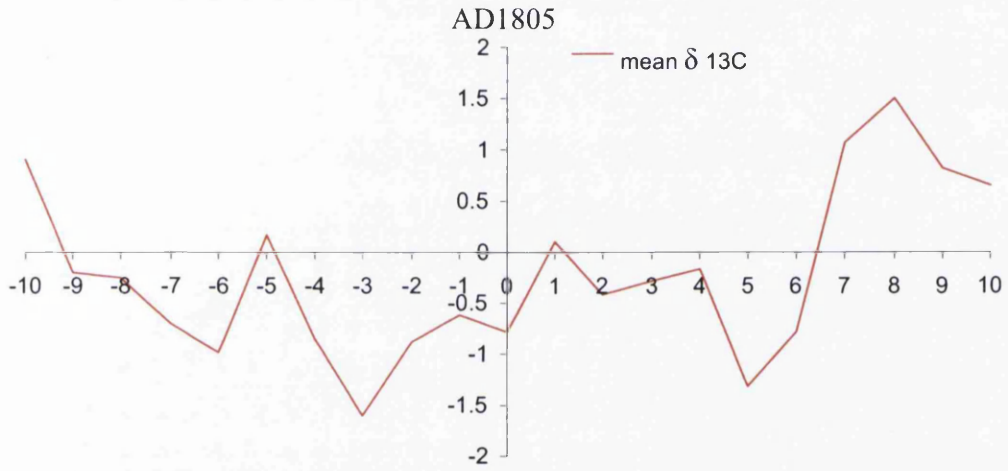

Figure 6.31 1805 'event' SEA showing the period 1795 to1815.

It is interesting that both the 1815 and 1805 volcanic eruptions, large as they were do not have as much effect on the Blanco carbon isotopes as is evident in ring width studies. In certain cases it may be the case (as shown in figure 6.33 and 6.34) that recovery to a mean level is much quicker in $\delta^{13}C$ than the evidence in ring widths would suggest.

6.4. $\delta^{13}C$ data analysis. AD1750-1799

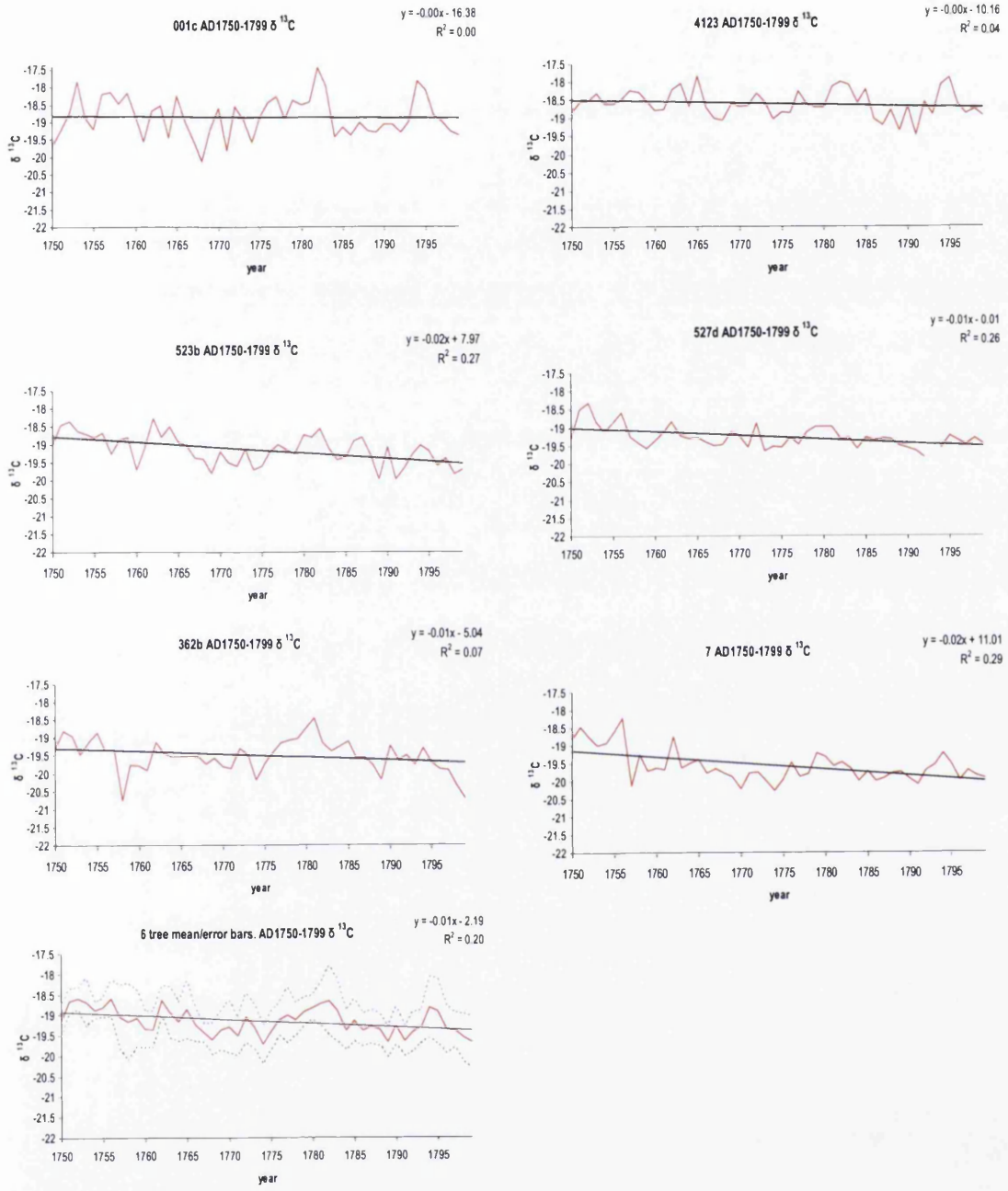

Figure 6.32. Individual trees $\delta^{13}C$ 1750-1799

Table 6.5 Tree details
Below: inter tree correlation $\delta^{13}C_{pin}$ 1750-1799

Tree	Most positive year (AD)	Most negative year(AD)	mean $\delta^{13}C$
001c	1782	1768	-18.87
523b	1762	1789	-19.15
362b	1781	1758	-19.51
4123	1765	1791	-18.61
527d	1752	1792	-19.27
007	1756	1774	-19.57
mean	**1756**	**1774**	**-19.16**

	001c	523b	362b	4123	527d
523b	0.39				
362b	0.28	0.53			
4123	0.68	0.46	0.34		
527d	0.24	0.57	0.49	0.27	
007	0.23	0.64	0.42	0.30	0.71
Mean r	0.44			**EPS**	0.82

A significant $\delta^{13}C$ decline is observed in three trees and the mean over this period. More positive values are associated with the period from 1750-1756 in all trees with a decline to 1768 and then a rise again to 1762-1765. More negative $\delta^{13}C$ values are then evident to 1775 before rising to a positive peak in 1781/1782. $\delta^{13}C$ then declines in all trees but rise in all trees for the period 1792-1796, with a positive peak at 1795.

Notable volcanic eruptions in the 18th century were those of Laki in Iceland and Assama Yama in Japan in 1783 and Vesuvius, Italy in 1785 (Oppenheimer, 2003).

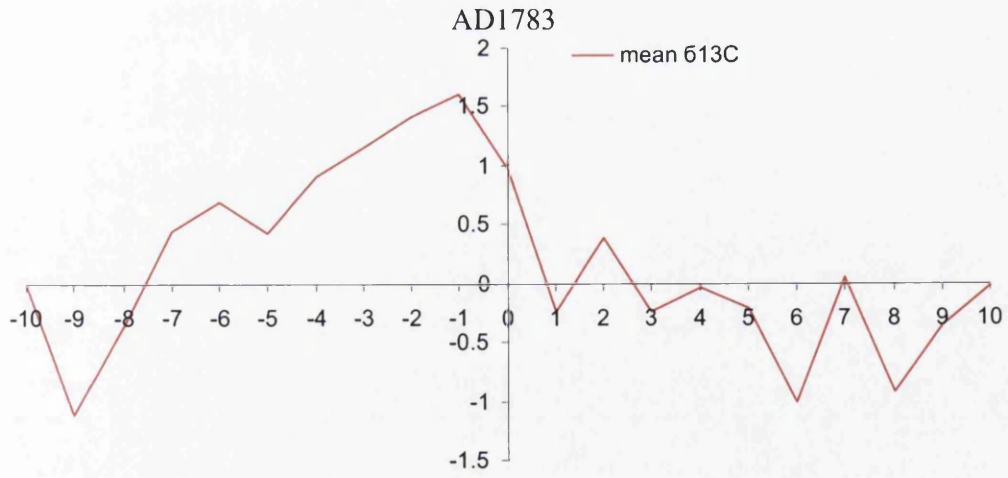

Figure 6.33 1783 SEA showing the period 1773 to 1793

The extreme positive $\delta^{13}C$ value of 1782 suggests dry/hot summer conditions and 1782 is in fact a well known narrow ring in the White Mountains bristlecone ring width chronologies. The 10 years following 1783 are generally depleted compared to the $\delta^{13}C$ values since 1774 suggesting cool or wet conditions following the three eruptions mentioned.

6.5. $\delta^{13}C$ data analysis AD1700-1749

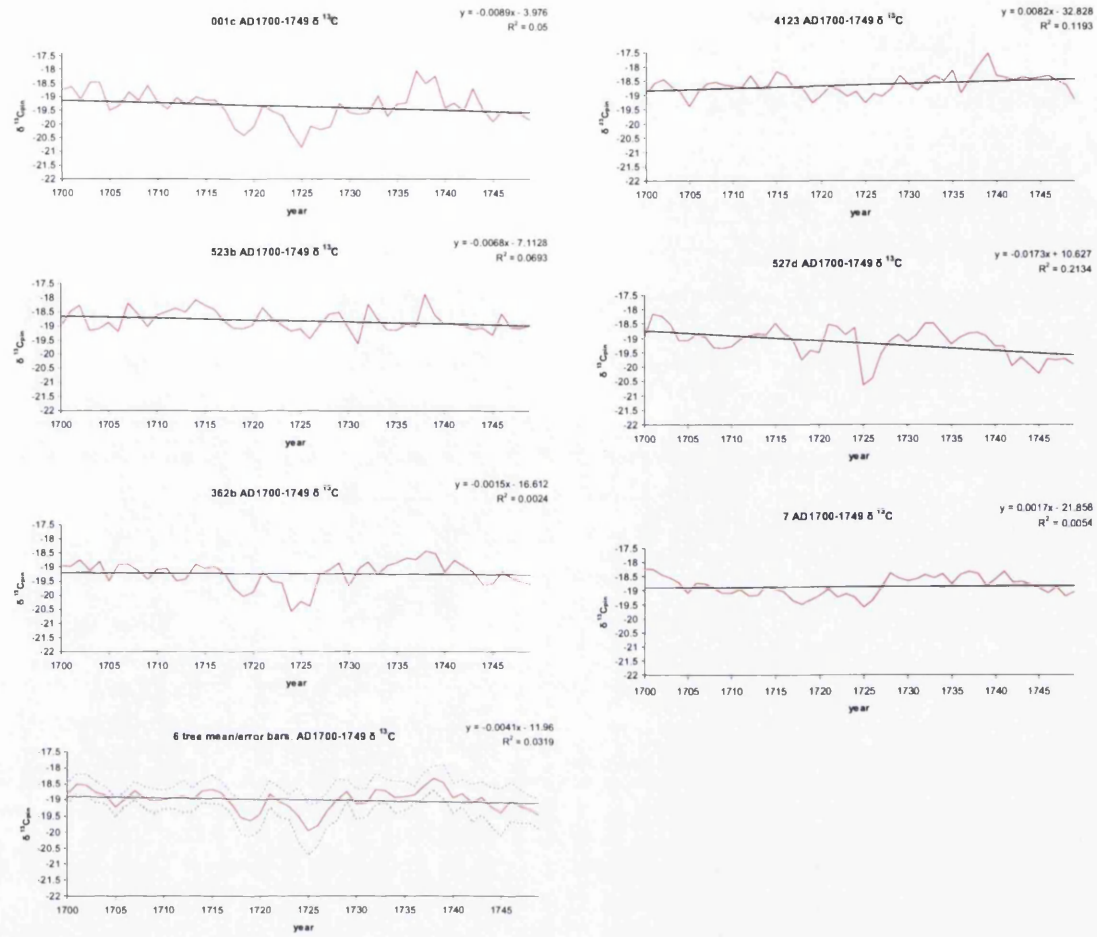

Figure 6.34. Individual trees $\delta^{13}C$ 1700-1749

Table 6.6: Tree details
Below: inter tree correlation $\delta^{13}C_{pin}$ 1700-1749

Tree	Most positive year (AD)	Most negative year(AD)	mean $\delta^{13}C$
001c	1737	1725	-19.35
523b	1738	1731	-18.83
362b	1738	1724	-19.25
4123	1739	1725	-18.63
527d	1701	1725	-19.16
007	1701	1725	-18.86
mean	1738	1725	**-19.01**

	001c	523b	362b	4123	527d
523b	0.35				
362b	0.71	0.47			
4123	0.54	0.38	0.53		
527d	0.51	0.51	0.50	0.21	
007	0.54	0.16	0.72	0.37	0.46
Mean r	0.46			**EPS**	0.84

With the exception of tree 527d no significant trends are observed in $\delta^{13}C$ for this period (1700-1749). Values decline gradually in all trees to a low in 1719. $\delta^{13}C$ rises in all trees to 1722 and then decline in all trees to 1724/1725. 1725 represents the lowest $\delta^{13}C$ value in four of the seven trees and the mean for this 50 year time period. Values then increase with a peak at 1737-1739 before declining toward 1749. The extreme positive value in 1738 may be related to drought identified in tree rings from Peña Nevada, Northeast Mexico from 1738-1743 (Villanueva *et al.*, 2006). 1725 is a noted frost ring in the bristlecone pines and 1732 is a ring width minima (LaMarche and Hirschboeck, 1984).

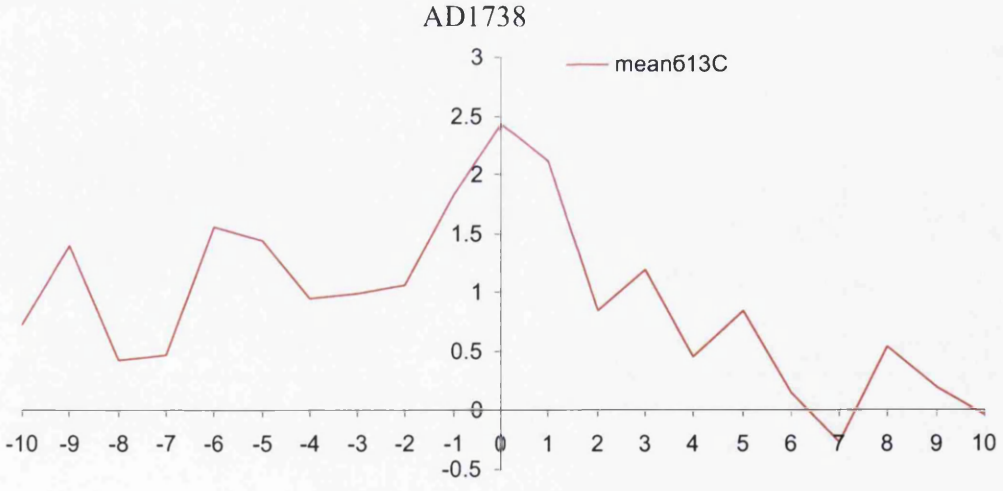

Figure 6.38 1738 event SEA showing the period 1728 to 1748

Ice core extremes are noted in 1729, 1731, 1732 and 1736 (LaMarche and Hirschboeck, 1984) and volcanic eruptions during this time have been attributed to the Guatemalan volcanoes of Sangay and Fuego (Amman and Naveau, 2003). The extreme depleted $\delta^{13}C$ value in 1725 is noted as a bristlecone frost ring year by Salzer and Hughes (2007).

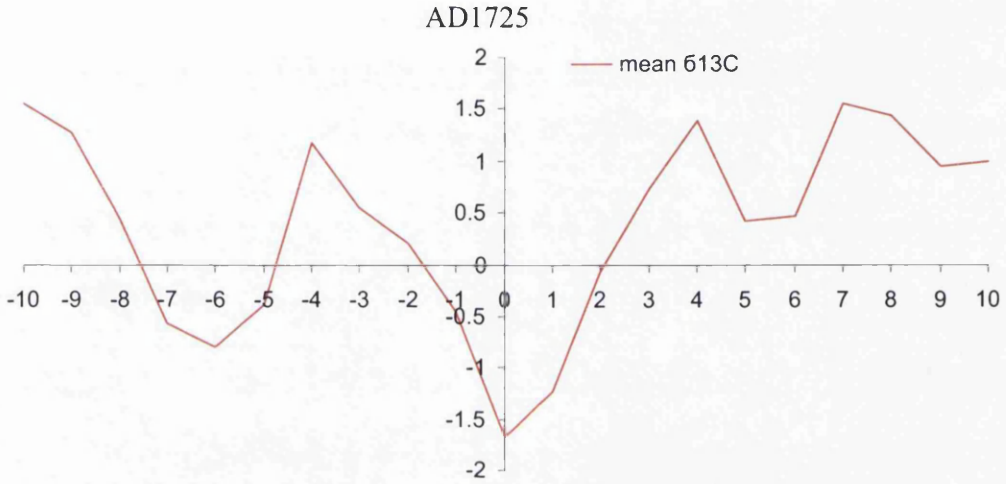

Figure 6.39 1725 event SEA showing the period 1715 to 1735

6.6: $\delta^{13}C$ data analysis AD1700-1849

Figure 6.40 (A,B,C,D,E,F,G) ($\delta^{13}C_{pin}$ from 1820-1849)

6.40A

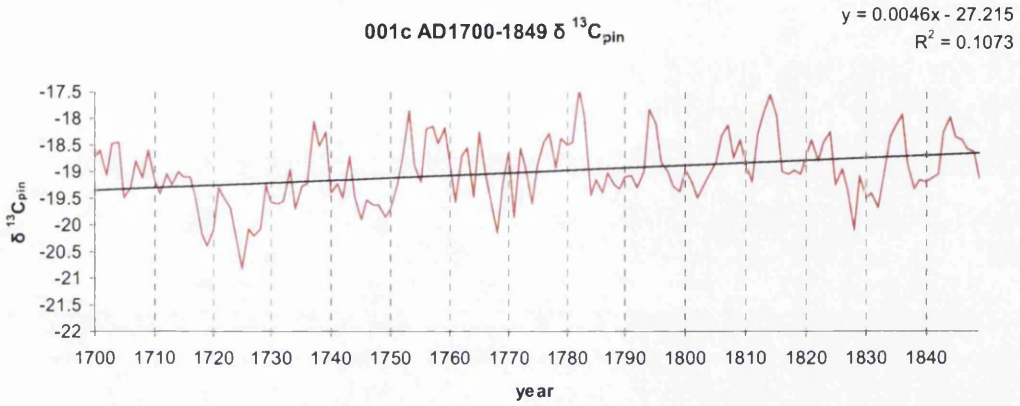

6.40B

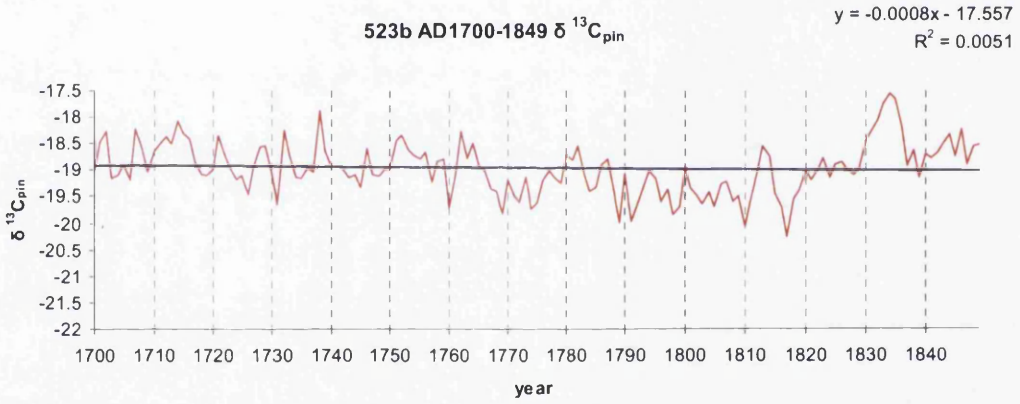

6.40C

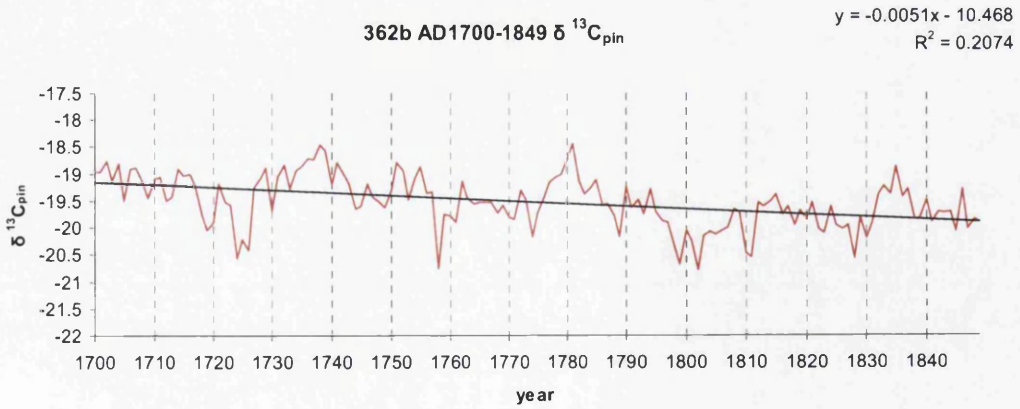

6.40D

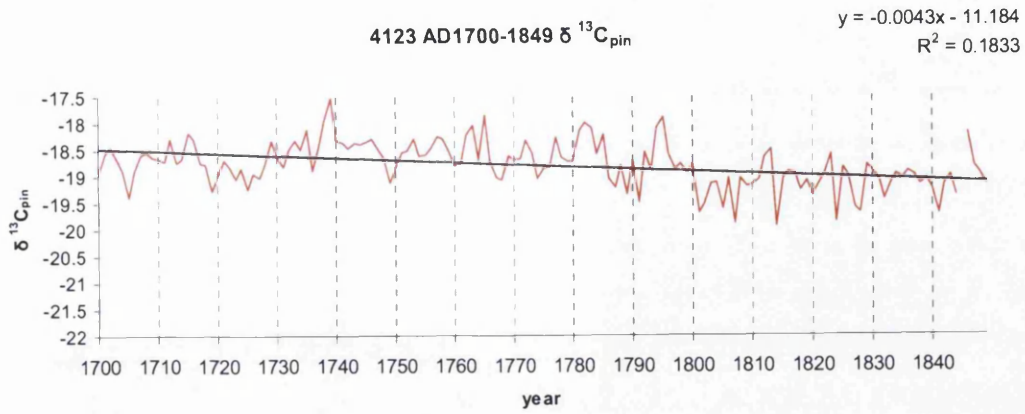
4123 AD1700-1849 δ 13Cpin
y = -0.0043x - 11.184
R2 = 0.1833
δ 13Cpin
-17.5
-18
-18.5
-19
-19.5
-20
-20.5
-21
-21.5
-22
1700 1710 1720 1730 1740 1750 1760 1770 1780 1790 1800 1810 1820 1830 1840
year

6.40E

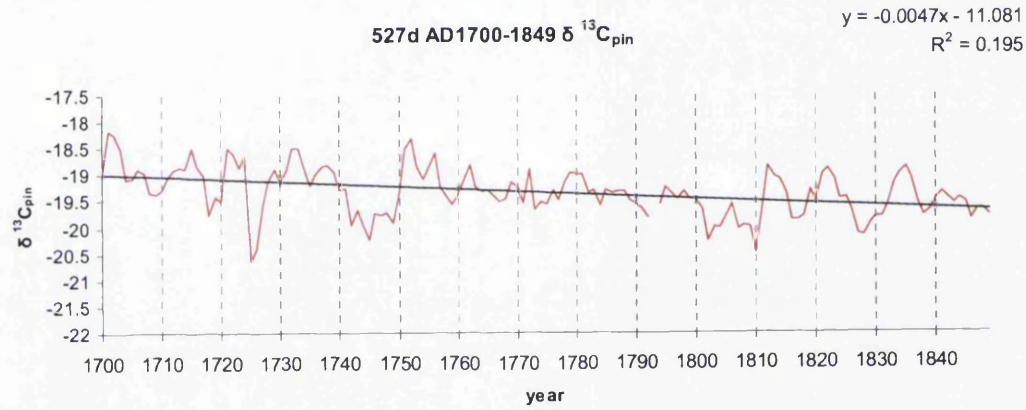
527d AD1700-1849 δ 13Cpin
y = -0.0047x - 11.081
R2 = 0.195
δ 13Cpin
-17.5
-18
-18.5
-19
-19.5
-20
-20.5
-21
-21.5
-22
1700 1710 1720 1730 1740 1750 1760 1770 1780 1790 1800 1810 1820 1830 1840
year

6.40F

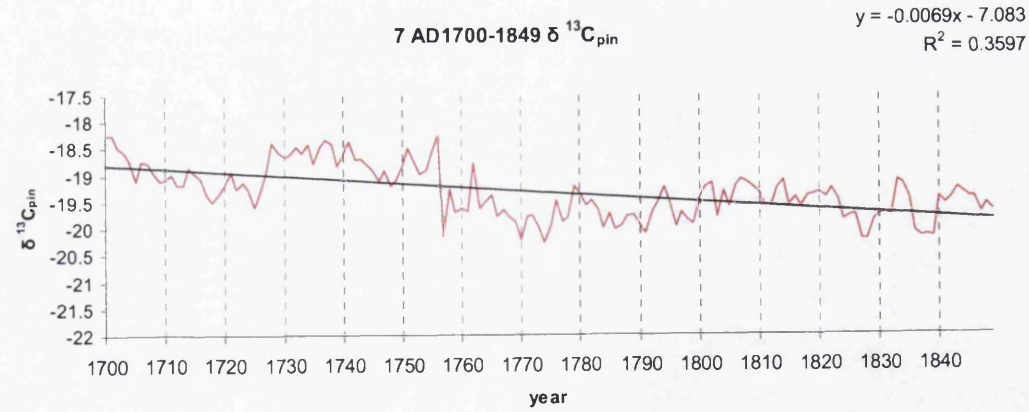
7 AD1700-1849 δ 13Cpin
y = -0.0069x - 7.083
R2 = 0.3597
δ 13Cpin
-17.5
-18
-18.5
-19
-19.5
-20
-20.5
-21
-21.5
-22
1700 1710 1720 1730 1740 1750 1760 1770 1780 1790 1800 1810 1820 1830 1840
year

6.40G

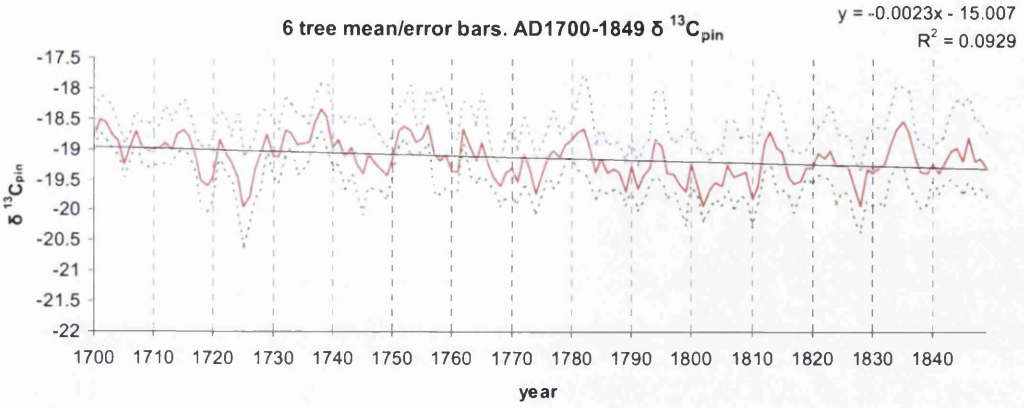

Table 6.7 Tree details
Below: inter tree correlation δ^{13}C1700-1849

Tree	Most positive year (AD)	Most negative year(AD)	mean δ^{13}C
001c	1782	1725	-19.00
523b	1834	1817	-18.97
362b	1781	1802	-19.53
4123	1739	1814	-18.79
527d	1701	1725	-19.34
007	1700/01	1774	-19.32
mean	**1738**	**1725**	**-19.14**

	001c	523b	362b	4123	527d
001c					
523b	0.18				
362b	0.21	0.44			
4123	0.21	0.22	0.51		
527d	0.24	0.44	0.59	0.39	
007	-0.01	0.33	0.54	0.31	0.47
	Mean r	0.34		**EPS**	0.75

A significant decline in δ^{13}C is evidenced between 1700-1849 in four of the six trees (362, 527, 7, 4123) and a significant positive trend is evident in tree 001c. The decline is not significant in the mean. The most positive δ^{13}C occurred in the mid 1730s, peaking in 1738/1739. The years 1700/1701, 1781/1782 and 1834 also represent extreme positive values in this 150 year period. The most negative values in two trees(001c/527d) and the mean are centred on 1725. Extreme negative excursions are also centred on 1802, 1814-1817 and 1774.

It is interesting to note that the drought reconstruction by Stahle *et al.,* (2007:136) indicates that 1833 may have been the wettest single year in the last 500 years, with

extreme wetness extending from the Great Plains into central Mexico. Early settlers in Texas reported high water from March till late June and in eastern Oklahoma and Arkansas record flooding occurred in the first week of June 1833 (Stahle *et al.*, 2007:136). As discussed in chapter 6.3 the Blanco $\delta^{13}C$ for the period from 1832 to 1836 is positive in the extreme indicating dry or hot conditions.

The after effects of volcanic eruptions are identifiable in the positive $\delta^{13}C$ of the mid 1830s including 1834 as the most positive value in tree 523b for the 150 year period 1700-1849. The period between 1737 and 1739 represents drought. The extreme positive values in 1700/1701 represent the after effects of a climatic event that caused frost or 'light' rings in a variety of high altitude or high latitude tree ring chronologies in 1699/1700 described by Hantemeriov (2007). The most extreme negative in this 150 year period of 1725 is of an unknown cause but is evident as a frost ring in bristlecone pines (Salzer and Hughes, 2007). The year 1726 was noted for catastrophic flooding in parts of Europe (Zielinski, 2000) and may be related to hemispheric cooling at the time.

6.7: $\delta^{13}C$ data analysis AD1650-1699

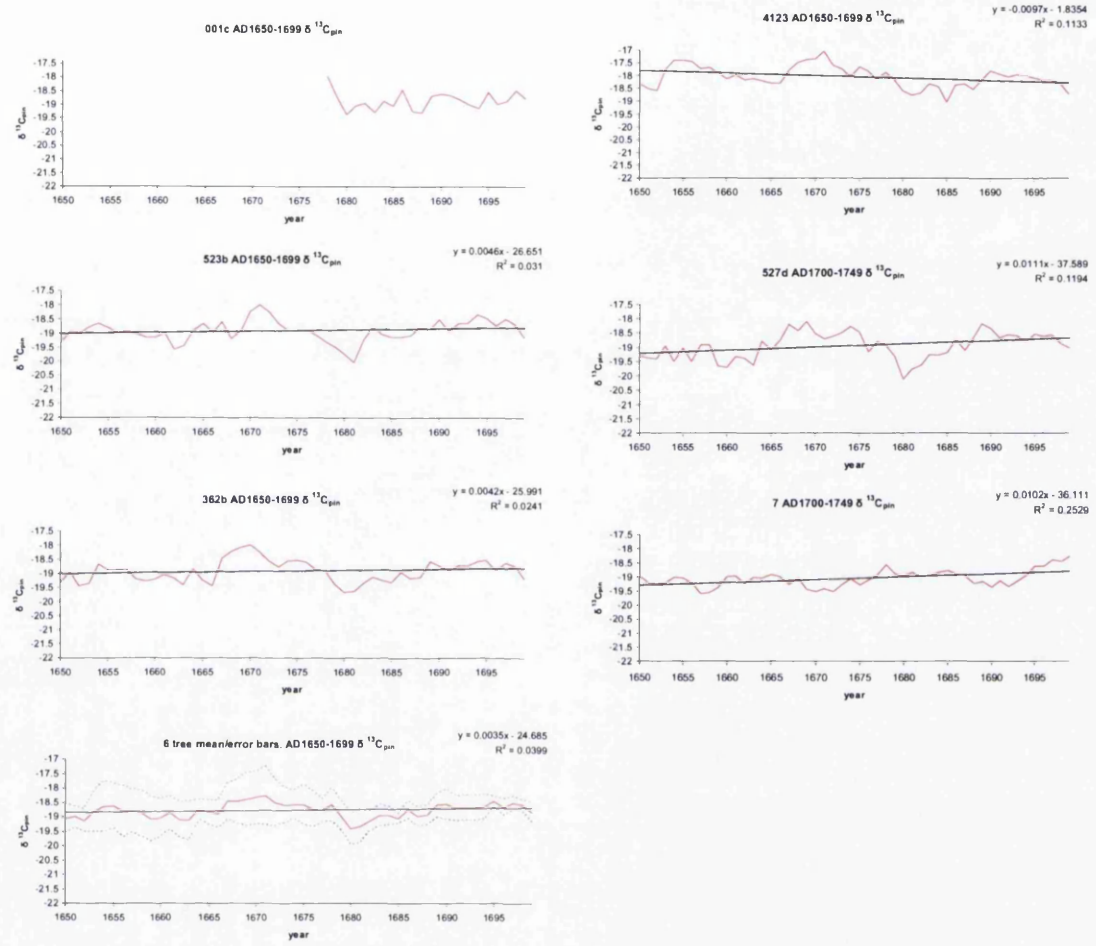

Figure 6.41 Individual trees $\delta^{13}C$ 1650-1699

Table 6.8 Tree details
Below: inter tree correlation $\delta^{13}C$1650-1699

Tree	Most positive year (AD)	Most negative year(AD)	mean $\delta^{13}C$
001c	1678	1680	-18.83
523b	1671	1681	-18.90
362b	1670	1680	-18.90
4123	1671	1685	-18.03
527d	1669	1680	-18.93
007	1699	1657	-19.04
mean	1671	1680	**-18.76**

	001c	523b	362b	4123	527d
523b	0.09				
362b	0.41	0.70			
4123	0.45	0.51	0.69		
527d	0.41	0.61	0.75	0.40	
007	0.29	-0.22	-0.26	-0.53	-0.17
Mean r	0.28			**EPS**	0.70

In trees 001c, 362b, 4123, 527d and the mean this is the 50 year period (1650-1699) with the most positive $\delta^{13}C$ values in the whole chronology. Extreme positive $\delta^{13}C$ is observed between 1669 and 1678 in all trees except tree 007 and the mean, with the most positive values between 1669 and 1671. Negative $\delta^{13}C$ occurs with extreme low values centred on 1680/1681 persisting until 1685. The period 1690-1699 sees a return to positive $\delta^{13}C$ in all trees. Tree 007 does not appear to follow the same pattern as the other trees during this period. Lower values are observed in this tree between 1668 and 1673 but the values are not as extreme negatives as in the other trees. 1680/1681 is likewise not a major negative feature in this tree. The strong negative correlations between tree 007 and the other trees suggests it is responding differently to the climate of this 50 year period. This may also explain the low EPS for this period.

The second half of the 17th century witnesses some of the most positive isotope values in the whole chronology with positive $\delta^{13}C$ centred on 1669/1670 and 1671 indicating temperature or drought more extreme than the present day. The southwestern American drought of the late 1660s and early 1670s is believed to have led to widespread native American rebellion against Spanish rule that culminated in the Pueblo revolt of 1680 (Cook *et al.*, 1995; 2005; Weber, 1999). The widespread documentary evidence that the Spanish compiled during this period provides

evidence for the fragility of the environment and society in the southwest of America. One year of intense drought would be bad for the pueblo peoples, two or three years would be devastating for the corn based economy that both the pueblo peoples and the Spanish who taxed them depended upon (Diamond, 2005:153).

Figure 6.42 AD 1680-The Pueblo Revolt, by George Chacón, Taos Mural Project. http://en.wikipedia.org/wiki/Image:Cg-98-3.jpg

The Blanco $\delta^{13}C$ values between 1667 and 1681 change from extreme positive values centred on 1671 to extreme negative values centred on 1680. The extreme negative $\delta^{13}C$ value of 1680 appears as a widespread frost ring in bristlecone pines and may well be related to eruptions of two volcanoes in that year, Tongoko, Celebes and Krakatoa, Java . 1679 and 1680 also appear as light or frost rings in juniper and larch chronologies from northwest Siberia (Hantemirov *et al.*, 2004). The years 1672, 1675 and 1677 and 1681 are identified as ring width minima in bristlecone pine chronologies that correspond to an ice core signal (Hughes and Salzer, 2007:62). The years 1693 and 1694 have also been identified as years in which volcanic eruptions occurred but are not evidenced as ring width minima or frost rings in the bristlecones but do appear as extreme in ice core data (Hughes and Salzer, 2007). The year 1660 appears as a widespread frost ring in bristlecone pines with four volcanic eruptions attributed to that year

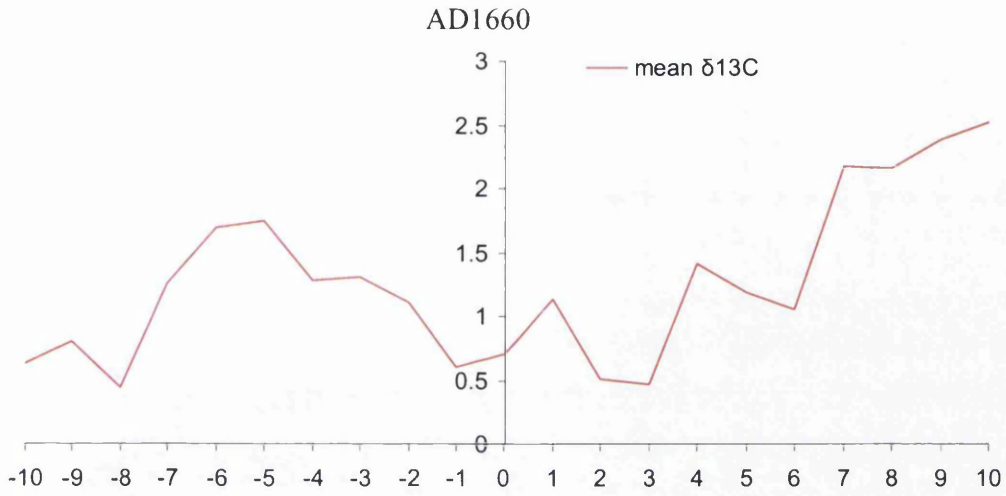

Figure 6.43.1660 SEA showing the period 1650 to 1670

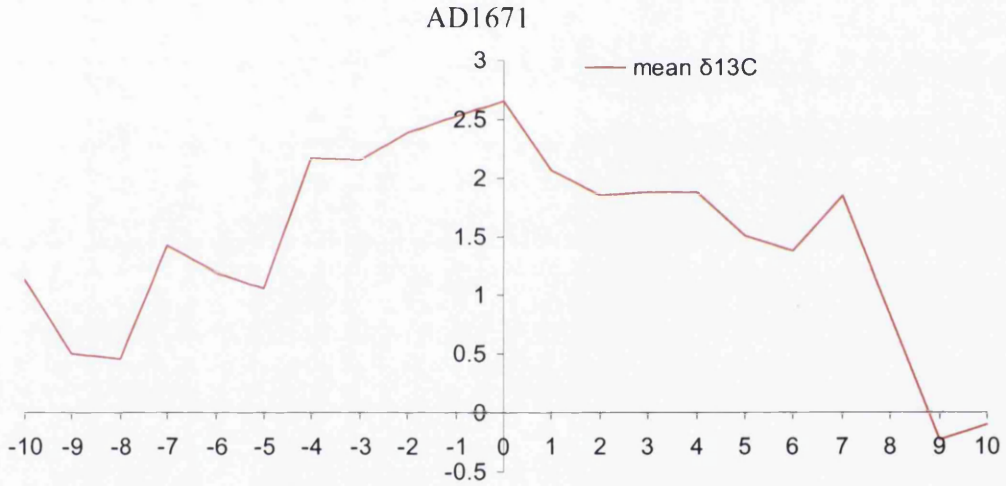

Figure 6.44.1671 drought SEA showing the period 1661 to 1681

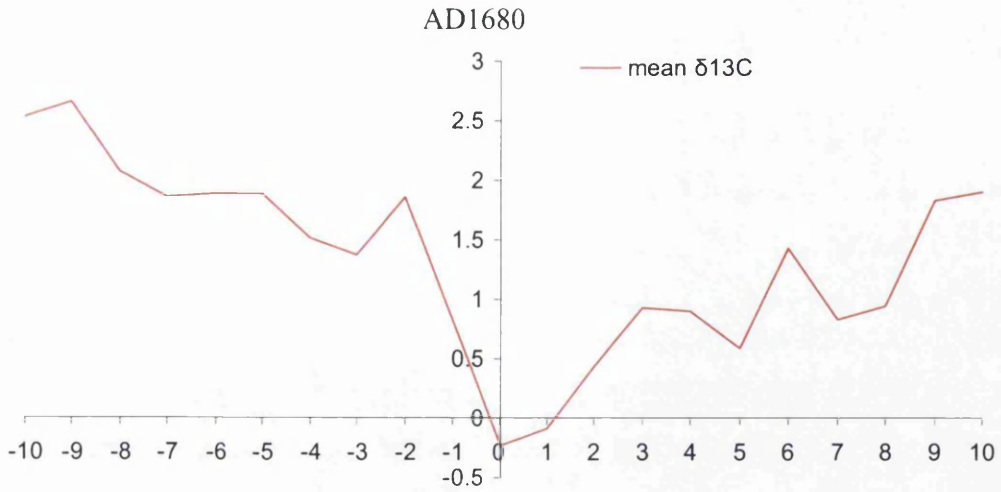

Figure 6.45.1680 eruption SEA showing the period 1670 to 1690

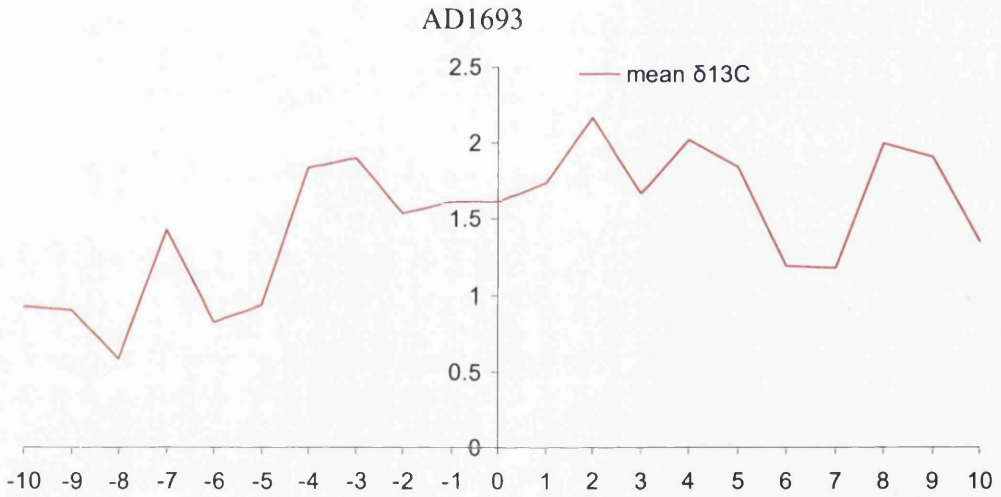

Figure 6.46.1693 eruption SEA showing the period 1683 and 1703

All the above SEA figures indicate a sustained period of positive mean $\delta^{13}C$. From around 1650 to the early 1700s there was extreme drought, the likes of which has not been paralleled since AD1150 and has not occurred from the 17th century until the present day.

6.8. $\delta^{13}C$ data analysis AD1600-1649

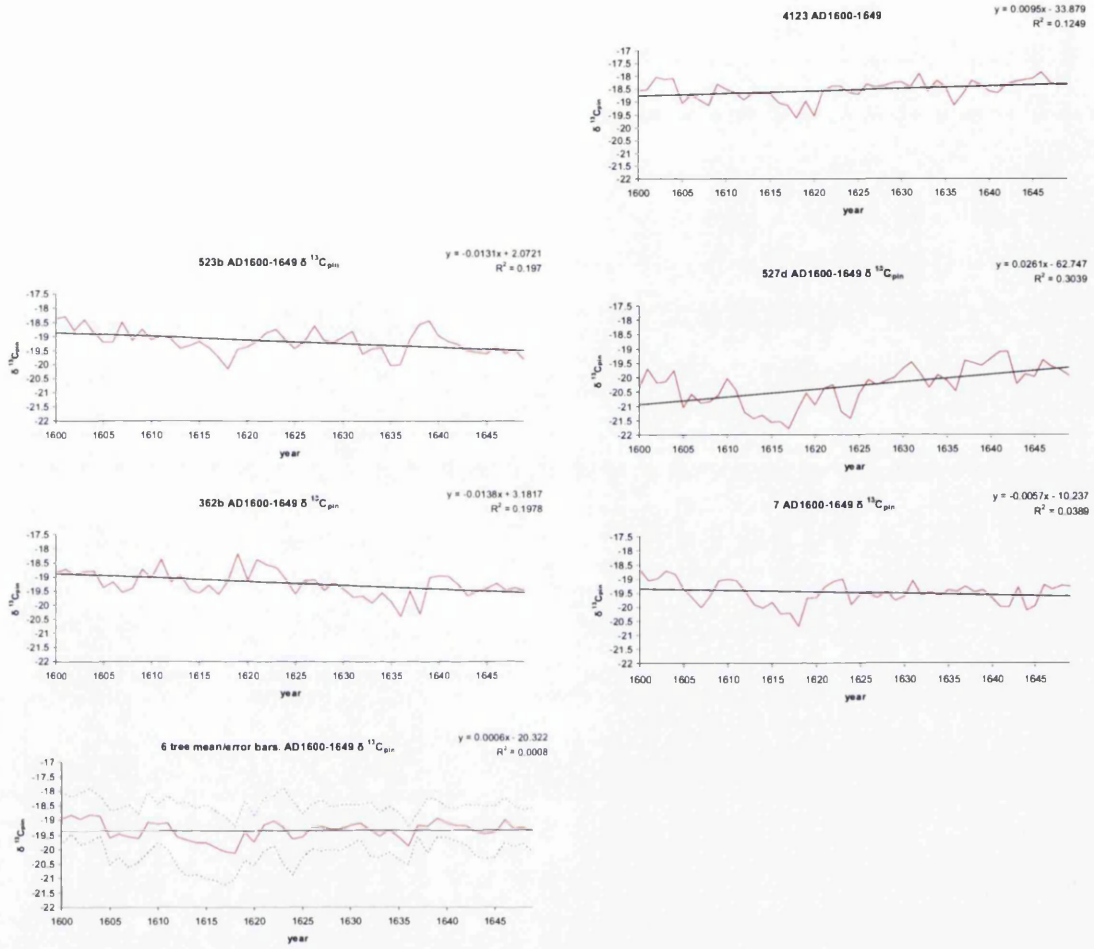

Figure 6.47: Individual trees $\delta^{13}C$ 1600-1649

Table 6.8: Tree details
Below: inter tree correlation $\delta^{13}C$1600-1649

Tree	Most positive year (AD)	Most negative year(AD)	mean $\delta^{13}C$
523b	1601	1618	-19.79
362b	1619	1636	-19.44
4123	1646	1618	-18.32
527d	1642	1617	-19.93
007	1600	1618	-19.24
mean	**1603**	**1618**	**-19.34**

	523	362	4123	527
362	0.40			
4123	0.26	-0.01		
527	0.16	-0.08	0.62	
007	0.50	0.26	0.44	0.34
Mean r	0.29		**EPS**	0.67

The first half of the seventeenth century contrasts with the second half in that in four trees (523,362,527,007) and the mean, $\delta^{13}C$ values are on average some of the most negative in the whole millennial chronology. There are extreme positive $\delta^{13}C$ values from 1600-1605 that decline to extreme negative values centred on 1617/1618. Values in all trees are generally positive between 1619-1632 and an extreme event then occurs centred on 1636, evidenced in all trees except tree 007. In the period between 1637 and 1646 $\delta^{13}C$ is generally positive with a negative event in 1644, with two positive $\delta^{13}C$ values either side of it (1642 and 1646).

Over the 50 years, a significant decline in $\delta^{13}C$ values is observed in trees 523 and 362 and a significant increase is observed in tree 527 which also displays the more negative mean values than the other trees during this period.

A notable volcanic eruption occurred in 1600 (Huynapatina, Peru) and possibly in 1605 (Momotombo, Nicaragua) (Amman and Naveau, 2003). The year 1601 is noted as a bristlecone and Siberian frost ring and the years 1602 and 1606 are noted as extreme ice core events and bristlecone ring width minima (Hughes and Salzer, 2007). The years 1605-1608 appear to be the most significant negative event in the Blanco isotopes between 1590 and 1610 (figure 6.48).

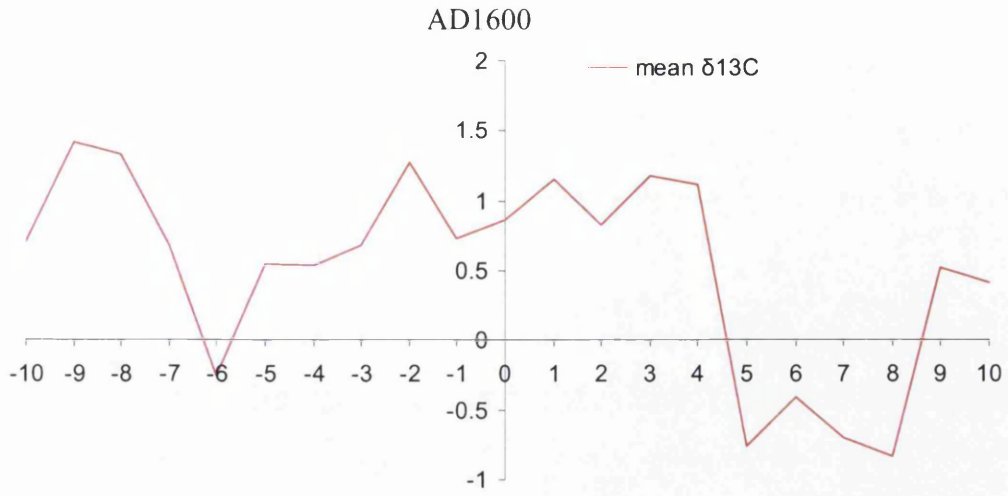

Figure 6.48.1600 SEA showing the period 1590 to 1610

The period is marked by low $\delta^{13}C$ inter tree correlation and EPS (chapter 4), although common features are observed in all the trees. All trees display the negative excursion at 1617/1618 and all trees exhibit relatively positive values between 1619 and the next negative excursion in 1636.

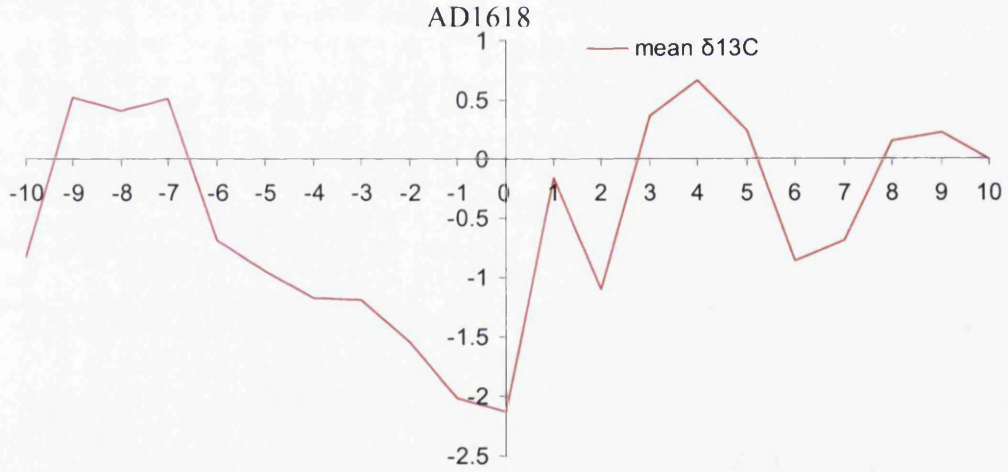

Figure 6.49.1618 SEA showing the period 1608 to 1628

The negative event that occurs in the Blanco $\delta^{13}C$ in 1618 is evident in a range of proxy and historical evidence. LaMarche and Hirschboeck (1984) note an eruption in the Little Sunda Islands in 1614 but do not note a bristlecone frost ring. Hughes and Salzer (2007) note a bristlecone ring width minima in 1618 and that ice core

signals occur in 1619, 1621, 1622 and 1625 and Finnish tree width minima from 1616-1620. Hantemirov *et al.*, (2004) note a Siberian frost/light ring in 1617. Historical and proxy evidence from Spain suggests that winter flooding in 1617 caused widespread catastrophic socio-economic damage and exceeded floods in the instrumental period (Thorndycraft *et al.*, 2006). In common with the Blanco $\delta^{13}C$ based reconstruction the first half of the 17th century in the northern hemisphere is often associated with a cooler phase of climate variability. From the southwestern USA Graumlich (1993) identifies the period between 1604 and 1623 and the period between 1628 and 1647 as being anomalously cool from foxtail pine in the Sierra Nevada. Salzer and Kipfmueller (2005) identify cool periods in Rocky Mountain bristlecone pine from 1599 to 1612 and 1636 to 1653 and wet periods from 1615 to 1622 and 1640 to 1647. Notable volcanic eruptions in the first half of the 17th century occurred in 1638 and 1640 (Mann and Jones, 2003). Hughes and Salzer (2007) note a bristlecone frost ring in 1640/1641 and Hantemirov *et al.*, (2004) note extreme years in Siberian trees in 1631 and 1634. The most extreme events in the Blanco $\delta^{13}C$ during the period 1600-1649 occur in 1636 (negative) and in 1639 (positive). Ammann and Naveau (2003) identify the eruption of Parker, Indonesia in 1641. The years 1644, 1645 and 1646 occur as ring width minima in bristlecone pines (Salzer and Hughes, 2007) and 1644 does occur as a negative $\delta^{13}C$ but this is minor compared to the negative $\delta^{13}C$ in 1636. The years 1637, 1638, 1639, 1641, 1644, 1645, 1646 and 1647 occur as ice core extremes (Salzer and Hughes, 2007).

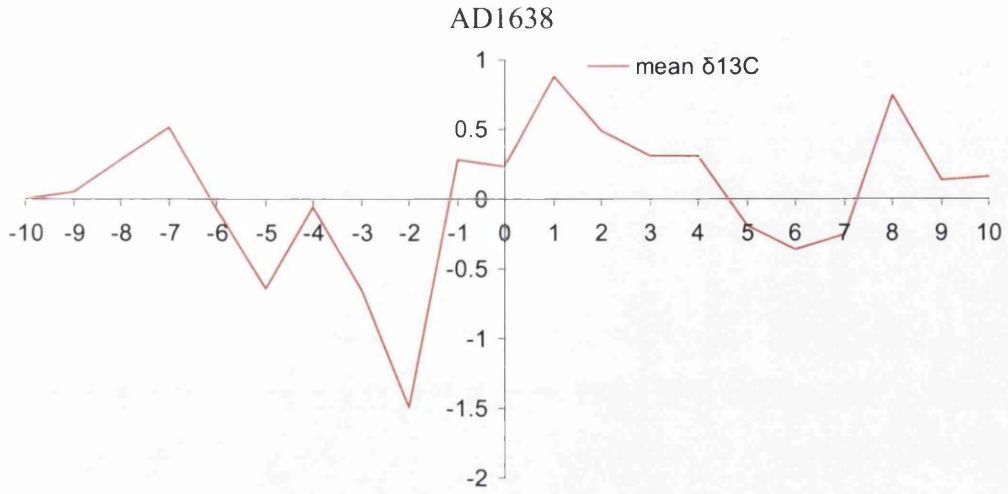

Figure 6.50.1638 SEA showing the period 1628 to 1648

6.9. $\delta^{13}C$ data analysis AD1550-1599

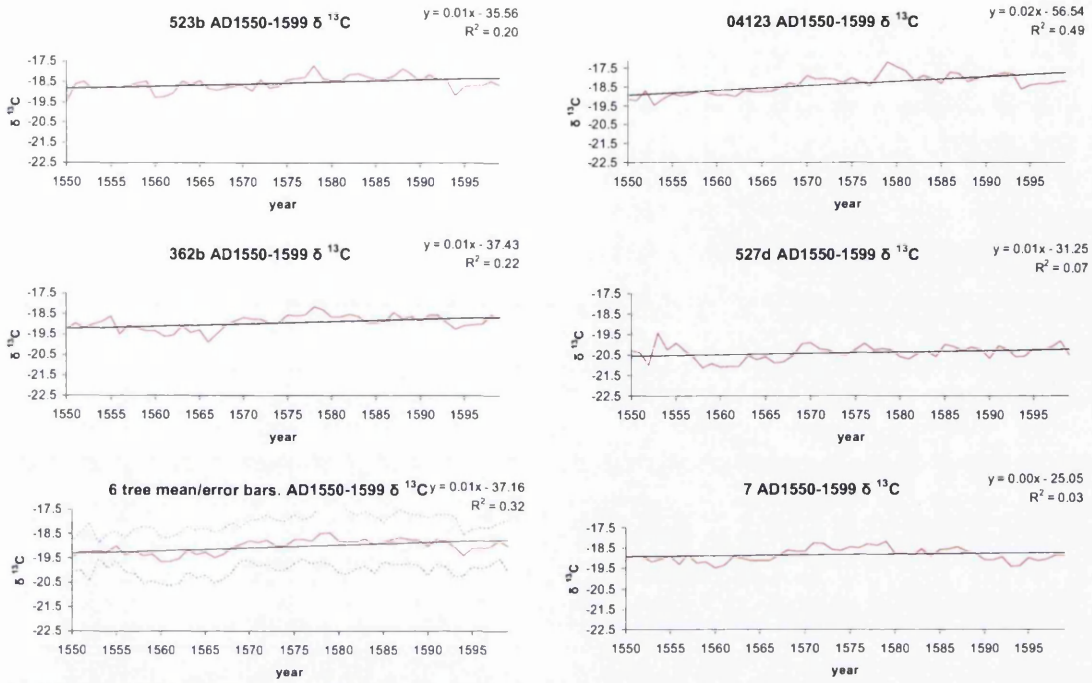

Figure 6.51 Individual trees $\delta^{13}C$ 1550-1599.

Tree	Most positive year (AD)	Most negative year(AD)	mean $\delta^{13}C$
523b	1578	1550	-18.58
362b	1578	1566	-18.94
4123	1579	1553	-18.35
527d	1553	1558	-20.41
007	1579	1560	-18.83
mean	**1579**	**1561**	**-19.02**

	523b	362b	4123	527d
362b	0.67			
4123	0.59	0.68		
527d	0.26	0.60	0.18	
007	0.45	0.65	0.55	0.41
Mean r	0.50		**EPS**	0.84

Table 6.10. Tree details and inter-tree correlation 1550-1599.

In three of the trees (523, 362 and 4123) and the mean, a significant $\delta^{13}C$ rise is evident in the period 1550-1599. All trees exhibit relatively positive $\delta^{13}C$ values except tree 527d.

The $\delta^{13}C$ values for this tree follow the general pattern of the other trees but are depleted by around 1.4‰.

The period begins with positive $\delta^{13}C$ at around 1553 and then a decline throughout the 1550s and 1560s with negative events at 1558, 1560/1561 and 1566. $\delta^{13}C$ values rise to a peak in all trees at 1570, then declines slightly to 1575 before rising to a peak centred on 1578/1579. The significance of this is discussed further in chapter 6.8. $\delta^{13}C$ values fall a little in all trees but remain relatively positive and decline in the 1590's with a negative excursion centred on 1594. Values rise slightly towards 1599.

Notable volcanic eruptions during this 50 year period occurred in 1586 at Kelut in Java and in 1595 at Raung, Java and Ruiz, Columbia (Amman and Naveau, 2003). No bristlecone frost ring for this year is noted by LaMarche and Hirschboeck (1984) although frost ring occurs in Siberian trees in 1585 (Hantemirov *et al.*, 2004). No noticeable effect from the 1586 Kelut eruption occurs in the Blanco $\delta^{13}C$.

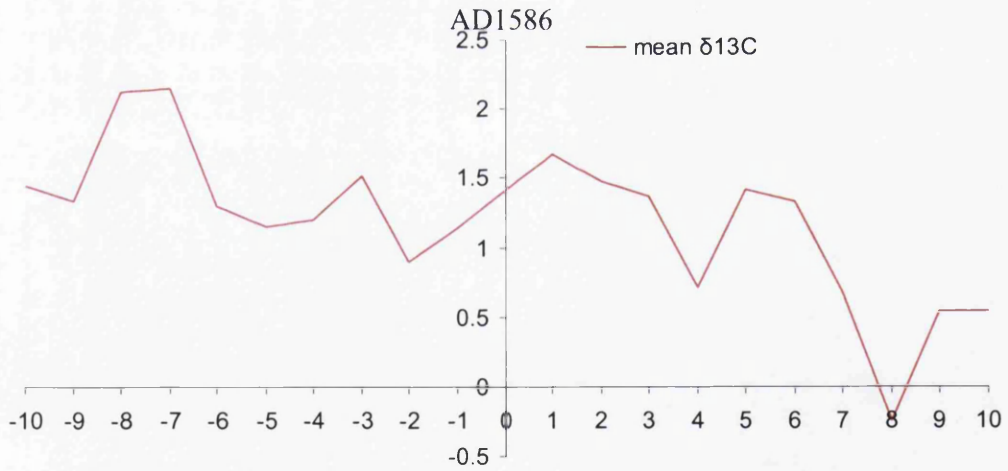

Figure 6.52 1586 SEA showing the period 1576 to 1596

6.10. $\delta^{13}C$ data analysis AD1550-1699

Figure 6.53 (A,B,C,D,E,F,G)

6.53A

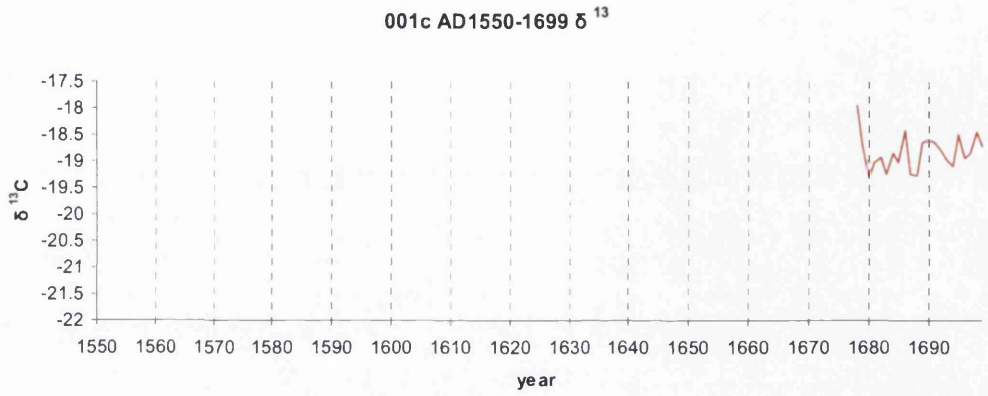

6.53B

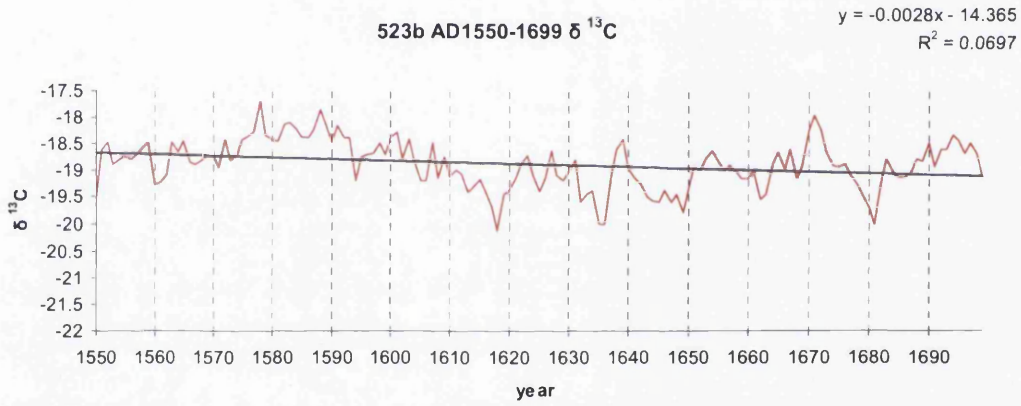

6.53C

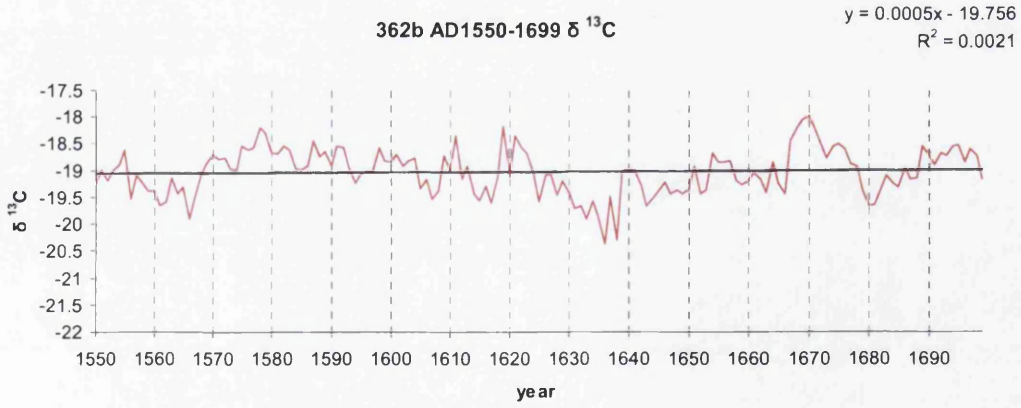

6.53D

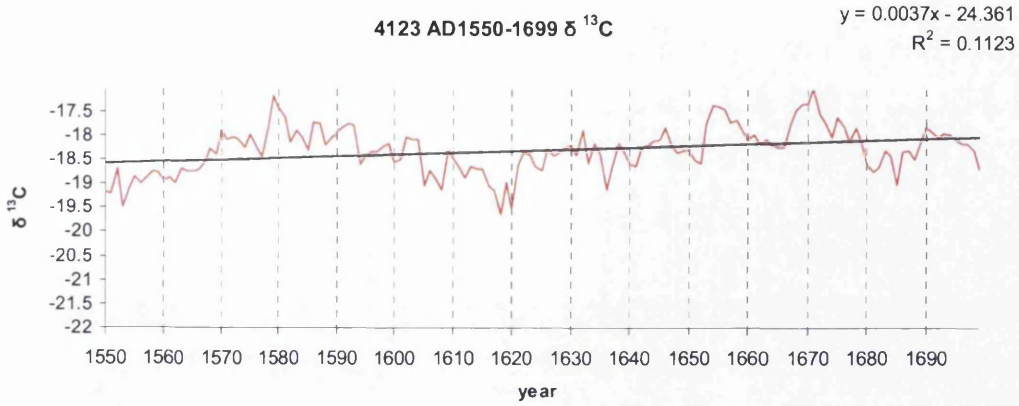

6.53E

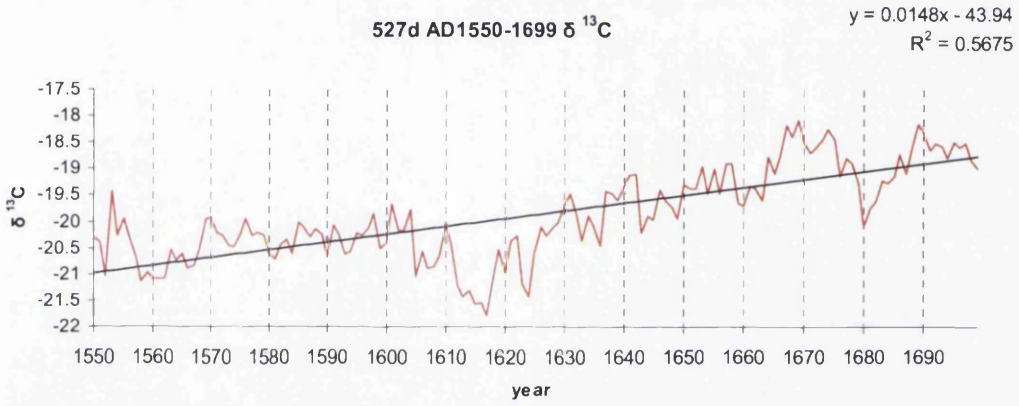

6.53F

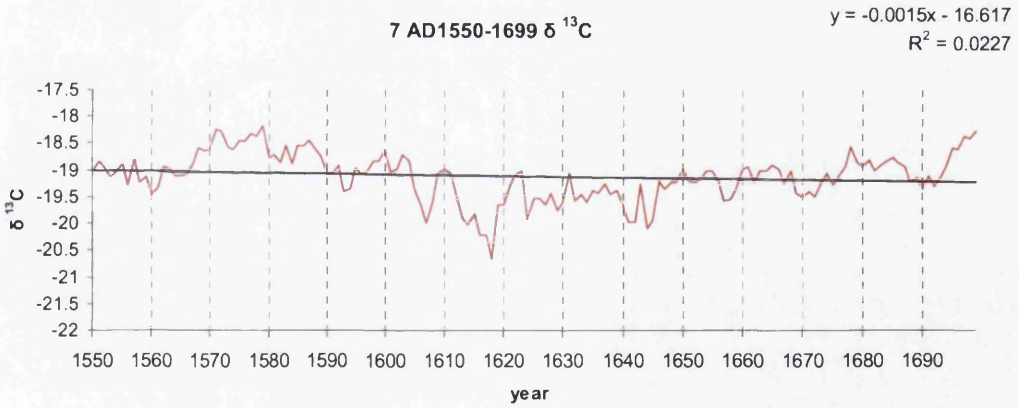

6.53G

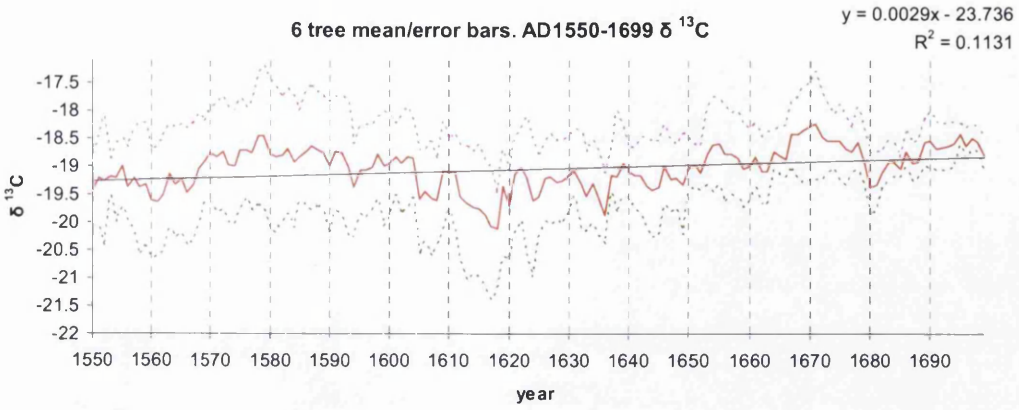

Table 6.11: Tree details
Below: inter tree correlation δ^{13}C1550-1699

Tree	Most positive year (AD)		Most negative year(AD)		mean δ^{13}C
001c	1678		1680		-18.83
523b	1578		1618		-18.88
362b	1670		1636		-19.02
4123	1671		1618		-18.30
527d	1669		1617		-19.88
007	1579		1618		-19.12
mean	**1671**		**1618**		**-19.04**

	001c	523b	362b	4123	527d
523b	0.09				
362b	0.41	0.59			
4123	0.45	0.41	0.50		
527d	0.41	0.11	0.32	0.53	
007	0.29	0.51	0.35	0.29	0.18
	Mean r	0.36		**EPS**	0.74

The increasing significant trend in δ^{13}C values observed from 1550-1699 is evident in two trees and the mean. Tree 001c ends in 1678.

The three major features of the period are generally positive δ^{13}C values between 1570-1604 with the most extreme positive values centred on 1578/1579, an excursion to generally negative values between 1605-1652, with the most negative values centred on 1617/1618 and 1636.

Values then rise gradually to a second positive excursion centred on 1655, with the most positive values in 1669/1670/1671 followed by a negative excursion centred on 1680. Minor positive excursions also occur between 1598-1605 and 1625-1632.

The Blanco $\delta^{13}C$ time series compares well to other climate reconstructions. The extreme positive $\delta^{13}C$ values of the late 16th century centred on 1578 similar to the ring width/historical drought reconstructions offered by Stahle *et al.*, (2007).

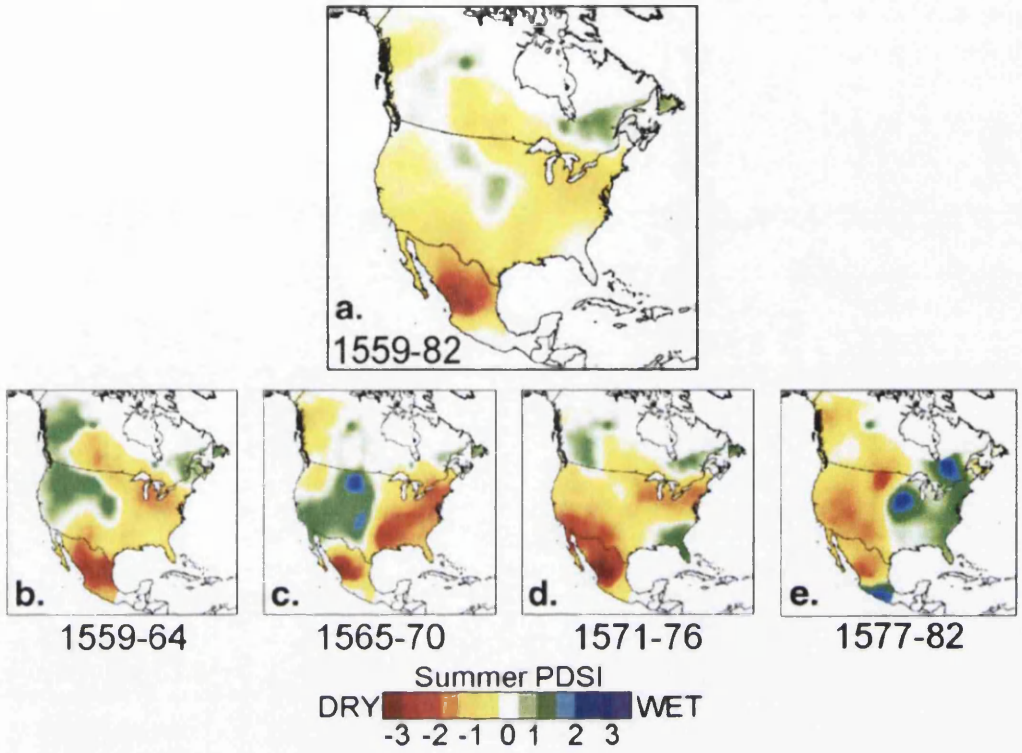

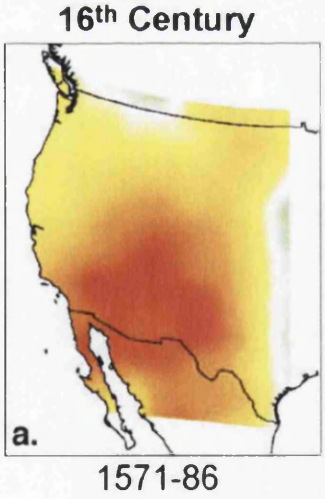

Figure 6.54. 16th century American megadrought (Stahle et al., 2007:143,144).

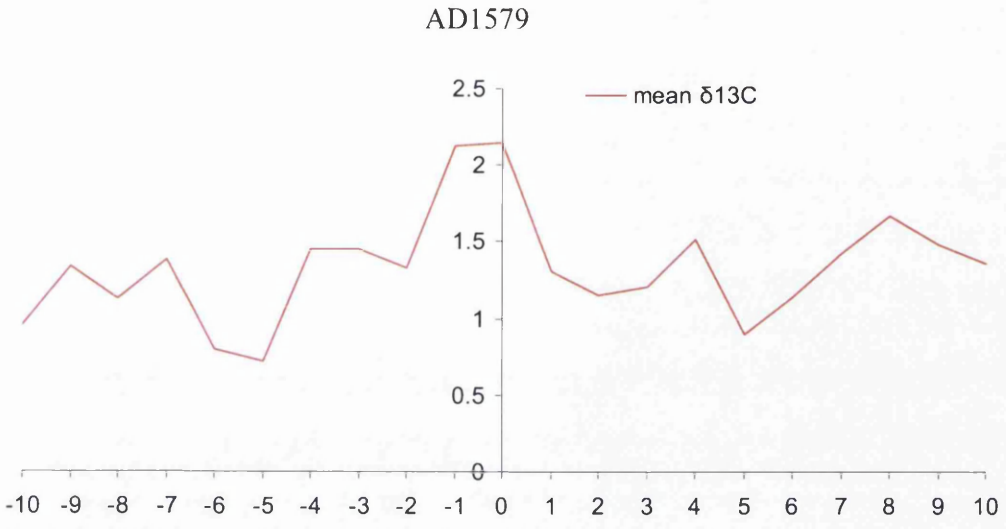

Figure *6.55.1579 SEA showing the period 1568 and 1588*

As can be seen from figure 6.55 this climatic event is of a greater magnitude than other drought periods. It appears to last longer than the 20 years and apart from a negative $\delta^{13}C$ value in 1594 the drought continues till 1604. This megadrought probably originated in Mexico in the 1540s and spread north and east over the next 60 years. Anomalous sea surface temperatures in the central and eastern equatorial Pacific may have been responsible for this drought (Stahle *et al.*,2007). It does correspond well to the periods of most intense drought in the west identified by Stahle *et al.*, (2007), from 1571 to 1582. This drought is believed to have had devastating socio-economic effects on early American settlers and may have been responsible for the disappearance of Sir Walter Raleigh's settlers from Roanoke Island, North Carolina, 1587 and the abandonment of settlement in Carolina in noted by Spanish documentary sources (Stahle *et al.*, 2007). Bizzare weather was reported by Sir Francis Drake from the coast of California in the summer of 1579 but it is interesting to note that it was extreme cold and dryness, rather than extreme heat that is described Drakes account:

"In 38 deg. 30 min. we fell with a convenient and fit harbor,1 and June 17 came to anchor there, where we continued till the 23 day of July following. During all which time, notwithstanding it was in the height of summer, and so near the sun, yet were

we continually visited with like nipping colds as we had felt before; insomuch that if violent exercises of our bodies, and busy employment about our necessary labors, had not sometimes compelled us to the contrary, we could very well have been contented to have kept about us still our winter clothes; yea (had our necessities suffered us) to have kept our beds; neither could we at any time, in whole fourteen days together, find the air so clear as to be able to take the height of sun or star [latitude]. And here having so fit occasion (notwithstanding it may seem to be besides the purpose of writing the history of this our voyage), we will a little more diligently inquire into the causes of the continuance of the extreme cold in these parts, as also into the probabilities or unlikelihoods of a passage to be found that way. Neither was it (as has formerly been touched) the tenderness of our bodies, coming so lately out of the heat, whereby the pores were opened, that made us so sensible of the colds we here felt: in this respect, as in many others, we found our God a provident Father and careful Physician for us. . . ."

(Drake, F, 1628- The world encompassed by Sir Francis Drake)

6.11. $\delta^{13}C$ data analysis AD1500-1549

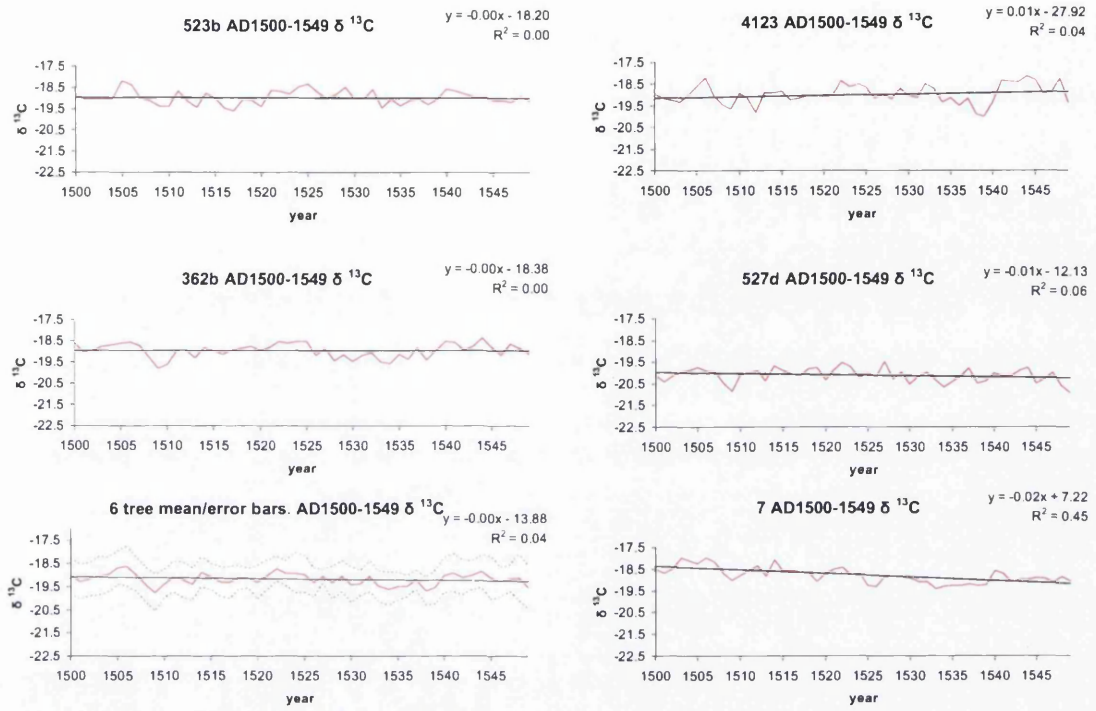

Figure 6.56 Individual trees $\delta^{13}C$ 1500-1549

Tree	Most positive year (AD)	Most negative year(AD)	mean $\delta^{13}C$
523b	1505	1517	-18.99
362b	1544	1509	-18.96
4123	1544	1539	-18.99
527d	1527	1549	-20.12
007	1503	1533	-18.79
mean	1506	1509	**-19.17**

	523b	362b	4123	527d
362b	0.54			
4123	0.46	0.49		
527d	0.41	0.62	0.34	
007	0.26	0.44	0.11	0.43
Mean r	0.41		**EPS**	0.78

Table 6.12 Tree details and inter tree correlation $\delta^{13}C$1500-1549

A significant $\delta^{13}C$ decline is evident in one tree (007). There are negative excursions centred on 1509, 1533-1539 and 1549. Positive values predominate in the period 1503-1506, 1520-1530 and 1540-1544.

6.12. $\delta^{13}C$ data analysis AD1450-1499

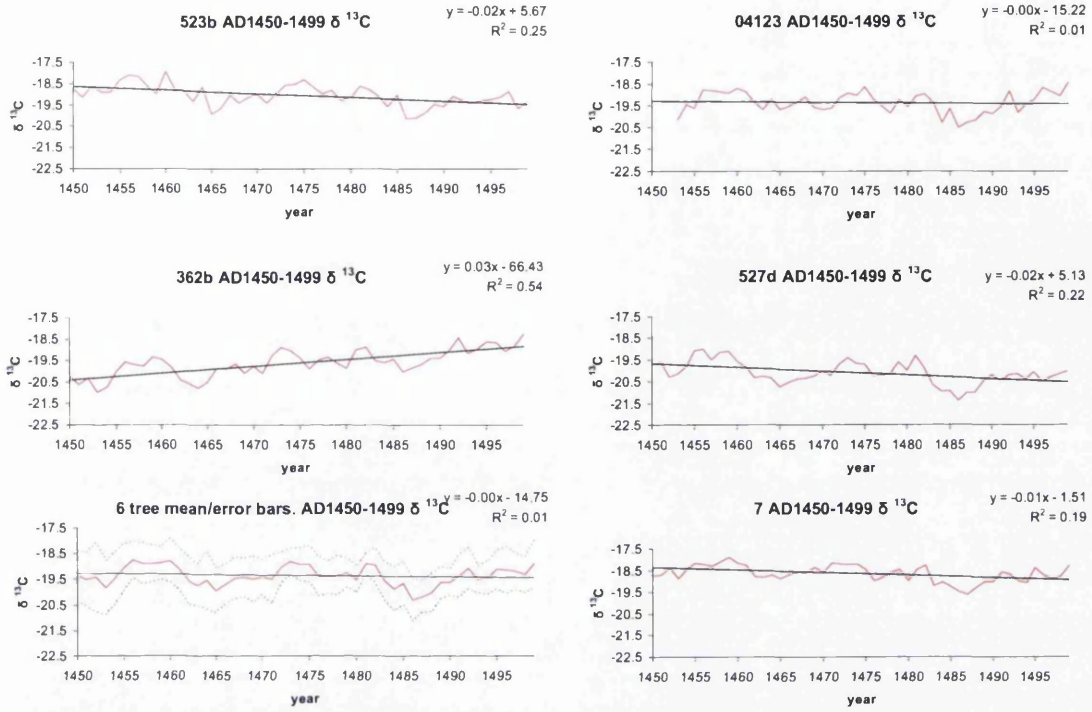

Figure 6.57 Individual trees $\delta^{13}C$ 1450-1499

Table 6.13 Tree details
Below: inter tree correlation $\delta^{13}C$1450-1499

Tree	Most positive year (AD)	Most negative year(AD)	mean $\delta^{13}C$
523b	1460	1486	-19.05
362b	1499	1453	-19.62
4123	1499	1486	-19.36
527d	1456	1486	-20.10
007	1459	1487	-18.64
mean	1456	1486	**-19.36**

	523b	362b	4123	527d
362b	0.00			
4123	0.62	0.46		
527d	0.74	0.10	0.63	
007	0.64	0.14	0.67	0.80
	Mean r	0.47	**EPS**	0.82

The period begins with a rise in $\delta^{13}C$ from 1450-1455, with more negative $\delta^{13}C$ in all trees in 1453, followed by generally positive $\delta^{13}C$ between 1455 -1460. The period between1460-1470 is marked by generally negative values centred on 1465. The period 1470-1475 is marked by positive values, values are negative in all trees till 1477 and then values generally decline to negative $\delta^{13}C$ centred on 1486/1487.

Values then rise again toward 1499. This 50 year period is marked by generally negative $\delta^{13}C$ in all trees compared with other 50 year periods in the chronology. It is the 14^{th} most negative 50 year period of 21 covering the 1000 year chronology.
A significant decline is observed in three trees (007, 527 and 523) and a significant increase in one tree (362b).

6.13. $\delta^{13}C$ data analysis AD1400-1449

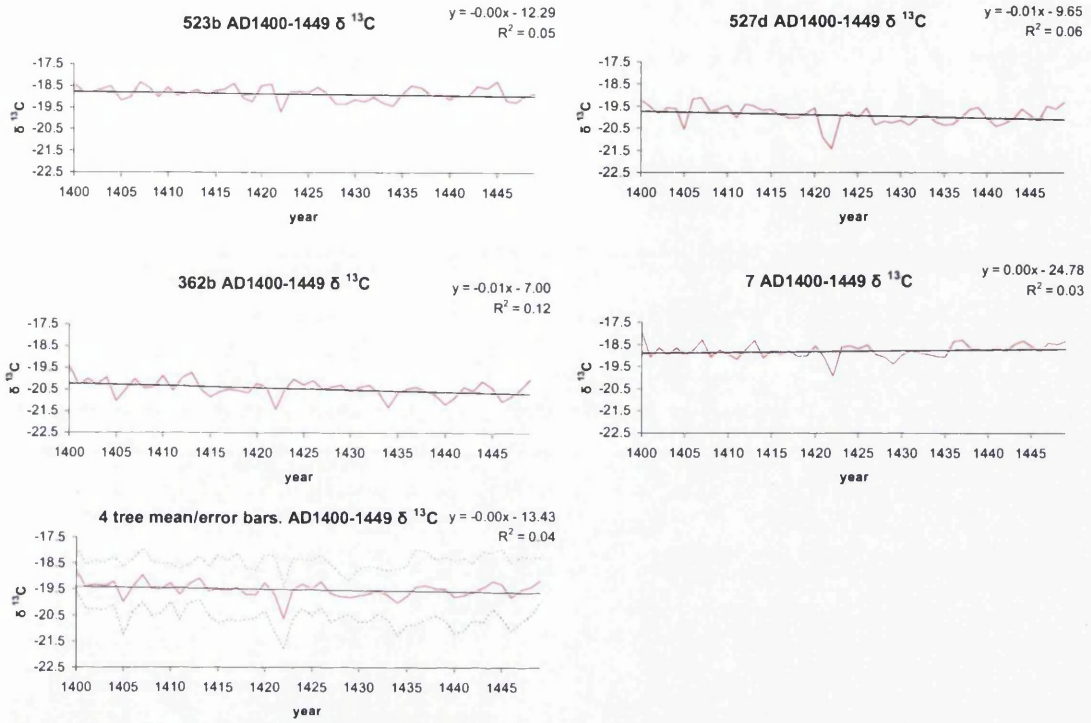

Figure 6.58 Individual trees $\delta^{13}C$ 1400-1449

Table 6.14 Tree details
Below: inter tree correlation $\delta^{13}C$1400-1449

Tree	Most positive year (AD)	Most negative year(AD)	mean $\delta^{13}C$
523b	1445	1422	-18.88
362b	1400	1422	-20.46
527d	1407	1422	-19.92
007	1400	1422	-18.80
mean	1400	1422	**-19.51**

	523b	362b	527d
362b	0.60		
527d	0.41	0.58	
007	0.58	0.54	0.60
Mean r	0.55	**EPS**	0.83

A significant $\delta^{13}C$ decline is observed in one tree (362b). The early part of this 50 year period is marked by generally positive values. The most notable feature of this 50 year period is the negative excursion of 1422. This is the most negative value of the millennium in three trees (363, 527 and 007) and also in the mean. Negative $\delta^{13}C$ is also associated with the years 1405 and around 1435 to 1440 in all trees.

6.14. $\delta^{13}C$ data analysis AD1400-1549

Figure 6.59(A,B,C,D,E,F)

6.59A

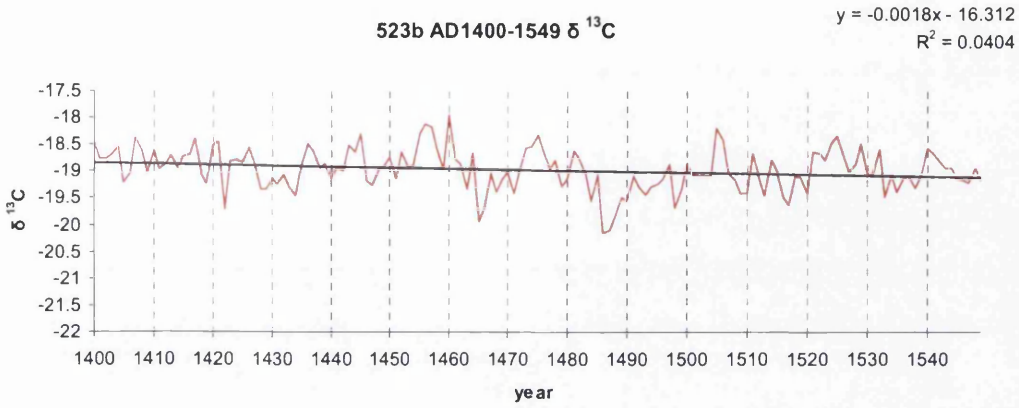

6.59B

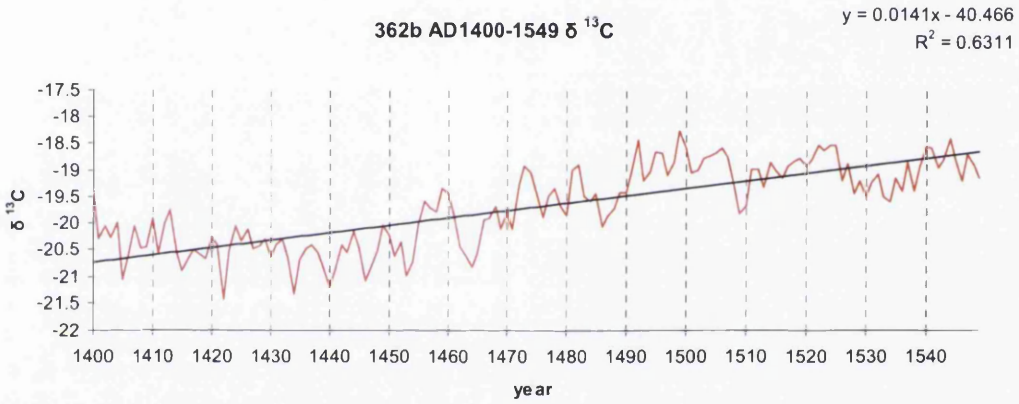

6.59C

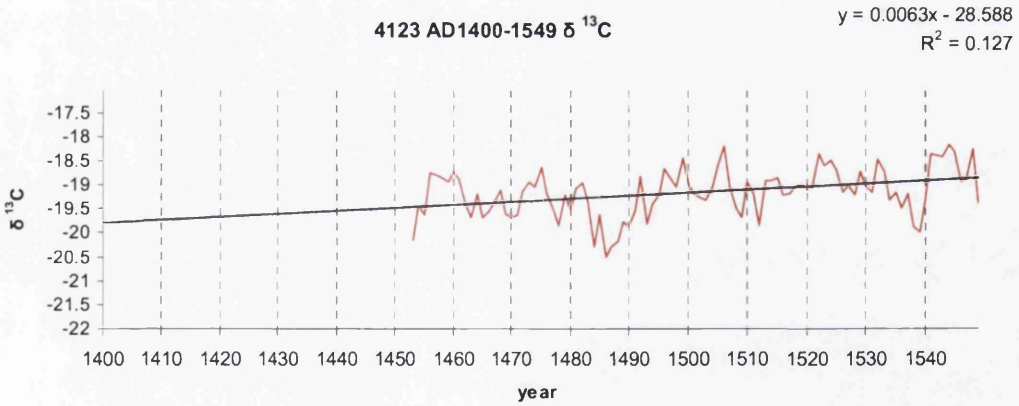

6.59D

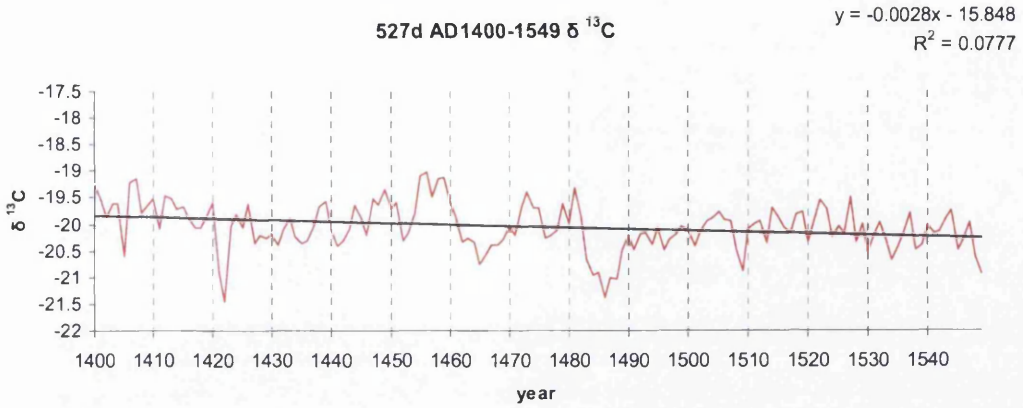

6.59E

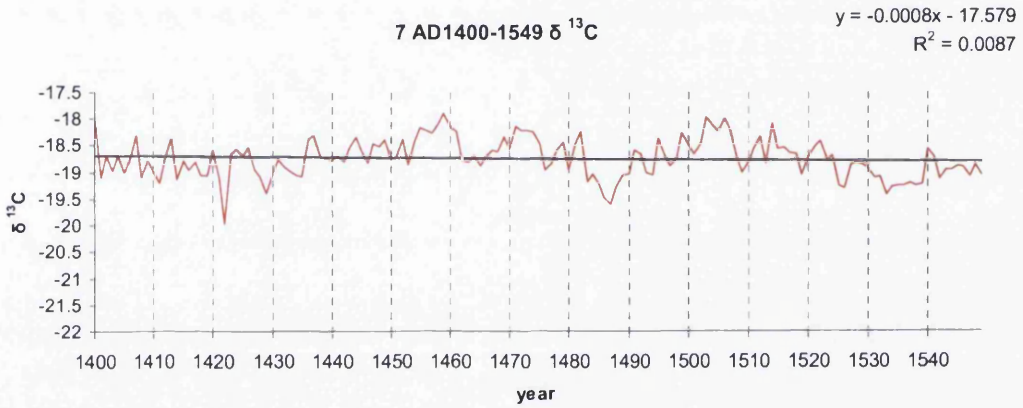

6.59F

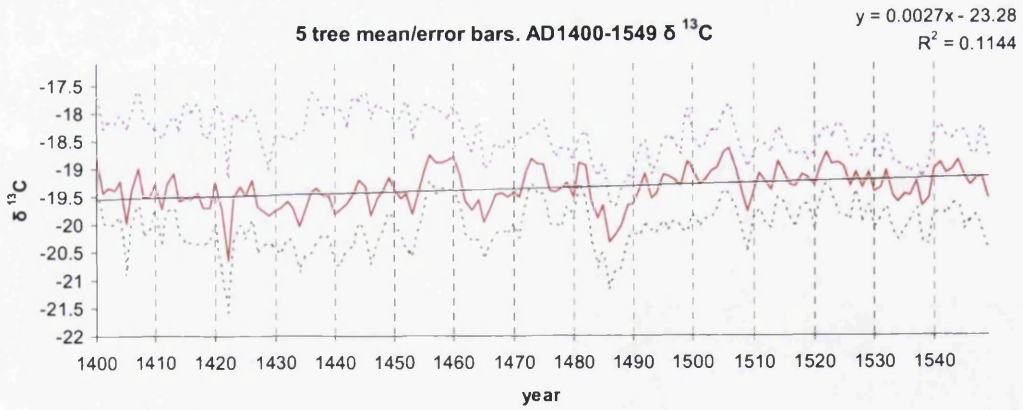

Table 6.15 Tree details
Below: inter tree correlation $\delta^{13}C$1400-1449

Tree	Most positive year (AD)	Most negative year(AD)	mean $\delta^{13}C$
523b	1460	1486	-18.97
362b	1499	1422	-19.68
4123	1544	1486	-19.17
527d	1456	1422	-20.05
007	1459	1422	-18.74
mean	**1506**	**1422**	**-19.35**

	523b	**362b**	**4123**	**527d**
362b	0.04			
4123	0.54	0.56		
527d	0.59	0.04	0.47	
007	0.46	0.21	0.30	0.59
	Mean r	0.38	**EPS**	0.75

A significant rise in $\delta^{13}C$ occurs between 1400-1549 in two trees (4123/362) and in the mean. The longest period of prolonged generally positive $\delta^{13}C$ is centred on the period 1456-1460. Gradually declining values are evident between 1400 to the extreme negative value in 1422 in all trees. 1405 and 1418 are more minor negative excursions during this period. Following a gradual rise in $\delta^{13}C$ and a negative event in 1453 values are generally positive 1455-1460. The period 1460-1470 is marked by generally negative $\delta^{13}C$ centred between1463- 1466.

Figure 6.60 Continental drought during the 15th century (Stahle 2007:145).

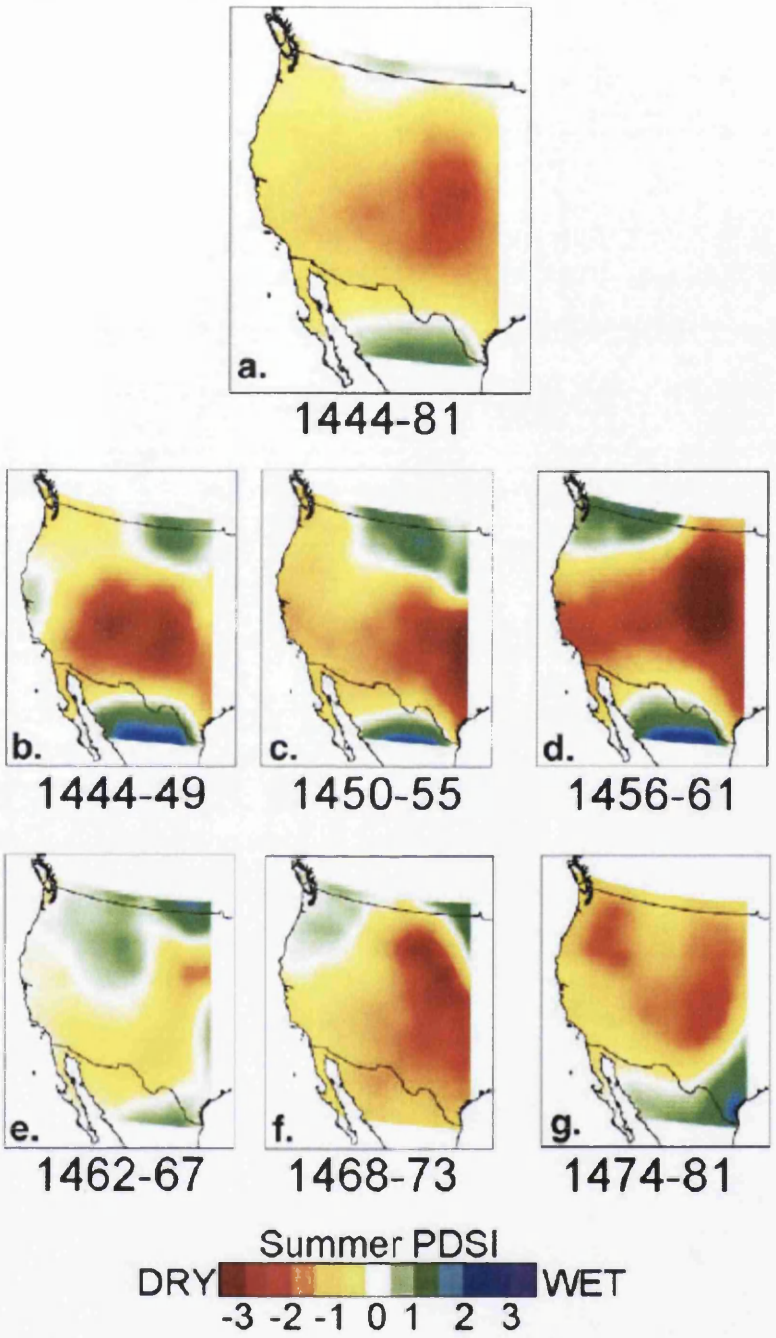

The bristlecone pine mean $\delta^{13}C$ displays two phases of positive values between 1444-1481. The first phase occurs from 1455-1463. The most positive values are between 1456-1460 (figure 6.61) with 1456 and 1460 being the two most positive values. This corresponds well to the period of greatest drought in the White

Mountains areas (figure 6.62). A second phase of positive $\delta^{13}C$ occurs between 1472 and 1478 with a peak in 1473. A final peak occurs in 1481 before values sharply decline to 1486. The positive phases evident in the bristlecone isotopes during the fifteenth century correspond well to previous drought reconstructions and provide a detailed regional picture of the fifteenth century megadrought discussed by Stahle *et al.* (2007).

The most negative $\delta^{13}C$ during the fifteenth century are also worthy of discussion. LaMarche and Hirschboek (1984) identify a widespread bristlecone frost ring in 1453 that may be related to the eruption of Kelud, Java in 1451, and also note low acidity values in Greenland ice core data for 1453-1454.

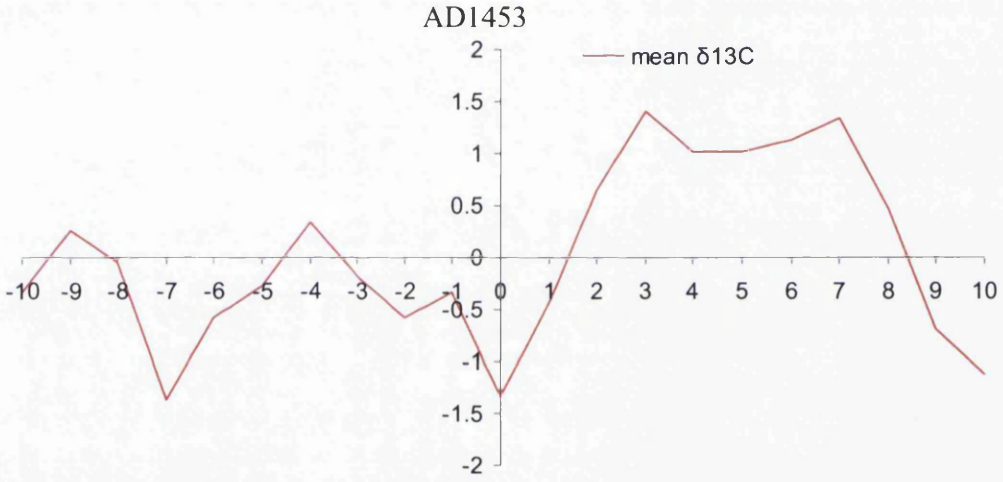

Figure 6.61.1453 SEA showing the period 1443 and 1463

The negative $\delta^{13}C$ that occurs in 1465 and 1486 may well be related to volcanic eruptions that have been inferred from proxy data and historical evidence. LaMarche and Hirschboeck (1984) identify a bristlecone frost ring in both the White mountains and the Rockies in 1485. Hughes and Salzer (2007) identify 1464 and 1466 as bristlecone ring width minima and frost rings. The climatic after effects of a large volcanic eruption of Kelut in eastern Java in 1463 may be responsible for the evidence offered in the tree rings and ice cores (Ammann and Naveau 2003). Depleted isotope values in the 1440s, early 1450s may be related to this and the possible eruption of Soufriere de Guadeloupe that is ^{14}C dated to c.1440 (Ammann and Neveau, 2003).

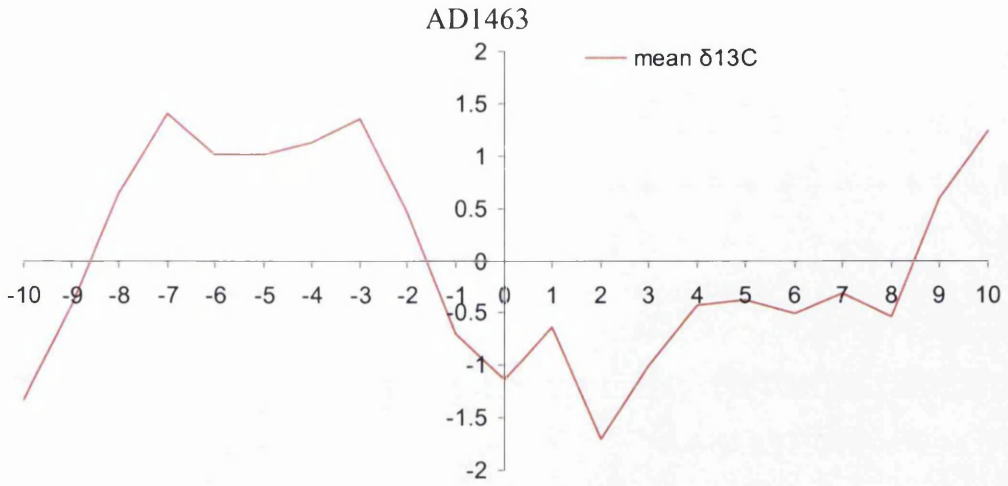

Figure 6.62. 1463 SEA showing years between 1453 and 1473. The sub decadal drought from 1456 to1460 is also evident in this figure.

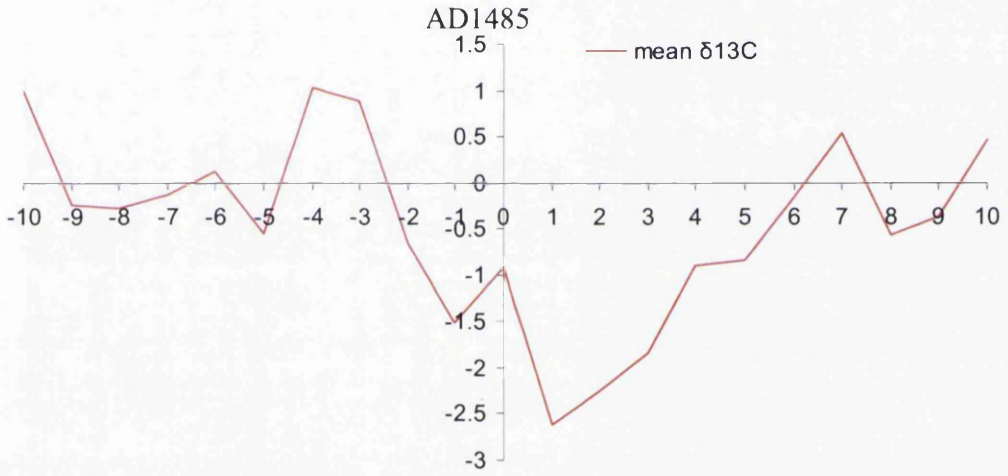

Figure 6.63_1485 SEA showing the period 1475 to 1495

An ice core volcanic signal is evident in both 1464 and 1484 and Finnish tree rings display a frost ring in 1484 (Hughes and Salzer, 2007:65). The year 1481 is an extreme year in Siberian tree rings (Hantemirov *et al.*, 2004). The negative $\delta^{13}C$ in 1422 evident in all trees is more difficult to explain, but in both the temperature and precipitation reconstructions undertaken using the Blanco isotope data (and also in the raw isotope values) the first half of the fifteenth century appears to have been colder or wetter than average (figure 6.1), and 1422 is the most depleted mean $\delta^{13}C$ (including PIN corrected data for 1850-2005) in the millennial series. That the first half of the 15th century witnessed below average temperatures through much of the

northern hemisphere is evidenced in ice core evidence and in historic evidence. By the 1420s proxy evidence suggests large variability in summer climate and this may have been an intense period of cold in Greenland that culminated (along with a variety of other factors) in the eventual abandonment by Norse peoples (Diamond, 2005; Fitzhugh and Ward, 2000).

As Diamond (2005) suggests, such societies existing on environmental 'margins' are highly susceptible to annual fluctuations and extremes. One bad summer would be disastrous for the hay harvest that the Norse inhabitants of Greenland depended on to feed their cattle. The KNMI spatial analysis tool (Oldenborgh & Burgers, 2005) suggests that maybe there may be some link between the summer climate of the White Mountains and that of Greenland (figure 6.64). Although the correlations over Greenland are in the region of r=0.3-0.4, they do suggest that there may be a link between the climate of Greenland and the White Mountains. Cut off from the ameliorating effects of the Gulf stream and bathed by Arctic air, Greenland experiences summers that are much colder (5 to 10° Celsius mean summer temperature) than those in Northern Europe. In common with the White Mountains, summer weather in Greenland is subject to large changes over short distances and there is great variation from year to year in both summer precipitation and mean summer temperature (Diamond, 2005).

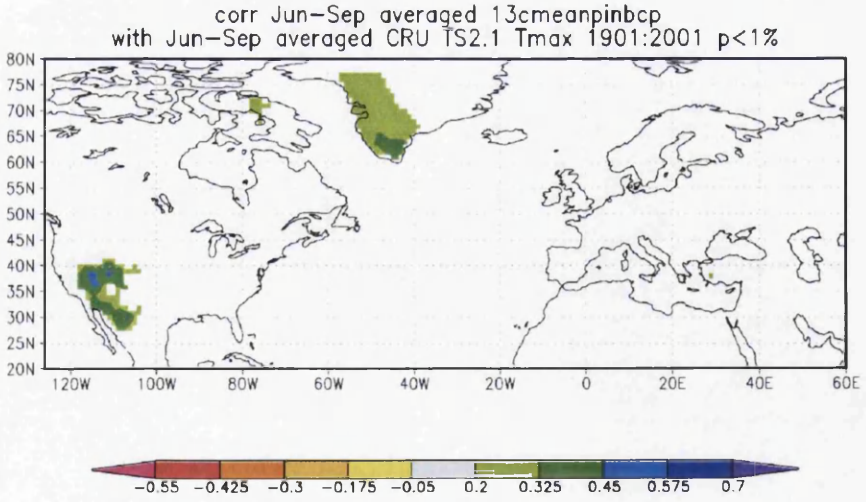

Figure 6.64. KNMI generated 1° spatial analysis- June-September average maximum temperature.

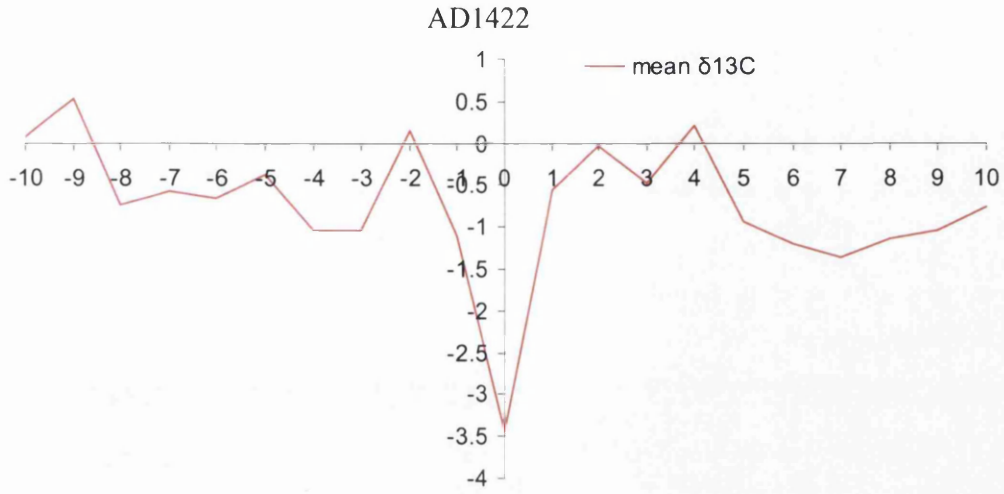

Figure 6.65.1422 SEA showing the period 1412 to 1432. AD1422 represents the coldest/wettest year in the millennial chronology.

6.15. $\delta^{13}C$ data analysis AD1350-1399

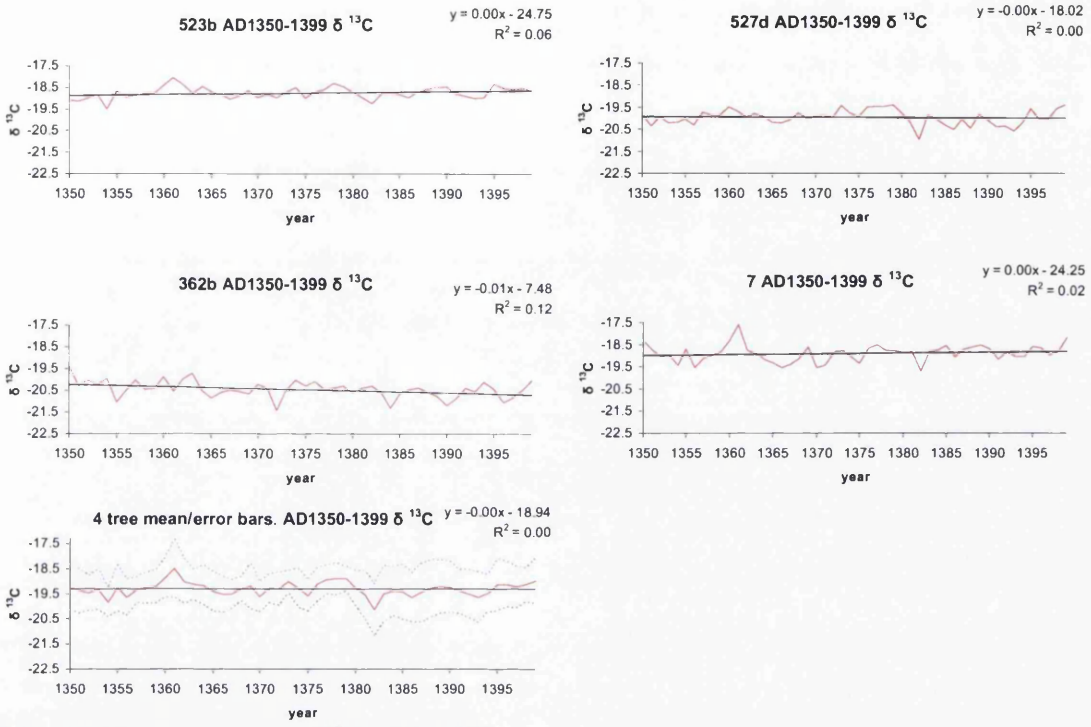

Figure 6.66 Individual trees $\delta^{13}C$ 1350-1399

Table 6.16 Tree details
Below: inter tree-correlation $\delta^{13}C$1350-1399

Tree	Most positive year (AD)	Most negative year(AD)	mean $\delta^{13}C$
523b	1361	1354	-18.76
362b	1361	1382	-19.63
527d	1379	1382	-19.98
007	1361	1382	-18.89
mean	**1361**	**1382**	**-19.31**

	523b	**362b**	**527d**
362b	0.54		
527d	0.54	0.41	
007	0.60	0.27	0.44
Mean r	0.47	**EPS**	0.78

The most positive $\delta^{13}C$ in three of the four trees and the mean is 1361. The most negative value in three of the four trees and the mean is 1382.

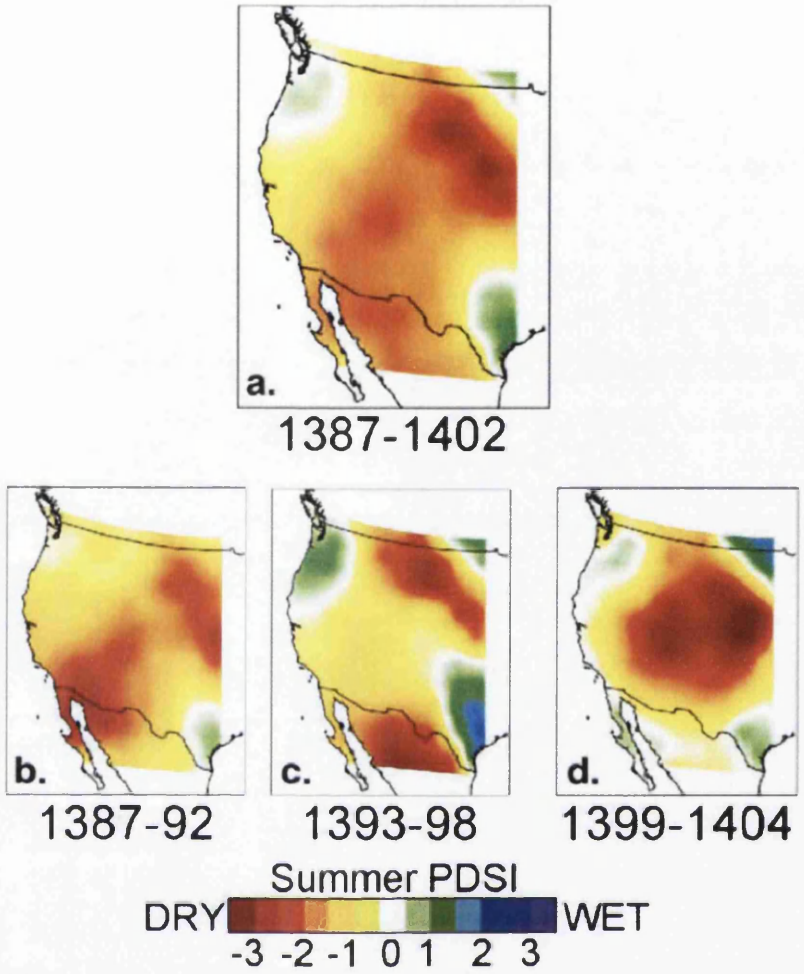

Figure 6.67 14th century drought in the western United States (Stahle, 2007:144)

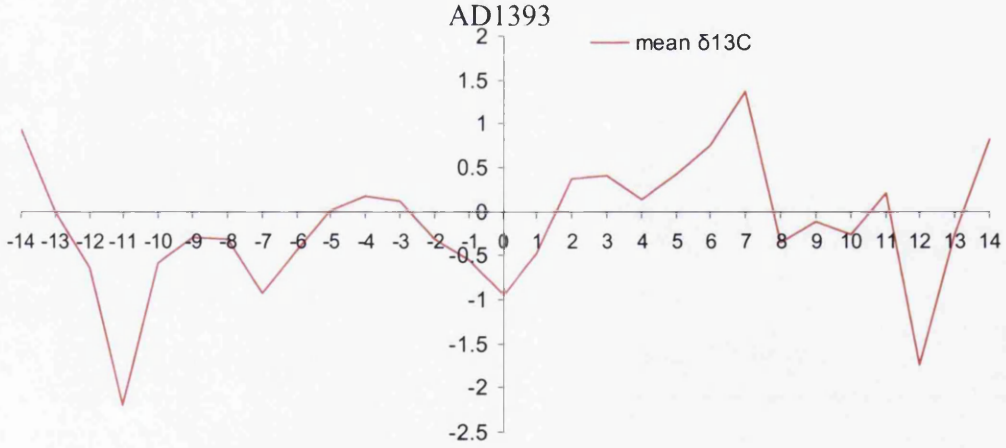

Figure 6.68.1393 SEA showing period 1379 to 1407.

Two periods of possible drought occur over the 29 year portrayed in the above figure. There is a small period of drought from 1388 to 1390 and a more extended period of drought from 1395 to 1400, with the most positive $\delta^{13}C$ occurring in 1400. The 23 years between 1382-1405 (figure 6.68) represent a comparatively dry period for the 14th and early 15th century. This compares well with the drought reconstruction by Stahle *et al.*, (2007) shown in figure 6.67.

With regard to extreme environmental events the years 1350, 1355, 1357 and 1360 are noted by Hughes and Salzer (2007:62) as being bristlecone pine ring width minima. The last eruption of the volcanoes that form the Inyo craters (within 100 miles of the White Mountains) probably occurred in AD1350 (Millar *et al.*, 2006). A series of strong earthquakes are also associated with this and other Inyo eruptions that occurred around 1350 (Bursik *et al.*, 2003). A light of frost ring is noted in Siberian trees in 1350 (Hantemirov *et al.*, 1350).

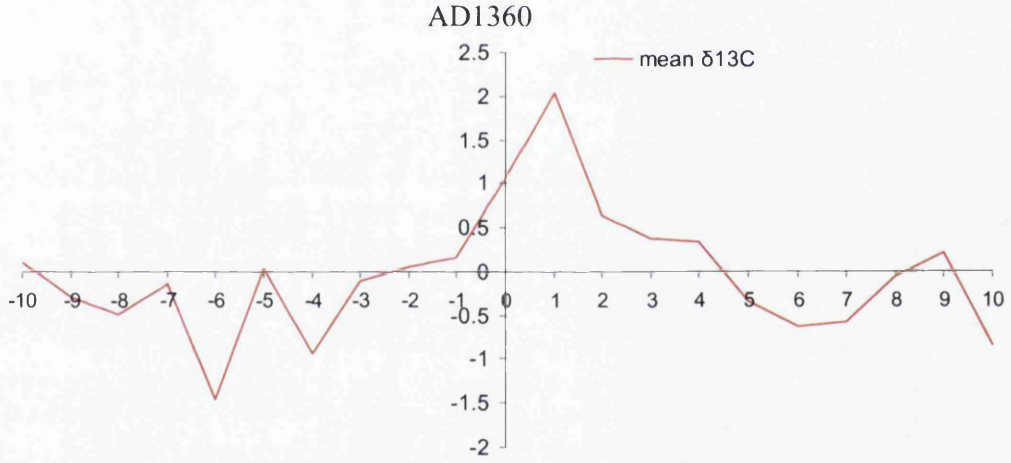

Figure 6.69.1360 SEA showing 20 years between 1350 and 1370.

6.16. $\delta^{13}C$ data analysis AD1300-1349

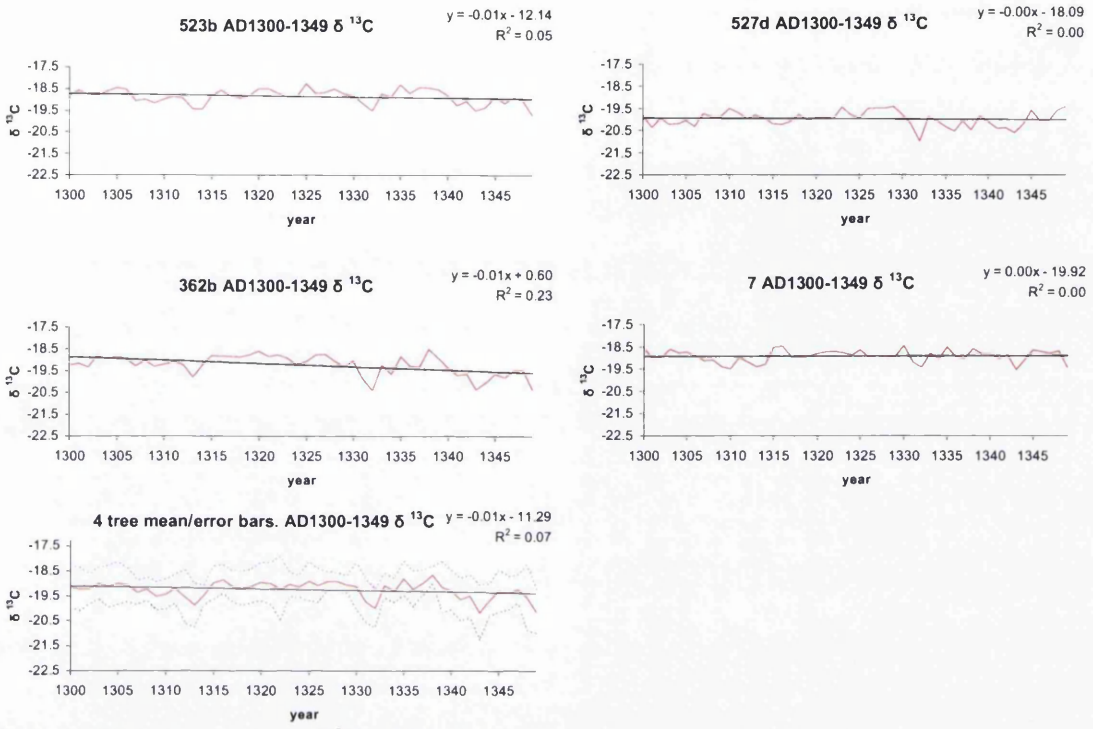

Figure 6.70 Individual trees $\delta^{13}C$ 1300-1349

Table 6.17 Tree details
Below: inter tree-correlation $\delta^{13}C$1300-1349

Tree	Most positive year (AD)	Most negative year(AD)	mean $\delta^{13}C$
523b	1325	1349	-18.87
362b	1338	1332	-19.23
527d	1338	1343	-19.97
007	1330	1343	-18.92
mean	**1338**	**1343**	**-19.25**

	523b	**362b**	**527d**
362b	0.775033		
527d	0.629596	0.57914	
007	0.668117	0.573135	0.441515
Mean r	0.61	**EPS**	0.86

The most notable positive $\delta^{13}C$ values occur in the 1320s and in the late 1330s.

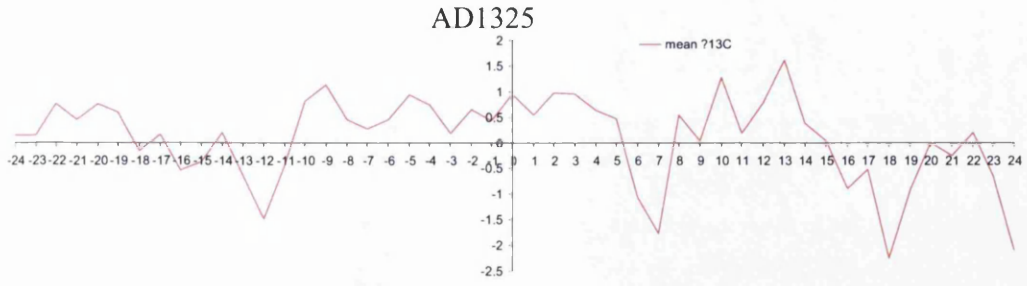

Figure 6.71. 1325 SEA showing years 1301 to 1349

The period from 1315 to 1330 is mainly positive $\delta^{13}C$ and may represent a period of sustained drought in the White Mountains. Salzer and Kipfmueller (2005) conversely identify the period between 1325 and 1334 as being very wet in Colorado and New Mexico. This dry period is flanked by two periods of depleted $\delta^{13}C$ from 1312 to 1314 and from 1331 to 1332. 1335 and 1338 are positive years and from 1341 to 1344 a negative excursion occurs. The years 1348 and 1349 are depleted values compared to the mean.

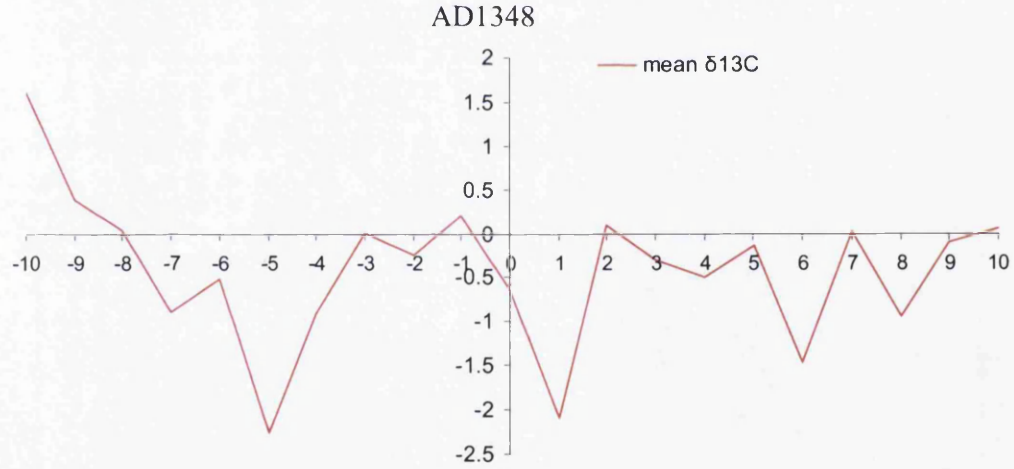

Figure 6.72.1348 SEA showing the period 1338 and 1358

The year 1348 is a noted bristlecone ring width minimum that corresponds with an ice core signal in 1346 and 1348 and Siberian ring width minima in 1347 (Hughes and Salzer, 2007:65). The year 1312 is a noted frost ring in Siberian trees (Hantemirov *et al.*, 2004) and famine and crop failure affected large parts of Europe

due to wet weather between 1310 and 1315. Aside from 1343 and 1348, 1313 represents the most negative mean value in this 50 year period. The succession of poor harvests in the early 14th century may have led in part to the devastating plague (Black Death) that swept through much of the world in the 1340s

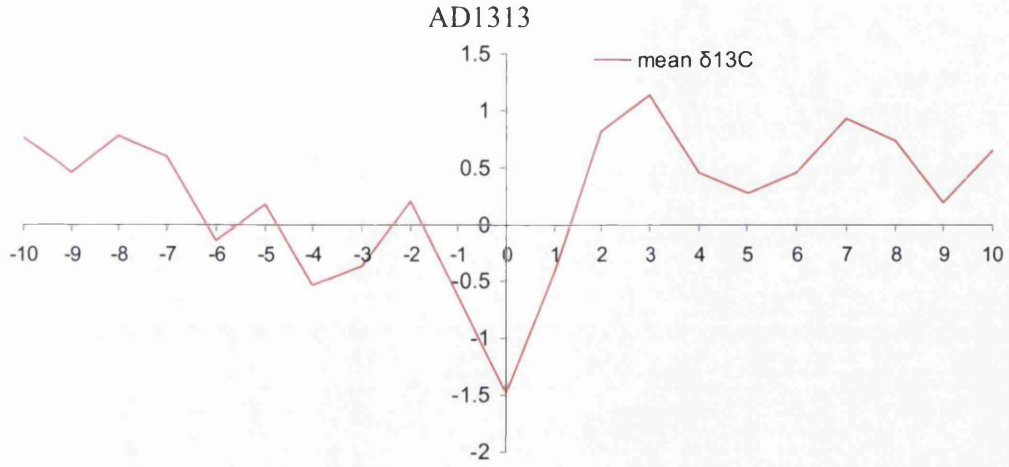

Figure 6.73.1313 SEA showing the period 1303 and 1323

6.17. $\delta^{13}C$ data analysis AD1250-1299

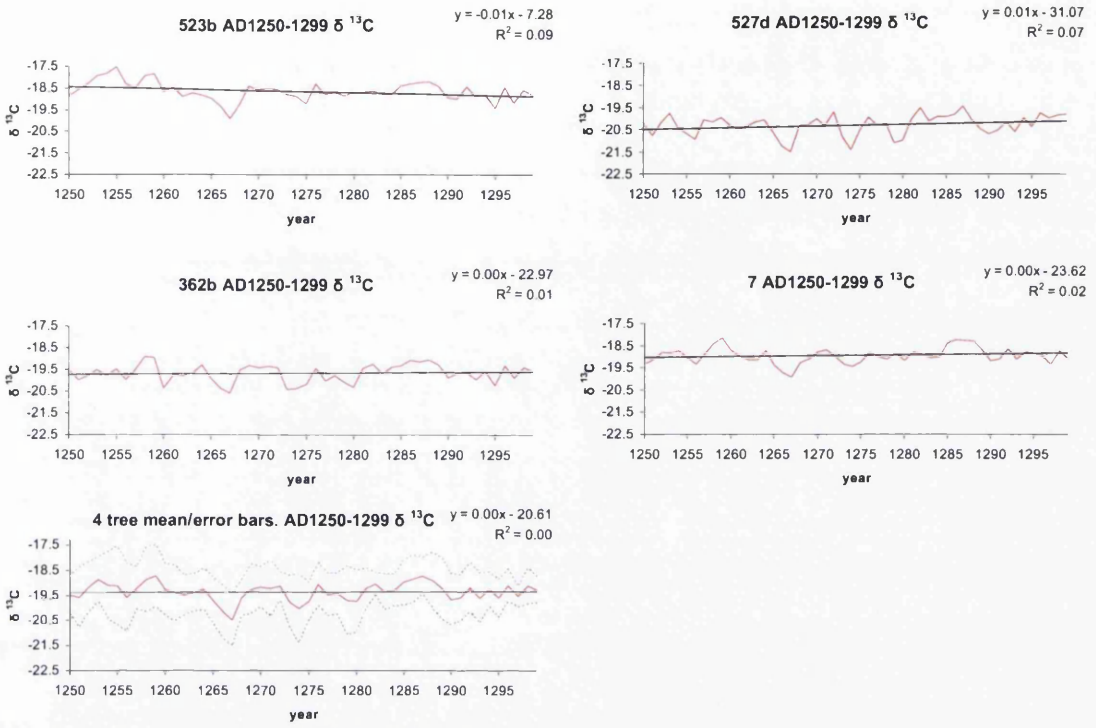

Figure 6.74 Individual trees $\delta^{13}C$ 1250-1299

Table 6.18 Tree details
Below: inter tree correlation $\delta^{13}C$1250-1299

Tree	Most positive year (AD)	Most negative year(AD)	mean $\delta^{13}C$
523b	1255	1267	-18.65
362b	1258	1267	-19.66
527d	1253	1267	-20.19
007	1259	1267	-18.95
mean	**1259**	**1267**	**-19.36**

	523b	362b	527d
362b	0.78		
527d	0.63	0.58	
007	0.67	0.57	0.44
Mean r	0.61	**EPS**	0.86

The most extreme positive $\delta^{13}C$ in this 50 year period occur in the 1250s. The years 1258 and 1259 are significant in that some believe that the largest volcanic eruption in the last 7000 years may have occurred in either 1258 or 1259 (Stothers, 2000). On the basis of ice core evidence, Hammer *et al.*, (1980) date the eruption of this 'super volcano' to 1258. Historical evidence from Europe indicates unusual dry for in 1258

and 1259 (Stothers, 2000) and unusual weather is reported in historic documents into the early 1260's. Along with the 1230s and 1240s during the period 1258-1261 grain prices in Europe are either incomplete from the records or very high (Bascome, 1848). While the years 1258 and 1259 are not among the top 10 most positive $\delta^{13}C$ values in the Blanco $\delta^{13}C$ chronology, the most negative $\delta^{13}C$ value in this 50 year block (1267) is among the top ten most depleted values in the last 1000 years. If a massive volcanic eruption occurred in 1258 that affected climate for much of the world for the following decade the effects as represented in the Blanco $\delta^{13}C$ appear very similar to those following the eruption of Krakotoa in 1883. As with the eruption of Krakotoa, the effect on the years 1883 and 1884 is not that noticeable in the $\delta^{13}C$ values, but huge storms that caused massive socio-economic damage occurred from 1889 to 1891 (Kuhn and Shepherd, 1984), some five to seven years after the volcano.

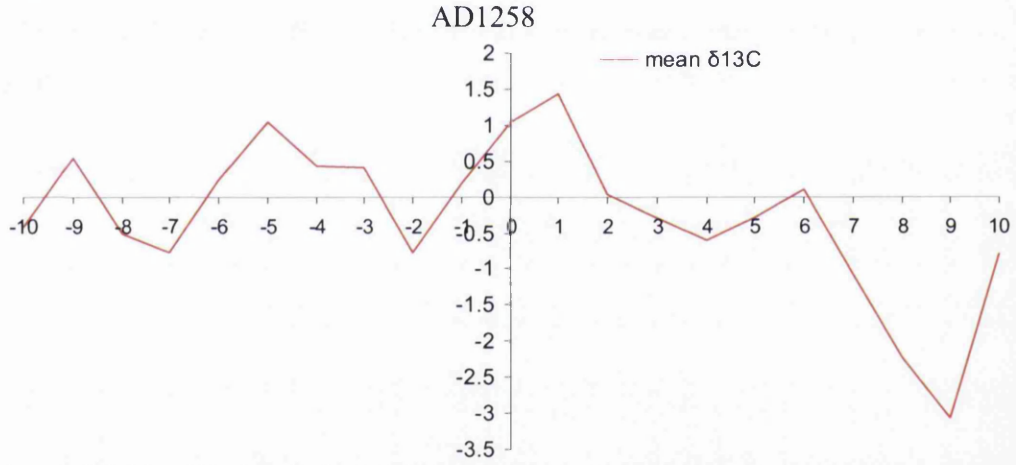

Figure 6.75 .1258 SEA showing the period 1248 to 1268

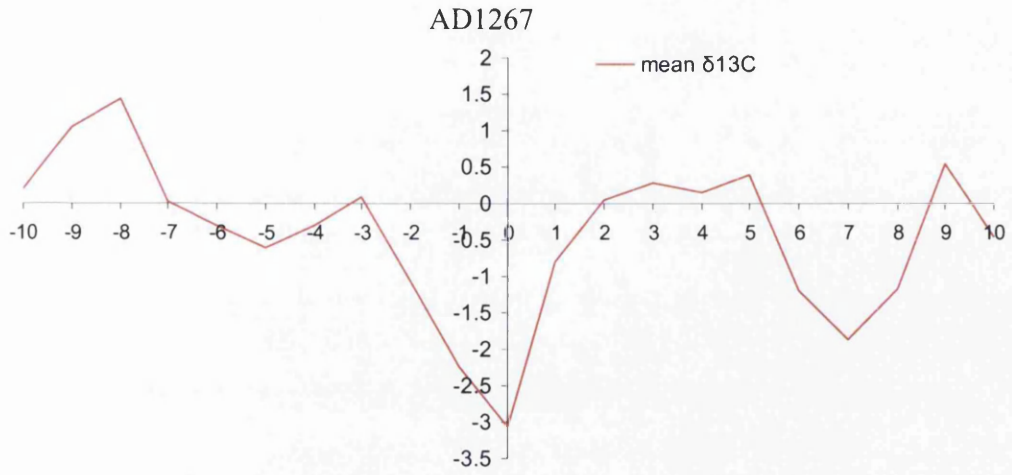

Figure 6.76. 1267 SEA *showing the period 1257 to 1277.*

The years 1225,1257,1259,1275,1277,1280 and 1287 are all noted bristlecone frost ring years (Salzer and Hughes, 2007:64). The years between 1195 and 1219 and 1258 to 1271 are identified by Salzer and Kipfmueller (2005) as being anomalously cool.

6.18. $\delta^{13}C$ data analysis AD1250-1399

Figure 6.77 (A,B,C,D,E) $\delta^{13}C$ AD 1250-1399 individual trees

6.77A

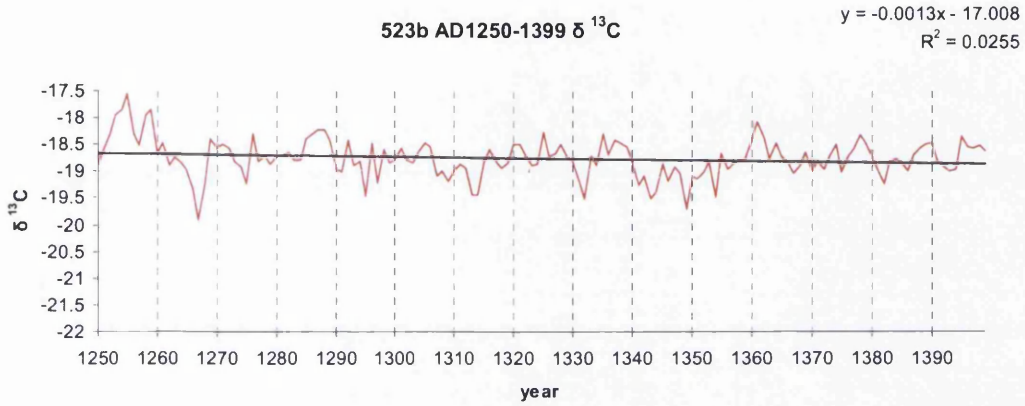

6.77B

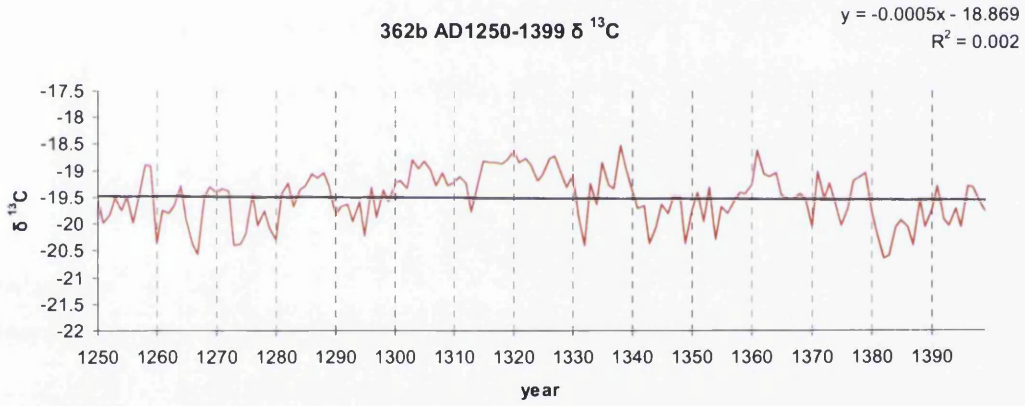

6.77C

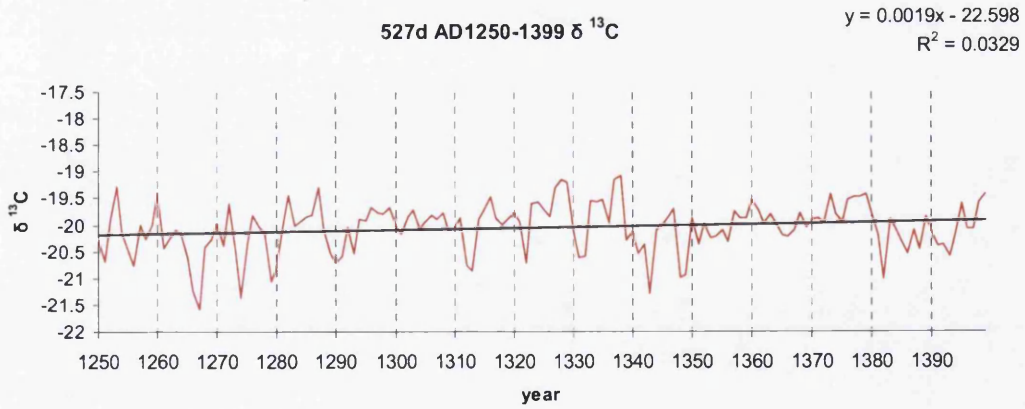

6.77D

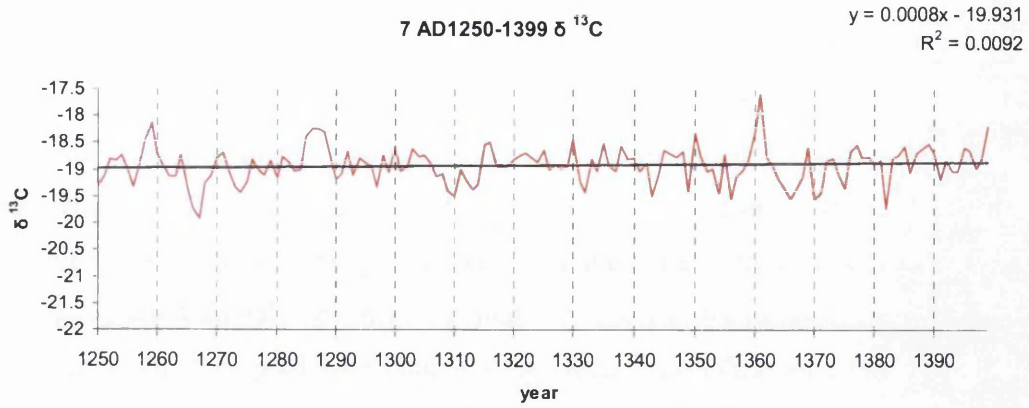

6.77E

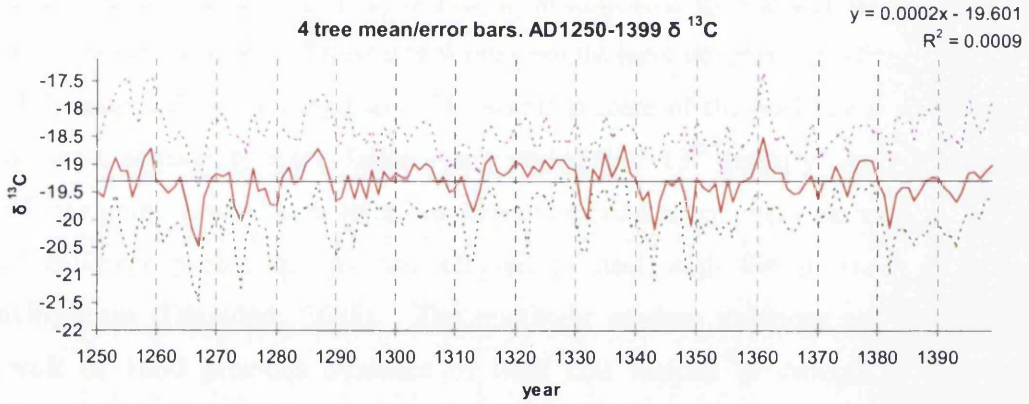

Table 6.19 Tree details

Below: inter tree correlation $\delta^{13}C$1250-1399

Tree	Most positive year (AD)	Most negative year(AD)	mean $\delta^{13}C$
523b	1255	1267	-18.76
362b	1338	1382	-19.51
527d	1338	1267	-20.05
007	1361	1267	-18.92
mean	**1361**	**1267**	**-19.31**

	523b	362b	4123	527d
362b	0.04			
4123	0.54	0.56		
527d	0.59	0.04	0.47	
007	0.46	0.21	0.30	0.59
	Mean r	0.38	**EPS**	0.75

The biggest $\delta^{13}C$ event in the 150 year period between 1250 and 1399 is the shift from positive to negative values that occurs from 1255/1258 to the most extreme depleted isotope values in 1267. Sustained positive values are evident in the late 1280's, from 1315 to 1330, in 1361 and in the late 1370's. These periods indicate

drought. The periods from 1264 to 1269, 1273 to 1275, 1312 to 1314, 1341 to 1345, 1348/1349 and 1382 witness depleted $\delta^{13}C$. The late 13th century is also an important period in terms of population movement and pueblo abandonment in the southwestern USA (Farmer, 1957; Graves *et al.*, 1982; Shwartz, 1957). Anthropological and tree ring evidence from the area indicate that the Anasazi people suggest a complex picture of climate change and social upheaval that led to the abandonment of pueblos throughout the area they inhabited (Arizona, Utah, Colorado and Nevada). Tree ring evidence (Dean, 1988; Shwartz, 1957) suggests that the normal pattern of heavy winter snow followed by summer monsoons had become unpredictable, and unseasonal rains would have devastating effects on crops and the populations farming them. The whole picture of the pueblo cultures of the southwest appears to have fallen apart during the 13th century. Archaeological evidence points toward inter tribal warfare and a breakdown of the various strategies that different pueblo groups had adopted to deal with life in such a fragile environment (Diamond, 2005). The relatively modern analogue of the Pueblo Revolt of 1680 provides evidence of what can happen to drought susceptible cultures should several dry growing seasons occur in a row, or if unseasonal rains occur.

6.19. $\delta^{13}C$ data analysis AD1200-1249

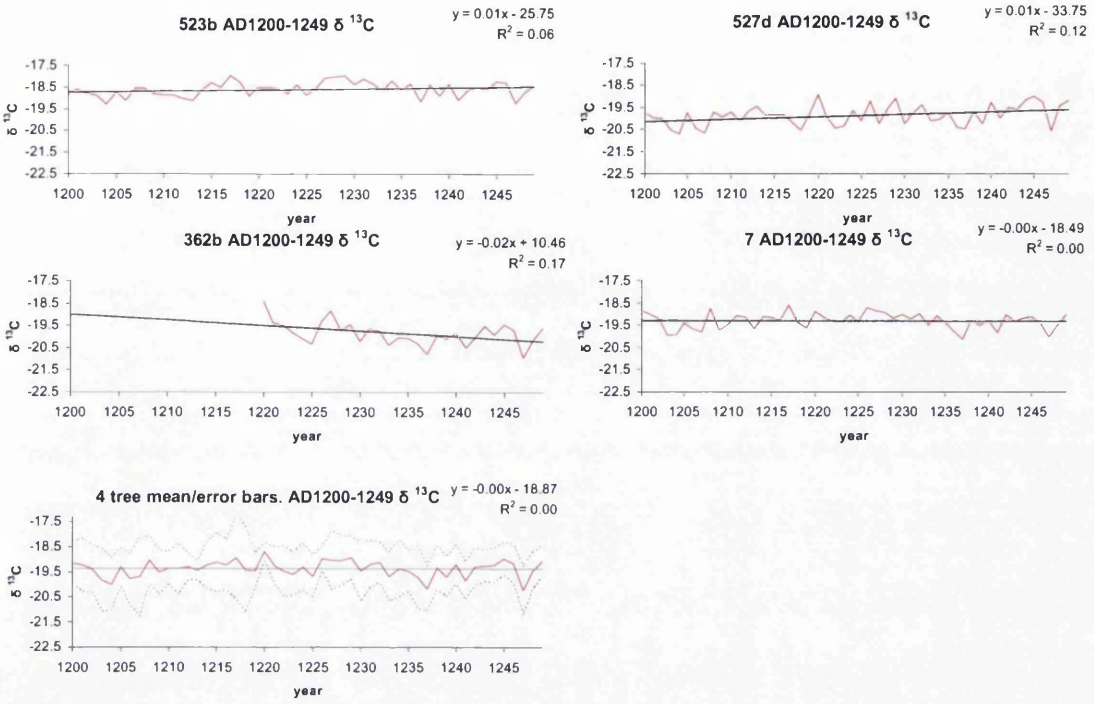

Figure 6.78 Individual trees $\delta^{13}C$ 1200-1249

Table 6.19 Tree details
Below: inter tree correlation $\delta^{13}C$1200-1249

Tree	Most positive year (AD)	Most negative year(AD)	mean $\delta^{13}C$
523b	1229	1204	-18.61
362b	1220	1247	-19.86
527d	1220	1204	-19.88
007	1217	1237	-19.32
mean	1220	1247	**-19.37**

	523b	**362b**	**527d**
362b	0.61		
527d	0.36	0.54	
007	0.65	0.75	0.51
Mean r	0.57	**EPS**	0.84

The only earlywood frost ring noted during this research (1227) occurred in two of the trees analysed (523b and 362b). LaMarche and Hirschboeck (1984), note 1227 as a widespread bristlecone frost ring in the both the Rockies and White Mountains and 1200 is also a bristlecone frost ring year. Hughes and Salzer (2007) note the years 1201, 1204 and 1230 are ring width minima that correspond to an ice core signal, and note 1225 as a bristlecone frost ring. The years 1229 and 1231 are frost ring years in Finnish trees and ice core signals occur in 1227 and 1229 (Hughes and

Salzer, 2007). Frost or light rings are noted in 1201 and 1209 in Siberian trees (Hantemirov *et al.*, 2004). The mean Blanco isotope values for the period from 1226 to 1229 are positive suggesting dry or hot conditions. The year 1220 is a positive $\delta^{13}C$ value suggesting dry or hot conditions.

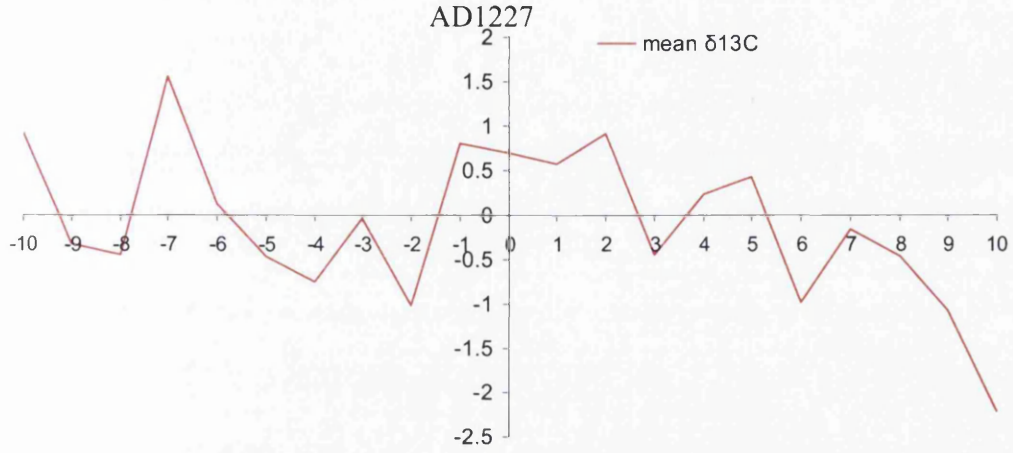

Figure 6.79. 1227 SEA showing 20 years between 1217 and 1237

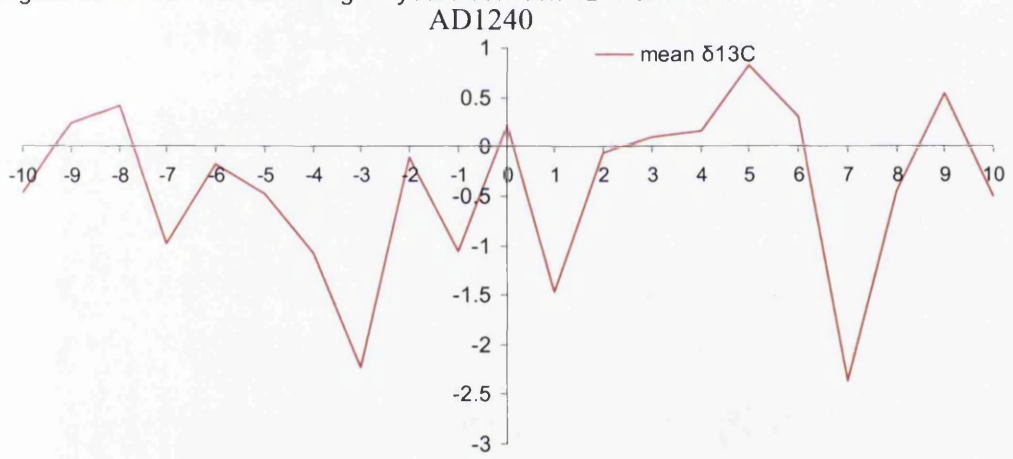

Figure 6.80.1240 SEA showing 20 years between 1230 and 1250

Generally positive $\delta^{13}C$ is observed between 1242 and 1246 and a negative $\delta^{13}C$ value occurs in 1247. The negative $\delta^{13}C$ values in 1237 and 1247 may be related to as yet unknown environmental events. The years 1238 and 1239 were 'destructive years in Europe' and in 1233 it was reported that the Mediterranean froze over and that 'all vegetation was destroyed in England' (Bescome, 1848:40).

6.20. $\delta^{13}C$ data analysis AD1150-1199

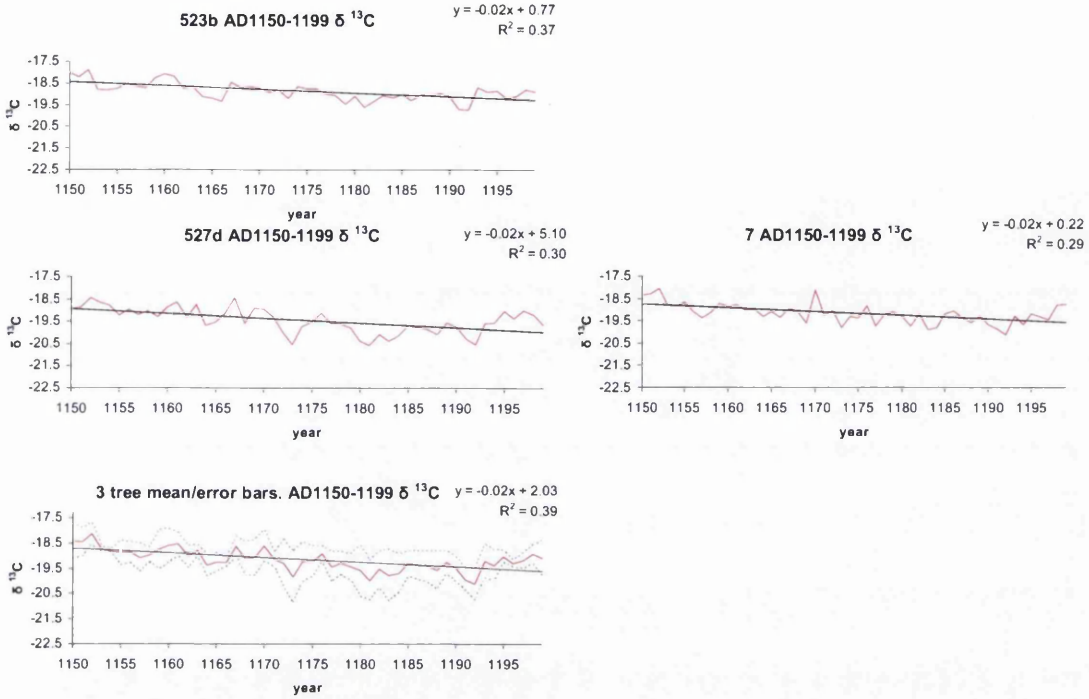

Figure 6.81 Individual trees $\delta^{13}C$ 1150-1199

Table 6.20 Tree details
Below: inter tree correlation $\delta^{13}C$1150-1199

Tree	Most positive year (AD)	Most negative year(AD)	mean $\delta^{13}C$
523b	1152	1192	-18.86
527d	1152	1181	-19.46
007	1152	1192	-19.16
mean	1152	1192	**-19.16**

	523b	**527d**	
527d	0.73		
007	0.70	0.69	
Mean r	0.71	**EPS**	0.88

6.21. $\delta^{13}C$ data analysis AD1100-1149

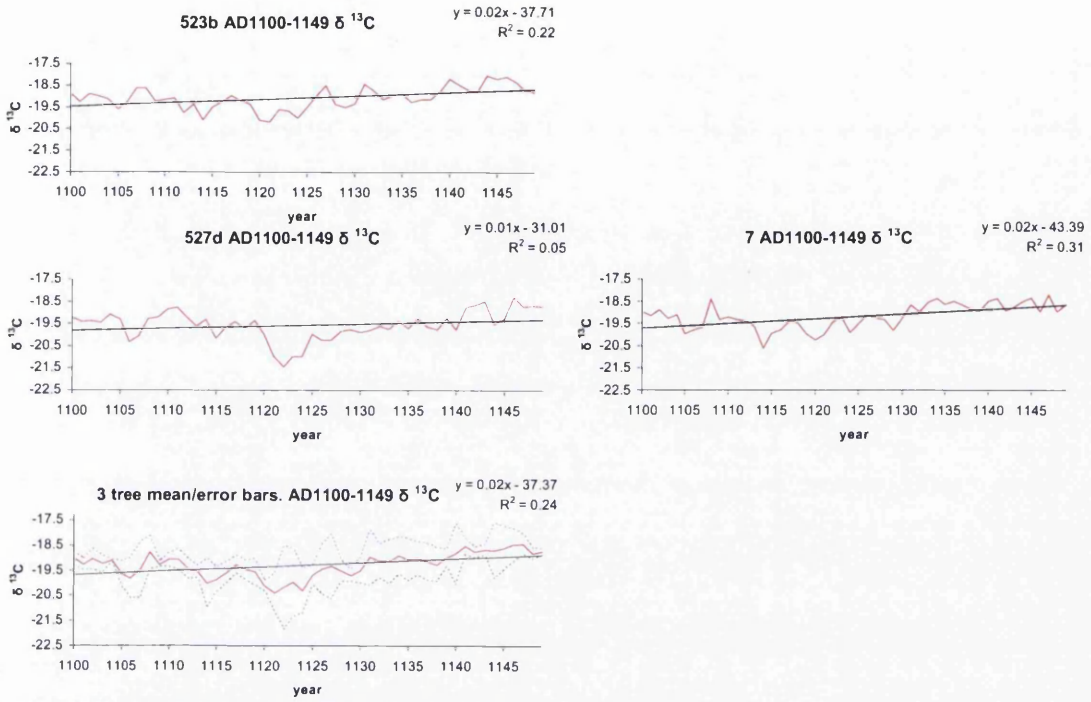

Figure 6.82Individual trees $\delta^{13}C$ 1100-1149

Table 6.21 Tree details

Below: inter tree correlation $\delta^{13}C$1100-1149

Tree	Most positive year (AD)	Most negative year(AD)	mean $\delta^{13}C$
523b	1144	1121	-19.09
527d	1146	1122	-19.58
007	1147	1114	-19.19
mean	1147	1121	**-19.29**

	523b	527d	
527d	0.50		
007	0.76	0.41	
Mean r	0.56	**EPS**	0.79

6.22. $\delta^{13}C$ data analysis AD1100-1249

Figure 6.83(A,B,C,D,E) individual trees $\delta^{13}C$ AD1100-1249

6.83A

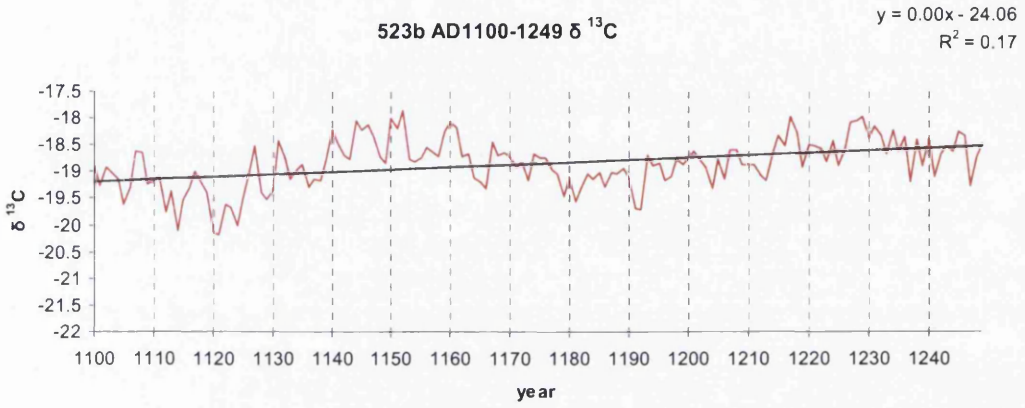

6.83B

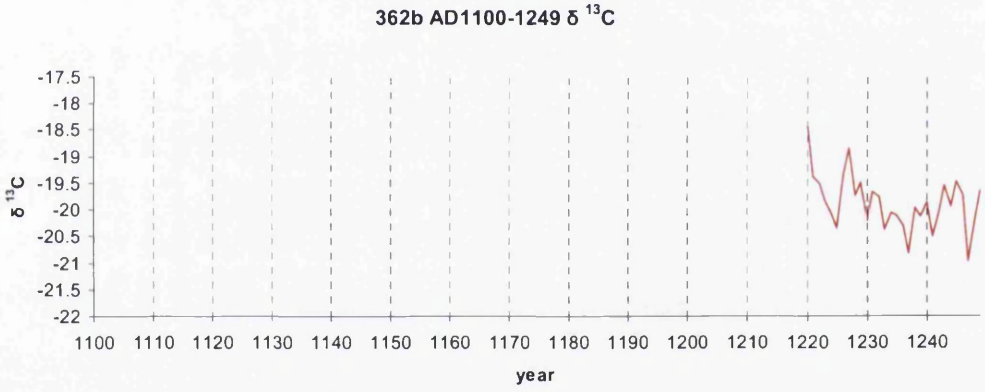

6.83C

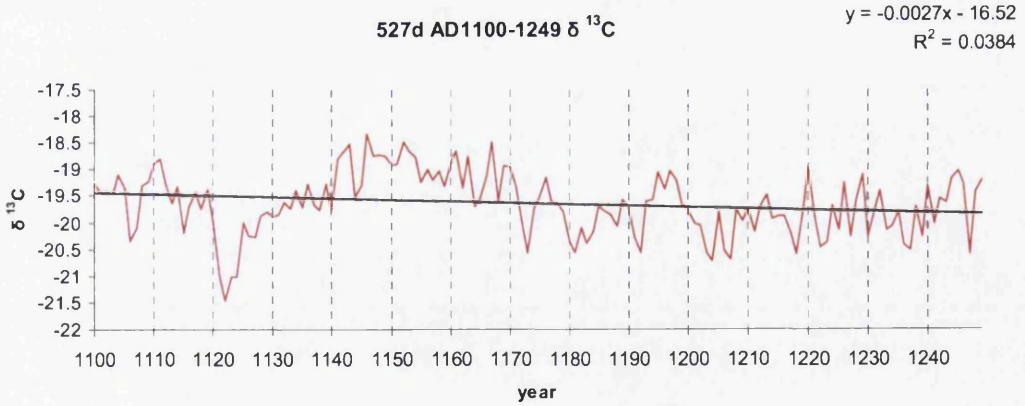

6.83D

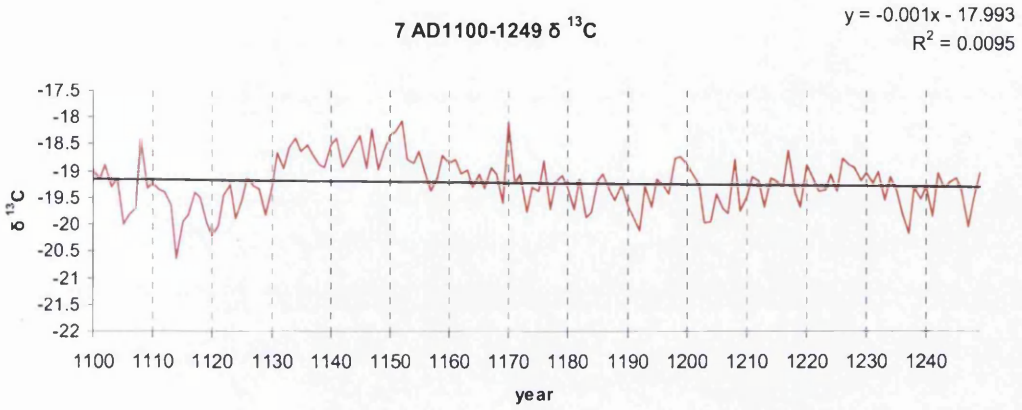

6.83E

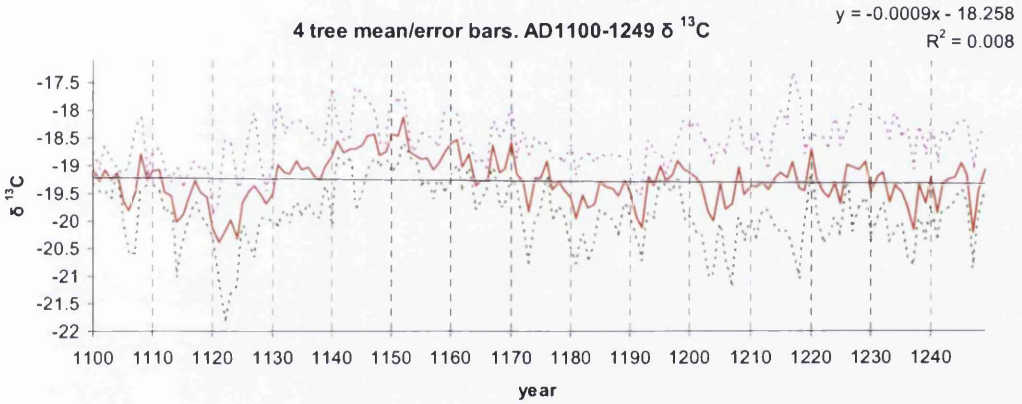

Table 6.22 Tree details

Below: inter tree correlation $\delta^{13}C$1100-1249

Tree	Most positive year (AD)	Most negative year(AD)	mean $\delta^{13}C$
523b	1152	1121	-18.85
362b	1220	1247	-19.86
527d	1146	1122	-19.64
007	1152	1114	-19.22
mean	**1152**	**1121**	**-19.27**

	523b	**362b**	**527d**
362b	0.61		
527d	0.38	0.54	
007	0.60	0.75	0.54
Mean r	**0.57**	**EPS**	**0.84**

The series of positive $\delta^{13}C$ that occurs in the 1140's and 1150's is the most sustained period of positive values in the millennial isotope chronology. The drought appears to have lasted for approximately 26 years (figure 6.105). The period just before this witnesses two prolonged periods of isotopic depletion that lasted in the region of a decade each centred on the mid 1080's and the 1110's/1120's.

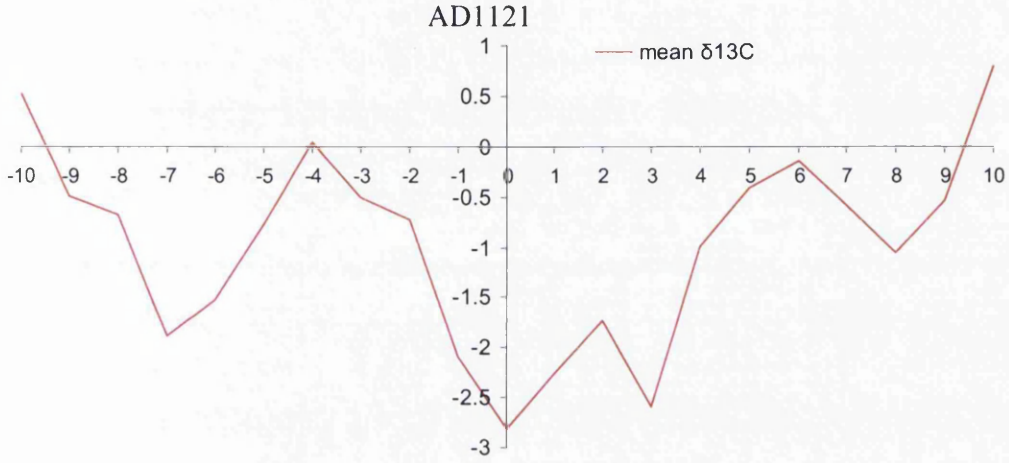

Figure 6.84.1121 SEA showing the period 1111 and 1131

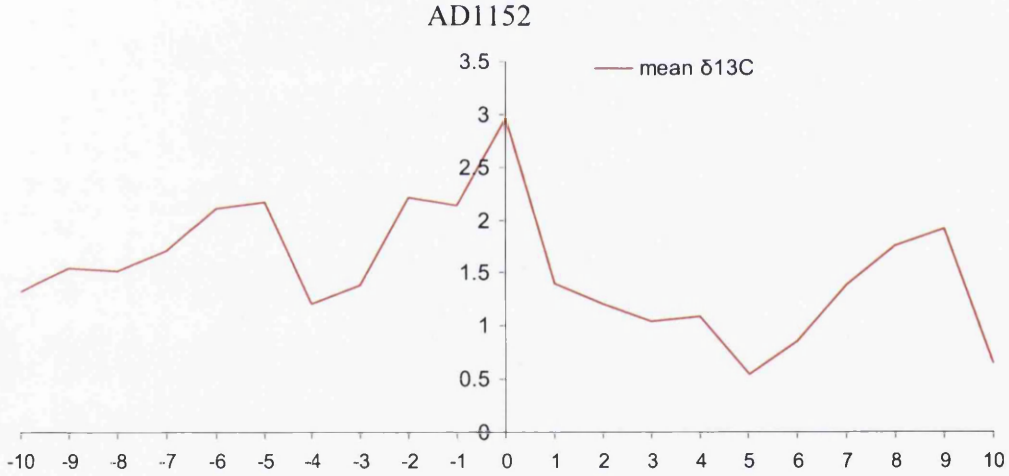

Figure 6.85.1152 SEA showing the period 1142 and 1162.

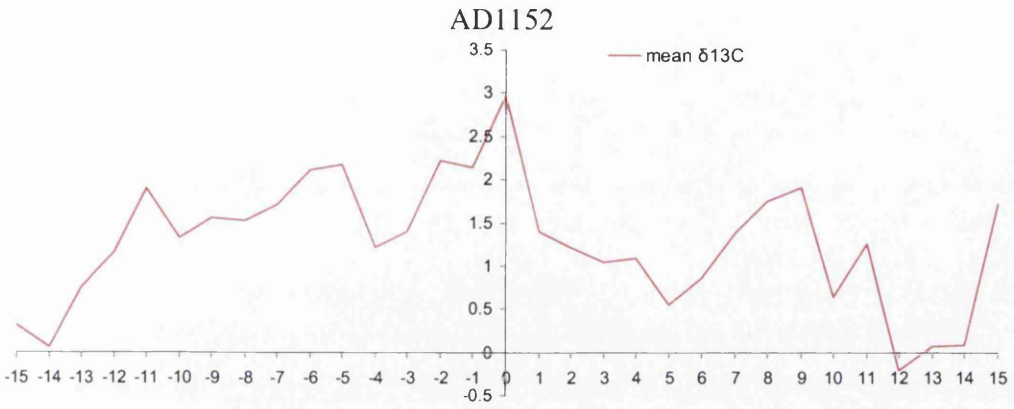

Figure 6.86.1152 31 year SEA showing 31 years 1137 to 1167.

The years 1109, 1172, 1180, 1201 and 1209 are all frost or light rings in Siberian trees (Hantemirov *et al.*, 2004). In the bristlecone pines, Salzer and Hughes (2007:62) note 1114 as a ring width minima, 1121 as a ring width minima and 1109,1118,1134,1139,1142,1171 and 1190 as frost rings. 1201 is a ring width minima and frost ring and the years 1204 and 1230 are also bristlecone ring width minima.

The extreme depleted $\delta^{13}C$ in the mid 1110's, 1120's, followed by the long period of positive $\delta^{13}C$ centred on 1152 can be linked to archaeological evidence from the southwestern USA (Larson and Michaelsen, 1990). Based on archaeological evidence and climatic reconstruction from bristlecone pines at Charleston Peak, Larson and Michaelsen (1990) attribute the climatic events between 1120 and 1150 as a major factor in causing the Virgin Branch Anasazi to abandon their settlements.

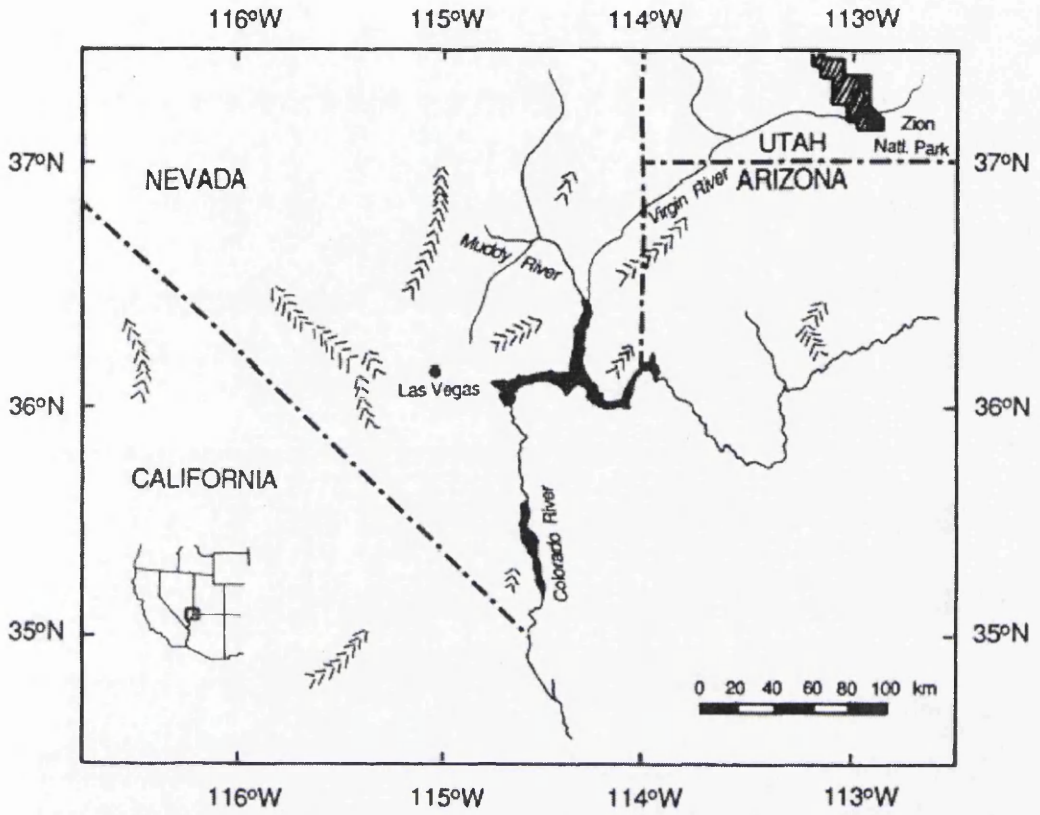

Figure 6.87. Virgin Branch Anasazi area as studied by Larson and Michaelsen (1990:229).

As can be seen in the figure 6.87, the area that the Virgin Branch Anasazi occupied from AD100 to AD1150 corresponds closely with some of the area that the Blanco isotope series has significant instrumental climate correlations with. As mentioned, two episodes of climate change that caused significant changes in the adaptive strategies of the Anasazi occurred between AD1000-1015 and the second occurred after 150 years of favourable conditions between AD1120-1150. The major, unpredictable climatic shifts evident in the Blanco isotopic evidence that occur between 1120 and 1150 (extreme wet/cold to extreme prolonged heat/drought) are exactly the type of events that, when coupled with the previous rapid population growth can lead to the failure of adaptive strategies that in less stressful periods with a lower population may be successful. It is worth bearing in mind that the areas occupied by the Anasazi and other native American cultures in the southwest were very densely populated and farmed in the past (Diamond, 2005). Today much of the

areas containing these ancient ruins are unsuitable for farming of any kind and are very sparsely populated, demonstrating clearly the fragility of the environment.

6.23: $\delta^{13}C$ data analysis AD1050-1099

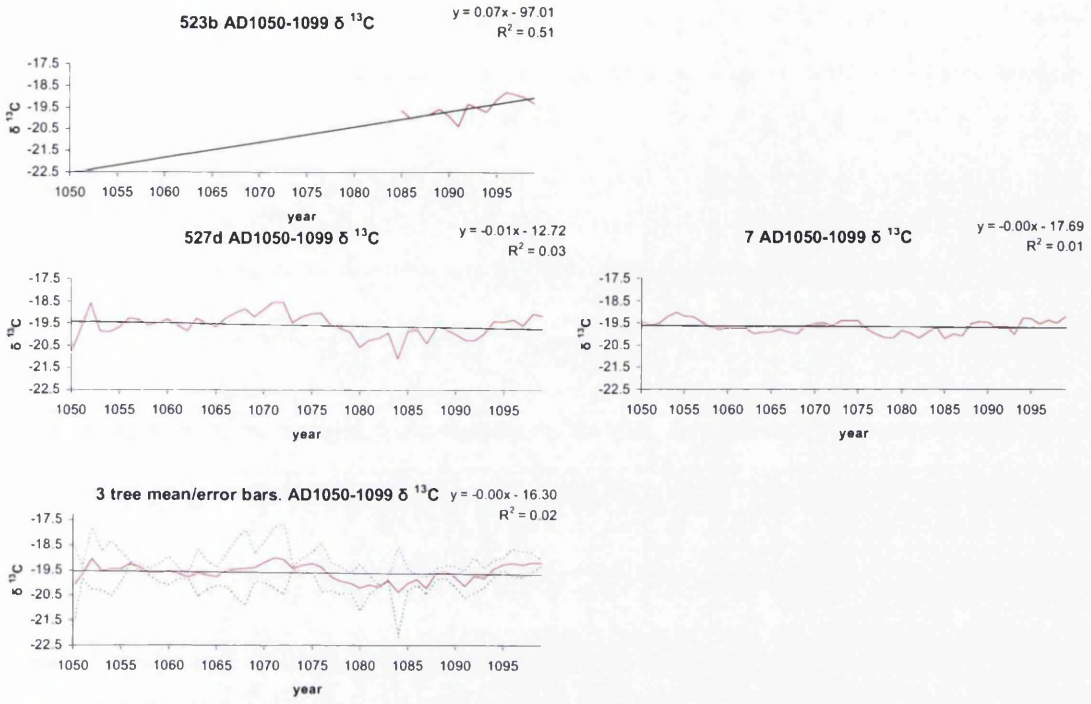

Figure 6.88 Individual trees $\delta^{13}C$ 1050-1099

Table 6.22 Tree details

Below: inter tree correlation $\delta^{13}C$1050-1099

Tree	Most positive year (AD)		Most negative year(AD)	mean $\delta^{13}C$
523b	1096		1091	-19.44
527d	1072		1084	-19.59
007	1054		1085	-19.67
mean	**1071**		**1084**	**-19.62**

	523b	527d	
523b			
527d	0.64		
007	0.29	0.21	
Mean r	0.38	**EPS**	0.65

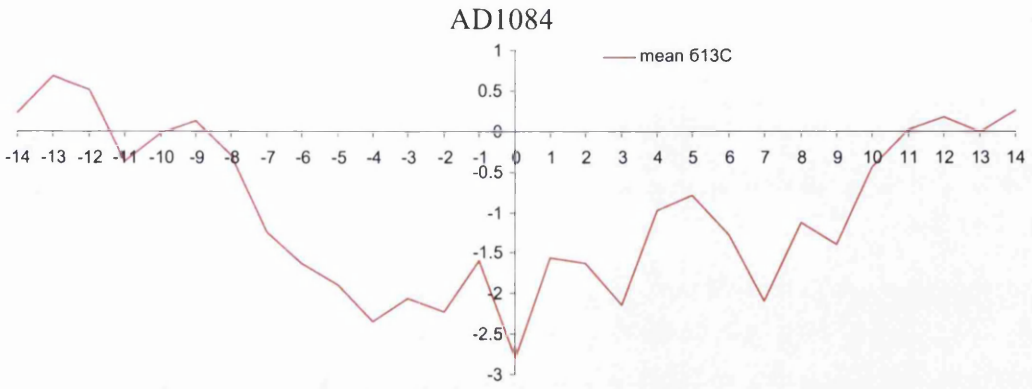

Figure 6.89: 1084 28 year SEA showing years 1070 to 1098. The 19 year period between 1076 and 1095 and, to a slightly lesser degree the 10 year period between 1118 and 1127 represent the most prolonged period of depleted $\delta^{13}C$ values in the millennial chronology (excluding 20th century $\delta^{13}C_{raw}$ values).

6.24. $\delta^{13}C$ data analysis AD1005-1049

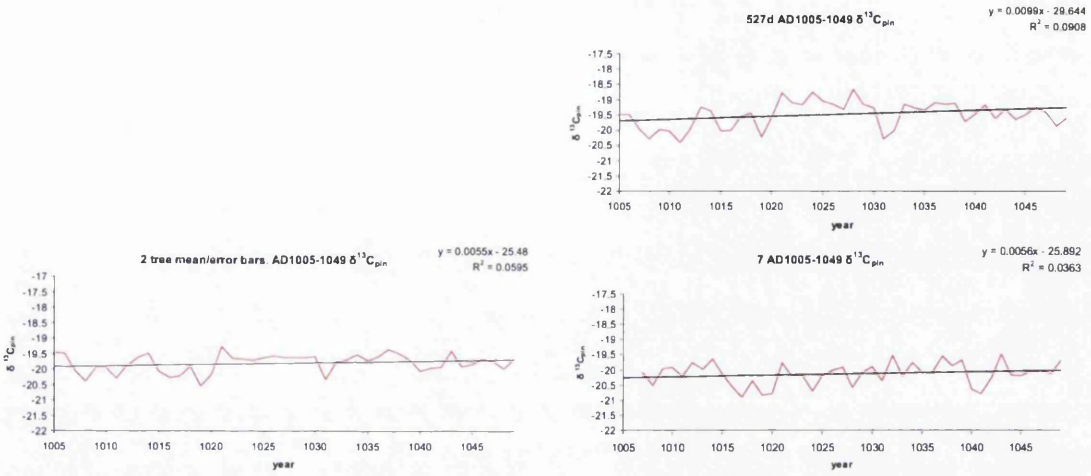

Figure 6.90 Individual trees $\delta^{13}C$ 1005-1049.

Table 6.23 Tree details
Below: inter tree correlation $\delta^{13}C$1005-1049

Tree	Most positive year (AD)	Most negative year(AD)	mean $\delta^{13}C$
527d	1024	1011	-19.48
007	1032	1017	-20.13
mean	**1021**	**1019**	**-19.79**

	527d
527d	
007	0.06
Mean r	**.06**

6.25 Summary of chapter 6

The major findings from breaking down the data into discrete 'blocks' is that many of the climatic events apparent in the Blanco $\delta^{13}C$ series are reflecting regional climatic events evident in other proxy records. Many of the sub decadal/ decadal droughts evident in the 1000 year $\delta^{13}C$ record correspond to droughts identified by other researchers. The high frequency (i.e annual) events that other researchers have explained in terms of the after effects of volcanic eruptions are in many cases not apparent in the Blanco $\delta^{13}C$ series. Whereas the frost rings identified by other researchers are the result of several days sub zero summer temperature, the $\delta^{13}C$ values are more reflective of summer conditions as a whole. The major annual negative excursions in $\delta^{13}C$ apparent in the Blanco series may reflect years when the weather throughout the summer was cold or wet rather than only several days being extremely cold or wet. The effects of certain large eruptions, known both through historical study and analysis of light/frost tree rings are absent from the Blanco $\delta^{13}C$ series. The climatic after effects of the eruptions of Laki in 1783 and Tambora in 1815 are well documented but are not represented in the Blanco $\delta^{13}C$ series. The greatest departures from the mean (both annual and low frequency) may reflect the effects of climatic events that were either of a regional nature or the after effects of climate phenomena such as volcanoes only when such phenomena affected the weather in this particular part of western North America. In summary, the main climatic events present in the Blanco $\delta^{13}C$ series may represent local climatic events, and to a lesser extent global or hemispheric climate events.

7.1 Introduction

The following chapter places the Blanco $\delta^{13}C$ series into a climatic context and compares the Blanco $\delta^{13}C$ climate reconstruction against other bristlecone pine records.

7.2 Comparison with 5 year pooled bristlecone isotope data (Leavitt, 1994; Leavitt and Long, 1992).

The most obvious data to compare the Blanco isotope data against would be any other bristlecone isotope and ring width chronologies. Professor S.W Leavitt provided previously published data (Leavitt, 1994; Leavitt and Long, 1992) for direct comparison with the Blanco carbon isotope chronology. The three chronologies used by Leavitt (1994) and Leavitt and Long (1992) comprise Methuselah A (AD1420-1984- four pooled trees of five year pentads), Methuselah B (AD925-1654 two pooled trees of five year pentads) and Patriarch (eight pooled trees- five year pentads).

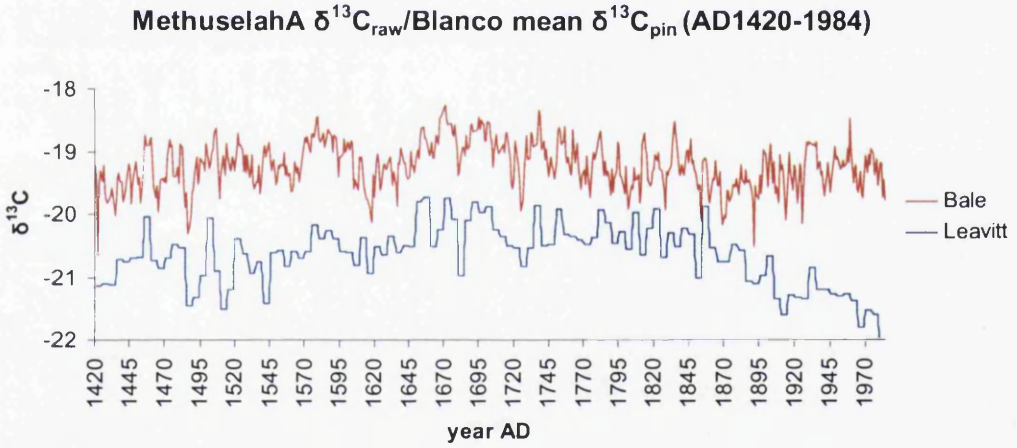

Figure 7.1 Methuselah A $\delta^{13}C_{raw}$/Blanco mean $\delta^{13}C_{pin}$ (AD1420-1984). Methuselah A chronology consists of four trees cut up into 5 year (Pentads) pooled samples (e.g 1420-1424, 1425-1429 etc).

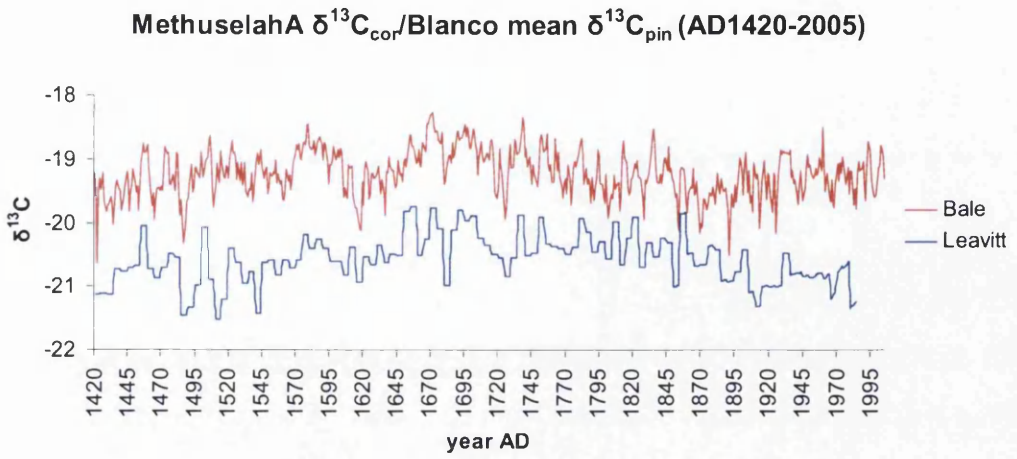

Figure 7.2 Methuselah A $\delta^{13}C_{cor}$/Blanco mean $\delta^{13}C_{pin}$ (AD1420-1984).

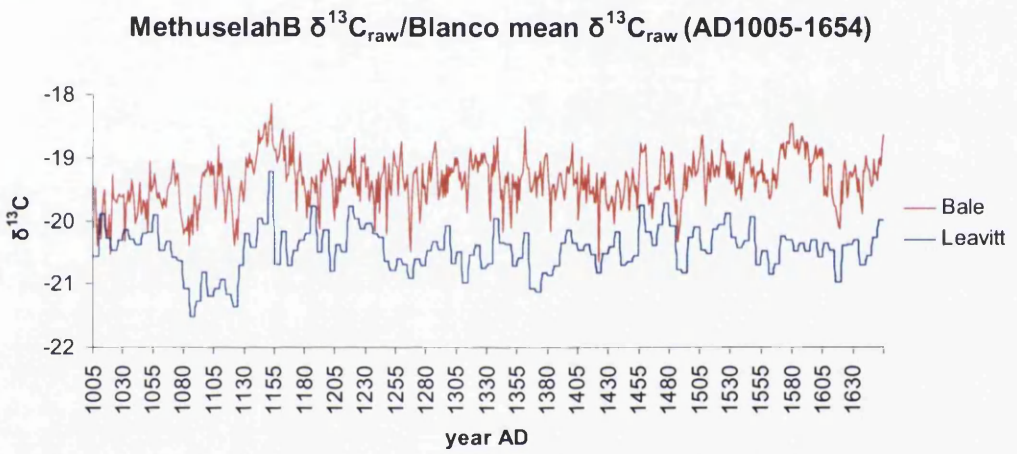

Figure 7.3 Methuselah B $\delta^{13}C_{raw}$/Blanco mean $\delta^{13}C$ (AD1005-1654). Methuselah A chronology consists of four trees cut up into 5 year (Pentads) pooled samples (e.g 1005-1009, 1010-1014 etc).

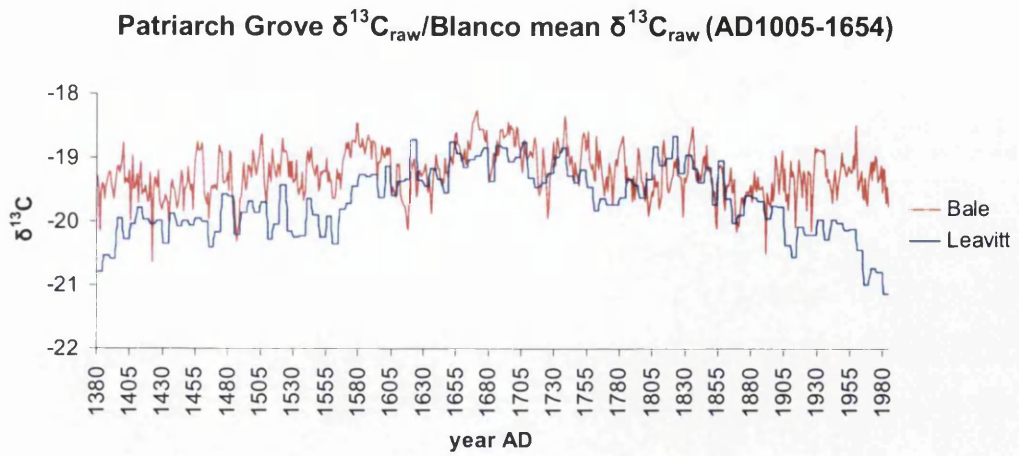

Figure 7.4 Patriarch $\delta^{13}C_{raw}$/Blanco mean $\delta^{13}C_{pin}$ (AD1380-1984). Methuselah A chronology consists of four trees cut up into 5 year (Pentads) pooled samples (e.g 1380-1384, 1385-1389 etc).

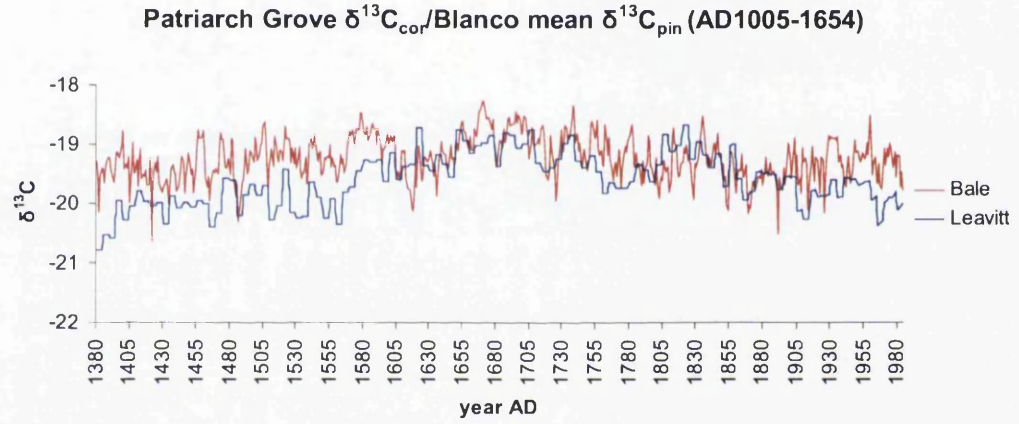

Figure 7.5 Patriarch $\delta^{13}C_{cor}$ (Leavitt and Long, 1992)/ Blanco mean $\delta^{13}C_{pin}$ (AD1380-1984). Methuselah A chronology consists of four trees cut up into 5 year (Pentads) pooled samples (e.g 1380-1384, 1385-1389 etc).

As evident from the above comparisons with the data of Leavitt (1994), there are many similarities between the carbon isotope datasets (figure 7.1 to 7.5). Both the Methuselah $\delta^{13}C$ data and the Patriarch $\delta^{13}C$ data appear to correlate well with the annually resolved Blanco $\delta^{13}C$ data. The absolute Patriarch $\delta^{13}C$ values are closer to the absolute $\delta^{13}C$ values of the Blanco values. The trees at Methuselah are growing at c.3000m a.s.l and the trees at Patriarch are growing at c.3500m a.s.l. The similarities between the absolute values of the Blanco and Patriarch isotope chronologies are probably due to the trees growing at similar altitudes. The effects of altitude on bristlecone pine tree ring cellulose have already been studied by

Leavitt and Long (1992). An altitudinal gradient of c.1.2‰ per km^{-1}, attributable to reduced pressure of internal to external CO_2 is apparent from studies of the $\delta^{13}C$ composition of leaves of different tree species (Körner *et al.*, 1988). With regard to the bristlecone pines themselves, Leavitt and Long (1992:179) notes "*The Patriarch site is consistently isotopically heavier ($\delta^{13}C$ -enriched) over this time period with an average $\delta^{13}C$ value of - 19.82‰, whereas the Methuselah average is -20.91‰. The average $\delta^{13}C$ difference between the two sites is 1.09‰. This gradient of 2.2‰ km -1 is about twice that found by Körner et al., (1988).*"

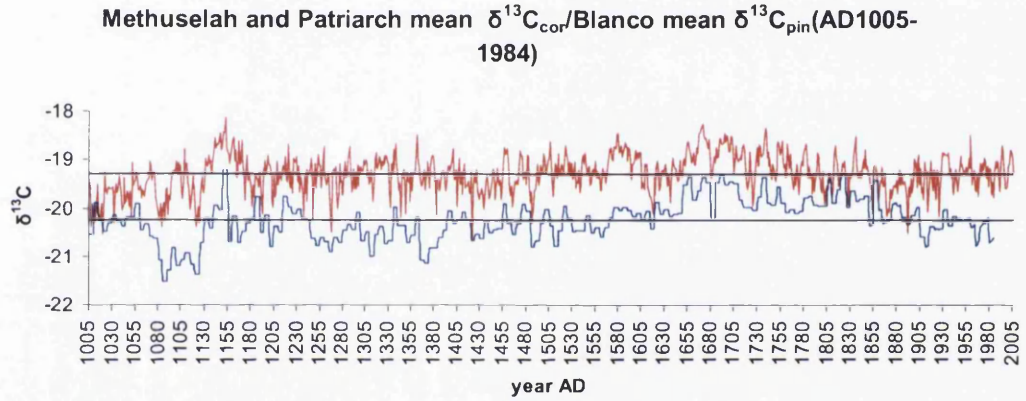

Figure 7.6 Mean of all (Methuselah A+B and Patriarch Leavitt, 1994; Leavitt & Long, 1992) $\delta^{13}C_{cor}$ AD1005-1984 /Blanco mean $\delta^{13}C_{pin}$ (AD1005-2005).

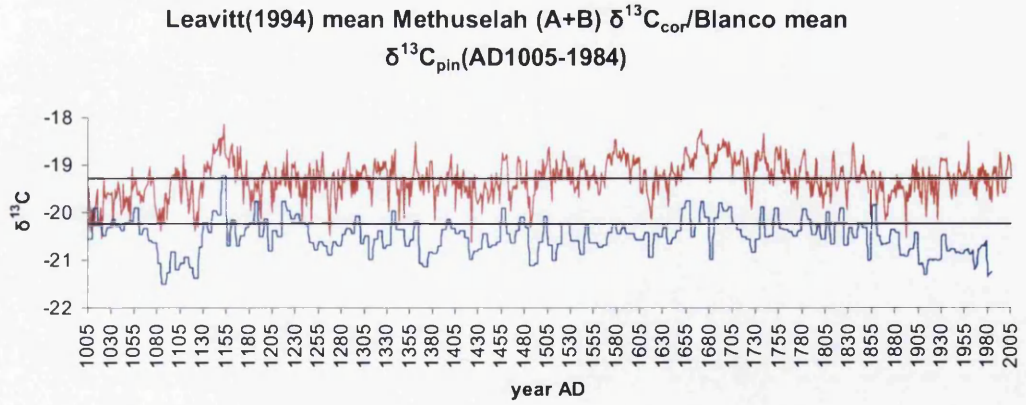

Figure 7.7 Mean Methuselah (blue) A+B $\delta^{13}C_{cor}$ AD1420-1984, AD 1005-1654 respectively (Leavitt, 1994) and Blanco (red) 2-7 tree mean $\delta^{13}C_{pin}$ (AD1005-2005).

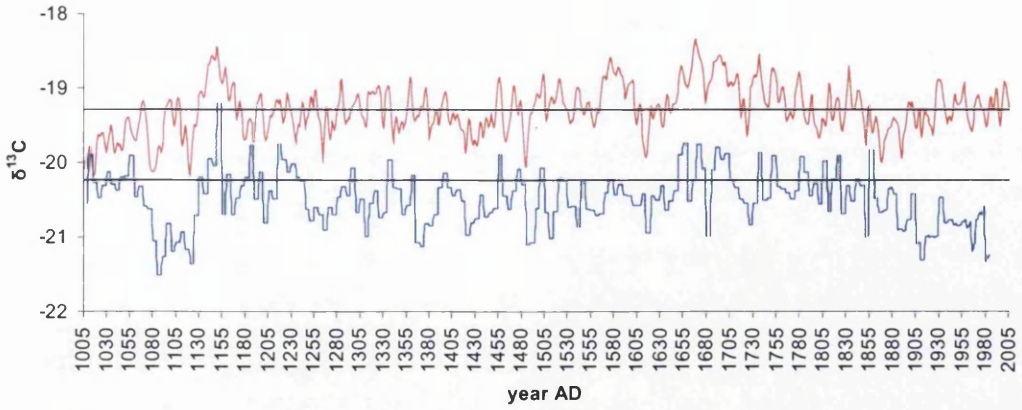

Figure 7.8.mean Methuselah A+B $\delta^{13}C_{cor}$ AD1420-1984, AD 1005-1654 respectively (Leavitt, 1994) and Blanco 2-7 tree mean 5 yr centred mean (e.g AD1005-1009 centred on AD1007) $\delta^{13}C_{pin}$ (AD1005-2005).

7.3: Correlation of Methuselah A $\delta^{13}C_{cor}$ and Blanco $\delta^{13}C_{cor}$ / $\delta^{13}C_{pin}$ with gridded instrumental climate data.

This chapter compares the 5 year $\delta^{13}C_{cor}$ pentad data of Leavitt (1994) and the Blanco $\delta^{13}C_{cor}$ /$\delta^{13}C_{pin}$ against gridded climate data using the KNMI spatial analysis tool (Oldenborgh & Burgers, 2005). This has been undertaken to ascertain possible differences in climatic influence between the two sites (Methuselah and Blanco) and also any differences in climate correlation between the five year pooled Methuselah data and the annually resolved Blanco data.

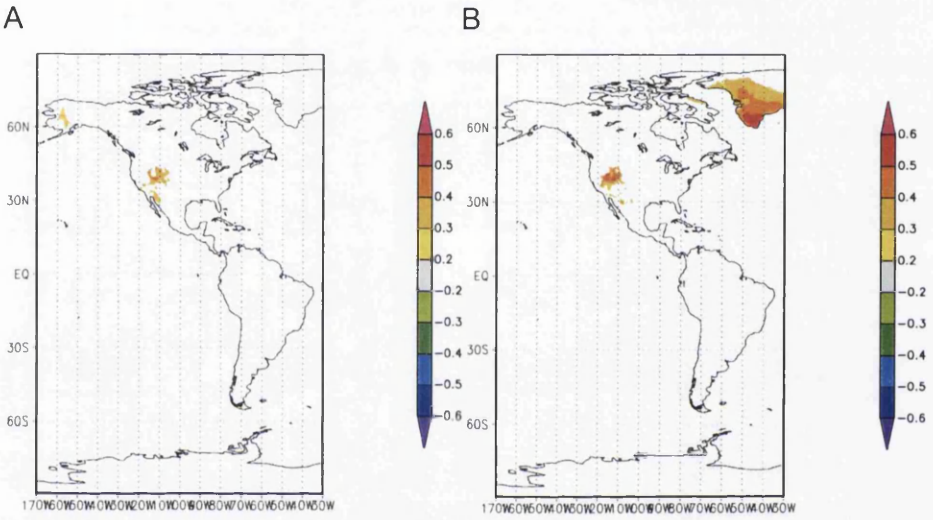

Figure 7.9 .KNMI generated map-A) Leavitt (1994)-Methuselah A ($\delta^{13}C_{cor}$)/ June-August average maximum temperature 1901-1984. B) Blanco mean ($\delta^{13}C_{cor}$) for the same time period (1901-1984). Both sets of $\delta^{13}C_{cor}$ data (both Methuselah and Blanco) appear to reflect average summer maximum temperature for the USA. The annually resolved Blanco $\delta^{13}C_{cor}$ data does however correlate significantly with Greenland maximum average summer temperature, suggesting a possible teleconnection. The fact that the 5 year pentad data reflects summer temperature adds support to the possibility that the low frequency trends in $\delta^{13}C_{cor}$ reflect summer temperature.

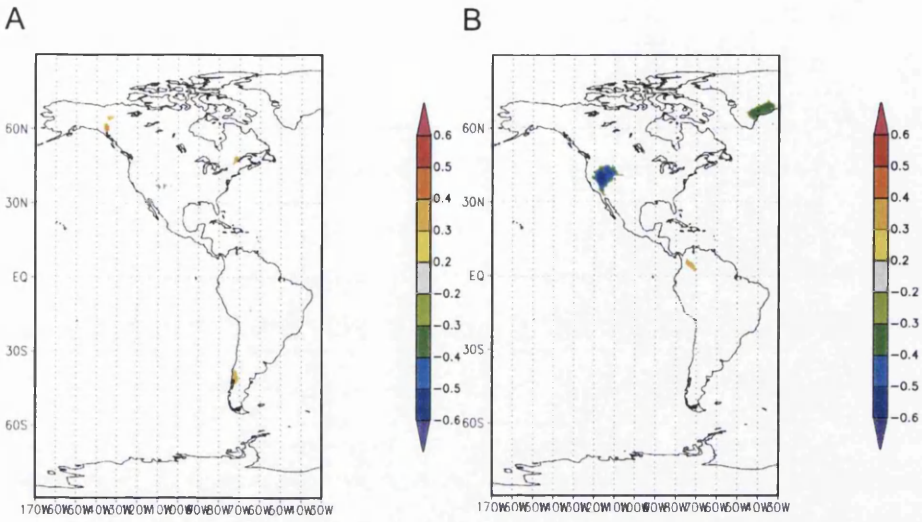

Figure 7.10 .KNMI generated map- Leavitt (1994)-Methuselah A) ($\delta^{13}C_{cor}$)/June-August average precipitation 1901-1984. B) Blanco mean ($\delta^{13}C_{cor}$) for the same time period (1901-1984). The annually resolved Blanco $\delta^{13}C_{cor}$ data has a stronger correlation with average summer precipitation than the 5 year pentad data. As with summer temperature there is also significant correlation between the annually resolved Blanco data and Greenland precipitation.

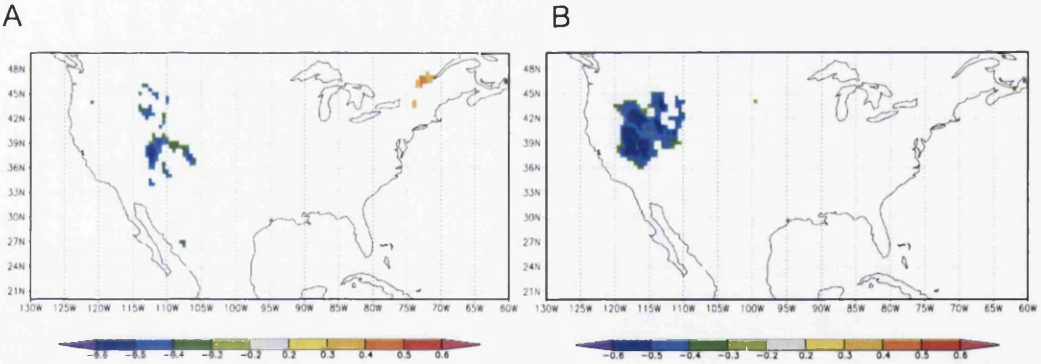

Figure 7.11.KNMI generated map- Leavitt (1994)-Methuselah A) $\delta^{13}C_{cor}$/June-August PDSI 1901-1984. B)- Blanco mean $\delta^{13}C_{cor}$ for the same time period (1901-1984).

7.4: Correlation of Patriarch $\delta^{13}C_{cor}$ and Blanco $\delta^{13}C_{cor}$ with gridded instrumental climate data.

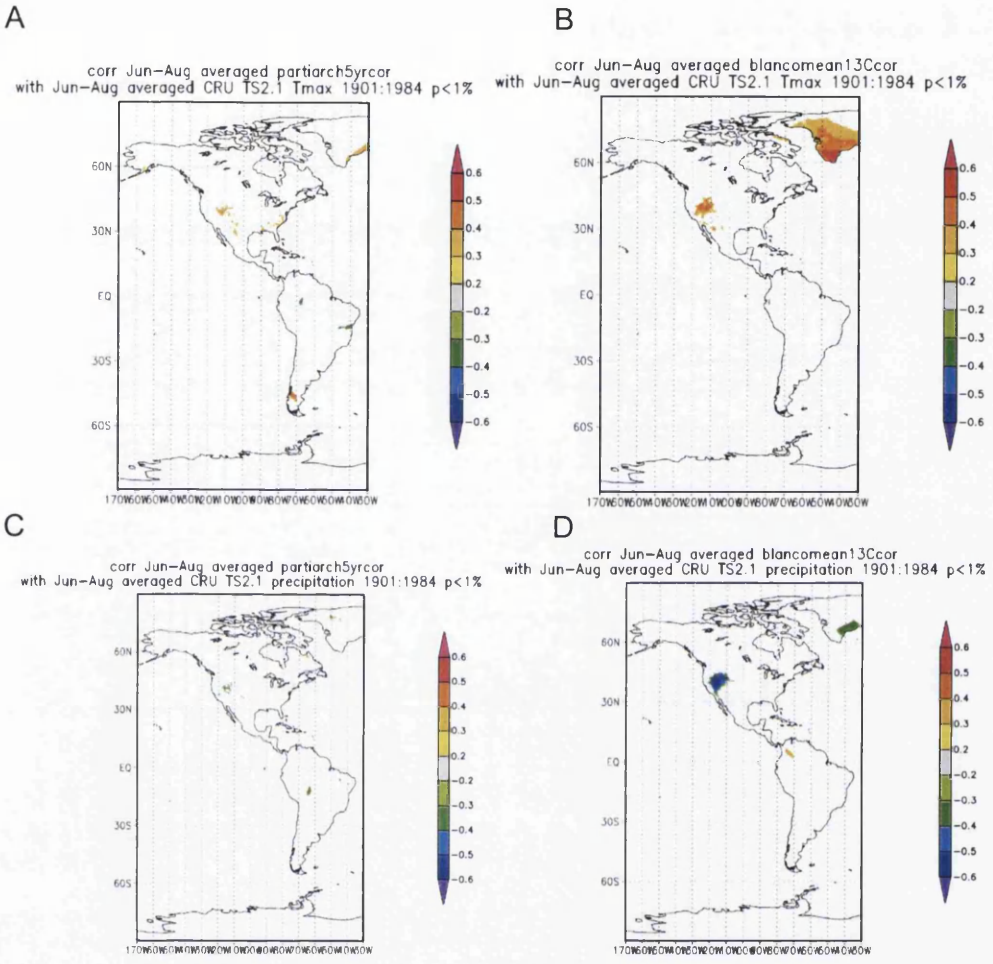

Figures 7.12 .KNMI generated maps- A) Leavitt (1994)-Patriarch ($\delta^{13}C_{cor}$)/ June-August average maximum temperature 1901-1984. B) Blanco mean ($\delta^{13}C_{cor}$) for the same time period (1901-1984). C and D) June- August average precipitation for the same period (1901-1984) for Patriarch and Blanco $\delta^{13}C_{cor}$.

As can be seen using annually resolved $\delta^{13}C$ data from bristlecone pine (7.12 D) rather than five year pentad data (7.12C) from sites at similar locations improves the degree of correlation with instrumental climate data.

7.5 Correlations of annual and smoothed Blanco $\delta^{13}C_{pin}$ and $\delta^{13}C_{cor}$ data and pooled data (Leavitt, 1994; Leavitt & Long, 1992) with climate.

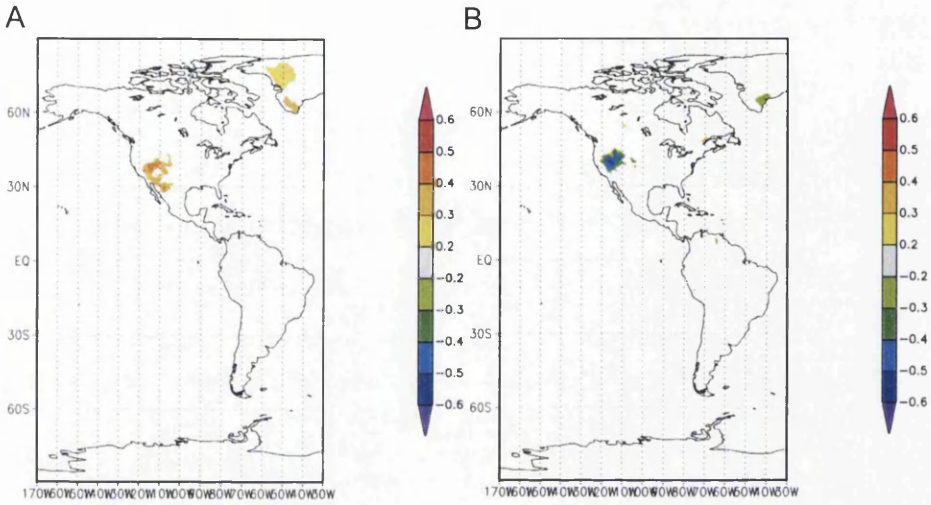

Figure 7.13 .KNMI generated maps. A) mean Blanco ($\delta^{13}C_{pin}$)/June-August average maximum temperature for the time period AD1901-2002.B) mean Blanco ($\delta^{13}C_{pin}$)/June-August average precipitation for the time period AD1901-2002.

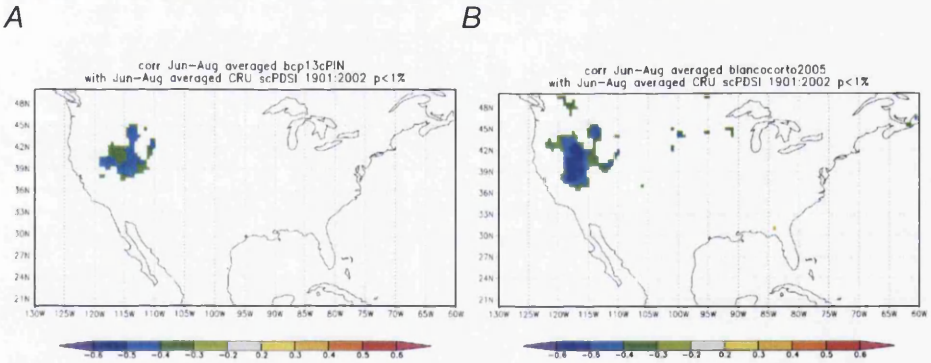

Figure 7.14 A) Mean Blanco $\delta^{13}C_{pin}$ / June, July, August averaged PDSI.B) Blanco $\delta^{13}C_{cor}$/June, July August PDSI.

However the application of the PIN correction (McCarroll *et al.*, in press), weakens the correlation slightly with precipitation and PDSI, but increases correlation with temperature (chapter 5.1). As mentioned previously (chapter 5.7) smoothing the annually resolved isotope data to three, four, five year averages increases the correlation with temperature (figures 7.16 to 7.18).

A B

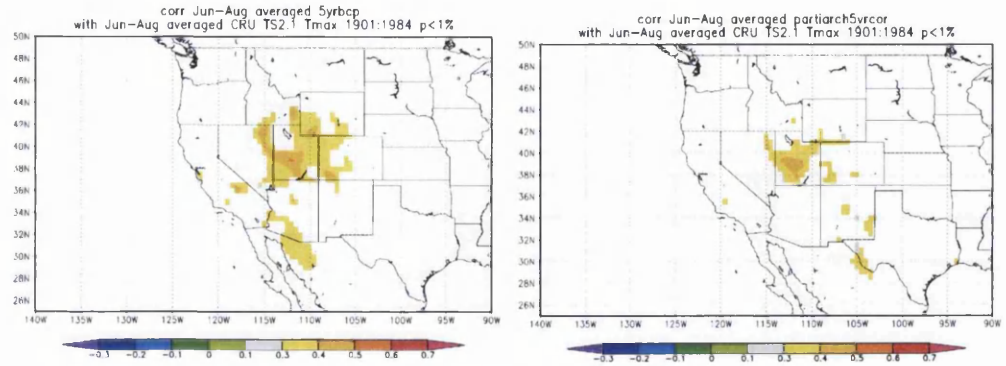

Figure 7.15.A) Patriarch $\delta^{13}C_{cor}$ / B) Methuselah A $\delta^{13}C_{cor}$. Maximum summer temperature (June, July and August average) 1901-1984

A B

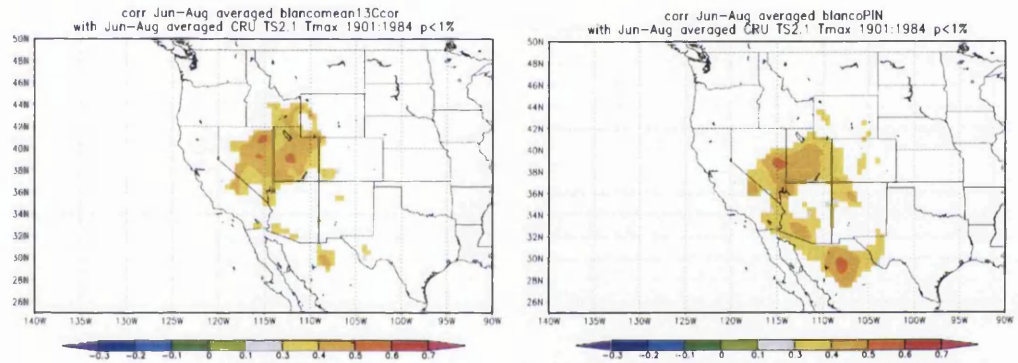

Figure 7.16.A) Blanco $\delta^{13}C_{cor}$ and B) Blanco $\delta^{13}C_{pin}$ maximum summer temperature (June, July and August average) 1901-1984

A B

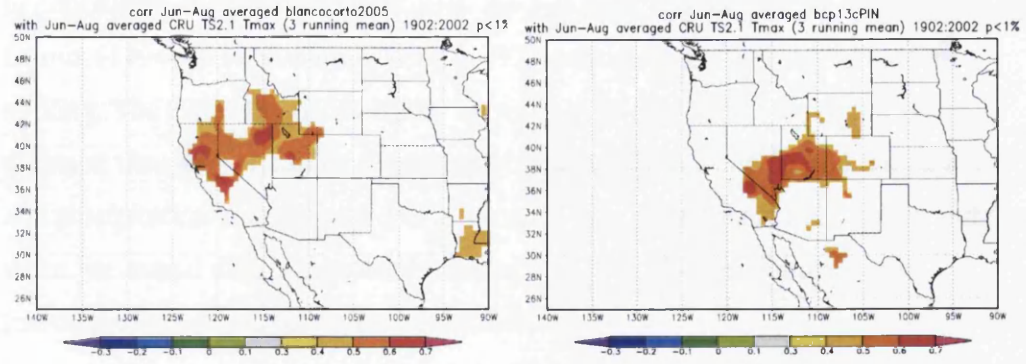

Figure 7.17.A) Blanco $\delta^{13}C_{cor}$ and B) Blanco $\delta^{13}C_{pin}$ three year running mean correlation with maximum summer temperature (June, July and August average) 1903-2002

A B

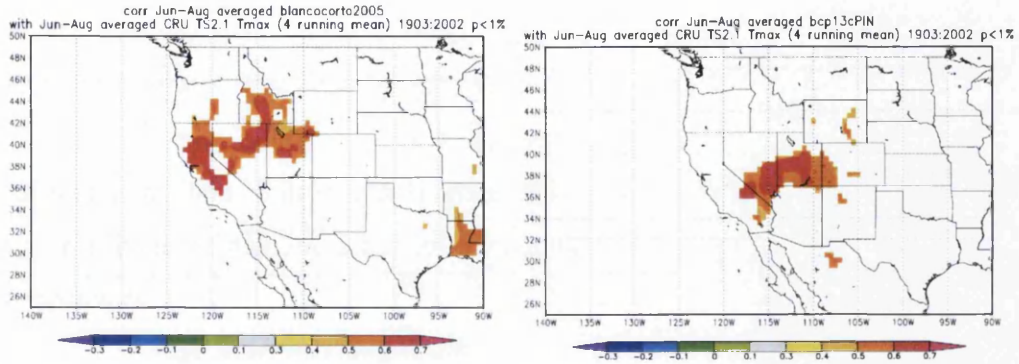

Figure 7.18. . Blanco $\delta^{13}C_{cor}$ and Blanco $\delta^{13}C_{pin}$ four year running mean correlation with maximum summer temperature (June, July and August average) 1903-2002.

A B

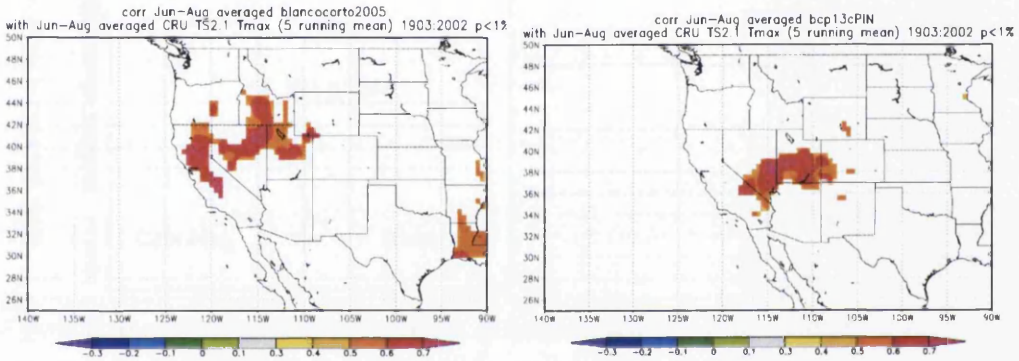

Figure 7.19.A) Blanco $\delta^{13}C_{cor}$ and B) Blanco $\delta^{13}C_{pin}$ five year running mean correlation with maximum summer temperature (June, July and August average) 1903-2002.

In conclusion, the similarities between the five year 'blocks' of data as presented by Leavitt (1994) and Leavitt and Long (1992) and the annually resolved data are striking. The lower frequency trends between trees from different altitudes and different sites appear similar. However, correlation between $\delta^{13}C$ and temperature and precipitation instrumental data is stronger than with pooled pentad data and yet when the annual data is smoothed (figures 7.17 to 7.19), the climate signal (particularly with temperature) is enhanced.

7.6 Comparison of Blanco $\delta^{13}C$ with millennial bristlecone ring width chronologies/climate reconstructions.

With a tree species living in a harsh, semi arid environment it would be expected that ring size would be heavily influenced by moisture. Previous ring width studies (Ferguson, 1968, LaMarche, 1974, Graybill and Funkhouser, 1995, Salzer and Kipfmueller, 2005, Salzer and Hughes, 2007) have emphasised the sensitivity of lower altitude bristlecone pines to precipitation and those trees at high altitude to temperature.

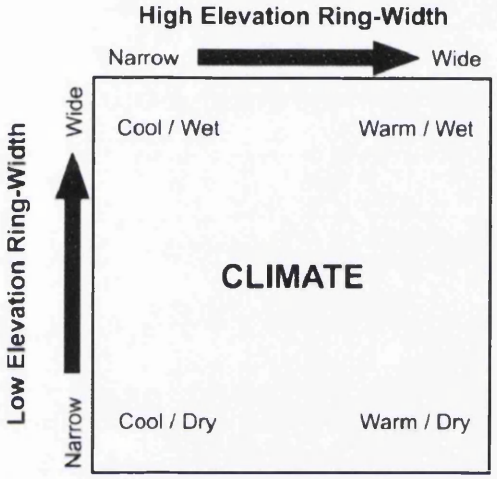

Figure 7.20 . Hypothetical link between altitude/climate and ring widths. From Salzer and Kipfmueller (2005: 467).

If the $\delta^{13}C$ values are also influenced by moisture then there should be some degree of similarity between the two series. The following figures (7.21 to 7.29) examine the similarities between the Blanco $\delta^{13}C$ and ring widths for the same two to seven tree mean.

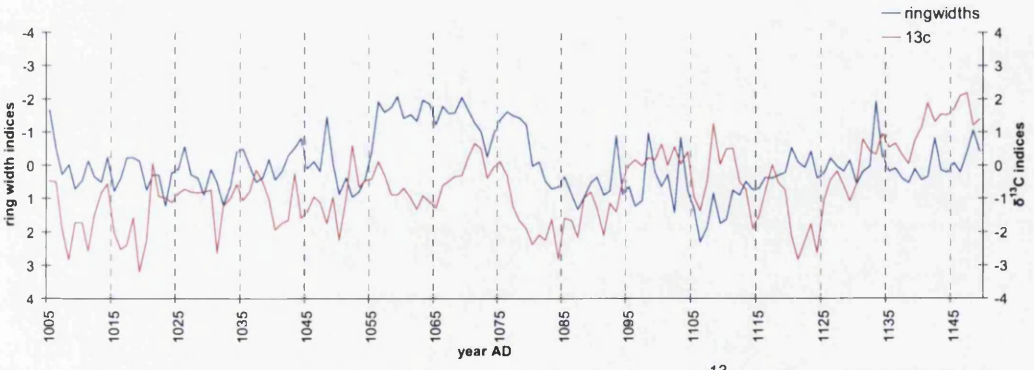

Figure 7.21.Blanco mean ring width indices and Blanco mean $\delta^{13}C$ indices AD1005-1149.

More negative ring width indices indicate narrow rings and more positive $\delta^{13}C$ indices indicate dry or hot conditions.

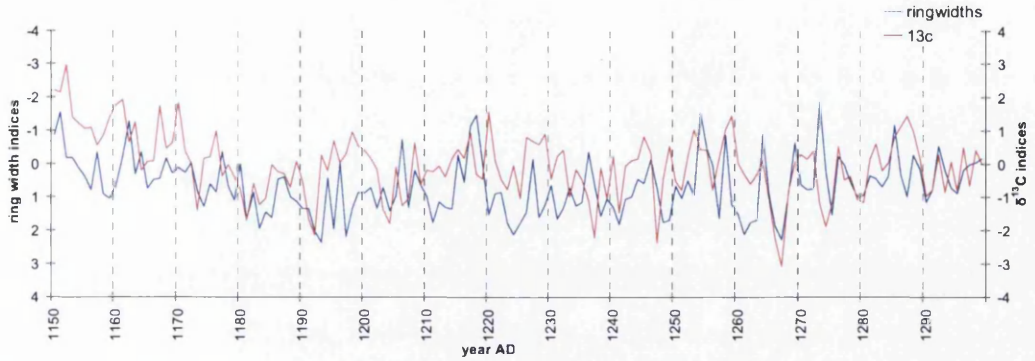

Figure 7.22. Blanco Ring width indices and mean $\delta^{13}C$ indices AD1150-1299.

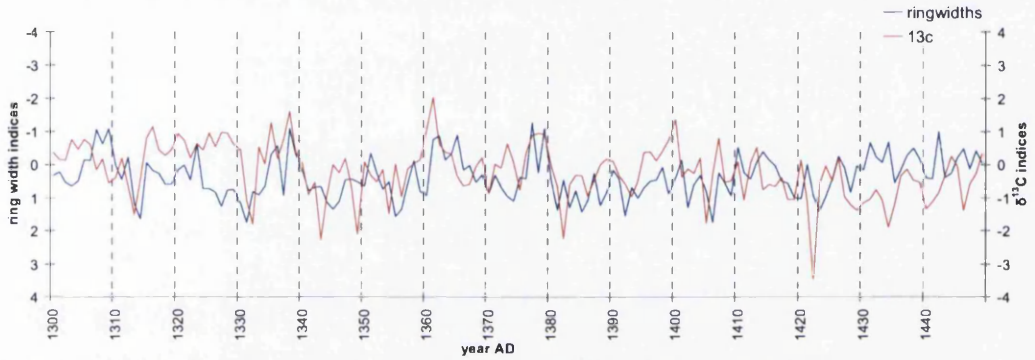

Figure 7.23. Blanco Ring width indices and mean $\delta^{13}C$ indices AD1300-1449.

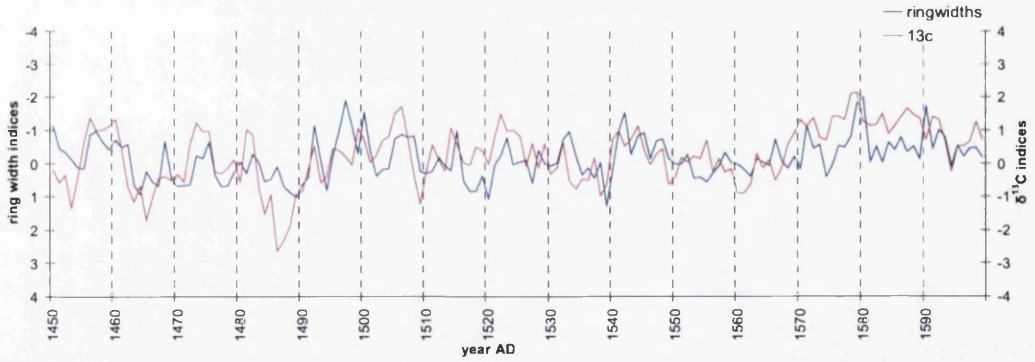

Figure 7.24. Blanco Ring width indices and mean $\delta^{13}C$ indices AD1450-1599

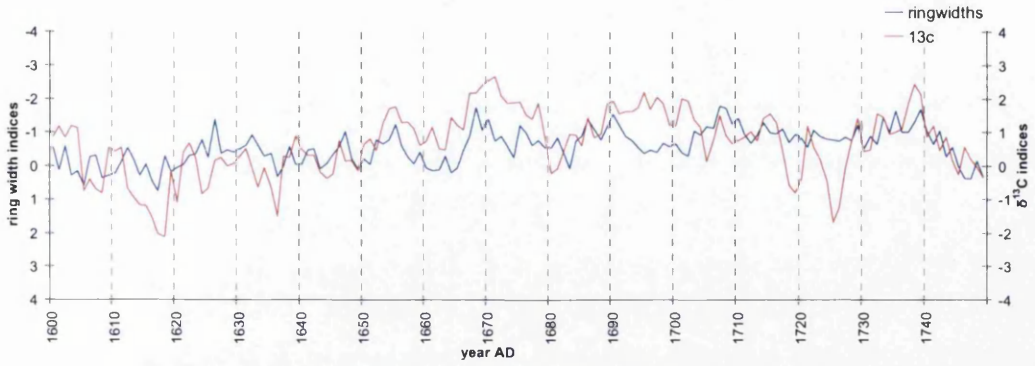

Figure 7.25. Blanco Ring width indices and mean $\delta^{13}C$ indices AD1600-1749

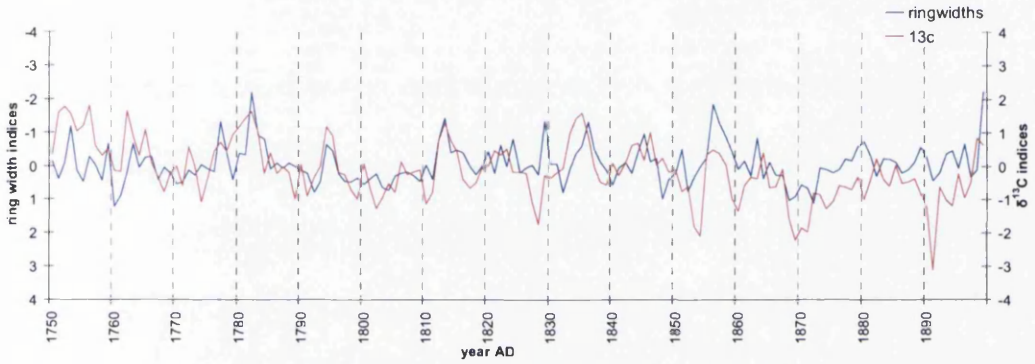

Figure 7.26. Blanco Ring width indices and mean $\delta^{13}C$ indices AD1750-1899

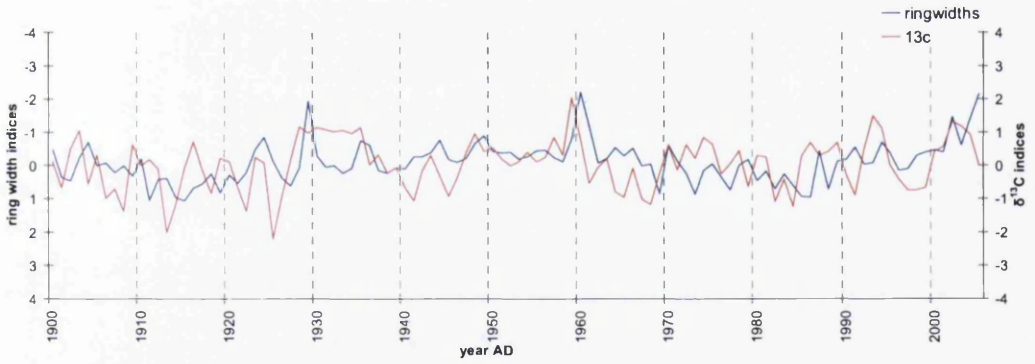

Figure 7.27 . Blanco Ring width indices and mean $\delta^{13}C$ indices AD1900-2005

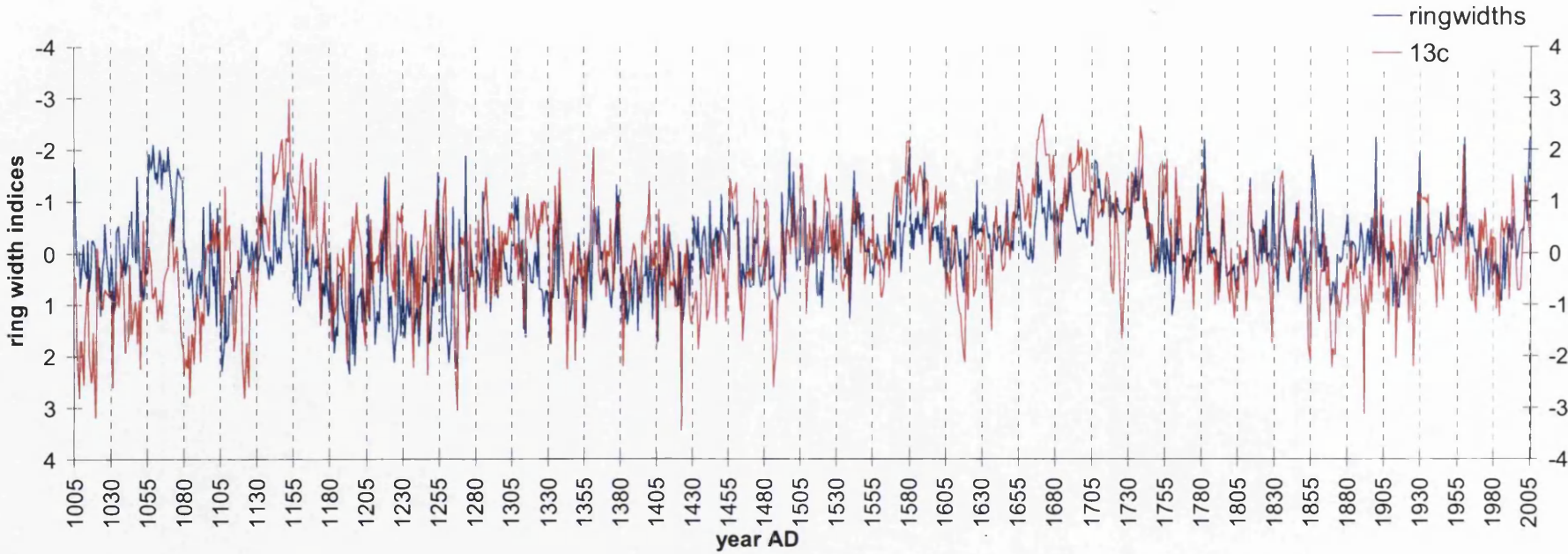

Figure 7.28. Blanco Ring width indices and mean $\delta^{13}C$ indices AD1005-2005

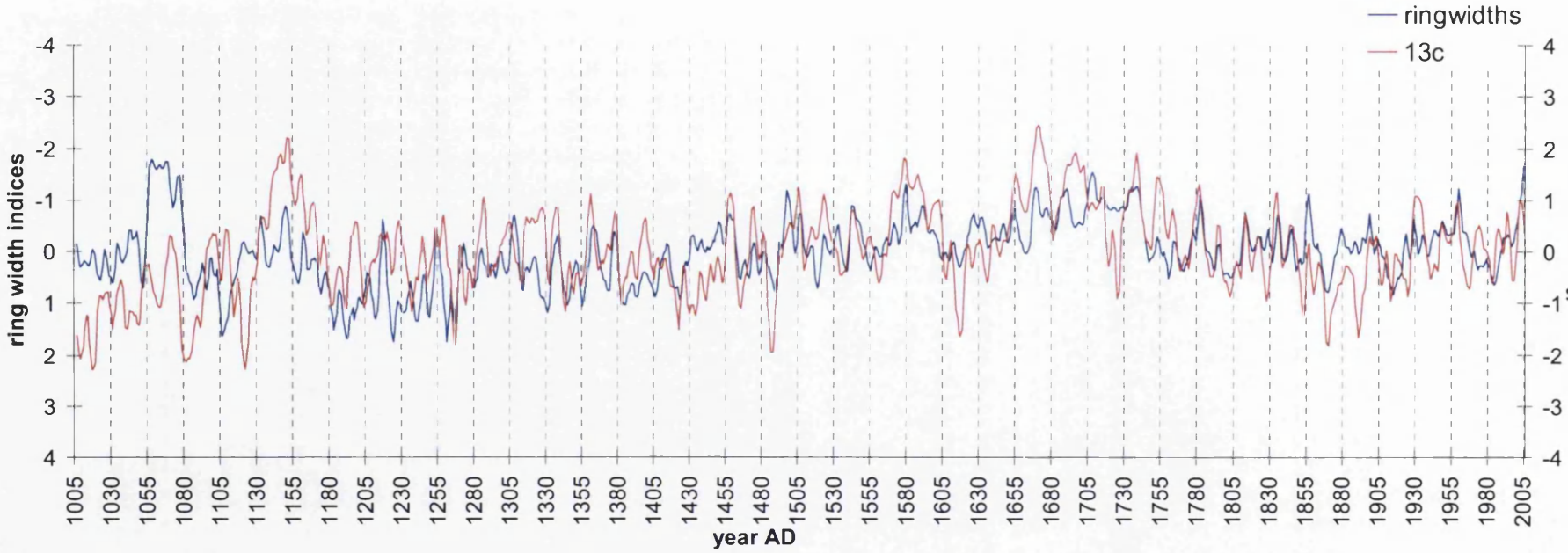

Figure 7.29 . 5 year centred Blanco mean ring width normalised indices and mean $\delta^{13}C$ indices AD1005-2005

The degree of similarity between the ring width indices and the $\delta^{13}C$ indices of the seven Blanco trees is in places striking. It is no surprise in such a water stressed environment that there is a high degree of association between the $\delta^{13}C$ and the ring width series. However, using the raw ring width or even normalised ring width values in comparison to the $\delta^{13}C$ series is not really appropriate. Ring width series require detrending because of age related trends, and such trends are clearly evident in the raw ring widths and will be inherited into the normalised indices. It is also worth comparing the $\delta^{13}C$ reconstruction against other bristlecone pine climate reconstructions based on ring widths from many more trees.

Extreme $\delta^{13}C$ values often occur one year before the event is visible as a narrow ring. Notable examples of this appear to occur in 1579, 1738, 1835, 1929 and 1959 when extreme positive $\delta^{13}C$ values precede extreme narrow rings. It may well be the case that the addition of many more trees to the ring width series would improve climate correlations, although for extreme narrow years at least it seems unlikely as the rings appear narrow in all the Blanco trees and the master chronologies used during cross dating. Despite the similarities between the ring widths and isotopes, the controls that affect $\delta^{13}C$ uptake in trees are better understood (Farquhar *et al.*, 1982; Vogel, 1980) than those that contribute to the formation of an annual ring so it is probable that $\delta^{13}C$ ratios represent a more precise proxy for summer, growing season conditions than do the ring widths, being as they are, an integration of many factors.

This presents problems with calibrating ring widths with climate evidenced by the way that complicated data treatment is often used (e.g Salzer and Kipfmueller, 2005) and the climate parameter used for calibration often comprising both the previous and subsequent year's temperature and precipitation. The Blanco $\delta^{13}C$ can be correlated and calibrated directly with the actual growing season conditions.

Ring width series used for climate reconstruction are often detrended to remove growth trends (Cook and Kariukistis, 1990). The first bristlecone pine ring width

data set used for comparison was a White Mountain master indices obtained from the International Tree Ring Data Base (ITRDB) and compiled by Ferguson *et al.*, (1962). This chronology comprises from 15 to 30 trees and covers the period AD1005 to AD1962.

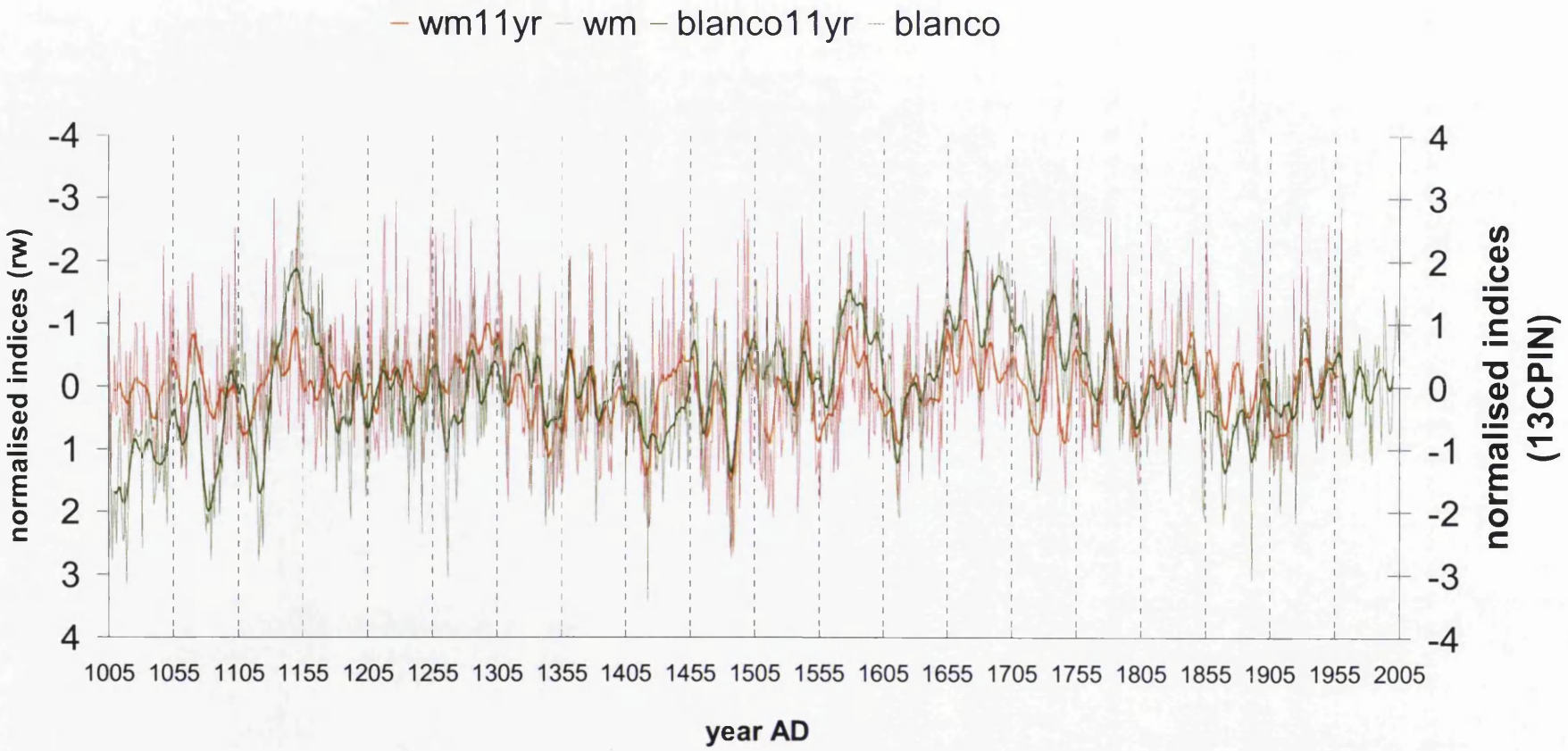

Figure 7.30. White Mountain master ring width indices (Ferguson et al.,1962) and Blanco $\delta^{13}C_{PIN}$. (r=-0.32 over period 1005-1962. r=-0.48 for 11 year mean correlation between Blanco $\delta^{13}C$ and ring width indices)

There is a high degree of correlation between the two series (figure 7.31). The high frequency changes are well represented in both the ring width indices and the $\delta^{13}C$ indices. The positive peaks in the $\delta^{13}C$ often precede the ring widths by one year. The low frequency changes appear similar but with some noticeable differences. There is less annual variability with the isotopes but lower frequency changes appear to be equally if not better represented by the isotopes. The major significant negative excursions that occur around AD1100 and the first half of the 15th century appear better represented in the $\delta^{13}C$. The droughts centred on AD1152, AD1579, AD1671 and the drought between AD1929 and 1934 being examples where the $\delta^{13}C$ appears to contain a clearer low frequency signal than the ring width indices. Looking at the correlation (*r* values) between the two series can provide numerical proof of similarity and divergence within records.

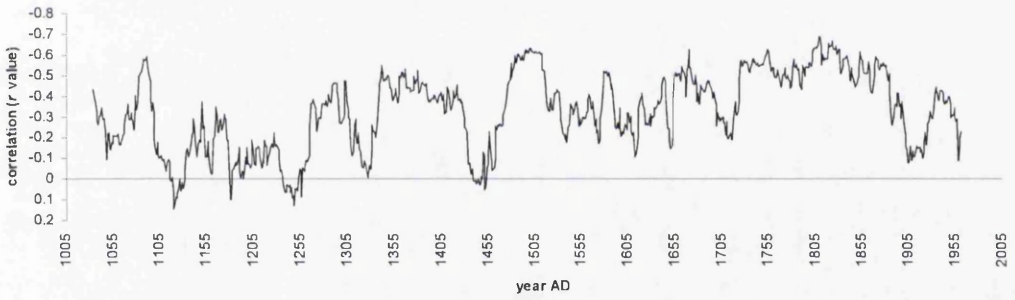

Figure 7.31.30 year running correlation between White Mountain master indices and Blanco mean $\delta^{13}C$ (AD1005-1962). The periods of low correlation between the Blanco $\delta^{13}C$ and the White Mountain ring width master may occur at time of particularly wet or cool climatic conditions (see figure 6.1 for further details). Low correlation between ring widths indices and $\delta^{13}C$ is particularly evident in the early 12th, 13th, mid 14th, mid 15th and late 19th century.

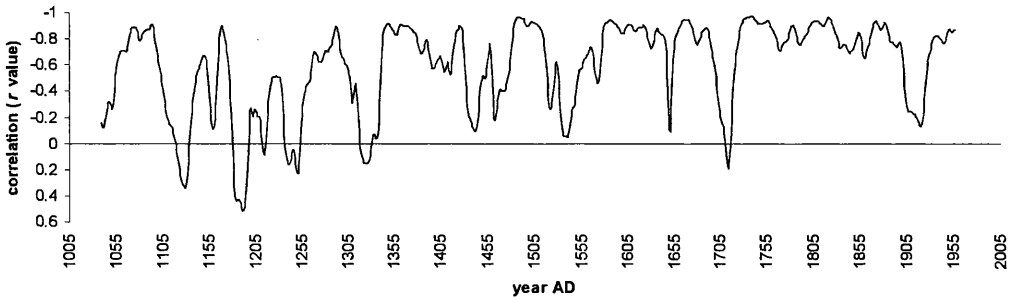

Figure 7.32.30 year running correlation between 31 year centred mean White Mountain master ring width indices/Blanco mean $\delta^{13}C$ (AD1005-1962).

As is evidenced in figure 7.32 there are periods of great similarity between the annual data and the 31 year smoothed data. It would appear that the periods of lowest correlation may occur during some of the most negative $\delta^{13}C$ phases (i.e cool/wet). The early 12th , mid 13th, early 14th, the first half of the 15th, mid 17th,early 18th and late 19th/ early 20th centuries are all phases of low correlation between the two series. This may be a reflection of a difference in response of ring widths and isotopes to extreme wet or cold events. The ring widths are very good at reflecting drought in such a moisture stressed environment but may not be so good at reflecting extreme or prolonged cold/wet periods. Leavitt (1994) suggested this may be the case for bristlecone pine.

More recent climate reconstructions using bristlecone pine ring widths have been created from other sites within the bristlecone pine range. Salzer and Kipfmueller (2005) describe a *Pinus aristata* millennial length temperature and precipitation reconstruction from the Southern Colorado Plateau. Both of these are compared to the Blanco $\delta^{13}C$ series and differences and similarities discussed.

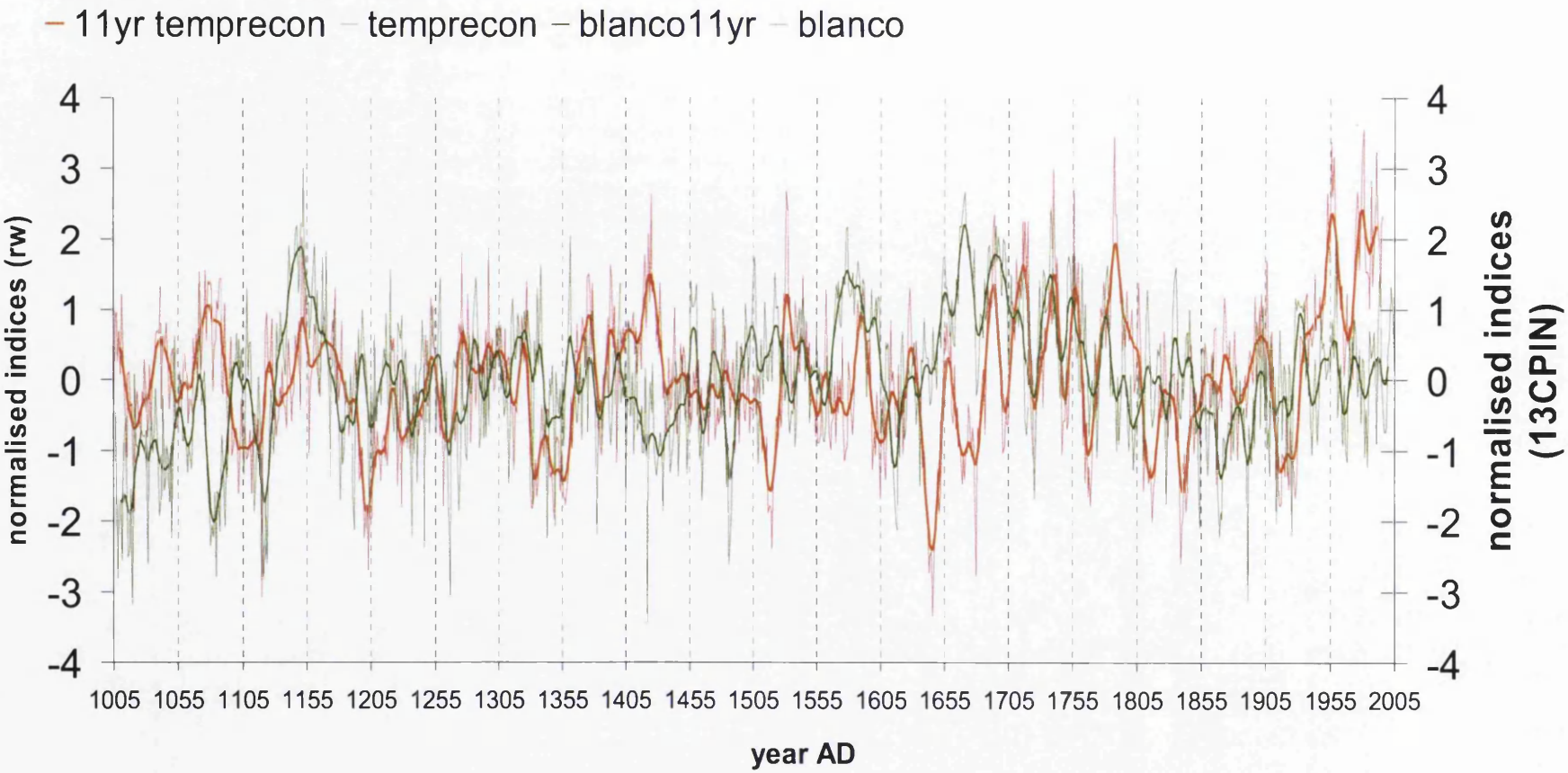

Figure 7.33. Salzer and Kipfmueller (2005) ring width (rw) temperature reconstruction and Blanco $^{13}C_{PIN}$ normalised indices. (r=0-.32 over period 1005-1962. r=-0.48 for 11 year means

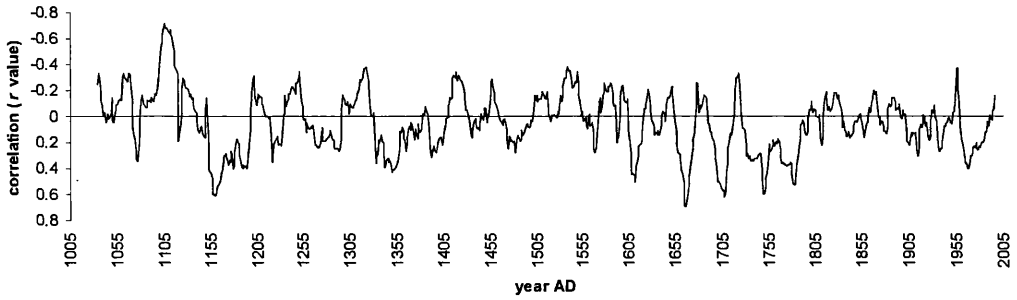

Figure 7.34.30 year running correlation between Salzer and Kipfmueller (2005) temperature reconstruction indices and Blanco mean $\delta^{13}C$ (AD1005-1996)

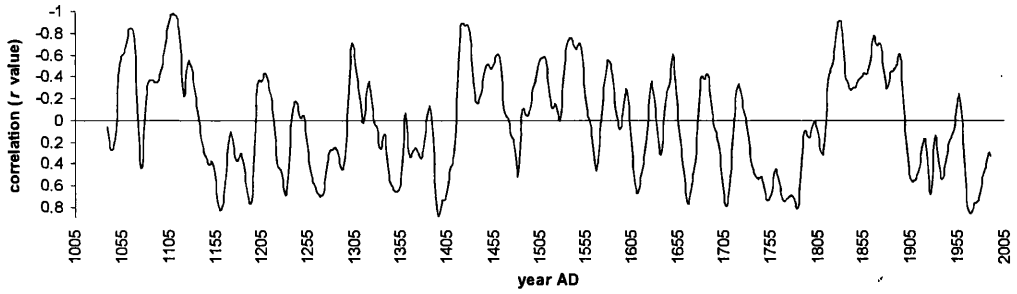

Figure 7.35.30 year running correlation between Salzer and Kipfmueller (2005) 31 year centred smoothed mean temperature reconstruction indices and Blanco mean $\delta^{13}C$ indices (AD1005-1996)

As with the White Mountain ring width climate indices there are numerous similarities with this ring width reconstruction despite the fact that the trees are from around 500 miles to the east (San Francisco Peaks, northeast Arizona) and at higher elevation than the Blanco trees (around 3500m a.s.l).

Of particular note is that the high frequency correlation is low during much of the late 18th and early 19th century (figure 7.34) but is much higher at lower frequencies (figure 7.35). This suggests that the late 19th and early 20th century witnessed cool or wet conditions that are reflected in many regional proxy records but that regionally, and at annual resolution the climate change that occurred during this period is complex. The high positive correlations evident in mid 12th, mid 17th, early and mid 18th centuries likely reflect the influence of regional or perhaps continental heat or drought. Where divergence occurs it is likely that more local factors are affecting

climate or a difference in the response to temperature or precipitation at the two sites. As the Blanco $\delta^{13}C$ record has been shown to be sensitive to both growing season temperature and precipitation this may well be likely. It is interesting to note that after AD1960 until 1996 the two records diverge and the correlations between the two series are low.

The precipitation reconstruction described by Salzer and Kipfmueller (2005) is based on three lower elevation (1890m to 2290m a.s.l) tree ring chronologies from the Flagstaff area of Arizona from three different species, ponderosa pine, pinon pine and Douglas fir. Despite periods of low correlation, reasonable annual correlation is apparent in the late 14th and 15th century and in the mid 17th century. Low frequency correlation is particularly strong in the late 16th/early 17th century, the late 17th century and the 19th century. Again as with temperature, the similarities and differences reflect the spatial and temporal complexity and patterns of drought in the southwest USA. Low high frequency correlation may reflect temporal complexity and regional climate but high low frequency correlations at the same time period may indicate regional climate influence over a long time period. Alternatively, if the bristlecone ring width chronology of Salzer and Kipfmueller (2005) is more temperature sensitive than the Blanco $\delta^{13}C$ chronology, which in turn may be more precipitation sensitive, then it is could be that the divergence in correlation between the two is reflecting hot/dry or cold/wet conditions. The early 15th century in the White Mountains may have been unusually wet and hot, the late 16th and mid to late 17th centuries in the White Mountains may well have been unusually cold and dry as evidenced in the divergence between the two records. Where the high frequency changes are in good agreement with each other it suggests a high degree of common forcing over a wide geographic area.

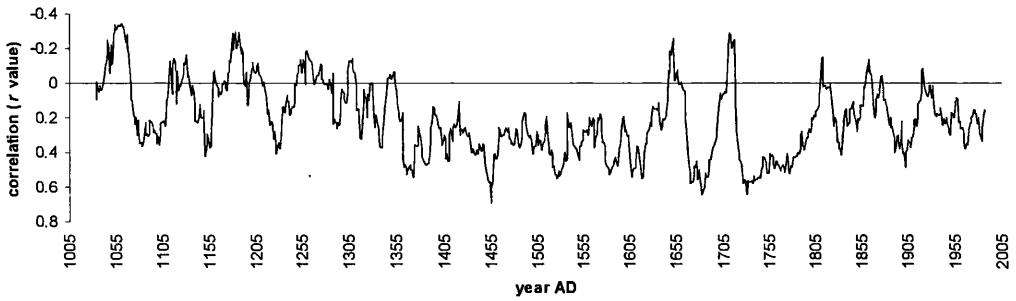

Figure 7.36.30 year running correlation between Salzer and Kipfmueller (2005) precipitation reconstruction and Blanco mean $\delta^{13}C$ (AD1005-1987)

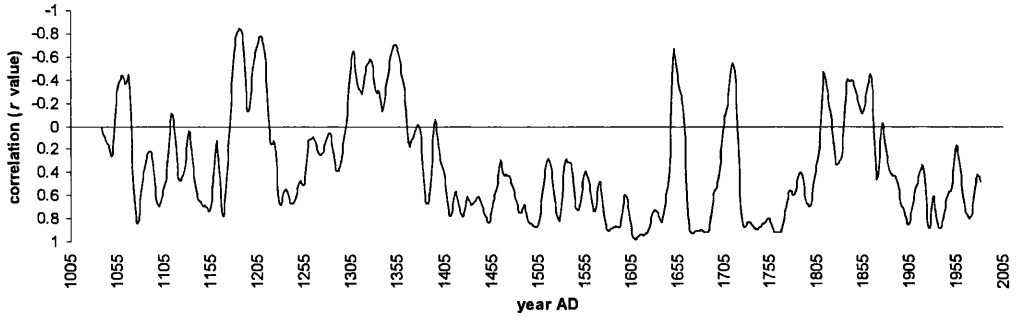

Figure 7.37.30 year running correlation between Salzer and Kipfmueller (2005) 30 year mean precipitation reconstruction and Blanco mean $\delta^{13}C$ (AD1005-1987)

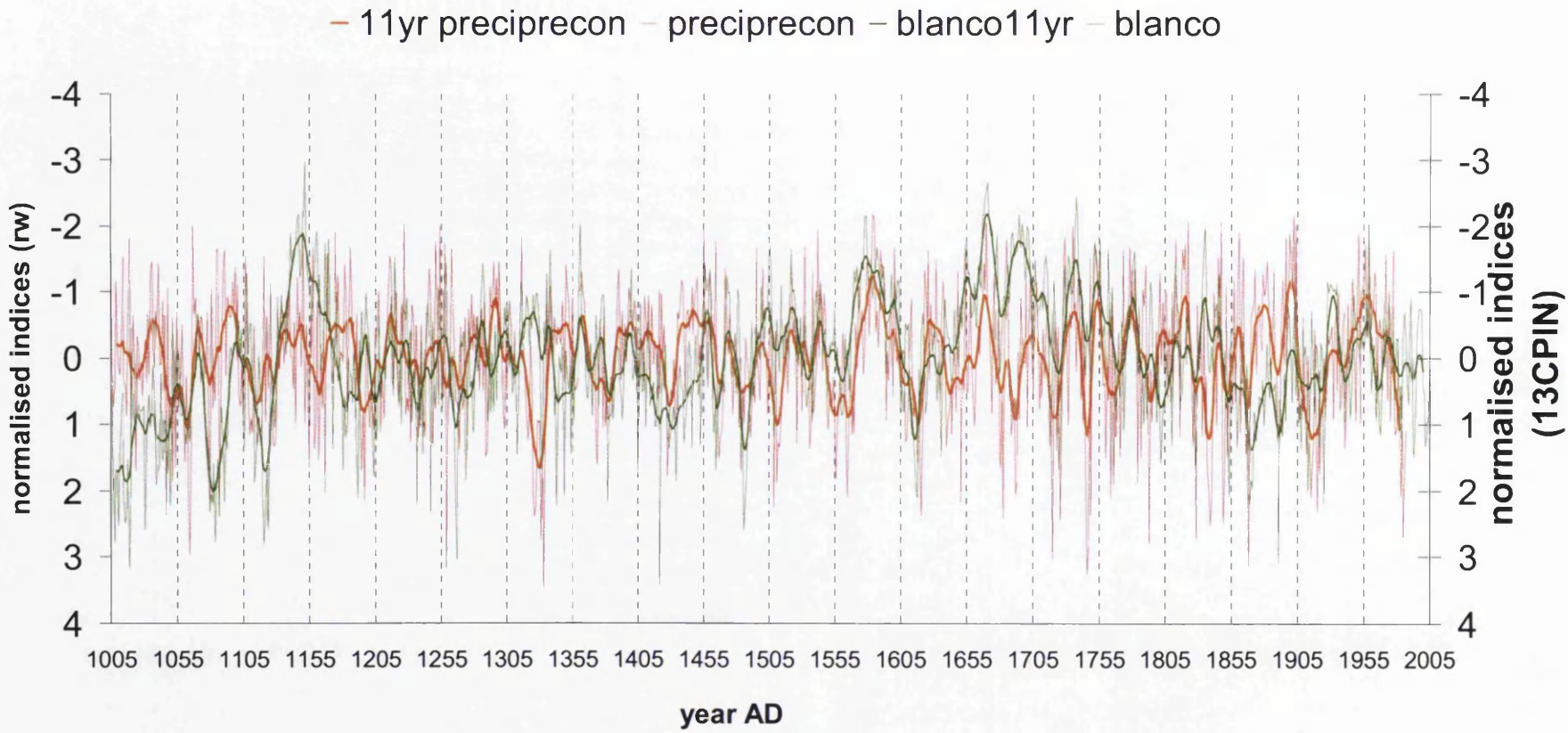

Figure 7.38. Salzer and Kipfmueller (2005) ring width (rw) precipitation reconstruction and Blanco $\delta^{13}C_{PIN}$ normalised indices (r=0.15).7.8 20th century climate change

8:0: Conclusions

This thesis has addressed the three major research questions outlined in chapter 1.10. A 1000 year $\delta^{13}C$ chronology from individual bristlecone pine trees has successfully been created. Direct comparison of the Blanco annually resolved carbon isotope data with the five year pentad carbon isotope data Leavitt (1994) and Leavitt and Long (1992) indicates a high degree of similarity in the different chronologies from different sites. The lower frequency changes appear similar for much of the chronologies but obviously extreme annual events are not picked up by the five year pentad data. Such extreme annual events may not be as important in climatic terms as low frequency changes but would be extremely important in terms of understanding of the effects of extreme climatic events on human populations and the exact nature and magnitude (in annual terms) of volcanic, drought and other environmental events. In addition, with annually resolved data, more exact calibration with instrumental climate data is possible. The climate calibration obtained from the annually resolved data could be used to calibrate the previous five year pentad data by Leavitt (1994) and Leavitt and Long (1992).

With reference to the late 11^{th}/ early 12^{th} century 'event' of particularly depleted $\delta^{13}C$ values the Blanco trees seem to show a great similarity with previous studies (Leavitt, 1994), but with the added benefit of annual resolution. There are depleted $\delta^{13}C$ from around 1080-1095 with extremes in the mean at 1082, 1084, 1087 and 1091. There is a shift to positive values from c.1096-1113, with smaller negative δ13Cs in 1108 and 1114. There is then a second negative period centred on extremes in 1121 and 1124. This has followed by comparatively positive values in the 1140s and 1150s, suggesting a major drought. The negative values during the late 11^{th}/early 12^{th} century event are some of the most negative in the whole chronology. The values are similar to raw values (not PIN or fossil fuel corrected) for the modern period and it certainly looks like the most prolonged period of negative values in the whole millennial chronology. There are more extreme $\delta^{13}C$ negatives, notably AD1267 and 1422 but these are annual extremes and not prolonged periods of $\delta^{13}C$

depletion. Unfortunately only three trees were analysed back to 1086 and only two back to 1005. The first part (perhaps the first 100-250 years of the chronology (AD1005-1250) would benefit from enhanced sample replication.

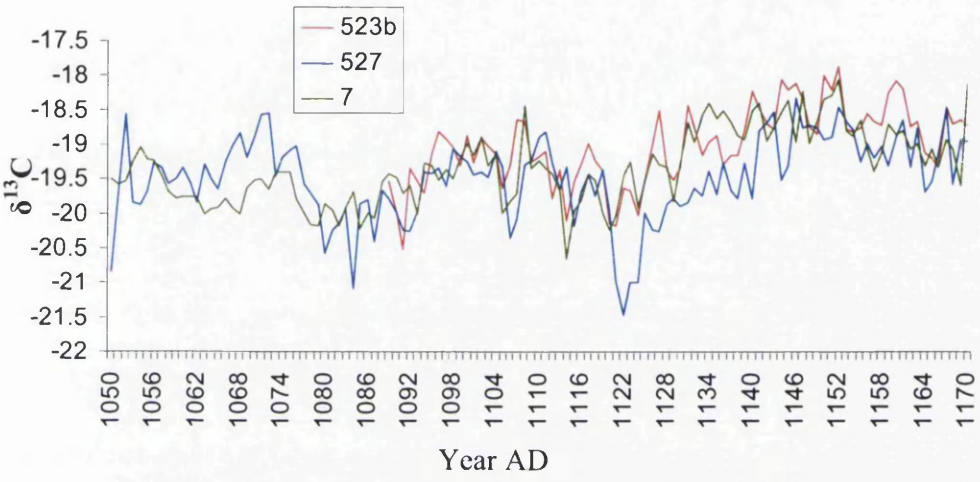

Figure 8.1 3 trees $\delta^{13}C$ from AD1050-1170.

The data reflects low temperature and higher precipitation during the late 19th century, with extreme years known from historical and tree ring evidence reflected in the isotopes. 1863, 1891 and 1913 are three examples of this. In one of the trees (4123) the second half of the 19th century shows the most depleted $\delta^{13}C$ in the entire 550 year length of the core. The data suggests the first half of the 15th century, the first half the 17th century and the 11th/early 12th century were generally cold and wet. Prolonged periods of dry/hot conditions are centred on the mid 12th century, the late 16th century and the late 17th century. The droughts look similar to those in a paper by Stahle *et al.*, (2007) outlining tree ring width reconstructed 'megadroughts' in continental north America and the Western United States. One notable exception to the similarities is that they report 1833 to be the wettest single year over the last 500 years in much of the United States. In the Blanco $\delta^{13}C$ the years 1832,1833,1834,1835 and 1836 display positive values suggesting dry or hot conditions. One explanation for this may be the question of how carbon isotopes in tree rings behave if it is very dry but also very cold. As freezing during the growing season dehydrates the tree and narrows stomata, this may lead to positive $\delta^{13}C$

values that could be interpreted as a signal of high temperature rather than cold/dry conditions.

Regarding any 'Juvenile' effect in the bristlecone $\delta^{13}C$ series, only one of the cores analysed for isotopes appeared to reach anywhere near the pith (001c; dated AD1678-2005). The core appeared to be close to the centre of the tree and using traditional pith estimate techniques it would appear that this core was perhaps close to the date that the tree started to grow. However the $\delta^{13}C$ of tree core 001c does not show depleted values close to the 'pith' and, in fact, follows the same pattern as the other trees.

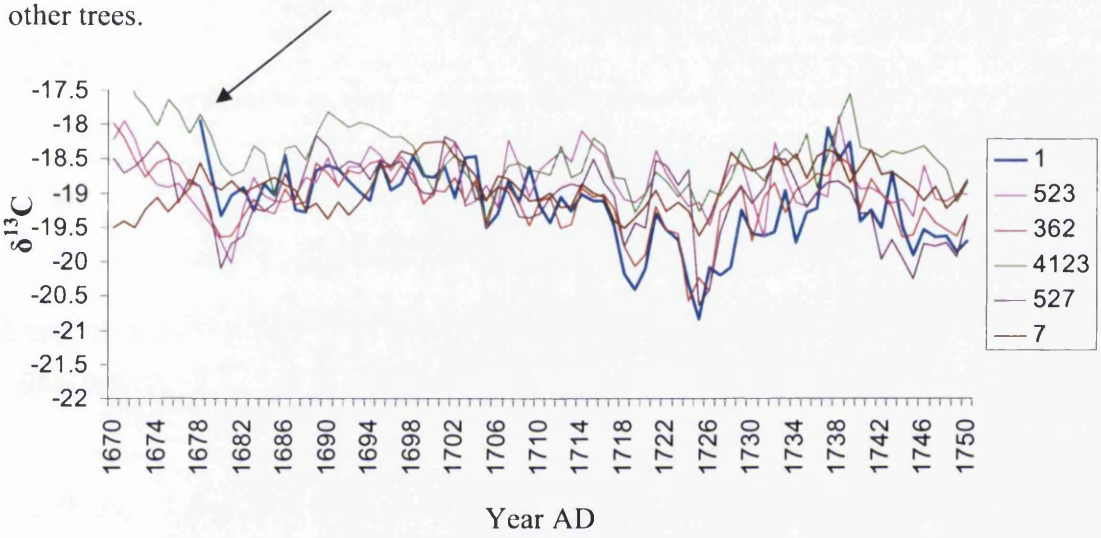

Figure 8.2 Blanco all trees $\delta^{13}C$ AD1670-1750.This figure shows all trees $\delta^{13}C$ from AD1670-1750. Tree 001 is the blue line that starts at AD1678.

The $\delta^{13}C$ isotope data was divided into two parts for the purpose of calibration/validation with instrumental climate data (RE/CE statistics). Both individual station and regional instrumental data were examined and the longest instrumental data that correlated best with the isotopes (regional sub division data for Nevada climate division 3 from 1895-2005). The reason that the Nevada instrumental data correlates best may be due to continental and Gulf influence dominating over Pacific influence during the summer months. Powell and Klieforth (1991), in their synopsis of weather in the White-Inyo Range state that although pacific influence dominates the Sierra, and to a lesser degree the White Mountains for most of the year, during the summer, and particularly July, continental influence

often dominates, bringing intense storms with high rainfall to the White mountains, sited as they are, at the centre of two competing weather fronts.

The summer temperature/isotope relationships seem as good as the summer precipitation /isotope relationships for the shorter instrumental weather data, as in the examples below from using PIN corrected data and Bishop meteorological data.

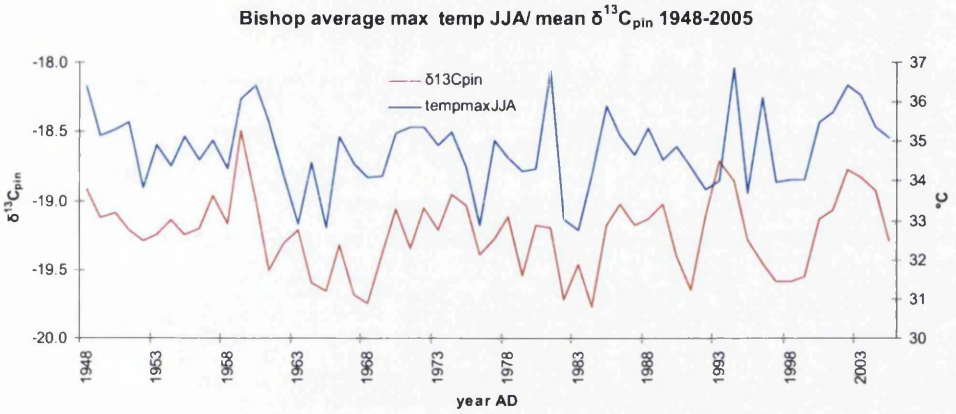

Copy of figure 5.5 Mean $\delta^{13}C_{pin}$ and Bishop average maximum JJA temperature 1948-2005 (r=0.55).

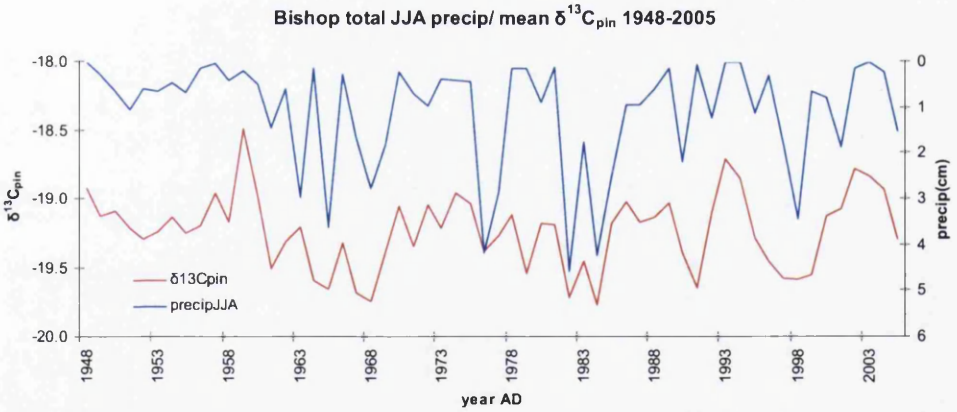

Copy of figure 5.6 Total summer (JJA) precipitation (Bishop) and mean $\delta^{13}C_{pin.}$ (r=.-0.58)

The high frequency (annual) $\delta^{13}C$ correlations with climate are strongest with precipitation. Temperature also seems to correlate well with $\delta^{13}C$ and correlations over 0.7 are evident if the data is smoothed to a three or five year centred mean. The temperature relationship appears strongest for the period 1895-1949 using four of

the seven trees, and using this period as a calibration period seems to work quite well in predicting reconstructed values for the period 1950-2005 (figure5.24). RE and CE values are positive when using the first period for reconstruction (figure 5.24)

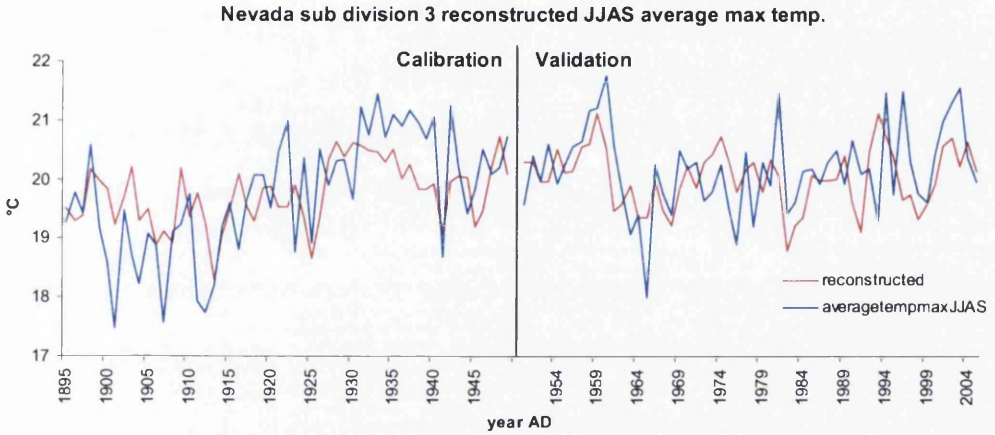

Copy of figure 5.24.Calibration based on the relationship between temperature and three –four tree $\delta^{13}C_{pin}$ relationship for the period 1895-1949 (r^2=0.29).

However, calibrating using the period 1950-2005 (figure 5.39) is not as effective as using the period 1895-1949 (figure 5.24). This may be due to the low temperatures evident in the late 19th/early 20th century.

The RE values using the period 1950-2005 are still positive but the CE value is 0, suggesting it may not be so suitable for reconstruction (National Research Council, 2006). Using all trees $\delta^{13}C_{pin}$ compared to temperature produces similar looking results but with lower correlations, more error and negative CE values. The reason three to four trees are used for temperature reconstruction is that these trees have the highest correlation with temperature.

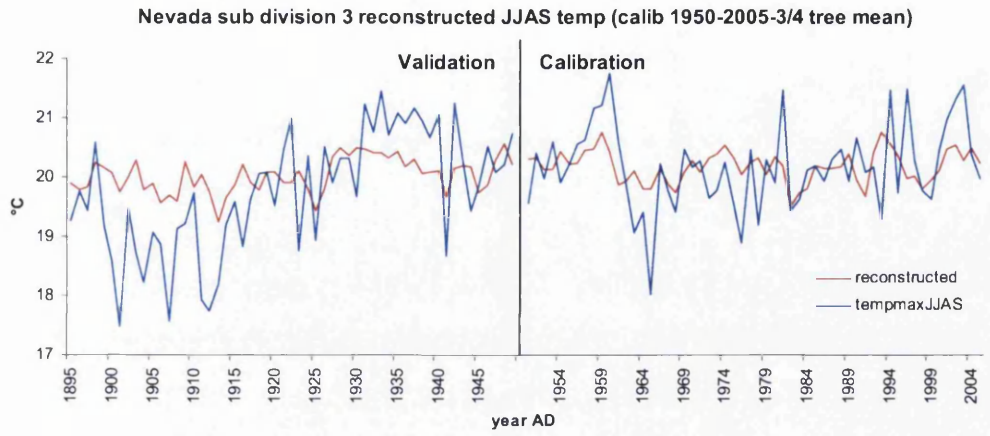

Copy of figure 5.39: Calibration based on the relationship between temperature and three to four tree $\delta^{13}C_{pin}$ relationship for the period 1950-2005

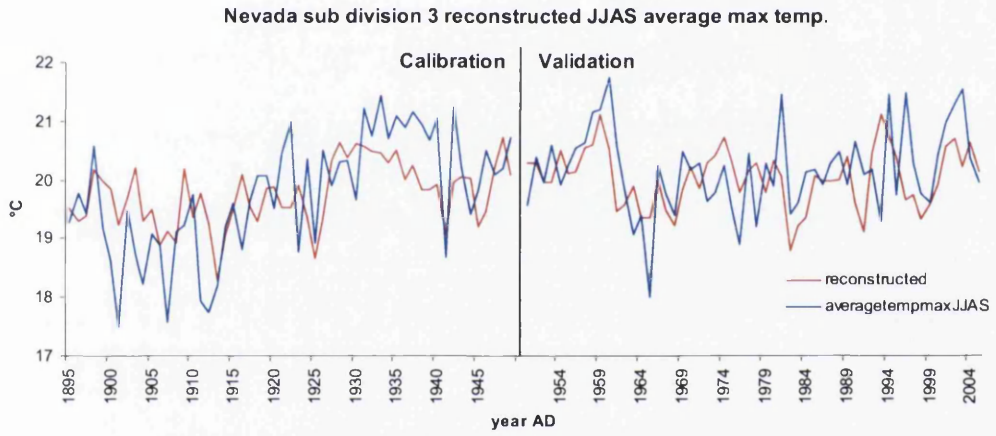

Copy of figure 5.36. Calibration based on the relationship between temperature and three to four tree $\delta^{13}C_{pin}$ relationship for the period 1895-1949.

Below Copy of figure 5.52

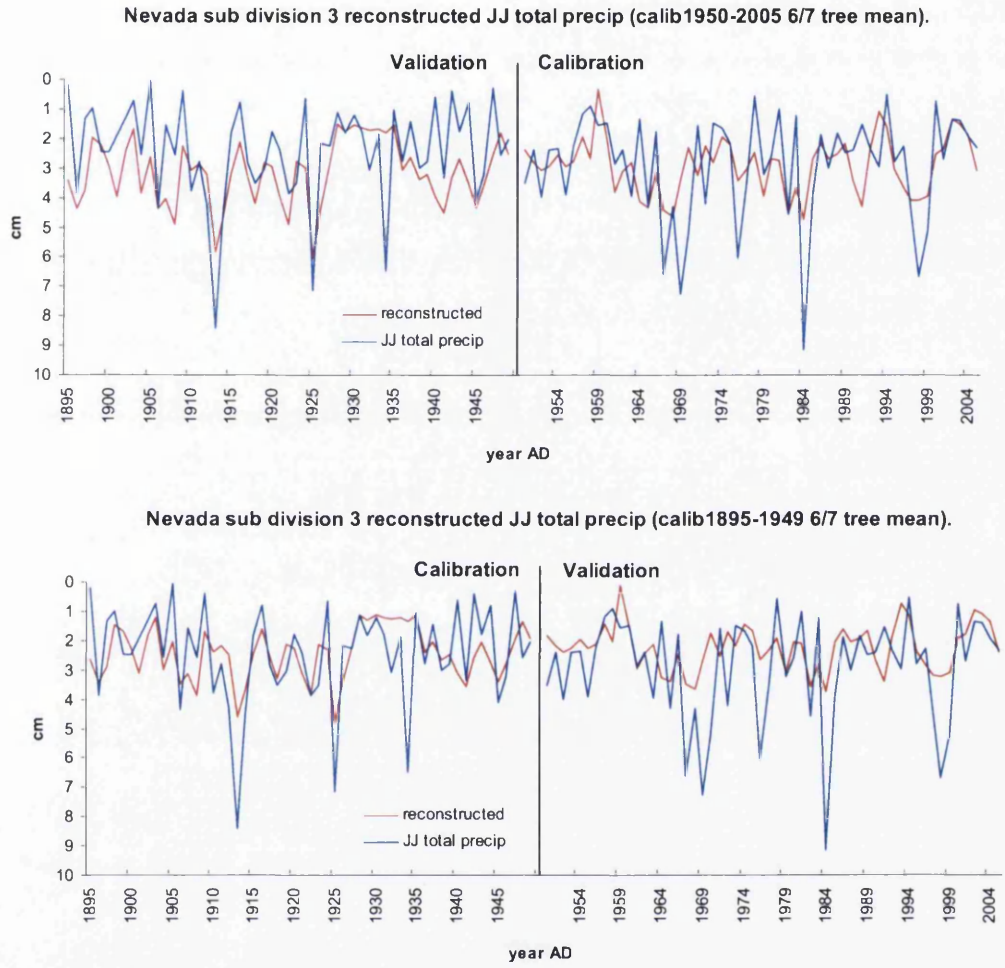

Above: Copy of figure 5.54.

With the precipitation data the calibration/validation works well for both halves of the data. As is seen, carbon isotopes reflect the annual changes in precipitation and the reconstruction may work better for precipitation. However, temperature also correlates with $\delta^{13}C$ and low frequency changes in $\delta^{13}C$ may be more related to temperature. In addition, individual trees seem more responsive to either temperature, precipitation or PDSI. Tree 362, for example, appears to be particularly temperature sensitive (figure 5.17).

Correlations are significant with precipitation using PIN and fossil fuel corrected data. Correlation with temperature is improved significantly by applying the PIN correction. Particularly after 1950, the fossil fuel corrected values show a significant decline that is hard to explain climatically and may be related to the trees reaction to increasing CO_2.

Originally the idea for this research was to use four trees of 1000 years each for isotopic analysis. The problems with this approach are that there are very narrow and some missing rings in the older trees, particularly in the all-important modern period. Using a variety of different aged trees has meant that more certainty can be placed in the calibration period and there is at least one tree (4123) that covers the last 550 years with no missing rings. The oldest trees used (527 and 007) were particularly difficult to cut for the modern period with very narrow rings.

Regarding the key question of 20th century warming and the 'hockey stick' shape of 20th century warming (Mann *et al.*, 1999; Jansen *et al.*, 2007), and its context in the climate of the last millennium, there is a significant rising trend in the $\delta^{13}C_{pin}$ corrected data for the period 1850-2005 (figure 4.23H). The fossil fuel corrected data displays no significant trend for the same period (figures 4.15H and 4.23H). The $\delta^{13}C_{raw}$ data displays a strong significant trend toward increasingly depleted values, with $\delta^{13}C_{raw}$ values for the 20th century more depleted than at any other time in the last 1000 years.

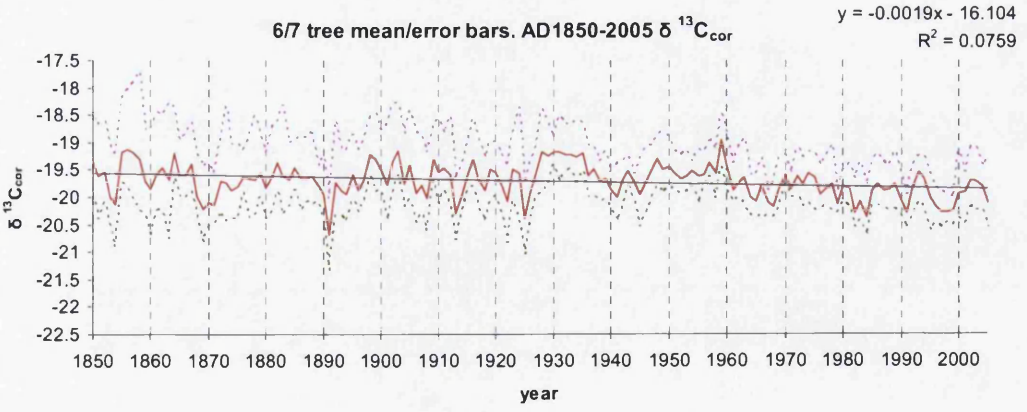

Copy of figure 4.15H (page119): fossil fuel corrected mean data AD1850-2005

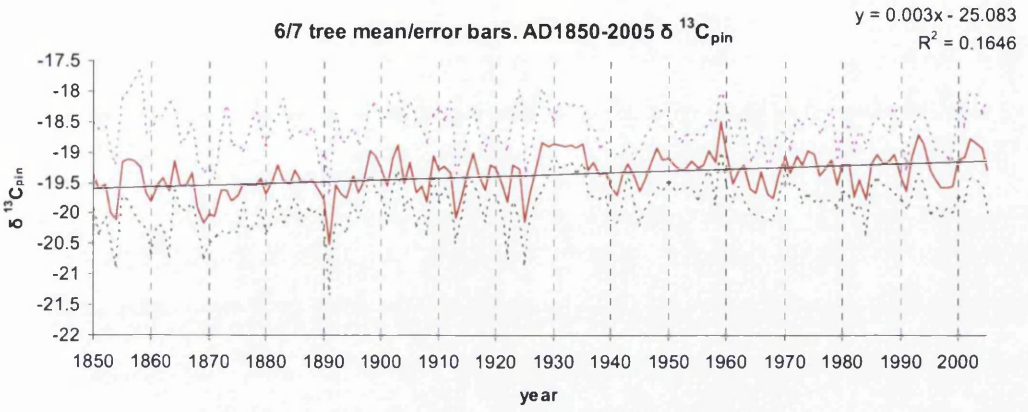

Copy of figure 4.23H (page129): mean PIN corrected data AD1850-2005

The longest regional instrumental climate data suggests a similar warming trend over the period from 1895-2005. As a whole 150 year period, 1850-2005 sees the most significant increase in isotope values compared to previous 150 year periods. This is however a bit misleading as there does appear to have been hotter/drier periods in the past. The late 16th and late 17th century appear as significantly warmer or drier than the present. There are several possible explanations. Temperatures in the past have been hotter in this region in the past than they are today, although recent warming in the last 150 years is evidenced in the $\delta^{13}C_{pin}$. There may have been a change in the way trees are reacting to increased CO_2 over the last 150 years and that the $\delta^{13}C$/temperature relationship is different in the modern period to the $\delta^{13}C$/temperature relationship in the past. An example of this would be that the hotter/drier periods of the late 16th and late 17th century are a reflection of extreme drought rather than extreme heat. Although drought and heat often occur together it is not always the case and extreme positive $\delta^{13}C$ may at times be reflecting cold dry conditions during summer. The relative influence of temperature/precipitation on $\delta^{13}C$ isotopes may have changed over time. This may be particularly important to the 20th century isotope values, where increased CO_2 may be leading to increased water use efficiency in trees. Just looking at $\delta^{13}C$ alone may not be enough to determine unusual weather or climate episodes such as cold/dry or warm/wet. There are periods in the $\delta^{13}C$ chronology where inter tree correlation (EPS) over the whole of

the last millennium is quite low, well below the threshold value of 0.85 (figure 8.3). Further analysis of ring widths may help further understanding of whether the climate has been cold/dry, cold/wet or warm/dry, warm/wet. Analysis of stable oxygen isotopes may also help address this question, in addition to providing information about source water and how precipitation patterns of the 20th century compare to previous centuries. Further analysis of $\delta^{18}O$ would be extremely useful as part of future bristlecone pine research.

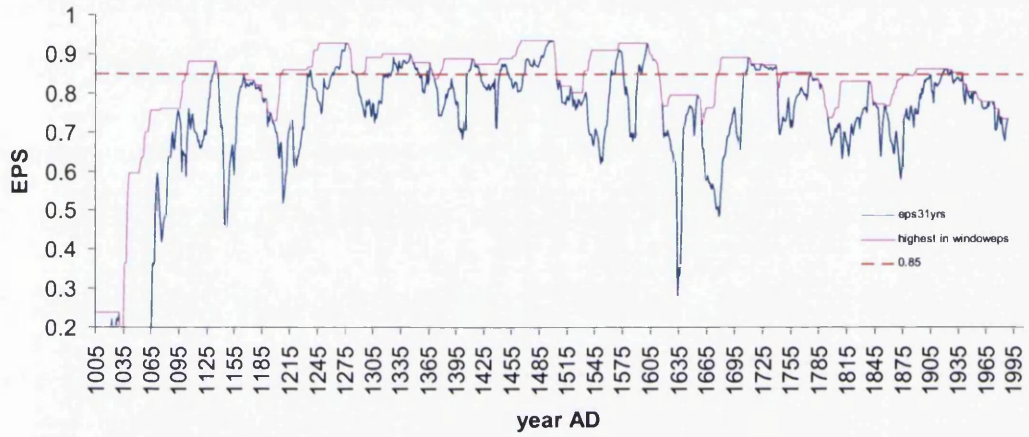

Figure 8.3: Measure of inter tree correlation (EPS) over the millennial $\delta^{13}C$ series AD1005-2005. Inter tree correlation (EPS) over moving 31 year increments is shown in blue. The pink line shows the highest EPS value in any given moving 31 year window. The red dashed line indicates EPS level of 0.85.

.

The simplest explanation for the 20th century not appearing as hot/dry as periods in the past, and also the explanation based on the climate correlations, would be that the $\delta^{13}C$ values are providing a good representation of summer precipitation/temperature and that there have been warmer and/or drier periods in this part of North America in the last 1000 years than the last 150 years.

References.

Adams, J. B., Mann, M. E., and Ammann, M. (2003). Proxy evidence for an El Niño-like response to volcanic forcing. *Nature* **426,** 274-278.

Anderson, W. T., Bernasconi, S. M., McKenzie, J. A., and Saurer, M. (1998). Oxygen and carbon isotopic record of climatic variability in tree ring cellulose (*Picea abies*): an example from central Switzerland (1913-1995). *J. of Geophysical Research* **103,** 625-31,636.

Baillie, M. (1995). "A slice through time- dendrochronology and precision dating." London.

Barbour, M. M., Walcroft, A. S., and Farquhar, G. D. (2002). Seasonal variation in $\delta^{13}C$ and $\delta^{18}O$ of cellulose from growth rings of *Pinus radiata. Plant, Cell and Environment.* **25,** 1483-1499.

Bascome, E. (1848). "A history of epidemic pestilences from the earliest ages, 1495 Years before the birth of our saviour to 1848 with researches into their causes and prophylaxis." John Churchill, London.

Beasley, R. S., and Klemmedson, J. O. (1980). Ecological Relationships of Bristlecone Pine. *American Midland Naturalist* **104,** 242-252.

Becker, B. (1993). A 11000 year oak and pine chronology for radiocarbon calibration. *Radiocarbon* **35,** 201-213.

Bert, D., Leavitt, S. W., and Dupouey, J.-L. (1997). Variations of wood $\delta^{13}C$ and water-use efficiency of Abies alba during the last century. *Ecology* **78,** 1588-1596.

Borella, S., Leuenberger, M., Saurer, M., and Siegwolf, R. (1998). Reducing uncertainties in $\delta^{13}C$ analysis of tree rings: pooling, milling, and cellulose extraction. *Journal of Geophysical Research* **103,** 19519-19526.

Boswijk, G., Fowler, A., Lorrey, A., Palmer, J., and Ogden, J. (2006). Extension of the New Zealand kauri (Agathis australis) chronology to 1724 BC. *The Holocene* **16,** 188-199.

Briffa, K., Osborn, T. J., Schweingruber, F., Harris, I. C., Jones, P. D., Shiyatov, S. G., and Vaganov, E. A. (2001). Low-frequency temperature variations from

a northern tree ring density network. *Journal of Geophysical Research* **106,** 2929–2941.

Briffa, K., Schweingruber, F. H., Jones, P. D., Osborn, T. J., Shiyatov, S. G., and Vaganov, E. A. (1998). Reduced sensitivity of recent treegrowth to temperature at high northern latitudes. . *Nature* **391,** 678–682.

Briffa, K. R. (2000). Annual climate variability in the Holocene: interpreting the message of ancient trees. *Quaternary Science Reviews* **19,** 87-105.

Briffa, K. R., Osborn, T. J., and Schweingruber, F. H. (2004). Large-scale temperature inferences from tree rings: a review. *Global Planet. Change* **40,** 11–26.

Brown, P. M. (1996). OLDLIST: A database of maximum tree ages. *In* "Tree rings, environment, and humanity." (J. S. Dean, D. M. Meko, and T. W. Swetnam, Eds.), pp. 727-731. Department of Geosciences, The University of Arizona, Tucson.

Castello, A. F., and Shelton, M. L. (2004). Winter precipitation on the US pacific coast and El Niño–Southern Oscillation events. *International Journal of Climatology* **24,** 481–497.

Cernusak, L. A., Marshall, J. D., Comstock, J. P., and Balster, N. J. (2001). Carbon isotope discrimination in photosynthetic bark. *Oecologia* **128**

Chacón, G. Taos Mural Project. (http://en.wikipedia.org/wiki/Image:Cg-98-3.jpg) Date accessed: 25/09/2008.

Cook, E. R., Briffa, K. R., Meko, D. M., Graybill, A., and Funkhouser, G. (1995). The 'segment length curse' in long tree-ring chronology development for palaeoclimatic studies. *The Holocene* **5,** 229-237.

Cook, E. R., Buckley, B. M., Palmer, J. G., Fenwick, P., Peterson, M. J., Boswijk, G., and Fowler, A. (2006). Millennia-long tree-ring records from Tasmania and New Zealand: a basis for modelling climate variability and forcing, past, present and future. *Journal of Quaternary Science* **21,** 689-699.

Cook, E. R., Esper, J., and D'Arrigo, R. D. (2004a). Extra-tropical Northern Hemisphere land temperature variability over the past 1000 years. *Quaternary Science Reviews* **23,** 2063–2074.

Cook, E. R., and Kairiukstis, L. A. (1990). Methods of Dendrochronology-applications in the environmental sciences. Kluwer Academic, Dordrecht.

Cook, E. R., Krusic, P. J., and Jones, P. D. (2003). Dendroclimatic signals in long tree ring chronologies from the Himalayas of Nepal. *International Journal of Climatology* **23,** 707-732.

Cook, E. R., Palmer, J. G., Cook, B. I., Hogg, A., and D'Arrigo, R. D. (2002). A multi-millennial palaeoclimatic resource from Lagarostrobos colensoi tree-rings at Oroko Swamp, New Zealand. *Global and Planetary Change* **33,** 209-220.

Cook, E. R., Woodhouse, C. A., Eakin, C. M., Meko, D. M., and Stahle, D. W. (2004b). Long-term aridity changes in the western United States. *Science* **306,** 1015-1018.

Craig, H. (1954). Carbon-13 variations in sequoia rings and the atmosphere. *Science* **119,** 141-143.

D'Arrigo, Wilson, R., and Jacoby, R. (2006). On the long-term context for late twentieth century warming. *J. Geophys. Res* **111**.

Dean, J. S. (1988). Dendrochronology and palaeoenvironmental reconstruction on the Colorado Plateaus. *In* "The Anasazi in a changing environment." (G. J. Gumerman, Ed.). Cambridge University Press, New York.

Diamond, J. (2005). Collapse- how societies choose to fail or survive. Allen Lane.

Drake, F (1628). The World Encompassed by Sir Francis Drake. (http://www.mcn.org/2/oseeler/climate.htm) date accessed: 29/09/2008

Dunwiddie, P., and LaMarche Jr, V. (1980). A climatically responsive tree-ring record from Widdringtonia cedarbergensis, Cape Province, South Africa. *Nature* **286,** 796–797.

Duquesnay, A., Breda, N., Stievenard, M., and Dupouey, J. L. (1998). Changes of tree-ring $\delta^{13}C$ and water-use efficiency of beech (*Fagus sylvatica* L.) in north-eastern France during the past century. *Plant, Cell and Environment* **21**.

Edwards, T. W. D. (1993). Interpreting past climate from stable isotopes in continental organic matter. *In* "Climate Change in Continental Isotopic

Records." (Swart P.K., K. C. Lohmann, J. McKenzie, and S. Savin, Eds.), pp. 333-341. American Geophysical Union, Washington, D.C.

Ehleringer, J. R., and Cerling, T., E. (1995). Atmospheric CO2 and the ratio of intercellular to ambient CO2 concentrations in plants *Tree Physiology* **15** 105–111.

Ehleringer, J. R., Hall, A. E., and Farquhar, G. D. (1993). Stable Isotopes and Plant Carbon- Water Relations. Academic, San Diego.

Elliot Fisk, D. L. (1991). Geomorphology. *In* "Natural History of the White/Inyo range." (C. A. Hall, Ed.), pp. 27-41. University of California, Berkeley.

Elliot Fisk, D. L., and Peterson, A. M. (1991). Trees. *In* "Natural history of the White-Inyo range." (J. Hall, C.A, Ed.), pp. 87-107. University of California, Los Angeles.

Epstein, S., and Krishnamurthy, R. V. (1990). Environmental information in the isotope record in trees. *Phil. Trans. R. Soc. Lond.*, 427-439.

Epstein, S., and Yapp, C. J. (1976). Climatic implications of the D/H ratios of hydrogen in C-H groups in tree cellulose. *Earth and Planetary Science Letters* **30,** 252.

Esper, J., Cook, E. R., and Schweingruber, F. H. (2002). Low-frequency signals in long tree ring chronologies for reconstructing past temperature variability. *Science* **295,** 2250-2252.

Farmer, D. L. (1957). Some Grain Price Movements in Thirteenth century England. *The Economic History Review* **10,** 207-220.

Farmer, J. G., and Baxter, M. S. (1974). Atmospheric carbon dioxide levels as indicated by the stable isotope record in wood. *Nature* **247,** 273-275.

Farquhar, G. D., Ehleringer, J. R., and Hubick, K. T. (1989). Carbon isotope discrimination and photosynthesis. *Annual review of plant physiology and plant molecular biology* **40,** 503-537.

Farquhar, G. D., O'Leary, M. H., and Berry, J. A. (1982). On the relationship between carbon isotope discrimination and the intercellular carbon dioxide concentration in leaves. *Australian journal of plant physiology* **9,** 121-137.

Feng, X. (1998). Long-term ci/ca response of trees in western North America to atmospheric CO_2 concentration derived from carbon isotope chronologies. *Oecologia* **117,** 19-25.

Feng, X. (1999). Trends in intrinsic water-use efficiency of natural trees for the past 100-200 years: A response to atmospheric CO_2 concentration. *Geochimica et Cosmochimica Acta* **63,** 1891-1903.

Feng, X., and Epstein, S. (1994). Climatic implications of an 8000-year hydrogen isotope time series from bristlecone pine trees. *Science* **265,** 1079-1081.

Feng, X., and Epstein, S. (1995). Carbon isotopes of trees from arid environments and implications for reconstructing atmospheric CO2 concentration. *Geochimica et Cosmochimica Acta* **59,** 2599-2608.

Feng, X., and Epstein, S. (1996). Climatic trends from isotopic records of tree rings: The past 100-200 years. *Climatic Change* **33,** 551-562.

Ferguson, C. W. (1968). Bristlecone Pine:Science and Esthetics. *Science* **159,** 839-846.

Ferguson, C. W. (1979). Dendrochronology of bristlecone pine, Pinus longaeva. *Environment International* **2,** 209-214.

Ferguson, C. W., Schulman, E., and Fritts, H. C. (1962). WHITE MOUNTAINS MASTER CHRONOLOGY -5141 BC- AD 1962

Fitzhugh, W. W., and Ward, E. I. (2000). Vikings: the North Atlantic Saga. Smithsonian Institution Press in association with the National Museum of Natural History, 2000, Washington

Francey, R. J., Allison, C. E., Etheridge, D. M., Trudinger, C. M., Enting, I. G., Leuenberger, M., Langenfelds, R. L., Michel, E., and Steele, L. P. (1999). A 1000-year high precision record of d13C in atmospheric CO_2. *Tellus* **51B,** 170-193.

Francey, R. J., and Farquhar, G. D. (1982). An explanation of $^{13}C/^{12}C$ variations in tree rings. *Nature* **297,** 28-31.

Freidli, H., Lotsher, H., Oeschger, H., and Siegenthaler, U. (1986). Ice core record of $^{13}C/^{12}C$ ratio of atmospheric CO_2 in the past two centuries. *Nature* **324,** 327-328.

Freyer, H. D. (1981). Recent $^{13}C/^{12}C$ trends in atmospheric CO_2 and tree rings. *Nature* **293,** 679-680.

Friedrich, M., Remmele, S., Kromer, B.,Hofmann,J., Spurk,M Kaiser, K.F., Orcel,C., Küppers,M (2004) The 12,460-Year Hohenheim oak and pine tree-ring chronology from central Europe—A unique annual record for radiocarbon calibration and palaeoenvironment reconstructions. *Radiocarbon*, **46**,3,1111–1122.

Fritts, H. (1969). "Bristlecone pine in the White Mountains of California: Growth and ring width characteristics." University of Tucson, Arizona.

Fritts, H. (1976). "Tree rings and climate." Academic press, New York.

Gagen, M., McCarroll, D., and Edouard, J. L. (2004). The effect of site conditions on pine tree ring width, density and $\delta^{13}C$ series in a dry sub-Alpine environment. *Arctic, Antarctic, and Alpine Research* **36.**

Gagen M, McCarroll D, Loader N J, Robertson I, Jalkanen R and Anchukaitis K J. (2007).Exorcising the 'segment length curse': summer temperature reconstruction since AD 1640 using non-detrended stable carbon isotope ratios from pine trees in northern Finland. The Holocene **17**(4), 435-446,

Glock, W. S. (1951). Cambial frost injuries and multiple growth layers at Lubbock, Texas. *Ecology* **32,** 28-36.

Graves, M. W., Longacre, W. A., and Holbrook, S. J. (1982). Aggregation and abandonment at Grasshopper Pueblo, Arizona. *Journal of Field Archaeology* **9,** 193-206.

Graybill, D. A. (1980). Methuselah Walk California Great Basin Bristlecone pine 2805M. -6000BC AD1979

Green, J. W. (1963). Wood cellulose. *In* "Methods in carbohydrate chemistry III." (R. L. Whistler, Ed.). Academic press, New York.

Grinsted, M. J., Wilson, A. T., and Ferguson, C. W. (1979). $^{13}C/^{12}C$ ratio variations in Pinus longaeva (bristlecone pine) cellulose during the last millennium. *Earth and Planetary Science Letters* **42,** 251-253.

Grissino-Mayer, H.D., (2001). Evaluating crossdating accuracy: a manual and tutorial for the computer program COFECHA. Tree-ring research **57**, 205-21.

Grudd, H., Briffa, K., Karlen, W., Bartholin, T. S., Jones, P. D., and Kromer, B. (2002). A 7400-year tree-ring chronology in northern Swedish Lapland: natural climatic variability expressed on annual to millennial timescales. *The Holocene* **12,** 657-665.

Guiot, J., Nicault, A., Rathberger, C., Edouard, J.L., Guibal, F., Pichard, G., Till, C. (2005). Last-millennium summer-temperature variations in Western Europe based on proxy data *The Holocene* **15,** 489–500.

Hantemirov, R. M., Gorlanova, L. A., and Shiyatov, S. G. (2004). Extreme temperature events in summer in northwest Siberia since AD742 inferred from tree rings. *Palaeogeography, Palaeoclimatology, Palaeoecology* **209,** 155-164.

Hantemirov, R. M., and Shiyatov, S. G. (2002). A continuous multimillennial ring-width chronology in Yamal, northwestern Siberia. *The Holocene* **12,** 717-726.

Hays, G., Imbrie, J., and Shackleton, N. J. (1976). Variations in the earth's orbit: Pacemaker of the ice ages. *Science* **194,** 1121-1132.

Helle, G., and Schleser, G. H. (2004). Beyond CO_2-fixation by Rubisco – an interpretation of $^{13}C/^{12}C$ variations in tree rings from novel intra-seasonal studies on broad-leaf trees. *Plant, Cell and Environment* **27,** 367–380.

Hendy, E. J., Gagan, M. K., Alibert, C. A., McCulloch, M. T., Lough, J. M., and Isdale, P. J. (2002). Abrupt decrease in tropical Pacific sea surface salinity at end of Little Ice Age. *Science* **295,** 1511-1514.

Hill, S. A., Waterhouse, J. S., Field, E. M., Switsur, V. R., and ap Rees, T. (1995). Rapid recycling of triose phosphates in oak stem tissue. *Plant, Cell and Environment* **18,** 931–936.

Holmes, R.L., (1983). Computer-assisted quality control in tree-ring dating and measurement. Tree-ring bulletin **43,** 69-78.

http://www.cdc.noaa.gov/cgi-bin/Timeseries/timeseries1.pl.
Date accessed: 10/5/2007

http://www.cpc.noaa.gov/products/analysis_monitoring/regional_monitoring/CLIM_DIVS/nevada.gif.

Date accessed: 10/5/2007

http://www.wrcc.dri.edu/summary/Climsmnv.html.

Date accessed: 10/5/2007

Hughes, M. K., and Funkhouser, G. (1998). Extremes of moisture availability reconstructed from tree rings for recent millennia in the Great Basin of Western North America. *In* "The Impacts of Climate Variability on Forests." (M. Beniston, and J. Innes, Eds.), pp. 99-107. Springer, Berlin.

Hughes, M. K., and Graumlich, L. (1998). Multimillennial dendroclimatic studies from the western United States. *In* "Climatic variations and forcing mechanisms of the last 2000 years." (P. D. Jones, R. S. Bradley, and J. Jouzel, Eds.), pp. 109-124. NATO ASI. Spriger Verlag, Berlin Heidlberg.

Hultine, K. R., and Marshall, J. D. (2000). Altitude trends in conifer leaf morphology and stable carbon isotope composition. *Oecologia* **123,** 32-40.

Imbrie, J., Hays, J. D., Martinson, D. G., McIntyre, A., Mix, A. C., Morley, J. J., Pisias, N. G., Prell, W. L., and Shackleton, N. J. (1984). The orbital theory of Pleistocene climate:support from a revised chronology of the marine $\delta\ ^{18}O$ record. *In* "Milankovitch and climate." (A. Berger, J. Imbrie, G. Hays, G. Kukla, and B. Saltzman, Eds.), pp. 269-306. Reidel, Dordrecht.

Jansen, E. J., Overpeck, K. R., Briffa, K., Duplessy, J. C., Joos, F., Masson-Delmotte, V., Olago, D., Otto- Bliesner, B., Peltier, W. R., Rahmstorf, S., Ramesh, R., Raynaud, D., Rind, D., Solomina, O., Villalba, R., and Zhang, D. (2007). Palaeoclimate. *In* "Climate Change 2007: The Physical Science Basis. Contribution of Working Group 1 to the Fourth Assessment Report of the Intergovernmental Panel on Climate Change." (S. D. Solomon, D. Qin, M. Manning, Z. Chen, M. Marquis, K. B. Averyt, M. Tignor, and H. L. Miller, Eds.), pp. 434-497. Cambridge University Press, Cambridge.

Jones, P. D., Briffa, K. R., Barnett, T. P., and Tett, S. F. B. (1998). High-resolution palaeoclimatic records for the last millennium:interpretation, integration and

comparison with General Circulation Model control-run temperatures. *The Holocene* **8,** 455-471.

Keeling, C. D. (1979). The Suess effect: 13Carbon-14Carbon interrelations. *Environment International* **2,** 229-300.

Korner, C. (2003). Carbon limitations in trees. *Journal of Ecology* **91,** 4-17.

Kromer, B., and Spurk, M. (1998). Revision and Tentative Extension of the Tree-Ring Based 14C Calibration, 9200-11,855 Cal BP. *Radiocarbon* **40** 1117-1125.

Kuniholm, P. I., Kromer, B., Manning, S. W., Newton, M. W., Latini, C. E., and Bruce, M. J. (1996). Anatolian tree rings and the absolute chronology of the eastern Mediterranean, 2220-718 BC. *Nature* **381** 780- 783.

LaMarche, J., V.C. (1974). Paleoclimatic inferences from long tree-ring records. *Science* **183,** 1043-1048.

LaMarche, V. C. (1969). Environment in relation to age of bristlecone pine. *Ecology* **50,** 53-59.

LaMarche, V. C., and Hirschboeck, K. K. (1984). Frost rings in trees as records of major volcanic eruptions. *Nature* **307,** 121-126.

Lamb, H. H. (1995). "Climate, History and the modern world." Routledge, New York.

Lara, A., and Villalba, R. (1993). A 3620-year temperature record from Fitzroya cupressoides tree-rings in Southern South America *Science* **260** 1104-1106.

Lazear, G. D., and Harlan, T. P. (2001). Crossdate- a tool for tree ring dating.

Leavitt, S. W. (1993). Environmental information from $^{13}C/^{12}C$ ratios in wood. *In "Climate Change in Continental Isotopic Records."* (P. K. Swart, K. C. Lohmann, J. McKenzie, and S. Savin, Eds.), pp. 325-331. American Geophysical Union.

Leavitt, S. W. (1994). Major wet interval in White Mountains Medieval Warm Period evidenced in $\delta^{13}C$ of bristlecone pine tree rings. *Climatic Change* **26,** 299-307.

Leavitt, S. W., and Long, A. (1984). Sampling strategy for stable carbon isotope analysis for tree rings in pine. *Nature* **311,** 145- 147.

Leavitt, S. W., and Long, A. (1991). Seasonal stable-carbon isotope variability in tree-rings:possible paleoenvironmental signals. *Chemical Geology* **87,** 59-70.

Leavitt, S. W., and Long, A. (1992). Altitudinal Differences in $\delta^{13}C$ of Bristlecone Pine Tree Rings. *Naturwissenschaften* **79**. 178-180.

Leuenberger, M., Siegenthaler, U., Langway, C. C., and (1992). Carbon isotope composition of atmospheric CO2 during the last ice age from an Antarctic ice core. *Nature* **357** 488-490.

Loader, N. J. (1995). High resolution stable isotope analysis of tree-rings: implications of 'microdendroclimatology' for palaeoenvironmental research. *The Holocene* **5,** 457-460.

Loader, N. J., Robertson, I., Barker, A. C., Switsur, V. R., and Waterhouse, J. S. (1997). An improved technique for the batch processing of small wholewood samples to [alpha]-cellulose. *Chemical Geology* **136,** 313-317.

Loader N J, Santillo P M, Woodman-Ralph J P, Rolfe J E, Hall M A, Gagen M, Robertson I, Wilson R, Froyd C A and McCarroll D, Multiple stable isotopes from oak trees in southwestern Scotland and the potential for stable isotope dendroclimatology in maritime climatic regions. *Chemical Geology* **252**(1-2), 62-71.

Lowe, J. J., and Walker, M. J. C. (1997). "Reconstructing Quaternary Environments." Longman.

Luterbacher, J.,(2004). European seasonal and annual temperature variability, trends, and extremes since 1500. *Science* **303** 1499–1503.

Macfarlane, C., Warren, C., White, D., and Adams, M. (1999). A rapid and simple method for processing wood to crude cellulose for analysis of stable carbon isotopes in tree rings. *Tree Physiology* **19,** 831-835.

Manley, G., Central England temperatures: monthly means 1659 to 1973. *Quarterly Journal of the Royal Meteorological Society* 100, 389-405, 1974.

Mann, M. E., Bradley, R. S., and Hughes, M. K. (1999). Northern hemisphere temperatures during the past millennium: Inferences, uncertainties, and limitations. *Geophys. Res. Lett* **26,** 759–762.

Mann, M. E., and Jones, P. D. (2003). Global surface temperatures over the past two millennia. *Geophysical research letters* **30,** 51-54.

Mann, M. E., Rutherford, S., Wahl, E., and Ammann, C. (2005). Testing the fidelity of methods used in proxy-based reconstructions of past climate. *Journal of climate* **10**.

McCarroll, D., Gagen, M., Loader, N. J., Robertson, I., Anchukaitis, K., Los, S., Jalkanen, R., Kirchhefer, A., and Waterhouse, J. S. (In Press). Objective correction of tree ring stable carbon isotope chronologies for changes in the carbon dioxide content of the atmosphere

McCarroll, D., Jalkanen, S., Hicks, M., Tuovinen, M., Gagen, M., Pawellek, F., Eckstein, D., Schmitt, U., Autio, J., and Heikkenen, O. (2003). Multiproxy dendroclimatology: a pilot study in northern Finland. *Holocene* **13,** 820-838.

McCarroll, D., and Loader, N. J. (2004). Stable Isotopes in Tree Rings. *Quaternary Science Reviews* **23,** 771-801.

McCarroll, D., and Pawellek, F. (1998). Stable carbon isotope ratios of latewood cellulose in *Pinus sylvestris* from northern Finland: variability and signal-strength. *The Holocene* **8,** 675-684.

McCormick, P. M., Thomason, L. W., and Trepte, C. R. (1995). Atmospheric effects of the Mt Pinatubo eruption. *Nature* **373,** 399-404.

McDonald, G.M. (2003). Biogeography, Space, Time and Life. John Wiley and Sons.

McDowell, N., Phillips, N., Lunch, C., Bond, B. J., and Ryan, M. G. (2002). An investigation of hydraulic limitation and compensation in large, old Douglas-fir trees *Tree Physiology* **22** 763–774.

McIntyre, A., and McKitrick, R. (2003). Corrections to the Mann *et al.* (1998) proxy database and northern hemispheric average temperature series. *Energy Environ* **14,** 751–771.

McIntyre, S., and McKitrick, R. (2005a). The MandM critique of the MBH98 Northern Hemisphere climate index: Update and implications *Energy Environ.,* **T16,** 69–99.

McIntyre, S., and McKitrick, R. (2005b). Reply to comment by von Huybers on "Hockey sticks, principal components, and spurious significance". *Geophys. Res. Lett.*, **32**.

Moberg, A., Sonechkin, D. M., Holmgren, K., Datsenko, N. and Karlen, W. (2005). Highly variable northern hemisphere temperatures reconstructed from low- and high-resolution proxy data. *Nature* **433,** 613-617.

Monserud, R. A., and Marshall, J. D. (2001). Time-series analysis of d13C from tree rings. I. Time trends and autocorrelation *Tree Physiology* **21** 1087–1102.

Mooney, H. A., West, M., and Brayton, R. (1966). Field measurements of the metabolic responses of Bristlecone Pine and big Sagebrush in the White Mountains of California. *Botanical Gazzette* **127,** 105-113.

Muscheler, R. (2007). Solar activity during the last 1000 years inferred from radionuclide records. *Quaternary Science Reviews* **26** 82-97.

National Research Council (2006). Surface temperature reconstructions for the last 2000 years. National Research Council. (http://www.nap.edu/catalog/11676.html) Date accessed: 25/09/2008

Nelson, C. A., Hall, J. C. A., and Ernst, W. G. (1991). Geologic History of the White -Inyo Range. *In* "Natural History of the White/Inyo range." (C. A. Hall, Ed.), pp. 42-55. University of California, Berkeley.

Norström, E., Homgren, K., Mörth, C.M. (2005). Rainfall driven variations in

Oerlemans, J. (2005). Extracting a climate signal from 169 glacier records. *Science* **308,** 675–677.

Oldenborgh, G.J., van and G. Burgers (2005). Searching for decadal variations in ENSO precipitation teleconnections. *Geophysical Research Letters*. **32**, 15. (http://climexp.knmi.nl) Date accessed: 25/9/2008.

Oppenheimer, C. (2003). Climatic, environmental and human consequences of the largest known historic eruption: Tambora volcano (Indonesia) 1815. *Progress in Physical Geography* **27,** 230-259.

Petit, J. R., Jouzel, J., Raynaud, D., Barkov, N. I., Barnola, J.-M., Basile, I., Bender, M., Chappellaz, J., Davis, M., Delaygue, G., Delmotte, M., Kotlyakov, V. M., Legrand, M., Lipenkov, V. Y., Lorius, C., PEpin, L., Ritz, C., Saltzman,

E., and Stievenard, M. (1999). Climate and atmospheric history of the past 420,000 years from the Vostok ice core, Antarctica. *Nature* **399,** 429-436.

Pettersen, R. C. (1984). The chemical composition of wood. *In* "The chemistry of solid wood." (R. Rowell, Ed.), pp. 57-126. American chemical soiciety, Washington, D.C.

Pilcher, J. R., Baillie, M., Scmidt, B., and Becker, B. (1984). A 7272 year tree ring chronology for Western Europe. *Nature* **312,** 150-152.

Powell, D. R., and Klieforth, H. E. (1991). Weather and climate. *In* "Natural History of the White/Inyo range." (C. A. Hall, Ed.), pp. 3-27. University of California, Berkeley.

Raynaud, D., Barnola, J.-M., Chappellaz, J., Blunier, T., Indermuhle, A., and Stauffer, B. (2000). The ice record of greenhouse gases: a view in the context of future changes. *Quaternary Science Reviews* **19,** 9-17.

Rinne K T, Boettger T, Loader N J, Robertson I, Switsur V R and Waterhouse J S, On the purification of α-cellulose from resinous wood for stable isotope (H, C and O) analysis, *Chemical Geology* 222, 75-82, 2005.

Robertson, A., Overpeck, J., Rind, D., Mosley-Thompson, E., Zielinski, G., Lean, J., Koch, D., Penner, J., Tegen, I., and Healy, R. (2001). Hypothesized climate forcing time series for the last 500 years. *Journal of Geophysical Research* **106,** 14783–14803.

Robertson, I., Loader, N. J., McCarroll, D., Carter, A. H. C., Cheng, L., and Leavitt, S. W. (2004). $\delta^{13}C$ of tree-ring lignin as an indirect measure of climate change. *Water, Air and Soil Pollution:Focus* **4,** 531-544.

Robertson, I., Switsur, V. R., Carter, A. H. C., Barker, A. C., Waterhouse, J. S., Briffa, K. R., and Jones, P. D. (1997). Signal strength and climate relationships in $^{13}C/^{12}C$ ratios of tree ring cellulose from oak in east England. *Journal of Geophysical Research* **102,** 19507–19519.

Robertson I, Leavitt S, Loader N J and Buhay B, (2008) Progress in isotope dendroclimatology, *Chemical Geology* **252**(1-2), Ex1-4,.

Rutherford, S. (2005). Proxy-based Northern Hemisphere surface temperature reconstructions: Sensitivity to method, predictor network, target season, and target domain. *J. Clim* **2308–2329,** 13.

Ryan, M. G., and Yoder, B. J. (1997). Hydraulic limits to tree height and tree growth. *Bioscience* **47,** 235–242.

Salzer, M. W., and Hughes, M. K. (2007). Bristlecone pine tree rings and volcanic eruptions over the last 5000 yr. *Quaternary Research* **67,** 57-68.

Salzer, M. W., and Kipfmueller, K. F. (2005). Reconstruted temperature and precipitation from on a millennial timescale from tree rings in the southern Colorado Plateau, U.S.A. *Climatic Change* **70,** 465-487.

Saurer, M., Borella, S., Schweingruber, F., and Siegwolf, R. (1997). Stable carbon isotopes in tree rings of beech: climatic versus site-related influences. *Trees* **11,** 291–297.

Saurer, M., and Siegenthaler, U. (1989). $^{13}C/^{12}C$ ratios in tree rings are sensitive to relative humidity. *Dendrochronologia* **7,** 9-13.

Saurer, M., Siegenthaler, U., and Schweingruber, F. (1995). The climate–carbon isotope relationship in tree rings and the significance of site conditions. *Tellus* **47B,** 320–330.

Saurer, M., Siegwolf, R. T. W., and Schweingruber, F. (2004). Carbon isotope discrimination indicates improving water-use efficiency of trees in northern Eurasia over the last 100 years. *Global Change Biology* **10** 2109–2120.

Schleser, G. H., Helle, G., Lucke, A., and Vos, H. (1999). Isotope signals as climate proxies: the role of transfer functions in the study of terrestrial archives. *Quaternary Science Reviews* **18,** 927-943.

Schleser, G. H., and Jayasekera, R. (1985). $\delta^{13}C$ variations in leaves of a forest as an indication of reassimilated CO2 from the soil. *Oecologia* **65.**

Schulman, E. (1954). Longevity under adversity in conifers. *Science* **119,** 396-399.

Schulman, E. (1958). Bristlecone Pine, Oldest known Living Thing. *National Geographic Magazine* **113,** 355-372.

Schulze, B., Wirth, C., Linke, P., Brand, W. A., Kuhlmann, I., Horna, V., and Shulze, E. D. (2004). Laser ablation-combustion-GC-IRMS-a new method

for online analysis of intra-annual variation of $\delta^{13}C$ in tree rings. *Tree Physiology* **24,** 1193-1201.

Schulze, E. D., Mooney, H. A., and Dunn, E. L. (1967). WIntertime photosynthesis of Bristlecone Pine (Pinus Aristata) in the White Mountains of California. *Ecology* **48,** 1044-1047.

Scuderi, L. A. (1993). A 2000 year tree ring record of annual temperatures in the Sierra Nevada Mountains. *Science* **259,** 1433-1436.

Shwartz, D. W. (1957). Climate change and culture history in the Grand Canyon Region. *American Antiquity* **22,** 372-377.

Shweingruber, F. H. (1996). "Tree rings and environment dendroecology." Haupt, Vienna.

Soon, W., and Baliunas, S. (2003). Proxy climatic and environmental changes of the past 1000 years. *Climatic Research* **23,** 89–110.

Stahle, D. W., Fye, F. K., Cook, E. R., and Griffin, R. D. (2007). Tree ring reconstructed megadroughts over North America since A.D. 1300. *Climatic Change* **83,** 133-149.

Stokes, M. A., and Smiley, T. L. (1996). An introduction to tree-ring dating. University of Arizona press, Tucson.

Stuiver, M., and Braziunas, T. F. (1987). Tree cellulose $^{13}C/^{12}C$ isotope ratios and climatic change. *Nature* **328,** 58-60.

Switsur, V. R., and Waterhouse, J. S. (1998). Stable isotopes in tree ring cellulose. *In* "Stable Isotopes-intergration of biological, ecological and geochemical processes." (H. Griffiths, Ed.), pp. 303-321. Bios scientific.

Tang, K., Feng, X., and Ettle, G. J. (2000). The variations in δD of tree rings and the implications for climatic reconstruction. *Geochimica et Cosmochimica Acta* **64,** 1663-1673.

Tang, K., Feng, X., and Funkhouser, G. (1999). The $\delta^{13}C$ of tree rings in full-bark and strip-bark bristlecone pine trees in the White Mountains of California. *Global Change Biology* **5,** 33-40.

Tans, P., P, and Mook, W. G. (1980). Past atmospheric CO_2 levels and the $^{13}C/^{12}C$ ratios in tree rings. *Tellus* **32,** 268-283.

Thompson, L. G. (2000). A high-resolution millennial record of the South Asian Monsoon from Himalayan ice cores. *Science* **289,** 1916–1919.

Thorndycraft, V. L., Barriendos , M., Benito , G., Rico, M., and Casas, A. (2006). The catastrophic floods of AD 1617 in Catalonia (northeast Spain) and their climatic context. *Hydrological Sciences–Journal–des Sciences Hydrologiques, Special issue: Historical Hydrology* **51,** 899-912.

Treydte, K., Schleser, G. H., Schweingruber, F. H., and Winiger, M. (2001). The climatic significance of $\delta^{13}C$ in subalpine spruces (L. otschental, Swiss Alps).. *Tellus* **53B** 593–611.

Vogel, J. (1980). Fractionation of the carbon isotopes during photosynthesis I. *In* "Sitzungsberichte der Heidelberger Akademie der Wissenschaften." pp. 111–135. Springer-Verlag Berlin.

Wahl, E., and Ammann, C. (2007). Robustness of the Mann, Bradley,Hughes reconstruction of Northern Hemisphere surface temperatures:Examination of criticisms based on the nature and processing of proxy climate evidence. . *Climatic Change,(in press).*

Warren, C. R., McGrath, J. F., and Adams, M. A. (2001). Water availability and carbon isotope discrimination in conifers. *Oecologia* **127,** 476-486.

Weber, D. J. (1999). What Caused the Pueblo Revolt of 1680? St. Martin's Press, Bedford.

Wilson, A. T., and Grinsted, J. M. (1977). $^{12}C/^{13}C$ in cellulose and lignin as palaeothermometers. *Nature* **265,** 133-135.

Woodward, F. I., and Bazzaz, F. A. (1988). The responses of stomatal density to CO_2 partial pressure. *Journal of Experimental botany* **39,** 1771-1781.

Wright, R. D., and Mooney, H. A. (1965). Substrate orientated Distribution of Bristlecone Pine in the White Mountains of California. *American Midland Naturalist* **73,** 257-284.

Yapp, C. J., and Epstein, S. (1982). Climatic significance of the hydrogen isotope ratios in tree cellulose. *Nature* **297,** 636-639.

Zielinski, G. A. (2000). Use of paleo-records in determining variability within the volcanism-climate system. *Quaternary Science Reviews* **19,** 417-438.

Appendix 1

year AD	001c $\delta^{13}C$	523b $\delta^{13}C$	362b $\delta^{13}C$	4123 $\delta^{13}C$	007 $\delta^{13}C$	527d $\delta^{13}C$	487e $\delta^{13}C$	mean $\delta^{13}C$
1005						-19.47		-19.47
1006						-19.48		-19.48
1007					-20.10	-19.98		-20.04
1008					-20.52	-20.26		-20.39
1009					-19.95	-19.97		-19.96
1010					-19.91	-20.01		-19.96
1011					-20.20	-20.38		-20.29
1012					-19.77	-19.98		-19.87
1013					-20.00	-19.22		-19.61
1014					-19.64	-19.36		-19.50
1015					-20.14	-20.01		-20.08
1016					-20.55	-20.00		-20.27
1017					-20.92	-19.53		-20.22
1018					-20.37	-19.42		-19.90
1019					-20.84	-20.23		-20.54
1020					-20.77	-19.57		-20.17
1021					-19.77	-18.75		-19.26
1022					-20.21	-19.08		-19.65
1023					-20.18	-19.16		-19.67
1024					-20.70	-18.74		-19.72
1025					-20.19	-19.04		-19.61
1026					-20.01	-19.12		-19.57
1027					-19.91	-19.30		-19.60
1028					-20.59	-18.63		-19.61
1029					-20.07	-19.13		-19.60
1030					-19.89	-19.26		-19.58
1031					-20.36	-20.26		-20.31
1032					-19.52	-20.00		-19.76
1033					-20.22	-19.13		-19.67
1034					-19.75	-19.26		-19.51
1035					-20.07	-19.33		-19.70
1036					-20.09	-19.08		-19.59
1037					-19.55	-19.13		-19.34
1038					-19.85	-19.11		-19.48
1039					-19.66	-19.70		-19.68
1040					-20.62	-19.47		-20.04
1041					-20.78	-19.15		-19.96
1042					-20.24	-19.61		-19.93
1043					-19.47	-19.29		-19.38
1044					-20.17	-19.63		-19.90
1045					-20.18	-19.48		-19.83
1046					-20.05	-19.26		-19.66
1047					-20.04	-19.41		-19.72
1048					-20.11	-19.84		-19.97
1049					-19.70	-19.61		-19.65
1050					-19.49	-20.85		-20.17
1051					-19.57	-19.75		-19.66
1052					-19.53	-18.57		-19.05
1053					-19.24	-19.84		-19.54

1054					-19.04	-19.88		-19.46
1055					-19.20	-19.68		-19.44
1056					-19.23	-19.26		-19.24
1057					-19.45	-19.34		-19.40
1058					-19.68	-19.58		-19.63
1059					-19.77	-19.50		-19.64
1060					-19.76	-19.33		-19.55
1061					-19.75	-19.58		-19.66
1062					-19.77	-19.84		-19.80
1063					-20.00	-19.28		-19.64
1064					-19.93	-19.50		-19.71
1065					-19.92	-19.65		-19.78
1066					-19.77	-19.26		-19.52
1067					-19.91	-19.03		-19.47
1068					-20.00	-18.83		-19.41
1069					-19.62	-19.19		-19.40
1070					-19.51	-18.89		-19.20
1071					-19.50	-18.56		-19.03
1072					-19.64	-18.54		-19.09
1073					-19.41	-19.46		-19.43
1074					-19.40	-19.20		-19.30
1075					-19.40	-19.08		-19.24
1076					-19.78	-19.03		-19.40
1077					-19.99	-19.56		-19.78
1078					-20.15	-19.71		-19.93
1079					-20.18	-19.88		-20.03
1080					-19.85	-20.57		-20.21
1081					-19.96	-20.24		-20.10
1082					-20.18	-20.15		-20.16
1083					-19.91	-19.92		-19.91
1084					-19.69	-21.08		-20.39
1085					-20.22	-19.85		-20.04
1086					-19.99	-19.79		-19.89
1087					-20.07	-20.40		-20.23
1088					-19.54	-19.66		-19.60
1089		-19.54			-19.42	-19.78		-19.58
1090		-19.98			-19.47	-19.99		-19.81
1091		-20.51			-19.70	-20.23		-20.15
1092		-19.34			-19.60	-20.25		-19.73
1093		-19.53			-20.01	-19.96		-19.83
1094		-19.71			-19.26	-19.41		-19.46
1095		-19.13			-19.30	-19.42		-19.28
1096		-18.81			-19.51	-19.35		-19.22
1097		-18.92			-19.35	-19.60		-19.29
1098		-19.03			-19.49	-19.06		-19.19
1099		-19.31			-19.19	-19.17		-19.22
1100		-18.87			-18.99	-19.25		-19.03
1101		-19.27			-19.16	-19.43		-19.29
1102		-18.91			-18.90	-19.39		-19.07
1103		-19.02			-19.31	-19.47		-19.27
1104		-19.13			-19.14	-19.10		-19.12

1105		-19.62			-19.99	-19.33		-19.65
1106		-19.28			-19.82	-20.34		-19.82
1107		-18.63			-19.70	-20.09		-19.47
1108		-18.65			-18.42	-19.29		-18.79
1109		-19.25			-19.34	-19.22		-19.27
1110		-19.18			-19.23	-18.88		-19.09
1111		-19.10			-19.34	-18.80		-19.08
1112		-19.77			-19.41	-19.26		-19.48
1113		-19.37			-19.66	-19.64		-19.56
1114		-20.11			-20.65	-19.32		-20.03
1115		-19.53			-19.95	-20.18		-19.89
1116		-19.28			-19.82	-19.68		-19.59
1117		-18.99			-19.41	-19.42		-19.27
1118		-19.22			-19.51	-19.74		-19.49
1119		-19.38			-19.98	-19.36		-19.57
1120		-20.13			-20.23	-19.97		-20.11
1121		-20.18			-20.03	-20.97		-20.39
1122		-19.62			-19.44	-21.46		-20.18
1123		-19.67			-19.24	-20.99		-19.97
1124		-20.02			-19.91	-21.00		-20.31
1125		-19.52			-19.53	-19.99		-19.68
1126		-18.99			-19.13	-20.24		-19.45
1127		-18.51			-19.28	-20.26		-19.35
1128		-19.38			-19.32	-19.86		-19.52
1129		-19.51			-19.81	-19.78		-19.70
1130		-19.34			-19.28	-19.89		-19.50
1131		-18.43			-18.67	-19.83		-18.98
1132		-18.75			-18.97	-19.62		-19.11
1133		-19.15			-18.56	-19.75		-19.15
1134		-18.97			-18.39	-19.38		-18.92
1135		-18.87			-18.63	-19.72		-19.07
1136		-19.28			-18.51	-19.27		-19.02
1137		-19.15			-18.68	-19.66		-19.16
1138		-19.16			-18.87	-19.77		-19.27
1139		-18.79			-18.93	-19.26		-18.99
1140		-18.22			-18.51	-19.78		-18.84
1141		-18.46			-18.39	-18.79		-18.54
1142		-18.70			-18.94	-18.68		-18.77
1143		-18.77			-18.75	-18.53		-18.68
1144		-18.05			-18.52	-19.51		-18.69
1145		-18.21			-18.35	-19.30		-18.62
1146		-18.11			-18.96	-18.32		-18.46
1147		-18.34			-18.22	-18.75		-18.44
1148		-18.73			-18.99	-18.72		-18.81
1149		-18.84			-18.64	-18.75		-18.74
1150		-18.00			-18.34	-18.93		-18.42
1151		-18.20			-18.27	-18.89		-18.45
1152		-17.86			-18.06	-18.46		-18.13
1153		-18.78			-18.79	-18.65		-18.74
1154		-18.81			-18.86	-18.77		-18.82
1155		-18.75			-18.64	-19.25		-18.88

1156		-18.54			-19.06	-18.98		-18.86
1157		-18.65			-19.37	-19.19		-19.07
1158		-18.72			-19.12	-19.02		-18.95
1159		-18.24			-18.70	-19.30		-18.75
1160		-18.07			-18.85	-18.88		-18.60
1161		-18.18			-18.79	-18.65		-18.54
1162		-18.73			-19.05	-19.33		-19.04
1163		-18.66			-18.98	-18.75		-18.80
1164		-19.11			-19.31	-19.69		-19.37
1165		-19.19			-19.06	-19.54		-19.26
1166		-19.32			-19.32	-19.12		-19.26
1167		-18.45			-18.93	-18.46		-18.61
1168		-18.69			-19.06	-19.58		-19.11
1169		-18.65			-19.59	-18.91		-19.05
1170		-18.71			-18.10	-18.93		-18.58
1171		-18.91			-19.22	-19.29		-19.14
1172		-18.81			-19.05	-20.01		-19.29
1173		-19.17			-19.78	-20.55		-19.84
1174		-18.66			-19.31	-19.71		-19.23
1175		-18.75			-19.37	-19.52		-19.21
1176		-18.75			-18.82	-19.14		-18.90
1177		-18.97			-19.73	-19.59		-19.43
1178		-19.04			-19.21	-19.63		-19.29
1179		-19.46			-19.08	-19.78		-19.44
1180		-19.09			-19.30	-20.36		-19.58
1181		-19.57			-19.73	-20.57		-19.96
1182		-19.32			-19.15	-20.08		-19.52
1183		-19.03			-19.87	-20.39		-19.76
1184		-19.13			-19.78	-20.16		-19.69
1185		-19.02			-19.18	-19.68		-19.29
1186		-19.28			-19.05	-19.80		-19.37
1187		-19.01			-19.36	-19.84		-19.40
1188		-19.05			-19.55	-20.07		-19.56
1189		-18.95			-19.26	-19.55		-19.25
1190		-19.11			-19.66	-19.71		-19.49
1191		-19.69			-19.85	-20.26		-19.93
1192		-19.71			-20.11	-20.55		-20.12
1193		-18.68			-19.28	-19.59		-19.18
1194		-18.89			-19.67	-19.56		-19.37
1195		-18.84			-19.15	-19.04		-19.01
1196		-19.17			-19.29	-19.36		-19.27
1197		-19.08			-19.42	-19.01		-19.17
1198		-18.77			-18.76	-19.19		-18.91
1199		-18.86			-18.73	-19.64		-19.08
1200		-18.74			-18.88	-19.77		-19.13
1201		-18.61			-19.05	-20.00		-19.22
1202		-18.79			-19.25	-20.02		-19.35
1203		-18.92			-19.98	-20.57		-19.82
1204		-19.31			-19.96	-20.71		-19.99
1205		-18.76			-19.43	-19.78		-19.32
1206		-19.14			-19.70	-20.50		-19.78

1207		-18.59			-19.81	-20.69		-19.69
1208		-18.59			-18.77	-19.75		-19.04
1209		-18.86			-19.76	-19.97		-19.53
1210		-18.87			-19.48	-19.72		-19.36
1211		-18.88			-19.10	-20.16		-19.38
1212		-19.06			-19.17	-19.70		-19.31
1213		-19.16			-19.68	-19.47		-19.44
1214		-18.63			-19.12	-19.92		-19.22
1215		-18.31			-19.18	-19.87		-19.12
1216		-18.51			-19.29	-19.86		-19.22
1217		-17.98			-18.62	-20.18		-18.93
1218		-18.26			-19.41	-20.57		-19.41
1219		-18.93			-19.67	-19.80		-19.46
1220		-18.49	-18.40		-18.90	-18.94		-18.68
1221		-18.51	-19.38		-19.17	-19.92		-19.24
1222		-18.56	-19.50		-19.37	-20.46		-19.47
1223		-18.82	-19.82		-19.35	-20.35		-19.58
1224		-18.41	-20.07		-19.05	-19.67		-19.30
1225		-18.89	-20.35		-19.37	-20.14		-19.69
1226		-18.58	-19.33		-18.75	-19.23		-18.97
1227		-18.08	-18.85		-18.88	-20.27		-19.02
1228		-18.05	-19.73		-18.92	-19.56		-19.07
1229		-17.97	-19.48		-19.19	-19.10		-18.93
1230		-18.37	-20.20		-19.04	-20.26		-19.47
1231		-18.15	-19.64		-19.23	-19.76		-19.20
1232		-18.33	-19.76		-19.01	-19.39		-19.12
1233		-18.66	-20.36		-19.54	-20.14		-19.67
1234		-18.21	-20.04		-19.10	-20.07		-19.35
1235		-18.63	-20.09		-19.38	-19.78		-19.47
1236		-18.34	-20.30		-19.78	-20.41		-19.71
1237		-19.18	-20.80		-20.16	-20.50		-20.16
1238		-18.39	-19.94		-19.29	-19.69		-19.33
1239		-18.90	-20.12		-19.52	-20.27		-19.70
1240		-18.38	-19.85		-19.28	-19.29		-19.20
1241		-19.10	-20.49		-19.85	-20.01		-19.86
1242		-18.66	-20.01		-19.04	-19.54		-19.31
1243		-18.52	-19.52		-19.34	-19.62		-19.25
1244		-18.61	-19.92		-19.21	-19.18		-19.23
1245		-18.24	-19.46		-19.14	-19.02		-18.96
1246		-18.31	-19.71		-19.39	-19.27		-19.17
1247		-19.26	-20.96		-20.06	-20.58		-20.22
1248		-18.73	-20.16		-19.52	-19.42		-19.46
1249		-18.46	-19.61		-19.04	-19.20		-19.08
1250		-18.88	-19.49		-19.33	-20.25		-19.49
1251		-18.59	-19.97		-19.12	-20.69		-19.59
1252		-18.30	-19.82		-18.80	-19.89		-19.20
1253		-17.94	-19.50		-18.83	-19.26		-18.88
1254		-17.85	-19.75		-18.73	-20.14		-19.12
1255		-17.54	-19.48		-19.02	-20.48		-19.13
1256		-18.29	-19.98		-19.33	-20.77		-19.59
1257		-18.51	-19.50		-18.87	-19.98		-19.22

1258		-17.95	-18.88		-18.43	-20.27		-18.88
1259		-17.85	-18.92		-18.14	-19.99		-18.73
1260		-18.66	-20.37		-18.70	-19.39		-19.28
1261		-18.48	-19.75		-18.96	-20.44		-19.41
1262		-18.90	-19.81		-19.13	-20.25		-19.52
1263		-18.75	-19.65		-19.14	-20.08		-19.41
1264		-18.85	-19.28		-18.73	-20.15		-19.25
1265		-18.97	-19.88		-19.37	-20.61		-19.71
1266		-19.34	-20.37		-19.73	-21.24		-20.17
1267		-19.90	-20.56		-19.91	-21.59		-20.49
1268		-19.24	-19.49		-19.26	-20.42		-19.60
1269		-18.40	-19.31		-19.11	-20.26		-19.27
1270		-18.58	-19.40		-18.78	-19.96		-19.18
1271		-18.49	-19.34		-18.69	-20.40		-19.23
1272		-18.56	-19.39		-19.01	-19.58		-19.13
1273		-18.82	-20.40		-19.33	-20.48		-19.76
1274		-18.91	-20.38		-19.44	-21.35		-20.02
1275		-19.24	-20.18		-19.24	-20.34		-19.75
1276		-18.29	-19.42		-18.80	-19.80		-19.08
1277		-18.81	-20.01		-19.01	-20.05		-19.47
1278		-18.72	-19.75		-19.11	-20.14		-19.43
1279		-18.86	-20.07		-18.84	-21.06		-19.71
1280		-18.71	-20.29		-19.17	-20.78		-19.74
1281		-18.71	-19.44		-18.76	-20.02		-19.23
1282		-18.64	-19.23		-18.87	-19.45		-19.05
1283		-18.79	-19.67		-19.02	-20.00		-19.37
1284		-18.80	-19.36		-19.01	-19.93		-19.27
1285		-18.40	-19.29		-18.38	-19.83		-18.98
1286		-18.30	-19.06		-18.23	-19.81		-18.85
1287		-18.23	-19.13		-18.25	-19.30		-18.73
1288		-18.21	-19.04		-18.28	-20.08		-18.90
1289		-18.42	-19.28		-18.68	-20.54		-19.23
1290		-18.95	-19.85		-19.18	-20.70		-19.67
1291		-19.02	-19.68		-19.09	-20.57		-19.59
1292		-18.43	-19.63		-18.65	-20.03		-19.19
1293		-18.89	-19.94		-19.10	-20.54		-19.62
1294		-18.82	-19.57		-18.78	-19.88		-19.26
1295		-19.46	-20.21		-18.85	-19.92		-19.61
1296		-18.48	-19.30		-18.94	-19.66		-19.10
1297		-19.21	-19.87		-19.34	-19.77		-19.55
1298		-18.60	-19.36		-18.74	-19.80		-19.12
1299		-18.84	-19.58		-19.07	-19.66		-19.29
1300		-18.80	-19.23		-18.56	-20.00		-19.15
1301		-18.56	-19.18		-19.03	-20.15		-19.23
1302		-18.79	-19.34		-18.96	-19.84		-19.23
1303		-18.84	-18.79		-18.62	-19.71		-18.99
1304		-18.64	-18.96		-18.77	-20.07		-19.11
1305		-18.46	-18.82		-18.74	-19.93		-18.99
1306		-18.54	-18.98		-18.89	-19.80		-19.05
1307		-19.09	-19.27		-19.14	-19.89		-19.35
1308		-19.00	-19.03		-19.09	-19.76		-19.22

1309		-19.18	-19.29		-19.41	-20.12		-19.50
1310		-19.00	-19.20		-19.49	-20.04		-19.43
1311		-18.87	-19.11		-19.01	-19.86		-19.21
1312		-18.95	-19.22		-19.20	-20.77		-19.53
1313		-19.44	-19.79		-19.39	-20.87		-19.87
1314		-19.43	-19.22		-19.29	-19.89		-19.46
1315		-18.83	-18.80		-18.53	-19.71		-18.97
1316		-18.59	-18.83		-18.49	-19.46		-18.84
1317		-18.83	-18.83		-18.93	-19.86		-19.11
1318		-18.93	-18.86		-18.97	-19.98		-19.18
1319		-18.85	-18.78		-18.94	-19.88		-19.11
1320		-18.50	-18.61		-18.81	-19.77		-18.92
1321		-18.49	-18.84		-18.74	-19.94		-19.00
1322		-18.70	-18.75		-18.70	-20.71		-19.21
1323		-18.89	-18.89		-18.79	-19.58		-19.04
1324		-18.86	-19.18		-18.86	-19.57		-19.12
1325		-18.26	-19.06		-18.65	-19.68		-18.91
1326		-18.71	-18.76		-19.00	-19.83		-19.07
1327		-18.68	-18.72		-18.92	-19.30		-18.90
1328		-18.50	-19.04		-18.99	-19.13		-18.92
1329		-18.75	-19.29		-18.92	-19.20		-19.04
1330		-18.83	-19.05		-18.44	-20.10		-19.10
1331		-19.18	-19.83		-19.19	-20.60		-19.70
1332		-19.52	-20.39		-19.42	-20.59		-19.98
1333		-18.73	-19.23		-18.80	-19.55		-19.08
1334		-18.89	-19.62		-19.02	-19.56		-19.27
1335		-18.30	-18.84		-18.51	-19.51		-18.79
1336		-18.70	-19.26		-18.94	-19.96		-19.21
1337		-18.43	-19.32		-19.04	-19.15		-18.98
1338		-18.48	-18.51		-18.57	-19.06		-18.65
1339		-18.54	-18.94		-18.80	-20.28		-19.14
1340		-18.81	-19.37		-18.80	-20.10		-19.27
1341		-19.27	-19.71		-19.04	-20.53		-19.64
1342		-19.08	-19.64		-18.88	-20.35		-19.49
1343		-19.52	-20.37		-19.51	-21.28		-20.17
1344		-19.38	-20.05		-19.08	-20.08		-19.65
1345		-18.86	-19.64		-18.64	-20.01		-19.28
1346		-19.18	-19.80		-18.72	-19.83		-19.38
1347		-18.92	-19.48		-18.77	-19.68		-19.21
1348		-19.03	-19.48		-18.67	-20.97		-19.54
1349		-19.71	-20.36		-19.43	-20.92		-20.11
1350		-19.10	-19.72		-18.31	-19.86		-19.25
1351		-19.13	-19.40		-18.73	-20.35		-19.40
1352		-19.01	-19.94		-19.03	-19.95		-19.48
1353		-18.83	-19.31		-18.99	-20.24		-19.34
1354		-19.50	-20.28		-19.46	-20.21		-19.86
1355		-18.66	-19.67		-18.70	-20.08		-19.28
1356		-18.96	-19.81		-19.56	-20.32		-19.66
1357		-18.86	-19.60		-19.13	-19.73		-19.33
1358		-18.77	-19.42		-19.01	-19.87		-19.27
1359		-18.78	-19.44		-18.83	-19.86		-19.23

1360		-18.40	-19.26		-18.31	-19.51		-18.87
1361		-18.06	-18.62		-17.59	-19.71		-18.49
1362		-18.38	-19.05		-18.76	-19.97		-19.04
1363		-18.76	-19.11		-18.90	-19.79		-19.14
1364		-18.46	-19.03		-19.19	-19.95		-19.16
1365		-18.72	-19.46		-19.33	-20.18		-19.42
1366		-18.85	-19.52		-19.56	-20.22		-19.54
1367		-19.03	-19.54		-19.39	-20.10		-19.51
1368		-18.90	-19.44		-19.14	-19.77		-19.31
1369		-18.65	-19.52		-18.60	-20.04		-19.20
1370		-18.98	-20.06		-19.56	-19.90		-19.62
1371		-18.83	-19.02		-19.42	-19.85		-19.28
1372		-18.97	-19.53		-18.84	-19.95		-19.32
1373		-18.72	-19.22		-18.79	-19.43		-19.04
1374		-18.49	-19.67		-19.08	-19.78		-19.26
1375		-19.02	-20.01		-19.37	-19.94		-19.58
1376		-18.71	-19.71		-18.66	-19.51		-19.15
1377		-18.60	-19.18		-18.53	-19.46		-18.94
1378		-18.31	-19.10		-18.78	-19.46		-18.91
1379		-18.48	-19.03		-18.77	-19.41		-18.92
1380		-18.74	-19.78		-18.89	-19.75		-19.29
1381		-18.97	-20.19		-18.83	-20.18		-19.54
1382		-19.23	-20.64		-19.72	-21.00		-20.15
1383		-18.82	-20.58		-18.79	-19.88		-19.52
1384		-18.77	-20.04		-18.73	-20.07		-19.40
1385		-18.84	-19.92		-18.56	-20.34		-19.41
1386		-18.99	-20.05		-19.06	-20.52		-19.66
1387		-18.69	-20.39		-18.69	-20.08		-19.46
1388		-18.57	-19.52		-18.61	-20.45		-19.29
1389		-18.49	-20.05		-18.52	-19.83		-19.22
1390		-18.47	-19.72		-18.68	-20.11		-19.25
1391		-18.81	-19.27		-19.17	-20.38		-19.41
1392		-18.91	-19.90		-18.84	-20.37		-19.51
1393		-19.00	-20.01		-19.03	-20.59		-19.66
1394		-18.97	-19.70		-19.04	-20.19		-19.48
1395		-18.34	-20.05		-18.59	-19.58		-19.14
1396		-18.54	-19.27		-18.64	-20.05		-19.13
1397		-18.57	-19.31		-18.98	-20.07		-19.23
1398		-18.53	-19.57		-18.82	-19.56		-19.12
1399		-18.63	-19.75		-18.19	-19.42		-19.00
1400		-18.45	-19.37		-17.97	-19.23		-18.76
1401		-18.78	-20.29		-19.10	-19.54		-19.43
1402		-18.76	-20.04		-18.68	-19.86		-19.34
1403		-18.69	-20.27		-19.00	-19.61		-19.39
1404		-18.54	-19.98		-18.68	-19.62		-19.21
1405		-19.21	-21.06		-19.02	-20.61		-19.97
1406		-19.03	-20.54		-18.79	-19.23		-19.39
1407		-18.37	-20.05		-18.33	-19.14		-18.97
1408		-18.62	-20.47		-19.11	-19.78		-19.50
1409		-19.05	-20.44		-18.77	-19.65		-19.48
1410		-18.62	-19.90		-18.98	-19.52		-19.25

1411		-18.97	-20.58		-19.20	-20.08		-19.71
1412		-18.87	-19.99		-18.73	-19.45		-19.26
1413		-18.72	-19.74		-18.36	-19.50		-19.08
1414		-18.93	-20.53		-19.14	-19.71		-19.58
1415		-18.73	-20.88		-18.80	-19.66		-19.52
1416		-18.69	-20.63		-18.96	-19.90		-19.54
1417		-18.40	-20.49		-18.81	-20.06		-19.44
1418		-19.07	-20.58		-19.07	-20.07		-19.70
1419		-19.25	-20.67		-19.05	-19.82		-19.70
1420		-18.51	-20.24		-18.58	-19.59		-19.23
1421		-18.44	-20.40		-19.11	-20.92		-19.72
1422		-19.71	-21.44		-19.96	-21.45		-20.64
1423		-18.82	-20.52		-18.66	-20.04		-19.51
1424		-18.79	-20.04		-18.57	-19.81		-19.30
1425		-18.84	-20.31		-18.70	-20.06		-19.48
1426		-18.57	-20.09		-18.54	-19.62		-19.20
1427		-18.84	-20.47		-18.96	-20.37		-19.66
1428		-19.34	-20.41		-19.09	-20.21		-19.76
1429		-19.35	-20.29		-19.41	-20.25		-19.83
1430		-19.13	-20.63		-19.00	-20.18		-19.74
1431		-19.24	-20.39		-18.77	-20.37		-19.69
1432		-19.06	-20.29		-18.90	-20.08		-19.58
1433		-19.30	-20.64		-18.99	-19.89		-19.70
1434		-19.46	-21.33		-19.06	-20.23		-20.02
1435		-18.92	-20.68		-19.09	-20.35		-19.76
1436		-18.49	-20.47		-18.39	-20.32		-19.42
1437		-18.62	-20.39		-18.31	-20.03		-19.34
1438		-18.94	-20.55		-18.70	-19.68		-19.47
1439		-18.86	-20.81		-18.73	-19.56		-19.49
1440		-19.15	-21.21		-18.78	-20.08		-19.80
1441		-18.93	-20.89		-18.68	-20.41		-19.73
1442		-18.98	-20.39		-18.80	-20.31		-19.62
1443		-18.53	-20.55		-18.53	-20.09		-19.42
1444		-18.64	-20.14		-18.34	-19.64		-19.19
1445		-18.29	-20.45		-18.59	-19.90		-19.31
1446		-19.20	-21.08		-18.83	-20.20		-19.83
1447		-19.27	-20.83		-18.46	-19.52		-19.52
1448		-18.96	-20.48		-18.52	-19.64		-19.40
1449		-18.88	-20.02		-18.39	-19.33		-19.15
1450		-18.74	-20.22		-18.75	-19.72		-19.36
1451		-19.13	-20.63		-18.71	-19.60		-19.52
1452		-18.65	-20.34		-18.39	-20.30		-19.42
1453		-18.91	-20.98	-20.15	-18.86	-20.16		-19.81
1454		-18.90	-20.72	-19.45	-18.43	-19.79		-19.46
1455		-18.29	-20.02	-19.63	-18.17	-19.09		-19.04
1456		-18.12	-19.58	-18.76	-18.21	-19.03		-18.74
1457		-18.17	-19.71	-18.81	-18.27	-19.49		-18.89
1458		-18.60	-19.78	-18.86	-18.10	-19.13		-18.89
1459		-18.97	-19.32	-18.95	-17.89	-19.11		-18.85
1460		-17.95	-19.42	-18.71	-18.15	-19.58		-18.76
1461		-18.76	-19.83	-18.87	-18.24	-19.83		-19.11

1462		-18.87	-20.45	-19.38	-18.79	-20.34		-19.56
1463		-19.35	-20.59	-19.69	-18.80	-20.25		-19.73
1464		-18.68	-20.81	-19.19	-18.70	-20.33		-19.54
1465		-19.94	-20.53	-19.69	-18.87	-20.76		-19.96
1466		-19.68	-19.91	-19.55	-18.72	-20.57		-19.69
1467		-19.04	-19.91	-19.35	-18.59	-20.39		-19.46
1468		-19.40	-19.68	-19.11	-18.62	-20.38		-19.44
1469		-19.14	-20.11	-19.59	-18.35	-20.28		-19.49
1470		-19.02	-19.77	-19.67	-18.57	-20.04		-19.42
1471		-19.42	-20.09	-19.62	-18.15	-20.22		-19.50
1472		-18.99	-19.28	-19.12	-18.21	-19.69		-19.06
1473		-18.57	-18.91	-18.94	-18.21	-19.40		-18.81
1474		-18.55	-19.04	-19.04	-18.23	-19.68		-18.91
1475		-18.31	-19.41	-18.63	-18.46	-19.70		-18.90
1476		-18.64	-19.88	-19.20	-18.96	-20.26		-19.39
1477		-18.96	-19.48	-19.53	-18.83	-20.21		-19.40
1478		-18.80	-19.33	-19.85	-18.59	-20.12		-19.34
1479		-19.30	-19.64	-19.22	-18.43	-19.60		-19.24
1480		-19.15	-19.86	-19.56	-18.96	-19.99		-19.50
1481		-18.61	-18.99	-19.07	-18.46	-19.30		-18.89
1482		-18.76	-18.88	-18.96	-18.24	-19.86		-18.94
1483		-19.07	-19.49	-19.35	-19.19	-20.65		-19.55
1484		-19.57	-19.58	-20.28	-19.03	-20.96		-19.88
1485		-19.06	-19.42	-19.62	-19.23	-20.91		-19.65
1486		-20.15	-20.04	-20.52	-19.47	-21.39		-20.32
1487		-20.11	-19.85	-20.29	-19.60	-21.02		-20.17
1488		-19.87	-19.69	-20.19	-19.29	-21.02		-20.01
1489		-19.49	-19.40	-19.78	-19.05	-20.48		-19.64
1490		-19.57	-19.41	-19.88	-19.04	-20.20		-19.62
1491		-19.10	-19.02	-19.56	-18.59	-20.48		-19.35
1492		-19.28	-18.42	-18.83	-18.67	-20.18		-19.08
1493		-19.43	-19.17	-19.82	-19.01	-20.15		-19.52
1494		-19.30	-19.01	-19.42	-19.07	-20.38		-19.44
1495		-19.23	-18.65	-19.23	-18.37	-20.07		-19.11
1496		-19.14	-18.65	-18.67	-18.69	-20.49		-19.13
1497		-18.86	-19.07	-18.89	-18.88	-20.29		-19.20
1498		-19.69	-18.82	-19.05	-18.76	-20.18		-19.30
1499		-19.35	-18.25	-18.44	-18.28	-20.03		-18.87
1500		-18.84	-18.57	-18.97	-18.50	-20.11		-19.00
1501		-19.08	-19.03	-19.18	-18.67	-20.40		-19.27
1502		-19.08	-18.97	-19.27	-18.46	-20.14		-19.18
1503		-19.08	-18.75	-19.33	-17.98	-19.95		-19.02
1504		-19.08	-18.71	-19.04	-18.12	-19.89		-18.97
1505		-18.20	-18.65	-18.61	-18.23	-19.76		-18.69
1506		-18.41	-18.57	-18.21	-17.99	-19.91		-18.62
1507		-19.03	-18.74	-19.05	-18.19	-19.94		-18.99
1508		-19.16	-19.28	-19.49	-18.71	-20.47		-19.42
1509		-19.42	-19.81	-19.68	-19.01	-20.87		-19.76
1510		-19.42	-19.65	-18.94	-18.81	-20.09		-19.38
1511		-18.66	-18.96	-19.18	-18.56	-19.98		-19.07
1512		-19.13	-18.96	-19.85	-18.34	-19.93		-19.24

1513		-19.46	-19.31	-18.91	-18.83	-20.37		-19.38
1514		-18.79	-18.83	-18.91	-18.09	-19.69		-18.86
1515		-19.00	-18.98	-18.85	-18.56	-19.89		-19.05
1516		-19.48	-19.12	-19.23	-18.53	-20.05		-19.28
1517		-19.63	-18.92	-19.19	-18.63	-20.16		-19.31
1518		-19.08	-18.82	-19.06	-18.65	-19.82		-19.09
1519		-19.12	-18.75	-19.01	-19.05	-19.76		-19.14
1520		-19.42	-18.92	-19.11	-18.71	-20.34		-19.30
1521		-18.65	-18.79	-19.04	-18.51	-19.89		-18.98
1522		-18.66	-18.52	-18.37	-18.41	-19.53		-18.70
1523		-18.80	-18.61	-18.61	-18.76	-19.72		-18.90
1524		-18.46	-18.52	-18.51	-18.70	-20.24		-18.88
1525		-18.34	-18.52	-18.68	-19.25	-20.03		-18.96
1526		-18.72	-19.19	-19.17	-19.31	-20.19		-19.32
1527		-19.02	-18.85	-19.02	-18.85	-19.49		-19.05
1528		-18.86	-19.43	-19.22	-18.83	-20.33		-19.33
1529		-18.50	-19.17	-18.73	-18.86	-19.98		-19.05
1530		-19.06	-19.47	-19.03	-18.93	-20.55		-19.41
1531		-19.04	-19.21	-19.16	-19.10	-20.18		-19.34
1532		-18.60	-19.05	-18.48	-19.09	-19.97		-19.04
1533		-19.49	-19.49	-18.71	-19.43	-20.33		-19.49
1534		-19.07	-19.58	-19.34	-19.28	-20.67		-19.59
1535		-19.39	-19.13	-19.15	-19.25	-20.40		-19.46
1536		-19.13	-19.37	-19.50	-19.26	-20.16		-19.48
1537		-19.08	-18.83	-19.18	-19.20	-19.78		-19.21
1538		-19.31	-19.39	-19.89	-19.26	-20.48		-19.67
1539		-19.09	-18.94	-19.99	-19.22	-20.39		-19.53
1540		-18.57	-18.53	-19.33	-18.57	-20.01		-19.00
1541		-18.66	-18.57	-18.37	-18.71	-20.16		-18.89
1542		-18.81	-18.94	-18.39	-19.13	-20.14		-19.08
1543		-18.94	-18.78	-18.43	-18.95	-19.89		-19.00
1544		-18.94	-18.38	-18.17	-18.96	-19.74		-18.84
1545		-19.14	-18.79	-18.31	-18.90	-20.47		-19.12
1546		-19.16	-19.19	-18.93	-18.92	-20.29		-19.30
1547		-19.21	-18.68	-18.88	-19.09	-19.97		-19.17
1548		-18.95	-18.88	-18.26	-18.87	-20.61		-19.11
1549		-19.17	-19.12	-19.38	-19.06	-20.93		-19.53
1550		-19.52	-19.26	-19.15	-19.03	-20.29		-19.45
1551		-18.61	-18.98	-19.22	-18.85	-20.39		-19.21
1552		-18.46	-19.19	-18.69	-18.93	-21.04		-19.26
1553		-18.89	-19.02	-19.49	-19.14	-19.42		-19.19
1554		-18.79	-18.89	-19.12	-19.03	-20.27		-19.22
1555		-18.74	-18.62	-18.87	-18.89	-19.92		-19.01
1556		-18.79	-19.53	-18.99	-19.27	-20.29		-19.37
1557		-18.72	-19.08	-18.88	-18.79	-20.65		-19.22
1558		-18.58	-19.23	-18.75	-19.23	-21.14		-19.39
1559		-18.47	-19.37	-18.78	-19.14	-20.95		-19.34
1560		-19.27	-19.38	-18.94	-19.46	-21.09		-19.63
1561		-19.24	-19.64	-18.89	-19.32	-21.08		-19.64
1562		-19.09	-19.57	-19.00	-18.93	-21.08		-19.53
1563		-18.46	-19.12	-18.69	-18.99	-20.52		-19.16

1564		-18.65	-19.43	-18.75	-19.10	-20.74		-19.34
1565		-18.44	-19.30	-18.76	-19.10	-20.61		-19.24
1566		-18.84	-19.89	-18.72	-19.08	-20.89		-19.48
1567		-18.90	-19.51	-18.56	-18.87	-20.82		-19.33
1568		-18.82	-19.07	-18.28	-18.58	-20.54		-19.06
1569		-18.73	-18.87	-18.38	-18.64	-19.97		-18.92
1570		-18.72	-18.69	-17.89	-18.62	-19.91		-18.77
1571		-18.93	-18.78	-18.08	-18.24	-20.20		-18.85
1572		-18.42	-18.75	-18.04	-18.27	-20.25		-18.75
1573		-18.81	-18.95	-18.09	-18.56	-20.47		-18.98
1574		-18.73	-18.98	-18.24	-18.60	-20.49		-19.01
1575		-18.41	-18.55	-17.99	-18.44	-20.23		-18.72
1576		-18.35	-18.61	-18.25	-18.46	-19.95		-18.72
1577		-18.26	-18.57	-18.45	-18.31	-20.25		-18.77
1578		-17.70	-18.18	-17.84	-18.36	-20.22		-18.46
1579		-18.35	-18.29	-17.17	-18.17	-20.26		-18.45
1580		-18.43	-18.67	-17.42	-18.77	-20.61		-18.78
1581		-18.45	-18.68	-17.63	-18.72	-20.71		-18.84
1582		-18.13	-18.53	-18.13	-18.87	-20.44		-18.82
1583		-18.10	-18.62	-17.90	-18.53	-20.34		-18.70
1584		-18.23	-18.96	-18.02	-18.88	-20.60		-18.94
1585		-18.36	-18.98	-18.32	-18.55	-20.00		-18.84
1586		-18.38	-18.90	-17.73	-18.54	-20.12		-18.73
1587		-18.22	-18.45	-17.77	-18.44	-20.29		-18.63
1588		-17.84	-18.73	-18.21	-18.62	-20.14		-18.71
1589		-18.11	-18.63	-18.04	-18.75	-20.25		-18.75
1590		-18.47	-18.91	-17.94	-19.05	-20.68		-19.01
1591		-18.14	-18.55	-17.84	-19.07	-20.07		-18.73
1592		-18.37	-18.57	-17.75	-18.91	-20.23		-18.77
1593		-18.38	-18.94	-17.79	-19.40	-20.61		-19.02
1594		-19.18	-19.22	-18.61	-19.35	-20.57		-19.39
1595		-18.75	-19.07	-18.41	-18.95	-20.21		-19.08
1596		-18.69	-19.02	-18.34	-19.08	-20.26		-19.08
1597		-18.66	-19.00	-18.33	-19.02	-20.11		-19.02
1598		-18.48	-18.57	-18.23	-18.83	-19.85		-18.79
1599		-18.69	-18.81	-18.17	-18.83	-20.51		-19.00
1600		-18.37	-18.84	-18.55	-18.62	-20.38		-18.95
1601		-18.28	-18.69	-18.51	-19.04	-19.67		-18.84
1602		-18.78	-18.90	-18.02	-18.97	-20.16		-18.97
1603		-18.40	-18.80	-18.10	-18.70	-20.15		-18.83
1604		-18.82	-18.77	-18.09	-18.83	-19.76		-18.85
1605		-19.18	-19.34	-19.05	-19.34	-21.03		-19.59
1606		-19.18	-19.15	-18.72	-19.64	-20.56		-19.45
1607		-18.48	-19.53	-18.91	-20.01	-20.89		-19.56
1608		-19.14	-19.37	-19.13	-19.59	-20.85		-19.62
1609		-18.74	-18.70	-18.30	-19.05	-20.62		-19.08
1610		-19.11	-19.02	-18.48	-18.99	-20.03		-19.13
1611		-18.99	-18.34	-18.64	-19.05	-20.42		-19.09
1612		-19.07	-19.16	-18.90	-19.45	-21.21		-19.56
1613		-19.41	-18.92	-18.65	-19.89	-21.43		-19.66
1614		-19.30	-19.43	-18.69	-20.03	-21.30		-19.75

1615		-19.17	-19.55	-18.68	-19.82	-21.56		-19.76
1616		-19.38	-19.27	-19.05	-20.23	-21.53		-19.89
1617		-19.70	-19.60	-19.13	-20.21	-21.77		-20.08
1618		-20.14	-19.10	-19.62	-20.68	-21.08		-20.12
1619		-19.44	-18.16	-18.97	-19.66	-20.54		-19.35
1620		-19.37	-19.10	-19.53	-19.66	-20.96		-19.72
1621		-19.15	-18.34	-18.60	-19.27	-20.36		-19.14
1622		-18.86	-18.56	-18.37	-19.08	-20.25		-19.02
1623		-18.73	-18.66	-18.39	-19.01	-21.18		-19.19
1624		-19.10	-19.04	-18.64	-19.91	-21.43		-19.62
1625		-19.40	-19.57	-18.72	-19.53	-20.57		-19.56
1626		-19.15	-19.09	-18.29	-19.53	-20.08		-19.23
1627		-18.61	-19.07	-18.41	-19.65	-20.25		-19.20
1628		-19.10	-19.45	-18.36	-19.42	-20.11		-19.29
1629		-19.18	-19.18	-18.24	-19.74	-20.00		-19.27
1630		-19.02	-19.40	-18.21	-19.59	-19.68		-19.18
1631		-18.80	-19.71	-18.42	-19.05	-19.46		-19.09
1632		-19.60	-19.65	-17.89	-19.58	-19.86		-19.32
1633		-19.44	-19.89	-18.58	-19.46	-20.35		-19.54
1634		-19.39	-19.54	-18.16	-19.59	-19.89		-19.31
1635		-20.01	-19.86	-18.40	-19.38	-20.10		-19.55
1636		-20.00	-20.37	-19.14	-19.42	-20.46		-19.88
1637		-19.09	-19.48	-18.67	-19.25	-19.41		-19.18
1638		-18.58	-20.30	-18.17	-19.46	-19.48		-19.20
1639		-18.43	-19.01	-18.33	-19.37	-19.58		-18.94
1640		-18.97	-18.96	-18.57	-19.67	-19.33		-19.10
1641		-19.15	-18.98	-18.64	-19.98	-19.11		-19.17
1642		-19.25	-19.26	-18.29	-19.98	-19.08		-19.17
1643		-19.49	-19.66	-18.20	-19.27	-20.22		-19.37
1644		-19.56	-19.51	-18.12	-20.10	-19.88		-19.43
1645		-19.59	-19.37	-18.08	-19.94	-19.97		-19.39
1646		-19.36	-19.21	-17.84	-19.20	-19.38		-19.00
1647		-19.59	-19.44	-18.22	-19.34	-19.59		-19.24
1648		-19.44	-19.36	-18.37	-19.24	-19.72		-19.23
1649		-19.79	-19.44	-18.32	-19.24	-19.93		-19.34
1650		-19.35	-19.33	-18.31	-18.95	-19.29		-19.05
1651		-18.92	-18.92	-18.49	-19.21	-19.35		-18.98
1652		-18.98	-19.43	-18.57	-19.23	-19.37		-19.12
1653		-18.76	-19.35	-17.75	-19.19	-18.94		-18.80
1654		-18.62	-18.66	-17.38	-19.00	-19.47		-18.63
1655		-18.79	-18.84	-17.39	-19.02	-19.00		-18.61
1656		-18.98	-18.84	-17.44	-19.20	-19.47		-18.79
1657		-18.90	-18.82	-17.72	-19.57	-18.89		-18.78
1658		-19.01	-19.18	-17.67	-19.54	-18.89		-18.86
1659		-19.13	-19.26	-17.89	-19.36	-19.64		-19.06
1660		-19.13	-19.19	-18.10	-18.97	-19.68		-19.01
1661		-18.98	-19.03	-17.97	-18.94	-19.31		-18.85
1662		-19.55	-19.16	-18.16	-19.24	-19.36		-19.09
1663		-19.44	-19.40	-18.10	-19.01	-19.59		-19.11
1664		-18.87	-18.83	-18.20	-19.01	-18.76		-18.74
1665		-18.64	-19.23	-18.26	-18.90	-19.09		-18.82

1666		-18.97	-19.43	-18.26	-18.97	-18.74		-18.88
1667		-18.59	-18.44	-17.76	-19.25	-18.17		-18.44
1668		-19.15	-18.19	-17.48	-19.01	-18.38		-18.44
1669		-18.89	-18.05	-17.35	-19.43	-18.06		-18.36
1670		-18.21	-17.97	-17.34	-19.50	-18.48		-18.30
1671		-17.94	-18.19	-17.02	-19.40	-18.69		-18.25
1672		-18.21	-18.52	-17.57	-19.50	-18.60		-18.48
1673		-18.64	-18.75	-17.72	-19.24	-18.45		-18.56
1674		-18.88	-18.55	-18.02	-19.06	-18.25		-18.55
1675		-18.91	-18.50	-17.63	-19.27	-18.44		-18.55
1676		-18.86	-18.58	-17.80	-19.10	-19.14		-18.70
1677		-19.06	-18.85	-18.12	-18.93	-18.80		-18.75
1678	-17.95	-19.25	-18.90	-17.85	-18.55	-18.89		-18.56
1679	-18.68	-19.45	-19.36	-18.15	-18.87	-19.27		-18.96
1680	-19.33	-19.70	-19.64	-18.57	-18.94	-20.09		-19.38
1681	-19.03	-20.01	-19.62	-18.74	-18.82	-19.74		-19.33
1682	-18.92	-19.21	-19.33	-18.66	-19.00	-19.61		-19.12
1683	-19.26	-18.76	-19.09	-18.30	-18.91	-19.22		-18.92
1684	-18.85	-19.02	-19.23	-18.42	-18.83	-19.26		-18.93
1685	-19.03	-19.11	-19.30	-19.02	-18.75	-19.15		-19.06
1686	-18.43	-19.12	-18.93	-18.34	-18.86	-18.71		-18.73
1687	-19.24	-19.05	-19.15	-18.31	-18.94	-19.08		-18.96
1688	-19.28	-18.76	-19.12	-18.51	-19.23	-18.63		-18.92
1689	-18.65	-18.83	-18.54	-18.12	-19.14	-18.14		-18.57
1690	-18.59	-18.48	-18.70	-17.81	-19.36	-18.32		-18.54
1691	-18.65	-18.91	-18.89	-17.91	-19.11	-18.64		-18.69
1692	-18.81	-18.60	-18.67	-18.03	-19.32	-18.53		-18.66
1693	-18.97	-18.60	-18.71	-17.95	-19.14	-18.57		-18.66
1694	-19.10	-18.31	-18.54	-17.99	-18.93	-18.79		-18.61
1695	-18.51	-18.43	-18.51	-18.08	-18.60	-18.50		-18.44
1696	-18.94	-18.67	-18.84	-18.16	-18.61	-18.59		-18.64
1697	-18.85	-18.46	-18.59	-18.17	-18.37	-18.53		-18.49
1698	-18.45	-18.66	-18.72	-18.31	-18.43	-18.83		-18.57
1699	-18.73	-19.12	-19.15	-18.69	-18.26	-18.99		-18.82
1700	-18.76	-19.03	-18.95	-18.97	-18.24	-19.00		-18.82
1701	-18.61	-18.48	-18.97	-18.58	-18.24	-18.16		-18.51
1702	-19.07	-18.27	-18.75	-18.44	-18.46	-18.24		-18.54
1703	-18.47	-19.17	-19.12	-18.71	-18.57	-18.51		-18.76
1704	-18.46	-19.10	-18.80	-18.90	-18.74	-19.08		-18.85
1705	-19.50	-18.88	-19.50	-19.39	-19.11	-19.08		-19.24
1706	-19.30	-19.20	-18.92	-18.89	-18.74	-18.89		-18.99
1707	-18.81	-18.21	-18.89	-18.59	-18.77	-18.98		-18.71
1708	-19.13	-18.59	-19.13	-18.54	-18.92	-19.33		-18.94
1709	-18.60	-19.04	-19.46	-18.64	-19.10	-19.36		-19.03
1710	-19.18	-18.64	-19.10	-18.68	-19.09	-19.30		-19.00
1711	-19.43	-18.51	-19.05	-18.72	-18.98	-19.05		-18.96
1712	-19.04	-18.38	-19.50	-18.31	-19.19	-18.92		-18.89
1713	-19.25	-18.53	-19.44	-18.76	-19.17	-18.86		-19.00
1714	-19.01	-18.08	-18.91	-18.68	-18.85	-18.90		-18.74
1715	-19.11	-18.29	-19.04	-18.18	-18.99	-18.48		-18.68
1716	-19.10	-18.42	-19.00	-18.31	-19.05	-18.84		-18.79

1717	-19.47	-18.84	-19.22	-18.76	-19.39	-19.02		-19.12
1718	-20.17	-19.09	-19.76	-18.78	-19.51	-19.77		-19.51
1719	-20.40	-19.12	-20.05	-19.27	-19.35	-19.42		-19.60
1720	-20.09	-18.98	-19.89	-19.01	-19.17	-19.50		-19.44
1721	-19.30	-18.35	-19.18	-18.69	-18.94	-18.50		-18.83
1722	-19.53	-18.71	-19.53	-18.82	-19.26	-18.59		-19.07
1723	-19.67	-18.97	-19.57	-19.05	-19.13	-18.87		-19.21
1724	-20.32	-19.18	-20.57	-18.86	-19.25	-18.64		-19.47
1725	-20.83	-19.12	-20.22	-19.26	-19.61	-20.63		-19.95
1726	-20.07	-19.47	-20.41	-18.94	-19.34	-20.40		-19.77
1727	-20.19	-18.95	-19.25	-19.03	-18.93	-19.55		-19.32
1728	-20.08	-18.58	-19.09	-18.78	-18.39	-19.11		-19.01
1729	-19.24	-18.54	-18.88	-18.33	-18.57	-18.89		-18.74
1730	-19.57	-19.06	-19.70	-18.62	-18.66	-19.14		-19.13
1731	-19.61	-19.63	-19.05	-18.82	-18.61	-18.92		-19.11
1732	-19.56	-18.24	-18.83	-18.50	-18.46	-18.49		-18.68
1733	-18.95	-18.73	-19.27	-18.33	-18.58	-18.49		-18.73
1734	-19.71	-19.13	-18.94	-18.49	-18.42	-18.84		-18.92
1735	-19.27	-19.17	-18.85	-18.13	-18.78	-19.20		-18.90
1736	-19.22	-18.96	-18.70	-18.91	-18.46	-18.98		-18.87
1737	-18.04	-19.04	-18.74	-18.43	-18.35	-18.84		-18.57
1738	-18.52	-17.87	-18.46	-17.94	-18.42	-18.81		-18.34
1739	-18.25	-18.64	-18.56	-17.53	-18.84	-18.94		-18.46
1740	-19.40	-18.93	-19.21	-18.32	-18.60	-19.29		-18.96
1741	-19.23	-18.92	-18.78	-18.38	-18.36	-19.27		-18.82
1742	-19.51	-19.00	-19.01	-18.47	-18.72	-19.96		-19.11
1743	-18.69	-19.14	-19.19	-18.37	-18.69	-19.68		-18.96
1744	-19.48	-19.09	-19.64	-18.41	-18.80	-19.95		-19.23
1745	-19.91	-19.34	-19.60	-18.36	-18.92	-20.24		-19.39
1746	-19.53	-18.59	-19.19	-18.31	-19.11	-19.73		-19.08
1747	-19.63	-19.08	-19.43	-18.49	-18.90	-19.77		-19.22
1748	-19.62	-19.11	-19.53	-18.64	-19.22	-19.71		-19.30
1749	-19.85	-19.00	-19.62	-19.13	-19.07	-19.92		-19.43
1750	-19.70	-19.00	-19.31	-18.84	-18.80	-19.31		-19.16
1751	-19.25	-18.44	-18.79	-18.56	-18.48	-18.51		-18.67
1752	-18.74	-18.34	-18.94	-18.53	-18.77	-18.31		-18.61
1753	-17.85	-18.62	-19.47	-18.31	-18.99	-18.84		-18.68
1754	-18.88	-18.71	-19.09	-18.62	-18.91	-19.10		-18.88
1755	-19.21	-18.80	-18.85	-18.61	-18.59	-18.87		-18.82
1756	-18.19	-18.68	-19.35	-18.47	-18.24	-18.60		-18.59
1757	-18.14	-19.24	-19.32	-18.24	-20.13	-19.25		-19.05
1758	-18.48	-18.84	-20.76	-18.29	-19.25	-19.42		-19.17
1759	-18.17	-18.80	-19.74	-18.54	-19.69	-19.57		-19.09
1760	-18.84	-19.71	-19.77	-18.80	-19.62	-19.36		-19.35
1761	-19.57	-19.10	-19.90	-18.78	-19.68	-19.12		-19.36
1762	-18.70	-18.27	-19.12	-18.22	-18.76	-18.83		-18.65
1763	-18.54	-18.79	-19.45	-18.04	-19.62	-19.23		-18.94
1764	-19.47	-18.50	-19.56	-18.70	-19.51	-19.31		-19.17
1765	-18.25	-18.93	-19.53	-17.84	-19.39	-19.29		-18.87
1766	-19.04	-19.02	-19.53	-18.73	-19.78	-19.41		-19.25
1767	-19.54	-19.37	-19.53	-19.02	-19.64	-19.51		-19.44

1768	-20.15	-19.41	-19.72	-19.07	-19.78	-19.47		-19.60
1769	-19.24	-19.81	-19.58	-18.62	-19.87	-19.13		-19.38
1770	-18.62	-19.19	-19.79	-18.70	-20.23	-19.23		-19.29
1771	-19.84	-19.49	-19.84	-18.67	-19.78	-19.54		-19.53
1772	-18.56	-19.60	-19.30	-18.33	-19.74	-18.88		-19.07
1773	-18.94	-19.13	-19.48	-18.57	-19.99	-19.65		-19.29
1774	-19.60	-19.71	-20.18	-19.05	-20.27	-19.52		-19.72
1775	-18.88	-19.60	-19.72	-18.85	-19.95	-19.56		-19.43
1776	-18.45	-19.20	-19.43	-18.86	-19.47	-19.29		-19.12
1777	-18.28	-19.01	-19.16	-18.28	-19.88	-19.49		-19.02
1778	-18.93	-19.15	-19.07	-18.64	-19.81	-19.13		-19.12
1779	-18.38	-19.26	-19.02	-18.73	-19.22	-18.98		-18.93
1780	-18.51	-18.72	-18.72	-18.73	-19.33	-19.00		-18.83
1781	-18.44	-18.81	-18.45	-18.14	-19.58	-18.98		-18.73
1782	-17.44	-18.55	-19.14	-18.01	-19.49	-19.33		-18.66
1783	-17.96	-19.09	-19.37	-18.10	-19.65	-19.29		-18.91
1784	-19.44	-19.42	-19.25	-18.60	-20.00	-19.59		-19.38
1785	-19.15	-19.34	-19.10	-18.23	-19.72	-19.28		-19.14
1786	-19.40	-18.91	-19.57	-19.04	-20.01	-19.35		-19.38
1787	-19.02	-18.80	-19.54	-19.22	-19.94	-19.31		-19.30
1788	-19.26	-19.30	-19.77	-18.79	-19.77	-19.32		-19.37
1789	-19.32	-19.98	-20.18	-19.36	-19.76	-19.50		-19.68
1790	-19.09	-19.07	-19.23	-18.70	-19.96	-19.57		-19.27
1791	-19.07	-19.97	-19.62	-19.50	-20.09	-19.65		-19.65
1792	-19.31	-19.67	-19.49	-18.56	-19.71	-19.82		-19.43
1793	-19.01	-19.28	-19.74	-18.91	-19.54			-19.30
1794	-17.83	-19.02	-19.29	-18.09	-19.23	-19.57		-18.84
1795	-18.09	-19.17	-19.71	-17.91	-19.51	-19.24		-18.94
1796	-18.82	-19.59	-19.87	-18.61	-19.97	-19.36		-19.37
1797	-19.00	-19.37	-19.91	-18.88	-19.70	-19.48		-19.39
1798	-19.28	-19.83	-20.35	-18.77	-19.84	-19.31		-19.56
1799	-19.38	-19.69	-20.69	-18.94	-19.92	-19.45		-19.68
1800	-18.94	-18.91	-20.04	-18.77	-19.44	-19.47		-19.26
1801	-19.19	-19.34	-20.24	-19.69	-19.23	-19.67		-19.56
1802	-19.49	-19.49	-20.80	-19.53	-19.15	-20.26		-19.79
1803	-19.25	-19.63	-20.14	-19.15	-19.80	-20.00		-19.66
1804	-19.05	-19.41	-20.06	-19.13	-19.31	-20.01		-19.50
1805	-18.83	-19.68	-20.12	-19.62	-19.59	-19.75		-19.60
1806	-18.32	-19.26	-20.05	-19.05	-19.21	-19.56		-19.24
1807	-18.12	-19.22	-20.00	-19.89	-19.09	-20.04		-19.39
1808	-18.76	-19.60	-19.65	-19.06	-19.15	-19.95		-19.36
1809	-18.40	-19.50	-19.70	-19.20	-19.22	-19.98		-19.33
1810	-18.86	-20.07	-20.46	-19.17	-19.36	-20.48		-19.73
1811	-19.21	-19.60	-20.53	-19.08	-19.61	-19.58		-19.60
1812	-18.31	-19.04	-19.53	-18.64	-19.58	-18.84		-18.99
1813	-17.84	-18.54	-19.61	-18.49	-19.25	-19.03		-18.79
1814	-17.55	-18.74	-19.50	-19.96	-19.10	-19.09		-18.99
1815	-17.95	-19.44	-19.37	-19.06	-19.57	-19.36		-19.12
1816	-19.00	-19.69	-19.76	-18.93	-19.43	-19.86		-19.44
1817	-19.06	-20.25	-19.60	-18.95	-19.60	-19.87		-19.56
1818	-18.97	-19.53	-19.94	-19.28	-19.40	-19.79		-19.49

1819	-19.04	-19.40	-19.68	-19.09	-19.38	-19.30		-19.32
1820	-18.69	-18.99	-19.84	-19.38	-19.33	-19.52		-19.29
1821	-18.40	-19.18	-19.53	-19.15	-19.43	-19.00		-19.12
1822	-18.79	-19.00	-20.03	-18.98	-19.26	-18.90		-19.16
1823	-18.45	-18.78	-20.10	-18.61	-19.47	-19.10		-19.09
1824	-18.25	-19.14	-19.59	-19.88	-19.85	-19.46		-19.36
1825	-19.26	-18.90	-19.94	-18.86	-19.77	-19.43		-19.36
1826	-18.95	-18.85	-20.02	-18.99	-19.74	-19.70		-19.38
1827	-19.33	-19.00	-19.95	-19.61	-20.22	-20.14		-19.71
1828	-20.11	-19.09	-20.57	-19.70	-20.21	-20.17		-19.98
1829	-19.07	-18.97	-19.79	-18.81	-19.84	-19.94		-19.40
1830	-19.51	-18.44	-20.19	-18.92	-19.74	-19.81		-19.44
1831	-19.40	-18.28	-19.92	-19.06	-19.73	-19.82		-19.37
1832	-19.67	-18.05	-19.39	-19.44	-19.78	-19.59		-19.32
1833	-19.09	-17.76	-19.23	-19.14	-19.11	-19.17		-18.92
1834	-18.36	-17.56	-19.38	-18.97	-19.19	-18.98		-18.74
1835	-18.16	-17.66	-18.85	-19.04	-19.45	-18.87		-18.67
1836	-17.92	-18.18	-19.44	-18.93	-20.08	-19.08		-18.94
1837	-18.86	-18.91	-19.29	-19.01	-20.18	-19.55		-19.30
1838	-19.33	-18.61	-19.85	-19.18	-20.15	-19.78		-19.48
1839	-19.15	-19.15	-19.82	-19.07	-20.18	-19.69		-19.51
1840	-19.20	-18.70	-19.47	-19.25	-19.42	-19.48		-19.25
1841	-19.13	-18.76	-19.90	-19.73	-19.55	-19.34		-19.40
1842	-19.04	-18.66	-19.71	-19.17	-19.46	-19.45		-19.25
1843	-18.26	-18.50	-19.72	-19.01	-19.25	-19.56		-19.05
1844	-17.97	-18.32	-19.71	-19.37	-19.32	-19.47		-19.03
1845	-18.34	-18.75	-20.07		-19.43	-19.53		-19.22
1846	-18.39	-18.23	-19.27	-18.20	-19.44	-19.87		-18.90
1847	-18.59	-18.88	-20.02	-18.81	-19.73	-19.66		-19.28
1848	-18.62	-18.55	-19.85	-18.96	-19.54	-19.67		-19.20
1849	-19.13	-18.51	-19.89	-19.18	-19.68	-19.78		-19.36
1850	-18.74	-18.71	-19.92	-18.70	-20.12	-19.81		-19.33
1851	-19.34	-18.58	-20.01	-18.76	-20.56	-20.31		-19.59
1852	-19.06	-18.91	-20.61	-19.97	-18.85	-19.78		-19.53
1853	-19.25	-19.64	-20.99	-19.53	-20.74	-19.83		-20.00
1854	-19.08	-19.38	-20.38	-21.03	-20.92	-19.85		-20.11
1855	-18.47	-18.19	-20.30	-19.28	-19.47	-19.26		-19.16
1856	-18.45	-17.83	-20.17	-19.10	-19.66	-19.45		-19.11
1857	-18.22	-17.66	-20.13	-19.49	-20.09	-19.27		-19.14
1858	-18.01	-17.86	-20.87	-19.07	-20.08	-19.78		-19.28
1859	-19.00	-18.72	-20.50	-19.40	-20.41	-19.98		-19.67
1860	-18.85	-18.68	-20.41	-20.30	-21.16	-19.53		-19.82
1861	-18.97	-18.19	-20.69	-19.68	-20.03	-19.56		-19.52
1862	-19.24	-18.08	-19.88	-19.64	-20.67	-19.04		-19.42
1863	-19.07	-17.87	-20.60	-20.09	-19.91	-19.12		-19.44
1864	-18.59	-18.30	-19.92	-19.25	-19.57	-19.21		-19.14
1865	-19.71	-18.66	-20.20	-19.71	-19.48	-19.51		-19.55
1866	-19.14	-18.95	-20.43	-19.20	-20.04	-19.45		-19.54
1867	-19.33	-18.29	-20.06	-19.02	-19.76	-19.52		-19.33
1868	-19.98	-19.30	-20.84	-19.48	-20.06	-19.76		-19.90
1869	-20.43	-19.37	-20.62	-19.62	-21.11	-19.80		-20.16

1870	-20.32	-19.17	-20.71	-20.05	-20.40	-19.46		-20.02
1871	-19.69	-19.47	-20.69	-20.03	-20.55	-19.96		-20.06
1872	-19.24	-18.39	-20.03	-20.38	-20.19	-19.43		-19.61
1873	-19.59	-18.13	-21.29	-19.23	-19.95	-19.57		-19.63
1874	-19.75	-18.66	-20.66	-19.58	-20.26	-19.83		-19.79
1875	-19.73	-18.70	-20.22	-19.14	-20.58	-19.86		-19.71
1876	-19.52	-18.99	-20.11	-19.30	-19.77	-19.43		-19.52
1877	-19.28	-19.03	-19.60	-18.92	-20.95	-19.42		-19.53
1878	-19.55	-18.33	-20.98	-19.15	-20.06	-19.32		-19.56
1879	-19.15	-18.57	-19.99	-19.48	-20.18	-19.17		-19.42
1880	-19.63	-18.67	-19.84	-20.78	-19.76	-19.46		-19.69
1881	-19.50	-18.32	-20.07	-18.78	-20.28	-19.80		-19.46
1882	-19.08	-18.30	-19.72	-18.64	-19.92	-19.57		-19.21
1883	-19.10	-18.18	-20.89	-18.69	-20.17	-19.66		-19.45
1884	-19.36	-18.81	-20.02	-18.95	-20.24	-19.78		-19.53
1885	-19.09	-18.51	-19.60	-19.06	-19.77	-19.70		-19.29
1886	-19.21	-18.61	-19.96	-18.87	-20.41	-19.90		-19.49
1887	-19.43	-18.71	-20.25	-18.97	-19.79	-19.73		-19.48
1888	-19.42	-18.44	-20.23	-18.96	-20.12	-19.50		-19.44
1889	-19.34	-19.30	-19.85	-19.37	-20.23	-19.59		-19.61
1890	-20.05	-18.56	-20.18	-19.46	-20.23	-20.17		-19.78
1891	-20.92	-19.12	-20.42	-21.16	-21.19	-20.26		-20.51
1892	-19.32	-18.63	-20.97	-18.81	-19.95	-19.54		-19.54
1893	-19.66	-18.68	-20.51	-19.29	-20.16	-19.83		-19.69
1894	-19.80	-18.76	-20.62	-19.34	-20.50	-19.53		-19.76
1895	-18.96	-18.69	-20.21	-18.94	-19.73	-19.76		-19.38
1896	-19.86	-18.97	-20.56	-19.24	-19.86	-19.49		-19.67
1897	-19.57	-18.96	-20.50	-19.15	-19.32	-19.41		-19.49
1898	-18.71	-18.46	-19.69	-18.47	-19.18	-19.30		-18.97
1899	-18.42	-18.72	-19.58	-18.17	-19.87	-19.51		-19.05
1900	-18.97	-18.55	-20.11	-18.87	-19.60	-19.38		-19.25
1901	-19.40	-18.81	-20.86	-18.55	-20.22	-19.51		-19.56
1902	-18.89	-18.43	-20.49	-18.39	-19.01	-19.36		-19.10
1903	-18.80	-18.50	-19.99	-18.25	-18.85	-18.86		-18.88
1904	-19.17	-18.86	-20.84	-19.47	-19.40	-19.34		-19.51
1905	-18.77	-18.68	-20.27	-18.25	-19.25	-19.75		-19.16
1906	-19.18	-19.05	-21.12	-18.97	-20.10	-19.62		-19.67
1907	-19.16	-19.05	-21.18	-19.18	-19.45	-19.69	-19.23	-19.56
1908	-19.22	-18.94	-21.24	-19.47	-20.45	-20.10	-19.35	-19.82
1909	-18.56	-18.48	-20.03	-18.77	-19.42	-19.28	-18.78	-19.05
1910	-18.20	-18.97	-20.74	-18.51	-19.77	-19.85	-18.98	-19.29
1911	-18.67	-18.58	-20.15	-18.86	-19.44	-19.67	-19.15	-19.22
1912	-17.93	-18.68	-20.94	-19.15	-19.38	-20.02	-19.21	-19.33
1913	-19.61	-19.57	-20.92	-19.52	-20.28	-20.79	-19.90	-20.08
1914	-19.37	-18.99	-20.63	-19.54	-20.03	-20.11	-19.59	-19.75
1915	-18.80	-19.11	-19.98	-18.98	-19.19	-19.45	-19.74	-19.32
1916	-18.66	-18.38	-20.17	-18.44	-19.23	-19.60	-18.61	-19.01
1917	-18.91	-18.78	-19.98	-18.94	-19.47	-20.15	-19.19	-19.35
1918	-19.25	-19.13	-20.68	-19.87	-19.50	-20.09	-18.84	-19.62
1919	-18.64	-18.92	-19.77	-18.72	-19.76	-19.87	-18.77	-19.21
1920	-18.85	-18.48	-19.78	-18.80	-19.76	-19.94	-19.11	-19.25

1921	-19.03	-18.91	-20.06	-19.04	-20.55	-19.99	-19.18	-19.53
1922	-18.73	-18.84	-20.34	-20.72	-21.14	-19.88	-19.09	-19.82
1923	-18.52	-18.37	-20.20	-18.97	-19.65	-20.00	-18.69	-19.20
1924	-17.75	-18.57	-20.99	-18.58	-19.94	-20.51	-18.51	-19.26
1925	-19.86	-19.35	-21.23	-19.90	-21.01	-20.54	-19.17	-20.15
1926	-19.86	-19.24	-20.42	-18.92	-20.18	-19.82	-19.13	-19.65
1927	-19.27	-18.02	-19.97	-19.24	-19.87	-19.38	-18.83	-19.23
1928	-18.07	-18.15	-19.81	-18.15	-20.22	-19.33	-18.12	-18.84
1929	-18.73	-18.48	-19.53	-18.10	-19.43	-19.44	-18.64	-18.91
1930	-18.45	-18.44	-19.21	-18.87	-19.14	-19.04	-18.79	-18.85
1931	-18.89	-18.40	-19.31	-17.99	-19.58	-18.79	-19.11	-18.87
1932	-18.29	-18.42	-19.34	-18.40	-19.72	-18.80	-19.28	-18.89
1933	-18.56	-18.46	-19.77	-18.50	-19.22	-18.82	-18.84	-18.88
1934	-18.71	-18.34	-19.78	-18.12	-19.31	-19.50	-18.67	-18.92
1935	-18.87	-18.09	-19.61	-18.41	-18.92	-19.24	-18.81	-18.85
1936	-19.52	-18.45	-19.87	-18.57	-19.93	-19.40	-19.27	-19.29
1937	-18.92	-18.35	-19.59	-18.89	-19.92	-19.77	-18.69	-19.16
1938	-19.21	-18.77	-19.43	-19.02	-20.00	-19.85	-19.36	-19.38
1939	-19.44	-18.65	-19.46	-18.63	-19.79	-19.78	-19.50	-19.32
1940	-19.40	-18.40	-19.70	-19.77	-20.45	-19.72	-19.39	-19.55
1941	-19.56	-18.76	-20.26	-19.15	-19.99	-20.50	-19.72	-19.71
1942	-19.26	-19.08	-19.34	-18.93	-20.23	-19.76	-18.91	-19.36
1943	-18.84	-18.77	-19.33	-19.11	-19.38	-19.59	-19.20	-19.17
1944	-19.46	-18.79	-19.42	-19.55	-19.94	-19.77	-18.93	-19.41
1945	-19.82	-19.09	-20.26	-18.63	-20.13	-20.31	-19.29	-19.65
1946	-19.47	-18.83	-19.84	-18.33	-19.97	-20.16	-19.45	-19.44
1947	-18.48	-18.50	-19.44	-19.08	-19.96	-19.86	-18.66	-19.14
1948	-18.39	-17.88	-19.17	-18.94	-19.89	-19.54	-18.61	-18.92
1949	-18.78	-18.43	-19.92	-18.73	-19.58	-19.45	-18.97	-19.12
1950	-19.15	-18.46	-20.10	-18.69	-19.44	-19.11	-18.63	-19.08
1951	-19.29	-18.39	-19.64	-18.84	-20.05	-19.16	-19.10	-19.21
1952	-19.43	-18.65	-19.40	-18.78	-19.73	-19.53	-19.51	-19.29
1953	-19.09	-18.72	-20.11	-18.92	-19.60	-19.37	-18.90	-19.24
1954	-19.26	-18.59	-19.41	-19.27	-19.68	-19.15	-18.58	-19.13
1955	-19.04	-18.94	-19.91	-18.76	-20.18	-19.36	-18.52	-19.24
1956	-19.17	-18.53	-19.57	-18.85	-19.68	-19.25	-19.33	-19.20
1957	-18.92	-18.12	-19.14	-18.67	-19.49	-19.19	-19.19	-18.96
1958	-18.77	-18.02	-19.06	-19.43	-20.44	-19.26	-19.20	-19.17
1959	-18.03	-18.24	-18.72	-17.85	-19.26	-19.07	-18.22	-18.49
1960	-18.25	-18.40	-19.79	-18.83	-20.08	-19.18	-18.35	-18.98
1961	-18.88	-18.85	-20.19	-19.98	-19.32	-19.65	-19.62	-19.50
1962	-19.06	-18.94	-19.96	-18.60	-19.42	-19.57	-19.59	-19.31
1963	-18.75	-18.54	-19.55	-18.16	-20.30	-19.70	-19.44	-19.21
1964	-18.94	-19.19	-19.73	-19.48	-20.17	-20.05	-19.61	-19.60
1965	-19.52	-18.72	-20.16	-19.32	-20.18	-19.98	-19.70	-19.66
1966	-19.63	-18.72	-19.60	-18.36	-20.17	-20.07	-18.66	-19.32
1967	-19.35	-19.04	-20.02	-19.97	-20.21	-19.87	-19.29	-19.68
1968	-19.59	-18.69	-20.60	-19.81	-19.91	-19.99	-19.63	-19.75
1969	-18.86	-18.58	-19.88	-19.06	-20.35	-19.40	-19.52	-19.38
1970	-18.64	-18.60	-19.38	-19.12	-19.21	-19.28	-19.17	-19.06
1971	-19.24	-18.85	-19.70	-19.68	-19.10	-19.57	-19.25	-19.34

1972	**-19.21**	**-18.53**	**-19.59**	**-18.13**	**-19.71**	**-19.30**	**-18.87**	**-19.05**
1973	**-19.23**	**-18.28**	**-19.69**	**-18.82**	**-20.45**	**-19.19**	**-18.79**	**-19.21**
1974	**-18.31**	**-18.66**	**-19.29**	**-19.10**	**-20.04**	**-19.28**	**-18.00**	**-18.95**
1975	**-18.27**	**-18.93**	**-19.43**	**-18.79**	**-19.95**	**-19.78**	**-18.08**	**-19.03**
1976	**-18.73**	**-18.67**	**-20.24**	**-19.43**	**-20.05**	**-19.46**	**-19.12**	**-19.38**
1977	**-18.84**	**-18.30**	**-20.04**	**-19.15**	**-20.30**	**-19.19**	**-19.07**	**-19.27**
1978	**-18.73**	**-18.50**	**-19.76**	**-18.19**	**-20.61**	**-19.08**	**-18.93**	**-19,12**
1979	**-19.48**	**-19.09**	**-20.02**	**-19.58**	**-20.18**	**-19.40**	**-19.01**	**-19.54**
1980	**-19.27**	**-18.40**	**-19.52**	**-18.86**	**-19.91**	**-19.43**	**-18.81**	**-19.17**
1981	**-18.80**	**-18.43**	**-19.80**	**-18.82**	**-19.89**	**-19.81**	**-18.78**	**-19.19**
1982	**-19.21**	**-19.60**	**-20.64**	**-19.01**	**-19.83**	**-19.98**	**-19.75**	**-19.72**
1983	**-18.45**	**-18.89**	**-20.34**	**-19.27**	**-19.58**	**-19.97**	**-19.67**	**-19.45**
1984	**-20.33**	**-18.62**	**-20.49**	**-18.91**	**-20.58**	**-19.86**	**-19.62**	**-19.77**
1985	**-19.39**	**-18.25**	**-19.49**	**-18.68**	**-19.36**	**-19.70**	**-19.37**	**-19.18**
1986	**-18.66**	**-18.83**	**-19.29**	**-18.05**	**-19.40**	**-19.74**	**-19.15**	**-19.02**
1987	**-18.56**	**-18.38**	**-19.66**	**-19.13**	**-19.48**	**-19.76**	**-19.23**	**-19.17**
1988	**-18.41**	**-18.98**	**-19.45**	**-18.85**	**-19.67**	**-19.70**	**-18.83**	**-19.13**
1989	**-18.35**	**-17.94**	**-20.04**	**-18.98**	**-19.84**	**-19.59**	**-18.43**	**-19.02**
1990	**-19.43**	**-18.60**	**-20.00**	**-18.71**	**-19.69**	**-19.97**	**-19.35**	**-19.39**
1991	**-19.34**	**-19.61**	**-19.97**	**-19.26**	**-19.76**	**-20.18**	**-19.40**	**-19.65**
1992	**-18.45**	**-18.35**	**-19.12**	**-19.26**	**-20.11**	**-19.68**	**-18.73**	**-19.10**
1993	**-18.62**	**-18.10**	**-18.41**	**-18.86**	**-19.20**	**-19.52**	**-18.25**	**-18.71**
1994	**-18.12**	**-18.19**	**-18.67**	**-19.22**	**-19.48**	**-19.71**	**-18.57**	**-18.85**
1995	**-19.40**	**-18.01**	**-19.53**	**-19.81**	**-19.67**	**-20.02**	**-18.52**	**-19.28**
1996	**-19.07**	**-19.02**	**-20.12**	**-19.24**	**-20.02**	**-19.75**	**-18.93**	**-19.45**
1997	**-19.79**	**-18.63**	**-19.92**	**-19.15**	**-20.51**	**-19.65**	**-19.40**	**-19.58**
1998	**-19.64**	**-19.47**	**-20.14**	**-18.81**	**-20.00**	**-19.59**	**-19.41**	**-19.58**
1999	**-19.31**	**-19.46**	**-20.15**	**-19.46**	**-20.10**	**-19.52**	**-18.84**	**-19.55**
2000	**-18.24**	**-18.22**	**-20.68**	**-18.87**	**-19.56**	**-19.63**	**-18.67**	**-19.12**
2001	**-18.41**	**-18.55**	**-18.81**	**-19.37**	**-20.12**	**-19.62**	**-18.60**	**-19.07**
2002	**-19.33**	**-17.97**	**-19.73**	**-17.96**	**-18.86**	**-19.46**	**-18.13**	**-18.78**
2003	**-19.27**		**-19.62**	**-17.85**	**-18.51**	**-19.31**	**-18.41**	**-18.83**
2004	**-18.03**	**-18.64**	**-19.19**	**-19.09**	**-19.93**	**-19.09**	**-18.53**	**-18.93**
2005	**-19.66**	**-18.46**	**-19.71**				**-19.33**	**-19.29**

Bold above=$\delta^{13}C_{pin}$

year AD	001c $\delta^{13}C$	523b $\delta^{13}C$	362b $\delta^{13}C$	4123 $\delta^{13}C$	007 $\delta^{13}C$	527d $\delta^{13}C$	487e $\delta^{13}C$	mean $\delta^{13}C$
	Italic below=$\delta^{13}C_{cor}$							
1850	*-18.75*	*-18.73*	*-19.93*	*-18.70*	*-19.82*	*-20.12*		*-19.34*
1851	*-19.36*	*-18.60*	*-20.03*	*-18.76*	*-20.32*	*-20.56*		*-19.60*
1852	*-19.08*	*-18.94*	*-20.63*	*-19.97*	*-19.80*	*-18.85*		*-19.54*
1853	*-19.27*	*-19.67*	*-21.01*	*-19.53*	*-19.85*	*-20.74*		*-20.01*
1854	*-19.11*	*-19.42*	*-20.41*	*-21.03*	*-19.88*	*-20.92*		*-20.13*
1855	*-18.50*	*-18.23*	*-20.33*	*-19.28*	*-19.29*	*-19.47*		*-19.18*
1856	*-18.49*	*-17.88*	*-20.20*	*-19.10*	*-19.48*	*-19.66*		*-19.14*
1857	*-18.22*	*-17.72*	*-20.17*	*-19.49*	*-19.31*	*-20.09*		*-19.17*
1858	*-17.93*	*-17.93*	*-20.91*	*-19.07*	*-19.82*	*-20.08*		*-19.29*
1859	*-19.05*	*-18.79*	*-20.55*	*-19.40*	*-20.03*	*-20.41*		*-19.71*
1860	*-18.91*	*-18.76*	*-20.46*	*-20.29*	*-19.58*	*-21.15*		*-19.86*
1861	*-19.03*	*-18.28*	*-20.74*	*-19.68*	*-19.62*	*-20.03*		*-19.56*
1862	*-19.30*	*-18.17*	*-19.94*	*-19.64*	*-19.11*	*-20.67*		*-19.47*
1863	*-19.14*	*-17.97*	*-20.66*	*-21.30*	*-19.19*	*-19.91*		*-19.70*

1864	-18.67	-18.41	-19.99	-19.25	-19.29	-19.57		-19.20
1865	-19.79	-18.78	-20.28	-19.71	-19.59	-19.48		-19.61
1866	-19.23	-19.07	-20.51	-19.20	-19.54	-20.04		-19.60
1867	-19.42	-18.43	-20.15	-19.02	-19.61	-19.76		-19.40
1868	-20.07	-19.44	-20.93	-19.48	-19.86	-20.06		-19.97
1869	-20.52	-19.52	-20.72	-19.61	-19.90	-21.10		-20.23
1870	-20.42	-19.33	-20.81	-20.04	-19.57	-20.40		-20.10
1871	-19.80	-19.64	-20.80	-20.02	-20.07	-20.54		-20.15
1872	-19.37	-18.58	-20.15	-20.36	-19.56	-20.19		-19.70
1873	-19.72	-18.34	-21.40	-19.23	-19.70	-19.95		-19.72
1874	-19.88	-18.88	-20.78	-19.57	-19.97	-20.26		-19.89
1875	-19.87	-18.93	-20.36	-19.14	-20.00	-20.57		-19.81
1876	-19.67	-19.23	-20.25	-19.30	-19.59	-19.77		-19.64
1877	-19.44	-19.28	-19.76	-18.92	-19.59	-20.93		-19.65
1878	-19.71	-18.60	-21.12	-19.15	-19.49	-20.06		-19.69
1879	-19.33	-18.85	-20.15	-19.47	-19.35	-20.18		-19.56
1880	-19.80	-18.96	-20.01	-20.75	-19.65	-19.77		-19.82
1881	-19.68	-18.63	-20.24	-18.79	-19.99	-20.28		-19.60
1882	-19.28	-18.63	-19.90	-18.65	-19.77	-19.92		-19.36
1883	-19.31	-18.52	-21.05	-18.70	-19.86	-20.17		-19.60
1884	-19.57	-19.15	-20.21	-18.95	-19.99	-20.24		-19.69
1885	-19.31	-18.87	-19.80	-19.06	-19.92	-19.78		-19.46
1886	-19.43	-18.98	-20.16	-18.88	-20.12	-20.40		-19.66
1887	-19.66	-19.09	-20.44	-18.97	-19.96	-19.80		-19.65
1888	-19.65	-18.84	-20.43	-18.96	-19.74	-20.12		-19.62
1889	-19.58	-19.69	-20.06	-19.36	-19.84	-20.23		-19.79
1890	-20.27	-18.99	-20.38	-19.45	-20.41	-20.23		-19.96
1891	-21.12	-19.54	-20.62	-21.10	-20.50	-21.16		-20.67
1892	-19.58	-19.08	-21.16	-18.82	-19.81	-19.95		-19.73
1893	-19.91	-19.14	-20.71	-19.28	-20.10	-20.16		-19.88
1894	-20.05	-19.23	-20.82	-19.33	-19.81	-20.49		-19.96
1895	-19.25	-19.18	-20.43	-18.95	-20.04	-19.74		-19.60
1896	-20.12	-19.46	-20.77	-19.24	-19.79	-19.87		-19.88
1897	-19.85	-19.46	-20.71	-19.15	-19.72	-19.35		-19.71
1898	-19.02	-18.99	-19.93	-18.49	-19.62	-19.22		-19.21
1899	-18.75	-19.25	-19.83	-18.21	-19.83	-19.88		-19.29
1900	-19.28	-19.10	-20.34	-18.88	-19.71	-19.62		-19.49
1901	-19.70	-19.36	-21.06	-18.57	-19.84	-20.22		-19.79
1902	-19.22	-19.01	-20.70	-18.42	-19.70	-19.06		-19.35
1903	-19.14	-19.09	-20.23	-18.29	-19.23	-18.91		-19.15
1904	-19.49	-19.44	-21.04	-19.45	-19.69	-19.43		-19.76
1905	-19.12	-19.28	-20.49	-18.29	-20.09	-19.29		-19.43
1906	-19.51	-19.65	-21.30	-18.98	-19.97	-20.10		-19.92
1907	-19.50	-19.66	-21.36	-19.18	-20.04	-19.48	-19.23	-19.78
1908	-19.56	-19.56	-21.42	-19.45	-20.44	-20.44	-19.36	-20.03
1909	-18.93	-19.14	-20.26	-18.79	-19.66	-19.46	-18.80	-19.29
1910	-18.60	-19.61	-20.94	-18.54	-20.21	-19.79	-19.02	-19.53
1911	-19.05	-19.25	-20.38	-18.87	-20.04	-19.48	-19.20	-19.47
1912	-18.35	-19.36	-21.12	-19.15	-20.38	-19.42	-19.27	-19.58
1913	-19.94	-20.21	-21.10	-19.50	-21.11	-20.28	-19.96	-20.30
1914	-19.72	-19.67	-20.83	-19.52	-20.47	-20.04	-19.67	-19.99

1915	-19.18	-19.79	-20.21	-18.99	-19.85	-19.25	-19.82	-19.58
1916	-19.05	-19.11	-20.39	-18.48	-19.99	-19.29	-18.72	-19.29
1917	-19.29	-19.50	-20.21	-18.95	-20.52	-19.51	-19.19	-19.66
1918	-19.61	-19.83	-20.87	-19.83	-20.46	-19.54	-18.97	-19.87
1919	-19.04	-19.64	-20.01	-18.74	-20.26	-19.79	-18.91	-19.48
1920	-19.24	-19.24	-20.02	-18.82	-20.33	-19.79	-19.25	-19.53
1921	-19.41	-19.65	-20.28	-19.04	-20.38	-20.53	-19.33	-19.80
1922	-19.13	-19.59	-20.55	-20.62	-20.28	-21.09	-19.26	-20.07
1923	-18.94	-19.16	-20.41	-18.98	-20.39	-19.69	-18.87	-19.49
1924	-18.22	-19.35	-21.15	-18.61	-20.87	-19.96	-18.71	-19.55
1925	-20.19	-20.09	-21.38	-19.85	-20.90	-20.96	-19.37	-20.39
1926	-20.19	-19.99	-20.62	-18.93	-20.23	-20.19	-19.34	-19.93
1927	-19.64	-18.86	-20.20	-19.23	-19.82	-19.90	-19.05	-19.53
1928	-18.52	-18.99	-20.05	-18.21	-19.78	-20.23	-18.37	-19.16
1929	-19.14	-19.30	-19.79	-18.17	-19.88	-19.49	-18.88	-19.24
1930	-18.88	-19.27	-19.49	-18.89	-19.51	-19.22	-19.04	-19.19
1931	-19.29	-19.24	-19.58	-18.07	-19.28	-19.63	-19.11	-19.18
1932	-18.73	-19.26	-19.61	-18.45	-19.29	-19.76	-19.53	-19.23
1933	-18.98	-19.30	-20.01	-18.54	-19.31	-19.30	-19.11	-19.22
1934	-19.12	-19.20	-20.02	-18.19	-19.95	-19.38	-18.96	-19.26
1935	-19.27	-18.97	-19.86	-18.46	-19.71	-19.02	-19.10	-19.20
1936	-19.87	-19.31	-20.10	-18.61	-19.86	-19.96	-19.56	-19.61
1937	-19.31	-19.23	-19.84	-18.91	-20.20	-19.95	-19.01	-19.49
1938	-19.58	-19.62	-19.69	-19.03	-20.28	-20.03	-19.67	-19.70
1939	-19.79	-19.51	-19.72	-18.67	-20.21	-19.83	-19.81	-19.65
1940	-19.75	-19.29	-19.94	-19.72	-20.16	-20.44	-19.71	-19.86
1941	-19.90	-19.62	-20.46	-19.15	-20.88	-20.02	-20.04	-20.01
1942	-19.62	-19.92	-19.61	-18.94	-20.20	-20.24	-19.26	-19.68
1943	-19.24	-19.64	-19.60	-19.11	-20.04	-19.46	-19.55	-19.52
1944	-19.81	-19.66	-19.68	-19.52	-20.21	-19.97	-19.30	-19.74
1945	-20.14	-19.94	-20.46	-18.67	-20.70	-20.15	-19.66	-19.96
1946	-19.81	-19.70	-20.07	-18.40	-20.57	-20.00	-19.82	-19.77
1947	-18.90	-19.41	-19.70	-19.09	-20.29	-19.99	-19.07	-19.49
1948	-18.82	-18.84	-19.46	-18.96	-20.00	-19.93	-19.04	-19.29
1949	-19.18	-19.35	-20.14	-18.77	-19.91	-19.65	-19.40	-19.49
1950	-19.52	-19.38	-20.31	-18.74	-19.60	-19.52	-19.09	-19.45
1951	-19.64	-19.32	-19.89	-18.88	-19.65	-20.08	-19.55	-19.57
1952	-19.77	-19.56	-19.67	-18.83	-19.99	-19.79	-19.95	-19.65
1953	-19.46	-19.62	-20.31	-18.96	-19.84	-19.67	-19.38	-19.61
1954	-19.61	-19.50	-19.68	-19.28	-19.64	-19.75	-19.09	-19.51
1955	-19.41	-19.82	-20.13	-18.83	-19.83	-20.21	-19.05	-19.61
1956	-19.53	-19.45	-19.82	-18.92	-19.73	-19.77	-19.83	-19.58
1957	-19.30	-19.07	-19.43	-18.77	-19.68	-19.61	-19.72	-19.37
1958	-19.17	-18.99	-19.36	-19.47	-19.74	-20.48	-19.74	-19.56
1959	-18.51	-19.19	-19.06	-18.06	-19.57	-19.43	-18.84	-18.95
1960	-18.71	-19.34	-20.02	-18.96	-19.67	-20.18	-18.98	-19.41
1961	-19.28	-19.75	-20.38	-20.01	-20.09	-19.52	-20.20	-19.89
1962	-19.44	-19.84	-20.17	-18.79	-20.02	-19.62	-20.19	-19.72
1963	-19.17	-19.49	-19.80	-18.42	-20.13	-20.43	-20.07	-19.64
1964	-19.34	-20.08	-19.96	-19.61	-20.44	-20.33	-20.25	-20.00
1965	-19.86	-19.67	-20.35	-19.49	-20.38	-20.35	-20.36	-20.07

1966	-19.96	-19.68	-19.85	-18.66	-20.46	-20.36	-19.42	-19.77
1967	-19.71	-19.97	-20.23	-20.10	-20.29	-20.41	-20.03	-20.11
1968	-19.93	-19.67	-20.74	-19.97	-20.40	-20.16	-20.37	-20.18
1969	-19.29	-19.58	-20.12	-19.33	-19.89	-20.56	-20.29	-19.87
1970	-19.10	-19.61	-19.69	-19.41	-19.79	-19.57	-20.00	-19.60
1971	-19.63	-19.83	-19.98	-19.91	-20.06	-19.49	-20.10	-19.86
1972	-19.60	-19.56	-19.89	-18.59	-19.84	-20.03	-19.78	-19.61
1973	-19.62	-19.35	-19.98	-19.21	-19.76	-20.68	-19.74	-19.76
1974	-18.83	-19.68	-19.64	-19.48	-19.85	-20.33	-19.05	-19.55
1975	-18.80	-19.92	-19.76	-19.24	-20.30	-20.26	-19.15	-19.63
1976	-19.20	-19.70	-20.46	-19.81	-20.04	-20.35	-20.11	-19.95
1977	-19.30	-19.39	-20.29	-19.60	-19.83	-20.57	-20.08	-19.87
1978	-19.21	-19.57	-20.06	-18.81	-19.76	-20.84	-19.97	-19.75
1979	-19.85	-20.07	-20.28	-20.02	-20.05	-20.48	-20.05	-20.11
1980	-19.68	-19.49	-19.87	-19.44	-20.09	-20.26	-19.88	-19.82
1981	-19.29	-19.52	-20.11	-19.43	-20.43	-20.25	-19.85	-19.84
1982	-19.64	-20.50	-20.82	-19.62	-20.59	-20.20	-20.71	-20.30
1983	-19.01	-19.91	-20.57	-19.86	-20.60	-20.00	-20.64	-20.08
1984	-20.58	-19.69	-20.70	-19.58	-20.52	-20.83	-20.59	-20.36
1985	-19.81	-19.38	-19.88	-19.41	-20.41	-19.82	-20.37	-19.87
1986	-19.22	-19.86	-19.73	-18.92	-20.46	-19.85	-20.18	-19.75
1987	-19.15	-19.49	-20.04	-19.83	-20.49	-19.91	-20.24	-19.88
1988	-19.04	-19.98	-19.88	-19.62	-20.46	-20.07	-19.89	-19.85
1989	-19.00	-19.13	-20.37	-19.74	-20.39	-20.20	-19.55	-19.77
1990	-19.89	-19.66	-20.35	-19.54	-20.71	-20.08	-20.33	-20.08
1991	-19.83	-20.47	-20.33	-20.00	-20.90	-20.13	-20.37	-20.29
1992	-19.13	-19.45	-19.66	-20.02	-20.52	-20.41	-19.80	-19.86
1993	-19.28	-19.25	-19.11	-19.71	-20.41	-19.68	-19.39	-19.55
1994	-18.90	-19.32	-19.33	-20.01	-20.58	-19.90	-19.66	-19.67
1995	-19.93	-19.17	-20.03	-20.49	-20.84	-20.05	-19.62	-20.02
1996	-19.69	-19.96	-20.50	-20.05	-20.65	-20.32	-19.95	-20.16
1997	-20.27	-19.65	-20.36	-19.99	-20.59	-20.70	-20.33	-20.27
1998	-20.17	-20.30	-20.54	-19.74	-20.56	-20.30	-20.34	-20.28
1999	-19.93	-20.28	-20.56	-20.25	-20.52	-20.37	-19.87	-20.25
2000	-19.13	-19.32	-20.98	-19.80	-20.63	-19.95	-19.73	-19.93
2001	-19.28	-19.57	-19.56	-20.19	-20.64	-20.38	-19.67	-19.90
2002	-20.01	-19.12	-20.28	-19.12	-20.53	-19.41	-19.29	-19.68
2003	-19.98		-20.21	-19.04	-20.43	-19.15	-19.51	-19.72
2004	-19.06	-19.62	-19.90	-19.98	-20.28	-20.22	-19.61	-19.81
2005	-20.32	-19.48	-20.31				-20.24	-20.09

underlined below=$\delta^{13}C_{raw}$

	001c $\delta^{13}C$	523b $\delta^{13}C$	362b $\delta^{13}C$	4123 $\delta^{13}C$	007 $\delta^{13}C$	527d $\delta^{13}C$	487e $\delta^{13}C$	mean $\delta^{13}C$
1850	-18.76	-18.74	-19.94	-18.71	-19.83	-20.13		-19.35
1851	-19.38	-18.62	-20.05	-18.78	-20.34	-20.58		-19.63
1852	-19.10	-18.96	-20.65	-19.99	-19.82	-18.87		-19.57
1853	-19.30	-19.70	-21.04	-19.56	-19.88	-20.77		-20.04
1854	-19.14	-19.45	-20.44	-21.06	-19.91	-20.95		-20.16
1855	-18.53	-18.26	-20.36	-19.31	-19.32	-19.50		-19.21
1856	-18.53	-17.92	-20.24	-19.14	-19.52	-19.70		-19.18
1857	-18.26	-17.76	-20.21	-19.53	-19.35	-20.13		-19.21

1858	-17.98	-17.98	-20.96	-19.12	-19.87	-20.13		-19.34
1859	-19.10	-18.84	-20.60	-19.45	-20.08	-20.46		-19.76
1860	-18.97	-18.82	-20.52	-20.35	-19.64	-21.21		-19.92
1861	-19.09	-18.34	-20.80	-19.74	-19.68	-20.09		-19.62
1862	-19.37	-18.24	-20.01	-19.71	-19.18	-20.74		-19.54
1863	-19.21	-18.04	-20.73	-21.37	-19.26	-19.98		-19.77
1864	-18.74	-18.48	-20.06	-19.32	-19.36	-19.64		-19.27
1865	-19.87	-18.86	-20.36	-19.79	-19.67	-19.56		-19.69
1866	-19.31	-19.15	-20.59	-19.28	-19.62	-20.12		-19.68
1867	-19.51	-18.52	-20.24	-19.11	-19.70	-19.85		-19.49
1868	-20.16	-19.53	-21.02	-19.57	-19.95	-20.15		-20.06
1869	-20.62	-19.62	-20.82	-19.71	-20.00	-21.20		-20.33
1870	-20.52	-19.43	-20.91	-20.14	-19.67	-20.50		-20.20
1871	-19.91	-19.75	-20.91	-20.13	-20.18	-20.65		-20.26
1872	-19.48	-18.69	-20.26	-20.47	-19.67	-20.30		-19.81
1873	-19.83	-18.45	-21.51	-19.34	-19.81	-20.06		-19.83
1874	-20.00	-19.00	-20.90	-19.69	-20.09	-20.38		-20.01
1875	-19.99	-19.05	-20.48	-19.26	-20.12	-20.69		-19.93
1876	-19.80	-19.36	-20.38	-19.43	-19.72	-19.90		-19.77
1877	-19.57	-19.41	-19.89	-19.05	-19.72	-21.06		-19.78
1878	-19.85	-18.74	-21.26	-19.29	-19.63	-20.20		-19.83
1879	-19.47	-18.99	-20.29	-19.61	-19.49	-20.32		-19.70
1880	-19.95	-19.11	-20.16	-20.90	-19.80	-19.92		-19.97
1881	-19.83	-18.78	-20.39	-18.94	-20.14	-20.43		-19.75
1882	-19.43	-18.78	-20.05	-18.80	-19.92	-20.07		-19.51
1883	-19.47	-18.68	-21.21	-18.86	-20.02	-20.33		-19.76
1884	-19.73	-19.31	-20.37	-19.11	-20.15	-20.40		-19.85
1885	-19.48	-19.04	-19.97	-19.23	-20.09	-19.95		-19.63
1886	-19.60	-19.15	-20.33	-19.05	-20.29	-20.57		-19.83
1887	-19.84	-19.27	-20.62	-19.15	-20.14	-19.98		-19.83
1888	-19.83	-19.02	-20.61	-19.14	-19.92	-20.30		-19.80
1889	-19.76	-19.87	-20.24	-19.54	-20.02	-20.41		-19.97
1890	-20.46	-19.18	-20.57	-19.64	-20.60	-20.42		-20.15
1891	-21.31	-19.73	-20.81	-21.29	-20.69	-21.35		-20.86
1892	-19.78	-19.28	-21.36	-19.02	-20.01	-20.15		-19.93
1893	-20.11	-19.34	-20.91	-19.48	-20.30	-20.36		-20.08
1894	-20.26	-19.44	-21.03	-19.54	-20.02	-20.70		-20.17
1895	-19.46	-19.39	-20.64	-19.16	-20.25	-19.95		-19.81
1896	-20.34	-19.68	-20.99	-19.46	-20.01	-20.09		-20.10
1897	-20.07	-19.68	-20.93	-19.37	-19.94	-19.57		-19.93
1898	-19.24	-19.21	-20.15	-18.71	-19.84	-19.44		-19.43
1899	-18.98	-19.48	-20.06	-18.44	-20.06	-20.11		-19.52
1900	-19.51	-19.33	-20.57	-19.11	-19.94	-19.85		-19.72
1901	-19.94	-19.60	-21.30	-18.81	-20.08	-20.46		-20.03
1902	-19.46	-19.25	-20.94	-18.66	-19.94	-19.30		-19.59
1903	-19.39	-19.34	-20.48	-18.54	-19.48	-19.16		-19.40
1904	-19.74	-19.69	-21.29	-19.70	-19.94	-19.68		-20.01
1905	-19.38	-19.54	-20.75	-18.55	-20.35	-19.55		-19.69
1906	-19.77	-19.91	-21.56	-19.24	-20.23	-20.36		-20.18
1907	-19.76	-19.92	-21.62	-19.44	-20.30	-19.74	-19.49	-20.04
1908	-19.83	-19.83	-21.69	-19.72	-20.71	-20.71	-19.63	-20.30

1909	-19.20	-19.41	-20.53	-19.06	-19.93	-19.73	-19.07	-19.56
1910	-18.88	-19.89	-21.22	-18.82	-20.49	-20.07	-19.30	-19.81
1911	-19.33	-19.53	-20.66	-19.15	-20.32	-19.76	-19.48	-19.75
1912	-18.64	-19.65	-21.41	-19.44	-20.67	-19.71	-19.56	-19.87
1913	-20.23	-20.50	-21.39	-19.79	-21.40	-20.57	-20.25	-20.59
1914	-20.02	-19.97	-21.13	-19.82	-20.77	-20.34	-19.97	-20.29
1915	-19.48	-20.09	-20.51	-19.29	-20.15	-19.55	-20.12	-19.88
1916	-19.35	-19.41	-20.69	-18.78	-20.29	-19.59	-19.02	-19.59
1917	-19.60	-19.81	-20.52	-19.26	-20.83	-19.82	-19.40	-19.89
1918	-19.92	-20.14	-21.18	-20.14	-20.77	-19.85	-19.28	-20.18
1919	-19.36	-19.96	-20.33	-19.06	-20.58	-20.11	-19.23	-19.80
1920	-19.56	-19.56	-20.34	-19.14	-20.65	-20.11	-19.57	-19.85
1921	-19.74	-19.98	-20.61	-19.37	-20.71	-20.86	-19.66	-20.13
1922	-19.46	-19.92	-20.88	-20.95	-20.61	-21.42	-19.59	-20.40
1923	-19.28	-19.50	-20.75	-19.32	-20.73	-20.03	-19.21	-19.83
1924	-18.56	-19.69	-21.49	-18.95	-21.21	-20.30	-19.05	-19.89
1925	-20.53	-20.43	-21.72	-20.19	-21.24	-21.30	-19.71	-20.73
1926	-20.54	-20.34	-20.97	-19.28	-20.58	-20.54	-19.69	-20.28
1927	-19.99	-19.21	-20.55	-19.58	-20.17	-20.25	-19.40	-19.88
1928	-18.88	-19.35	-20.41	-18.57	-20.14	-20.59	-18.73	-19.52
1929	-19.50	-19.66	-20.15	-18.53	-20.24	-19.85	-19.24	-19.60
1930	-19.25	-19.64	-19.86	-19.26	-19.88	-19.59	-19.41	-19.56
1931	-19.66	-19.61	-19.95	-18.44	-19.65	-20.00	-19.48	-19.54
1932	-19.11	-19.64	-19.99	-18.83	-19.67	-20.14	-19.91	-19.61
1933	-19.36	-19.68	-20.39	-18.92	-19.69	-19.68	-19.49	-19.60
1934	-19.50	-19.58	-20.40	-18.57	-20.33	-19.76	-19.34	-19.64
1935	-19.66	-19.36	-20.25	-18.85	-20.10	-19.41	-19.49	-19.59
1936	-20.26	-19.70	-20.49	-19.00	-20.25	-20.35	-19.95	-20.00
1937	-19.71	-19.63	-20.24	-19.31	-20.60	-20.35	-19.41	-19.89
1938	-19.98	-20.02	-20.09	-19.43	-20.68	-20.43	-20.07	-20.10
1939	-20.20	-19.92	-20.13	-19.08	-20.62	-20.24	-20.22	-20.06
1940	-20.16	-19.70	-20.35	-20.13	-20.57	-20.85	-20.12	-20.27
1941	-20.32	-20.04	-20.88	-19.57	-21.30	-20.44	-20.46	-20.43
1942	-20.04	-20.34	-20.03	-19.36	-20.62	-20.66	-19.68	-20.10
1943	-19.66	-20.06	-20.02	-19.53	-20.46	-19.88	-19.97	-19.94
1944	-20.24	-20.09	-20.11	-19.95	-20.64	-20.40	-19.73	-20.17
1945	-20.57	-20.37	-20.89	-19.10	-21.13	-20.58	-20.09	-20.39
1946	-20.25	-20.14	-20.51	-18.84	-21.01	-20.44	-20.26	-20.21
1947	-19.34	-19.85	-20.14	-19.53	-20.73	-20.43	-19.51	-19.93
1948	-19.27	-19.29	-19.91	-19.41	-20.45	-20.38	-19.49	-19.74
1949	-19.63	-19.80	-20.59	-19.22	-20.36	-20.10	-19.85	-19.94
1950	-19.98	-19.84	-20.77	-19.20	-20.06	-19.98	-19.55	-19.91
1951	-20.10	-19.78	-20.35	-19.34	-20.11	-20.54	-20.01	-20.03
1952	-20.23	-20.02	-20.13	-19.29	-20.45	-20.25	-20.41	-20.11
1953	-19.93	-20.09	-20.78	-19.43	-20.31	-20.14	-19.85	-20.08
1954	-20.08	-19.97	-20.15	-19.75	-20.11	-20.22	-19.56	-19.98
1955	-19.89	-20.30	-20.61	-19.31	-20.31	-20.69	-19.53	-20.09
1956	-20.01	-19.93	-20.30	-19.40	-20.21	-20.25	-20.31	-20.06
1957	-19.79	-19.56	-19.92	-19.26	-20.17	-20.10	-20.21	-19.86
1958	-19.66	-19.48	-19.85	-19.96	-20.23	-20.97	-20.23	-20.05
1959	-19.01	-19.69	-19.56	-18.56	-20.07	-19.93	-19.34	-19.45

1960	-19.21	-19.84	-20.52	-19.46	-20.17	-20.68	-19.48	-19.91
1961	-19.78	-20.25	-20.88	-20.51	-20.59	-20.02	-20.70	-20.39
1962	-19.96	-20.36	-20.69	-19.31	-20.54	-20.14	-20.71	-20.24
1963	-19.72	-20.04	-20.35	-18.97	-20.68	-20.98	-20.62	-20.19
1964	-19.92	-20.66	-20.54	-20.19	-21.02	-20.91	-20.83	-20.58
1965	-20.47	-20.28	-20.96	-20.10	-20.99	-20.96	-20.97	-20.68
1966	-20.59	-20.31	-20.48	-19.29	-21.09	-20.99	-20.05	-20.40
1967	-20.37	-20.63	-20.89	-20.76	-20.95	-21.07	-20.69	-20.77
1968	-20.62	-20.36	-21.43	-20.66	-21.09	-20.85	-21.06	-20.87
1969	-20.01	-20.30	-20.84	-20.05	-20.61	-21.28	-21.01	-20.59
1970	-19.85	-20.36	-20.44	-20.16	-20.54	-20.32	-20.75	-20.35
1971	-20.40	-20.60	-20.75	-20.68	-20.83	-20.26	-20.87	-20.63
1972	-20.40	-20.36	-20.69	-19.39	-20.64	-20.83	-20.58	-20.41
1973	-20.45	-20.18	-20.81	-20.04	-20.59	-21.51	-20.57	-20.59
1974	-19.69	-20.54	-20.50	-20.34	-20.71	-21.19	-19.91	-20.41
1975	-19.69	-20.81	-20.65	-20.13	-21.19	-21.15	-20.04	-20.52
1976	-20.12	-20.62	-21.38	-20.73	-20.96	-21.27	-21.03	-20.87
1977	-20.24	-20.33	-21.23	-20.54	-20.77	-21.51	-21.02	-20.81
1978	-20.18	-20.54	-21.03	-19.78	-20.73	-21.81	-20.94	-20.72
1979	-20.85	-21.07	-21.28	-21.02	-21.05	-21.48	-21.05	-21.11
1980	-20.71	-20.52	-20.90	-20.47	-21.12	-21.29	-20.91	-20.85
1981	-20.35	-20.58	-21.17	-20.49	-21.49	-21.31	-20.91	-20.90
1982	-20.72	-21.58	-21.90	-20.70	-21.67	-21.28	-21.79	-21.38
1983	-20.12	-21.02	-21.68	-20.97	-21.71	-21.11	-21.75	-21.19
1984	-21.72	-20.83	-21.84	-20.72	-21.66	-21.97	-21.73	-21.50
1985	-20.98	-20.55	-21.05	-20.58	-21.58	-20.99	-21.54	-21.04
1986	-20.42	-21.06	-20.93	-20.12	-21.66	-21.05	-21.38	-20.95
1987	-20.37	-20.71	-21.26	-21.05	-21.71	-21.13	-21.46	-21.10
1988	-20.29	-21.23	-21.13	-20.87	-21.71	-21.32	-21.14	-21.10
1989	-20.28	-20.41	-21.65	-21.02	-21.67	-21.48	-20.83	-21.05
1990	-21.20	-20.97	-21.66	-20.85	-22.02	-21.39	-21.64	-21.39
1991	-21.17	-21.81	-21.67	-21.34	-22.24	-21.47	-21.71	-21.63
1992	-20.50	-20.82	-21.03	-21.39	-21.89	-21.78	-21.17	-21.23
1993	-20.67	-20.64	-20.50	-21.10	-21.80	-21.07	-20.78	-20.94
1994	-20.32	-20.74	-20.75	-21.43	-22.00	-21.32	-21.08	-21.09
1995	-21.38	-20.62	-21.48	-21.94	-22.29	-21.50	-21.07	-21.47
1996	-21.17	-21.44	-21.98	-21.53	-22.13	-21.80	-21.43	-21.64
1997	-21.78	-21.16	-21.87	-21.50	-22.10	-22.21	-21.84	-21.78
1998	-21.70	-21.83	-22.07	-21.27	-22.09	-21.83	-21.87	-21.81
1999	-21.49	-21.84	-22.12	-21.81	-22.08	-21.93	-21.43	-21.81
2000	-20.72	-20.91	-22.57	-21.39	-22.22	-21.54	-21.32	-21.52
2001	-20.90	-21.19	-21.18	-21.81	-22.26	-22.00	-21.29	-21.52
2002	-21.66	-20.77	-21.93	-20.77	-22.18	-21.06	-20.94	-21.33
2003	-21.65		-21.88	-20.71	-22.10	-20.82	-21.18	-21.39
2004	-20.75	-21.31	-21.59	-21.67	-21.97	-21.91	-21.30	-21.50
2005	-22.03	-21.19	-22.02				-21.95	-21.80